



MONASH University

**FUNCTIONAL CHARACTERISATION OF THE
CALCITONIN RECEPTOR**

Anna Ostrovskaya

Master of Science

A thesis submitted for the degree of Doctor of Philosophy at
Monash University in June, 2019

Drug Discovery Biology
Monash Institute of Pharmaceutical Sciences
Faculty of Pharmacy and Pharmaceutical Sciences
Monash University

Copyright notice

© Anna Ostrovskaya (2019).

I certify that I have made all reasonable efforts to secure copyright permissions for third-party content included in this thesis and have not knowingly added copyright content to my work without the owner's permission.

Table of Contents

Abstract	i
Declaration	iii
Communications during enrolment	iv
Thesis including published works declaration	v
Acknowledgements	viii
List of abbreviations	x
CHAPTER 1	1
General introduction	1
1.1 G protein-coupled receptors (GPCRs)	2
1.1.1 General introduction	2
1.1.2 Structural characteristics of GPCRs	2
1.1.3 Classification of GPCRs	2
1.1.4 Functional characteristics of GPCRs	5
1.1.4.1 G protein dependent signalling	5
1.1.4.2 GPCR desensitisation and internalisation	7
1.1.4.3 G protein independent signalling	9
1.1.4.4 The concept of efficacy and biased agonism	9
1.2 The law of mass action and pharmacological quantification using the operational model	11
1.2.1 The Law of Mass Action	11
1.2.2 The operational model of agonism	12
1.3 Secretin-like, Class B1 GPCRs	12
1.3.1 secretin-like subfamily	12
1.3.2 Ligand binding site and two domain model of secretin-like GPCRs	13
1.3.3 secretin-like structural characteristics	15
1.3.4 Comparisons between rhodopsin-like and secretin-like	17
1.3.5 secretin-like GPCRs biased agonism	18
1.3.6 Accessory proteins and receptor heterocomplexes with RAMPs	19
1.3.7 Calcitonin family of peptides – their sites of production, physiological roles and receptors	20
1.3.7.1 Calcitonin	21
1.3.7.2 Amylin	23
1.3.7.3 α CGRP and β CGRP	23

1.3.7.4 Adrenomedullin and Intermedin	24
1.3.7.5 Novel CTR peptides	24
1.4 Calcitonin receptor	25
1.4.1 CTR isoforms and splice variants	25
1.4.2 CTR structure and activation	26
1.4.3 CTR signalling	28
1.4.4 CTR trafficking and regulation	30
1.4.5 Biological actions CTR	31
1.4.5.1 Bone actions	31
1.4.5.2 Renal actions	33
1.4.5.3 Central actions	33
1.4.5.4 CTR roles in cancer	33
1.4.5.5 CTR in Glioblastoma Multiforme	36
1.4.5.6 Other actions of CTR	36
1.5 Aims	37
CHAPTER 2	40
Materials and methods	40
2.1 MATERIALS	41
2.1.1 Peptides	41
2.1.2 Antibodies	41
2.1.3 General reagents	41
2.1.4 Plasmids and primers	42
2.2 Molecular biology	42
2.2.1 Generation of single alanine point mutations of the cMycCTRaLeu in pENTR11 vector	42
2.2.2 Transformation	43
2.2.3 DNA amplification, extraction	43
2.2.4 Sequence confirmation	43
2.2.5 Recombination into destination vector	43
2.3 Tissue culture	44
2.3.1 Mammalian cell culture	44
2.3.2 Stable transfection of mammalian FlpIn cells	44
2.4 Functional Assays	45
2.4.1 Iodination of sCT(8-32)	45
2.4.2 Heterologous whole cell radioligand competition binding	45

2.4.3 cAMP accumulation Assay	45
2.4.4 ERK1/2 Phosphorylation Assay	46
2.4.5 p38 phosphorylation	46
2.4.6 Ca ²⁺ mobilization	47
2.4.7 Assessing cell proliferation using live cell imaging (Operetta)	47
2.4.8 MTT assay	47
2.5 Assessing receptor cell surface expression by flow cytometry	48
2.6 Quantitative Real-time Reverse Transcription Polymerase Chain Reaction (RT-qPCR)	48
2.7 Public data analysis	49
2.8 Equations and data analysis	50
2.8.1 Equations to fit experimental data	50
2.8.2 Error propagation	52
2.8.3 Statistics	52
CHAPTER 3	53
Expression and activity of the calcitonin receptor family in a sample of primary human high-grade gliomas	53
CHAPTER 4	66
Effects of alanine mutations of residues within calcitonin receptor (hCTR) binding pocket on the CTR cell surface expression and binding of calcitonin agonists	66
4.1 Introduction	67
4.2 Results	69
4.2.1 Effects of the CTR TM mutations on CTR cell surface expression	72
4.2.2 Effects of CTR TM mutations on equilibrium affinity and cAMP functional affinity of calcitonin peptide agonists	76
4.2.3 Effects of the CTR TM mutations on CTR cAMP functional affinity in response to α CGRP and rAMY	91
4.2.4 Effects of the CTR TM mutations on CTR pERK1/2 functional affinity	97
4.3 Discussion	107
4.3.1 Effects of the CTR TM mutations on CTR cell surface expression	107
4.3.2 Effects of CTR TM mutations on calcitonin agonists equilibrium and functional cAMP affinity	108
4.3.3 Effects of the CTR TM mutations on CTs pERK1/2 functional affinity	118
4.3.4 Effects of CTR TM mutations on the CTR cAMP and pERK1/2 functional affinity in response to α CGRP and rAMY	120
4.4 Summary	123
CHAPTER 5	125

Effects of alanine mutations of residues within calcitonin receptor (hCTR) binding pocket on intracellular signalling to cAMP and ERK pathways	125
5.1 Introduction	126
5.2 Results	127
5.2.1 Effects of the CTR TM mutations on CTR cAMP signalling	127
5.2.1.1 cAMP signalling in response to calcitonins	127
5.2.1.2 cAMP signalling in response to α CGRP and rAMY	136
5.2.2 Effects of the CTR TM mutations on CTR pERK1/2 signalling	142
5.2.2.1 Assessment of pERK1/2 in response to calcitonins	142
5.2.2.2 Assessment of pERK1/2 in response to α CGRP and rAMY	154
5.3 Discussion	160
Effects of the CTR TM mutations on CTR cAMP and pERK1/2 efficacy	160
5.4 Summary	168
CHAPTER 6	170
General discussion and future directions	170
6.1 Research Focus	171
6.2 CTR role in GBM signalling and proliferation: main findings and discussion	171
6.3 Mutagenesis of CTR binding pocket: main findings and discussion	173
6.4 Concluding remarks	178
REFERENCES	181
APPENDIX 1	209
APPENDIX 2	221
Expression and activity of the calcitonin receptor family in a sample of primary human high-grade gliomas	221
APPENDIX 3	234
Calcitonin	234

Section 1.4 is largely reproduced from Ostrovskaya A, Findlay DM, Sexton PM, SGB F. Calcitonin. Reference Module in Neuroscience and Biobehavioral Psychology. Amsterdam: Elsevier; 2017. p. 1–12. <https://doi.org/10.1016/B978-0-12-809324-5.03223-5>. This book chapter is primarily my own work.

ABSTRACT

Calcitonin receptor (CTR) is a member of the class B G protein-coupled receptor (GPCR) family, with roles in calcium and bone homeostasis, and other roles, including cell growth and differentiation and is implicated in the pathophysiology of various cancers. These diverse roles may, partly, be due to CTR's pleiotropic coupling to signalling pathways including cAMP, ERK1/2 phosphorylation and intracellular Ca^{2+} mobilization.

This thesis examines the putative role of pleiotropic coupling of the CTR in the pathophysiological setting of Glioblastoma Multiforme (GBM) (a type of brain cancer), followed by a molecular dissection of agonist-dependent activation of the CTR using alanine scanning mutagenesis.

Pharmacological characterization of the CTR receptor family present in four high grade glioma cell lines that were derived from individual patient tumours and are capable of recapitulating the original disease phenotype in xenograft models was performed. Gene expression analysis using TaqMan qPCR confirmed CTR and calcitonin receptor-like receptor (CLR) expressed at the mRNA level in each of the four cell lines. However, performing cAMP assay using a panel of CTR- and (CLR) agonists showed that only one out of four studied cell lines, SB2b, expressed functional CTR, while the other three cell lines (Pb1, WK1 and JK2) displayed a CLR-receptor phenotype. Consistent with low CTR expression, SB2b showed no activation of pERK1/2, p38 MAPK, or Ca^{2+} mobilization. The absence of CTR-mediated MAPK-signaling in the SB2b was consistent with no effects of CTR stimulation/inhibition on cell metabolism and proliferation. Based on these results I concluded that targeting CTR pharmacologically is unlikely to be viable strategy for GBM treatment and that more comprehensive and systematic analysis is required in order to understand CTR's role in this cancer. Additionally, I established no correlation between GBM subtype and CTR expression profile.

Class B GPCRs are known to adopt a two-domain binding mode of their peptide agonists, where both extracellular (ECD) and transmembrane domains (TM) of the receptor participate in ligand binding and receptor activation. For the CTR this is supported by both structural cryo-EM data as well as by the mutational studies of the CTR ECD domains. To gain insight into how CTR ligand binding and signaling activation is mediated within the TM region of the receptor, I performed Alanine mutagenesis analysis of residues within this region. I identified residues with common and unique effects on affinity of CTR agonists and these were interpreted using CTR structural data and molecular dynamics simulations. Binding in response to salmon calcitonin (sCT) was less affected by individual Ala substitutions, consistent with the slow dissociation

kinetics and higher persistency of sCT-CTR interactions. Assessment of cAMP and pERK1/2 signalling pathways revealed pathway-specific effects, with only limited effects on cAMP efficacy while pERK1/2 efficacy was profoundly decreased across all CTR ligands. Comparison of mutational effects on binding affinity and efficacy between CTR and other class B receptors revealed certain commonalities (such as the importance of conserved polar network in binding and signal transduction) and differences (arising from distinct structures of the class B receptors' binding pockets and peptides).

DECLARATION

This thesis contains no material which has been accepted for the award of any other degree or diploma at any university or equivalent institution and that, to the best of my knowledge and belief, this thesis contains no material previously published or written by another person, except where due reference is made in the text of the thesis.

Signature:



Print Name: Anna Ostrovskaya

Date: 12.06.2019

COMMUNICATIONS DURING ENROLMENT

PEER REVIEWED ARTICLES

Ostrovskaya, A., Findlay, D. M., Sexton, P. M., Furness, S. G. B. 2017. Calcitonin. Reference Module in Neuroscience and Biobehavioral Psychology. Elsevier.

Ostrovskaya, A., Hick, C., Hutchinson, D. S., Stringer, B. W., Wookey, P. J., Wootten, D., Sexton, P. M., Furness, S. G. B. 2019. Expression and activity of the calcitonin receptor family in a sample of primary human high-grade gliomas. BMC Cancer, 19, 157.

CONFERENCE PROCEEDINGS

Ostrovskaya A., Hick C., Sexton P. M., Furness S.G.B. (2016). Expression and signalling of calcitonin family receptors in four patient-derived GBM cell lines. Poster presentation. 9th meeting of the Molecular Pharmacology of G Protein Coupled Receptors (ASCEPT-MPGPCR-2016). Melbourne, Australia.

Ostrovskaya A., Hick C., Wootten D., Sexton P. M., Furness S.G.B. (2017). Pharmacological analysis of the calcitonin receptor family in patient-derived high-grade glioma cell lines. Poster presentation. The British Pharmacological Society's annual meeting "Pharmacology-2017". London, United Kingdom

Ostrovskaya A., Hick C., Sexton P. M., Wootten D., Furness S.G.B. (2018). Structure-Function Studies of the Calcitonin Receptor Binding Pocket. Poster presentation. 10th meeting of the Molecular Pharmacology of G Protein Coupled Receptors (BPS-MPGPCR-2018) meeting. Melbourne, Australia.

THESIS INCLUDING PUBLISHED WORKS DECLARATION

I hereby declare that this thesis contains no material which has been accepted for the award of any other degree or diploma at any university or equivalent institution and that, to the best of my knowledge and belief, this thesis contains no material previously published or written by another person, except where due reference is made in the text of the thesis.

This thesis includes one original paper published in peer reviewed journal. The core theme of the thesis is functional characterisation of the calcitonin receptor. The ideas, development and writing up of all the papers in the thesis were the principal responsibility of myself, the candidate, working within the department of Drug Discovery Biology under the supervision of Dr. Sebastian Furness, Prof. Denise Wootten, Prof. Patrick Sexton.

(The inclusion of co-authors reflects the fact that the work came from active collaboration between researchers and acknowledges input into team-based research.)

In the case of *Chapter 3* my contribution to the work involved the following:

Thesis Chapter	Publication Title	Status (published, in press, accepted or returned for revision, submitted)	Nature and % of student contribution	Co-author name(s) Nature and % of Co-author's contribution*	Co-author(s), Monash student Y/N*
3	Expression and activity of the calcitonin receptor family in a sample of primary human high-grade gliomas	Published	Assisted with project design, performed the majority of experiments, analysed data, prepared, reviewed and edited the manuscript. (75%)	CH assisted with cell signaling experiments, reviewing & editing, DSH assisted with qPCR experiments, reviewing & editing; PJW performed western blot experiments, reviewing & editing; BWS provided high-grade glioma cell lines, reviewing & editing. DW and PMS assisted with project design, reviewing & editing. SGBF overall conception, analysis of publicly available data, manuscript preparation.	No No No No No, No No

I have not renumbered sections of published papers in order to generate a consistent presentation within the thesis.



Student signature:

Date: 12.06.2019

The undersigned hereby certify that the above declaration correctly reflects the nature and extent of the student's and co-authors' contributions to this work. In instances where I am not the responsible author I have consulted with the responsible author to agree on the respective contributions of the authors.



Main Supervisor signature:

Date: 12.06.2019

ACKNOWLEDGEMENTS

I would like to express my sincere gratitude to all of my amazing supervisors, Dr. Sebastian Furness, Prof. Patrick Sexton, Assoc. Prof. Denise Wootten and Dr. Caroline Hick, who provided me with excellent guidance and enabled me to grow and develop as a scientist. Under your supervision I discovered for myself a new field, mastered new scientific methods and matured my scientific writing.

To Sebastian, thank you for your time and patience, and for teaching me so much in these 4 years. Your fresh and innovative views enabled me to look at the issues in a different light. I appreciate that I could always turn to you for useful guidance and advice. To Patrick, thank you for your wisdom, challenging me intellectually and prompting me to see the bigger picture. To Denise, thank you for taking me under your wing. Your invaluable comments and suggestions always helped me to see things more clearly and logically. To Caroline, thank you for always being so caring, empathetic and optimistic. I wouldn't be able to achieve such results without your kind support.

Huge thanks to my PhD panel members, Dr John Haynes, Dr. Simon Murray and Cameron Nowell for your valuable guidance and insights.

Thanks to all family B/Metabolic group members for creating a supportive and friendly atmosphere.

Many thanks to everyone who helped me in the lab, and especially to Emma (Dr. Emma Dal Maso) who has always been my lifesaver. Thank you Dr. Dana Hutchinson for teaching me RNA extraction and qPCR experiments, for your thorough approach and patience. Many thanks to George Christopoulos and to Dr. Stewart Fabb for teaching me a lot of tricks in molecular biology that made my experiments work. I would like to acknowledge Dr. Peter Wookey for providing me with GBM cell lines. Another thanks to Cameron Nowell for helping me with microscopy experiments and data analysis.

I would like to thank the DDB theme, Faculty of Pharmacy and Pharmaceutical Sciences and Monash University for the generous funding support (without which my PhD would be

impossible) and for providing me with an opportunity to be a part of this fantastic world-leading PhD program.

I would like to thank my parents, who are far away, but are always supporting me and believing in me. My best friend and mentor, Natasha, for always being the source of my inspiration and a positive outlook. To, Arseni, for being such a loving and caring partner and a true friend, for going with me throughout my numerous PhD ups and downs. To all of my DDB friends and colleagues, and especially to Emma, Diana and Paulina – for being there for me, for our talks, laughs and for your immense support and advice.

LIST OF ABBREVIATIONS

AC	adenylyl cyclase
ACTH	adrenocorticotrophic hormone
Ala	alanine
AM1	adrenomedullin 1
AM2/IMD	adrenomedullin 2/ intermedin
AM₁, AM₂	adrenomedullin receptors 1 and 2
Amy	amylin peptide
AMY	amylin receptor
ANOVA	analysis of variance
ATP	adenosine triphosphate
BRET	bioluminescence resonance energy transfer
BSA	bovine serum albumin
BW	Ballesteros-Weinstein numbering
CALCR	calcitonin receptor protein coding gene
cAMP	cyclic adenosine monophosphate
cCT	chicken calcitonin
CGRP	calcitonin gene-related peptide
CLR	calcitonin-like receptor
CNS	central nervous system
CT	calcitonin peptide
C-terminus	carboxyl terminus
CTR	calcitonin receptor
CREB	cAMP response element-binding protein
cpm	counts per minute
CRFR1	corticotropin-releasing factor receptor 1
CRFR2	corticotropin-releasing factor receptor 2
CRSPs	CTR-stimulating peptides
Cryo-EM	cryogenic electron microscopy
CV-1	<i>Cercopithecus aethiops</i> kidney cells
DAG	diacylglycerol
DNA	deoxyribonucleic acid
DMEM	Dulbecco's modified eagle's medium
EC₅₀	half maximal effective concentration

ECD	extracellular domain
ECL	extracellular loops
E_{max}	maximal response
EPAC	cAMP-regulated guanine nucleotide exchange factor proteins directly activated by cAMP
ER	endoplasmic reticulum
ERK1/2	extracellular signal-regulated kinases 1/2
ERK5	extracellular signal-regulated kinases 5
FACS	fluorescence-activated cell sorting
FBS	foetal bovine serum
FDA	US Food and Drug Administration
Forskolin	(3 <i>R</i> ,4 <i>aR</i> ,5 <i>S</i> ,6 <i>S</i> ,6 <i>aS</i> ,10 <i>S</i> ,10 <i>aR</i> ,10 <i>bS</i>)-6,10,10 <i>b</i> -Trihydroxy- 3,4 <i>a</i> ,7,7,10 <i>a</i> -pentamethyl-1-oxo-3-vinyldodecahydro-1 <i>H</i> - benzo[<i>f</i>]chromen-5-yl acetate
FPKM	Fragments Per Kilobase of transcript per Million mapped reads
FRET	Förster resonance energy transfer
Gα	Guanine nucleotide binding protein (G protein), alpha (α) subunit (of the G protein heterotrimer)
Gαi	G α that inhibits adenylate cyclase
Gαq	G α subunit that activates phospholipase C
Gαs	G α subunit that activates adenylate cyclase
G$\beta\gamma$	beta (β) and gamma (γ) subunits of the G protein heterotrimer
GABA	gamma-aminobutyric acid
GASPs	GPCR-associated sorting proteins
GBM	glioblastoma multiforme
GCGR	glucagon receptor
GDP	guanosine diphosphate
GEF	guanine nucleotide exchange factor
GHRH	growth hormone-releasing hormone
GIP	glucose-dependent insulintropic peptide
GIPR	gastric inhibitory polypeptide receptor
GIRK	g protein-coupled inwardly rectifying potassium channel
GLP-1	glucagon-like peptide 1

GLP-1R	glucagon-like peptide 1 receptor
GLP-2R	glucagon-like peptide 2 receptor
GTP	guanosine triphosphate
GTPase	a family of hydrolase enzymes that can bind and hydrolyze guanosine triphosphate (GTP)
GPCR	g protein–coupled receptor
GRAFS	GPCR classification system (Glutamate, Rhodopsin, Adhesion, Frizzled/taste2 and Secretin)
GRK	g protein–coupled receptor kinase
H8	helix VIII/8
HBSS	Hanks' balanced salt solution
hCT	human calcitonin
hCTR_aLeu	human calcitonin receptor variant, with a leucine polymorphism in the third intracellular C-terminal domain lacking a 16 amino acid insertion in the first intracellular loop
HD	heptahelical domain
HEF1	human enhancer of filamentation 1
HEPES	4-(2-hydroxyethyl)-1-piperazineethanesulfonic acid
IκBα	nuclear factor of kappa light polypeptide gene enhancer in β -cells inhibitor, alpha
ICL	intracellular loops
IP1	inositol monophosphate
IP₃	inositol triphosphate
JNK	c-jun n-terminal kinase
MAPK	mitogen-activated protein kinases
MD	molecular dynamics
MDM2	mouse double minute 2 homolog
MTC	medullary thyroid cancer
N.D.	not determined
NTD	N-terminal domain
p300	histone acetyltransferase p300 (transcriptional co-activator)
p38	p38 mitogen-activated protein kinase
p53	tumor protein 53
PAC1/ADCYAP1R1	pituitary adenylate cyclase-activating polypeptide receptor

PCR	polymerase chain reaction
pCT	porcine calcitonin
PI3K	phosphoinositide 3-kinase
PIP2	phosphatidylinositol 4,5-bisphosphate
pdb	protein data bank
PDZ	post synaptic density protein (PSD95), Drosophila disc large tumor suppressor (Dlg1), and zonula occludens-1 protein (zo-1) homology domain
PHM-27	human peptide histidine-methionine 27
PLC-β (Cβ)	phospholipase C β
PLD	phospholipase d
pK_A	functional affinity, derived from operational model of agonism
PKA	protein kinase a
PKB/AKT	protein kinase b
PKC	protein kinase c
pK_i	equilibrium affinity defined by competition radioligand binding
PTH	parathyroid hormone
PTHrP	parathyroid hormone-related peptides
PTHR1, PTHR2	parathyroid hormone receptors 1 and 2
Raf	mitogen-activate protein kinase
RAMP	receptor activity modifying protein
rAMY	rat amylin peptide
RAR	retinoic acid receptor
RGS	regulators of G protein signalling
RFU	relative fluorescence units
RNA	ribonucleic acid
RT qPCR	quantitative reverse transcription polymerase chain reaction
sCT	salmon calcitonin
SCTR	secretin receptor
SD	standard deviation
SEM	standard error of the mean
SNP	single nucleotide polymorphism

TM	transmembrane
uPA	urokinase-type plasminogen activator
V2	vasopressin receptor
VIP	vasoactive intestinal polypeptide
Wnt	wingless/integration 1
WT	wild-type

CHAPTER 1

General introduction

1.1 G PROTEIN-COUPLED RECEPTORS (GPCRs)

1.1.1 GENERAL INTRODUCTION

G protein-coupled receptors (GPCRs) are the largest family of cell surface receptors that mediate many cellular responses to hormones and neurotransmitters, and are responsible for senses such vision, taste and smell. They play key roles in all aspects of physiology and pathophysiology and as such are the targets of ~50% of all pharmaceuticals (Rask-Andersen *et al.*, 2011). In response to ligand binding, GPCRs can pleiotropically couple to G proteins and β -arrestins allowing parallel signalling to multiple cellular pathways (Pal *et al.*, 2013, Tuteja, 2009).

Approximately 150 of the GPCRs found in the human genome have unknown ligands and are referred as orphan GPCRs (Davenport *et al.*, 2013).

1.1.2 STRUCTURAL CHARACTERISTICS OF GPCRs

GPCRs are transmembrane proteins that have both extracellular and intracellular domains. A distinguishing feature of a GPCR is the presence of a heptahelical domain (HD) consisting of seven transmembrane α -helices (TMs) that span the plasma membrane to form 3 extracellular and 3 intracellular loops (ECL and ICL respectively) of various length (Lagerstrom *et al.*, 2008). GPCRs receive stimuli (such as hormones, neurotransmitters, light etc.) from the extracellular environment (Fredriksson *et al.*, 2003). Receptor activation by external stimuli results in structural rearrangements that are associated with the movement of transmembrane helices. These conformational changes facilitate opening of intracellular transducer binding pocket allowing recruitment of intracellular transducers (Lagerstrom *et al.*, 2008).

Some GPCRs dimerize and can form homo- or heterodimers (Terrillon *et al.*, 2004, Roed *et al.*, 2012, Angers *et al.*, 2002, George *et al.*, 2002). At present, the mechanism and functional role of receptor dimerization of most receptor families is largely unclear. In contrast, class C receptors can only exist and function as obligate dimers and are well characterised dimers (Moller *et al.*, 2017, Geng *et al.*, 2016, Geng *et al.*, 2013).

1.1.3 CLASSIFICATION OF GPCRs

The superfamily of G-protein-coupled receptors (GPCRs) is very diverse in structure and function, with almost 800 GPCR sequences found in the human genome; with ~ 400 non-olfactory GPCRs (Lagerstrom *et al.*, 2008, Stevens *et al.*, 2013).

Various systems to classify GPCRs have been proposed. One of the more recent, and widely used systems, is the GRAFS classification system, proposed by (Fredriksson *et al.*, 2003).

It uses alignment of the amino-acid sequences of the predicted transmembrane helices to derive a phylogeny of all human GPCRs resulting in five main families: Glutamate, Rhodopsin, Adhesion, Frizzled/taste2 and Secretin (Fredriksson *et al.*, 2003) (Figure 1.1). The GRAFS (glutamate (G), rhodopsin (R), adhesion (A), frizzled/taste2 (F) and secretin (S)) system differs from earlier systems which grouped the Secretin and Adhesion family into a single class.

The Rhodopsin-like family (known also as Class A) is the largest group of GPCRs accounting for about 80% of all GPCRs. This family includes receptors for hormones, neurotransmitters, olfactory- and light-activated receptors and are further subdivided into 19 subfamilies plus orphan GPCRs (Wolf *et al.*, 2015, Lagerstrom *et al.*, 2008). Despite a huge diversity of their ligands, all class A receptors are believed to have some common sequence and structural organisation of seven TM helices with a pattern of highly conserved residues at specific positions, followed by the eighth helix and a palmitoylated cysteine at the C terminal tail. Rhodopsin-like receptors have N-terminal domain of variable length (Palczewski *et al.*, 2000, Lagerstrom *et al.*, 2008, Wolf *et al.*, 2015, Katritch *et al.*, 2013).

The older classification of Class B GPCRs consists of 48 receptors in humans and forms 2 families in the GRAFS scheme: the secretin-like receptors (or Class B1) and adhesion receptors (or class B2). Characteristic of Class B1 is a long N-terminal domain consisting of around 120 residues that is stabilized by 3 conserved disulphide bonds (Lagerstrom *et al.*, 2008, Hollenstein *et al.*, 2014, Culhane *et al.*, 2015).

The secretin-like (Class B1) are a small family of 15 endocrine hormone receptors. These receptors include calcitonin and calcitonin-like receptors (CTR, CLR); corticotropin-releasing factor receptors (CRFR1, CRFR2); the glucagon receptor (GCGR); the gastric inhibitory polypeptide receptor (GIPR); the glucagon-like peptide receptors (GLP-1R, GLP2R); the growth-hormone-releasing hormone receptor (GHRHR); the adenylate cyclase activating polypeptide receptor (PAC1/ADCYAP1R1); the parathyroid hormone receptors (PTH1R, PTH2R); the secretin receptor (SCTR) and the vasoactive intestinal peptide receptor (VPAC1R/VPAC2R) (Mayo *et al.*, 2003, Culhane *et al.*, 2015, Fredriksson *et al.*, 2003). These receptors are important existing or candidate targets for treatment of many human diseases and conditions, including diabetes, obesity, bowel disorders, osteoporosis, hyper- and hypoglycaemia, neurodegeneration and psychiatric disorders, cardiovascular disease, migraine, pain and cancer (as reviewed by (Culhane *et al.*, 2015, Pal *et al.*, 2012, Bortolato *et al.*, 2014).

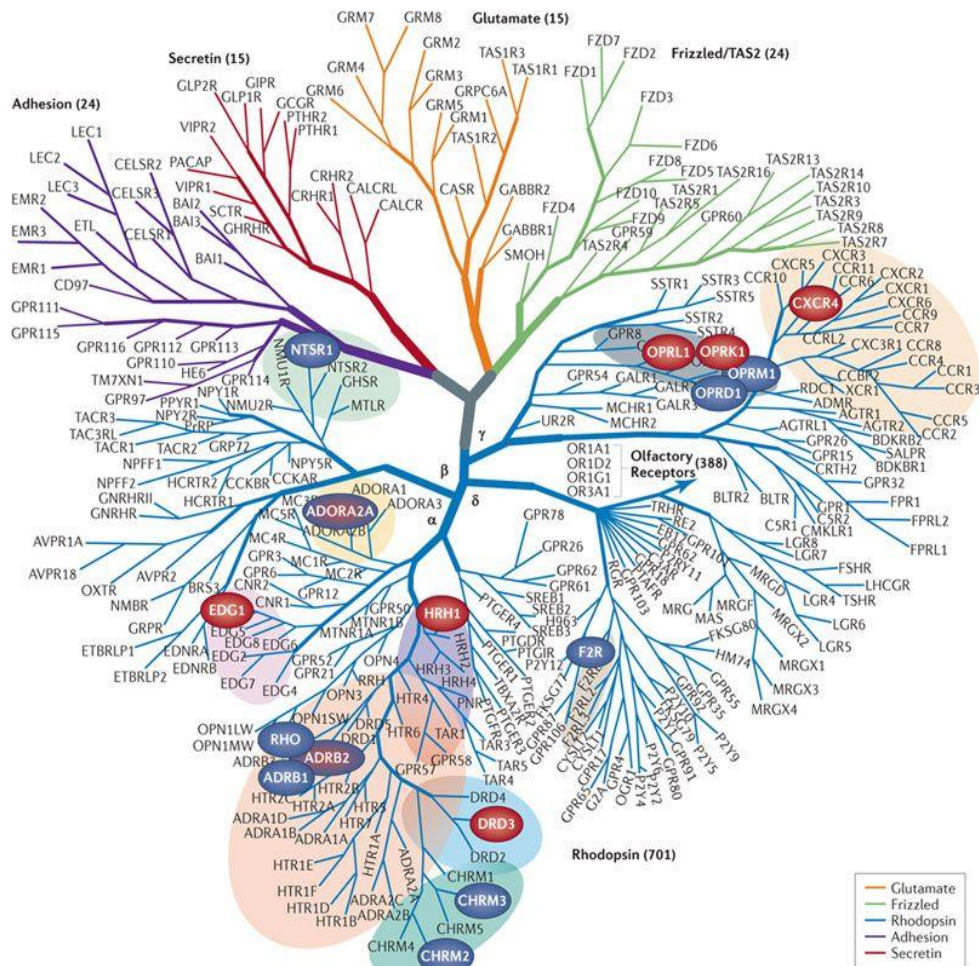


Figure 1.1. Phylogenetic tree showing 5 major GPCR families: Rhodopsin; Secretin; Adhesion; Glutamate and Frizzled/taste receptors (adopted from (Stevens *et al.*, 2013)).

The adhesion GPCRs (or Class B2) have 33 members in humans and are the second largest family of GPCRs. These receptors are structurally distinct from class B1: they have a large extracellular N-terminus with multiple structural domains. Most cell-adhesion GPCRs are orphan receptors with no known ligands and are poorly studied at a molecular level (Nordström *et al.*, 2009). The known roles for these receptors are in mediation and regulation of cytoskeletal organization, regulation of cell adhesion and migration; regulation of cell cycle and development, roles in immune system and in neuronal development (Hamann *et al.*, 2015, Fredriksson *et al.*, 2003).

The glutamate family (or Class C) includes metabotropic glutamate, GABA (gamma-aminobutyric acid), calcium-sensing and taste receptors. The distinctive feature of these GPCRs is a large hydrophilic extracellular ligand-binding domain that has a number of conserved cysteine residues. Another characteristic feature of the glutamate GPCRs family is their dimerization, either homo- or hetero-dimers, which is obligatory for their function (Kniazeff *et*

al., 2011). This family has roles in many important physiological processes, which include synaptic transmission, taste sensation and calcium homeostasis (Moller *et al.*, 2017, Geng *et al.*, 2016, Geng *et al.*, 2013).

Fungal mating pheromone receptors (Class D) and cAMP receptors in slime molds (class E) have 7 hydrophobic TM helix domains organised in a manner similar to rhodopsin-like receptors resulting in their classification as GPCRs but are not included in the GRAFS system as they have no homologues in animals (Valentine *et al.*, 2001, Nakayama *et al.*, 1985, Burkholder *et al.*, 1985, Marsh *et al.*, 1988, Klein *et al.*, 1988, Saxe *et al.*, 1993, Johnson *et al.*, 1993).

The frizzled family (Class F) includes frizzled, smoothened receptors and a series of taste receptors that do not form a clade with the glutamate family. Frizzled receptors have a cysteine-rich extracellular domain that couples these receptors to Wnt (Wingless/integration 1) signalling pathways. Consequently, frizzled receptors play roles in embryonic development, cell fate regulation, cell proliferation, cell polarity and in formation of neural synapses (Nusse *et al.*, 1992, Nusslein-Volhard *et al.*, 1980, Cadigan *et al.*, 1997, Yang-Snyder *et al.*, 1996, Wang *et al.*, 1996, Hsieh *et al.*, 1999, Nichols *et al.*, 2013). The smoothened receptor is a protein that, in humans, is encoded by the SMO gene that can function as an oncogene. The smoothened receptor is a component of the hedgehog signalling pathway; both smoothened and the hedgehog pathway are important cancer drug targets (Ayers *et al.*, 2010, Philipp *et al.*, 2009, Luchetti *et al.*, 2016, Huang *et al.*, 2018).

1.1.4 FUNCTIONAL CHARACTERISTICS OF GPCRS

1.1.4.1 G PROTEIN DEPENDENT SIGNALLING

Among the main cellular transducers of GPCRs are hetero-trimeric G proteins that are members of the GTPase enzyme family (a family of hydrolase enzymes that bind and hydrolyze guanosine triphosphate (GTP)). Hetero-trimeric G proteins can receive and transmit signals from various stimuli outside of the cell by acting as molecular switches, whose activity is regulated by the nucleotide binding subunit. Upon agonist stimulation of a GPCR, a G protein heterotrimer, consisting of α , β and γ subunits, is recruited to the intracellular face and GDP (bound by the α -subunit) is exchanged for GTP followed by the rearrangement/dissociation between the α and $\beta\gamma$ subunits of the complex. The G_{α} -GTP and $G_{\beta\gamma}$ subunits can modulate the activity of different cellular effectors (Hamm, 2001, Tuteja, 2009, Oldham *et al.*, 2008).

There are multiple G protein heterotrimer isoforms. In the human genome there are 16 G_{α} subunits, 5 G_{β} subunits and 12 G_{γ} subunits. These subunit isoforms can form a large combination of heterotrimer combinations that may allow selective recognition between GPCRs and G_{α}

proteins and engender differential downstream transducer/effector coupling. All this may regulate specific physiological targeting of responses to particular stimuli.

G protein α subunits are classified into 4 groups based on their sequence homology and function: $G_{\alpha s}$, $G_{\alpha q}$, $G_{\alpha i/o}$ and $G_{\alpha 12/13}$ (Offermanns, 2003, Cabrera-Vera *et al.*, 2003, Milligan *et al.*, 2006, Downes *et al.*, 1999) with different G_{α} subunits activating distinct second messenger signalling cascades.

The $G_{\alpha s}$ family includes $G_{\alpha s}$, which has several splice variants and $G_{\alpha olf}$ (Simon *et al.*, 1991). $G_{\alpha s}$ proteins stimulate cyclic adenosine monophosphate (cAMP) production via activation of adenylyl cyclase which catalyses the conversion of adenosine triphosphate (ATP) into cAMP. cAMP can bind to inactive protein kinase A (PKA), causing a rearrangement within PKA leading to its activation (Cheng *et al.*, 2008, Marinissen *et al.*, 2001). PKA, as the name suggests, is a kinase whose targets include L-type Ca^{2+} channels (Bunemann *et al.*, 1999), enzymes involved in sugar and lipid metabolism (Pilkis *et al.*, 1988), proteins in the vesicle secretory pathway (Seino *et al.*, 2009, Leenders *et al.*, 2005) and transcription factors (e.g. cAMP response element-binding protein (CREB)) (Delghandi *et al.*, 2005). cAMP can also directly regulate the activity of Epac proteins (Epac1 and Epac2, guanine exchange factor (GEF) proteins directly activated by cAMP) in a PKA-independent manner. Epac can in turn activate the Ras superfamily small GTPase members Rap1 and Rap2, which are responsible for a plethora of important cell functions, such as cell adhesion, formation of cell-cell junctions, cell growth and differentiation, apoptosis and exocytosis (as reviewed in (Cheng *et al.*, 2008). cAMP and PKA can both stimulate or inhibit mitogen-activated protein kinases (MAPKs) that include extracellular signal-regulated kinases 1/2 (ERK1/2), extracellular signal-regulated kinases 5 (ERK5) and p38 mitogen-activated protein kinase (p38) (Waltereit *et al.*, 2003, Cheng *et al.*, 2008, Goldsmith *et al.*, 2007). cAMP also regulates the activity of cyclic nucleotide-gated channels in sensory organs (Nakamura *et al.*, 1987).

The $G_{\alpha i/o}$ family includes $G_{\alpha i1}$, $G_{\alpha i2}$, $G_{\alpha i3}$, $G_{\alpha o}$, $G_{\alpha z}$, $G_{\alpha gust}$, $G_{\alpha t-r}$, and $G_{\alpha t-c}$. Activated G_i proteins inhibit adenylyl cyclase activity, lowering cellular cAMP with a concomitant cAMP-dependent decrease in PKA activity (Taussig *et al.*, 1993). The $G_{\alpha i/o}$ pathway regulates multiple physiological processes such as leukocyte chemotaxis (Chung *et al.*, 2001, Xu *et al.*, 2003, Sun *et al.*, 2012, Cubillos *et al.*, 2010), locomotor activity (Funada *et al.*, 1993), and neurite outgrowth (Strittmatter *et al.*, 1990, Strittmatter *et al.*, 1994). $G_{\alpha i/o}$ is also attributed a minor role in activation of the phospholipase C pathway (PLC) where this PLC activation is mediated by $G_{\beta\gamma}$ subunit linked to $G_{\alpha i/o}$ pathway (Kelley *et al.*, 2004).

The $G_{\alpha q/11}$ family includes $G_{\alpha q}$, $G_{\alpha 11}$, $G_{\alpha 14}$, $G_{\alpha 15}$, and $G_{\alpha 16}$. This family of G proteins is coupled to the activation of phospholipase C β (PLC- β) (Rhee *et al.*, 1992). PLC- β hydrolyzes the

phosphorylated lipid phosphatidylinositol 4,5-bisphosphate (PIP₂) to produce inositol triphosphate (IP₃) and diacylglycerol (DAG) (Axelrod *et al.*, 1988). Where IP₃ activates intracellular Ca²⁺ mobilization and DAG activates protein kinase C (PKC), together they promote regulation of multiple physiological processes including vascular function, channel regulation, contraction, neuronal regulation and transcription (Moscat *et al.*, 2003, Ueda *et al.*, 1996).

The G_{α12} family includes G_{α12} and G_{α13}. G_{α12/13} proteins were shown to couple to multiple cellular effectors and pathways and through them regulate numerous cellular functions such as myocardial function (through coupling to Na⁺/H⁺ exchanger), transcription and proliferation (through coupling to cadherin and RAS pathway), actin cytoskeleton and cell movement (through Rho GTPase and phospholipase D (PLD) pathways) (Kozasa *et al.*, 1998, Hart *et al.*, 1998). Constitutively active G_{α12} and G_{α13} can act as oncogenes due to their coupling to Rho signalling through guanine nucleotide exchange factors for Rho/Rac/Cdc42-like GTPases (RhoGEFs), such as p115-RhoGEF, PDZ-RhoGEF, and leukemia-associated RhoGEF (LARG) (Dhanasekaran *et al.*, 1996, Fromm *et al.*, 1997, Fukuhara *et al.*, 2001).

G_{βγ} acts as one functional unit. There are 5 G_β -isoforms and 14 different G_γ -subunit isoforms in humans. G_{βγ} can activate its own signalling cascades (Clapham *et al.*, 1997). Among G_{βγ} downstream effectors are the G protein-coupled inwardly rectifying potassium channels (GIRK), N-type Ca²⁺ channels, adenylyl cyclase, phospholipases Cβ1, Cβ2, Cβ3 and phosphoinositide 3-kinase (PI3K). Correspondingly, G_{βγ} signalling mediates regulation of the following biological functions: cardiac function, neurotransmitter release, platelet aggregation, neutrophil migration, chemotaxis and others (Gautam *et al.*, 1998, Schwindinger *et al.*, 2001, Yan *et al.*, 1996, Wang *et al.*, 1999).

While traditionally, GPCR signal transduction was believed to only occur at the plasma membrane, more recent studies proved that GPCR signalling can also occur from intracellular receptors (as reviewed by (Jong *et al.*, 2018, Calebiro *et al.*, 2010, Eichel *et al.*, 2018)). A number of GPCRs display post-internalisation G protein-mediated signalling from endosomes (Eichel *et al.*, 2018, Ferrandon *et al.*, 2009, Feinstein *et al.*, 2013, Jensen *et al.*, 2017, Jong *et al.*, 2018). Additionally, there are examples of GPCRs that can be activated *in situ* by diffusion of permeable ligands or active transport of non-permeable ligands, or via *de novo* ligand synthesis (as reviewed by (Jong *et al.*, 2018)).

1.1.4.2 GPCR DESENSITISATION AND INTERNALISATION

The duration of GPCR activation and signalling is finely regulated. GPCR desensitisation or receptor uncoupling means loss of response after agonist administration (Hausdorff *et al.*,

1990). This loss of responsiveness can happen after repeated or prolonged administration (for example, few hours), but might as well take place after a short time stimulation of few seconds (Kelly *et al.*, 2008). GPCR desensitisation can happen via either homologous or heterologous mechanism.

The best characterised mechanism for GPCR desensitisation is homologous desensitisation via phosphorylation of serine or threonine residues in the 3rd ICL or the carboxy-terminus of the receptor by one or more of the seven different G protein-coupled receptor kinase (GRK) isoforms, followed by β -arrestin recruitment (Ferguson *et al.*, 1998, Hausdorff *et al.*, 1990, Lefkowitz, 1998, Luttrell *et al.*, 2002, Smith *et al.*, 2016).

β -arrestins are adaptor proteins that typically bind to phosphorylated GPCRs with high affinity to uncouple them from G protein dependant pathways by sterically inhibiting the G protein interaction. Upon binding, β -arrestins can facilitate the targeting of receptors for clathrin-mediated endocytosis by acting as adaptors for clathrin and $\beta(2)$ adaptin (Ferguson *et al.*, 1996, Goodman *et al.*, 1996, Laporte *et al.*, 1990). There are 2 isoforms of β -arrestin – β -arrestin 1 and 2, that share 78 % sequence homology. Studies have shown, that while some GPCRS do not distinguish between the two β -arrestin isoforms and can internalise with either isoform, other GPCRs can only internalise with one β -arrestin isoform and not with the other (Smith *et al.*, 2016). The kinetics of β -arrestin – GPCR interactions can follow two distinct patterns. Depending on this pattern GPCR – β -arrestin interaction can be classified in either "Class A" (low affinity, transient binding between a GPCR and β -arrestin resulting in fast receptor recycling after its internalisation) and "Class B" (high affinity and long duration interaction with β -arrestin resulting in formation of a stable GPCR- β -arrestin complex that internalizes together to endosomes and with slower receptor recycling rates) (Oakley *et al.*, 2000).

If signalling at one GPCR results in activation (desensitization) of an unrelated GPCR, such desensitisation is called heterologous. Another form of GPCR heterologous desensitisation is GPCR desensitisation mediated by its own second messenger systems, such as PKA and PKC. The proposed mechanism of desensitisation is via kinase phosphorylation of serines and threonines in the C-terminal tail of a GPCR that impairs receptor–G protein coupling. This mechanism of a GPCR desensitisation can happen in the absence of ligand (Bouvier *et al.*, 1988, Benovic *et al.*, 1985, Lefkowitz, 1993).

Although the GRK- β -arrestin mechanism is widespread for GPCR internalisation, there are examples of GPCR desensitization occurring via GRK- and β -arrestin independent mechanisms (Hardy *et al.*, 2005, Cho *et al.*, 2007). Additionally, β -arrestins can activate signalling cascades independently of G protein activation.

1.1.4.3 G PROTEIN INDEPENDENT SIGNALLING

It is now accepted that GPCRs can signal via G-protein-independent mechanisms. One such mechanism is via β -arrestins, which can activate diverse cellular signalling responses. These responses include MAPK signalling, ERK1/2, c-Jun N-terminal kinases (JNK3), p38 and signalling through PI3K downstream target of protein kinase B (PKB or AKT) in cytosol (Luttrell *et al.*, 1997, DeFea *et al.*, 2000, Luttrell *et al.*, 2001, Povsic *et al.*, 2003, Goel *et al.*, 2004). Additionally, β -arrestins can also regulate nuclear processes such as transcription by utilising a number of distinct mechanisms, such as association with transcription factors (nuclear factor of kappa light polypeptide gene enhancer in B-cells inhibitor, alpha ($\text{I}\kappa\text{B}\alpha$) and mouse double minute 2 homolog (MDM2) in the cytoplasm, activating nuclear receptors (Retinoic acid receptor (RAR) and associating with transcription co-factors and co-activators (CREB, Histone acetyltransferase p300 (p300)). Through these functions β -arrestins can regulate growth and apoptosis. (Sen *et al.*, 1986, Gao *et al.*, 2004, Luan *et al.*, 2005, Piu *et al.*, 2006, Kang *et al.*, 2005). These signalling cascades may be spatially and temporally distinct from G protein signalling resulting in unique cellular outcomes.

Additionally, GPCRs exhibit a capacity to interact with a wide variety of accessory proteins that can modulate GPCR-G-protein coupling, receptor trafficking, desensitisation, internalisation, and, in some cases, elicit G-protein independent signalling. Among GPCR interaction partners are receptor activity modifying proteins (RAMPs), regulators of G-protein signalling (RGS), GPCR-associated sorting proteins (GASPs), homer proteins, small G proteins, PDZ domain containing proteins, spinophilin, calmodulin, protein phosphatases and others (as reviewed in (Magalhaes *et al.*, 2012).

1.1.4.4 THE CONCEPT OF EFFICACY AND BIASED AGONISM

Efficacy is a concept that relates receptor occupancy to cellular response (Kenakin, 2002, Neubig *et al.*, 2003). In the simplest sense any ligand that can act at a receptor must have affinity for that receptor. Ligands may have the property that they bind to a receptor but do not produce an effect and we would call these antagonists. On the other hand, ligands that bind to a receptor and produce an effect can be said to have efficacy. The extent to which a particular ligand is able to elicit an effect says something about the magnitude of that particular ligand's efficacy. For almost every receptor that has been extensively studied ligands exist which display a range of efficacies. A sub-phenomenon of differential efficacy is signalling bias; the phenomenon that different ligands acting at the same GPCR can engender different cellular responses (Figure 1.2), presumably by engaging alternative transducer subsets (that can include different G proteins as well as β -arrestins) (Kenakin, 2011, Kenakin *et al.*, 2013). GPCRs are dynamic structures

capable of adopting a variety of conformational states corresponding to individual energy minima (Kenakin *et al.*, 2010, Deupi *et al.*, 2010). Biased signalling is generally thought to be the result of ligands stabilizing different parts of a GPCR's conformational landscape allowing differential transducer coupling (Deupi *et al.*, 2010, Burgen, 1981, Kenakin *et al.*, 2010, Mary *et al.*, 2012).

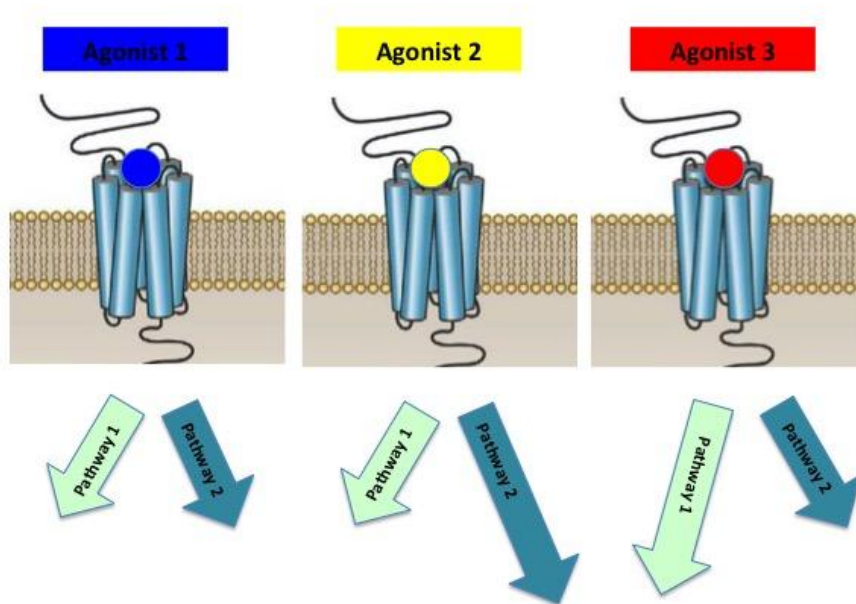


Figure 1.2. Schematic representation of biased agonism principle. GPCR (can pleiotropically couple to more than one intracellular effector. Agonists (Agonist, Agonist 2 and Agonist 3) can couple the receptor to individual signalling pathways with differential efficacy thus producing various patterns of signalling outcomes.

1.2 THE LAW OF MASS ACTION AND PHARMACOLOGICAL QUANTIFICATION USING THE OPERATIONAL MODEL

The following sections contain a brief overview of the main principles of quantifications for ligand-receptor interactions in pharmacology, as well as an introduction to the Operational Model of agonism that was used to analyse data in the Chapters 4 and 5.

1.2.1 THE LAW OF MASS ACTION

In order that ligand activity at a receptor may be quantitated the binding of a ligand A to its receptor R is considered to follow the law of mass action, which can be described by an equilibrium:



The rates, K_{on} and K_{off} depend on the concentration of reactants, and at equilibrium the product of concentration and rates must be equal:

$$K_{on}([A][R]) = K_{off}[AR] \quad (\text{Equation 1.2})$$

Therefore, where K_d is the equilibrium dissociation constant, $K_d = K_{off}/K_{on}$, at equilibrium,

$$K_d = [L][R]/[AR] \quad (\text{Equation 1.3})$$

For 1:1 stoichiometry concentration of a drug-ligand complex, if $[R_T]$ (total receptor concentration) is substituted into the above (where $[R_T] = [R] + [AR]$ and the equation is simplified by assuming $[R_T] \ll K_d$ then $[AR]$ can be described by a sigmoidal curve plotted against the logarithmic molar ligand concentration:

$$[AR] = \frac{[R_T][A]}{[A] + K_A} \quad (\text{Equation 1.4})$$

Where $[A]$ is the concentration of ligand; $[R_T]$ is the total number of receptors; $[R]$ is the concentration of free receptors (not occupied by ligand) and $K_A = K_{off}/K_{on}$ equilibrium dissociation constant of the ligand characterising the strength with which ligand binds to the receptor (moles per litre).

Black and Leff Operational Model of agonism was developed to take into account the experimental data showing that receptor occupancy (as driven by the Law of mass action) was insufficient to account for tissue response. In this model, transducer functions (e.g. receptor – G

protein binding) necessarily also follow a sigmoidal curve (on a log scale, presumably governed by mass action) and the product of mass action occupancy with a mass action transducer function will produce a cellular response proteins and can be also described by a sigmoidal curve

1.2.2 THE OPERATIONAL MODEL OF AGONISM

Black and Leff introduced the operational model in 1983. The Operational Model describes agonism using 3 parameters: the dissociation constant of the agonist-receptor complex K_A ; the total receptor concentration $[R_0]$; and a parameter K_E , defining the transduction of agonist-receptor complex into pharmacological effect. The ‘transducer ratio’ $[R_0]/K_E$ equals efficacy τ . τ , also defined as operational efficacy, measures the efficiency with which occupied receptors are able to transduce a signal (Black *et al.*, 1983):

$$Response = \frac{[A] * \tau * E_{max}}{[A] * (\tau + 1) + K_A}, \quad (\text{Equation 1.5})$$

where $[A]$ is the concentration ligand; E_{max} is the maximum response of the system.

Equation 1.5 Describes response curves for the functions with slopes of unity. The Operational model equation for a variable slope (Equation 1.6) is used for experimental dose-response curves with slopes other than unity and for the situations when stimulus-response system cooperativity effects need to be considered:

$$Response = \frac{[A]^n * \tau^n * E_{max}}{([A] + K_A)^n + \tau^n + [A]^n} \quad (\text{Equation 1.6})$$

where n is the “transducer slope” for the function linking agonist concentration to measured response (Kenakin *et al.*, 2012).

1.3 SECRETIN-LIKE, CLASS B1 GPCRS

1.3.1 SECRETIN-LIKE SUBFAMILY

The secretin-like (class B1) GPCRs are a relatively small group of receptors for secretin, vasoactive intestinal polypeptide (VIP), glucagon, glucagon-like peptides (GLP), glucose-dependent insulintropic peptide (GIP), growth hormone-releasing hormone (GHRH), calcitonin (CT), calcitonin gene-related peptide (CGRP), corticotropin-releasing factor (CRF), parathyroid hormone (PTH) and parathyroid hormone-related peptides (PTHrP) (Mayo *et al.*, 2003) (Structures of the solved active peptide-bound class B GPCRs are shown on Figure 1.3). Members of this group are clinical or proposed clinical targets for many medically important

disorders, including the management of diabetes, obesity, bone disease, headache, pain and stress (Mayo *et al.*, 2003).

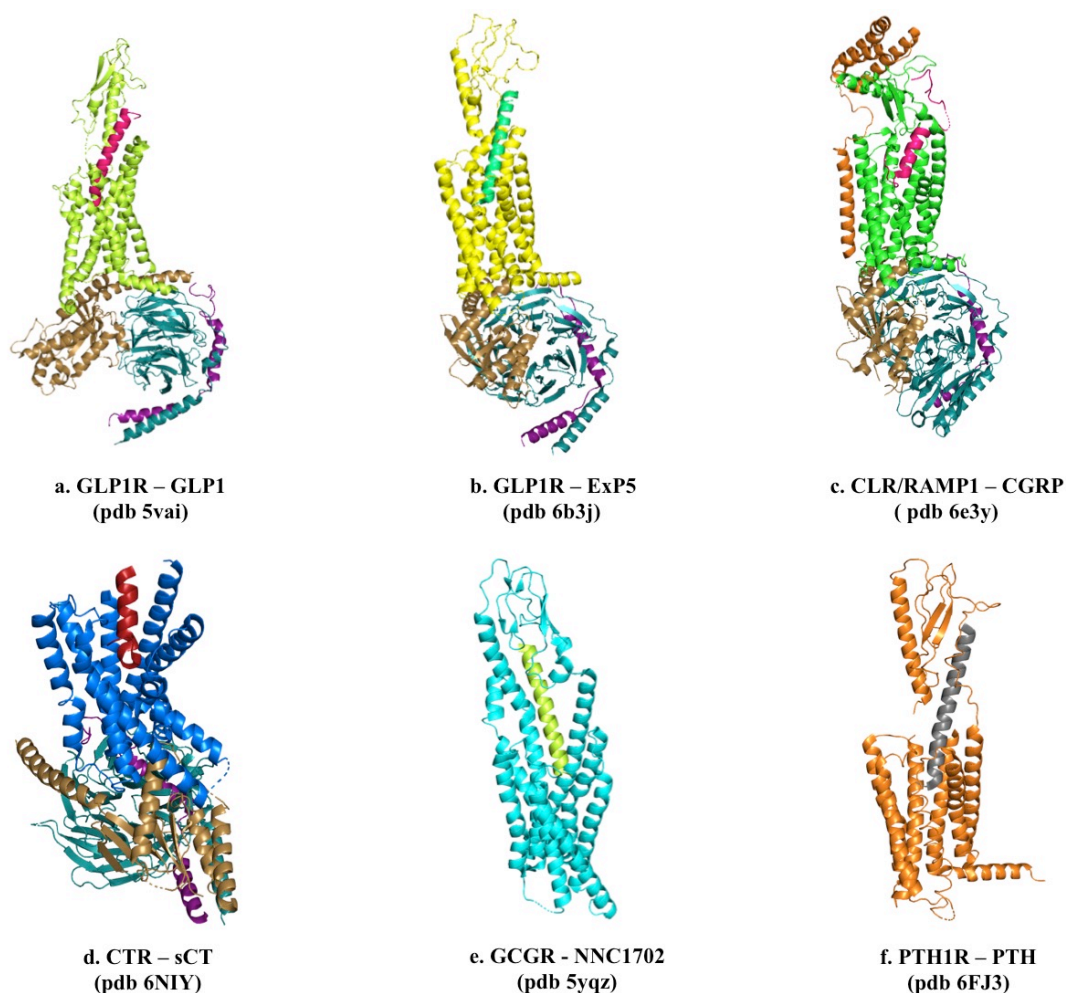


Figure 1.3. Peptide agonist bound, active class B GPCR structures: (a) active state GLP-1R (lime) bound to GLP-1 (pink) and heterotrimeric G protein (pdb:5vai); (b) active state GLP-1R (yellow) bound to the biased agonist exendin-P5 (green) and heterotrimeric G protein (pdb:6b3j); (c) active state CGRPR, comprised of CLR (green) and RAMP1 (orange) bound to CGRP (pink) and heterotrimeric G protein (PDB:6e3y); (d) active state CTR (blue, n-terminal domain not shown) bound to sCT (red) and heterotrimeric G protein (pdb 6NIY); (e) active state GCGR (cyan) bound to the partial agonist NNC1702 (lime) (pdb 5yqz); (f) active state PTH1R (orange) bound to agonist PTH (gray) (pdb 6FJ3); G protein heterotrimer subunits are coloured sand for G_α , deep teal for G_β , and purple for G_γ (figures a-d).

1.3.2 LIGAND BINDING SITE AND TWO DOMAIN MODEL OF SECRETIN-LIKE GPCRS

It is now well accepted in the field that secretin-like GPCRs are activated by their peptide agonists according to a 2 domain binding model which is supported by recent structural studies (Liang *et al.*, 2017, Liang *et al.*, 2018b, Liang *et al.*, 2018a, Zhang *et al.*, 2017b) as well as earlier chimera studies (Bergwitz *et al.*, 1996, Unson *et al.*, 2002) and the kinetic data (Vilardaga *et al.*, 2011). According to the 2 domain model, initial interaction between agonist's C terminal domain and receptor's extracellular domain enables positioning of peptide's N-terminus into a

transmembrane (TM) binding pocket (Neumann *et al.*, 2008, Dong *et al.*, 2014, Wootten *et al.*, 2016c, Koole *et al.*, 2012b). According to the two-domain model, and supported by photoaffinity cross-linking and by mutagenesis studies, the juxtamembrane domain (ECLs and stalk) is involved not only in ligand binding but also in receptor activation (Dong *et al.*, 2011, Gkountelias *et al.*, 2009, Barwell *et al.*, 2011) (Figure 1.4).

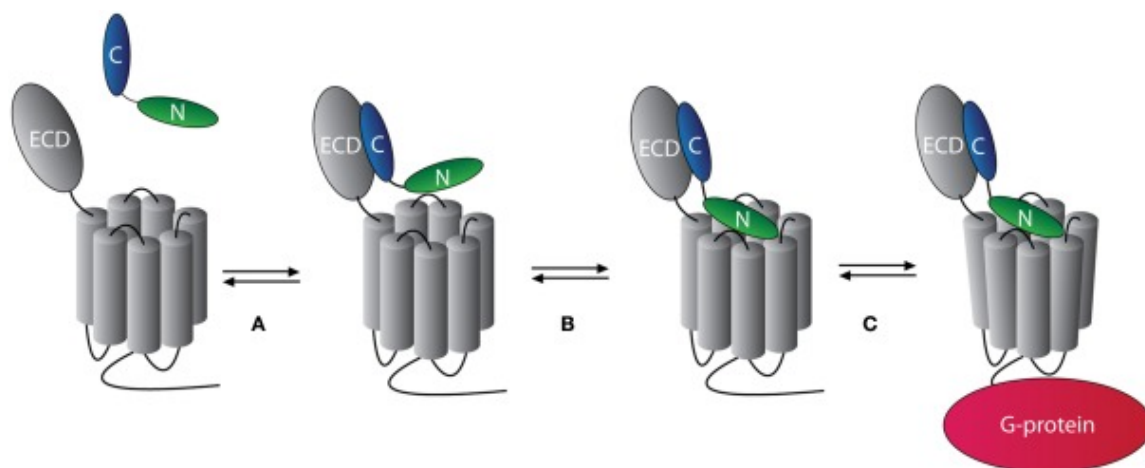


Figure 1.4. The two-step model of peptide ligand binding to class B GPCRs. (A) the C-terminal portion of the peptide (blue) binds to the N-terminal domain of the receptor. In step (B), the N-terminus of the ligand (green) binds to the TM domain of the receptor. This activates the receptor and promotes recruitment of intracellular effectors (G-proteins) (step (C)) (adopted from Roed *et al.*, 2012).

The initial interaction with receptor N-terminus is well characterised, including crystal and cryo-EM data supported by cross-linking and mutagenesis data (Liang *et al.*, 2018a, Liang *et al.*, 2017b, Zhang *et al.*, 2017a, Zhang *et al.*, 2017b, Siu *et al.*, 2013b, Hollenstein *et al.*, 2013, Dong *et al.*, 2011, Nicole *et al.*, 2000, Adelhors *et al.*, 1994). The C-terminus of the peptide penetrates between inner β -sheet layers of the α - β - β/α fold like a “hotdog in a bun” manner (Hollenstein *et al.*, 2014, Dong *et al.*, 2011).

The second step of the two-domain binding model is the interaction between peptide N-terminus and TM domain that is accompanied by rearrangements within receptor TMs and within polar residue networks.

In class B peptides the N terminus is important for receptor activation; its truncation results in competitive antagonists (Feyen *et al.*, 1992). Additionally, the N-terminal regions of class B peptide hormones have conserved helix-capping motifs (Neumann *et al.*, 2008). The calcitonin family of peptides are distinguished by a cysteine ring structure at their N-termini (Schwartz *et al.*, 1981). Presence of a cysteine ring results in a slightly different shape of the TM binding pocket compared to other class B1 receptors providing additional ligand-recognition specificity (Liang *et al.*, 2018a, Liang *et al.*, 2017b).

1.3.3 SECRETIN-LIKE STRUCTURAL CHARACTERISTICS

The extracellular domain of the secretin-like family comprises the N-terminal domain of 100-160 residues with 3 conserved disulphide bonds and a juxtamembrane domain. The juxtamembrane domain consists of the three extracellular loops (with ECL1 being the longest loop, ECL2 is the intermediate and ECL3 – the shortest loop) and the peptide fragment at the junction between the N-terminal domain and TM1 (also known as stalk) (Hollenstein *et al.*, 2014).

The sequence homology of class B GPCRs' extracellular domains is very low and is limited to about 18 residues, including 6 cysteines forming disulphide bonds, and 4 conserved residues stabilizing receptor tertiary structure (D113, W118, P132, and W154). The N-terminal domain of Class B1 GPCRs adopts distinct fold of their peptide-binding domain, also known as “secretin family recognition fold” α - β - β/α arrangement formed by the N-terminal α -helix, 2 antiparallel β -sheet core and an additional short outer α -helix (for some receptors) (Hollenstein *et al.*, 2014, Culhane *et al.*, 2015, Parthier *et al.*, 2009, Dong *et al.*, 2014). This fold is stabilised by 3 conserved disulphide bonds. Presence of such conserved fold in all class B1 GPCRs, despite their low sequence homology, suggests common ligand recognition and binding mechanisms for these receptors (Hollenstein *et al.*, 2014), which is supported by the active structures of CTR, GLP-1R and CGRP. Extracellular loops are important for initiating peptide hormone recognition and binding as shown by structural data (Zhang *et al.*, 2017b, Liang *et al.*, 2018a, Liang *et al.*, 2018b) along with mutagenesis and cross-linking studies (Dal Maso *et al.*, 2018b, Wootten *et al.*, 2016c, Dong *et al.*, 2016, Dong *et al.*, 2014, Koole *et al.*, 2012b, Woolley *et al.*, 2017a). ECLs vary significantly by their size and sequence, thus opening possibilities for ligand specificity. For different class B GPCR different residues and residue networks in the ECLs are important for ligand bias (Koole *et al.*, 2012b, Koole *et al.*, 2012a, Wootten *et al.*, 2016c).

Transmembrane region plays key role in receptor activation and signal transmission. TM1, TM6, TM7 on one side and TM2 and TM5 on the other side form a large solvent-filled cavity of a V shape to accommodate peptide N-terminus (Hollenstein *et al.*, 2014, Culhane *et al.*, 2015). Receptor activation upon ligand binding results in structural rearrangements within TMs that enable opening of a binding pocket on the cytoplasmic side of the receptor accessible for signalling transducers. This process includes TM6 and TM7 reorientation to point away from the TM core centre (Liang *et al.*, 2017a, Liang *et al.*, 2018a, Zhang *et al.*, 2017a).

Class B TM domains contain conserved networks of polar residues that play key roles in TM reorganisation during receptor activation and for receptor signalling and bias. A central polar network formed by residues N^{2.60}, N^{3.43}, Q^{6.52} and Q^{7.49} (residue numbers are according to the

class B Wootten numbering system (Wootten *et al.*, 2013)) is preserved in both active and inactive class B receptor structures, however upon receptor activation it undergoes re-ordering that affects relative orientation of residues and the strengths of their interactions (Liang *et al.*, 2017a, Wootten *et al.*, 2013, Liang *et al.*, 2018b). While conserved for the entire secretin-like family, study of GLP1-R showed that these conserved polar residues are important for receptor stabilization, activation and for ligand-directed signalling bias (Liang *et al.*, 2018a, Wootten *et al.*, 2013). CTR cryo-EM structure has also revealed Y^{2.57} to be a part of this network in CTR (Liang *et al.*, 2017a). The second conserved polar motif between TMs 2, 3, 6 and 7 is H^{2.50}-E^{3.50}-T^{6.42}-Y^{7.57}. This motif is thought to constrain receptor activation; these interactions break upon receptor activation to allow for TM rearrangement and particularly TM6 reorientation (Frimurer *et al.*, 1999). Mutation of these residues results in constitutive receptor activation (Vohra *et al.*, 2013a). This polar network was also shown to be important in biased signalling (Wootten *et al.*, 2013, Furness *et al.*, 2018).

Cytoplasmic domain is responsible for G protein coupling and undergoes structural rearrangements upon receptor activation (Liang *et al.*, 2017a, Zhang *et al.*, 2017a, Liang *et al.*, 2018a). ICLs were shown to play important roles in G protein binding. Studies were undertaken to understand the importance of each ICL. ICL3 was shown to be of major importance as it can activate all different types of G proteins (Liang *et al.*, 2017a, Zhang *et al.*, 2017a, Cypess *et al.*, 1999, Bavec *et al.*, 2003, Conner *et al.*, 2006). Other loops have subsidiary roles, also participate in G protein binding, and are likely to play important roles in G protein selectivity (Hallbrink *et al.*, 2001, Cypess *et al.*, 1999, Conner *et al.*, 2006). For example, naturally occurring polymorphism in the CTR ICL1 alters ligand binding and signalling in both ligand- and pathway-specific manner (Dal Maso *et al.*, 2018a). Additionally, selectivity of G protein binding can also depend on the ligand and on accessory proteins (Kenakin *et al.*, 2013, Sato, 2013, Gingell *et al.*, 2016). The molecular mechanism behind the selectivity remains largely unknown. A short amphipathic helix, known as helix VIII/8 (H8) is located at the start of the carboxyl (C)-terminus; H8 forms interactions with G_{βγ} G-protein subunit (Liang *et al.*, 2017a, Liang *et al.*, 2018a, Zhang *et al.*, 2017a). Deletions of the C-terminus in both CTR and CLR support the importance of H8 in receptor stability and cell surface expression and Gs-mediated cAMP signalling (Liang *et al.*, 2017b, Conner *et al.*, 2008).

There is another conserved polar network sitting below TM2-3-6-7 network towards receptor cytoplasmic interface – R^{2.46}, R/K^{6.37}, N^{7.61} and E^{8.41} (TM2-6-7-H8 network). According to the CTR homology model and the GCGR inactive structure these residues interact with each other with two salt bridges formed, one between E^{8.41} and R^{2.46} and the second between E^{8.41} and

R/K^{6.37}. As a part of receptor activation process these residues undergo rearrangement and the salt bridge between K^{6.37} and E^{8.41} is broken (between E^{8.41} and R^{2.46} is likely to be preserved in the active structure). These rearrangements free TM6 from the inactive state constraints (Liang *et al.*, 2017a, Zhang *et al.*, 2017a).

1.3.4 COMPARISONS BETWEEN RHODOPSIN-LIKE AND SECRETIN-LIKE

Overall, rhodopsin-like and secretin-like GPCRs have similar organisation of TM helices but quite divergent organisation of NTDs. Whereas secretin-like receptors have 100-150 amino acid long ECD that adopts a characteristic α - β - β/α fold, different rhodopsin-like receptors have variable length of N-termini (although, predominantly they have a relatively short N-termini).

The TM and cytoplasmic domain organisation between different classes is well conserved reflecting the general activation, signal transduction and transducer recruitment mechanisms for all GPCRs. Activation of both rhodopsin-like and secretin-like receptors results in rearrangement within the TM bundle associated with an outward movement of TM6 at the base of the receptor. This movement of the cytoplasmic end of TM6 away from TM3 happens around the conserved in class A P^{6.50} (Ballesteros-Weinstein (BW) numbering system, (Ballesteros *et al.*, 1995)) and conserved in class B G^{6.50} (Wooten, (Wooten *et al.*, 2013)) that acts as a hinge allowing for accommodation of α -helix of G $_{\alpha}$ (Shi *et al.*, 2002, Seidel *et al.*, 2017). What is unique for secretin-like GPCRs is that the TM6 kink is of greater amplitude than in rhodopsin-like and it is also associated with the outward movement of TM7 and an inward movement of the extracellular top of TM1.

The common activation mechanism for GPCRs of different classes can be followed through the conserved polar networks in TM domains. TMs 2-3-6-7 motif (H^{2.50}-E^{3.50}-T^{6.42}-Y^{7.57}) (Wooten, (Wooten *et al.*, 2013)) in secretin-like GPCRs is thought to be analogous of the rhodopsin-like D(E)R^{3.50}Y motif (BW, (Ballesteros *et al.*, 1995)) which forms an ionic lock at the base of TMs 2,3,6 in an inactive state and is disrupted upon receptor activation (Liang *et al.*, 2017b, Zhang *et al.*, 2017a, Ballesteros *et al.*, 2001, Rovati *et al.*, 2007, Rasmussen *et al.*, 2011b, Rasmussen *et al.*, 2011a). Mutations in both locks (secretin-like and rhodopsin-like) result in higher receptor constitutive activity (Vohra *et al.*, 2013a, Ballesteros *et al.*, 2001, Montanelli *et al.*, 2004).

NPXXY^{7.53} (BW, Ballesteros *et al.*, 1995) motif is another conserved motif in rhodopsin-like GPCRs and is located in TM7. It plays a role in receptor packing, activation (receptor transition from receptor ground state to its active state) and receptor-mediated signalling and internalization (Fritze *et al.*, 2003, Hausdorff *et al.*, 1991, He *et al.*, 2001). Based on previous

mutagenesis studies and molecular simulation VXXXXY(F)^{7.53} (BW, Ballesteros *et al.*, 1995) motif has been proposed as an equivalent in secretin-like GPCRs.

Organisation of C-terminal tail into an amphipathic α -helix (H8) is similar in both rhodopsin-like and secretin-like receptors where H8 plays role in receptor expression, internalisation and G protein recruitment. In secretin-like receptors H8 appears to be longer than in rhodopsin-like receptors and the recent cryo-EM class B structures showed that H8 interacts with ICL1 and G β which hasn't been described for rhodopsin-like receptors (Huynh *et al.*, 2009, Liang *et al.*, 2017b, Zhang *et al.*, 2017b, Song *et al.*, 2017).

1.3.5 SECRETIN-LIKE GPCRS BIASED AGONISM

The phenomenon of bias is described by the ability of distinct ligands to elicit differential signalling outcomes while acting at the same receptor (Kenakin *et al.*, 2013, Violin *et al.*, 2014). This phenomenon is of great therapeutic potential as it opens potential to tailor agonists with targeted pharmacological and therapeutical properties. Secretin-like GPCRs can be activated by various natural and synthetic ligands and can be pleiotropically coupled to different G proteins and can also recruit β -arrestins (Wootten *et al.*, 2017). GLP-1R is the most well characterised secretin-like receptor with respect to biased agonism with multiple endogenous and exogenous agonists tested including studies to understand the mechanistic basis for this phenomenon (as reviewed by (Wootten *et al.*, 2017, Wootten *et al.*, 2018). Previous studies have shown that different parts of GLP-1R are responsible for biased signalling, including receptor stalk region, ECLs and tops of TMs (Koole *et al.*, 2012a, Koole *et al.*, 2012b, Lei *et al.*, 2018, Wootten *et al.*, 2016c). Residues forming conserved receptor polar networks were extensively studied and confirmed as important triggers for both pathway- and ligand-specific bias (Wootten *et al.*, 2013, Wootten *et al.*, 2016a).

Mutagenesis studies of the CTR have revealed how mutation of individual residues within CTR ECL2 and ECL3 resulted in ligand- and pathway- specific effects on receptor binding and signalling supporting the idea that individual ligands use distinct amino acid networks and stabilise certain receptor conformations which can result in biased signalling and can be used to design biased drugs with desired properties (Dal Maso *et al.*, 2018b).

Among other examples of biased agonism in secretin-like GPCRs are a PTH peptide (D-Trp(12),Tyr(34))-PTH(7-34) that was reported to act as inverse agonist in cAMP pathway while activating ERK1/2 and beta-arresting pathways in osteoblasts that is of therapeutic potential (Gesty-Palmer *et al.*, 2009). Other examples include PACAP-responsive receptors in primary rat glia cultures, where PACAP-38, but not PACAP-27, activated ERK in glia, while both forms stimulated cellular cAMP production (Walker *et al.*, 2014).

1.3.6 ACCESSORY PROTEINS AND RECEPTOR HETEROCOMPLEXES WITH RAMPS

The function of secretin-like GPCRs can be influenced by the co-expression of RAMPs. RAMPs are single-pass transmembrane proteins with an ~100-amino acid extracellular N-terminal domains and very short C-terminal cytoplasmic domains. RAMP association with the CTR or with CLR generates multiple distinct receptor phenotypes with different specificities for the CT peptide family (Figure 1.5, Table 1.1) (Poyner *et al.*, 2002, Hay *et al.*, 2016). Thus, for example, amylin (AMY) receptors are composed of CTR together with one of the three types of receptor activity-modifying proteins (RAMPs 1, 2 and 3 generating amylin 1, 2 and 3 type receptors, respectively (AMY1, AMY2 and AMY3), each with a distinct agonist and antagonist pharmacology. Although AMY2 is rather poorly characterized and may not be a physiologically relevant receptor for Amy (Christopoulos *et al.*, 1999, Morfís *et al.*, 2008a). In addition, CTR by itself is the high affinity receptor for CT.

Unlike CTR, CLR does not appear to traffic to the cell surface in the absence of RAMPs. CLR together with RAMP1 forms a CGRP (calcitonin gene related peptide) receptor. It is now accepted in the CGRP field that the AMY1 receptor, comprising CTR and RAMP1, is also a receptor for the CGRPs (Leuthauser *et al.*, 2000, Tilakaratne *et al.*, 2000, Walker *et al.*, 2015, Walker *et al.*, 2018, Hay *et al.*, 2017). CLR forms AM1 (Adrenomedullin 1) and AM2 (Adrenomedullin 2) receptors when paired with RAMP2 or RAMP3, respectively (McLatchie *et al.*, 1998).

While RAMPs engender significant pharmacology switches to these receptors, all current evidence points to this occurring via allosteric modulation of the receptor ligand-binding site and through direct contacts with CGRP, AM₁ and AM₂ C-terminal residues (Booe *et al.*, 2015, Booe *et al.*, 2018). In the published CLR–RAMP1– α CGRP complex (Liang *et al.* 2018a), interactions between the ligand and RAMPs contribute <10% to the buried surface.

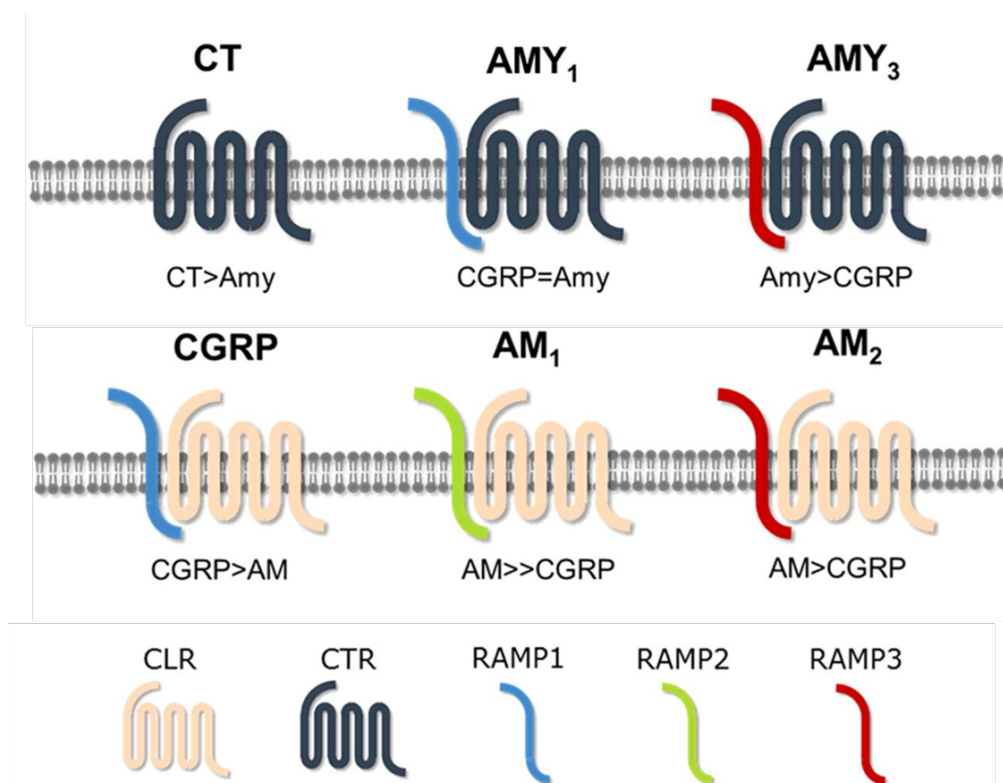


Figure 1.5. Composition of receptors of the calcitonin family and their interactions with RAMPs (Adopted from (Hay et al., 2016)).

Table 1.1. Composition of receptors of the calcitonin family: their interactions with RAMPs and pharmacological properties.

Receptor	Heteromers	Peptides rank order of potency (human)
CTR	CTR	$sCT \geq hCT > AMY$, $\alpha CGRP > AM$, <i>intermedin</i>
AMY1	CTR + RAMP1	$sCT \geq AMY \geq \alpha CGRP > intermedin \geq hCT > AM$
AMY2	CTR + RAMP2	<i>Poorly defined</i>
AMY3	CTR + RAMP3	$sCT \geq AMY > \alpha CGRP > intermedin \geq hCT > AM$
GCRP	CLR + RAMP1	$\alpha CGRP > AM \geq intermedin > AMY \geq sCT$
AM ₁	CLR + RAMP2	$AM > intermedin > \alpha\text{-CGRP}$, $AMY > sCT$
AM ₂	CLR + RAMP3	$AM \geq intermedin \geq \alpha\text{-CGRP} > AMY > SCT$

1.3.7 CALCITONIN FAMILY OF PEPTIDES – THEIR SITES OF PRODUCTION, PHYSIOLOGICAL ROLES AND RECEPTORS

There are five members of the calcitonin family of peptides that are all structurally related but biologically diverse: CT, two distinct forms calcitonin gene-related peptides (α CGRP and β CGRP), amylin (AMY), adrenomedullin 1 (AM1) and adrenomedullin 2/ intermedin (AM2/IMD). The CT family of peptides shares a common disulphide bridge and C-terminal amidation, which is required for activity; beyond this the sequence homology is low (Figure 1.6).

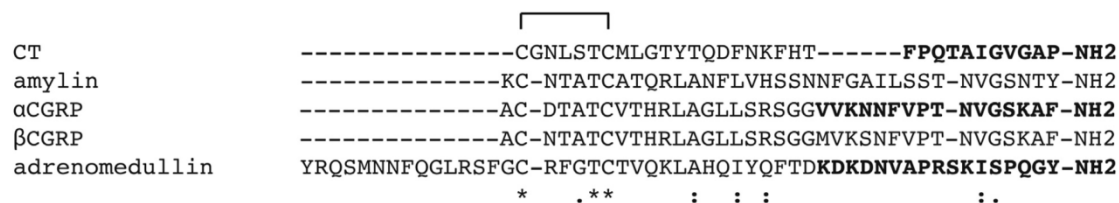


Figure 1.6. Primary amino acid sequence alignment calcitonin family of peptides: human calcitonin, amylin, αCGRP, βCGRP, and adrenomedullin. Conservation of residues is denoted by symbols: identical residues (*), conservative substitutions (:) and semi-conservative substitutions (.). While having generally low sequence conservation all peptides have conserved cysteine disulphide bridge toward the N- terminal and a C-terminal amidation. Highlighted in bold are the sequences that have been shown by crystallography to make contacts with the receptor N-terminal domain. For all peptides, truncation after the second cysteine generates an antagonist, highlighting the importance of the peptide N-terminus in activating the receptor.

1.3.7.1 CALCITONIN

CT is a 32-amino-acid peptide synthesized by the C cells of the thyroid gland in mammals. CT is processed from a 141 amino acid pre-pro-calcitonin encoded by the CALCA gene (Figure 1.7); several other processed peptides have also been identified in human plasma. Procalcitonin (pro-CT) is a 116-amino acid peptide that is found in the plasma of healthy individuals at about 10% of the level of mature CT.

CT lowers blood Ca^{2+} levels by direct inhibition of osteoclast-mediated bone resorption and by enhancing calcium excretion by the kidney (Fujikawa *et al.*, 1996a, Fujikawa *et al.*, 1996b, Ardaillou, 1975, Friedman *et al.*, 1965, Raisz *et al.*, 1969). It has been used clinically in the treatment of bone disorders, including Paget's disease, osteoporosis, and hypercalcaemia due to malignancy (Williams *et al.*, 1978, Kanis *et al.*, 1999, Overgaard, 1994).

A number extrathyroidal sites were identified to produce hCT peptide. These include kidney, pituitary, prostate gland, lung, and central nervous system (CNS) (Davis *et al.*, 1989, Cochran *et al.*, 1970, Ren *et al.*, 2001, Gosney *et al.*, 1985, Henke *et al.*, 1983, Sexton *et al.*, 1991). The physiological role for CT in these tissues is largely unknown but seems to be uninvolved in calcium homeostasis regulation.

CT from different species shows limited sequence homology, with all CT peptides having 32 amino acid sequence, a conserved disulphide bridge between cysteine residues at positions 1 and 7 and a carboxy-terminal proline amide. CTs from different species are classified into three groups based on their sequence homology: artiodactyl group (porcine (pCT), bovine, and ovine CT); primate/rodent group (human (hCT) and rat CT) and teleost/avian group (salmon (sCT), eel, goldfish, and chicken (cCT) CT) (Figure 1.8) (Sexton *et al.*, 1999). Presence of basic amino acids in mid-region of a CT molecule promotes helical structure yielding higher affinity, longer plasma half-life and in some cases higher potency of physiological response. Thus, sCT and non-

mammalian calcitonins have higher helicity and can be more potent than hCT. The order of biological potency for CT is teleost > artiodactyl > human (Here, comparison of the order of biological potency (with respect to a hypocalcemic response) relates to various species. The studies have been conducted with CTR receptors in humans and other animal species (rat, mouse, etc.) (Galante *et al.*, 1971, O'Dor *et al.*, 1969, Keutmann *et al.*, 1970, reviewed by Sexton *et al.*, 1999)).

human	MGFQKFSPFLALSILVLLQAGSLHAAPFRSALESSPADPATLSEDEARLLLAALVQNYVQ
rat	MGFLKFSPFLVVSILLLYQACGLQAVPLRSTLESSPGM-ATLSEEEAR-LLAALVQNYMQ
pig	MGFGKSSPFLAFSILVLCQAGSLQATPLRSALETLP-DPGPLSEKEGRLLLAALVKAYVQ
cow	MGFGKSSPFLAFSILVLCQAGSLQATPLRSALETLP-DPGALSEKEGRLLLAALVKAYVQ
chicken	MVMLKISSFLAVYALVVCQMSDFQAAPVRPGLESIT-DRVTLSDYEARRLLNALVKEFIQ
salmon	MVMLKISAFVLVAYALVICQMYSSQAAPSRPGIESMT-DRVTLTDYEARRLLNAIVKEFVQ
	* : * * *. *:: * . :*. * * :: *:: *:: *.* ** *::: :*
human	MKASELEQE--Q-EREGSSLDSPRSKRCGNLSTCMLGTYTQDFNKFHTFPQTAIGVGAPG
rat	MKVRELEQEEEQ-EAEGSSLDSPRSKRCGNLSTCMLGTYTQDLNKFHTFPQTSIGVGAPG
pig	RKTNELEQEEEQ-ETEGSSLDSSRAKRCNLSTCVLSAYWRNLNNFHRFSGMGFGPETPG
cow	RKTNELEQEEEQEETEDSSLDGSRKRCNLSTCVLSAYWKDLNNYHRFSGMGFGPETPG
chicken	MTAEELEQA-----SEGNLDRPISKRCASLSTCVLGKLSQELHKLQTYPRTDVGAGTPG
salmon	MTAEELEQQENE-GNEGNSMERPITKRCNLSTCVLGKLSQDLHKLQTFPRTDVGAGTPG
	.. **** * .*: : :***..*****: : : : : : .* :*
human	KKRDMSSDLERDHRPHVSMPOQAN
rat	KKRDMAKDLETNHHYPYFGN-----
pig	KKSDIASSLERD-LFPRGMPQDAN
cow	KKRDVANSLERDHSFHFVGPQDAN
chicken	KKRNVLNDLDHERYANYGETLGNN
salmon	KKRSAP---ESERYASYGKTFDSI
	** . : : .

Figure 1.7. Primary amino acid sequence alignment of the sequences for the predicted pre-pro-calcitonin (CT) peptide from various species. The first 25 amino acids comprise a signal peptide. Highlighted in red is the sequence for the N-terminus of pro-CT (which continues to the very C-terminus), blue is fully processed CT while in black dashes is katalcalcin (adopted from Ostrovskaya *et al.*, 2017).

cCT	CASLSTCVLGKLSQELHKLQTYPRTDVGAGTP
sCT	CSNLSTCVLGKLSQELHKLQTYPRNTGSGTP
hCT	CGNLSTCMLGTYTQDFNKFHTFPQTAIGVGAP
pCT	CSNLSTCVLSAYWRNLNNFHRFSGMGFGPETP

Figure 1.8. Primary amino acid sequence alignment calcitonin peptides from different species (chicken, salmon, human and porcine CTs). The CT sequences have been aligned and residues are colour-coded according to their sequence conservation: identical amino acids are coloured in green; conservative substitutions are coloured in blue; semi-conservative substitutions are coloured in orange; and non-conserved residues are coloured in black.

CTR is a class B GPCR. For many years, the research on CTR and CT was largely focused on their function in calcium homeostasis. Expression of CT and its receptors has been demonstrated in many different cell types and tissues suggesting multiple, biologically diverse roles for this peptide.

1.3.7.2 AMYLIN

Amy is co-secreted with insulin from pancreatic β -cells and acts to inhibit gastric emptying and signal satiety, thus reducing post-prandial glucose excursion (Westermarck *et al.*, 1986, Reda *et al.*, 2002). In common with the other CT family members, the mature 37-amino acid amylin hormone is C-terminally amidated and has an internal disulphide bond between residues 2 and 6 (Roberts *et al.*, 1989). Its stable analogue, pramlintide, is used in combination therapy with insulin for treatment of types 1 and 2 diabetes (Kruger *et al.*, 2004, Kleppinger *et al.*, 2003, Ryan *et al.*, 2008). There are three recognized receptors for amylin, AMY1 (CTR/RAMP1), AMY2 comprising CTR/RAMP2, and AMY3 comprising CTR/RAMP3, although AMY2 is rather poorly characterized and may not be a physiologically relevant receptor for Amy (Poyner *et al.*, 2002, Morfis *et al.*, 2008b).

1.3.7.3 α CGRP AND BCGRP

α CGRP is encoded by the same gene as CT (CALCA) and arises through tissue-specific alternative splicing of the primary mRNA transcript. The CT/ α CGRP gene was one of the first recognized examples of a cellular gene exhibiting alternative, tissue-specific processing and has served as an important paradigm to study the molecular mechanisms of RNA splicing (Emeson *et al.*, 1989). Mature α CGRP is a 37-amino acid peptide with low sequence homology to CT but sharing cysteine cyclization at the amino end and amidated C-terminus. α CGRP is predominantly produced in the nervous system (Amara *et al.*, 1982). It is a potent vasodilator and is strongly implicated in the pathophysiology of migraine (Muff *et al.*, 1995, Bell *et al.*, 1996, Durham, 2006). α CGRP's inotropic actions on the heart are mediated through activation of the sympathetic nervous system (Sato *et al.*, 1986, Ishikawa *et al.*, 1988, Fujioka *et al.*, 1991, Kawasaki *et al.*, 1990). Of note, α CGRP expression and secretion is upregulated in a wide range of tissues during sepsis and, in animal models, has a protective effect against septic mortality (Joyce *et al.*, 1990, Holzmann, 2013).

β CGRP is encoded by a different, but closely related gene with the mature peptide identical at 34 of 37 residues to CGRP. β CGRP is expressed in the gastrointestinal tract and has a role in modulating gastric motility and gastric acid secretion (Sternini *et al.*, 1992, Mulderry *et al.*, 1988). Historically the primary receptor for the CGRPs was considered to be the CGRP

receptor composed of CLR and RAMP1. It is now accepted in the GPCR field that the AMY1 receptor, comprising CTR and RAMP1, is also a receptor for the CGRPs (Christopoulos *et al.*, 1999, Walker *et al.*, 2015)

1.3.7.4 ADRENOMEDULLIN AND INTERMEDIN

AM, initially identified from the adrenal medulla of a patient with pheochromocytoma, is widely distributed and produced predominantly in vascular smooth muscle and endothelial cells (Kitamura *et al.*, 1993). Mature AM is a 52-amino acid peptide that is amidated at the C-terminus with a disulphide bond between residues 16 and 21. Much like α CGRP, AM is a potent vasodilator (Kitamura *et al.*, 2002). Other important actions include bronchodilation, natriuresis as well as regulation of cell growth, differentiation, and apoptosis (Hinson *et al.*, 2000, Lopez *et al.*, 2002, Otjacques *et al.*, 2011). AM2/IMD remains poorly understood. It has a wide range of effects on the cardiovascular system (vasodilator function and protection against oxidative stress), CNS (a neurotransmitter or modulator stimulating the sympathetic nervous system to increase blood pressure) and endocrine system (paracrine/autocrine regulator in the hypothalamo-pituitary-adrenal axis stimulating the release of adrenocorticotrophic hormone, prolactin, and oxytocin, but suppressing growth hormone release) (Taylor *et al.*, 2005b, Roh *et al.*, 2004, Taylor *et al.*, 2005a). There are two receptors showing high potency response to AM, both comprising heteromers: CLR/RAMP2 (the AM₁ receptor) and CLR/RAMP3 complex (the AM₂ receptor) (Roh *et al.*, 2004, Zhang *et al.*, 1999). CLR/RAMP3 complex was named the AM₂ receptor before AM2/IMD peptide was discovered. Although, perhaps serendipitously, AM2/IMD displays some preferential selectivity towards CLR/RAMP3 complex (as reviewed by (Hay *et al.*, 2018)). Adrenomedullin expression has been detected in glioblastoma biopsies where its expression correlates with the tumour grade, with highest expression in grade IV tumours (Metellus *et al.*, 2011, Ouafik *et al.*, 2002). AM expression is controlled by the hypoxia inducible factor 1 α , and cells overexpressing AM are resistant to hypoxia induced apoptosis (Metellus *et al.*, 2011, Ouafik *et al.*, 2002).

1.3.7.5 NOVEL CTR PEPTIDES

Several novel peptides with the ability to stimulate CTR have been reported. One of them is PHM-27 that is synthesized from the precursor protein pre-pro-VIP and was found in human neuroblastoma and neuroendocrine tumours (Itoh *et al.*, 1983). PHM-27 and hCT share limited sequence homology. PHM-27 has been initially published to be full agonist of hCTR with potency and efficacy similar to hCT, although when tested in our laboratory this peptide acts as a weak partial agonist in all pathways tested (Ma *et al.*, 2004).

A family of peptides that are most closely related to the CT/ α CGRP primary transcript, known as CTR-stimulating peptides (CRSPs), CRSP-1, CRSP-2, and CRSP-3, have been identified in the brain and the thyroid gland of the pig, dog, and cow, but not in man and mouse (Ogoshi, 2016). CRSP-1 has been shown to transiently decrease plasma calcium concentration when administrated into rats (as reviewed by (Katafuchi *et al.*, 2009). CRSP peptides bind effectively to CTR and stimulate cAMP production in COS-7 cells expressing recombinant CTR.

1.4 CALCITONIN RECEPTOR

1.4.1 CTR ISOFORMS AND SPLICE VARIANTS

Various CTR mRNA isoforms were previously cloned and described for different species, including humans, rat, pork and rabbit. Although not all these isoforms were well characterised and many of them are likely to represent aberrant mRNA from transformed cell lines (Sexton *et al.*, 1993, Zolnierowicz *et al.*, 1994, Shyu *et al.*, 1997, Seck *et al.*, 2005).

The most common example for human CTR splicing is an insertion of extra 16 amino acids in the ICL1 of the receptor (Gorn *et al.*, 1992, Kuestner *et al.*, 1994) giving rise to two CTR isoforms CTRa (insert negative) and CTRb (insert positive). This insert is encoded by a separate exon in human CTR gene. Although it has been shown by some groups that there is no consistent difference in binding affinities between the two CTR isoforms (Moore *et al.*, 1995), more recent direct comparison of binding affinities and signalling for various human CTR isoforms has shown increased affinity for both high affinity agonists, sCT and cCT, for CTRb isoform versus CTRa. Whereas lower affinity CTR agonists, hCT and pCT, and an antagonist, sCT(8-32) showed no significant differences in affinity between CTR splice variants (Dal Maso *et al.*, 2018a). Numerous studies showed that the insert positive CTR receptor loses its Gq-coupled signalling component that is manifested in complete loss of intracellular calcium accumulation and inositol monophosphate (IP1) signalling (Nakamura *et al.*, 1995, Kuestner *et al.*, 1994, Gorn *et al.*, 1992, Dal Maso *et al.*, 2018a). The insert positive CTR isoform was also commonly associated with profoundly reduced cAMP response in a cell type-dependent manner (Moore *et al.*, 1995, Raggatt *et al.*, 2000, Dal Maso *et al.*, 2018a). This is consistent with recent CTR structural data (Liang *et al.*, 2017) (showing that ICL1 packs against the $G_{\alpha\beta\gamma}$ heterotrimer and the 16-amino acid insert would be predicted to cause steric hindrance for this interaction. Insert positive CTR variant has been shown to be less efficient in activating ERK1/2 phosphorylation pathway in two different cellular backgrounds compared with the insert negative isoform (Dal Maso *et al.*, 2018a).

The physiological significance of the two human CTR isoforms remains to be established. CTR isoforms are differentially expressed in different cell types, suggesting that

alternative splicing is highly regulated and that receptor variants do have physiological roles. Additionally, there are some clues in literature demonstrating possible presence of more than one CTR splice variant in a single cancer cell line (Albrandt *et al.*, 1995, Beaudreuil *et al.*, 2004). This would enable both tissue-specific and isoform-specific regulation of receptors in under physiological and pathophysiological conditions.

In humans, the CTR gene contains a common single nucleotide polymorphism in the coding sequence that results in encoding either a leucine (T) or a proline (C) at amino acid 447 (463 for ICL1 insert positive) in the C-terminal tail (Kuestner *et al.*, 1994, Wolfe *et al.*, 2003). This polymorphism more commonly encodes leucine in Caucasian populations and much more commonly encodes proline in Asian populations (Wolfe *et al.*, 2003, Nakamura *et al.*, 1997). In other mammals this codon encodes proline (Dal Maso *et al.*, 2018a). In Asian populations there are reports of association between this polymorphism and a predisposition to osteoporosis in postmenopausal women. Some studies have shown that, in those (Asian) populations, women with leucine homozygote (TT) displayed lower spine bone density compared to either proline (CC) homozygotes or heterozygotes (Nakamura *et al.*, 1997, Masi *et al.*, 1998, Taboulet *et al.*, 1998, Wolfe *et al.*, 2003, Nakamura *et al.*, 2001, Tsai *et al.*, 2003). No statistically significant difference in the constitutive receptor activity to stimulate production of basal levels of cAMP in the absence of agonist stimulation was observed between the proline and leucine forms (Wolfe *et al.*, 2003). Recent direct *in vitro* comparison between CTR leucine and CTR proline polymorphisms it was observed that proline polymorphism biases receptor signalling away from cAMP production (this effect was observed in 2 different cell backgrounds) and also away from Ca^{2+} in one of the two cellular backgrounds signalling relative to the leucine variant. However, the magnitude of these effects was quite modest (Dal Maso *et al.*, 2018a).

1.4.2 CTR STRUCTURE AND ACTIVATION

Structural data on the CTR and CGRP receptor (Liang *et al.*, 2018a, Liang *et al.*, 2017b) along with the data on structure of the isolated NTD (N-terminal domain) in complex with truncated sCT and the NTD of CLR:RAMP1 (CGRP) and CLR:RAMP2 (AM1) bound to truncated CGRP and AM provide useful information on differences between binding of CT family peptides to their receptors compared with other secretin-like GPCRs (Johansson *et al.*, Booe *et al.*, 2015) (Figure 1.3). These structures reveal that CT family peptides occupy a similar cleft in the NTD of the receptor but unlike other class B peptides they do not adopt an extended alpha helix (Parthier *et al.*, 2009). These peptides do not adopt any strong secondary structure when bound, with the exception of a b-turn at their extreme C-terminus. This b-turn allows the C-terminal amide in all three structures to bury into a pocket that allows hydrogen bonding with

the receptor backbone carbonyl group and complementary hydrogen bonding between the receptor backbone amide and the ligand C-terminal carbonyl (Booe *et al.*, 2015, Johansson *et al.*). This appears to explain the observed requirement for C-terminal amidation among all CT family peptides.

Mutational studies of the CTR ECLs revealed the importance of residues in the CTR ECL2 for conformational propagation linked to Gs signalling. The GLP-1 receptor also utilizes ECL2 for its ligand binding and activation of intracellular signalling, however ECL2 is engaged in different manner in CTR (Dal Maso *et al.*, 2018b, Koole *et al.*, 2012a, Koole *et al.*, 2012b). In addition, individual residues and residue networks within both GLP-1R and CTR ECL3 were shown to be important for distinct ligand- and pathway specific effects (Wootten *et al.*, 2016c, Koole *et al.*, 2012a, Dal Maso *et al.*, 2018b).

Comparison of the active CTR cryo-EM structure to the homology model of apo-CTR suggests that agonists bind to receptor's hydrophobic binding pocket that is formed by large an outward movement of the receptor's extracellular ends of transmembrane regions 6 and 7 (Liang *et al.*, 2017) (Figure 1.9). TM helix 6 also forms a 60° kink with an intracellular end of this helix pointing outwards to open a binding pocket for interactions with G protein heterotrimer (Liang *et al.*, 2017). When compared with the binding pocket of the GLP-1R active structure (Zhang *et al.*, 2017a) it is apparent that the CTR orthosteric binding site sits higher than that for GLP-1R (Liang *et al.*, 2017b) and also as predicted for other secretin-like GPCRs, with the N-terminus residing approximately 1 helical turn above a network of conserved secretin-like family polar residues (Siu *et al.*, 2013b, Wootten *et al.*, 2016c, Dods *et al.*, 2016) (Figure 1.3). This difference is determined by a structural difference in the N-terminus of CTR ligands that have a cyclic ring that creates a steric hindrance compared to linear N-termini of other class B peptides (Schwartz *et al.*, 1981). The recently solved active CGRP receptor structure (CLR:RAMP1 with α CGRP) displays a similar organisation of the binding pocket to CTR to accommodate a bulky cyclic ring at CGRP N-terminus (Liang *et al.*, 2018a). An extended intracellular H8 contributes to receptor stability and CTR engagement with the G β subunit of G protein (Liang *et al.*, 2017).

As discussed above, CTR activation by different agonists occurs via distinct engagement of the receptor. Indeed the low affinity agonist hCT is commonly equipotent with the high affinity agonist sCT, a fact that, until recently, remained unexplained. The mechanistic explanation for this effect is based on the ability of hCT to stabilize distinct conformations for CTR in complex with G protein that have higher affinity to GTP and thus enable faster G protein turnover leading to higher accumulation rates for downstream second messengers (in this instance, cAMP) (Furness *et al.*, 2016). Comparison of 1 μ s molecular dynamics (MD) simulations demonstrates that when bound to CTR hCT displays more conformational mobility

and a bigger number of rearrangements within the side chains and in the ECL2 compared to sCT (Dal Maso *et al.*, 2018b).

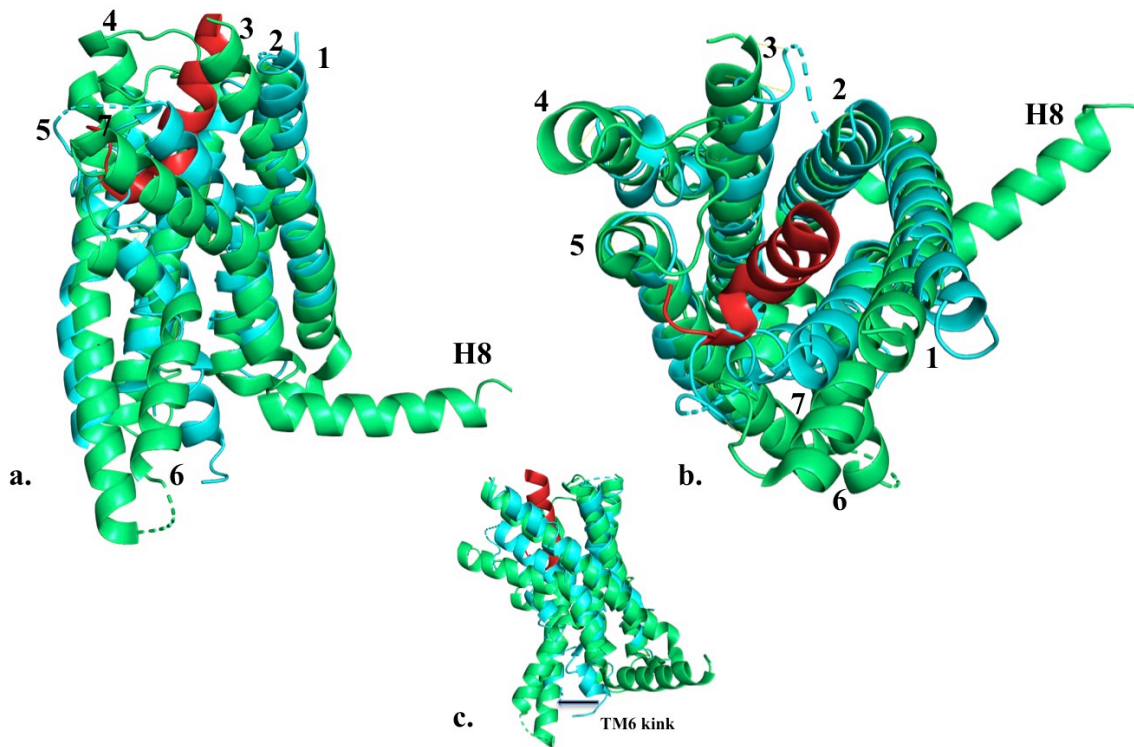


Figure 1.9. Comparison between active and inactive CTR structures. (a., c.) side and (b.) extracellular views of the sCT/CTR active structure (green) in complex with sCT (red) (pdb 6NIY) relative to CTR inactive model based on GCGR receptor structure (cyan, pdb 5EE7). All TM domains are numbered accordingly.

1.4.3 CTR SIGNALLING

CTR is known to pleiotropically couple to multiple G proteins and downstream signalling pathways (Figure 1.10). Coupling of the CTR to either $G_{\alpha s}$ or $G_{\alpha q}$ can activate AC or PLC, respectively. AC catalyses the conversion of ATP to cAMP (Sexton *et al.*, 1993, Houssami *et al.*, 1994, Moore *et al.*, 1995) while PLC cleaves PIP_2 to form DAG and IP_3 (Essen *et al.*, 1997) and hence leads to increased cytosolic calcium (via IP_3 activation of IP_3 receptors in endoplasmic reticulum (ER) that promote Ca^{2+} diffusion from ER into the cytoplasm where increased intracellular Ca^{2+} levels activate IP_3 receptors in cytosol that further promote Ca^{2+} mobilization) (Chabre *et al.*, 1992, Naro *et al.*, 1998, Force *et al.*, 1992). In osteoclasts, there is evidence that signalling through both cAMP and intracellular calcium is important in CT action (Chambers *et al.*, 1985). In kidneys, CTR couples to either AC or PLC pathways depending on the region of the nephron (Goldring *et al.*, 1978, Chabardes *et al.*, 1976, Murphy *et al.*, 1986, Suzuki *et al.*,

1989). While in hepatocytes CTR is likely to couple to G proteins, other than G_{as}, with some evidence towards CTR signalling linked to intracellular calcium mobilization (Yamaguchi, 1989, Yamaguchi, 1991). In the CNS CT inhibits AC activity through G_i-independent mechanism (Rizzo *et al.*, 1981, Nicosia *et al.*, 1986, Guidobono *et al.*, 1991a).

There is some evidence in literature that CTR can also couple to PLD signal transduction pathway (Naro *et al.*, 1998). However, this study did not investigate activation of which G protein by the CTR is responsible for the activation of this pathway. Perhaps, this could be CTR activation of G_{12/13} (based on the information on signalling pathways of other GPCRs), but more investigation of this is needed. CTR coupling to G_{ai} was seen in cells overexpressing the insert-negative CTR isoform, in which pertussis toxin enhanced the cAMP response to CT (Lacroix *et al.*, 1998, Chen *et al.*, 1998).

CTR-mediated activation of the ERK1/2 MAPK pathway has also been described. Rapid or sustained activation of MAPK has been observed under different circumstance (Robinson *et al.*, 1997, Chen *et al.*, 1998). However, a sustained activation of the ERK1/2 MAPK pathway and cell-growth suppression by CT is also associated with growth inhibition and accumulation of cells in G2 phase, has been observed in HEK-293 cell lines overexpressing hCTR (Raggatt *et al.*, 2000). CTR ERK1/2 signalling can be mediated by multiple G proteins and requires further investigation (Morfis *et al.*, 2008). Possible role for beta gamma G protein subunits in ERK1/2 activation should be also considered, as is commonly the case for other GPCRs. There is also evidence that CT, acting via CTR, can influence cell–cell and cell–extracellular matrix interactions. This can occur by modulating components of focal adhesions and the cytoskeleton as well as tight junction components. CTR activation was shown to induce tyrosine phosphorylation of the p130Cas-like protein human enhancer of filamentation 1 (HEF1) which leads to the formation of a complex with adhesion-related proteins HEF1, paxillin, and focal adhesion kinase (FAK) and through this CTR can mediate changes in cell shape and motility (Zhang *et al.*, 1999). In prostate cancer cell lines has been shown that CT-activated CTR can also destabilize tight junctions and this requires its C-terminal PDZ docking site (Zhang *et al.*, 1999, Aljameeli *et al.*, 2017, Aljameeli *et al.*, 2016). It is not yet clear how these in vitro CT actions correlate with in vivo physiology; however these effects may have relevance to cancer, particularly cell migration, invasion and metastasis development.

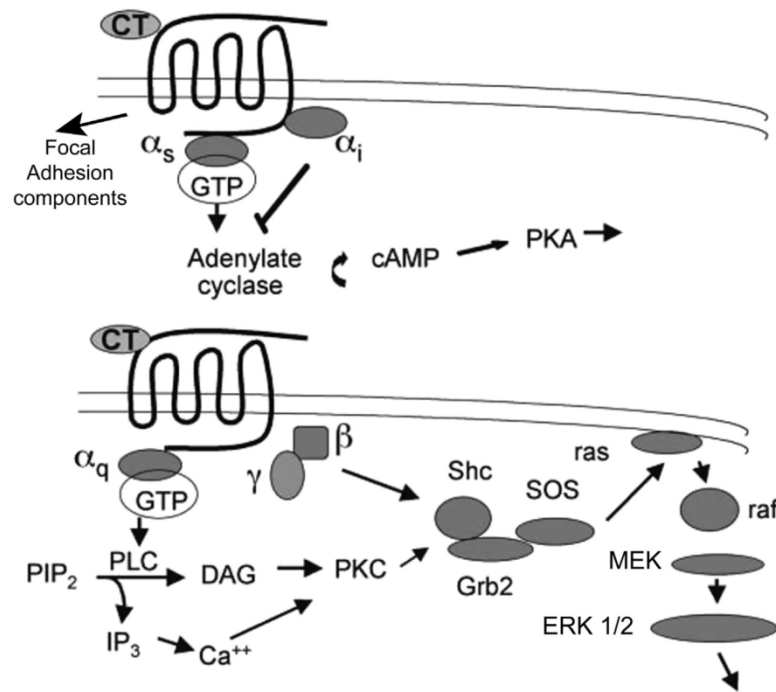


Figure 1.10. Signalling capability of the calcitonin receptor (CTR), showing some of the major intracellular signalling pathways that are activated on binding of calcitonin (CT) to the CTR. CTR coupling to G_s and G_q proteins activates AC and PLC, respectively. Downstream pathways activated include those involving PKC, PKA, MAPK (ERK), and components of the focal adhesions. (Adopted from (Ostrovskaya *et al.*, 2017).

These studies reveal that CTR activation and signalling is dependant on many factors, such as the particular receptor splice variant or polymorph as well as cellular background. Understanding how these factors are linked to the regulation of physiological and pathophysiological CTR responses is still unclear.

1.4.4 CTR TRAFFICKING AND REGULATION

Previous studies are inconsistent on whether CTR is able to recruit β -arrestins. The controversy between this data and the earlier data showing recruitment to hCTR α Leu may be because of the construct used in second study (Andreassen *et al.*, 2014, Dal Maso *et al.*, 2018a). Andreassen and colleagues in their study used a CTR modified C-terminus with that of vasopressin (V2) receptor that has a property of efficient β -arrestin recruitment (Oakley *et al.*, 1999). Although is not clear whether the CTR can couple to β -arrestin, in cell backgrounds where this does not occur, CTR exhibits constitutive internalization, independent of splice variant and polymorphism and this profile appears unaltered by peptide binding (Dal Maso *et al.*, 2018b). Preliminary data in our lab also supports fast constitutive internalisation of human CTR in human osteoclasts. Insufficient work has been done to know how widespread this phenomenon is amongst different cell types.

A number of earlier studies support the idea of CTR homologous regulation via CT (Findlay *et al.*, 1996, Findlay *et al.*, 1982, Findlay *et al.*, 1984, Michelangeli *et al.*, 1983); this

regulation was used to explain the well-known effect of loss of responsiveness to CT by patients the calcitonin “escape phenomenon” that can be observed in patients after only several days of CT treatment) (Wilkinson, 1984, Takahashi *et al.*, 1995). This regulation appears to be cell type- and tissue-specific. For, example, in murine osteoclasts prolonged CTR stimulation (24 hours incubation) by CT results in CTR downregulation through decrease of CTR mRNA expression mechanistically linked to PKA activation (Ikegame *et al.*, 1994, Wada *et al.*, 1995, Takahashi *et al.*, 1995, Wada *et al.*, 1996). On the other hand, the mechanism of CTR regulation by CTs in human osteoclasts was shown to be predominantly through the activation of PKC leading to homologous CTR down-regulation and inhibition of bone resorption (Samura *et al.*, 2000). In the latter case, CTR down-regulation was due not only to internalization of the receptor, but also due to inhibition of *de novo* CTR synthesis, i.e. CTR mRNA transcription mediated through PKC pathway (Samura *et al.*, 2000). Same study has also showed that even short exposure to CT (of 1 hour) resulted in prolonged CTR downregulation and diminished CTR mRNA expression (up to 96 hours after CT removal) with expression recovered 72 hours after CT removal. It could be speculated that this mechanism is the one responsible for CT-induced tachyphylaxis in humans. It was also shown that that integrity of the C-terminal tail (a point of interaction with second messengers and kinases) is important for cellular internalization of the CTR (Seck *et al.*, 2003).

Co-administration of glucocorticoids, on the contrary, was shown to induce CTR up-regulation accompanied with increased mRNA expression, and enhanced responsiveness of CT-stimulated adenylate cyclase activity (heterologous regulation) (Wada *et al.*, 2001).

1.4.5 BIOLOGICAL ACTIONS CTR

1.4.5.1 BONE ACTIONS

The best understood physiological action of CT is on osteoclasts is to inhibit bone resorption under conditions of elevated plasma calcium (Copp *et al.*, 1962, Friedman *et al.*, 1965, Chambers *et al.*, 1985). There is also evidence of calcitonin role in prevention of bone loss during pregnancy, lactation, and growth (i.e. conserving bone during calcium stress) (Skinner *et al.*, 2015, Broulik, 2010). In thyroidectomized patients the decrease in serum calcium levels in response to short-term intravenous calcium infusion is delayed compared with patients with an intact thyroid, showing the role of CT in the acute control of bone resorption (Hirsch *et al.*, 1969).

Because of the known action to inhibit osteoclast-mediated bone resorption, CT has been used clinically for treatment of osteoporosis, Paget’s disease, prevention of bone loss due to sudden immobilization, and hypercalcemia of malignancy (Williams *et al.*, 1978, Kanis *et al.*, 1999, Overgaard, 1994). Recently the European Medicines Agency undertook a large

metaanalysis of data relating to the clinical use of CTs. The report concluded that there was limited evidence demonstrating improvements in osteoporosis, Paget's disease, and bone loss due to sudden immobilization but did conclude that there is evidence for benefit in treating hypercalcemia of malignancy. It did note that there is evidence that pharmacological use of CT is associated with increased risk of several cancers (see below). In the United States, CT is no longer used for treatment of osteoporosis or Paget's disease. It seems likely that the physiological activity of CT in humans with respect to bone is limited to development and protection from bone loss during lactation and that CT should be regarded as a regulator of the rate of bone remodelling (see below) (Ostrovskaya *et al.*, 2017).

The genetic disruption of CT and its receptor in mice would seem to provide the most direct means for analysis of the physiological actions of CT (at least in a model organism). Disruption of CALCA gene leads to loss of both CT and α CGRP, and these mice display increased bone density and increased bone turnover with age suggesting that the action of CT is to regulate the rate of bone turnover (Hoff *et al.*, 2002, Zaidi *et al.*, 2002). These authors also developed mice in which a translational termination codon was introduced into exon 5, effectively producing a functional deletion of α CGRP without affecting CT (Schinke *et al.*, 2004). These mice displayed a mild loss of bone density at all ages (osteopenia) due to decreased bone formation, arguing for a role of α CGRP in antagonizing CT action on osteoclasts. At 3 months of age these mice displayed increased bone density and there were no changes in osteoclast number, bone resorption, or serum calcium levels; however, at 12 months there were increased osteoclast numbers and increased bone resorption, even though there was still increased bone density (Schinke *et al.*, 2004, Lerner, 2006). This suggests that the physiological role of CT is to decrease the overall rate of bone turnover. Since α CGRP-deleted mice display decreased bone formation and there are no CTRs on osteoblasts, CT must exert an indirect anabolic effect on bone.

Two groups have developed CTR knockout mice. The first group reported that global knockout resulted in embryonic lethality; however, haploinsufficient mice showed normal serum calcium levels but developed high bone density due to increased bone formation (Dacquin *et al.*, 2004). Through the use of conditional knockout techniques, this group was able to generate animals that had >94 and <100% functional deletion of CTR (Davey *et al.*, 2008). Consistent with their haploinsufficient animals disruption, these animals displayed normal serum calcium and increased bone density due to increased bone formation. A second group generated CTR knockouts by using a conditional knockout strategy to remove the same exons; in contrast to the first group, global functional deletion was not embryonic lethal (Keller *et al.*, 2014a). These mice displayed normal plasma calcium and increased bone formation leading to increased bone

density from 3 to 18 months (Keller *et al.*, 2014a). This group then generated mice with osteoclast-specific disruption of CTR and was able to show that CT, acting through CTR on osteoclasts, inhibited sphingosine 1-phosphate release, which acts on osteoblasts to increase their activity (Keller *et al.*, 2014b). These data therefore support the role of CT, acting through the CTR as a modulator of bone remodelling rather than a regulator of plasma calcium levels and is consistent with observations in humans (above).

The preceding discussion relates largely to CT bone physiology in non-stress situations. In mice bearing the CALCA disruption, challenge with PTH or 1,25-dihydroxyvitamin D3 resulted in short-term elevation of serum calcium caused by excess bone resorption and this could be corrected by pharmacological dosing of CT (Hoff *et al.*, 2002). Similarly, mouse models in which CTR was disrupted in osteoclasts there was impaired acute regulation of serum calcium levels in response to 1,25-dihydroxyvitamin D3 (Davey *et al.*, 2008). This supports the idea that CT provides acute regulation of serum calcium via its actions at the CTR to inhibit osteoclast-mediated bone resorption. During lactation there are large demands for calcium, which are largely met by mobilization of calcium stores (Qing *et al.*, 2012).

1.4.5.2 RENAL ACTIONS

In kidneys, CT reduces serum calcium by decrease in the tubular resorption of calcium (Cochran *et al.*, 1970). This effect is the opposite of PTH effect on calcium. CTR also promotes urinary excretion of phosphorous, sodium, potassium, chloride and magnesium (Ardaillou *et al.*, 1967, Cochran *et al.*, 1970, Haas *et al.*, 1971). Under normocalcemic conditions calcitonin has an important role in the maintenance of serum 1,25-dihydroxyvitamin D3 (1,25(OH)₂D3) via promoting 1-hydroxylation of 25-hydroxyvitamin D in kidney (Jaeger *et al.*, 1986, Wongsurawat *et al.*, 1991). This has physiological importance during pregnancy, lactation, and early development.

1.4.5.3 CENTRAL ACTIONS

Activation of the CTRs expressed in the central nervous system induce effects such as analgesia, inhibition of appetite, regulation of gastric acid secretion, modulation of hormone secretion and alterations to membrane excitability of individual neurons (Guidobono *et al.*, 1991b, Morley *et al.*, 1981, Twery *et al.*, 1988, Morley *et al.*, 1991).

1.4.5.4 CTR ROLES IN CANCER

Neuroendocrine tumours including pheochromocytoma, small cell lung cancer, pancreatic islet, gastrointestinal and lung carcinoid as well as both neuroendocrine and

nonneuroendocrine breast tumours have been reported as secreting high levels of pro-CT (Chaftari *et al.*, 2015, Conlon *et al.*, 1988, Becker *et al.*, 2004, Jimeno *et al.*, 2004). Levels of pro-CT present in plasma from cancer patients are elevated compared with healthy individuals, and the levels are positively correlated with disease stage (Chaftari *et al.*, 2015). The role of pro-CT in this broad range of cancers is unknown, but a number of both prospective and retrospective studies have shown positive correlation with disease progression and morbidity (Jimeno *et al.*, 2004). This has led a number of clinical researchers to propose the use of pro-CT as a prognostic indicator (Shen *et al.*, 2017). Serum pro-CT levels are also massively increased by sepsis, and studies of cancer patients demonstrate that even with elevated baseline pro-CT, elevated pro-CT is still prognostic for septic infection (Patout *et al.*, 2014).

Medullary thyroid cancers secrete high levels of CT (Conlon *et al.*, 1988). It is widely assumed that this is simply a consequence of the tumour origin and there is currently no evidence that CT secretion is consequential to the disease pathology. On the other hand, CT is a useful biomarker for confirming complete surgical resection.

The expression of CTR has been demonstrated in a number of cancer cell lines and primary cancers including breast, prostate, thymic lymphoma, and glioblastoma (Wookey *et al.*, 2012, Nakamura *et al.*, 2007, Segawa *et al.*, 2001, Venkatanarayan *et al.*, 2015). Research on the role of CTR expression in cancer has been fragmentary, and any role for CTR in cancer pathology seems to be entirely dependent on the cancer type.

CTR mRNA is expressed in normal ductal cells but not elsewhere in the breast. CT has been found to be a potent inhibitor of the growth and invasion of a model human breast cancer cell line MB-MDA-231 *in vitro* (Qing *et al.*, 2012, Nakamura *et al.*, 2007). This is due to the ability of CT to suppress high basal MAPK activity as well as reducing expression of urokinase plasminogen activator (uPA), a protease at the top of the extracellular matrix degradation pathway (Nakamura *et al.*, 2007). In less invasive human breast cancer model cell lines, such as T47D and MCF-7, binding and activity data support the presence of CTR as AMY receptors (Nakamura *et al.*, 2007, Wada *et al.*, 1995, Iwasaki *et al.*, 1983, Martin *et al.*, 1980, Findlay *et al.*, 1981). The level of CTR in these cells is suppressed by estradiol, and CT is not reported to affect growth of these cells (Lacroix *et al.*, 1998). A study of CTR in surgically obtained human breast cancers identified receptor mRNA production in all cases examined, regardless of breast cancer subtype (Wang *et al.*, 2004). CTR expression by non-ductal tumours possibly represents a recapitulation of foetal expression, and it was recently reported that the CTR is expressed in several foetal tissues in the mouse, including the developing mammary gland, although it is absent in the same tissues postnatally. There is no data on the developmental expression of the CTR in humans, but it is reasonable to speculate that CTR expression in certain tumours

represents a reappearance of foetal expression. Of note, pro-CT is present at elevated levels in the serum of patients suffering from breast cancer (Chaftari *et al.*, 2015).

Basal epithelial cells of the prostate express mRNA for both CT and CTR, and primary prostate cells in culture secrete CT (Sabbisetti *et al.*, 2005b, Chien *et al.*, 2001). There is no evidence for expression of either CT or CTR elsewhere in normal prostate tissue. In prostate tumour biopsies there is a strong positive correlation between histological scoring of disease progression and co-expression of both CT and CTR mRNA (Sabbisetti *et al.*, 2005a). The LNCaP model human prostate cell line expresses CTR but not CT and responds to CT with increased growth (Sabbisetti *et al.*, 2005a). The PC-3 model cell line secretes CT but does not express CTR, on the other hand a highly metastatic clone PC-3M and the highly metastatic line DU-145 express both CT and CTR (Segawa *et al.*, 2001). In support of paracrine/autocrine signalling of CT/CTR, in vitro proliferation and invasiveness of LNCaP cells is increased by enforced expression of CT (Thomas *et al.*, 2008). Similarly, the proliferation and invasiveness of the PC-3 cell line could be increased by enforced CTR expression and that of the PC-3M line decreased by downregulation of either CT or CTR (Aljameeli *et al.*, 2016, Thakkar *et al.*, 2016, Thomas *et al.*, 2006, Thomas *et al.*, 2005). In these cell lines, autocrine CT/CTR signalling via PKA stimulates expression of urokinase-type plasminogen type activator (uPA) to promote correlates of invasiveness. In addition, CT activated CTR, via its C-terminal PDZ (postsynaptic density protein 95, desmoglein 1, zonula occludens-1) docking site, destabilizes tight junctions, which would also contribute to invasiveness (Zhang *et al.*, 1999, Aljameeli *et al.*, 2017, Aljameeli *et al.*, 2016). These data are consistent with the European Medicines Agency report, recommending close monitoring of prostate cancer during the clinical use of CT.

CTR is functionally expressed on normal B and T lymphocytes from healthy individuals as well as on B and T cells from leukemic patients and transformed lymphoid cell lines (Cafforio *et al.*, 2009, Body *et al.*, 1990, Moran *et al.*, 1978). In a genetically modified mouse model of thymic lymphoma, it has been shown that the tumour protein 53 (p53) family of tumour suppressors are upstream of amylin expression. CTR is expressed on malignant cells with RAMP3 as the AMY3 receptor (Venkatanarayan *et al.*, 2015). Stimulation of these lymphomas with pramlintide (a synthetic amylin analogue) causes CTR-dependent tumour regression via changes to cellular metabolism (Venkatanarayan *et al.*, 2015, Venkatanarayan *et al.*, 2016). This work was extended to show that a range of model human cancers also undergo a switch from glycolysis to mitochondrial respiration in response to amylin signalling via CTR/AMY3 and that this leads to increased oxidative stress and apoptosis (Venkatanarayan *et al.*, 2015). There are currently no data that address how signalling from CTR/AMY3 couples to changes in cellular metabolism and whether CT would also produce these effects.

Given the wide expression of pro-CT/CT/CTR in a variety of cancers and the differing effects observed, significantly more work needs to be done. Clearly, there needs to be better assessment of the potential receptor(s) for pro-CT and a better understanding of its possible metabolism to products with different activity. In addition, significantly more work is required to understand the coupling of CTR and AMY receptors in different cell backgrounds if expression of pro-CT, CT, or CTR is to be leveraged in cancer treatment.

1.4.5.5 CTR IN GLIOBLASTOMA MULTIFORME

Glioblastoma multiforme (GBM) is the most common and aggressive type of primary brain cancer (Louis *et al.*, 2007, Kleihues *et al.*, 1999). GBM arises from transformed precursors of astrocytes (Sanai *et al.*, 2005) and is characterized by high proliferation, vascularization and resistance to apoptosis. GBM can be classified into four subtypes: proneural, neural, classical and mesenchymal based on distinct genomic and proteomic profiles and with distinct responsiveness to the existing combined therapy protocol (Verhaak *et al.*, 2010). GBMs are highly heterogeneous tumours, comprising cells in various states of differentiation including a subpopulation of cells that display stem cell characteristics (Sanai *et al.*, 2005). Excessive blood vessel formation resulting from hypoxia, secretion of angiogenic growth factors by GBM cells and tumour stem cell differentiation into endothelial cells (vascular mimicry) contributes to rapid disease progression (Cheng *et al.*, 2013, Soda *et al.*, 2011, Ricci-Vitiani *et al.*, 2010, Wang *et al.*, 2010). With median survival of less than 15 months, even with best practice intervention, identification and validation of new GBM therapeutic targets is of critical importance (Das *et al.*, 2013).

In Glioblastoma tumour biopsies, CTR expression has been detected using CTR-specific antibodies (12 out of 14 GBM biopsies were CTR positive), with low or undetectable CTR expression in adjacent non-tumour tissue (Wookey *et al.*, 2012). Additionally, toxin conjugates of monoclonal anti-CTR antibody 2C4 promote cell death in JK2, SB2b and WK1 GBM-derived cell lines and in U87MG glioblastoma-derived cell line with effective concentrations in the picomolar range, supportive of CTR expression (Gilabert-Oriol *et al.*, 2017).

1.4.5.6 OTHER ACTIONS OF CTR

As discussed above CT and its receptor are found in a large number of cell types and tissues include kidney, brain, pituitary, testis, prostate, spermatozoa, lung, and lymphocytes (Cochran *et al.*, 1970, Ardaillou *et al.*, 1967, Ren *et al.*, 2001, Davis *et al.*, 1989, Silvestroni *et al.*, 1987, Gosney *et al.*, 1985, Henke *et al.*, 1983, Sexton *et al.*, 1991, Wu *et al.*, 1996, Body *et al.*, 1990, Cafforio *et al.*, 2009). This suggests multiple physiological roles for the CT/CTR. In

spite of this, and as discussed above, mice bearing a functional deletion of CT have no overt phenotype outside bone (Hoff *et al.*, 2002). The most thorough published data on mice carrying functional deletion of CTR in mice also show no overt phenotype in any of the above tissues (Davey *et al.*, 2008, Keller *et al.*, 2014b). Thus, physiological roles for CT/CTR outside bone homeostasis are likely to be to do with environmental adaptation. That there is a massive upregulation of pro-CT expression during sepsis and that neutralization of serum pro-CT improves outcome speaks to some involvement of (pro)-CT in immune modulation (Assicot *et al.*, 1993, Whang *et al.*, 1998, Muller *et al.*, 2000, Nysten *et al.*, 1998). Indeed, expression of CTR is a characteristic of most hematopoietic lineages and this expression occurs in two phases, one in very early precursors and another implicated in recruitment of mature cells to target tissues (Becker *et al.*, 2010). Similarly, there have been a number of reports that CTR is upregulated during wound healing and CT signalling may be involved in this process (Lupulescu *et al.*, 1978). Lastly CTR is expressed on muscle satellite cells, and CT signalling appears to play a role in maintaining their quiescence (Yamaguchi *et al.*, 2015).

1.5 AIMS

The calcitonin receptor is a member of the class B G-protein coupled receptor family and has a role in controlling calcium and bone homeostasis by regulating osteoclast activity and renal calcium excretion (reviewed in Ostrovskaya *et al.*, 2017). CTR expression in various cell types and tissues correlates with CTR's diverse roles extending beyond calcium regulation and bone homeostasis. For example, the CTR is expressed in the central nervous system, monocyte and macrophage precursors, a subset of T cells, muscle satellite cells, and proliferating fibroblasts. What the exact roles in CNS, immune system, wound healing, cell differentiation and tissue morphogenesis are not well researched and thus remain undefined (reviewed in Ostrovskaya *et al.*, 2017, Wookey *et al.*, 2010). Of particular interest is CTR expression in various cancers. Currently, the research on CTR's role in various cancers has been fragmentary and inconclusive regarding the potential link between the receptor and its role in cancer progression. Apparently, it seems that the effect of CTR stimulation/inhibition is both cancer-, and cell-type dependent (reviewed in Ostrovskaya *et al.*, 2017, Nakamura *et al.*, 2007, Aljameeli *et al.*, 2016, Thakkar *et al.*, 2016, Thomas *et al.*, 2005, Thomas *et al.*, 2006, Venkatanarayan *et al.*, 2014, Venkatanarayan *et al.*, 2016).

High CTR expression has been previously confirmed in Glioblastoma Multiforme (GBM) tumour biopsies using anti-CTR antibodies (Wookey *et al.*, 2012). GBM is an aggressive primary brain cancer, with no effective treatment available (Louis *et al.*, 2007, Kleihues *et al.*, 1999, Sanai *et al.*, 2005). Therefore, in the first project of my thesis (Chapter 3) I sought to

perform a pharmacological characterization of the CTR (along with other receptors of its family) in primary high-grade glioma cell lines and to test whether targeting CTR pharmacologically could be viable strategy for GBM treatment.

For this study I obtained four high-grade glioma cell lines that were derived from individual patient tumours. These cell lines are distinct from other conventional recombinant cell lines (growing on matrigel in the absence of serum and the ability to recapitulate the original GBM tumour when injected intracranially into mice), making them good representative models for our study (Day *et al.*, 2013). GBM is a highly heterogeneous tumour and is classified into 4 distinct subtypes that differ morphologically and by their responsiveness to therapy. I obtained 4 GBM cell lines that represent 3 out of 4 distinct GBM subtypes (SB2b and PB1 of classical GBM subtype; JK2 of proneural and WK1 of mesenchymal) and thus one of the aims was to understand whether there is any correlation between the GBM subtype and CTR expression profile in these lines.

Pharmacological characterization of the high-grade glioma cell lines was performed using a range of assays and a range of CTR and CLR agonists. Signaling was tested across different pathways that CTR is known to couple to, and that can be linked to cancer signaling. In order to assess the effects of CTR activation/suppression on the cell growth, I performed a number of assays measuring cell proliferation and cell metabolism, as well as direct cell counting using a high content imaging system. Additionally, I performed a correlation analysis between the CTR expression and patient survival using two public databases.

While there are gaps in the knowledge regarding CTR's roles in (patho)physiology, some of which I tried to address in the first project, there is also incomplete understanding about how CTR ligands activate the receptor and how CTR signaling to distinct signaling effectors is mediated. Class B GPCRs interact with their cognate peptide agonists according to the two-domain model, where both the N-terminal ECD and TM regions of the receptor participate in ligand binding. This mechanism is well accepted in the field and is supported by multiple studies (Stroop *et al.*, 1995, Holtmann *et al.*, 1995, Bergwitz *et al.*, 1996, Gelling *et al.*, 1997, Runge *et al.*, 2003). The full length CTR ternary complex structure solved in our laboratory initially had insufficient resolution for sCT to allow unambiguous modelling of the peptide side-chains and thus limiting our understanding of particular side-chain interactions between the CTR and sCT (Liang *et al.*, 2017). More generally, both X-ray and cryo-EM structural data provide a static picture of one (or a limited subset) of the receptor's possible conformations, limiting the ability of this structural information to fully inform receptor signalling. Additionally, each single structure can only describe an interaction between a receptor and a single agonist coupled to a single signaling pathway, (in case if the structure was solved in complex with a particular

transducer, i.e. a G protein). Therefore, while I had a reasonably good overall understanding about class B GPCRs binding and signaling, we still lacked many of the finer details regarding the mechanics of single amino acids interactions.

Previous mutagenesis studies have confirmed the importance of the CTR's ECD in ligand binding and signal transduction as well as revealing certain ligand-dependent differences for CTR-agonist interaction (Dal Maso *et al.*, 2018b, Dal Maso *et al.*, 2019). However, no such studies have been performed on the CTR TM region. It is understood, that distinct CTR agonists display different affinities and efficacies at the CTR, and this has been best studied for sCT and hCT (Furness *et al.*, 2016). Therefore, I aimed to perform Ala mutagenesis analysis of the residues in proximity of the CTR TM binding pocket. In this study I investigated the importance of individual interactions between the CTR and distinct agonists, to understand their importance in CTR binding and signalling.

For this study I used CTR agonists from the 3 major CT evolutionary branches (based on sequence conservation): sCT (avian/teleost), hCT (human/rodent) and pCT (artiodactyl) as well as 2 weak CTR agonists – CGRP and rAMY. The latter 2 become potent CTR agonists when the receptor is co-expressed with any RAMP and therefore can be used to assess the effects of RAMPs on CGRP and rAMY binding and signalling in comparison studies (when CTR is expressed with and without RAMPs) (Christopoulos *et al.*, 1999, Morfis *et al.*, 2008). In Chapter 4 I aimed to analyze mutational effects on global binding affinities for individual CTR agonists, obtained from radioligand competition binding. To assess the effects of the CTR TM mutations on receptor signaling I chose 2 signalling pathways – cAMP and pERK1/2. Functional affinity (calculated from the signaling data) is a measure of affinity when receptor-agonist complex is coupled to a particular signaling pathway. Therefore, we sought to compare how well CTR binding affinity correlates with its functional affinity for each signaling pathway (Chapter 4). I also aimed to understand both ligand- and pathway-specific commonalities and differences in how signal transduction is mediated through the CTR by assessing the effects of alanine mutations on the CTR efficacy (Chapter 5). As a common aim for the Chapters 4 and 5, I compared our CTR mutational data to currently available information on analogous mutagenesis of other class B GPCRs in order to establish commonalities and differences in the mechanisms of class B GPCRs activation and signaling.

CHAPTER 2

Materials and methods

2.1 MATERIALS

2.1.1 PEPTIDES

All peptides were purchased from Mimotopes Pty Ltd., Clayton, Victoria, Australia.

2.1.2 ANTIBODIES

Mouse anti-human-cMyc 9E10 was purified and harvested in house from hybridoma (ATCC CRL-1729) supernatant. MAb4614 anti-CTR antibody is from R&D Systems. Goat Anti-mouse AF647 was purchased from Thermofisher Scientific Australia Pty Ltd.

2.1.3 GENERAL REAGENTS

Dulbecco's Modified Eagle's Medium (DMEM) and heat-inactivated foetal bovine serum (FBS) were purchased from Thermofisher Scientific. StemPro® NSC SFM kit was purchased from Thermofisher Scientific (formerly Life Technologies). Matrigel was purchased from In Vitro Technologies, Melbourne, Australia. F12 GlutaMax medium was obtained from Thermofisher Scientific.

Selection antibiotics puromycin, zeocin and hygromycin B were acquired from InvivoGen (SanDiego, CA, USA), Sigma-Aldrich and Thermofisher Scientific respectively.

AlphaScreen™ reagents, LANCE HTRF cAMP kit and Lance Ultra cAMP assay kit were purchased from PerkinElmer Life Sciences (Waltham, MA, USA). SureFire™ ERK1/2 reagents were purchased from TGR Biosciences (Adelaide, SA, Australia) and PerkinElmer. Fluo-4 acetoxymethyl ester was purchased from Thermofisher Scientific. CellTiter 96® AQueous One Solution Cell Proliferation Assay was obtained from Promega. Optiplates were purchased from PerkinElmer Life Sciences.

Q5 polymerase kit was acquired from New England Biolabs (Ipswich, MA, USA). LR Clonase II enzyme mix was obtained from Thermofisher Scientific. DpnI (10 U/ul) was purchased from Thermo Fisher Scientific.

DNA-free DNA removal kit as well as TaqMan Fast Advanced Master Mix was purchased from Thermo Fisher Scientific. iScript Reverse Transcription Supermix for reverse transcripton-qPCR (RT qPCR) was acquired through Bio-Rad (Hercules, CA, USA).

Wizard Plus SV Minipreps DNA Purification System kit was acquired from Promega and Plasmid Maxi Kit was purchased from QIAGEN.

Radioactive ¹²⁵I (~350 mCi/ml) was purchased from Perkin Elmer.

All other reagents were purchased from Sigma (St. Louis, MO, USA) or BDH Merck (Melbourne, Vic, Australia) and were of an analytical grade.

2.1.4 PLASMIDS AND PRIMERS

pENTR11, pEF5/FRT/V5 DEST, pOG44 and were obtained from Thermofisher Scientific. The CTR construct used in this study consists of sequence in pENTR11 vector containing kanamycin resistance gene (vector construct previously designed in our laboratory). For cMycCTRaLeu a 10 amino acid C-Myc tag (encoding EQKLISEEDL) was inserted immediately downstream of the predicted signal peptide at N-terminus cloned into pENTR11 vector as described in (Dal Maso *et al.*, 2018b) (Supplementary tables 1 and 2, Appendix 1).

Sequencing primers for pENTR11 and for pEF5/FRT/V5 (pENTR11 forward, pENTR11 reverse, T7 and BGH), were synthesised by GeneWorks. Primers for single CTR mutants were synthesized by Bioneer Pacific (Melbourne, Australia) (sequences for sequencing and mutagenesis primers are provided in Supplementary tables 3 and 4, Appendix 1).

Primers for TaqMan Gene Expression assays were purchased from Thermofisher Scientific (formerly Life Technologies): for CALCR (Hs01016882_m1), CALCRL (Hs00907738_m1), RAMP1 (Hs00195288_m1), RAMP2 (Hs01006937_g1), RAMP3 (Hs00389131_m1), CALCA (Hs01100741_m1), IAPP (Hs00169095_m1), and ACTB (Hs01060665_g1).

2.2 MOLECULAR BIOLOGY

2.2.1 GENERATION OF SINGLE ALANINE POINT MUTATIONS OF THE cMYCCTRALEU IN pENTR11 VECTOR

To verify functional importance of identified residues within CTR they were mutated to alanine. Residues that were initially alanine were mutated to either leucine (non-polar side chain, same as alanine, but two carbon atoms longer) or serine (same length as alanine, but contain polar -OH group). Mutations were introduced into the coding sequence of the human insert negative splice variant of CTR containing Leu polymorphism (hCTRaLeu) that is the most commonly studied CTR variant. Nucleotide substitutions encoding single amino-acid changes were introduced using oligonucleotides from Bioneer Pacific (Melbourne, Australia) and Q5 polymerase following supplier's standard protocol. Briefly, PCR was performed in Verti 96 well Thermal Cycler (Applied Biosystems). After initial denaturation for 3 minute at 98°C, 25 cycles were performed including denaturation (98°C, 10 seconds; annealing 72°C, 30 seconds; and extension 72°C, 2 minutes). A 10-minute final extension at 72°C was performed at the end of the cycling steps, and then samples were maintained at 4°C. PCR reaction was followed by 4 hours digestion of template DNA with DpnI enzyme in accordance with manufacturer's protocol.

2.2.2 TRANSFORMATION

Receptor clones in pENTR11 vector were used to transform DH5alpha strain of *E. coli* competent cells following the manufacturer's protocol for bacterial transformation. In brief, 2.5 µl of the PCR product was pre-incubated for 30 minutes on ice with 50 µl of DH5α cells followed by heat-shock for 40 seconds at 42°C and followed by 5 minute incubation on ice. Transformed bacteria were then incubated at 37°C for 1 hour in 250 µl of LB (10 g/l tryptone, 5 g/l yeast extract, 10 g/l NaCl) and plated on an agar plate with appropriate antibiotic selection (50 µg/ml Kanamycin for pENTR11 vector; 100 µg/ml Ampicillin for pEF5/FRT/V5 vector). Selection plates were incubated at 37°C overnight.

2.2.3 DNA AMPLIFICATION, EXTRACTION

Colonies were inoculated and grown overnight at 37°C in LB media with relevant antibiotic. Next day, culture broth was centrifuged at 15 minutes at 4°C, 1000 g. Pellets were re-suspended and plasmids were extracted using either Miniprep (Promega) or Maxiprep (Qiagen) DNA purification kits following manufacturer's protocol.

2.2.4 SEQUENCE CONFIRMATION

All cMycCTRaLeu alanine substitutions were confirmed by sequencing. For one sequencing reaction around ~400 ng of plasmid DNA was combined with ~10 ng of either forward (pENTR11 forward for pENTR11 vector and pT7 pEF5/FRT/V5 vector) or reverse (pENTR11 reverse for pENTR11 BGH for pEF5/FRT/V5 vector) primer. Sequencing of individual receptor clones was conducted as automated sequencing at the Melbourne branch of the Australian Genome Research Facility. All plasmids were sequenced in the full coding sequence to ensure there were no additional deleterious mutations.

2.2.5 RECOMBINATION INTO DESTINATION VECTOR

Correct mutant receptor clones as well as WT CTR were subsequently transferred into destination vector pEF5/FRT/V5-DEST using LR Clonase II enzyme mix following manufacturer's instructions. Receptor clones in the destination vector were transformed into competent cells; this was followed by DNA amplification, extraction and sequencing as described above.

2.3 TISSUE CULTURE

2.3.1 MAMMALIAN CELL CULTURE

Primary patient high-grade glioma (HGG) cell lines, *in vitro* surrogates of glioblastoma, were developed by QIMR-Berghofer Medical Research Institute (Brisbane, Australia) and represent 3 distinct GBM subtypes: SB2b and PB1 (classical), JK2 (proneural) and WK1(mesenchymal) (Day *et al.*, 2013). GBM cell lines were cultured as adherent monolayers on matrigel (BD Biosciences)-coated flasks using StemPro NSC SFM serum free cell culture medium (Thermo Fisher Scientific) supplemented with 20 ng/ml EGF and 20 ng/ml FGFb, 1% D-glutamine and 1 % of penicillin/ streptomycin (further referred as StemPro complete medium).

African Green Monkey kidney Flp-In CV-1 cells stably expressing either WT or single alanine point mutation of the CTRaLeu were cultured in DMEM supplemented with 5% FBS and 300 µg/ml hygromycin B.

All cells were cultured in 5% CO₂ / 95% humidified air at 37°C.

2.3.2 STABLE TRANSFECTION OF MAMMALIAN FLPIN CELLS

FlpIn CV-1 cells were chosen as they have no pharmacologically detectable CTR and no pharmacologically detectable RAMP expression. This was previously experimentally verified by the members of our laboratory by probing for an amylin phenotype upon transfection of CTR and assessment of CLR trafficking to the cell surface upon transfection, in the case of CTR transfection data from other members of our lab shows no measurable amylin phenotype and no cell surface expression of CLR in the absence of co-transfection with a RAMP family member . Flp-In-CV-1 cells were initially seeded in 25 cm² flasks in DMEM, 5% FBS, 100 µl zeocin and grown up to 70-80 % confluency. On the day of transfection, medium was replaced with serum and antibiotic-free DMEM. Transfection mixture was prepared by combining 0.5 µg pEF5/FRT/V5-DEST containing the WT or mutant hCTRaLeu constructs and 4.5 µg pOG44 vector (prepared in 250 µl of 150 nM sterile NaCl) with 30 µl PEI (also prepared in 150 nM sterile NaCl), shaking it vigorously and incubating at room temperature for 10 minutes. After that, the transfection mixture was drop-wise added to the cells. Following 48 hours post transfection media was replaced with DMEM containing 10% fetal bovine serum and 400 µg/ml hygromycin B. Cells were further maintained and selected in DMEM containing 10% fetal bovine serum and 400 µg/ml hygromycin B in a humidified environment at 37°C in 5% CO₂. 39 mutant cell lines plus the control cell line expressing wild type receptor have been generated. Backup frozen stocks have been made and placed into the vapour phase nitrogen storage.

2.4 FUNCTIONAL ASSAYS

2.4.1 IODINATION OF sCT(8-32)

Iodination reaction of sCT(8-32) was performed to obtain mono-iodo-tyrisyl. 10 µl of ^{125}I (as sodium iodide, concentration 350 mCi/mL) was added to 5 µl of 1 mg/ml freshly made chloramine T (in PBS, pH 7.4) and incubated together at room temperature for 60 seconds. This was followed by addition of 20 µl of PBS and 5 µl of 0.1 mM sCT(8-32) and incubation at room temperature for 10 seconds. 200 µl of KI (5 mg/ml prepared in PBS) was added to quench the reaction and adjusted with 260 µl of PBS to the final volume of 500 µl. ^{125}I -sCT(8-32) was purified with reverse phase HPLC (C-18 column; 0.1% TFA in H₂O to 0.1% TFA in acetonitrile gradient). Purified ^{125}I -sCT(8-32) was supplemented with 0.1 % final BSA, aliquoted and stored at -20°C.

2.4.2 HETEROLOGOUS WHOLE CELL RADIOLIGAND COMPETITION BINDING

CV-1 cells were plated at 25000 cells per well in DMEM, 5% FBS on a 96 wells plate and incubated at 37°C in humidified 5% CO₂ overnight. On the next day cell media was replaced with 80 µl of binding buffer (DMEM, 25 mM HEPES, 0.1% BSA, pH 7.4) and cells were chilled at 4°C for 4 hours to minimise receptor internalization. Approximately 20000 to 75000 cpm/well (corresponding to 50-150 pM) of ^{125}I -sCT(8-32) were added to each well followed by relevant dilution of competing non-iodinated ligand in the final volume of 100 µl. Plates were incubated overnight at 4°C. The following day, binding buffer was removed and wells were washed with ice cold PBS twice. 50 µl of 0.1M NaOH was added to each well and lysates were transferred into scintillation tubes. γ radiation was detected using a γ -counter (Wallac Wizard 1470 Gamma Counter, Perkin Elmer, 80% counter efficiency). Data analysis was performed using Graphpad Prism 7. Data was normalized between the total level of bound ^{125}I -sCT(8-32) and non-specific binding, defined by saturating concentration of competing non-iodinated sCT(8-32) (1 µM).

2.4.3 CAMP ACCUMULATION ASSAY

GBM cell lines were seeded at 38000 cells/well (SB2b) or 35000 cells/well (PB1, JK2 and WK1) in 96-well matrigel-coated plates and incubated for 24 hours at 37°C, 5% CO₂ in humidified incubator in StemPro complete medium. CV-1 cells were seeded at 25000 cells/well in 96-well clear FALCON culture plates and incubated overnight at 37°C, 5% CO₂ in humidified incubator in DMEM media (5% FBS, 300 µg/ml hygromycin B). Next day plating media was

replaced with stimulation buffer (phenol red free F12 media, 0.1 % BSA, 0.5 mM IBMX, pH 7.4). Cells were stimulated with agonists (sCT, hCT, pCT, rAmy, α CGRP or AM) at concentrations ranging from 10^{-6} M – 10^{-12} M, or 10^{-5} M forskolin, or vehicle for 30 minutes at 37°C. Stimulation buffer was aspirated, cells were lysed (0.3 % Tween 20, 5 mM Hepes, 0.1% BSA, pH 7.4) and 5 μ l of cell lysate from each well was transferred to a corresponding well of 384-well optiplate. Intracellular cAMP levels in the wells were determined using Lance Ultra cAMP assay kit (Perkin Elmer) according to the manufacturer's instructions and detected using an Envision multilabel 2103 reader. Raw relative fluorescence units (RFU) values were converted using a cAMP standard curve to give absolute cAMP concentrations. Data were analysed by three-parameter logistic curve and are presented as percentage of 10^{-5} M forskolin response (Chapter 3) or analysed by three-parameter logistic curve and normalized to WT response (present in each individual assay) (Chapters 4 and 5).

2.4.4 ERK1/2 PHOSPHORYLATION ASSAY

GBM cell lines were seeded at 38000 cells/well in 96-well matrigel-coated plates and incubated either overnight (for 4 hours growth factor starvation), or for 7 hours (for overnight starvation) at 37°C, 5% CO₂ in humidified incubator in StemPro complete medium. CV-1 cells were seeded at 25000 cells/well in 96-well clear culture plates and incubated overnight at 37°C, 5% CO₂ in humidified incubator in DMEM media (5% FBS, 300 μ g/ml hygromycin B). Culture media was replaced with DMEM/F12 GlutaMax medium (without growth factors) and incubated for either 6 hours on the day of experiment (for 6 hours growth factor starvation of SB2b or CV-1), or overnight (overnight starvation of SB2b) prior to stimulation experiment. An initial time-course was performed for each ligand (sCT, hCT, pCT, α CGRP and rAmy) at 0.1 - 1 μ M to assess the maximum peak of ERK1/2 phosphorylation. Following stimulation by ligands, media was removed and cells lysed in lysis buffer. For ERK1/2 inhibition, test cells were stimulated with agonists (sCT and hCT, at concentrations ranging from 10^{-6} M – 10^{-12} M in presence of 0.3 % FBS for 6 minutes). ERK1/2 phosphorylation was detected using AlphaScreen SureFire pERK1/2 (Thr202/Tyr204) Assay Kit according to the manufacturer's instructions and detected using an Envision multilabel 2103 reader.

2.4.5 P38 PHOSPHORYLATION

SB2b cells were seeded at 38000 cells/well in 96-well matrigel-coated plates and incubated either overnight (for 4 hours growth factor starvation), or for 7 hours (for overnight starvation) at 37°C, 5% CO₂ in humidified incubator in StemPro complete medium. Culture media was replaced with DMEM/F12 GlutaMax medium (without growth factors) and

incubated for either 4 hours (for 4 hours growth factor starvation), or overnight (overnight starvation). P38 phosphorylation was detected using AlphaScreen SureFire Total p38 MAPK Assay Kit according to the manufacturer's instructions and detected using an Envision multilabel 2103 reader.

2.4.6 Ca^{2+} MOBILIZATION

GBM cell lines were seeded at 38000 cells/well (SB2b) or 35000 cells/well (PB1 and WK1) in 96-well matrigel-coated plates and incubated for 24 hours at 37°C, 5% CO_2 in humidified incubator in StemPro complete medium. Cells were washed twice with Ca^{2+} Buffer (150 mM NaCl, 10 mM HEPES, 10 mM D-glucose, 2.6 mM KCl, 1.18 mM MgCl_2 , 2.2 mM CaCl_2 , 0.5% BSA, 4 mM probenecid, pH 7.4) before addition of 1 μM Fluo4-AM diluted in Ca^{2+} buffer. Cells were incubated at 37°C for 60 minutes before ligand addition and detection of Ca^{2+} mobilisation in a Flex Station 3 (Molecular Devices). The machine settings were as follows: 37°C, excitation 485 nm, emission 525 nm, baseline reads of 15 seconds before drug addition, fast drug dispense, 120 seconds reading.

2.4.7 ASSESSING CELL PROLIFERATION USING LIVE CELL IMAGING (OPERETTA)

SB2b cells were seeded at 10000 cells/well in 96-well matrigel-coated Cell-Carrier (0.18 mm bottom) 96-well plates and incubated overnight at 37°C, 5% CO_2 in humidified incubator in StemPro complete medium. After 14-18 hours, treatments including sCT (1 μM and 100 nM) and hCT (1 μM and 100 nM); 1 μM sCT:8-32, 10% FBS or vehicle (StemPro media), were added to individual wells. Following drug additions, cells were placed into the Perkin-Elmer Operetta chamber and were kept at 37°C and 5% CO_2 for the duration of the experiment. Cells were imaged every hour for 72 hours using a 10x PlanApo 0.3 NA objective. Both bright field and digital phase contrast images were captured at each time point. The number of cells and their morphology (length, breadth and area) were counted for every well and time point. Analysis was performed using Harmony 4.1 software by segmenting the digital phase.

2.4.8 MTT ASSAY

The CellTiter 96[®] AQueous One Solution Cell Proliferation Assay was used to quantify cell metabolism. The assay principle relies on MTS tetrazolium compound ([3-(4,5-dimethylthiazol-2-yl)-5-(3-carboxymethoxyphenyl)-2-(4-sulfophenyl)-2H-tetrazolium, inner salt; MTS^(a)]) bioreduction by metabolically active cells into a soluble colored formazan product. Metabolic activity of SB2b was assessed by an MTT assay in the presence (+GF) or

absence (-GF) of defined growth factors (GF, EGF + bFGF) in combination with 1 μ M of CTR agonists sCT or hCT or the CTR specific antagonist sCT(8-32). In brief, 15000 cells were plated per well in the Stem Pro media. For the (-GF) condition, cells were plated in complete STEM Pro media. Media was aspirated from the wells after cells had attached to the bottom (about 6 hours after plating) and was replaced with F12 DMEM without growth factors. For both (+GF) and (-GF) conditions 1 μ M of CTR agonists sCT or hCT or the CTR specific antagonist sCT(8-32) were added along with vehicle control (F12 DMEM) and cells were incubated for the next 24 hours in a humidified incubator at 37°C/5%CO₂. For MTT detection incubation media was discarded from the cells and replaced with serum-free media and MTT reagent and further incubated at 37°C for 4 hours in a humidified, 5% CO₂ incubator. Absorbance was measured at 490 nm using Envision multilabel 2103 reader.

2.5 ASSESSING RECEPTOR CELL SURFACE EXPRESSION BY FLOW CYTOMETRY

On the day of the assay cells were gently harvested using versene, pelleted at 350 xg for 3 minutes and resuspended in ice cold blocking buffer (HBSS, 25 mM HEPES, 5% BSA, pH7.4) for 30-60 minutes. Primary antibody incubation for 90 minutes was performed with a mix of 1 μ g/ml of MAb4614 anti-CTR antibody and 5 μ g/ml of 9E10 anti-cMyc antibody made up in FACS buffer (HBSS, 25 mM HEPES, 0.1 % BSA, pH7). The anti-c-Myc (9E10) antibody was purified and harvested in house from hybridoma (ATCC CRL-1729) supernatant; 9E10 recognizes the N-terminal epitope tag on the CTR; MAb4614 is a commercial monoclonal antibody from R&D Systems which binds to extracellular epitope at the folded CTR, these antibodies were used in combination to achieve sufficient sensitivity for accurate quantitation of cell surface expression. This was followed by two washes with FACS buffer and a 60 minutes incubation with a secondary antibody goat anti-mouse (to the final concentration of 1 μ g/ml AF647 in FACS buffer). After 2 washes cells were resuspended in FACS buffer containing Sytox blue at 0.5 μ M. Samples were analysed on a FACS CantoII (BD Biosciences) with minimum 20000 cells collected per sample. Data was analysed using FlowJo software. The mean AF647 fluorescence intensity for the live population of each sample was normalized to 0% (untransfected parental CV-1) and 100% (CV-1 stably expressing WT CTR).

2.6 QUANTITATIVE REAL-TIME REVERSE TRANSCRIPTION POLYMERASE CHAIN REACTION (RT-QPCR)

Cells were grown as indicated above in 6-well plates, rinsed in warm PBS, and plates rapidly frozen and stored at -80°C. Each n number refers to a different passage number of cells. Total RNA was extracted from 1 x 6-well plate using TriReagent (Sigma Aldrich, NSW,

Australia) as per the manufacturer's instructions. The yield and quality of RNA was assessed by measuring absorbance at 260 and 280 nm (Nanodrop ND-1000 Spectrophotometer; NanoDrop Technologies LLC, Wilmington DE USA) and by electrophoresis in 1.3% agarose gels. Any contaminating DNA was removed using the DNA-free DNA removal kit (Ambion, Thermo Fisher Scientific, Scoresby, Australia) as per manufacturer's instructions. RNA samples were stored at -80°C. For preparation of cDNA, 0.5 µg of RNA was reverse-transcribed using iScript Reverse Transcription Supermix for RT-qPCR according to the manufacturers instructions. Briefly, the reactions consisted of 2 µl of 5 x iScript reverse transcription supermix, 3 µl DNase/RNase free water, and 0.5 µg of RNA, in a final volume of 10 µl in 200 µl Eppendorf PCR tubes. Reactions were performed on an Applied Biosystems 2720 Thermal Cycler (Applied Biosystems, Foster City CA USA) as following: 25°C for 5 minutes, 42°C for 30 minutes, 85°C for 5 minutes, and then allowed to cool to 4°C. The cDNA was diluted with 190 µl DNase/RNase free water to obtain the equivalent of 2.5 ng/µl of starting RNA, and cDNA was stored at -20°C.

For each independent sample, qPCR was performed in duplicate using TaqMan Gene Expression assays for CALCR, CALCRL, RAMP1, RAMP2, RAMP3, CALCA, IAPP, and ACTB. Each reaction consisted of 4 µl cDNA, 0.5 µl TaqMan Gene Expression Assay, 0.5 µl DNase/RNase free water, and 5 µl TaqMan Fast Advanced Master Mix dispensed in Eppendorf twin.tec PCR plates. qPCR reactions were carried out using an Eppendorf Mastercycler Relapse Real-time PCR instrument. After initial heating at 50°C for 2 minutes and denaturation at 95°C for 10 minutes, fluorescence was detected over 40 cycles (95°C for 15 seconds, 60°C for 1 minute). Data are expressed as relative expression of the gene of interest to the reference gene ACTB where:

$$\text{Relative expression} = 2^{-((Cq \text{ of gene of interest}) - (Cq \text{ of ACTB}))} \quad (\text{Equation 2.1})$$

For some genes, no mRNA was detected. These samples are omitted were omitted from the graphs as indicated in the figure legends.

2.7 PUBLIC DATA ANALYSIS

Raw data from IVY-GAP was analysed as follows: patient tumour biopsies were manually curated to identify tumour blocks with RNA-seq expression of CALCR greater than 1.25 fragments per kilobase of transcript (FPKM) that also corresponded to histological grading consistent with GBM, resulting in the identification of 12 patients whose tumours were positive for CALCR expression. This threshold was then applied to the patient survival data to generate a Kaplan-Meier survival plot. Raw RNA-sequencing data from TCGA was used to identify tumour samples with CALCR gene expression, this data was used to filter the patient clinical data and

expression was converted to Log₂. This was used to generate an expression – survivorship plot. This data was used with an FPKM threshold of 1.25 to generate the Kaplan-Meier plot.

2.8 EQUATIONS AND DATA ANALYSIS

2.8.1 EQUATIONS TO FIT EXPERIMENTAL DATA

Data was analysed using GraphPad Prism 7.

Homologous competition binding was analysed using the equation for one site homologous competition binding:

$$y = \frac{B_{max} * [Hot]}{[Hot] + [A] + K_d} + Bottom \quad (\text{Equation 2.2})$$

where B_{max} is the maximum binding of ligand to receptors in cpm; [Hot] is the concentration of ¹²⁵I-sCT(8-32) in nM; [A] is concentration of unlabelled sCT(8-32) in nM; K_d is the equilibrium binding constant of ¹²⁵I-sCT(8-32) in nM; Bottom is a plateau in the units of Y axis.

Data from heterologous competition binding was analysed using the Cheng-Prusoff equation to derive the K_i values:

$$LogIC_{50} = Log(10^{logK_i} * \left(\frac{1 + [Hot]}{K_d}\right)) \quad (\text{Equation 2.3})$$

$$Y = Bottom + \frac{(Top - Bottom)}{1 + 10^{X - LogIC_{50}}} \quad (\text{Equation 2.4})$$

where [Hot] is the concentration of ¹²⁵I-sCT(8-32) in nM; K_d is the equilibrium binding constant of ¹²⁵I-sCT(8-32) in nM; LogIC₅₀ is the Log of the concentration of competitor that results in binding half-way between Bottom and Top; LogK_i is the log of the molar equilibrium dissociation constant of unlabelled ligand; Top and Bottom are plateaus in the units of Y axis.

Concentration response curves for cAMP and ERK data were analysed using three-parameter fit:

$$y = Bottom + \frac{(Top - Bottom)}{1 + 10^{LogEC_{50} - Log[A]}} \quad (\text{Equation 2.5})$$

where EC₅₀ is the concentration of agonist that gives a response half-maximum response; [A] is concentration of agonist; Top and Bottom are plateaus in the units of the Y axis.

In case when concentration responses were better fitted to a biphasic curve, the following equation was applied:

$$Span = Top - Bottom \quad (\text{Equation 2.6})$$

$$Section1 = Span \times \frac{Frac}{1 + 10^{LogEC_{501} - Log[A] \times nH1}} \quad (\text{Equation 2.7})$$

$$Section2 = Span \times \frac{1 - Frac}{1 + 10^{LogEC_{502} - Log[A] \times nH2}} \quad (\text{Equation 2.8})$$

$$Y = Bottom + Section1 + Section2 \quad (\text{Equation 2.9})$$

where 1 and 2 represent the 2 phases of the curve; [A] is concentration of agonist; Frac is the proportion of maximal response due to the more potent phase; EC₅₀ is the concentration of agonist that gives a half-maximum response; nH1 and nH2 are the Hill slopes, constrained to 1.0 for stimulation; Top and Bottom are plateaus in the units of the Y axis.

In order to derive the key efficacy value, τ that represents a ligand intrinsic efficacy for the pathway and a equilibrium dissociation constant of an agonist K_A (functional affinity) an equation for the Operational Model of partial agonism was applied:

$$y = Bottom + \frac{Emax - Bottom}{1 + \left(\frac{(10^{logK_A} + 10^{log[A]})^n}{10^{log\tau} + 10^{log[A]}} \right)} \quad (\text{Equation 2.10})$$

Where E_{max} is the maximal response of the system; [A] is concentration of agonist, n is the transducer slope.

$log\tau$ values were corrected for cell surface expression to obtain $log\tau_c$ using formula:

$$log\tau_c = log\tau - log\left(\frac{Mutant(X) expression}{WT expression}\right) \quad (\text{Equation 2.11})$$

2.8.2 ERROR PROPAGATION

Uncertainties due to experimental measurement limitations, such as SD and SEM, need to be considered. When combining experimental variables, the following equations were used to allow for error propagation:

$$\partial y = \sqrt{\partial a^2 + \partial b^2} \quad \text{for linear combination of variables (sum or difference)} \\ \text{(Equation 2.12)}$$

and

$$\partial y = |y| \sqrt{\left(\frac{\partial a}{a}\right)^2 + \left(\frac{\partial b}{b}\right)^2} \quad \text{(for non-linear combinations of variables (multiplication and division))}. \\ \text{(Equation 2.13)}$$

2.8.3 STATISTICS

Statistical analysis was performed using one-way ANOVA analysis of variance and Dunnett's post-hoc test using GraphPad Prism7. Statistical significance was accepted at $p < 0.05$.

CHAPTER 3

Expression and activity of the calcitonin receptor family in a sample of primary human high-grade gliomas


Anna Ostrovskaya, Caroline Hick, Dana S. Hutchinson, Brett
W. Stringer, Peter J. Wookey, Denise Wootten, Patrick M.
Sexton and Sebastian G. B. Furness

RESEARCH ARTICLE

Open Access



Expression and activity of the calcitonin receptor family in a sample of primary human high-grade gliomas

Anna Ostrovskaya¹, Caroline Hick¹, Dana S. Hutchinson¹, Brett W. Stringer², Peter J. Wookey³, Denise Wootten^{1,4}, Patrick M. Sexton^{1,4} and Sebastian G. B. Furness^{1*} 

Abstract

Background: Glioblastoma (GBM) is the most common and aggressive type of primary brain cancer. With median survival of less than 15 months, identification and validation of new GBM therapeutic targets is of critical importance.

Results: In this study we tested expression and performed pharmacological characterization of the calcitonin receptor (CTR) as well as other members of the calcitonin family of receptors in high-grade glioma (HGG) cell lines derived from individual patient tumours, cultured in defined conditions.

Previous immunohistochemical data demonstrated CTR expression in GBM biopsies and we were able to confirm CALCR (gene encoding CTR) expression. However, as assessed by cAMP accumulation assay, only one of the studied cell lines expressed functional CTR, while the other cell lines have functional CGRP (CLR/RAMP1) receptors. The only CTR-expressing cell line (SB2b) showed modest coupling to the cAMP pathway and no activation of other known CTR signaling pathways, including ERK_{1/2} and p38 MAP kinases, and Ca²⁺ mobilization, supportive of low cell surface receptor expression.

Exome sequencing data failed to account for the discrepancy between functional data and expression on the cell lines that do not respond to calcitonin(s) with no deleterious non-synonymous polymorphisms detected, suggesting that other factors may be at play, such as alternative splicing or rapid constitutive receptor internalisation.

Conclusions: This study shows that GPCR signaling can display significant variation depending on cellular system used, and effects seen in model recombinant cell lines or tumour cell lines are not always reproduced in a more physiologically relevant system and vice versa.

Keywords: Calcitonin receptor, Glioblastoma, GPCR, Signaling

Background

Glioblastoma (GBM) is the most common and aggressive type of primary brain cancer [1, 2]. GBM arises from transformed precursors of astrocyte-glia lineage [3] and is characterized by high proliferation, vascularization and resistance to apoptosis. GBM have been classified into four subtypes: proneural, neural, classical and mesenchymal based on distinct genomic and proteomic profiles, and these subtypes have distinct responsiveness to the existing combined therapy protocol [4]. GBMs are

highly heterogeneous tumours, comprising cells in various states of differentiation including a subpopulation of cells that display stem cell characteristics [3]. Excessive blood vessel formation resulting from hypoxia, secretion of angiogenic growth factors by GBM cells and glioma stem cell differentiation into endothelial cells and pericyte precursors (vascular mimicry) contributes to rapid disease progression [5–9]. With median survival of less than 15 months, even with best practice intervention, identification and validation of new GBM therapeutic targets is of critical importance.

The calcitonin family of receptors consist of the calcitonin receptor (gene:CALCR, protein:CTR) and the calcitonin receptor-like receptor (gene:CALRL, protein:CLR);

* Correspondence: sebastian.furness@monash.edu

¹Drug Discovery Biology and Department of Pharmacology, Monash Institute of Pharmaceutical Sciences, Monash University, Parkville, VIC 3052, Australia
Full list of author information is available at the end of the article



© The Author(s). 2019 **Open Access** This article is distributed under the terms of the Creative Commons Attribution 4.0 International License (<http://creativecommons.org/licenses/by/4.0/>), which permits unrestricted use, distribution, and reproduction in any medium, provided you give appropriate credit to the original author(s) and the source, provide a link to the Creative Commons license, and indicate if changes were made. The Creative Commons Public Domain Dedication waiver (<http://creativecommons.org/publicdomain/zero/1.0/>) applies to the data made available in this article, unless otherwise stated.

both are class B (or secretin-like) G protein-coupled receptors (GPCRs). CTR and CLR can form complexes with the accessory single-transmembrane-domain proteins known as the receptor activity-modifying proteins (RAMPs) [10] generating multiple distinct receptor phenotypes with different specificities for the calcitonin (CT) peptide family (Table 1) [11].

Although CTR is most commonly known for its role in bone and calcium homeostasis (reviewed in [12]), its expression has been demonstrated in a number of cancer cell lines and primary cancers including breast and prostate cancers, bone cancers, leukemia, multiple myeloma, thymic lymphoma and glioblastoma (reviewed in [12]). Research on the role of CTR expression in cancer has been fragmentary and any role for CTR in cancer pathology seems to be entirely dependent on the cancer type. For instance, in human breast cancer model cell lines with high constitutive ERK (Extracellular Signal Regulated Kinase 1/2) phosphorylation, activation of CTR suppresses ERK phosphorylation. CT treatment inhibits the growth of MDA-MB-231 xenograft tumours but not those generated from MCF-7 cells [13]. In the human prostate cancer cell line PC3, CT inhibits apoptosis and stimulates tumour growth and invasiveness by recruiting zonula occludens-1 and promoting PKA-mediated tight junctions disassembly [14, 15]. Further, a metastatic derivative cell line – PC3M – expresses both CT and CTR and this co-expression appears to form a positive feedback system that increases invasiveness, emphasizing the role of paracrine/autocrine signaling of CT/CTR in this cancer [16, 17]. These data are also consistent with the European Medicines Agency report, recommending close monitoring of prostate cancer during the clinical use of CT (EMA/109665/2013). Furthermore, in mouse thymic lymphoma models, where CTR is expressed as an amylin receptor, amylin treatment leads to metabolic reprogramming (switch from glycolysis to oxidative phosphorylation) resulting in increased susceptibility to apoptosis [18, 19].

In normal human brain, CTR expression has been demonstrated by immunohistochemistry in the hypothalamus,

limbic system and circumventricular organs in the brain stem [20] but not elsewhere, which is consistent with sites for radio-ligand binding and pharmacological effects in model animals (reviewed in [12]) and with data from the Human Protein Atlas [21]. Glioblastoma primary tumours are almost exclusively found in the cortex, being predominantly located in frontal and temporal lobes [22, 23], where CTR is not normally expressed. In glioblastoma biopsies, CTR expression has been detected using CTR-specific antibodies (12 out of 14 GBM biopsies were CTR positive), with low or undetectable CTR expression in adjacent non-tumour tissue [24]. This expression correlated with GBM stem cell morphology and co-expression of GBM stem cell markers, glial fibrillary acidic protein and CD133 [24]. Additionally, toxin conjugates of monoclonal anti-CTR antibody mAb2C4 promote cell death in JK2, SB2b and WK1 high-grade glioma and U87MG glioblastoma-derived cell lines with effective concentrations in the picomolar range, supportive of CTR expression [25]. Other recent reports show variable expression of CALCR mRNA with expression in only a subset 12/42 [26] or 115/152 [27] of primary tumours. In addition, Pal et al. [28] report a correlation between patient survival and non-synonymous mutations in CTR.

Other receptors of the CTR family were also found in GBMs. CALCRL/RAMP2 (Adrenomedullin 1 (AM1) receptor) and CALCRL/RAMP3 (Adrenomedullin 2 (AM2) receptor) mRNA has been detected in both human glioma biopsies and in GBM cell lines [29, 30]. Comparative expression of 138 different GPCRs has revealed high levels of CALCRL mRNA, specifically in human glioblastoma cancer stem-like cells compared to significantly lower expression in human brain tumour U87MG cells, human astrocytes and foetal neural stem cells [31], although CALCRL is widely expressed in normal brain [21] as it functions as the predominant receptor for the neuropeptide CGRP. It has also been shown that the degree of adrenomedullin peptide expression correlates with GBM tumour grade, with highest expression in grade IV tumours, where adrenomedullin is localised in proximity to large necrotic areas together with vascular endothelial growth factor (VEGF) [30, 32].

The existing data on the role of CTR in GBM are from correlative studies [24] and the study of Pal et al. [28] supports a model in which CTR is a tumour suppressor. There are currently no data that mechanistically address the role of CT/CTR in the progression of GBM. The widely available GBM model cell lines such as U87MG and A172 fail to recapitulate the original tumour in intracranial xenograft models and lose temozolomide resistance [33–35]. A new method of deriving GBM cell lines from single patient tumours has been established [36, 37]. These cell lines, grown in serum free media

Table 1 Calcitonin family of receptors [10, 11, 38]

Receptor	Heteromers	Peptides rank order of potency (human)
CTR	CTR	$sCT \geq hCT > AMY$; $aCGRP > AM$, <i>intermedin</i>
AMY1	CTR + RAMP1	$sCT \geq AMY \geq aCGRP > intermedin \geq hCT > AM$
AMY2	CTR + RAMP2	<i>Poorly defined</i>
AMY3	CTR + RAMP3	$sCT \geq AMY > aCGRP > intermedin \geq hCT > AM$
CGRP	CLR + RAMP1	$aCGRP > AM \geq intermedin > AMY \geq sCT$
AM1	CLR + RAMP2	$AM > intermedin > aCGRP$; $AMY > sCT$
AM2	CLR + RAMP3	$AM \geq intermedin \geq aCGRP > AMY > sCT$

Rank order of potency for endogenous peptide ligands for calcitonin receptor family of receptors. *sCT* Salmon CT, *hCT* Human CT, *AMY1* Amylin 1 receptor, *AMY2* Amylin 2 receptor, *AMY3* Amylin 3 receptor, *CGRP* Calcitonin gene related peptide receptor

with the addition of defined growth factors, fully recapitulate the primary GBM tumour when injected into mice [38].

In this study we investigated further the question of whether CTR (or its family members) could be a valid therapeutic target in GBM treatment, as has been argued elsewhere [28]. For this purpose, we characterized expression of the calcitonin family of receptors along with the ligands, calcitonin and amylin (as they have been implicated in autocrine regulation of tumour growth) and performed functional and pharmacological characterisation across the known CTR signalling pathways.

Methods

Cell culture

Primary patient high-grade glioma (HGG) cell lines, in vitro surrogates of glioblastoma, were developed by QIMR-Berghofer Medical Research Institute (Brisbane, Australia) and represent 3 distinct GBM subtypes: SB2b and PB1 (classical), JK2 (proneural) and WK1 (mesenchymal) [37], who supplied these directly for this study. GBM cell lines were cultured as adherent monolayers on matrigel (BD Biosciences)-coated flasks using StemPro NSC SFM serum free cell culture medium (Thermo Fisher Scientific) supplemented with 20 ng/ml EGF and 20 ng/ml FGFb, 1% D-glutamine and 1% of penicillin/ streptomycin (further referred as StemPro complete medium). Cells were cultured in 5% CO₂ / 95% humidified air at 37 °C.

cAMP (cyclic adenosine mono-phosphate) assay

GBM cell lines were seeded at 38000 cells/well (SB2b) or 35,000 cells/well (PB1, JK2 and WK1) in 96-well matrigel-coated plates and incubated for 24 h at 37 °C, 5% CO₂ in humidified incubator in StemPro complete medium. Media was replaced with stimulation buffer (phenol red free F12 media, 0.1% BSA, 0.5 mM IBMX, pH 7.4). Cells were stimulated with agonists (sCT, hCT, rAmy, CGRP or adrenomedullin) at concentrations ranging from 10⁻⁶ M – 10⁻¹² M, or 10⁻⁵ M forskolin, or vehicle for 30 min at 37 °C. Cells were lysed (0.3% Tween 20, 5 mM Hepes, 0.1% BSA, pH 7.4) and 5 µl of cell lysate from each well was transferred to a corresponding well of 384-well optiplate. Intracellular cAMP levels in the wells were determined using Lance Ultra cAMP assay kit (Perkin Elmer) according to the manufacturer's instructions and detected using an Envision multilabel 2103 reader. Raw RFU values were converted using a cAMP standard curve to give absolute cAMP concentrations. Data were analysed by three-parameter logistic curve and are presented as percentage of 10⁻⁵ M forskolin response.

ERK 1/2 phosphorylation

SB2b cells were seeded at 38000 cells/well in 96-well matrigel-coated plates and incubated either overnight

(for 4 h growth factor starvation), or for 7 h (for overnight starvation) at 37 °C, 5% CO₂ in humidified incubator in StemPro complete medium. Culture media was replaced with DMEM/F12 GlutaMax medium (without growth factors) (Invitrogen, Carlsbad, CA, USA) and incubated for either 4 h (for 4 h growth factor starvation), or overnight (overnight starvation). An initial time-course was performed for each ligand (sCT and hCT) at 1 µM to assess the maximum peak of ERK_{1/2} phosphorylation. Following stimulation by ligands, media was removed and cells lysed in lysis buffer (TGR Bioscience). For ERK_{1/2} inhibition, test cells were stimulated with agonists (sCT and hCT, at concentrations ranging from 10⁻⁶ M – 10⁻¹² M in presence of 0.3% FBS for 6 mins). ERK_{1/2} phosphorylation was detected using AlphaScreen SureFire pERK_{1/2} (Thr202/Tyr204) Assay Kit according to the manufacturer's instructions and detected using an Envision multilabel 2103 reader.

Ca²⁺ mobilization

GBM cell lines were seeded at 38000 cells/well (SB2b) or 35,000 cells/well (PB1 and WK1) in 96-well matrigel-coated plates and incubated for 24 h at 37 °C, 5% CO₂ in humidified incubator in StemPro complete medium. Cells were washed twice with Ca²⁺ Buffer (150 mM NaCl, 10 mM HEPES, 10 mM D-glucose, 2.6 mM KCl, 1.18 mM MgCl₂, 2.2 mM CaCl₂, 0.5% BSA, 4 mM probenecid, pH 7.4) before addition of 1 µM Fluo4-AM diluted in Ca²⁺ buffer. Cells were incubated at 37 °C for 60 min before ligand addition and detection of Ca²⁺ mobilisation in a FlexStation 3 (Molecular Devices). The machine settings were as follows: 37 °C, excitation 485 nm, emission 525 nm, baseline reads of 15 s before drug addition, fast drug dispense, 120 s reading.

Quantitative real-time reverse transcription polymerase chain reaction (qRT-PCR)

Cells were grown as indicated above in 6-well plates, rinsed in warm PBS, and plates rapidly frozen and stored at - 80 °C. Each n number refers to a different passage number of cells. Total RNA was extracted from 1 × 6-well plate using TriReagent (Sigma Aldrich, NSW, Australia) as per the manufacturer's instructions. The yield and quality of RNA was assessed by measuring absorbance at 260 and 280 nm (Nanodrop ND-1000 Spectrophotometer; NanoDrop Technologies LLC, Wilmington DE USA) and by electrophoresis in 1.3% agarose gels. Any contaminating DNA was removed using the DNA-free DNA removal kit (Ambion, Thermo Fisher Scientific, Scoresby, Australia) as per manufacturer's instructions. RNA samples were stored at - 80 °C. For preparation of cDNA, 0.5 µg of RNA was reverse-transcribed using iScript Reverse Transcription Supremix for RT-qPCR (Bio-Rad, Hercules, USA) according to the manufacturers instructions. Briefly, the reactions consisted of 2 µl of 5 × iScript reverse transcription

supermix, 3 µl DNase/RNase free water, and 0.5 µg of RNA, in a final volume of 10 µl in 200 µl Eppendorf PCR tubes. Reactions were performed on a Applied Biosystems 2720 Thermal Cycler (Applied Biosystems, Foster City CA USA) as following: 25 °C for 5 min, 42 °C for 30 min, 85 °C for 5 min, and then allowed to cool to 4 °C. The cDNA was diluted with 190 µl DNase/RNase free water to obtain the equivalent of 2.5 ng/µl of starting RNA, and cDNA was stored at − 20 °C.

For each independent sample, qPCR was performed in duplicate using TaqMan Gene Expression assays (Life Technologies, MA, USA) for CALCR (Hs01016882_m1), CALCRL (Hs00907738_m1), RAMP1 (Hs00195288_m1), RAMP2 (Hs01006937_g1), RAMP3 (Hs00389131_m1), CALCA (Hs01100741_m1), IAPP (Hs00169095_m1), and ACTB (Hs01060665_g1). Each reaction consisted of 4 µl cDNA, 0.5 µl TaqMan Gene Expression Assay, 0.5 µl DNase/RNase free water, and 5 µl TaqMan Fast Advanced Master Mix dispensed in Eppendorf twin.tec PCR plates. qPCR reactions were carried out using an Eppendorf Mastercycler ep Realplex Real-time PCR instrument. After initial heating at 50 °C for 2 min and denaturation at 95 °C for 10 min, fluorescence was detected over 40 cycles (95 °C for 15 s, 60 °C for 1 min). Data are expressed as relative expression of the gene of interest to the reference gene ACTB where:

$$\text{Relative expression} = 2^{-((Cq \text{ of gene of interest}) - (Cq \text{ of ACTB}))}$$

For some genes, no mRNA was detected. These samples are omitted from the graphs as indicated in the figure legends.

Western blotting

Cells were harvested by scraping into PBS containing 1x cOmplete Mini Protease Inhibitor Cocktail (Sigma-Aldrich) and 1 mM EDTA and subjected to small-scale subcellular protein fractionation to enrich for the membrane fraction. Briefly, cell suspensions were microfuged for 5 min at 350 g and 4 °C, supernatant discarded and cell pellet homogenised in 2.5 volumes of hypotonic buffer (10% glycerol, 10 mM pH 7.4 HEPES, 10 mM NaCl, 1.5 mM MgCl₂) supplemented with 1 mM dithiothreitol (DTT; Sigma-Aldrich), 1 mM PMSF (Sigma-Aldrich) and 1x cOmplete Mini Protease Inhibitor Cocktail (Sigma-Aldrich) and incubated for 30 min on ice followed by centrifugation for 30 min at 16,300 g and 4 °C. The supernatant was discarded and the cell pellet resuspended and homogenised in hypertonic buffer (10% glycerol, 420 mM NaCl, 10 mM pH 7.4 HEPES, 1.5 mM MgCl₂) with 1 mM DTT, 1 mM PMSF and 1x cOmplete Mini Protease Inhibitor Cocktail followed by 30 min on ice and centrifugation for 30 min at 16,300 g and 4 °C. The supernatant was discarded and the cell pellet resuspended and homogenised in

radio immunoprecipitation (RIPA) buffer [1% NP-40 (Sigma-Aldrich), 1% sodium deoxycholate, 0.1% SDS, 150 mM NaCl, 50 mM NaF, 10 mM pH 7.2 phosphate buffer, 0.2 mM EDTA] and with 1 mM DTT, 1 mM PMSF and 1x cOmplete Mini Protease Inhibitor Cocktail. Suspensions were kept on ice for 10 min to allow solubilisation of membrane proteins and centrifuged for 20 min at 16,300 g and 4 °C. The resulting supernatant (membrane protein fraction) was collected and all fractions stored at − 80 °C. 50 µg of BCA quantitated membrane fractions were denatured at room temperature in Laemmli sample buffer and subjected to electrophoresis on 8% gels and transfer to PVDF using standard methods. Membranes were probed with anti-CTR antibody (1H10 Welcome Receptor Antibodies, Melbourne, Australia; MCA2191, BioRad AbD Serotec, Kidlington, UK) followed by HRP-conjugated secondary, enhanced chemi-luminescence and detection with a LAS-3000 Imaging System (Fuji; Tokyo, Japan).

Public data analysis

Raw data from IVY-GAP was analysed as follows: patient tumour biopsies were manually curated to identify tumour blocks with RNA-seq expression of CALCR greater than 1.25 FPKM that also corresponded to histological grading consistent with GBM, resulting in the identification of 12 patients whose tumours were positive for CALCR expression. This threshold was then applied to the patient survival data to generate a Kaplan-Meier survival plot. Raw RNA-seq data from TCGA was used to identify tumour samples with CALCR gene expression, this data was used to filter the patient clinical data and expression was converted to Log₂. This was used to generate an expression – survivorship plot shown in Additional file 1: Figure S2. This data was used with an FPKM threshold of 1.25 to generate the Kaplan-Meier plot shown in Fig. 5d.

Results

Data from the Q-Cell database [37] for glioblastoma cell lines are reproduced in Table 2 showing key meta-data relating to donor age and survival for the cell lines examined.

We analysed our primary microarray data (normalised using Illumina BeadStudio) for expression in primary tumours, cell lines and xenograft tumours of calcitonin receptor family genes along with calcitonin and amylin by considering all microarray data with a detection *P*-value of < 0.05 (Fig. 1). In contrast to our previous data [24] and data available in public glioblastoma data bases (IVY-GAP [26] and TCGA [27]), CTR mRNA was only detected in 2/12 primary tumours, a single cell line and one xenograft (Fig. 1), possibly due to limitations in this approach as previously reported for GPCRs [39]. The CALCA message, which encodes both calcitonin and

Table 2 Key patient meta-data and derived cell line properties (adapted from Q-Cell database [35])

Cell line	Patient age (years)	Patient Survival (Days)	RB pathway LOF	Cell line doubling time (hours)	XG median survival (days)
BAH1	75	94	Yes	79.5 ± 3.3	210 ± 8
FPW1	68	242	Yes	48.1 ± 4.7	196 ± 4
HW1	54	89	Yes	55.8 ± 2.7	174 ± 14
JK2	75	178	Yes	94.2 ± 4.5	147 ± 9
MMK1	80	334	Yes	52.4 ± 3.3	157 ± 15
MN1	84	36	Yes	44.9 ± 1.0	258 ± 20
PB1	57	39	Yes	79.4 ± 6.3	71 ± 1
RK1	57	Alive (7 years)	No	72.9 ± 5.3	248 ± 6
RN1	56	243	Yes	37.5 ± 1.9	81 ± 2
SB2b	48	420	Yes	108.7 ± 6.9	120 ± 3.3
SJH1	72	45	Yes	67.3 ± 4.7	148 ± 4
WK1	77	121	Yes	46.2 ± 1.0	150 ± 2

Metadata for patient age and survival post-diagnosis along with retinoblastoma status, doubling time for the derived cell lines and median survival of mice carrying orthotopic tumours. *RB pathway LOF* Loss of function in one or more steps in the retinoblastoma tumour suppressor pathway. *XG median survival* Median survival for mice with orthotopic xenografts

α -CGRP, was not detected in any sample and the mRNA encoding amylin (IAPP) was only detected in one cell line and 2 xenografts, none of which were concordant with detection of CALCR (Fig. 1). In contrast, but consistent with public databases, all primary tumours had detectable message for CALCRL and all RAMPs with one cell line losing detectable CALCRL expression along with 3 xenografts, one xenograft losing RAMP2 and 7 cell lines and 5 xenografts having no detectable RAMP3 (Fig. 1). We therefore performed a preliminary screen by western blot for CALCR in our 4 HGG cell lines, which supported expressed protein of molecular weight and reactivity consistent with CTR in all 4 cell lines (see below).

From this preliminary experiment we chose to further characterise these 4 cell lines, which appeared to have detectable CTR and were previously used in an anti-CTR immunotoxin study [25]. These cells were grown as adherent cultures in a monolayer on matrigel with EGF and FGFb growth factors that, in the absence of serum, showed a consistent morphology to previous publications (Fig. 2a).

CALCR, CALCRL and RAMPs are expressed in each of four GBM cell lines

Due to the discrepancy between the microarray data and our initial western blot screen, cell lines WK1, JK2, SB2b and PB1 were selected for further analysis. We tested for mRNA expression using TaqMan qPCR, which has been reported as more reliable for detection of low expression GPCR transcripts [39]. This showed low level of expression of both CALCR and CALCRL mRNA in all of the 4 cell lines (Fig. 2b). The apparent discordance between mRNA level and western blotting suggests that CTR protein level is primarily regulated at the translational or post-translational level as has been widely reported for non-housekeeping genes, where the concordance between mRNA and protein levels is low [40–42]. CALCR mRNA expression was markedly lower than CALCRL, at levels that are consistent with low mRNA copy number that is commonly seen for GPCRs and is also consistent with the low FPKM values extracted from the IVYGAP [26] and TCGA databases [27] (below). RAMPs 1 and 2 mRNAs were expressed in all 4 cell lines (Fig. 2b). RAMP3 was not detected in the SB2b cell line but was present at levels just above the threshold in PB1 and WK1 (approximately one copy per cell), and at slightly higher level in JK2. Expression of CALCA (encoding calcitonin and α -CGRP) and IAPP (encoding amylin) mRNA were also assessed, neither of which were detectable, except for very low (below the threshold of 1 copy per cell) IAPP in PB1 and CALCA in JK2 (Fig. 2b). We

	CALCR			CALCRL			RAMP1			RAMP2			RAMP3			CALCA			IAPP			ACTB		
	1° cell line	XG		1° cell line	XG		1° cell line	XG		1° cell line	XG		1° cell line	XG		1° cell line	XG		1° cell line	XG		1° cell line	XG	
BAH1	N/D	N/D	N/D	7.3	10.7	4.9	9.7	8.8	5.9	8.1	6.4	7.6	8.0	7.5	5.3	N/D	N/D	N/D	N/D	N/D	N/D	14.9	15.2	13.5
FPW1	N/D	N/D	N/D	10.3	7.4	5.1	10.2	9.8	9.4	9.4	7.3	5.6	9.2	N/D	N/D	N/D	N/D	N/D	N/D	N/D	N/D	15.3	15.3	13.5
HW1	N/D	N/D	N/D	8.9	10.4	6.3	10.8	10.7	10.2	8.4	5.5	8.5	6.8	7.3	5.8	N/D	N/D	N/D	N/D	N/D	N/D	15.2	15.3	12.1
JK2	N/D	N/D	N/D	10.3	9.8	7.4	8.8	6.9	8.5	7.4	6.1	6.4	5.4	N/D	4.4	N/D	N/D	N/D	N/D	N/D	N/D	15.2	15.2	12.9
MMK1	N/D	N/D	N/D	8.4	11.7	3.4	9.2	8.0	N/D	8.4	4.7	6.0	9.7	8.0	N/D	N/D	N/D	N/D	N/D	N/D	6.5	15.0	15.1	13.5
MN1	N/D	N/D	N/D	5.8	5.0	N/D	9.9	11.6	7.2	8.9	5.4	4.7	5.9	N/D	N/D	N/D	N/D	N/D	N/D	N/D	N/D	15.0	15.3	13.6
PB1	N/D	N/D	N/D	7.7	N/D	4.8	10.3	6.1	7.7	8.5	7.5	7.8	6.8	N/D	4.1	N/D	N/D	N/D	N/D	N/D	N/D	15.2	15.2	13.1
RK1	N/D	7.4	N/D	7.4	6.1	N/D	10.4	7.5	7.8	8.4	6.6	6.8	7.0	N/D	N/D	N/D	N/D	N/D	N/D	N/D	N/D	15.3	15.2	12.8
RN1	5.0	N/D	4.4	6.9	10.6	N/D	11.3	9.1	9.5	9.8	6.1	9.0	7.8	6.7	N/D	N/D	N/D	N/D	N/D	N/D	N/D	15.3	15.3	13.4
SB2b	5.1	N/D	N/D	8.1	8.0	7.7	10.5	9.2	8.1	8.2	6.3	6.2	7.4	6.4	2.4	N/D	N/D	N/D	N/D	N/D	N/D	15.3	15.3	13.6
SJH1	N/D	N/D	N/D	7.1	6.2	6.1	11.2	8.4	5.1	7.1	5.8	6.7	6.5	N/D	3.4	N/D	N/D	N/D	N/D	N/D	5.0	15.2	15.1	13.3
WK1	N/D	N/D	N/D	10.2	9.1	6.6	10.5	9.9	8.4	7.0	7.0	7.3	7.6	N/D	3.9	N/D	N/D	N/D	N/D	N/D	4.7	15.2	15.3	13.4

Fig. 1 Microarray data for expression of calcitonin receptor family and selected calcitonin receptor family ligands. Log₂ expression of calcitonin receptor family mRNA from Illumina micro array on primary tumour biopsies (1°), derived cell lines and orthotopic xenografts (XG). Expression is intensity colour coded from green (lowest) through yellow (middle) to red (highest). N/D represents microarray data for which there was either no signal detected or the detection *P*-value fell above 0.05

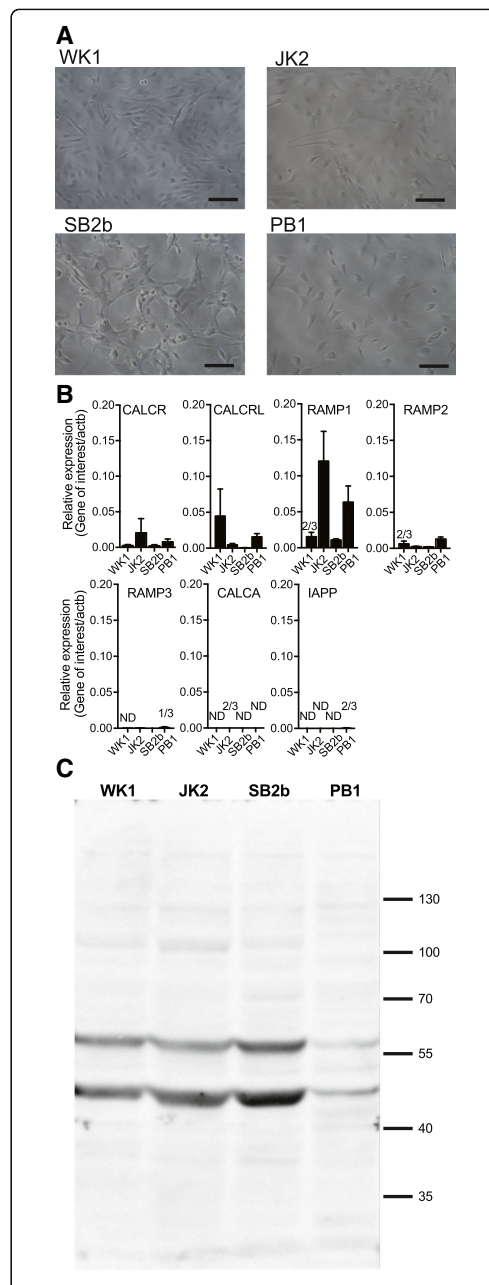


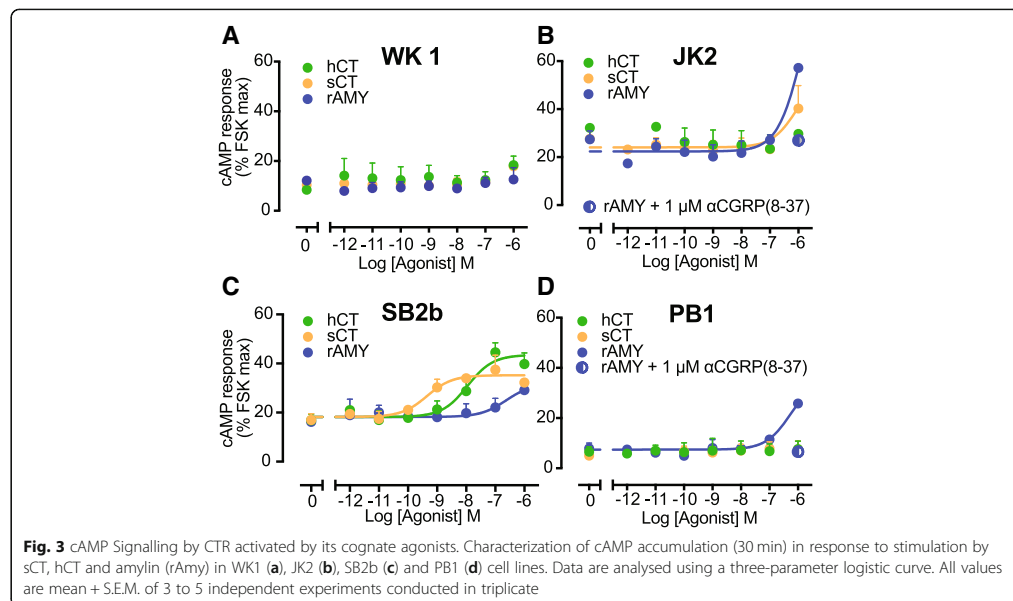
Fig. 2 Morphology and gene expression in the four GBM cell lines used in this study. **a** SB2b and PB1 of classical GBM subtype; JK2 of proneural subtype and WK1 of mesenchymal GBM subtype as adherent cultures on matrigel, scale bar represents 100 μ M. **b** Expression of CALCR, CALCRL, RAMP1, RAMP2, RAMP3, CALCA, and IAPP in SB2b, PB1, WK1 or JK2 cells. Data represent mean \pm SEM of 3 independent experiments, performed in duplicate, relative to β -actin expression. ND (not detected in all 3 samples), 2/3 (in 2 out of the 3 samples mRNA was detected), 1/3 (in 1 out of the 3 samples mRNA was detected). **c** Western blot for CTR, 50 μ g of membrane protein probed with anti-CTR 1H10, representative of 3 independent experiments

were most interested in expression of CALCR based on previous studies described above and therefore performed western blots using an anti-CTR Ab on purified membranes; these revealed antibody reactive bands corresponding to the expected size for unmodified (~ 50 kDa) and glycosylated (~ 60 kDa) CTR in all cell lines (Fig. 2c).

Individual HGG cell lines have distinct CTR/CLR-based pharmacology

In a wide variety of recombinant and ex vivo settings CTR is most strongly coupled to the stimulatory hetero-trimeric G_{α} subunit, Gas, that activates adenylate cyclase [43–47]. CTR function was therefore assessed using a cAMP accumulation assay. In the classical GBM model cell line, SB2b, we observed a robust, concentration dependent increase in cAMP in response to CTR agonists (Fig. 3c). The potency of the response to sCT ($pEC_{50} = 9.4 \pm 0.3$) and hCT ($pEC_{50} = 8.0 \pm 0.2$) were similar to the known affinities of these agonists for CTR. The similarities in affinity and cellular potency are consistent with low receptor expression and limited receptor reserve. We also observed a higher E_{max} for hCT (43% of forskolin) compared with sCT (35% of forskolin), consistent with higher efficacy of this lower affinity agonist [48]. The low potency amylin response ($pEC_{50} = 6.8 \pm 0.5$) is consistent with signalling via CTR in the absence of any RAMP [49] indicating there is unlikely to be functional interaction between CTR and RAMPs in this cell line.

No pharmacologically relevant responses to either sCT or hCT, in cAMP assays were detected in the other 3 cell lines (PB1, JK2 and WK1) (Fig. 3a, b & e). In the mesenchymal model line, WK1, we observed a small increase in cAMP in response to maximal concentrations of all 3 CTR agonists (Fig. 3a). To address whether this was due to poor receptor coupling to adenylate cyclase we performed co-stimulation experiments in the presence of a sub saturating concentration of forskolin (1 μ M). Application of 1 μ M forskolin increased the basal cAMP 4-fold and revealed a low potency sCT response with a pEC_{50} of 6.7 ± 0.6 (Additional file 2: Figure S1A) that is inconsistent with a CTR-mediated response. The low potency response to amylin in JK2 ($pEC_{50} = 5.9 \pm 0.5$) and PB1 ($pEC_{50} = 6.1 \pm 0.5$) is inconsistent with an AMY receptor



phenotype but is consistent with the CGRP (CLR/RAMP1) receptor, with application of 1 μ M of the CGRP antagonist (CGRP(8–37)) abolishing this response (Fig. 3b, d).

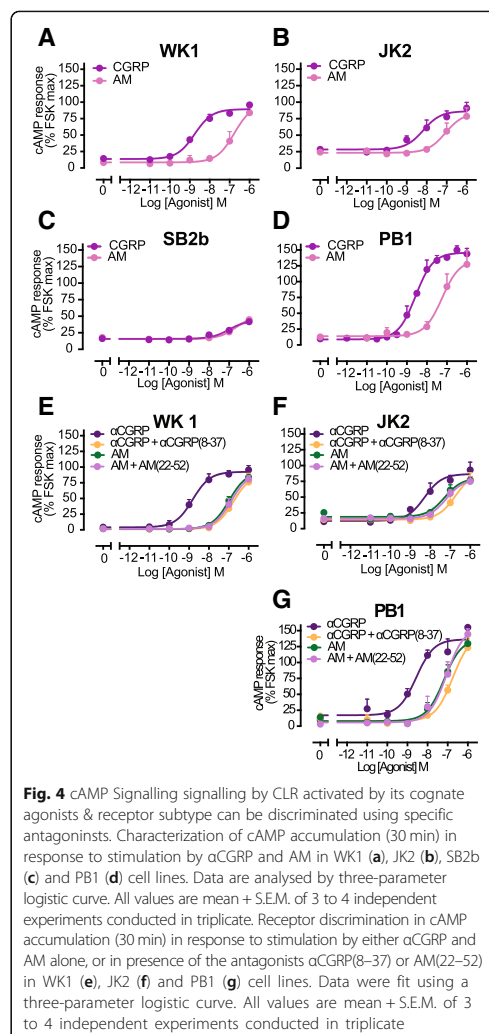
In addition to coupling to Gas, the CTR can couple to G α q, which stimulates phospholipase C leading to intracellular calcium mobilisation (Ca^{2+}) [46]. We were unable to detect functional CTR response in an Ca^{2+} mobilisation assay with sCT or amylin agonists in SB2b, WK1 or PB1 cell lines (Additional file 2: Figure S1B, C & D).

Quantitation of mRNA indicated that all cell lines expressed CLR and at least one RAMP family member. We therefore performed cAMP accumulation assays in the presence of adrenomedullin and α CGRP. No pharmacologically relevant response was seen in the SB2b cell line (Fig. 4c) suggesting that no functional CLR is present at the cell surface. The remaining three cell lines (PB1, JK2 and WK1) responded with high potency to stimulation with α CGRP ($\text{pEC}_{50} = 8.6 \pm 0.1$ for PB1, $\text{pEC}_{50} = 8.3 \pm 0.2$ for JK2 and $\text{pEC}_{50} = 8.8 \pm 0.1$ for WK1) and with lower potency to adrenomedullin ($\text{pEC}_{50} = 7.3 \pm 0.1$ for PB1, $\text{pEC}_{50} = 7.0 \pm 0.3$ for JK2 and $\text{pEC}_{50} = 6.8 \pm 0.3$ for WK1) (Fig. 4a, b and d). These data are most consistent with the reported pharmacology of a CLR/RAMP1 CGRP receptor phenotype. CLR generates 3, pharmacologically distinct receptor subtypes depending on its interaction with the 3 different RAMPs. To distinguish receptor subtypes present we measured cAMP concentration response to α CGRP and AM in the presence of 1 μ M subtype selective antagonists – α CGRP(8–37) and AM(22–52). Co-treatment of

PB1, JK2 and WK1 cell lines with α CGRP and its specific antagonist, α CGRP(8–37) led to an approximate 100-fold decrease in potency of α CGRP response reflected as 2 logarithmic unit shift in the EC_{50} (pEC_{50} from 8.6 to 6.7 in PB1; from 8.4 to 6.6 in JK2; and from 8.8 to 6.6 in WK1) (Fig. 4e, f and g). In contrast, co-treatment with AM and its specific antagonist, AM:22–52 caused no significant shift in potency of AM response (pEC_{50} of 7.2 versus 7.1 in PB1; 7.2 versus 7.3 in JK2; and 6.9 versus 6.7 in WK1). This is consistent with PB1, JK2 and WK1 cell lines expressing CGRP and not AM receptors, with the weak AM responses, mediated through the CGRP receptor.

Activation of CTR expressed in the SB2b cell line has no detectable effect on cell metabolism, proliferation, ERK phosphorylation or p38 phosphorylation

Activation of the CTR, as part of the amylin receptor, has been shown to cause metabolic reprogramming in some malignancies [18]. Others [28] have reported a change in GBM cell line proliferation in response to CTR stimulation and this has also been reported for a breast cancer cell line [50, 51], we therefore assessed whether activation (using both hCT and sCT) or blockade (using the antagonist sCT(8–32)) would alter metabolism in the SB2b cell line. Although growth factor deprivation had a significant effect on cellular metabolism (as assessed by an MTT assay, Fig. 5a) we saw no effect of any of the CTR ligands (Fig. 5a). In addition, we observed no changes in cell proliferation in the SB2b cell

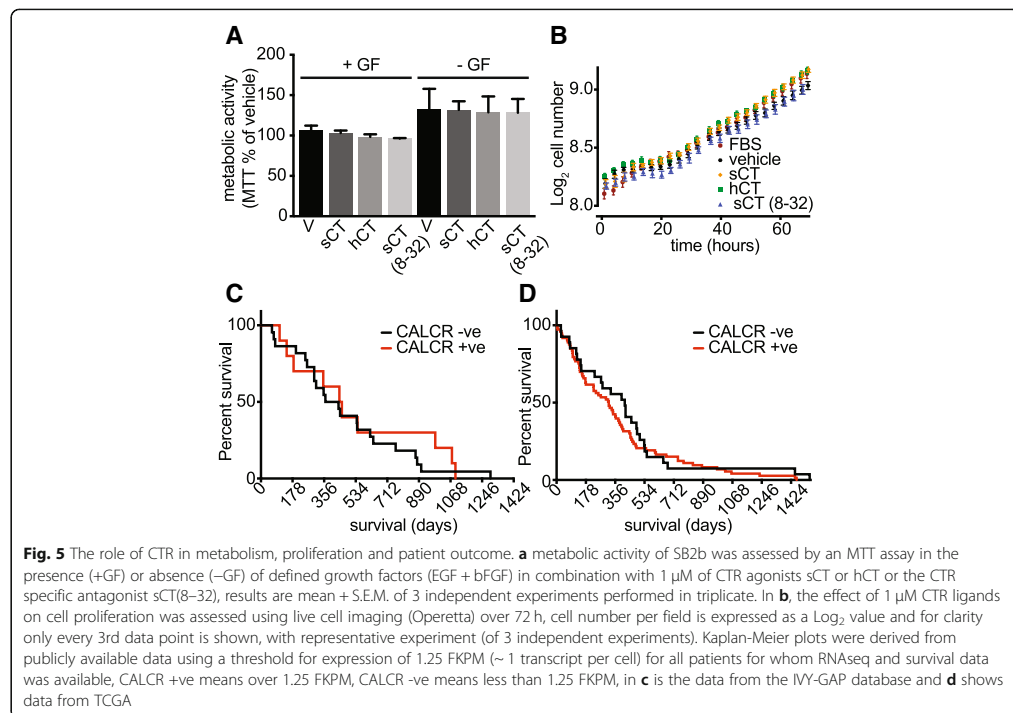


line by live cell imaging in the presence of CTR ligands (Fig. 5b) over 3 days, relative to the unstimulated control. To assess more proximal effects of CTR activation on pathways involved in cell proliferation, we directly assessed the ability of sCTR to activate pERK and p38 MAPKs, that have been implicated in tumour progression. We performed ERK_{1/2} and p38 phosphorylation assays as a time course in the SB2b cell line and were unable to detect any response (Additional file 1: Figure S2A and B). In some tumour cell lines, such as the glioblastoma model A172 [24] and the MDA-MB-231 breast cancer model

[13], CTR stimulation is inhibitory for ERK_{1/2} phosphorylation. We therefore tested for pERK_{1/2} suppression by either sCTR or hCTR in the presence of 0.1% FBS. We saw no detectable inhibition by either agonist over the concentrations tested (Additional file 1: Figure S2C) and conclude that CTR does not modulate pERK_{1/2} within the sensitivity we are able to measure.

CTR expression and survivorship

To understand what (if any) relationship CTR expression may have with tumour progression and patient outcome we extracted the raw expression data for CTR from two public databases (IVY-GAP [26] and TCGA [27]). We set an arbitrary cut-off for CTR expression corresponding to ~1 transcript per cell (\log_2 FPKM = 0.3) [52]. For patients for whom survival data were available, we used this threshold to generate Kaplan-Meier plots (Fig. 5c and d). In the IVY-GAP data, using our threshold, 12 out of 42 patient tumours (~28%) were positive for CTR and there was no relationship between CTR expression and survivorship (Fig. 5c). In the TCGA dataset, 115 of 152 patient tumours were CTR positive (~76%) by our criteria and similarly to the IVY-GAP dataset, there was also no relationship between CTR expression and survivorship (Fig. 5d); this result that was borne out when we plotted expression against survivorship for the TCGA dataset (Additional file 1: Figure S2D). Pal et al. [28] reported that several mutations of CTR were associated with loss-of-function (LOF) that correlated with poor patient outcome. To investigate the possibility that the lack of signalling of CTR that we report might be related to loss-of-function mutations we analysed whole exome sequencing data. The exome sequencing data showed that each of the cell lines bear a known polymorphism encoding leucine in the c-terminal tail of the protein (NM_001164737:c.T49C:p.S17P; JK2 (heterozygous), PB1 (homozygous), SB2b (homozygous) and WK1 (heterozygous)) that has a minor consequence on signalling [53]. The only other identified non-synonymous polymorphism was identified in the WK1 cell line (NM_001164738:c.G1369A:p.E457K, heterozygous), which would be predicted to result in a glutamine to lysine change in the distal C-terminus, an amino acid that is substituted with glycine, leucine and valine amongst mammals (Additional file 3: Figure S3) and a part of the c-terminus that can be deleted without altering cAMP coupling [54]. To contextualise the reported LOF mutations of Pal et al. [28], we mapped these to our current model of active CT bound CTR [54] (Additional file 3: Figure S3) and compared these residues across vertebrate species (Additional file 4: Figure S4). As shown in Additional file 3: Figure S3, our model would only predict that P100L and R404C



may effect receptor signalling and these mutations show the least LOF as reported by Pal et al. [28].

Discussion

Expression profiles revealed by RT qPCR indicate that each of the four model HGG cell lines investigated here generate mRNA encoding components of CTR, AMY, CGRP and AM_1 receptors, albeit that the CTR was expressed at low levels. Neither of the CTR activating peptides, hCT or amylin, were expressed at levels above threshold, suggesting there is no autocrine production of these peptides by these GBM cell lines. No coding polymorphisms, apart from the well-characterised c-terminal tail leucine/proline polymorphism [53], were detected by whole exome sequencing.

Although, RT qPCR data show mRNA encoding multiple receptors of the CTR family in the SB2b cell line (classical GBM subtype), functionally we were only able to confirm CTR. The potency with which CTR agonists elicit a cAMP response is consistent with a low level of endogenously expressed receptor. Weak responses to αCGRP , amylin and adrenomedullin can be attributed to CTR activation. In this cell line, sCT and hCT had distinct profiles with sCT demonstrating higher potency

but lower E_{max} than hCT. The molecular basis for the signalling profile observed in the SB2b GBM cell line is consistent with low or no receptor reserve but reveals apparent differences in efficacy, consistent with our data in recombinant systems [48], and further illustrates the complexity of signaling in (patho)physiologically relevant systems. In our assays we couldn't detect a response to sCT in Ca^{2+} mobilization assay suggesting limited Gq coupling of CTR in the SB2b cell line. Additionally, we were not able to detect either pERK $_{1/2}$ or p38 MAPK response in this cell consistent with no downstream effect of CTR activation on cellular metabolism or proliferation.

PB1, JK2 and WK1 cell lines (representing classical, proneural and mesenchymal types of GBM respectively) had detectable mRNA and western blot immuno-reactivity consistent with CTR expression (C-terminally directed antibody). In spite of this we could not detect a functional CTR response as assessed by cAMP accumulation (PB1, JK2, WK1) and Ca^{2+} assay (PB1 and WK1). However, we have previously shown that both JK2 and WK1 cell lines are susceptible to anti-CTR-immunotoxin (N-terminally directed) mediated cell killing [25]. In other systems, CTR has been reported to internalise extremely rapid in a ligand and independent receptor manner [53, 55], suggesting that

perhaps the CTR may not be present at the plasma membrane for sufficient time to generate detectable functional response in these GBM lines.

Despite a lack of functional CTR in PB1, JK2 and WK1 cell-lines, all three displayed a potent cAMP accumulation response to α CGRP, a less potent response to adrenomedullin, with a very weak response to amylin. In addition, specific CGRP and AM receptor antagonists confirmed the presence of CLR/RAMP1 type CGRP and not an AM receptor in these cells. This is in agreement with RT-qPCR gene expression data showing expression of both CLR and RAMP1. However, CGRP is unlikely to be tractable as a target for treating GBM given its broad expression in the brain. There was no clear correlation between pharmacological profiles and clinical classification of the originating GBM tumour subtype as SB2b and PB1, both of classical GBM subtype, had distinct pharmacological profiles of CTR and CLR/RAMP1 receptor.

Conclusion

Taken together this data indicates that we have a rather incomplete understanding of CTR (and related receptor) function in certain (patho)-physiological circumstances. While the CTR is expressed in a significant subset of GBM tumours it may only be tractable as a target by leveraging the compromised blood brain barrier characteristic of these tumours while taking advantage of the rapid cycling of CTR to deliver a toxic payload.

Our analysis of published CTR expression from IVY-GAP [26] or TCGA [27] databases do not support a correlation between CTR expression and patient outcome. We would therefore argue that CTR expression, while common in primary GBM tumours, is unlikely to be tractable to pharmacological intervention but may be suitable as a target for delivering cytotoxic agents.

Additional files

Additional file 1: Figure S2. MAP kinase response to sCT in SB2b cells and TCGA survival data. No detectable ERK_{1/2} phosphorylation (A) or p38 (B) in response to stimulation with 1 μ M sCT in SB2b cell line while a robust response to 10% FBS is seen; Data are presented as mean + S.E.M. of 3 replicates of a representative experiment. (C) ERK_{1/2} Phosphorylation response in SB2b cell line was induced by 0.1% FBS. No suppression of the induced response after stimulation sCT or hCT was seen at the concentrations tested (C). Data are presented as mean + S.E.M. of 3 replicates of a representative experiment. (D) Log₂ expression (FPKM) of CALCR transcript in patients with survival data from the TCGA database plotted as a scatter plot against survival. (PDF 915 kb)

Additional file 2: Figure S1. cAMP and Ca^{2+} mobilization in response to CTR agonists. A, Characterization of cAMP accumulation (30 min) in WK1 cells in response to stimulation by sCT alone or in presence of 1 μ M forskolin. Data are presented as mean + S.E.M. of 3 replicates of a representative experiment. Absence of intracellular calcium mobilization response to sCT and rAMY in WK1 (B), SB2b (C) and PB1(D) cell lines while maintaining robust response to 10 μ M ATP and 1 μ M ionomycin. Data are presented as peak values of response measured in relative

fluorescence units. Data are presented as mean + or - S.E.M. of 3 replicates of a representative experiment. (PDF 907 kb)

Additional file 3: Figure S3. Mapping reported CTR mutations to our a molecular model of the CTR [48]. A, mutations reported to be associated with LOF at the CTR are shown in space fill red, mapped onto our active, G protein bound, model derived from Cryo-EM data; the peptide (sCT) is shown in orange, receptor in blue, G α subunit in yellow, G β in teal and G γ in purple. B, the reported LOF residues, their substitution, mammalian conservation structural location, potential side-chain interaction and likely effect on receptor function are shown as a table. (PDF 3120 kb)

Additional file 4: Figure S4. Alignment of vertebrate CTR sequences. Alignment of a subset of validated and predicted CTR sequences from mammals and aves with reptile and amphibian sequences used as outgroups. Sequences were obtained from NCBI homologue filtering for reference sequences only. These were then manually curated and an alignment was performed using Clustalw Omega. Conserved asparagine (yellow) and cysteine (purple) residues in the N-terminus have been manually annotated and TMMHM used to predict TM helices which were manually curated and are indicated in blue. Putative LOF mutations are highlighted in red. (PDF 211 kb)

Abbreviations

ACTB: Actin b (gene); AM: Adrenomedullin; Amy: Amylin; BCA: Bicinchoninic acid assay; CALCA: Calcitonin related polypeptide alpha (gene); CALCR: Calcitonin receptor (gene); CALCL: Calcitonin-like receptor (gene); cAMP: 3', 5'-cyclic adenosine monophosphate; CGRP: Calcitonin gene related peptide (peptide); CLR: Calcitonin-like receptor (protein); cDNA: Complimentary deoxyribose nucleic acid; CT: Calcitonin (peptide); CTR: Calcitonin receptor (protein); DMEM: Dulbecco's modified Eagle medium; DNA: Deoxy-ribose nucleic acid; DNase: Deoxyribose nuclease; EGF: Epidermal growth factor; ERK_{1/2}: Extracellular signal-regulated kinase 1 and 2; FBS: Fetal bovine serum; FGFb: Basic fibroblast growth factor; FPKM: Fragments Per Kilobase of transcript per Million mapped reads; GBM: Glioblastoma; GLP-1: Glucagon-like peptide-1; GPCR: G protein-coupled receptor; HGG: High-grade glioma; HRP: Horse radish peroxidase; IAPP: Islet amyloid polypeptide (gene); IBMX: 3-Isobutyl-1-methylxanthine; Ca^{2+} : Intracellular Calcium; IVY-GAP: Ivy Glioblastoma Atlas Project; LOF: Loss of function; mRNA: Messenger ribonucleic acid; NSC: Neural stem cell; PBS: Phosphate buffered saline; PCR: Polymerase chain reaction; PKA: Protein kinase A; PVDF: Polyvinylidene difluoride; RAMP: Receptor activity modifying protein; RNA: Ribonucleic acid; RNase: Ribonuclease; RT-qPCR: Reverse-transcription quantitative polymerase chain reaction; SFM: Serum-free media; TCGA: The Cancer Genome Atlas; VEGF: Vascular endothelial growth factor

Acknowledgments

We would like to thank Mr. Cameron Nowell from the core imaging facility at the Monash Institute of Pharmaceutical Sciences for assistance with cell proliferation experiments on the Operetta and their analysis. We would also like to thank Dr. Erica Sloan for advice on interpretation of publicly available GBM data.

Funding

This work was supported by the National Health and Medical Research Council of Australia (NHMRC) (project grants [1061044], [1065410] and [1126857], and NHMRC program grant [1055134]); P.M.S. is a NHMRC Principal Research Fellow. D.W. is a NHMRC Career Development Fellow. S.G.B.F. is an ARC Future Fellow.

Availability of data and materials

The datasets analysed during the current study are available in the Q-Cell database, <https://www.qimrberghofer.edu.au/our-research/commercialisation/q-cell/>, TCGA repository, <https://gdc.cancer.gov/> and IVY-GAP, <http://glioblastoma.alleninstitute.org/>

Authors' contributions

AO performed experimental work along with CH, DSH and PJW, all of whom assisted with manuscript preparation. BWS generated the high-grade glioma cell lines, assisted with data interpretation and manuscript preparation. DW and PMS assisted with project design and manuscript preparation. SGBF was responsible for overall conception of the project, analysis of publicly available data and manuscript preparation. All authors read and approved the final manuscript.

Ethics approval and consent to participate
Not applicable.

Consent for publication
Not applicable.

Competing interests
The authors declare that they have no competing interests.

Publisher's Note

Springer Nature remains neutral with regard to jurisdictional claims in published maps and institutional affiliations.

Author details

¹Drug Discovery Biology and Department of Pharmacology, Monash Institute of Pharmaceutical Sciences, Monash University, Parkville, VIC 3052, Australia. ²QIMR-Berghofer Medical Research Institute, Brisbane, QLD, Australia. ³Department of Medicine/Cardiology (Austin Health, Heidelberg), University of Melbourne, Lance Townsend Building, Level 10, Austin Campus, Studley Road, Heidelberg, VIC 3084, Australia. ⁴School of Pharmacy, Fudan University, Shanghai 201203, China.

Received: 20 August 2018 Accepted: 11 February 2019
Published online: 18 February 2019

References

- Louis DN, Ohgaki H, Wiestler OD, Cavenee WK, Burger PC, Jouvet A, et al. The 2007 WHO classification of tumours of the central nervous system. *Acta Neuropathol.* 2007;114:97–109.
- Kleihues P, Ohgaki H. Primary and secondary glioblastomas: from concept to clinical diagnosis. *Neuro-oncology.* 1999;1:44–51.
- Sanai N, Alvarez-Buylla A, Berger MS. Neural stem cells and the origin of gliomas. *N Engl J Med.* 2005;353:811–22.
- Verhaak RGW, Hoadley KA, Purdom E, Wang V, Qi Y, Wilkerson MD, et al. Integrated genomic analysis identifies clinically relevant subtypes of glioblastoma characterized by abnormalities in PDGFRA, IDH1, EGFR, and NF1. *Cancer Cell.* 2010;17:98–110.
- Cheng L, Huang Z, Zhou W, Wu Q, Donnola S, Liu JK, et al. Glioblastoma stem cells generate vascular pericytes to support vessel function and tumor growth. *Cell.* 2013;153:139–52.
- Soda Y, Marumoto T, Friedmann-Morvinski D, Soda M, Liu F, Michiue H, et al. Transdifferentiation of glioblastoma cells into vascular endothelial cells. *Proc Natl Acad Sci.* 2011;108:4274–80.
- Ricci-Vitiani L, Pallini R, Biffoni M, Todaro M, Iavernici G, Cenci T, et al. Tumour vascularization via endothelial differentiation of glioblastoma stem-like cells. *Nature.* 2010;468:824–8.
- Wang R, Chadalavada K, Wilshire J, Kowalik U, Hovinga KE, Geber A, et al. Glioblastoma stem-like cells give rise to tumour endothelium. *Nature.* 2010;468:829–33.
- Das S, Marsden PA. Angiogenesis in glioblastoma. *N Engl J Med.* 2013;369:1561–3.
- McLachlan LM, Fraser NJ, Main MJ, Wise A, Brown J, Thompson N, et al. RAMPs regulate the transport and ligand specificity of the calcitonin-receptor-like receptor. *Nature.* 1998;393:333–9.
- Just R, Simms J, Furness S, Christopoulos A, Sexton P. Understanding Amylin Receptors. The calcitonin gene-related peptide family; 2010. p. 41–57.
- Ostrovskaya A, Findlay DM, Sexton PM, SGB F. Calcitonin. Reference Module in Neuroscience and Biobehavioral Psychology. Amsterdam: Elsevier; 2017. p. 1–12. <https://doi.org/10.1016/B978-0-12-809324-5.03223-5>.
- Nakamura M, Han B, Nishishita T, Bai Y, Kakudo K. Calcitonin targets extracellular signal-regulated kinase signaling pathway in human cancers. *J Mol Endocrinol.* 2007;39:375.
- Aljameeli A, Thakkar A, Thomas S, Lakshminathan V, Iczkowski KA, Shah GV. Calcitonin receptor-zonula Occludens-1 interaction is critical for Calcitonin-stimulated prostate Cancer metastasis. *PLoS One.* 2016;11:e0150090.
- Thakkar A, Aljameeli A, Thomas S, Shah GV. A-kinase anchoring protein 2 is required for calcitonin-mediated invasion of cancer cells. *Endocr Relat Cancer.* 2016;23:1–14.
- Thomas S, Shah GM. Calcitonin induces apoptosis resistance in prostate cancer cell lines against cytotoxic drugs via the Akt/Survivin pathway - Cancer Biology & Therapy - volume 4, issue 11. *Cancer Biol Ther.* 2005;4(11):1226–33.
- Thomas S, Chigurupati S, Anbalagan M, Shah G. Calcitonin increases tumorigenicity of prostate cancer cells: evidence for the role of protein kinase a and urokinase-type plasminogen receptor. *Mol Endocrinol.* 2006;20:1894–911.
- Venkataranarayan A, Raulji P, Norton W, Chakravarti D, Coarfa C, Su X, et al. IAPP-driven metabolic reprogramming induces regression of p53-deficient tumours in vivo. *Nature.* 2014;517(7536):626–30.
- Venkataranarayan A, Raulji P, Norton W, Flores ER. Novel therapeutic interventions for p53-altered tumors through manipulation of its family members, p63 and p73. *Cell Cycle.* 2016;15:164–71.
- Bower RL, Efekhari S, Waldvogel HJ, Faull RLM, Tajti J, Edvinsson L, et al. Mapping the calcitonin receptor in human brain stem. *Am J Physiol Regul Integr Comp Physiol.* 2016;310:R788–93.
- Uhlén M, Fagerberg L, Hallström BM, Lindskog C, Oksvold P, Mardinoglu A, et al. Proteomics. Tissue-based map of the human proteome. *Science.* 2015;347:1260419.
- Larjavaara S, Mäntylä R, Salminen T, Haapasalo H, Raitanen J, Jääskeläinen J, et al. Incidence of gliomas by anatomic location. *Neuro-oncology.* 2007;9:319–25.
- Davis ME. Glioblastoma: overview of disease and treatment. *Clin J Oncol Nurs.* 2016;20:52–8.
- Wooley PJ, McLean CA, Hwang P, Furness SGB, Nguyen S, Kourakis A, et al. The expression of calcitonin receptor detected in malignant cells of the brain tumour glioblastoma multiforme and functional properties in the cell line A172. *Histopathology.* 2012;60:895–910.
- Gilbert-Oriol R, Furness SGB, Stringer BW, Weng A, Fuchs H, Day BW, et al. Dianthin-30 or gelonin versus monomethyl auristatin E, each configured with an anti-calcitonin receptor antibody, are differentially potent in vitro in high-grade glioma cell lines derived from glioblastoma. *Cancer Immunol Immunother.* 2017;66(9):1217–28.
- Puchalski RB, Shah N, Miller J, Dalley R, Nomura SR, Yoon J-G, et al. An anatomic transcriptional atlas of human glioblastoma. *Science.* 2018;360:660–3.
- Brennan CW, Verhaak RGW, McKenna A, Campos B, Nourmehri H, Salama SR, et al. The somatic genomic landscape of glioblastoma. *Cell.* 2013;155:462–77.
- Pal J, Patil V, Kumar A, Kaur K, Sarkar C, Somasundaram K. Loss-of-function mutations in Calcitonin receptor (CALCR) identify highly aggressive glioblastoma with poor outcome. *Clin Cancer Res.* 2018;24:1448–58.
- Benes L, Kappus C, McGregor GP, Bertalanffy H, Mennel HD, Hagner S. The immunohistochemical expression of calcitonin receptor-like receptor (CRLR) in human gliomas. *J Clin Pathol.* 2004;57:172–6.
- Metellus P, Voutsinos-Porche B, Nanni-Metellus I, Colin C, Fina F, Berenguer C, et al. Adrenomedullin expression and regulation in human glioblastoma, cultured human glioblastoma cell lines and pilocytic astrocytoma. *Eur J Cancer.* 2011;47:1727–35.
- Fève M, Saliou J-M, Zeniou M, Lennon S, Carapito C, Dong J, et al. Comparative expression study of the Endo-G protein coupled receptor (GPCR) repertoire in human glioblastoma Cancer stem-like cells, U87-MG cells and non malignant cells of neural origin unveils new potential therapeutic targets. *PLoS ONE. Public Library of Science.* 2014;9:e91519.
- Ouafik L, Sauze S, Boudouresque F, Chinot O, Delfino C, Fina F, et al. Neutralization of adrenomedullin inhibits the growth of human glioblastoma cell lines in vitro and suppresses tumor xenograft growth in vivo. *Am J Pathol.* 2002;160:1279–92.
- Huszthy PC, Daphu I, Niclou SP, Stieber D, Nigro JM, Sakariassen PØ, et al. In vivo models of primary brain tumors: pitfalls and perspectives. *Neuro-oncology.* 2012;14:979–93.
- Jacobs VL, Valdes PA, Hickey WF, De Leo JA. Current review of in vivo GBM rodent models: emphasis on the CNS-1 tumour model. *ASN Neuro.* 2011;3:e00063.
- Perazzoli G, Prados J, Ortiz R, Caba O, Cabeza L, Berdasco M, et al. Temozolomide resistance in glioblastoma cell lines: implication of MGMT, MMR, P-glycoprotein and CD133 expression. *PLoS One.* 2015;10:e0140131.
- Day BW, Stringer BW, Al-Ejeh F, Ting MJ, Wilson J, Ensley KS, et al. EphA3 maintains tumorigenicity and is a therapeutic target in glioblastoma multiforme. *Cancer Cell.* 2013;23:238–48.
- Day BW, Stringer BW, Wilson J, Jeffery RL, Jamieson PR, Ensley KS, et al. Glioma surgical aspirate: a viable source of tumor tissue for experimental research. *Cancers (Basel).* 2013;5:357–71.

38. Pollard SM, Yoshikawa K, Clarke ID, Danovi D, Stricker S, Russell R, et al. Glioma stem cell lines expanded in adherent culture have tumor-specific phenotypes and are suitable for chemical and genetic screens. *Cell Stem Cell*. 2009;4:568–80.
39. Sriam K, Zhou S, Lowy AM, Insel PA. Comparative analysis of methods to profile mRNA expression of G-protein coupled receptors. *The FASEB journal. Federation of American Societies for. Exp Biol*. 2016;30:10284.
40. Vogel C, Abreu R de S, Ko D, Le S-Y, Shapiro BA, Burns SC, et al. Sequence signatures and mRNA concentration can explain two-thirds of protein abundance variation in a human cell line. *Mol Syst Biol*. 2010;6:400.
41. Lundberg E, Fagerberg L, Klevebring D, Matic I, Geiger T, Cox J, et al. Defining the transcriptome and proteome in three functionally different human cell lines. *Mol Syst Biol EMBO Press*. 2010;6:450.
42. Wilhelm M, Schlegl J, Hahne H, Gholami AM, Lieberenz M, Savitski MM, et al. Mass-spectrometry-based draft of the human proteome. *Nature Nature Publishing Group*. 2014;509:582–7.
43. Iglesias-Bartolome R, Torres D, Marone R, Feng X, Martin D, Simaan M, et al. Inactivation of a Gαs-PKA tumour suppressor pathway in skin stem cells initiates basal-cell carcinogenesis. *Nat Cell Biol*. 2015;17:793–803.
44. Andreassen KV, Hjuler ST, Furness SG, Sexton PM, Christopoulos A, Nosjean O, et al. Prolonged calcitonin receptor signaling by salmon, but not human calcitonin, reveals ligand bias. *PLoS One*. 2014;9:e92042.
45. Purdue BW, Tilakaratne N, Sexton PM. Molecular pharmacology of the calcitonin receptor. *Recept Channels*. 2002;8:243–55.
46. Chabre O, Conklin BR, Lin HY, Lodish HF, Wilson E, Ives HE, et al. A recombinant calcitonin receptor independently stimulates 3',5'-cyclic adenosine monophosphate and Ca²⁺/inositol phosphate signaling pathways. *Mol Endocrinol*. 1992;6:551–6.
47. Lin HY, Harris TL, Flannery MS, Aruffo A, Kaji EH, Gorn A, et al. Expression cloning of an adenylate cyclase-coupled calcitonin receptor. *Science*. 1991; 254:1022–4.
48. Furness SGB, Liang Y-L, Nowell CJ, Halls ML, Wookey PJ, Dal Maso E, et al. Ligand-dependent modulation of G protein conformation alters drug efficacy. *Cell*. 2016;167:739–749.e11.
49. Morfis M, Tilakaratne N, Furness SGB, Christopoulos G, Werry TD, Christopoulos A, et al. Receptor activity-modifying proteins differentially modulate the G protein-coupling efficiency of amylin receptors. *Endocrinology*. 2008;149:5423–31.
50. Lacroix M, Siwek B, Body JJ. Breast cancer cell response to calcitonin: modulation by growth-regulating agents. *Eur J Pharmacol*. 1998;344:279–86.
51. Bai Y, Mori I, Kakudo K. Calcitonin inhibits invasion of breast cancer cells: involvement of urokinase-type plasminogen activator (uPA) and uPA receptor. *Int J Oncol*. 2006;28(4):807–14.
52. Trakhtenberg EF, Pho N, Holton KM, Chittenden TW, Goldberg JL, Dong L. Cell types differ in global coordination of splicing and proportion of highly expressed genes. *Sci Rep*. 2016;6:32249.
53. Dal Maso E, Just R, Hick C, Christopoulos A, Sexton PM, Wootten D, Furness SGB. Characterization of signalling and regulation of common calcitonin receptor splice variants and polymorphisms. *Biochem Pharmacol*. 2018 ;148: 111–129. <https://doi.org/10.1016/j.bcp.2017.12.016>. Epub 2017 Dec 23. PubMed PMID: 29277692.
54. Liang Y-L, Khoshouei M, Radjainia M, Zhang Y, Glukhova A, Tarrasch J, et al. Phase-plate cryo-EM structure of a class B GPCR-G-protein complex. *Nature*. 2017;546:118–23.
55. Furness S, Hare DL, Kourakis A, Turnley AM, Wookey PJ. A novel ligand of calcitonin receptor reveals a potential new sensor that modulates programmed cell death. *Cell Death Discov*. 2016;2:16062.

Ready to submit your research? Choose BMC and benefit from:

- fast, convenient online submission
- thorough peer review by experienced researchers in your field
- rapid publication on acceptance
- support for research data, including large and complex data types
- gold Open Access which fosters wider collaboration and increased citations
- maximum visibility for your research: over 100M website views per year

At BMC, research is always in progress.

Learn more biomedcentral.com/submissions



CHAPTER 4

Effects of alanine mutations of residues within calcitonin receptor (hCTR) binding pocket on the CTR cell surface expression and binding of calcitonin agonists

4.1 INTRODUCTION

In the last decade, much work has been done to understand GPCR structure and the relationship between receptor structure and downstream signalling. By comparing inactive and active receptor structures and through multiple biophysical studies it has become evident that different ligands can stabilize different conformations of a receptor allowing for selective transducer coupling (signalling bias) (Deupi *et al.*, 2010, Sauliere *et al.*, 2012, Mary *et al.*, 2013b, Dong *et al.*, 2014).

2017 was marked by significant advancements in class B GPCR structural biology due to breakthroughs in the use of cryo-EM to solve structures of GPCR complexes. The first GPCR structure solved using cryo-EM was that of the human CTR in complex with sCT (Liang *et al.*, 2017). This success was followed by two different GLP-1R structures and a CGRP cryo-EM structure (Liang *et al.*, 2018b, Liang *et al.*, 2018a, Zhang *et al.*, 2017b). More recently, our group has also solved the structure of the human CTR solved in complex with hCT (unpublished). All of these structures are active receptor structures, each bound by their agonist peptide ligands and in complex with the heterotrimeric G_s protein. Other published class B GPCR structures include full-length GCGR crystal structures either bound to a negative allosteric modulator and antigen-binding fragment of an inhibitory antibody or to a glucagon analogue (Zhang *et al.*, 2017b, Zhang *et al.*, 2018), a full length PTH1R structure in complex with a peptide agonist (Ehrenmann *et al.*, 2018) and the inactive isolated transmembrane regions of the GLP-1R, the GCGR and the CRF1R (Song *et al.*, 2017, Siu *et al.*, 2013, Dore *et al.*, 2017).

The full-length sCT-CTR-G_s structure solved in our laboratory (Liang *et al.*, 2017) had a global resolution of 4.1Å, and as such had limited density for sCT side chains, therefore only the backbone was modelled. More recently, we have improved the cryo-EM map for this complex reaching 3.4Å resolution, where we can now model the peptide and its interactions with the receptor in this static structure (pdb 6NIY, Dal Maso *et al.*, 2019). In this structure, sCT is positioned higher up in the transmembrane bundle than the GLP-1R peptide agonists bound to the GLP-1R (Zhang *et al.*, 2017, Liang *et al.*, 2018). This is likely due to the unique cyclic ring present at the N- termini of CT ligands and not other Class B ligands (Schwartz *et al.*, 1981). The cyclic N-termini of the calcitonin-like peptides provide an additional structural constraint and defines a distinct agonist conformation within the binding pocket relative to the published GLP-1R structures (Liang *et al.*, 2018b, Zhang *et al.*, 2017b).

While other fields have demonstrated that cryo-EM is capable of capturing aspects of the protein conformational landscape (Lu *et al.*, 2017, Frank *et al.*, 2016), it is not yet clear that this will be possible for GPCRs. Recent, unpublished data from our lab does suggest that, there are

several conformational classes within the cryo-EM data, however we are yet to determine the extent to which extent these provide insight into receptor activation. While providing valuable information regarding ligand and G protein binding, the current structures represent a static picture of one (or a limited subset of) conformations out of the possible receptor's repertoire and therefore large-scale mutagenesis of receptor domains helps to identify the networks of amino acids that initiate and propagate signalling and to separate out networks important for activation of individual pathways and their importance across different ligands (Koole *et al.*, 2012b, Koole *et al.*, 2012a, Wootten *et al.*, 2013, Wootten *et al.*, 2016b, Dal Maso *et al.*, 2018b, Dal Maso *et al.*, 2019).

Class B GPCRs are predicted to interact with their peptide agonists via a 2-domain mechanism in which the NTD provides a high affinity interaction site for the C-terminal end of their interacting peptides and the N-terminal end of these peptides interact with the receptor TM binding site (Stroop *et al.*, 1995, Holtmann *et al.*, 1995, Bergwitz *et al.*, 1996, Gelling *et al.*, 1997, Runge *et al.*, 2003). Previous work performed in our laboratory identified residues in CTR ECLs 1, 2 and 3, that when mutated to alanine, alter agonist affinity in a ligand-specific manner as well as altering the receptor's functional affinity in both ligand- and pathway-specific manners (Dal Maso *et al.*, 2018b, Dal Maso *et al.*, 2019). This is in agreement with the data on another prototypical class B GPCR, the GLP1-R, where distinct regions of the GLP1-R extracellular surface were identified to be either globally or selectively important in affinity of individual GLP-1R ligands (Wootten *et al.*, 2013, Wootten *et al.*, 2016a, Wootten *et al.*, 2017). However, in these studies, significant diversity was observed in how ECLs 2 and 3 engaged and contributed to peptide binding and propagation to conformational changes linked to efficacy between the GLP-1R and CTR (Dal Maso *et al.*, 2018).

X-ray (Zhang *et al.*, 2017a, Zhang *et al.*, 2018, Ehrenmann *et al.*, 2018) and cryo-EM (Liang *et al.*, 2017, Liang *et al.*, 2018b, Liang *et al.*, 2018a, Zhang *et al.*, 2017b) structures support the involvement of the TM region in class B receptors for binding and this is further supported with a number of mutagenesis studies that showed the importance of residues X^{1.36}, X^{1.40}, X^{1.43}, Y/H^{1.47}, X^{2.60}, X^{2.64}, X^{2.67}, X^{2.71}, X^{3.36}, X^{3.37}, X^{3.40}, X^{5.36}, X^{5.40}, X^{6.53}, X^{6.56}, X^{7.35}, X^{7.39}, X^{7.42} and X^{7.43} (class B numbering system (Wootten *et al.*, 2013)) in the affinity of peptide ligands for binding to individual class B GPCRs (including GCGR, GLP-1R, GIPR, secretin, VIPR1, VIPR2, PTH1R, CRF1 and CGRP receptors) (Siu *et al.*, 2013, Wootten *et al.*, 2016, Moon *et al.*, 2015, Dods *et al.*, 2015, Yang *et al.*, 2016, Wootten *et al.*, 2016, Perret *et al.*, 2002, Runge *et al.*, 2003, Di Paolo *et al.*, 1999, Di Paolo *et al.*, 1988, Solano *et al.*, 2001). Cross-linking studies also confirmed the involvement of residues, Y^{1.36}, N^{1.43}, W^{2.64}, V^{2.67}, V^{2.71}, Y^{3.36}, N^{3.37}, H^{3.40}, D^{5.36}, Q^{5.40}, Y^{6.53} in CRF-1R; L^{1.36} and Y^{1.40} in GLP-1R; Y^{6.56} in secretin receptor; and

L^{7.43} in VIPR1 receptor, for peptide ligand interactions (Coin *et al.*, 2013, Seidal *et al.*, 2017, Dond *et al.*, 2016, Miller *et al.*, 2011, Dong *et al.*, 2012, Assil-Kishawi *et al.*, 2008).

A common feature of all class B GPCRs is the presence of a conserved cluster of polar residues located at the base of a predicted peptide binding cavity within the transmembrane helical bundle (Liang *et al.* 2017, Wootten *et al.*, 2013, Wootten *et al.*, 2016a). These residues play both global and ligand-specific roles in propagation of signalling at the GLP-1R (Wootten *et al.*, 2013, Wootten *et al.*, 2016a, Wootten *et al.*, 2017). The importance of these residues (K/R/N^{2.60}; N3.43; Y/F^{3.44}; H/T/Q/E^{6.52}; and Q/H^{7.49}) in peptide agonist binding affinity of other class B GPCRs has also been confirmed for the GCGR, GLP-1R, GIPR, secretin, GHRHR, VIPR1, VIPR2, PTH1R and CRF1R (Song *et al.*, 2017, Schipani *et al.*, 1997, Tseng *et al.*, 1997, Yaqub *et al.*, 2010, Coopman *et al.*, 2011, Dong *et al.*, 2012, Spyridaki *et al.*, 2014, Cordomi *et al.*, 2015).

The aim of this study was to use Ala mutational analysis of residues in the transmembrane binding pocket to identify how CT peptides with distinct sequences bind and activate the CTR. Comparing this data with data from analogous studies on other class B receptors will help to reveal global and subclass-specific mechanisms of class B GPCR activation.

Analysis of the CTR TM binding pocket mutational data is described in Chapters 4 and 5. Operational analysis was applied to signaling data (cAMP and pERK1/2) to derive measures of functional affinity (pK_A , the measure of affinity of an agonist for the receptor when coupled to a particular pathway) and efficacy (τ , the efficiency with which occupied receptors are able to transduce a signal). While both Chapters 4 and 5 include Operational analysis of largely the same data sets, each of these chapters has separate focus on characterizing distinct phases of CTR-agonist interactions and hence analysing distinct parameters. Chapter 4 is focused on analysing the effects of mutations on CTR binding (both equilibrium and pathway dependent functional affinity) with a focus on comparison of equilibrium affinity (pK_i , derived from radioligand competition binding data) and functional affinity (pK_A , derived from signaling data). Chapter 5 focusses on the mutational effects on CTR signal transduction by analyzing effects on efficacy (derived from signaling data). Chapter 4 also includes analysis of CTR TM mutants effects on cell surface expression while Chapter 5 has the analysis of the original cAMP and pERK1/2 concentration-response data, and the key parameters derived from it.

4.2 RESULTS

In this study, 35 residues within the transmembrane region of CTR were initially identified within the peptide binding pocket from our initial cryo-EM structure (Liang *et al.*,

2017) (Figure 4.1.a). Single Ala mutants for each residue were generated using site-directed mutagenesis (4 alanine residues were mutated to either leucine (non-polar side chain, but two carbon atoms longer than Ala) or serine (same length as Ala, but polar). A total of 39 cell lines, each stably expressing a different single point-mutant, plus the control cell line stably expressing wild type receptor (WT) were generated in CV1 FlpIn cells. For the experimental Chapters 4 and 5, 23 of these individual mutants were selected for pharmacological characterization. These are located in the TM2, TM3, TM5, TM6 and TM7 and in regions predicted to undergo structural rearrangements upon receptor activation, with TM6 and TM7 undergoing the largest movement in order to accommodate intracellular G protein transducer. These selected residues include 4 residues that form the central polar network, which is predicted to reorganize when receptor is activated (Figure 4.1.a). Residues are numbered using the Wootten numbering system where the most conserved residue in each family TM domains assigned the position number of .50 (with the TM number before 0.50, all shown in superscript). All other residues are numbered by reference to the 0.50 residue in each TM domain (Wootten *et al.*, 2013).

Cell surface expression for each mutant was determined relative to the WT receptor using flow cytometry with anti-c-Myc antibody (9E10, that recognizes the N-terminal epitope tag on the receptor) and anti-CTR antibodies. Ligand affinity (pK_i) of the three CTR peptides (hCT, sCT and pCT (sequence alignment is shown on Figure 4.1.b) was determined by competition binding using a radiolabeled antagonist probe [125]I-sCT(8-32). The effect of the mutations on ligand-induced signalling was also assessed in two pathways, cAMP and pERK1/2. cAMP and pERK1/2 concentration response data was fitted using the operational model of agonism to derive pK_A (functional affinity) values for each signalling pathway. These results are reported in the following sections.

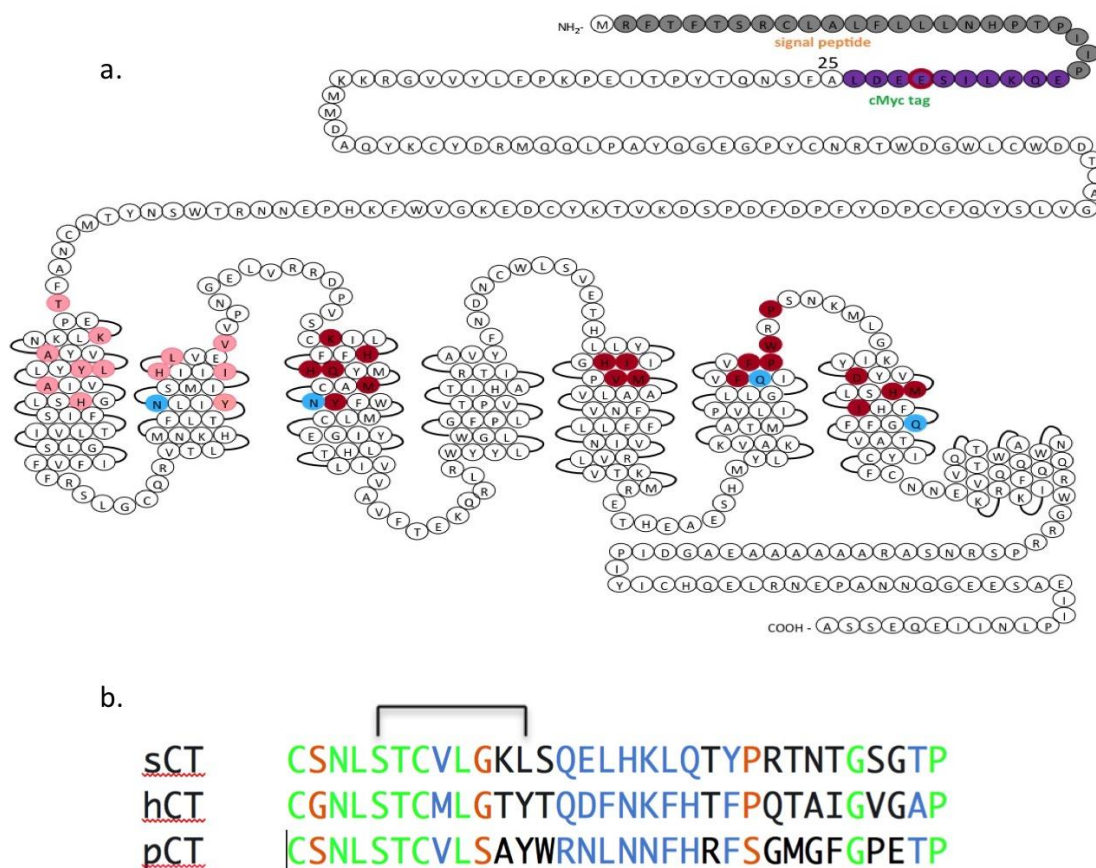


Figure 4.1. a. Snake diagram of the CTRaLeu construct used in this study and map of the CTR TM mutations introduced in CTR. Signal peptide in grey; cMyc-tag is in purple; TM residues mutated for this study are coloured in red and pink (in red are the residues that were characterized in this study and in pink are the residues that were mutated but their pharmacological characterization has not been performed; in blue are the central polar network residues). **b. Primary amino acid sequence alignment calcitonin peptides from different species (salmon, human and porcine CTs).** Conserved residues are in green, conservative substitutions are coloured blue, and semi-conservative substitutions are in orange. Black text indicates the non-conserved.

4.2.1 EFFECTS OF THE CTR TM MUTATIONS ON CTR CELL SURFACE EXPRESSION

Stable cell lines of the WT receptor and of each mutant receptor were generated by recombination using Flp recombinase which allows isogenic integration into host cells providing a single copy in the same genomic location under the same promoter with identical 3' and 5' untranslated regions. Under these conditions differences in the cell surface expression from that of the WT is interpreted as differences in protein stability and/or trafficking. While I didn't assess and compare effects of the CTR mutants on total expression, reduced cell surface expression relative to the WT is, by itself, an indicator that the particular mutant altered CTR protein stability/trafficking to the plasma membrane.

Many of the studied CTR TM mutants showed reduced cell surface expression relative to the WT receptor (Figure 4.2, Table 4.1). The only mutant for which cell surface expression could not be detected was Q355A (Q^{6.52}A). For H302A (H^{5.40}A) and Q383A (Q^{7.49}A) expression was below 20% of the WT; for N194A (N^{2.60}A), I301A (I^{5.39}A), F356A (F^{6.53}A), D373A (D^{7.39}A) and M376A (M^{7.42}A) expression was between 20% and 40% of the WT; for K220A (K^{3.30}A), Q227A (Q^{3.37}A), M230A (M^{3.40}A), N233A (N^{3.43}A), V305A (V^{5.43}A), M306A (M^{5.44}A) and P363A (P^{6.60}A) expression was between 40% and 60% of the WT expression. Expression of the mutants H223A (H^{3.33}A), H226A (H^{3.36}A), Y234A (Y^{3.44}A), F359A (F^{6.56}A), P360A (P^{6.57}A), W361A (W^{6.58}A) and H377A (H^{7.43}A) was not significantly different from the WT.

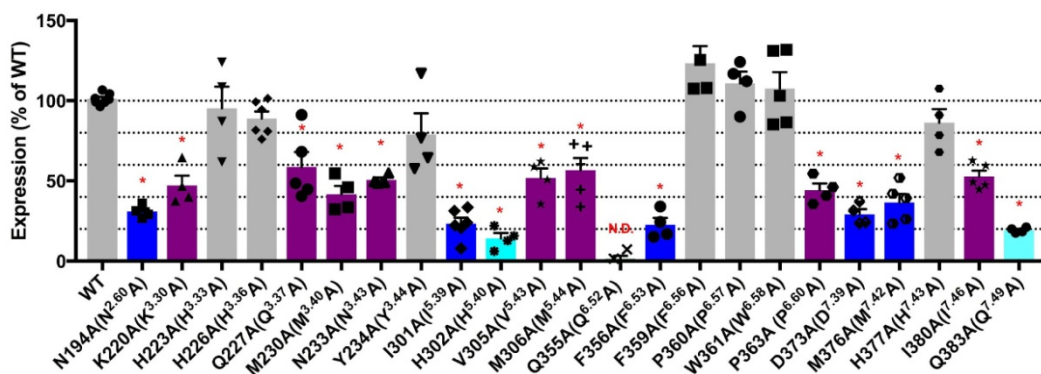


Figure 4.2. Cell surface expression of the hCTRLeu mutants stably expressed in CV-1-FlpIn cells. Expression of CTR mutant and WT receptors was determined by FACS using anti-cMyc and anti-CTR antibodies. All values are mean±S.E.M. of 3 to 6 independent experiments conducted in duplicate. Grey bars are not statistically different expression from wild-type, whereas coloured bars are statistically reduced expression relative to wild-type with purple being expression at 40-60% of wild-type, blue 20-40% of wild-type and cyan are <20%, of wild-type. Significant differences in receptor expression level were calculated via comparison of mutants to the WT receptor expression using a one-way analysis of variance (ANOVA) with Dunett's post-hoc test ($P < 0.05$ denoted by *). N.D. are data where there was no detectable expression.

Table 4.1. Cell surface expression of the hCTR α Leu mutants stably expressed in CV-1-FlpIn cells.

	Cell Surface Expression (%WT) \pm S.E.M
WT	101 \pm 1
N194A (N ^{2,60} A)	31* \pm 2
K220A (K ^{3,30} A)	47* \pm 6
H223A (H ^{3,33} A)	95 \pm 13
H226A (H ^{3,36} A)	89 \pm 4
Q227A (Q ^{3,37} A)	59* \pm 9
M230A (M ^{3,40} A)	42* \pm 5
N233A (N ^{3,43} A)	51* \pm 1
Y234A (Y ^{3,44} A)	79 \pm 13
I301A (I ^{5,39} A)	23* \pm 4
H302A (H ^{5,40} A)	14* \pm 3
V305A (V ^{5,43} A)	52* \pm 6
M306A (M ^{5,44} A)	57* \pm 8
Q355A (Q ^{6,52} A)	N.D.
F356A (F ^{6,53} A)	23* \pm 4
F359A (F ^{6,56} A)	123 \pm 11
P360A (P ^{6,57} A)	111 \pm 7
W361A (W ^{6,58} A)	108 \pm 10
P363A (P ^{6,60} A)	44* \pm 4
D373A (D ^{7,39} A)	29* \pm 3
M376A (M ^{7,42} A)	37* \pm 5
H377A (H ^{7,43} A)	86 \pm 9
I380A (I ^{7,46} A)	53* \pm 4
Q383A (Q ^{7,49} A)	19* \pm 1

*Expression of CTR in mutant and WT receptors was determined by FACS using anti-cMyc and anti-CTR antibodies. All values are mean \pm S.E.M. of 3 to 6 independent experiments conducted in duplicate. Significant differences in receptor expression level were calculated via comparison of mutants to the WT receptor expression using a one-way analysis of variance (ANOVA) with Dunett's post-hoc test with significant changes at $P<0.05$ denoted by *.*

For better visualization, the effects of the CTR TM mutations on the receptor cell surface were mapped onto the available cryo-EM structure of sCT bound to the CTR (only TM bundle shown) with residues within the receptor coloured according to their direction and magnitude of effect (Figure 4.3) (for the receptor expression the most relevant structure would be the structure of CTR alone in the absence of G protein or ligand, if such structure was available).

Residues with biggest effects on the CTR expression line the mid- and bottom portion of the peptide binding pocket as well as those sitting just below the binding pocket site and were concentrated in TMs 2, 5 and 7. On the other hand, residues with moderate effects on cell surface expression (40-69 % of the WT) were scattered across different parts of TM3, TM5, TM6 and TM7 (Figure 4.3).

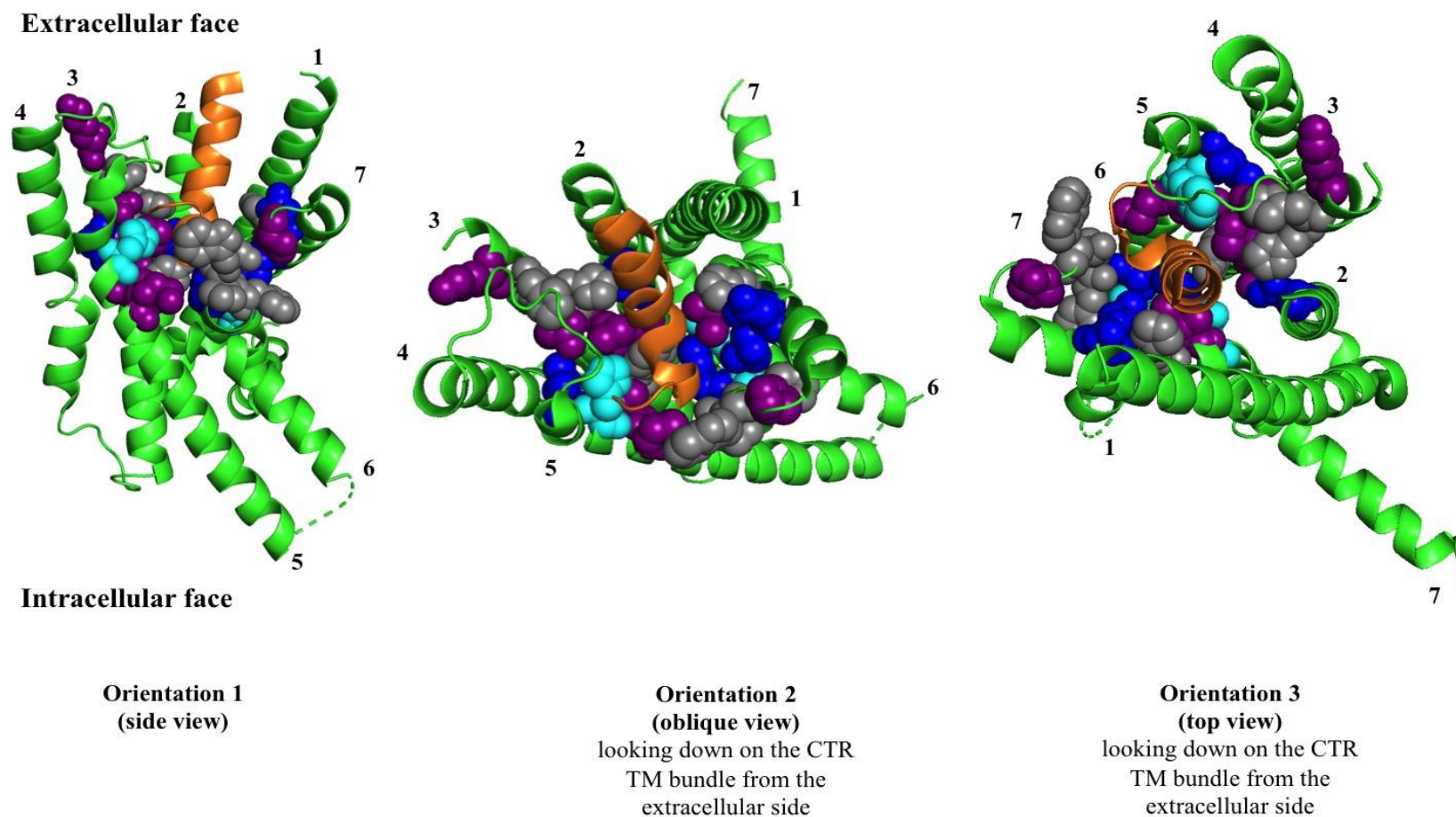


Figure 4.3. Effect of the CTR TM mutations on the receptor cell surface expression. Residues for sCT and pCT are mapped onto a Cryo-EM structure of CTR in complex with sCT and G_s protein (G_s protein and CTR N-terminal domain are not shown) (Dal Maso et. al., 2019). The receptor is shown in green and sCT ligand is shown in orange. Residues where produced significant changes in cell surface expression are shown as space-fill side chains and are coloured according to the level of effect; purple for the expression at 40-60% of wild type, blue are 20-40% of wild-type and cyan for the expression at <20% of wild type. Those of the studied residues that were expressed at levels not statistically different from the WT are shown in grey.

4.2.2 EFFECTS OF CTR TM MUTATIONS ON EQUILIBRIUM AFFINITY AND cAMP FUNCTIONAL AFFINITY OF CALCITONIN PEPTIDE AGONISTS

pK_i is the equilibrium dissociation constant that was determined for each peptide ligand and each receptor (WT and mutants) from competition binding (homologous for sCT(8-32) and heterologous for (sCT, hCT, pCT)) in presence of the labelled antagonist [125 I](sCT(8-32)). pK_i values ($pK_d \approx pK_i$) were calculated individually from each experiment using one site-homologous equation (for sCT(8-32)) and pK_i fit (for sCT, hCT and pCT) in Graphpad prism and are reported as the mean value \pm SEM in Table 4.2. Data was normalized between the total level of bound 125 I- sCT(8-32) (measured at concentrations 10^{-7} sCT, $10^{-5.5}$ hCT and 10^{-6} for pCT) and non-specific binding, defined by saturating concentration of competing non-iodinated sCT(8-32) (1 μ M) (in some cases, the observed % specific binding at zero competitor concentration is below 100% that is a result of measurement error where the highest specific binding was detected at second lowest competitor concentrations (rather than at zero competitor concentration). For the visualisation purposes, grouped binding data (both homologous and heterologous binding) was fitted using a three parameter logistic equation (one site competition in Graphpad prism) (Figures 4.4 – 4.7).

Functional affinity (pK_A) may be considered a measure of the affinity of an individual ligand when the receptor is coupled to a particular signalling pathway. pK_i and pK_A are both measures of affinity, however each of them may relate to different receptor populations, and therefore, they will not necessarily be the same. The CTR is most strongly coupled to G_{as} and previous studies revealed a good correlation between the measured pK_i from equilibrium binding assays and pK_A values measured for the cAMP accumulation assay, where receptor:ligand equilibrium is approached during the course of the experiment (Dal Maso *et al.*, 2018, Dal Maso *et al.*, 2019). In this study, concentration response data for cAMP was generated for each of the calcitonin peptides at each of the mutant and WT receptors and fitted to the operational model of agonism to derive pK_A (Figures 4.8 – 4.10, Table 4.2). ΔpK_i and ΔpK_A values for each mutant were obtained by subtracting WT pK_i and WT pK_A from each mutant's pK_i and pK_A values (respectively) and are summarized in Figures 4.11– 4.14. As per previous work, this study also identified a strong correlation between pK_i and pK_A derived from cAMP.

In homologous competition binding only the N194A ($N^{2.60}$ A) mutation significantly decreased binding affinity of the antagonist probe, sCT(8-32) (Figure 4.11, Table 4.2). The pK_i of H226A ($H^{3.36}$ A) for the antagonist probe was not statistically different from WT, although the magnitude of decrease was more than 3-fold (table 4.2).

For sCT, no alanine mutations had significant effects on pK_i values, although pK_i could not be determined for the K220A ($K^{3.30}A$) mutant (as a reliable window couldn't be obtained in order to accurately determine binding for this mutant). K220A ($K^{3.30}A$) was the only mutant that altered the cAMP pK_A relative to WT for sCT, with a statistically significant 8-fold decrease (Figure 4.12, Table 4.2).

Compared with sCT, a greater number of mutations exhibited statistically significantly reduced pK_i and cAMP derived pK_A for the lower affinity ligands, hCT and pCT, (Figures 4.13 – 4.14, Table 4.2).

For better visualization and comparison of the effects of the CTR TM mutations on pK_i and pK_A , residues that produced statistically significant changes for the cAMP-derived pK_A and the corresponding residues in pK_i were mapped onto the cryo-EM structure of either sCT bound the CTR (Dal Maso et al., 2019) (for sCT and pCT) or onto the provisional unpublished model of hCT bound the CTR (for hCT). These were colour coded according to the magnitude of effect. Any residue which gave a statistically significant change in pK_A (from cAMP) was mapped and although many of these residues had changes that failed to reach significance for the derived pK_i values, they were nonetheless included in this representation with the magnitude of change indicated according to colour (Figure 4.15).

For hCT, a number of mutants commonly reduced determined cAMP pK_A and pK_i values, with N194A ($N^{2.60}A$), Y234A ($Y^{3.44}A$), H302A ($H^{5.40}A$), F359A ($F^{6.56}A$) and P360 ($P^{6.57}A$) changing both measures of affinity to a similar extent (Figure 4.13, 4.15). Mutants such as I301A ($I^{5.39}A$), P363A ($P^{6.60}A$), D373A ($D^{7.39}A$) and M376A ($M^{7.42}A$) also decreased both measures of affinity, however the extent to which these changed pK_A was greater than the measured change in pK_i (Figure 4.13). In comparison, there were a series of residues, N233A ($N^{3.43}A$), Q355A ($Q^{6.52}A$) and F356A ($F^{6.53}A$), when mutated caused a selective decrease in cAMP pK_A with no change (or a non-significant increase) in pK_i (Figure 4.13). For pCT, N194A ($N^{2.60}A$), H226A ($H^{3.36}A$), P360 ($P^{6.57}A$) decreased and I380A ($I^{7.46}A$) increased both measures of affinity to a similar extent (Figure 4.14). While mutants such as K220A ($K^{3.30}A$), I301A ($I^{5.39}A$), P363A ($P^{6.60}A$), D373A ($D^{7.39}A$) and M376A ($M^{7.42}A$) also decreased both measures of affinity, however the extent to which these changed pK_A was greater than the measured change in pK_i for pCT (Figure 4.14). For sCT only pK_A for K220A ($K^{3.30}A$) was significantly decreased, and the magnitude K220A ($K^{3.30}A$) effect on sCT was smaller than for hCT and pCT (Figures 4.12 – 4.15).

Comparing cAMP pK_A data against the pK_i , allows a comparison between overall affinity effects and those effects that are related specifically to G_s coupling. Thus, for residues in which the magnitude and direction of change was similar for pK_A and pK_i the functional affinity loss

can be attributed to an global change in affinity not associated with specific G_s coupling. On the other hand, residues, such as N233A ($N^{3.43}A$), Q355A ($Q^{6.52}A$), F356A ($F^{6.53}A$) for hCT; K220A ($K^{3.30}A$), I301A ($I^{5.39}A$) for pCT; and P363A ($P^{6.60}A$), M376A ($M^{7.42}A$) for both hCT and pCT, where either the direction of change or magnitude was substantially different for cAMP pK_A compared with pK_i are likely to be functionally linked to activation of G_s (Figures 4.13-4.15).

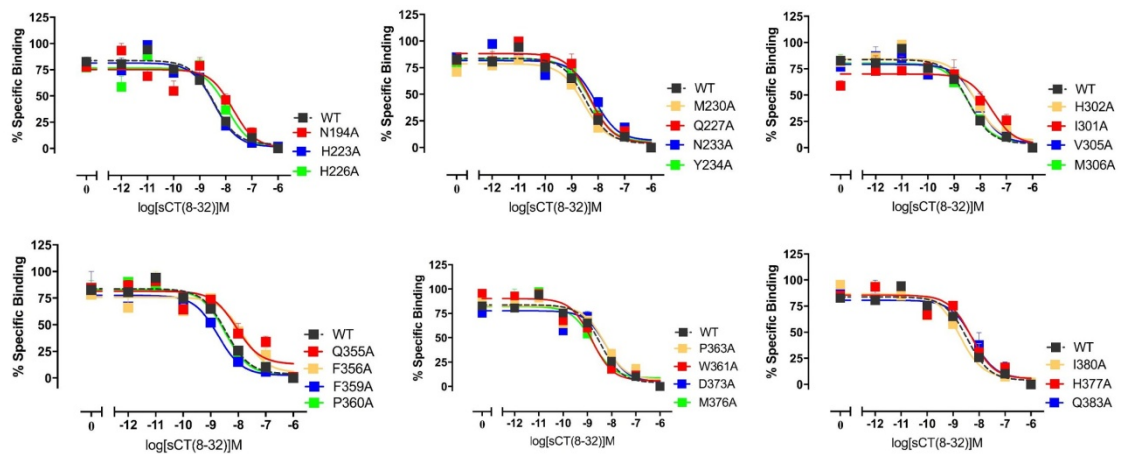


Figure 4.4. Homologous competition binding of sCT(8-32) for each of the hCTRaLeu mutants stably expressed in CV-1-FlpIn cells. Whole cell radioligand binding was performed for each mutant and for the WT receptor in the presence of ~ 50 - 150 pM 125 I-sCT(8-32) and competing concentrations sCT (as shown in the x axes). Non-specific binding was determined in the presence of 1 μ M of sCT(8-32) and was used to calculate % of specific binding. Data were fit with a three-parameter logistic equation (one-site competition in Graphpad prism). All values are mean \pm S.E.M. of 3 to 6 independent experiments, conducted in duplicate; for some data points error bars are not shown as they are smaller than the height of the symbol.

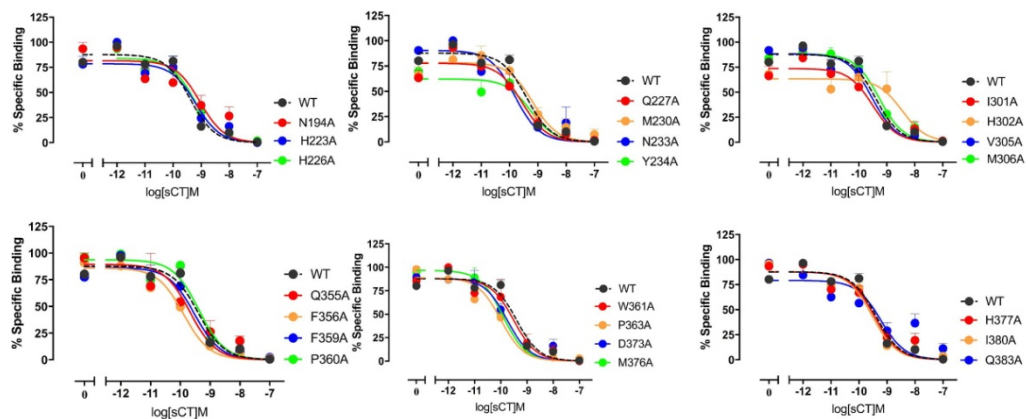


Figure 4.5 Heterologous competition binding of sCT for each of the hCTRaLeu mutants stably expressed in CV-1-FlpIn cells. Whole cell radioligand binding was performed for each mutant and for the WT receptor in the presence of ~ 50 - 150 pM 125 I-sCT(8-32) and competing concentrations sCT (as shown in the x axes). Non-specific binding was determined in the presence of 1 μ M of sCT(8-32) and was used to calculate % of specific binding. Data were fit with a three-parameter logistic equation (one-site competition in Graphpad prism). All values are mean \pm S.E.M. of 3 to 6 independent experiments, conducted in duplicate; for some data points error bars are not shown as they are smaller than the height of the symbol.

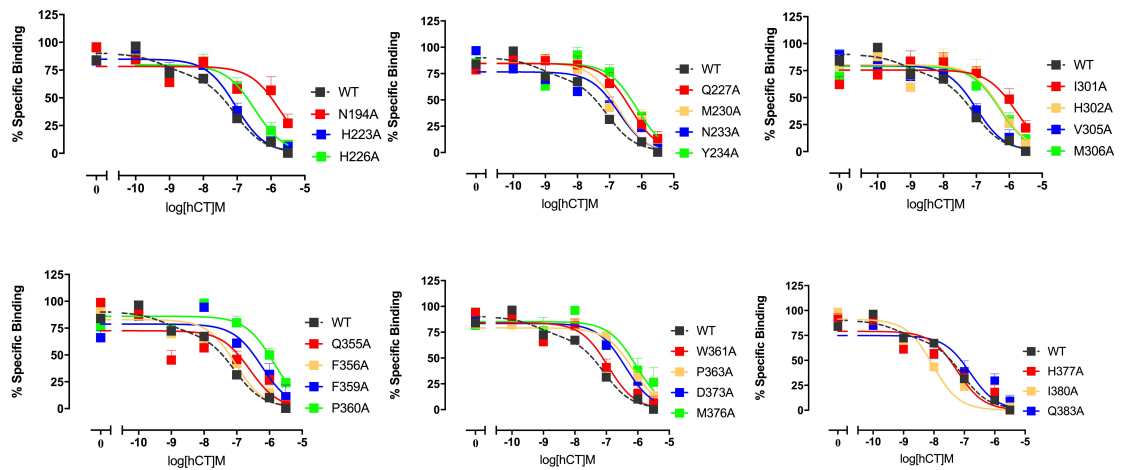


Figure 4.6. Heterologous competition binding of hCT for each of the hCTRaLeu mutants stably expressed in CV-1-FlpIn cells. Whole cell radioligand binding was performed for each mutant and for the WT receptor in the presence of ~ 50 - 150 pM 125 I-sCT(8-32) and competing concentrations hCT, as indicated on the x-axes. Non-specific binding was determined in the presence of 1 μ M of sCT(8-32) and was used to calculate % of specific binding. Data were fit with a three-parameter logistic equation (one-site competition in Graphpad prism). All values are mean+S.E.M. of 3 to 6 independent experiments, conducted in duplicate; for some data points error bars are not shown as they are smaller than the height of the symbol.

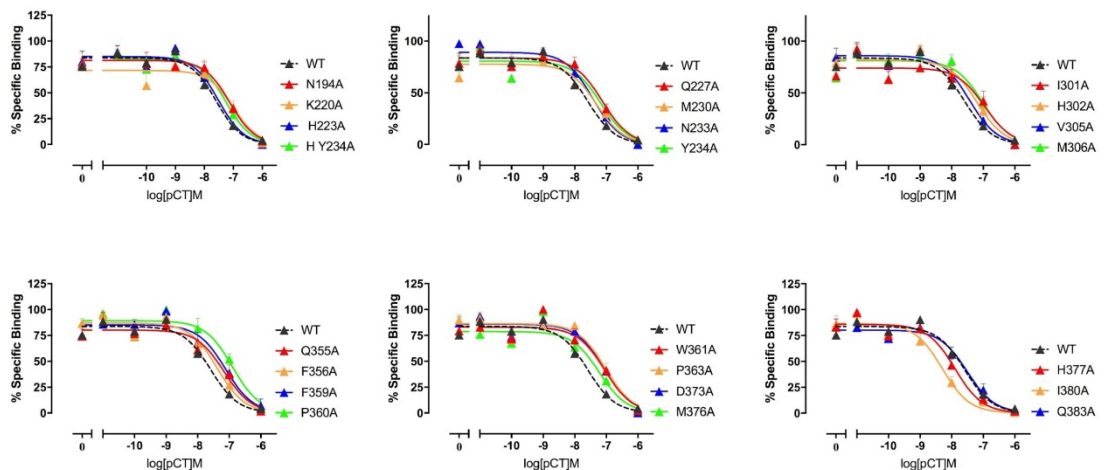


Figure 4.7. Heterologous competition binding of pCT for each of the hCTRaLeu mutants stably expressed in CV-1-FlpIn cells. Whole cell radioligand binding was performed for each mutant and for the WT receptor in the presence of ~ 50 - 150 pM 125 I-sCT(8-32) and competing concentrations pCT, as indicated on the x-axes. Non-specific binding was determined in the presence of 1 μ M of sCT(8-32) and was used to calculate % of specific binding. Data were fit with a three-parameter logistic equation (one-site competition in Graphpad prism). All values are mean+S.E.M. of 3 to 6 independent experiments, conducted in duplicate; for some data points error bars are not shown as they are smaller than the height of the symbol.

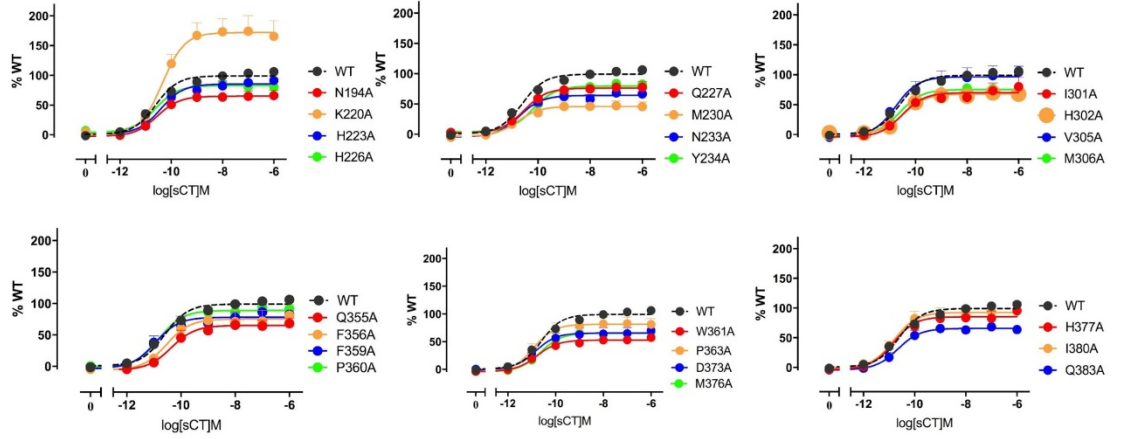


Figure 4.8. *cAMP accumulation profiles in response to sCT in CV-1-FlpIn cells stably expressing hCTRαLeu single alanine mutations in the receptor TM region. cAMP formation in the presence of sCT was fitted using three-parameter logistic equation and normalized to WT receptor response. Normalized data was fit using Black and Leff operational model, with a hill slope of 1. All values are mean+S.E.M. of 3 to 5 independent experiments conducted in duplicate; for some data sets error bars are not shown as they are smaller than the height of the symbol.*

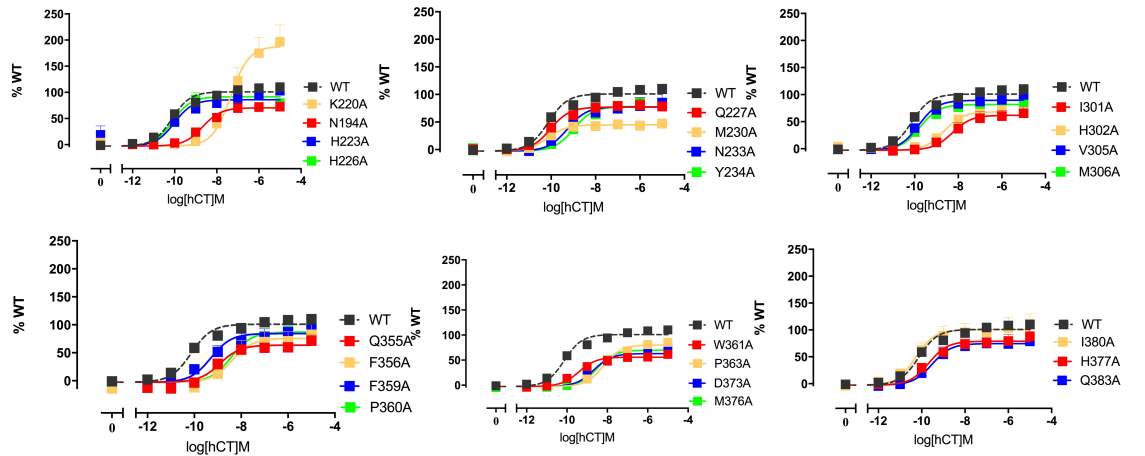


Figure 4.9. *cAMP accumulation profiles in response to hCT in CV-1-FlpIn cells stably expressing hCTRαLeu mutations in the receptor TM region. cAMP formation in the presence of hCT was fitted using three-parameter logistic equation and normalized to WT receptor response. Normalized data was fit using Black and Leff operational model, with a hill slope of 1. All values are mean+S.E.M. of 3 to 5 independent experiments conducted in duplicate; for some data sets error bars are not shown as they are smaller than the height of the symbol.*

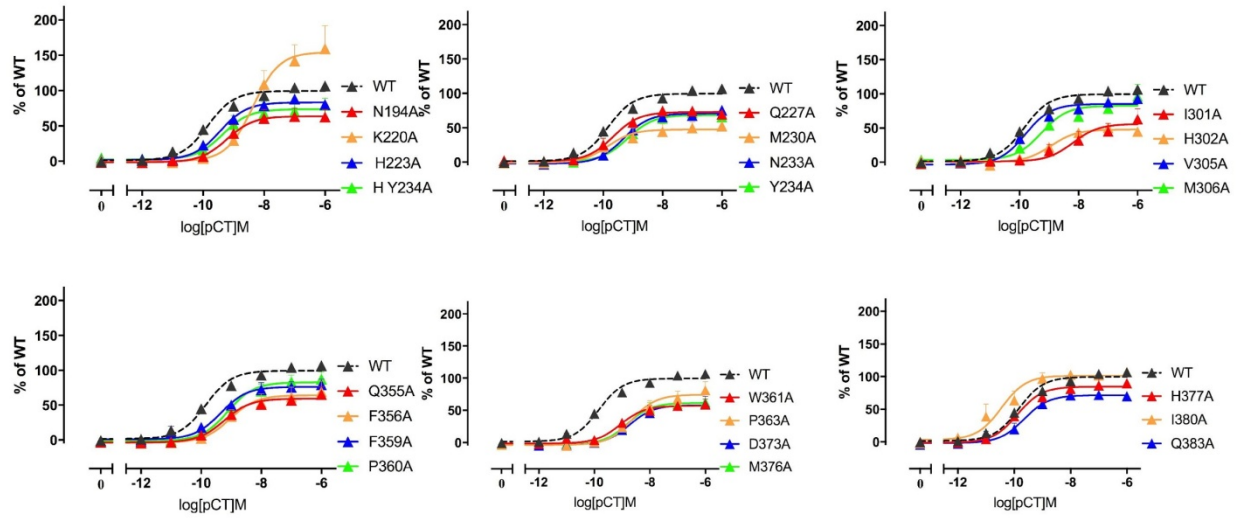


Figure 4.10. *cAMP* accumulation profiles in response to *pCT* in *CV-1-FlpIn* cells stably expressing *hCTRαLeu* mutations in the receptor *TM* region. *cAMP* formation in the presence of *pCT* was fitted using three-parameter logistic equation and normalized to WT receptor response. Normalized data was fit using Black and Leff operational model, with a hill slope of 1. All values are mean+S.E.M. of 3 to 5 independent experiments conducted in duplicate; for some data sets error bars are not shown as they are smaller than the height of the symbol.

Table 4.2. Effect of single alanine mutation in the CTR TM region on binding affinity (pK_i) and cAMP functional affinity (pK_A) of CT peptide agonists.

	pK _i sCT(8-32)			pK _i sCT			pK _A sCT			pK _i hCT			pK _A hCT			pK _i pCT			pK _A pCT		
WT	8.64	±	0.07	9.40	±	0.07	10.38	±	0.07	7.37	±	0.11	9.85	±	0.07	7.59	±	0.09	9.61	±	0.06
N194A(N ^{2.60} A)	7.67*	±	0.10	9.55	±	0.34	10.36	±	0.25	5.79*	±	0.45	8.49*	±	0.24	6.98*	±	0.11	9.05	±	0.24
K220A(K ^{3.30} A)	N.D.			N.D.			9.70*	±	0.09	N.D.			6.49*	±	0.15	N.D.			7.84*	±	0.12
H223A(H ^{3.33} A)	8.37	±	0.12	9.48	±	0.10	10.23	±	0.17	7.29	±	0.18	9.79	±	0.19	7.45	±	0.09	9.28	±	0.17
H226A(H ^{3.36} A)	7.94	±	0.16	9.02	±	0.10	10.50	±	0.19	6.37	±	0.24	9.85	±	0.16	7.07*	±	0.11	9.23	±	0.19
Q227A(Q ^{3.37} A)	8.38	±	0.19	9.73	±	0.19	10.41	±	0.21	7.21	±	0.48	9.83	±	0.20	7.01	±	0.11	9.52	±	0.25
M230A(M ^{3.40} A)	8.73	±	0.29	9.47	±	0.23	10.59	±	0.34	7.77	±	0.49	10.03	±	0.34	7.38	±	0.25	9.70	±	0.31
N233A(N ^{3.43} A)	8.98	±	0.46	9.83	±	0.27	10.48	±	0.29	7.68	±	0.43	9.06*	±	0.24	7.42	±	0.14	9.10	±	0.26
Y234A(Y ^{3.44} A)	8.31	±	0.19	9.56	±	0.02	10.08	±	0.20	6.27	±	0.11	8.77*	±	0.21	7.10	±	0.12	9.03	±	0.20
I301A(I ^{5.39} A)	8.51	±	0.24	9.56	±	0.29	10.28	±	0.23	6.28	±	0.38	8.10*	±	0.31	7.12	±	0.42	8.12*	±	0.30
H302A(H ^{5.40} A)	8.18	±	0.16	8.80	±	0.48	10.33	±	0.24	6.23	±	0.25	8.46*	±	0.26	7.15	±	0.14	8.83	±	0.36
V305A(V ^{5.43} A)	8.15	±	0.44	9.61	±	0.17	10.48	±	0.19	6.97	±	0.18	9.58	±	0.21	7.35	±	0.09	9.53	±	0.21
M306A(M ^{5.44} A)	8.70	±	0.24	9.46	±	0.18	10.41	±	0.21	6.42	±	0.29	9.55	±	0.20	6.89*	±	0.17	9.14	±	0.19
Q355A(Q ^{6.52} A)	8.11	±	0.14	9.94	±	0.01	10.11	±	0.24	7.42	±	0.61	8.75*	±	0.25	7.24	±	0.18	9.02	±	0.26
F356A(F ^{6.53} A)	8.11	±	0.43	9.78	±	0.38	10.27	±	0.22	7.68	±	0.57	8.19*	±	0.23	7.16	±	0.15	8.81*	±	0.24
F359A(F ^{6.56} A)	8.75	±	0.16	9.60	±	0.10	10.71	±	0.23	6.30	±	0.22	9.07*	±	0.23	7.33	±	0.27	9.19	±	0.24
P360A(P ^{6.57} A)	8.48	±	0.09	9.22	±	0.16	10.58	±	0.18	5.98	±	0.13	8.19*	±	0.20	6.83*	±	0.12	8.89*	±	0.19
W361A(W ^{6.58} A)	8.84	±	0.16	9.61	±	0.34	10.57	±	0.34	6.87	±	0.29	9.26	±	0.34	7.15	±	0.25	8.90	±	0.31
P363A(P ^{6.60} A)	8.58	±	0.28	9.43	±	0.37	10.67	±	0.19	6.57	±	0.44	7.97*	±	0.21	6.94*	±	0.11	8.37*	±	0.22
D373A(D ^{7.39} A)	8.32	±	0.14	9.07	±	0.46	10.69	±	0.23	6.46	±	0.22	8.51*	±	0.26	6.88*	±	0.10	8.51*	±	0.28
M376A(M ^{7.42} A)	8.59	±	0.43	9.88	±	0.15	10.42	±	0.29	6.55	±	0.17	8.32*	±	0.28	7.13	±	0.12	8.59*	±	0.30
H377A(H ^{7.43} A)	8.36	±	0.12	9.66	±	0.14	10.58	±	0.18	7.84	±	0.16	9.47	±	0.21	8.01	±	0.13	9.66	±	0.18
I380A(I ^{7.46} A)	8.94	±	0.39	9.52	±	0.10	10.57	±	0.20	8.23	±	0.34	10.00	±	0.19	8.21*	±	0.19	10.27	±	0.18
Q383A(Q ^{7.49} A)	8.31	±	0.39	9.50	±	0.46	10.43	±	0.28	7.40	±	0.46	9.33	±	0.26	7.63	±	0.16	9.44	±	0.25

pK_i for each mutant receptor was determined for each ligand using analysis of either homologous (sCT(8-32)) or heterologous (sCT, hCT, pCT) competition binding in presence of ~50-150 pM ¹²⁵I-sCT(8-32) using a three parameter logistic equation and pK_i derived by applying the Cheng-Prusoff equation to correct for radioligand occupancy. cAMP formation

*in the presence of each ligand was fitted using a three parameter logistic equation and normalized to the E_{max} calculated in the curve fit for the WT receptor response. The Black and Leff operational model, with a hill slope of 1, was then applied to separate efficacy (τ) and functional affinity (pK_A). All values are mean \pm S.E.M. of 3 to 5 independent experiments conducted in duplicate. Significance of changes in pK_i/pK_A were calculated via comparison of mutant pK_i/pK_A values to the WT pK_i/pK_A in a one-way analysis of variance (ANOVA) with Dunett's post-hoc test with significant changes ($P<0.05$ denoted by *).*

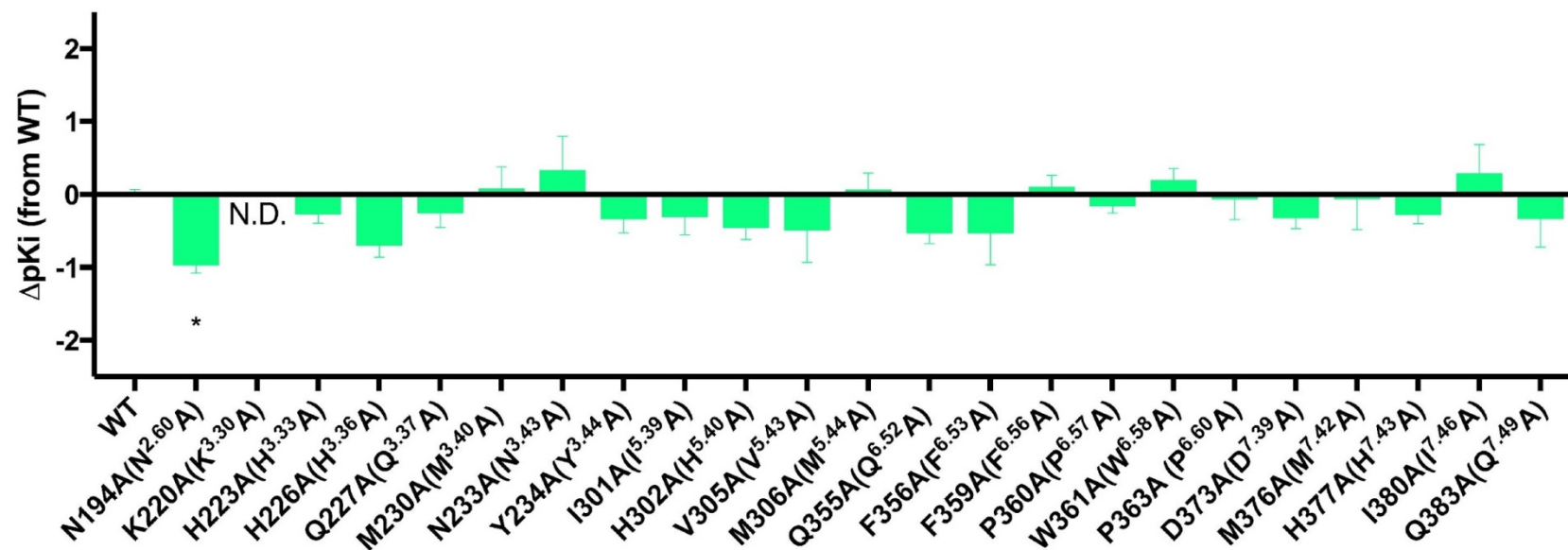


Figure 4.11. ΔpK_i values for sCT(8-32). ΔpK_i value for each mutant was obtained by subtracting WT pK_i from each mutant's pK_i value. All values are mean+S.E.M. of 3 to 5 independent experiments conducted in duplicate. Significance of changes were calculated via comparison of mutants to the WT receptor pK_i values in a one-way analysis of variance (ANOVA) with Dunett's post-hoc test with significant changes ($P < 0.05$ denoted by *).

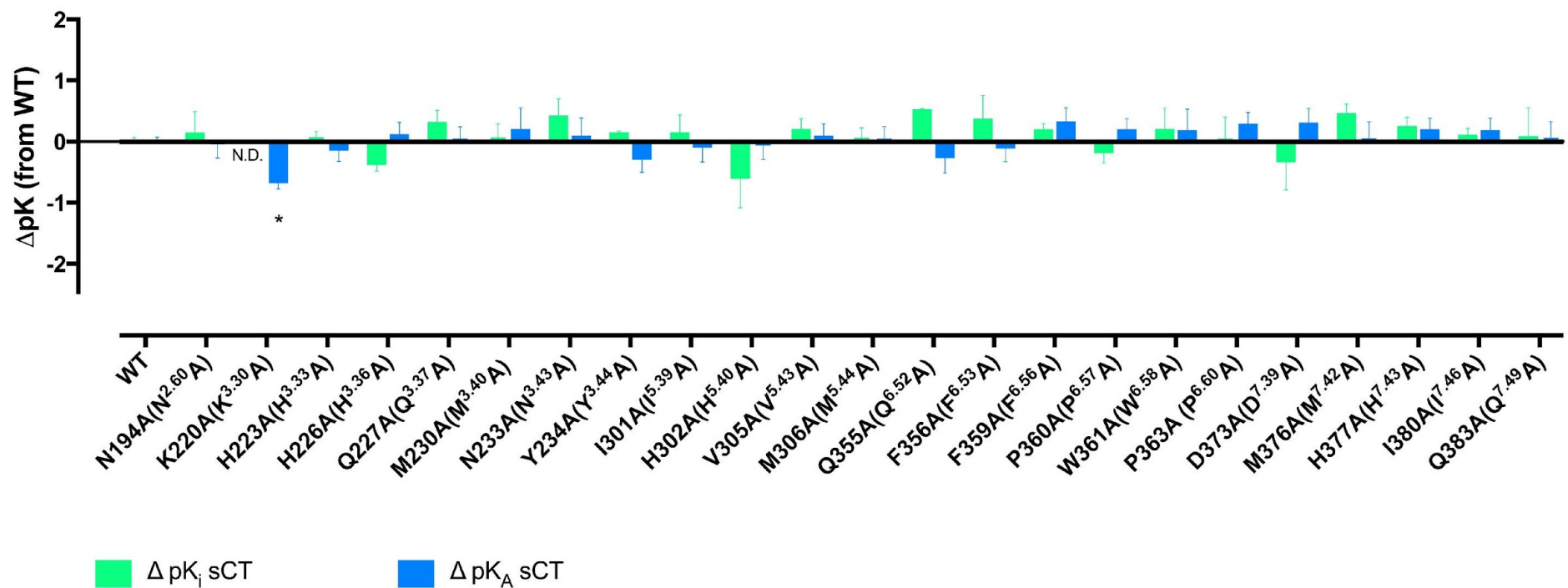


Figure 4.12. ΔpK_i and cAMP ΔpK_A values for sCT. ΔpK_i and ΔpK_A values for each mutant were obtained by subtracting WT pK_i and WT pK_A from each mutant's pK_i and pK_A values (respectively). All values are mean+S.E.M. of 3 to 5 independent experiments conducted in duplicate. Significance of changes were calculated via comparison of mutants to the WT receptor pK_i / pK_A values in a one-way analysis of variance (ANOVA) with Dunett's post-hoc test with significant changes ($P < 0.05$ denoted by *).

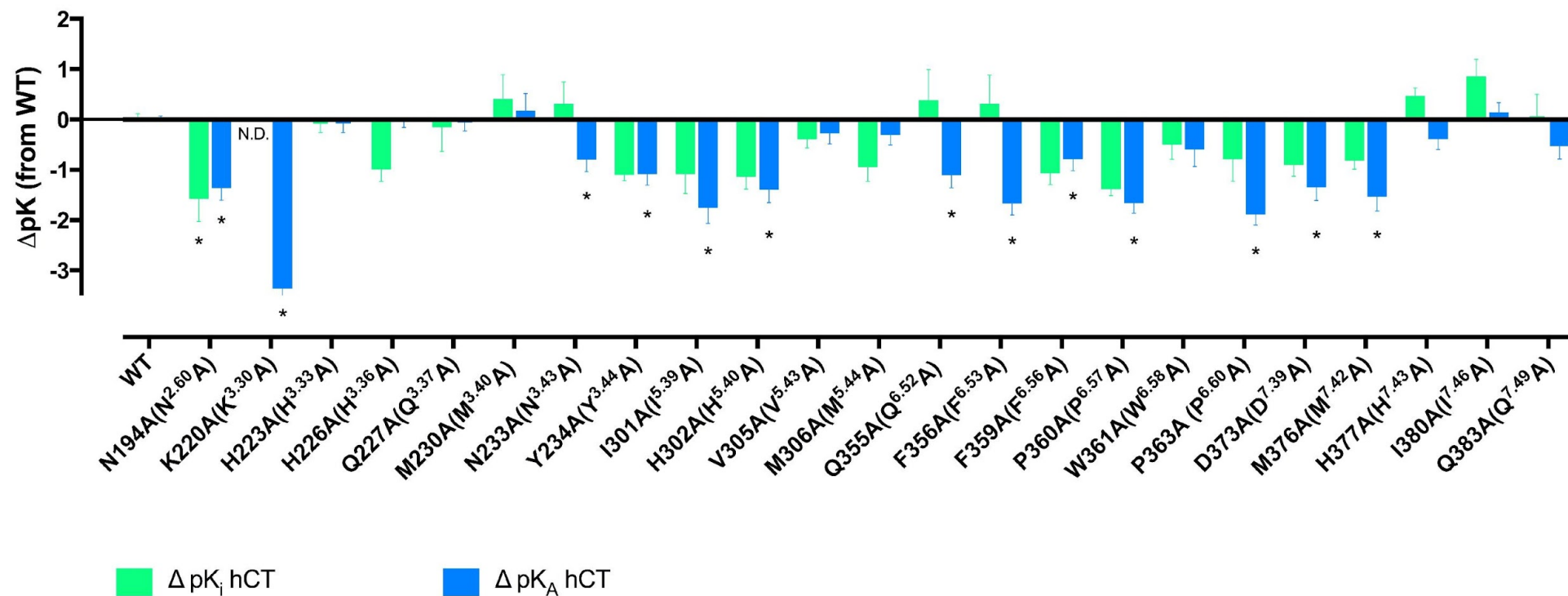


Figure 4.13. ΔpK_i and cAMP ΔpK_A values for hCT. ΔpK_i and ΔpK_A values for each mutant were obtained by subtracting WT pK_i and WT pK_A from each mutant's pK_i and pK_A values (respectively). All values are mean+S.E.M. of 3 to 5 independent experiments conducted in duplicate. Significance of changes were calculated via comparison of mutants to the WT receptor pK_i / pK_A values in a one-way analysis of variance (ANOVA) with Dunett's post-hoc test with significant changes ($P < 0.05$ denoted by *).

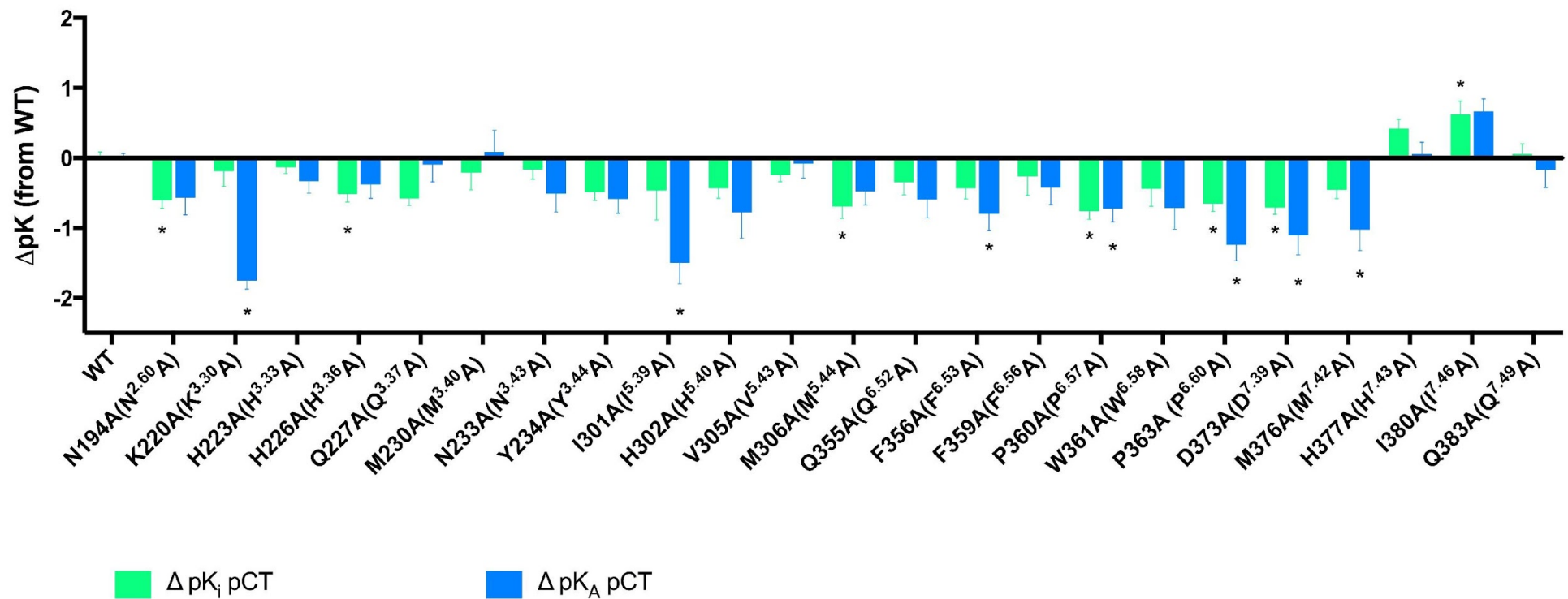


Figure 4.14. ΔpK_i and cAMP ΔpK_A values for pCT. ΔpK_i and ΔpK_A values for each mutant were obtained by subtracting WT pK_i and WT pK_A from each mutant's pK_i and pK_A values (respectively). All values are mean \pm S.E.M. of 3 to 5 independent experiments conducted in duplicate. Significance of changes were calculated via comparison of mutants to the WT receptor pK_i / pK_A values in a one-way analysis of variance (ANOVA) with Dunett's post-hoc test with significant changes ($P < 0.05$ denoted by *).

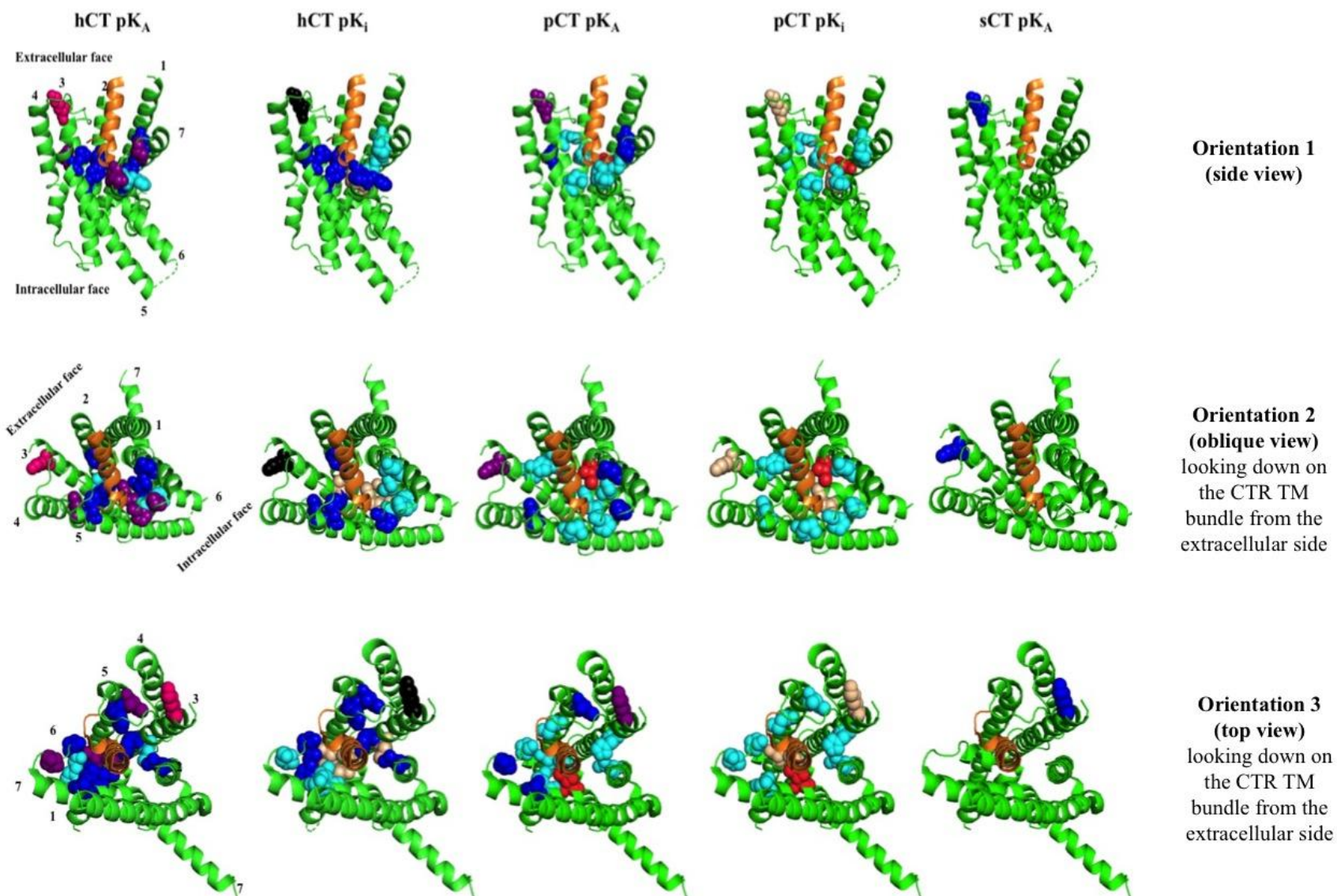


Figure 4.15 (previous page). Effect of the CTR TM mutations on pK_i and cAMP pK_A for hCT and pCT. Residues for sCT and pCT are mapped onto a Cryo-EM structure of CTR in complex with sCT and G_s protein (G_s protein and CTR N-terminal domain are not shown) (Dal Maso et. al., 2019) and for hCT onto a provisional Cryo-EM structure of CTR in complex with hCT and G_s protein (G_s protein and CTR N-terminal domain are not shown) (not published). The receptor is shown in green and CT ligand is shown in orange. Residues that produced significant changes either hCT or pCT pK_A and the corresponding residues in pK_i are shown as space-fill side chains (additionally, for pCT H226A, M306A and I380A are labelled, as they produced significant effects on pCT pK_i , whereas their pK_A effects were not significant. Residues are colour coded according to their effects on affinity (either pK_A or pK_i): reduced affinity $>5 < 10$ -fold are shown in cyan; reduced affinity $>10 < 15$ -fold are shown in blue; reduced affinity $>15 < 20$ -fold are shown in purple; reduced affinity >20 -fold are shown in fuchsia; those residues that increased affinity are shown in red. Residues pK_i effects for which were not detected are coloured black and those residues that showed no effects on pK_i (>5 -fold effect) are coloured beige. For sCT only pK_A effects are shown (as K220A was the only mutant that had effects on sCT pK_A and pK_i for this mutant could not be determined).

4.2.3 EFFECTS OF THE CTR TM MUTATIONS ON CTR cAMP FUNCTIONAL AFFINITY IN RESPONSE TO α CGRP AND rAMY

α CGRP and rAMY are low affinity CTR agonists in the absence of RAMPs and as such their affinity at each of the mutants could not be determined by radioligand binding, due to their inability to compete for the antagonist probe at the concentrations used. Since CTR is strongly coupled to $G_{\alpha S}$, we were able to measure the concentration response for this pathway (Figures 4.16 – 4.17), with only a few mutations failing to give a robust curve fit (P363A (P^{6.60}A) and D373A (D^{7.39}A) for both α CGRP and rAMY and H302A (H^{5.40}A) for rAMY). The latter were excluded from the subsequent operational analysis. Applying operational analysis to the cAMP data allowed us to derive functional affinity values that can be used as a surrogate measure of affinity (Table 4.3, Figures 4.18 – 4.19).

Alanine mutations of N194 (N^{2.60}), K220 (K^{3.30}), N233 (N^{3.43}), F356 (F^{6.53}) reduced cAMP functional affinity for both α CGRP and rAMY agonists and these mutations also reduced cAMP functional affinity of calcitonin peptides (Figures 4.18 – 4.19). H302A (H^{5.40}A) and Q355A (Q^{6.52}A) showed statistically significant reductions in α CGRP cAMP functional affinity and although they also reduced cAMP functional affinity for rAMY, this failed to reach statistical significance. On the other hand, I301A (I^{5.39}A) and P360A (P^{6.57}A) had statistically significant reductions in cAMP functional affinity for rAMY whereas the reductions in α CGRP cAMP functional affinity were smaller and did not reach statistical significance (Figures 4.18 – 4.19). The above mutations also displayed significant cAMP functional affinity reductions for at least one of the calcitonins, as described above. W361A (W^{6.58}A) significantly decreased cAMP pK_A for rAMY, consistent with the direction and magnitude of effect seen with hCT and pCT, although the reduction did not reach statistical significance for the calcitonins (Figures 4.13, 4.14, 4.19).

For better visualization effects of the CTR TM mutations on cAMP pK_A for α CGRP and rAMY, these were mapped onto a current CTR model (Dal Maso *et al.*, 2019) with residues coloured according to their effect direction and magnitude (Figure 4.20). Conservation of residues important for both α CGRP and rAMY cAMP pK_A was similar for some of the TM2 and TM3 residues, whereas more divergence was seen in the TM5 and TM6 region, with more residues altering cAMP pK_A for rAMY. Overall, this map was similar to the mapping of pK_A networks for the hCT, although the magnitude of effects for α CGRP and rAMY was generally smaller when compared to hCT. In contrast Y234A, M306A and W361A caused a greater loss in cAMP functional pK_A for rAMY compared to hCT. I380A had a 4-fold increase in cAMP functional pK_A to α CGRP compared to a 1.4-fold increase in response to hCT, while same

mutant produced a 4-fold decrease in pK_A in response to rAMY, although none of these changes reached statistical significance (Figures 4.13, 4.15, 4.18, 4.19, 4.20).

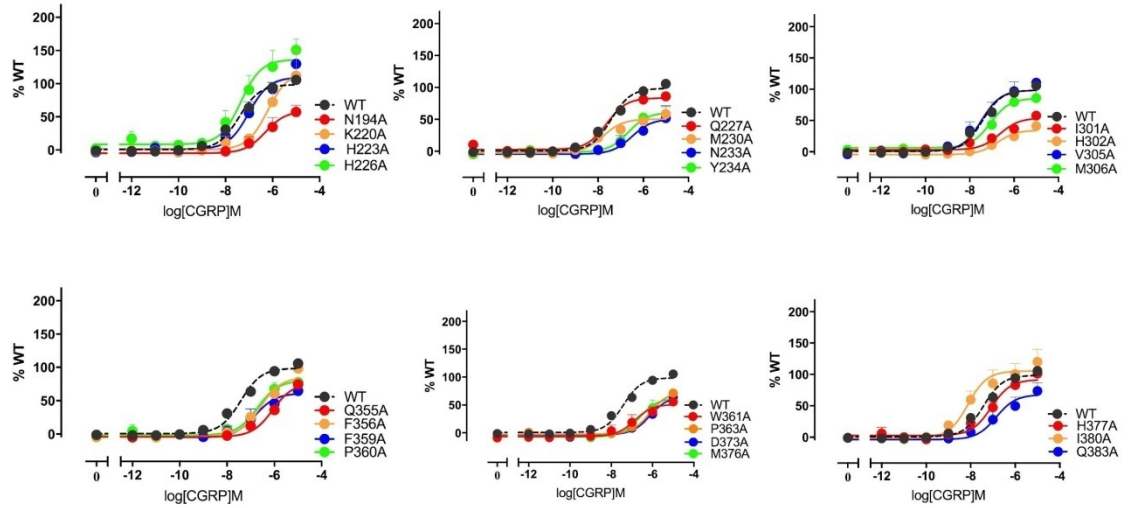


Figure 4.16. *cAMP accumulation profiles in response to α CGRP in CV-1-FlpIn cells stably expressing hCTR α Leu mutations in the receptor TM region. cAMP formation in the presence of α CGRP was fitted using three-parameter logistic equation and normalized to WT receptor response. Normalized data was fit using Black and Leff operational model, with a hill slope of 1. All values are mean+S.E.M. of 3 to 5 independent experiments conducted in duplicate; for some data points error bars are not shown as they are smaller than the height of the symbol.*

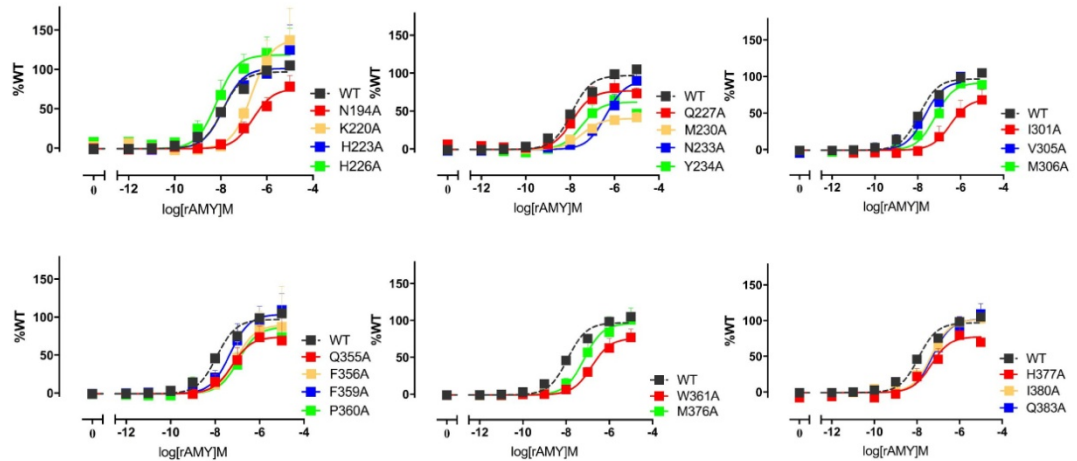


Figure 4.17. *cAMP accumulation profiles in response to rAMY in CV-1-FlpIn cells stably expressing hCTR α Leu mutations in the receptor TM region. cAMP formation in the presence rAMY was fitted using three-parameter logistic equation and normalized to WT receptor response. Normalized data was fit using Black and Leff operational model, with a hill slope of 1. All values are mean+S.E.M. of 3 to 5 independent experiments conducted in duplicate; for some data points error bars are not shown as they are smaller than the height of the symbol.*

Table 4.3. Effect of single alanine mutation in the CTR TM region on cAMP functional affinity (pK_A) of α CGRP and rAMY

	$pK_A \alpha$ CGRP			pK_A rAMY		
WT	7.25	±	0.08	7.69	±	0.08
N194A(N ^{2.60} A)	6.05*	±	0.34	6.41*	±	0.30
K220A(K ^{3.30} A)	5.96*	±	0.23	6.28*	±	0.16
H223A(H ^{3.33} A)	6.81	±	0.21	7.64	±	0.19
H226A(H ^{3.36} A)	7.20	±	0.15	7.87	±	0.15
Q227A(Q ^{3.37} A)	7.53	±	0.24	7.71	±	0.25
M230A(M ^{3.40} A)	7.58	±	0.33	7.34	±	0.57
N233A(N ^{3.43} A)	6.21*	±	0.39	6.15*	±	0.31
Y234A(Y ^{3.44} A)	6.53	±	0.42	7.34	±	0.40
I301A(I ^{5.39} A)	6.76	±	0.39	6.31*	±	0.39
H302A(H ^{5.40} A)	6.34*	±	0.54	N.D.		
V305A(V ^{5.43} A)	7.32	±	0.23	7.44	±	0.28
M306A(M ^{5.44} A)	7.10	±	0.21	6.96	±	0.22
Q355A(Q ^{6.52} A)	5.79*	±	0.37	7.06	±	0.29
F356A(F ^{6.53} A)	6.29*	±	0.31	6.85*	±	0.24
F359A(F ^{6.56} A)	6.55	±	0.35	7.08	±	0.20
P360A(P ^{6.57} A)	6.53	±	0.28	6.75*	±	0.27
W361A(W ^{6.58} A)	6.54	±	0.41	6.63*	±	0.27
P363A(P ^{6.60} A)	N.D.			N.D.		
D373A(D ^{7.39} A)	N.D.			N.D.		
M376A(M ^{7.42} A)	6.30	±	0.36	6.94	±	0.21
H377A(H ^{7.43} A)	6.97	±	0.22	7.13	±	0.33
I380A(I ^{7.46} A)	7.89	±	0.18	7.08	±	0.24
Q383A(Q ^{7.49} A)	6.62	±	0.31	7.00	±	0.20

cAMP formation for the wild type receptor in the presence of either α CGRP or rAMY was fitted using three-parameter logistic equation to determine the maximum response defined by the curve fit. All data were normalized to this WT receptor response. The Black and Leff operational model, with a hill slope of 1, was applied to separate efficacy (τ) and functional affinity (pK_A). All values are mean±S.E.M. of 3 to 5 independent experiments conducted in duplicate. Significance of changes in pK_A were calculated via comparison of mutant pK_A values to the WT pK_A in a one-way analysis of variance (ANOVA) with Dunett's post-hoc test with significant changes ($P<0.05$ denoted by *).

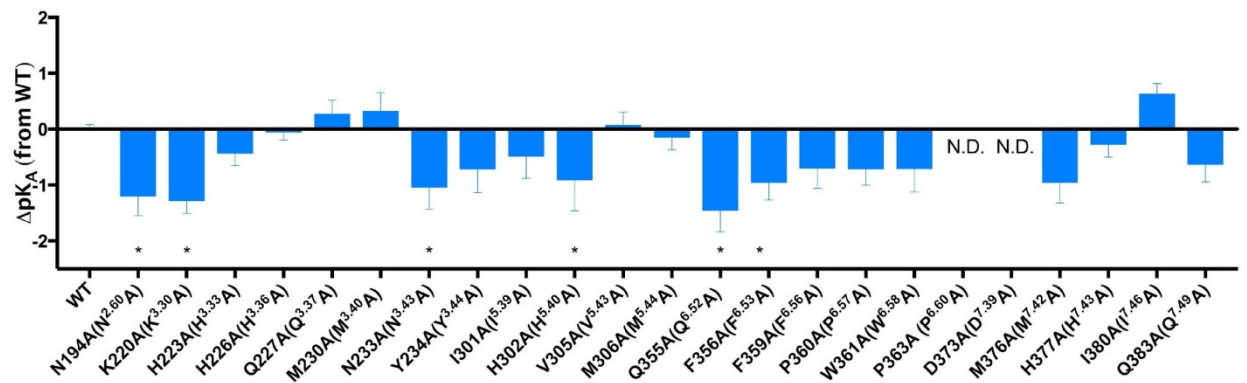


Figure 4.18. cAMP ΔpK_A values for α CGRP. ΔpK_A value for each mutant was obtained by subtracting WT pK_A from each mutant's pK_A value. All values are mean+S.E.M. of 3 to 5 independent experiments conducted in duplicate. Significance of changes were calculated via comparison of mutants to the WT receptor pK_A values in a one-way analysis of variance (ANOVA) with Dunnett's post-hoc test with significant changes ($P < 0.05$ denoted by *).

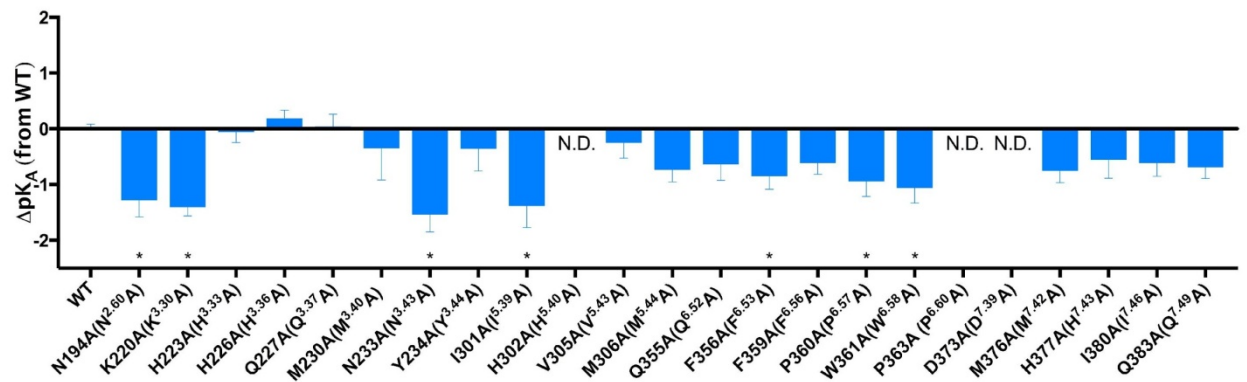


Figure 4.19. cAMP ΔpK_A values for rAMY. ΔpK_A value for each mutant was obtained by subtracting WT pK_A from each mutant's pK_A value. All values are mean+S.E.M. of 3 to 5 independent experiments conducted in duplicate. Significance of changes were calculated via comparison of mutants to the WT receptor pK_A values in a one-way analysis of variance (ANOVA) with Dunnett's post-hoc test with significant changes ($P < 0.05$ denoted by *).

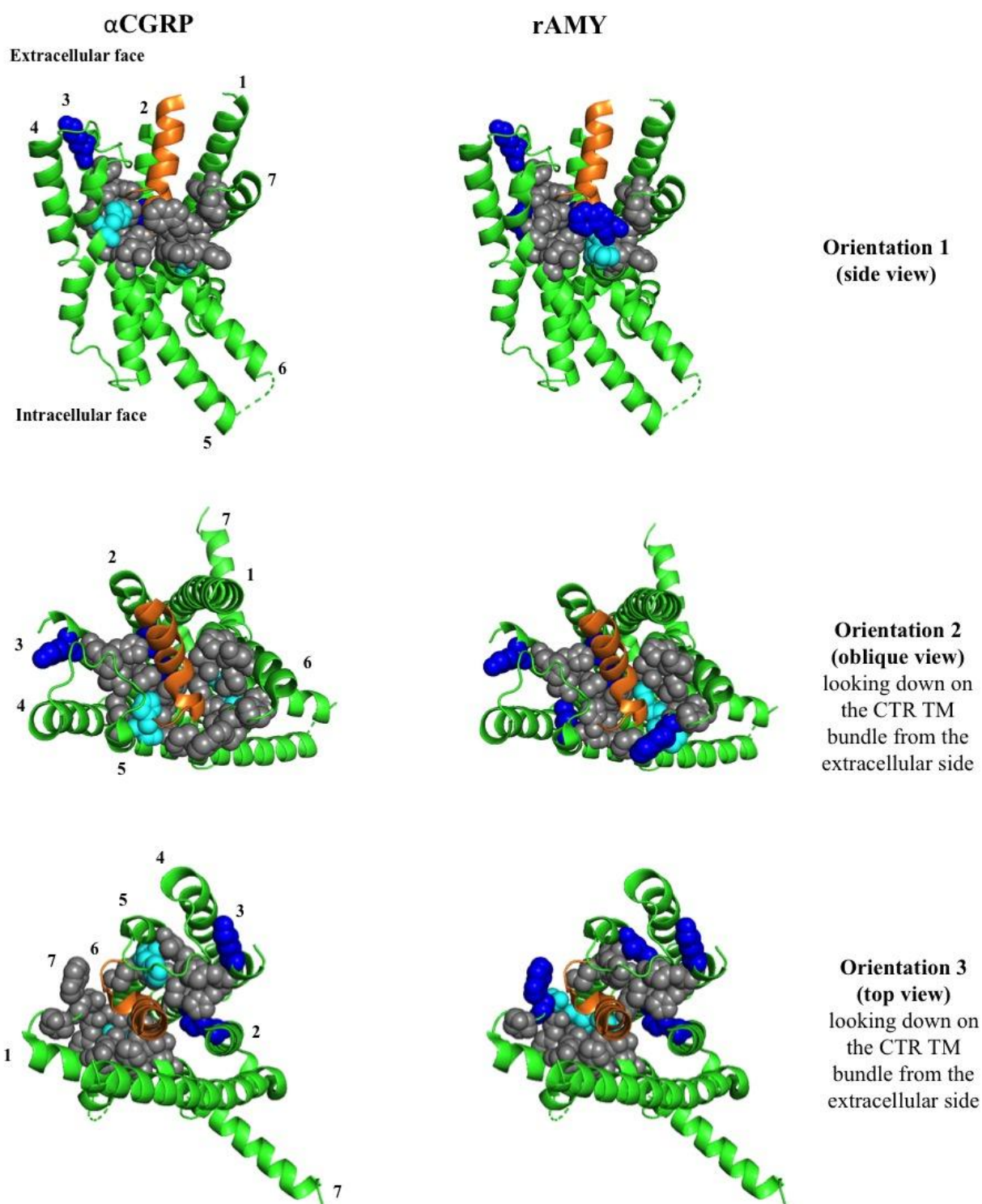


Figure 4.20. Effect of the CTR TM mutations on cAMP pK_A for α CGRP and rAMY. Residues are mapped onto a CTR active Cryo-EM structure in complex with sCT and G_s protein (G_s protein and CTR N-terminal domain are not shown) (Dal Maso et. al., 2019). The receptor is shown in green and sCT ligand is shown in orange. Residues that produced significant changes in functional affinity pK_A were coloured in either cyan (<10 decrease in pK_A) or in blue (>10 decrease in pK_A) and are shown as space-fill side chains. Residues that produced no significant change in efficacy were coloured in grey.

4.2.4 EFFECTS OF THE CTR TM MUTATIONS ON CTR pERK1/2 FUNCTIONAL AFFINITY

A high concentration of agonist (0.1 μ M for sCT and 1 μ M for hCT, pCT, α CGRP and rAMY) was used in time course studies to determine the peak response for WT and mutants in pERK1/2 phosphorylation (for traces see chapter 5 (Figures 5.10 – 5.12 and 5.21 – 5.22)). None of the mutants where a response could be detected displayed altered response kinetics. Concentration response curves were generated for each of the mutants and wild type and operational fitting was performed (Figures 4.21 – 4.25). pK_A values are reported in the Table 4.4. As pERK1/2 coupling was relatively weak, operational fitting was not carried out where there was inadequate data to support that the curve fit had passed the second inflection point such that there was limited confidence in the curve-fit estimate for the E_{max} . These included: F359A ($F^{6.56}A$) and M376A ($M^{7.42}A$) (for sCT); Y234A ($Y^{3.44}A$), F359A ($F^{6.56}A$), P360A ($P^{6.57}A$), W361A ($W^{6.58}A$), D373A ($D^{7.39}A$) and M376A ($M^{7.42}A$) (for hCT); H223A ($H^{3.33}A$), H226A ($H^{3.36}A$), N233A ($N^{3.43}A$), F359A ($F^{6.56}A$), P360A ($P^{6.57}A$), and M376A ($M^{7.42}A$) (for pCT); N194A ($N^{2.60}A$), K220A ($K^{3.30}A$), N223A ($H^{3.33}A$), I301A ($I^{5.39}A$), M306A ($M^{5.44}A$), Q355A ($Q^{6.52}A$), P360A ($P^{6.57}A$), P363A ($P^{6.60}A$), D373A ($D^{7.39}A$) and M376A ($M^{7.42}A$) (for α CGRP); H226A ($H^{3.36}A$), N233A ($N^{3.43}A$), H302A ($H^{5.40}A$), V305A ($V^{5.43}A$), Q355A ($Q^{6.52}A$), P360A ($P^{6.57}A$), W361A ($W^{6.58}A$), P363A ($P^{6.60}A$), D373A ($D^{7.39}A$), M376A ($M^{7.42}A$) and Q383A ($Q^{7.49}A$) (for rAMY) (Table 4.4, Figures 4.21 – 4.25). ΔpK_A value for each mutant was obtained by subtracting WT pK_A from each mutant's pK_A value (Figures 4.26 – 4.30).

For those mutants where operational modelling could be performed, there were selective significant effects detected with some mutants for sCT and rAMY relative to WT (Table 4.4, Figures 4.26, 4.30). For sCT, K220A ($K^{3.30}A$), I301A ($I^{5.39}A$) and H302A ($H^{5.40}A$) increased pERK1/2 pK_A by 59-fold, 158-fold and 59-fold, respectively (Figure 4.26). N194A ($N^{2.60}A$), Y234A ($Y^{3.44}A$) and M306A ($M^{5.44}A$) decreased pK_A for rAMY for 49-fold, 48-fold and 32-fold, respectively (Figure 4.30). Other mutants such as K220A ($K^{3.30}A$), M230A ($M^{3.40}A$), M306A ($M^{5.44}A$), F356A ($F^{6.53}A$), Q383A ($Q^{7.49}A$) (for both hCT, pCT), H223A ($H^{3.33}A$) (for hCT) and Q227A ($Q^{3.37}A$) (for pCT) displayed trends for increased pERK1/2 functional affinity. While Q227A ($Q^{3.37}A$), H377A (for hCT); P363A ($P^{6.60}A$) (for both hCT and pCT); and Y234A ($Y^{3.44}A$) (for pCT), trended towards decreased functional affinity (Table 4.4, Figures 4.27 – 4.28).

Mapping of the significant mutational effects for sCT and rAMY for the pERK1/2 pathway revealed distinct patterns of residues, while these effects were also of opposite directions (Figures 4.31, 4.32).

When comparing data between all CTR agonists, for the shared transducer slope n for CTs we saw that α CGRP and rAMY had apparent higher functional affinity in pERK1/2 compared to calcitonin agonists. Additionally, CT agonists had a general trend towards increased functional pK_A in pERK1/2 response for the CTR mutants whereas α CGRP and rAMY generally reduced pERK1/2 functional pK_A .

In order to accommodate both biphasic and monophasic concentration response curves seen in pERK1/2 for CT agonists (for pERK1/2 concentration response curves see chapter 5 (Figures 5.13 – 5.15)), we considered a number of ways to fit these data onto the operational model. The operational model assumes a common mechanism for ligands/mutations under investigation; it is therefore not possible to fit this model to a mixture of mono- and bi-phasic curves. In the original analysis (for the data described above) we used the operational fit where the transducer slope (n) was shared between all data sets for each CT agonist (in order to account for a common mechanism between mutant and the WT receptors) and the system E_{max} was set to 140 (based on pERK1/2 maximum response detected in my experiments). The limitation of this fit is, however, an apparent underestimate in the pK_A values at the WT receptor (between 6.2 and 6.6 for CT agonists). As an alternative fit we used the operational model with a shared transducer slope constrained to 0.4 (this was determined based on the hill slope obtained using 4-parameter fit for CT agonists at the WT receptor) and a system E_{max} constrained to 200 (previously used in (Dal Maso *et al.*, 2018, Dal Maso *et al.*, 2019) (Supplementary figures 1 – 3, Appendix 1). By constraining the transducer slope to 0.4 we, therefore, prioritised the transducer slope to fit the WT data as our reference control. The alternative operational fit resulted in higher apparent pK_A values for the WT (7.5 for all three CT agonists) and therefore in a slightly different pattern for ΔpK_A values, with the majority of mutants slightly decreasing (non-significantly) pK_A across all three CT agonists relative to the WT (Supplementary figure 4, Appendix 1). K220A ($K^{3.30}A$), I301A ($I^{5.39}A$) and H302A ($H^{5.40}A$), which under the shared transducer fit, had increased pK_A relative to the WT for sCT, still exhibited an increased pK_A but with reduced magnitude (6-fold, 10-fold and 5-fold, respectively, (Supplementary figures 1 and 4, Appendix 1). The pattern of effects was also more similar to the one seen for α CGRP and rAMY agonists, with the same overall direction of effects towards decreased pK_A (Figures 4.29 – 4.30, Supplementary figure 4, Appendix 1).

Table 4.4. Effect of single alanine mutation in the CTR TM region on pERK1/2 functional affinity (pK_A)

	pK_A sCT	pK_A hCT	pK_A pCT	pK_A α CGRP	pK_A rAMY
WT	6.23 \pm 0.32	6.63 \pm 0.24	6.36 \pm 0.39	7.58 \pm 0.13	7.67 \pm 0.10
N194A (N ^{2.60} A)	6.50 \pm 0.71	6.52 \pm 0.94	6.61 \pm 1.07	N.D.	5.97* \pm 1.16
K220A (K ^{3.30} A)	8.00* \pm 0.33	7.35 \pm 0.62	7.54 \pm 0.51	N.D.	7.19 \pm 0.52
H223A (H ^{3.33} A)	6.97 \pm 0.33	6.80 \pm 0.35	N.D.	7.58 \pm 0.59	6.75 \pm 0.25
H226A (H ^{3.36} A)	6.86 \pm 0.51	6.43 \pm 0.61	N.D.	7.20 \pm 0.79	N.D.
Q227A (Q ^{3.37} A)	7.03 \pm 0.29	6.21 \pm 0.47	6.82 \pm 0.39	7.47 \pm 0.59	6.49 \pm 0.35
M230A (M ^{3.40} A)	7.38 \pm 0.32	7.33 \pm 0.34	7.08 \pm 0.43	7.55 \pm 0.66	7.09 \pm 0.28
N233A (N ^{3.43} A)	6.61 \pm 0.88	6.82 \pm 0.85	N.D.	N.D.	N.D.
Y234A (Y ^{3.44} A)	7.02 \pm 0.34	N.D.	6.01 \pm 0.83	7.08 \pm 0.94	5.98* \pm 0.42
I301A (I ^{5.39} A)	8.42* \pm 0.39	7.63 \pm 0.56	7.58 \pm 0.56	N.D.	6.95 \pm 0.66
H302A (H ^{5.40} A)	8.00* \pm 0.40	6.96 \pm 0.61	6.65 \pm 0.63	6.87 \pm 0.94	N.D.
V305A (V ^{5.43} A)	6.74 \pm 0.45	6.94 \pm 0.49	6.25 \pm 0.77	6.99 \pm 0.58	N.D.
M306A (M ^{5.44} A)	6.88 \pm 0.42	7.02 \pm 0.49	6.65 \pm 0.63	N.D.	6.15* \pm 0.67
Q355A (Q ^{6.52} A)	6.38 \pm 0.72	6.75 \pm 0.52	7.08 \pm 0.63	N.D.	N.D.
F356A (F ^{6.53} A)	7.72 \pm 0.38	7.78 \pm 0.50	7.35 \pm 0.56	7.28 \pm 0.60	7.37 \pm 0.56
F359A (F ^{6.56} A)	N.D.	N.D.	N.D.	6.77 \pm 0.72	7.26 \pm 0.49
P360A (P ^{6.57} A)	6.07 \pm 0.58	N.D.	N.D.	N.D.	N.D.
W361A (W ^{6.58} A)	5.96 \pm 0.75	N.D.	6.19 \pm 0.78	6.76 \pm 0.70	N.D.
P363A (P ^{6.60} A)	6.40 \pm 0.44	5.68 \pm 0.93	5.99 \pm 0.86	N.D.	N.D.
D373A (D ^{7.39} A)	6.36 \pm 0.64	N.D.	6.30 \pm 1.03	N.D.	N.D.
M376A (M ^{7.42} A)	N.D.	N.D.	N.D.	N.D.	N.D.
H377A (H ^{7.43} A)	6.19 \pm 0.50	6.00 \pm 0.64	6.50 \pm 0.70	6.93 \pm 0.50	6.91 \pm 0.34
I380A (I ^{7.46} A)	6.54 \pm 0.47	6.77 \pm 0.45	6.65 \pm 0.67	7.08 \pm 0.44	7.12 \pm 0.66
Q383A (Q ^{7.49} A)	7.73 \pm 0.62	7.67 \pm 0.65	7.47 \pm 0.76	7.07 \pm 1.23	N.D.

*pERK1/2 response in the presence of CTR agonists (sCT, hCT, pCT, α CGRP and rAMY) was fit using Black and Leff operational model to derive pK_A values. All values are mean+S.E.M. of 3 to 5 independent experiments conducted in duplicate. Significance of changes in pK_A values were calculated via comparison of mutant pK_A values to the WT pK_A in a one-way Anova analysis of variance with Dunett's post-hoc test with significant changes $P < 0.05$ denoted by *.*

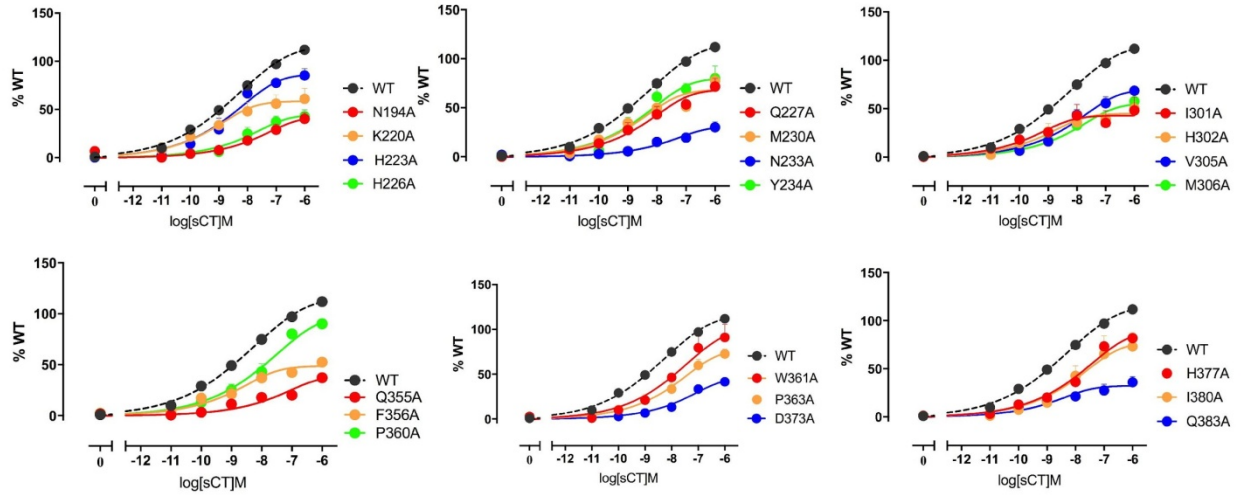


Figure 4.21. *pERK1/2* concentration response to sCT in CV-1-FlpIn cells stably expressing hCTRαLeu mutations in the receptor TM region. *pERK1/2* response in the presence of sCT was fit using Black and Leff operational model with hill slope (*n*) shared across all datasets and normalized to WT receptor response. All values are mean + S.E.M. of 3 to 5 independent experiments conducted in duplicate; for some data points error bars are not shown as they are smaller than the height of the symbol.

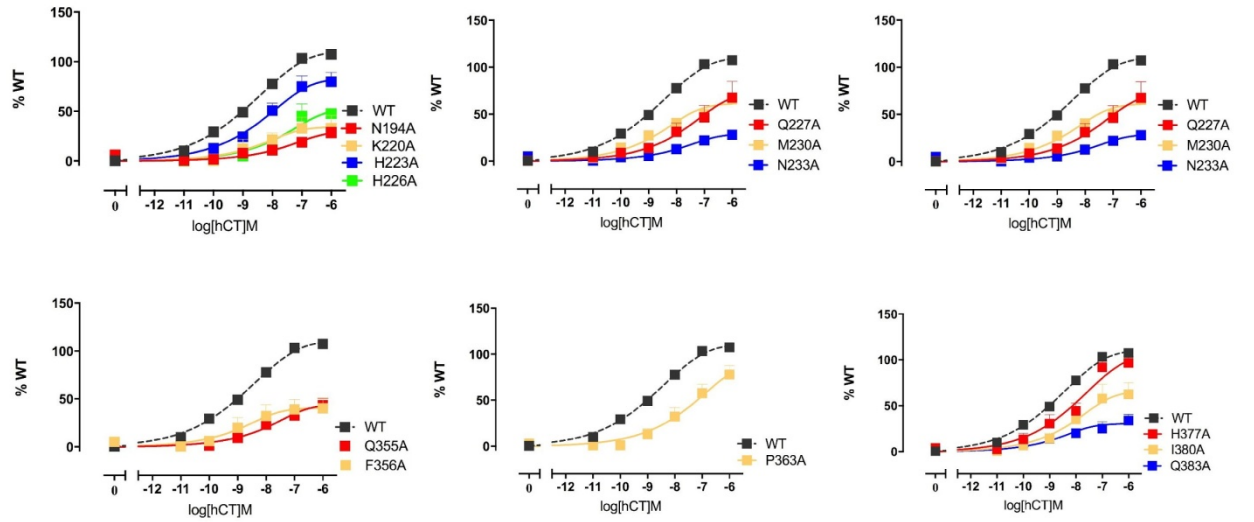


Figure 4.22. *pERK1/2* concentration response to hCT in CV-1-FlpIn cells stably expressing hCTRαLeu mutations in the receptor TM region. *pERK1/2* response in the presence of sCT was fit using Black and Leff operational model with hill slope (*n*) shared across all datasets and normalized to WT receptor response. All values are mean + S.E.M. of 3 to 5 independent experiments conducted in duplicate; for some data points error bars are not shown as they are smaller than the height of the symbol.

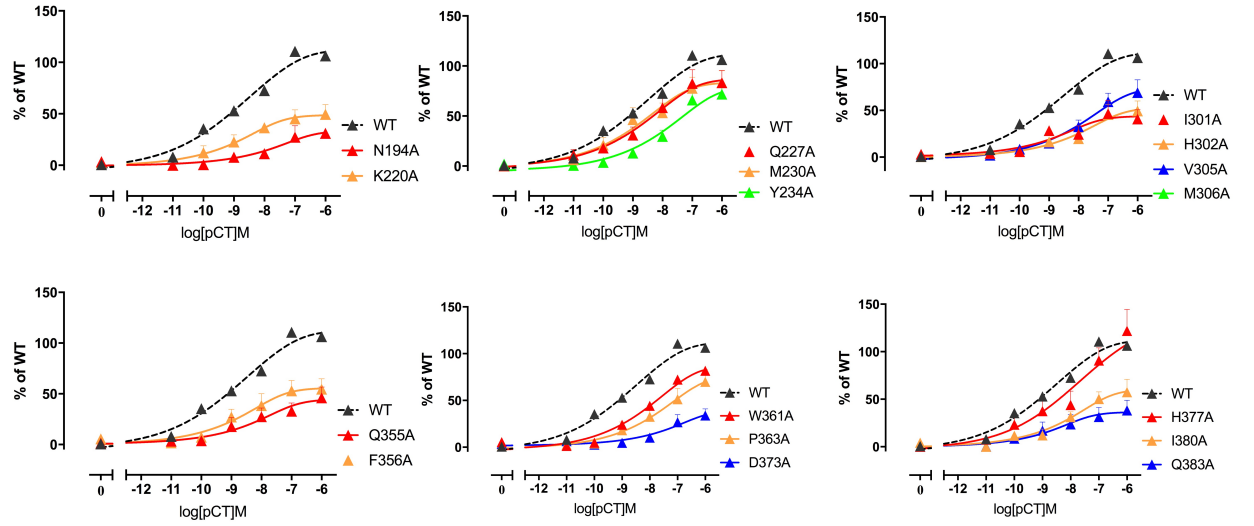


Figure 4.23. pERK1/2 concentration response to pCT in CV-1-FlpIn cells stably expressing hCTRaLeu mutations in the receptor TM region. pERK1/2 response in the presence of pCT was fit using Black and Leff operational model with hill slope (n) shared across all datasets and normalized to WT receptor response. All values are mean \pm S.E.M. of 3 to 5 independent experiments conducted in duplicate; for some data points error bars are not shown as they are smaller than the height of the symbol.

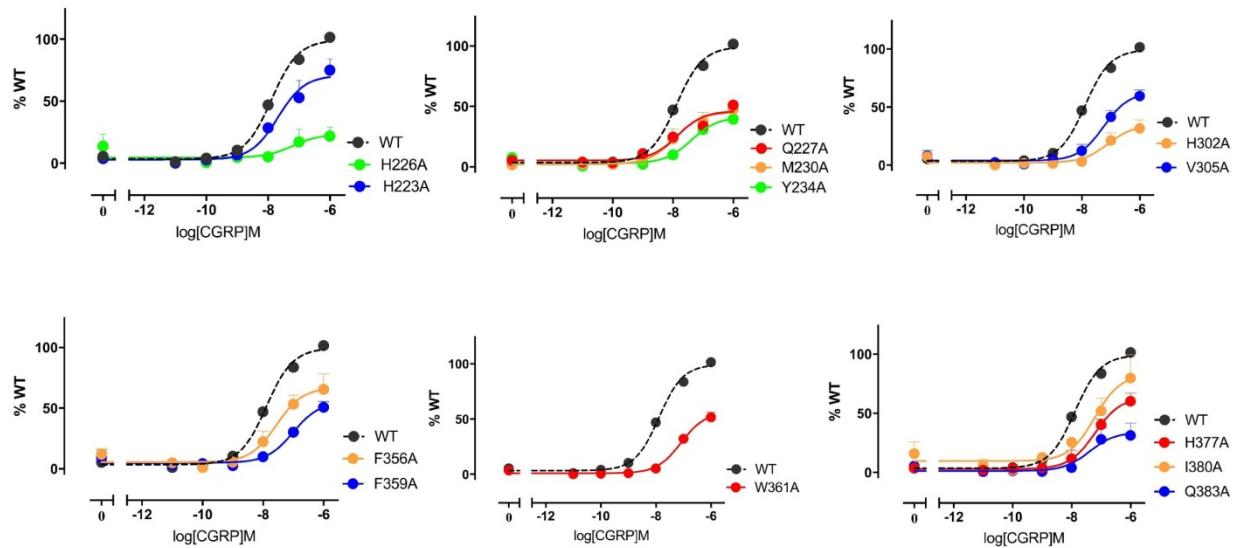


Figure 4.24. pERK1/2 concentration response to α CGRP in CV-1-FlpIn cells stably expressing hCTRaLeu single alanine mutations in the receptor TM region. pERK1/2 response in the presence of α CGRP was fit using three parameter logistic equation and normalized to WT receptor response. The Black and Leff operational model, with a hill slope of 1, was applied to separate efficacy (τ) and functional affinity (pK_A). All values are mean \pm S.E.M. of 3 to 5 independent experiments conducted in duplicate; for some data points error bars are not shown as they are smaller than the height of the symbol.

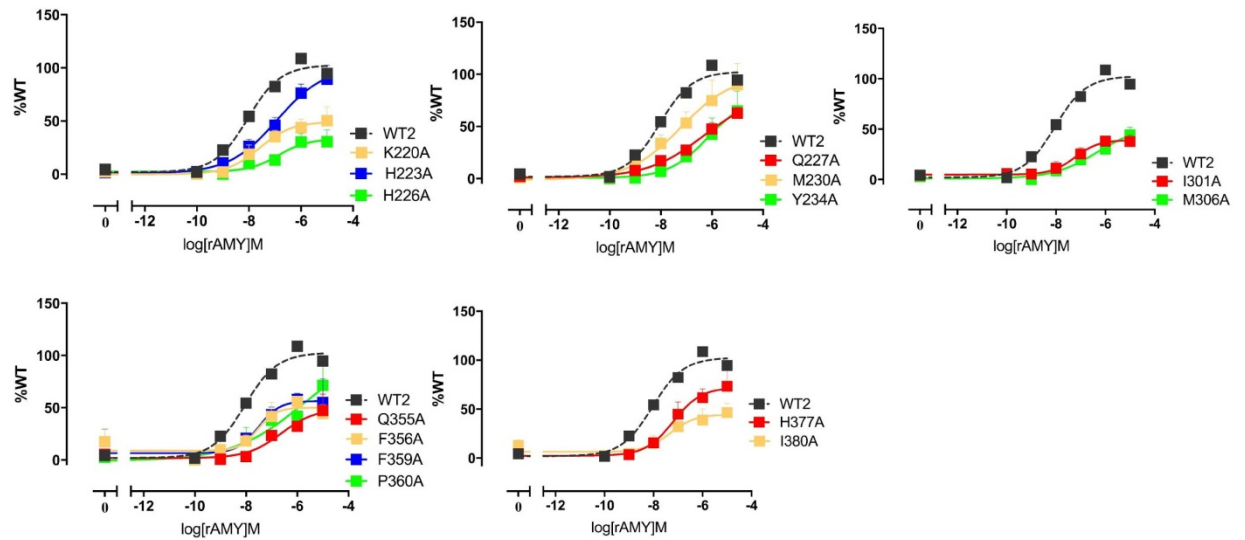


Figure 4.25. *pERK1/2* concentration response to *rAMY* in *CV-1-FlpIn* cells stably expressing *hCTR α Leu* single alanine mutations in the receptor TM region. *cAMP* formation in the presence of *rAMY* was fit using three parameter logistic equation and normalized to WT receptor response. The Black and Leff operational model, with a hill slope of 1, was applied to separate efficacy (τ) and functional affinity (pK_A). All values are mean \pm S.E.M. of 3 to 5 independent experiments conducted in duplicate; for some data points error bars are not shown as they are smaller than the height of the symbol.

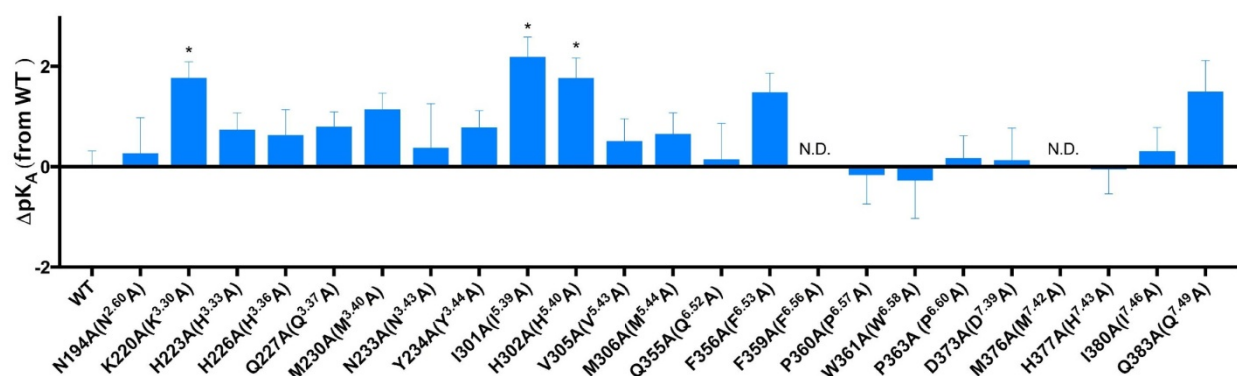


Figure 4.26. *p*ERK1/2 ΔpK_A values for sCT. ΔpK_A value for each mutant was obtained by subtracting WT pK_A from each mutant's pK_A value. All values are mean+S.E.M. of 3 to 5 independent experiments conducted in duplicate. Significance of changes were calculated via comparison of mutants to the WT receptor pK_A values in a one-way analysis of variance (ANOVA) with Dunett's post-hoc test with significant changes ($P < 0.05$ denoted by *).

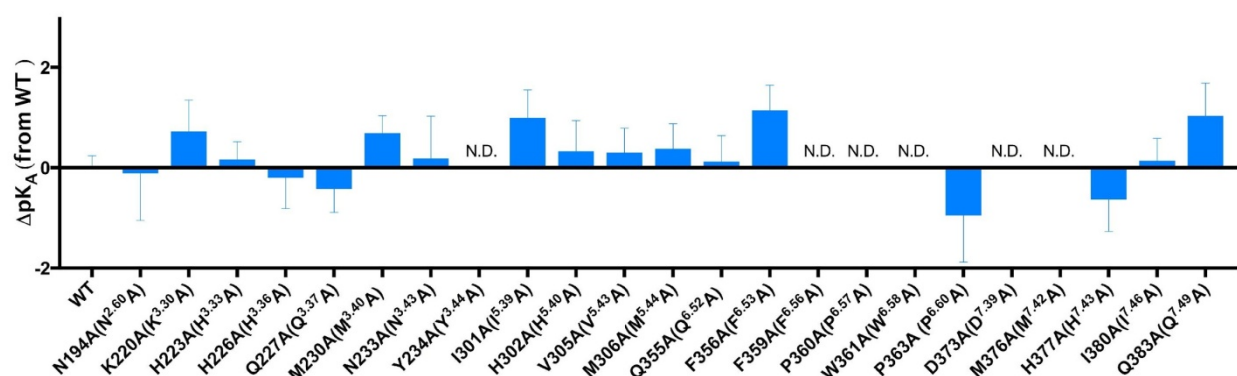


Figure 4.27. *p*ERK1/2 ΔpK_A values for hCT. ΔpK_A value for each mutant was obtained by subtracting WT pK_A from each mutant's pK_A value. All values are mean+S.E.M. of 3 to 5 independent experiments conducted in duplicate. Significance of changes were calculated via comparison of mutants to the WT receptor pK_A values in a one-way analysis of variance (ANOVA) with Dunett's post-hoc test with significant changes ($P < 0.05$ denoted by *).

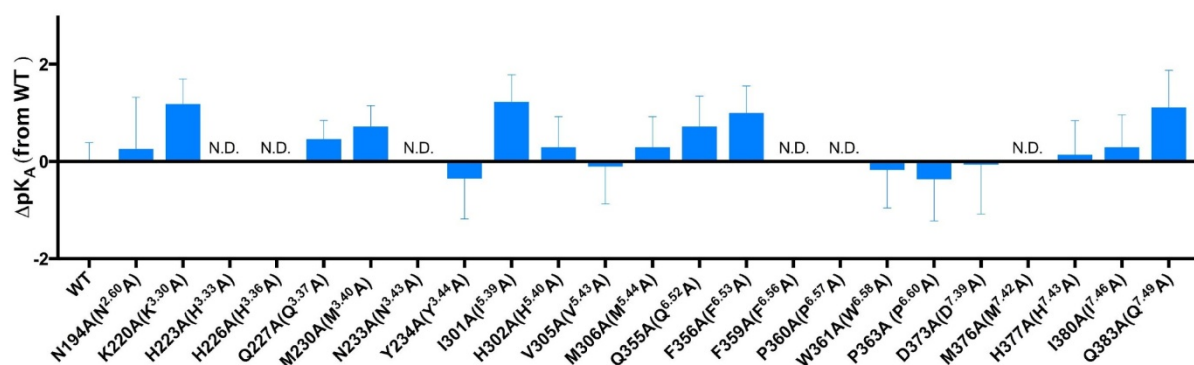


Figure 4.28. *p*ERK1/2 ΔpK_A values for pCT. ΔpK_A value for each mutant was obtained by subtracting WT pK_A from each mutant's pK_A value. All values are mean+S.E.M. of 3 to 5 independent experiments conducted in duplicate. Significance of changes were calculated via comparison of mutants to the WT receptor pK_A values in a one-way analysis of variance (ANOVA) with Dunett's post-hoc test with significant changes ($P < 0.05$ denoted by *).

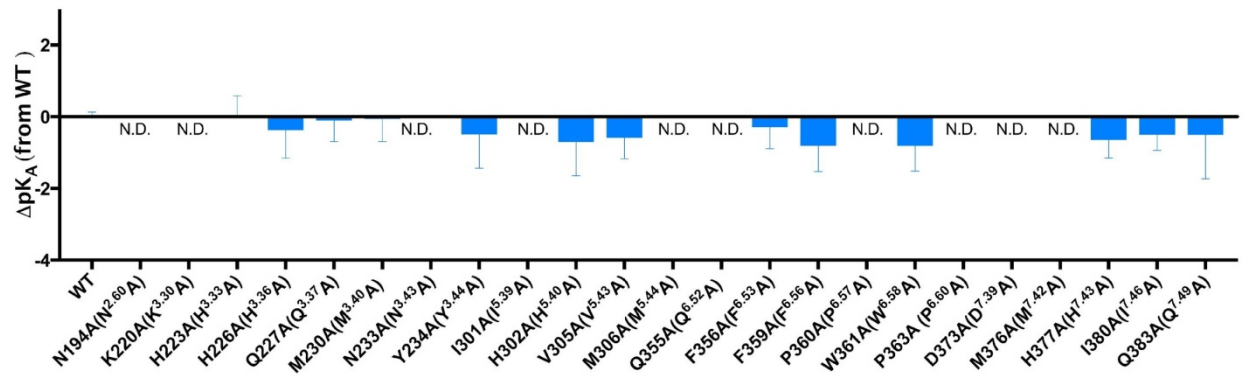


Figure 4.29. pERK1/2 ΔpK_A values for α CGRP. ΔpK_A value for each mutant was obtained by subtracting WT pK_A from each mutant's pK_A value. All values are mean+S.E.M. of 3 to 5 independent experiments conducted in duplicate. Significance of changes were calculated via comparison of mutants to the WT receptor pK_A values in a one-way analysis of variance (ANOVA) with Dunett's post-hoc test with significant changes ($P < 0.05$ denoted by *).

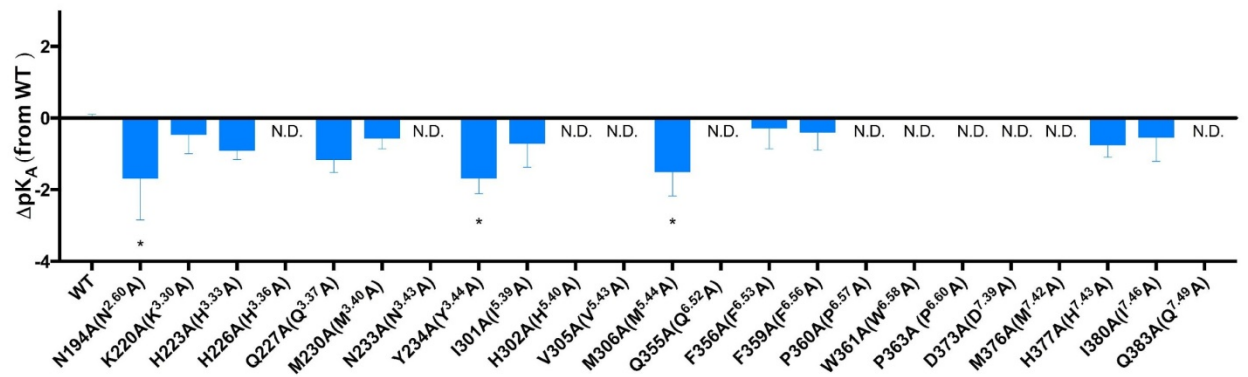


Figure 4.30. pERK1/2 ΔpK_A values for rAMY. ΔpK_A value for each mutant was obtained by subtracting WT pK_A from each mutant's pK_A value. All values are mean+S.E.M. of 3 to 5 independent experiments conducted in duplicate. Significance of changes were calculated via comparison of mutants to the WT receptor pK_A values in a one-way analysis of variance (ANOVA) with Dunett's post-hoc test with significant changes ($P < 0.05$ denoted by *).

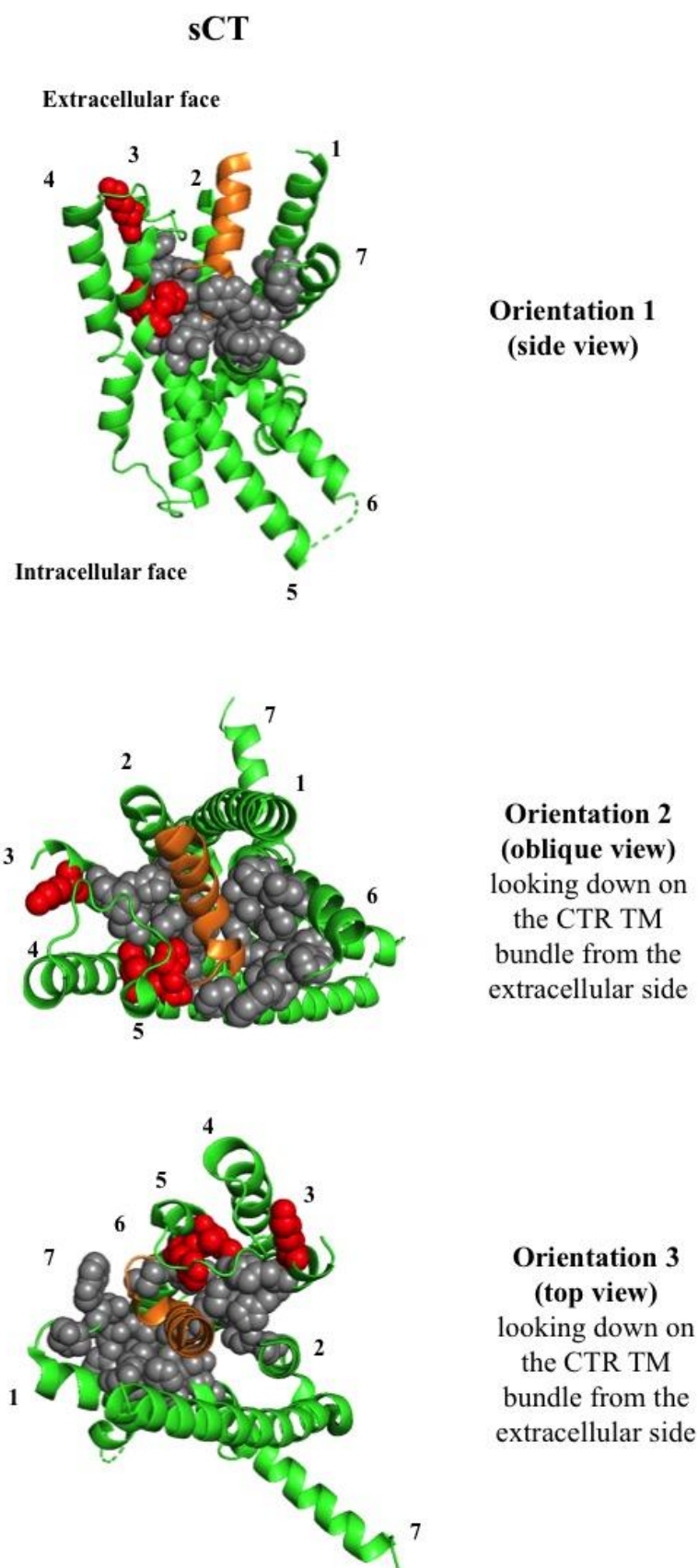
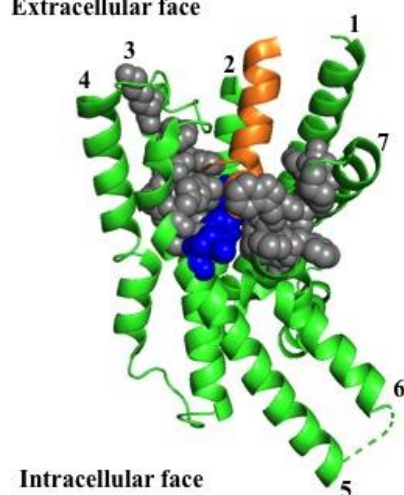


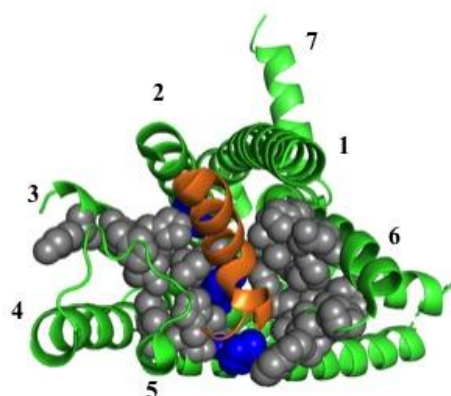
Figure 4.31. Effect of the CTR TM mutations on pERK1/2 affinity pK_A for sCT. Residues are mapped onto a CTR active Cryo-EM structure of CTR in complex with sCT and G_s protein (G_s protein is not shown, CTR N-terminal domain not shown) (Dal Maso et. al., 2019). The receptor is shown in green and sCT ligand is shown in orange. Residues that significantly increased pK_A (>10 increase in pK_A) are shown as space-fill side chains and were coloured in red. Residues that produced no significant change in affinity were coloured in gray.

rAMY

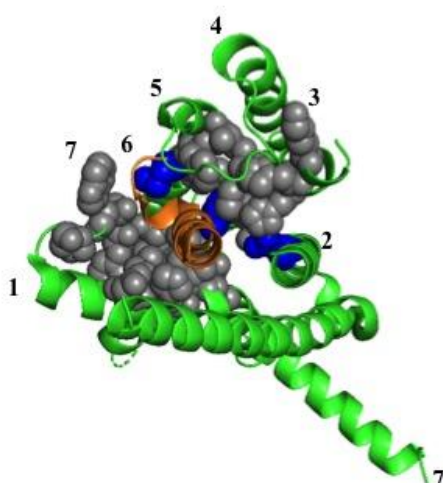
Extracellular face



Orientation 1
(side view)



Orientation 2
(oblique view)
looking down on
the CTR TM
bundle from the
extracellular side



Orientation 3
(top view)
looking down on
the CTR TM
bundle from the
extracellular side

Figure 4.32. Effect of the CTR TM mutations on pERK1/2 pK_A for rAMY. Residues are mapped onto a CTR active Cryo-EM structure of CTR in complex with sCT and G_s protein (G_s protein is not shown, CTR N-terminal domain not shown) (Dal Maso et. al., 2019). The receptor is shown in green and sCT ligand is shown in orange. Residues that significantly decreased pK_A (>10 decrease in pK_A) are shown as space-fill side chains and were coloured in blue. Residues that produced no significant change in affinity were coloured in gray.

4.3 DISCUSSION

4.3.1 EFFECTS OF THE CTR TM MUTATIONS ON CTR CELL SURFACE EXPRESSION

GPCR synthesis, folding and assembly starts in the endoplasmic reticulum, from endoplasmic reticulum properly folded receptors are targeted to Golgi apparatus where they become fully processed and are further targeted to plasma membrane (Dong *et al.*, 2007, Suzuki *et al.*, 2018). Poor cell surface expression observed for many of the studied mutants implies these residues are likely essential for proper folding and trafficking to plasma membrane. Alternatively, these residues could be also involved in maintaining receptor stability at the cell surface.

Mutations of residues that are a part of the central polar network resulted in significantly decreased cell surface expression: 20-50% of the WT (N194A (N^{2.60}A), N233A (N^{3.43}A) and Q383A (Q^{7.49}A); with no expression detected for Q355A (Q^{6.52}A) (Figures 4.2, 4.3). This is consistent with the central polar network being important for receptor stability and is consistent with corresponding mutations at the GLP-1R (Wootten *et al.*, 2013, Wootten *et al.*, 2016a, Wootten *et al.*, 2016b) and GCGR (as reviewed by (Siu *et al.*, 2013a)) as well as the structural data and computational data, which supports that these residues do, indeed form a polar stabilising network. In contrast mutation of same residues in GIPR did not significantly affect cell surface expression in transient transfection experiments (Yaqub *et al.*, 2010).

A subset of identical mutations that are described in this chapter were previously characterised and published by our lab as a part of a mutational study on ECL2/ECL3 of the CTR, for which cell lines were made as a separate transfection (Dal Maso *et al.*, 2018b). For F356A (F^{6.53}A), F359A (F^{6.56}A), P360A (P^{6.57}A), W361A (W^{6.58}A) there was no difference in the cell surface expression between studies. P363A (P^{6.60}A), D373A (D^{7.39}A) and M376A (M^{7.42}A) mutants showed significantly decreased cell surface expression compared to the WT in the current study, which is in contrast to the previous results where same mutations displayed receptor expression at levels not significantly different from the WT (with P363A (P^{6.60}A) having slightly reduced expression, at 81% of the WT) (Figure 4.2) (Dal Maso *et al.*, 2018b). In both studies cell lines were made using FlpIn system in which there is isogenic integration of the transgene. An additional integration of the gene of interest into a random gene location is unlikely, however could not be completely excluded. If this was the case, and CTR genes were integrated at an alternative site of the genome during transfections, that could potentially affected CTR gene expression levels and result in such discrepancy in CTR expression levels for the same mutants. Alternatively, the FlpIN CV-1 cell line may exhibit some heterogeneity with respect to the degree to which the FlpIN locus is accessible to the transcriptional machinery.

Regardless, all efficacy values for both studies were corrected for cell surface expression to allow appropriate comparison of derived pharmacological parameters independent of cell surface expression.

4.3.2 EFFECTS OF CTR TM MUTATIONS ON CALCITONIN AGONISTS EQUILIBRIUM AND FUNCTIONAL cAMP AFFINITY

Conformational selection is a model for describing the effect of the ligand on the distribution of the equilibrium between different energy states of a protein. According to this model, the unliganded receptor samples several distinct conformations, one or more of which is preferentially bound by a particular ligand. The effect of ligand binding is to shift the receptor conformational equilibrium towards a specific conformation (Deupi *et al.*, 2010, Sauliere *et al.*, 2012, Mary *et al.*, 2013). Since the agonist and transducer are allosterically coupled, this model may be extended to argue that a particular active receptor conformation will not only depend on the agonist but also on the particular transducer to which agonist-receptor complex is coupled (De Lean *et al.*, 1980, Furness *et al.*, 2016). Functional affinity (pK_A) describes the affinity of an agonist for the receptor when coupled to a particular pathway. Global (or equilibrium) affinity pK_i measures the strength of the binding interaction between a ligand and the receptor and is agnostic of whether the receptor is coupled to a transducer. The pK_i derived from experiments at equilibrium on whole cells is therefore a composite of all possible receptor affinity states and it is independent of coupling to a specific signalling pathway. Comparing cAMP pK_A data against the pK_i , allows a comparison between overall affinity effects and those effects that are related specifically to G_s coupling.

The central polar network ($N^{2.60}$, $N^{3.43}$, $Y^{3.44}$, $Q^{6.52}$ and $Q^{7.49}$) is conserved across class B GPCRs. $R^{2.60}$ in GLP-1R is predicted to form hydrogen bonds with the 3rd amino acid, E^9 , of the GLP-1 (Zhang *et al.*, 2017b, Wootten *et al.*, 2017). Whereas, due to a shallower binding pocket of the CTR, the central polar network sits one helical turn below the sCT binding pocket, which precludes these residues from forming direct interaction with the ligand (Figure 4.33). These differences in positioning of the central polar network relative to the binding pockets of CTR and GLP-1R imply different modes of interactions between the network residues and agonists for each receptor.

Ligand-specific effects on affinity were observed for a number of the central polar network residues in the CTR. One example is mutation of N194A ($N^{2.60}$ A) that resulted in significantly decreased pK_i of the antagonist probe sCT(8-32), hCT, pCT but not for full length sCT (Figures 4.11 – 4.14). The crystal structure of sCT(8-32) solved with the CTR NTD supports the role of CTR NTD in sCT(8-32) binding (Johansson *et al.*, 2016). Given the

positioning of N194A (N^{2.60}A) in the binding pocket relative to the peptide N-terminus (Figure 4.34), as well as the fact that sCT(8-32) does not contain the residues 1 – 7, still binds the CTR with high affinity (approx. 10-fold lower than sCT), and that N194A decreases sCT(8-32) affinity suggests there is an allosteric interaction between N194A (N^{2.60}A) and the extracellular face of the receptor. On the other hand, the fact that this residue was important for sCT(8-32), hCT and pCT pK_i, but not important for full length sCT indicates differential importance for the parts of the receptor responsible for high affinity engagement of sCT versus sCT(8-32), hCT and pCT. There was little variation between absolute values of cAMP levels at vehicle concentration of agonists between WT and mutant receptors, suggesting little difference between the level of the mutants' and WT CTR constitutive activity. Although there is some literature data suggesting that sCT(8-32) can act as an inverse agonist in the cell system with constitutive activity (Pozvek *et al.*, 1997), the data from our laboratory suggests that sCT(8-32) is a very weak partial agonist (unpublished). If sCT(8-32) were an inverse agonist, under the cubic ternary model, it would be expected to favour binding to the inactive state over the active state and hence for the mutant that increases receptor constitutive activity sCT(8-32) would have a reduced affinity. While N194A has reduced affinity to sCT(8-32), it's constitutive activity is no different from the WT CTR.

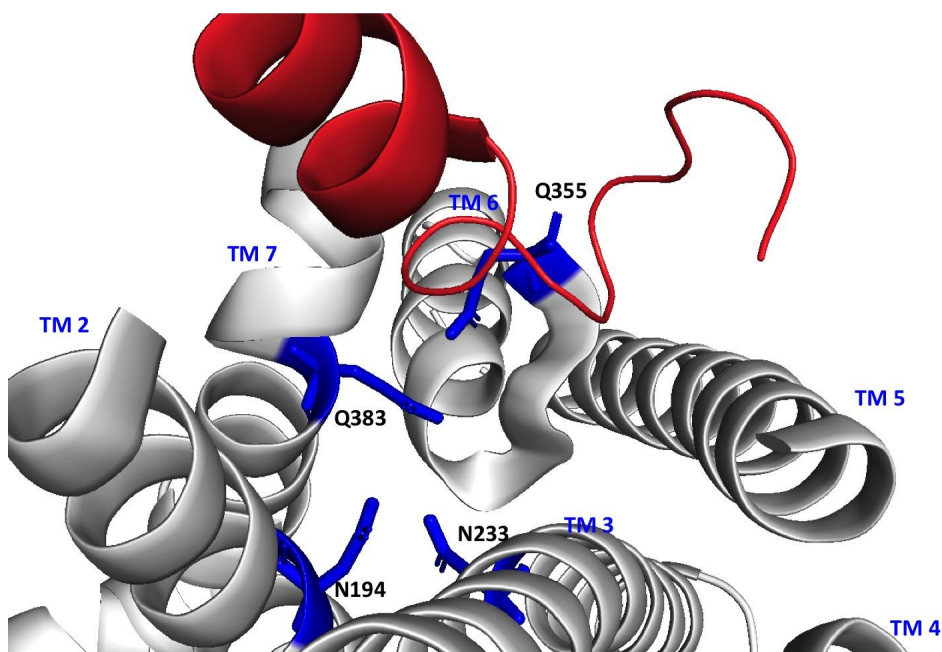


Figure 4.33. 3D model showing the central polar network of CTR. Ribbon representation of the TM bundle of the sCT-CTR complex based on the active Cryo-EM structure of CTR in complex with sCT (Dal Maso et. al., 2019). Receptor TMs 2,3,4,5,6 and 7 are shown in gray and ligand is shown in red (for better visualisation ECL and TM1 are not shown and sCT residues 1-10 are shown as ribbon).

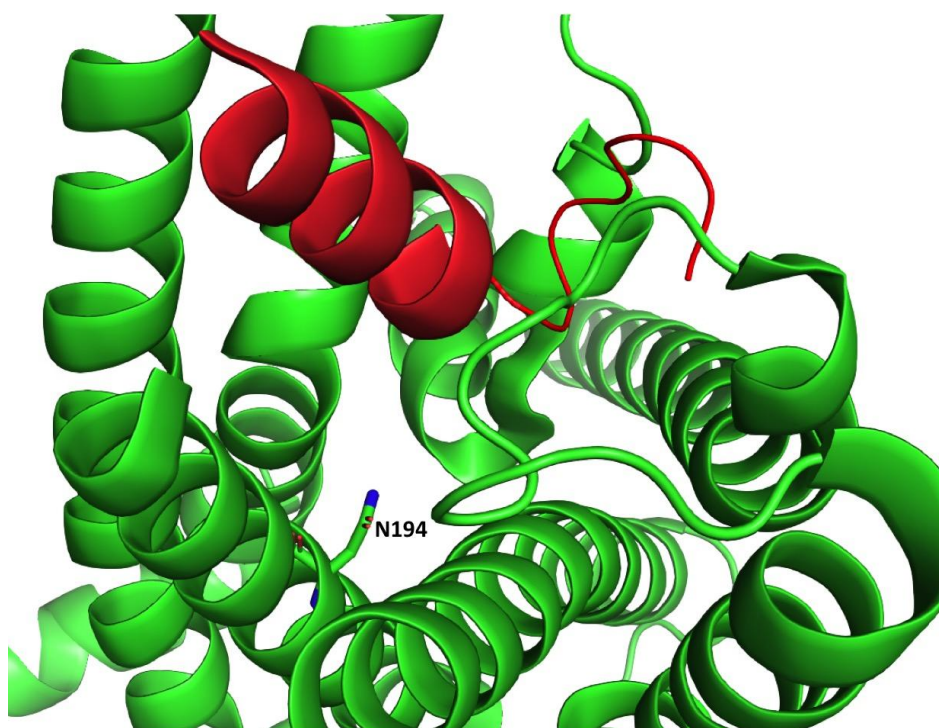


Figure 4.34. 3D model showing relative positions of N194 and sCT. Ribbon representation of the TM bundle of the sCT-CTR complex based on the active Cryo-EM structure of CTR in complex with sCT (Dal Maso et. al., 2019). Receptor TMs are shown in green and sCT is shown in red (sCT residues 1-7 that are absent in sCT(8-32) are shown as ribbon).

N233A (N^{3.43}A) and Q355A (Q^{6.52}A) were also differentially involved in affinity for distinct agonists. For instance, N233A (N^{3.43}A) had slightly increased pK_i for sCT and hCT (Figures 4.12 – 4.13). This same mutant, N233A (N^{3.43}A), as well as Q355A (Q^{6.52}A) showed significantly decreased G_s coupling affinity specifically for hCT, an effect not seen for other CT agonists (Figure 4.13). For pCT N233A (N^{3.43}A) and Q355A (Q^{6.52}A) slightly decreased pK_i, although this effect didn't reach statistical significance (Figure 4.14). Thus, we speculate, that affinity effects of N233A (N^{3.43}A) and Q355A (Q^{6.52}A) mutations may result from altering the shape of the binding pocket that in turn affects the peptide's binding conformation (or a range of conformations that the receptor is able to explore; or the rates of exchange between the different conformational states). Additionally, effects on G_s coupling affinity of N233A (N^{3.43}A) and Q355A (Q^{6.52}A) for hCT suggests an allosteric interaction between the bottom of ligand binding pocket and the G-protein binding site. Such allosteric networks that can transduce signal from the ligand binding site to the G protein binding site were previously observed in some class A GPCRs (Manglik *et al.*, 2015, Dror *et al.*, 2011, Miao *et al.*, 2013).

Analogous central polar network residues were previously extensively studied in a related GLP-1R. Similar to the observed CTR ligand-specific effects on both pK_i and cAMP functional affinity (pK_A), corresponding central polar network mutations (R^{2.60}A, N^{3.43}A, H^{6.52}A and Q^{7.49}A) affected GLP-1R equilibrium affinity (pK_i) in ligand- (GLP-1, exendin-4 and oxyntomodulin) and ligand isoform- (amidated, fully processed, extended or truncated GLP-1 isoforms; fully processed or truncated exendin-4) dependant manner (Wootten *et al.*, 2013, Furness *et al.*, 2018). In GLP-1R, R^{2.60}A, which corresponds to N194A (N^{2.60}A) in the CTR (decreased pK_i of sCT(8-32), hCT, pCT but not for sCT for CTR), resulted in decreased pK_i for amidated GLP-1(7-36)NH₂, truncated GLP-1(7-37)), exendin-4 and truncated exendin (9-39) but not for either the extended GLP-1(1-37) or oxyntomodulin isoforms. N^{3.43}A, which showed no effects on pK_i for CTR agonists, in GLP-1R decreased pK_i only for amidated GLP-1 (GLP-1(7-36)NH₂ and truncated GLP-1(7-37)), but not for either exendin-4, exendin (9-39), extended GLP-1(1-37) or oxyntomodulin (Wootten *et al.*, 2013, Furness *et al.*, 2018). H^{6.52}A, which only slightly decreased pK_i for pCT in the CTR, decreased pK_i only for amidated GLP-1(7-36)NH₂ and truncated GLP-1(7-37), exendin-4 and exendin (9-39), and oxyntomodulin, but not for the extended form of GLP-1 (GLP-1(1-37)). Interestingly, the Q383A (Q^{7.49}A) mutation that showed no change in pK_i or cAMP pK_A with any of the CT agonists (Figures 4.12 – 4.14) also had a more limited role on the equilibrium affinity of GLP-1 agonists, with only slight decrease of pK_i for the extended GLP-1(1-37) peptide isoform and no changes for other ligands or GLP-1 isoforms (Wootten *et al.*, 2013, Furness *et al.*, 2018). This is also consistent with limited role of this residue in peptide ligand affinity for other class B receptors where this has been assessed (as

reviewed by (de Graaf *et al.*, 2017)). This could perhaps indicate a lesser involvement of this residue in class B receptors orthosteric binding pocket and/or in the allosteric networks associated with the binding pocket, at least when coupled to G_s effector proteins.

Y234A (Y^{3.44}A) is located about one helical turn below the CTR binding pocket and for this receptor is likely to be involved in interactions with central polar residue network. Similar to N194A (N^{2.60}A), Y234A (Y^{3.44}A) mutation decreased pK_i for hCT and to a lesser degree for pCT (Figures 4.13, 4.14), indicating that this residue is likely to be involved in an allosteric interaction with the binding pocket.

Together, our results on CTR, along with data on GLP-1R (Wootten *et al.*, 2015, Furness *et al.*, 2018) and other class B receptors (as reviewed by (de Graaf *et al.*, 2017)) suggest that while there is a common involvement of the polar network residues in the affinity control of many class B GPCRs, the individual interactions differ in both receptor- and ligand-specific manner. This is unsurprising given the distinct structural features of the binding pockets and distinct positioning of the central polar network relative the peptide N-terminus for the different class B receptors.

K220A (K^{3.30}A) was the only mutation, which resulted in a significant loss of cAMP functional affinity across all three calcitonin agonists, including sCT. The magnitude of the effect was, however, differed for the different calcitonins: the highest impact was on hCT (approx. 2500-fold decrease relative to the WT); the impact on pCT was smaller (156-fold decrease relative to the WT); and the least affected was sCT (5-fold decrease relative to the WT) (Figures 4.12 – 4.14). Because of very low probe binding and inability to obtain a reliable window within our concentration range, pK_i for K220A (K^{3.30}A) were not detected, and so we are not able to compare them to pK_A effects. In our model this residue is positioned at the top of TM3, oriented away from the peptide agonist binding site. Its positioning is in proximity of the ECL2 backbone where it likely forms a hydrogen bond with the backbone of D287 in the middle of the loop (Figure 4.35). Although based on our static cryo-EM structure the distance between the two atoms is 3.6 Å, GPCRs are dynamic structures and distances between the residues can change, bringing the two atoms close together. It is known that D287^{ECL2} is located in the proximal region of the ECL2 and was shown to be important in binding affinity for all CTR peptides and thus K220 (K^{3.30}A) is likely to play role in stabilizing of the CTR ECL2 (Dal Maso *et al.*, 2018b). The equivalent residue in the GLP-1R, R^{3.30}A displayed a similar effect to observed in this study, where it substantially altered the affinity and cAMP potency of multiple GLP-1R peptide agonists (Wootten *et al.*, 2016b) as well as glucagon binding affinity for the GCGR (Siu *et al.*, 2013). Structures of the GLP-1R bound to peptide agonists also support a role

of the residue at 3.30 in stabilising ECL2, suggesting that this conserved residue may play a common role across the class B GPCR family.

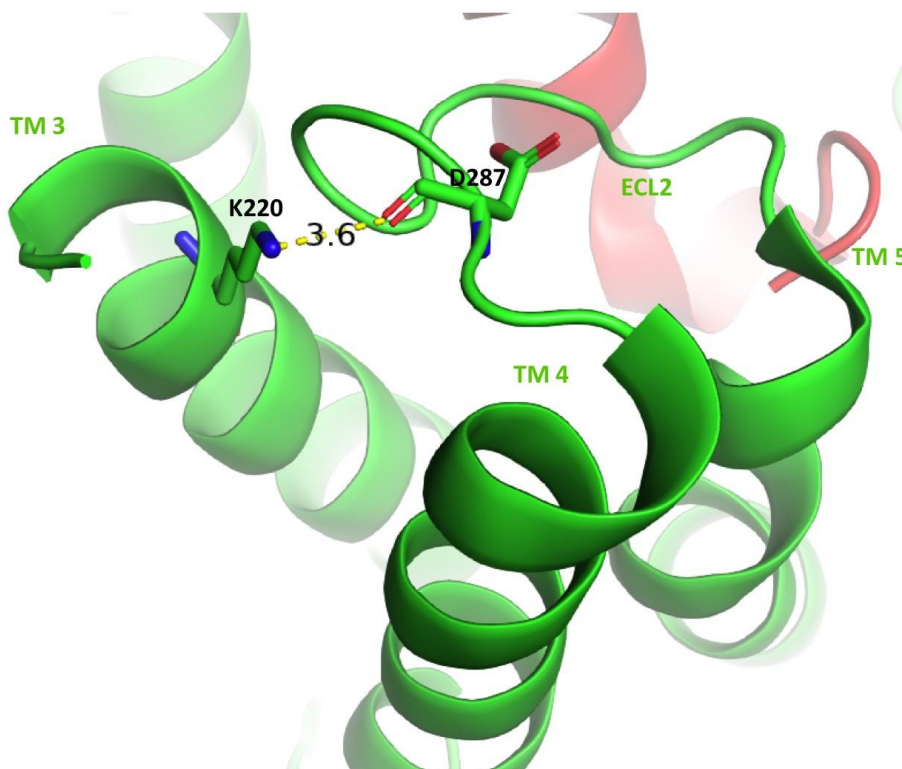


Figure 4.35. 3D model showing proximity between K220 and D287. Ribbon representation of the TM bundle of the sCT-CTR complex based on the active Cryo-EM structure of CTR in complex with sCT (Dal Maso *et al.*, 2019). Receptor is shown in green and ligand is shown in red. The distance measured between the atoms is shown by the yellow dash and equals 3.6 Å.

H302A (H^{5.40}A) mutation statistically significantly reduced hCT pK_i, with the pK_i of sCT and pCT also similarly reduced, although these did not reach statistical significance (Figure 4.12 – 4.14). Consistent with these detrimental effects on the equilibrium affinity, H302 (H^{5.40}) is predicted to directly interact with the T⁶ of the peptide in our current sCT (Dal Maso *et al.*, 2019) and the preliminary hCT-CTR (unpublished) models that were build into the cryo-EM density maps. The residue located at this position is likely to be important for peptide binding in all class B GPCRs. While a polar residue is located at 5.40 in all family members, the nature of the residue differs of across the family (for sequence alignment see Supplementary figure 7, Appendix 1). In the GLP-1R family, R5.40 forms interactions with peptide ligands in the currently available cryo-EM structures (Liang *et al.*, 2018a, Zhang *et al.*, 2017b). In addition, mutagenesis of the residue at this position has been shown to heavily reduce the affinity of multiple peptide ligands for the GLP-1R (Wootten *et al.*, 2016b), the GCGR (Siu *et al.*, 2013) and potency of the CLR cAMP response (Vohra *et al.*, 2013b).

M306A (M^{5.44}A) decreased pK_i for hCT and pCT (Figures 4.13, 4.14) is a TM5 residue located about one helical turn below the H302 (H^{5.40}). Based on its position, M306 (M^{5.44}A) could form hydrophobic interactions in the area surrounding the binding pocket. Other hydrophobic residues in this region also include L309 (L^{5.47}), V305 (V^{5.43}), F356 (F^{6.54}) and V357 (V^{6.53}) that form a pocket to accommodate L⁴ of the peptide (Figure 4.36). Our data indicate that the hydrophobic interactions in this region are important in maintaining of optimal binding pocket conformation for hCT and pCT.

Residues F356 (F^{6.53}), M376 (M^{7.42}) and F359 (F^{6.56}) are located in TMs 6 and 7 that undergo major conformational rearrangements upon receptor activation. These amino acids with hydrophobic side chains are predicted to pack together and were also previously implicated in CT peptide affinity consistent with the current results (Dal Maso *et al.*, 2018b). F359A (F^{6.56}A) decreased pK_i for both hCT and pCT. F356A (F^{6.53}A) affected G_s coupling affinity for hCT while P363A (P^{6.60}A) and M376A (M^{7.42}A) affected G_s coupling affinity for both hCT and pCT. Mutation of P363A (P^{6.60}A) led to a decrease in both pK_i and pK_A for hCT, however the change in pK_A was more than 10-fold greater than the change in pK_i supporting that this residue is more strongly involved in affinity with respect to G_s coupling (Figures 4.13 – 4.14). Neither P363A (P^{6.60}A) nor M376A (M^{7.42}A) had effects on sCT affinity, indicating that differential amino acid networks are important for individual ligands or that sCT is less sensitive to single mutations.

P360A (P^{6.57}) significantly impaired hCT and pCT equilibrium affinity (pK_i) and the pK_A derived from cAMP data (Figures 4.13 – 4.14). Prolines hydrogen bond to their backbone nitrogen and are often associated with breaks in secondary structure and kinks within helices (Richardson, 1981, Pace *et al.*, 1998). In the published CTR structure (Dal Maso *et al.*, 2019), the helical secondary structure with TM6 is disrupted at P360, where the top of the helix unwinds and is relatively mobile, but is also within proximity of Ser⁵ of the peptide ligand (Figure 4.37). Mutation to Ala may results in differences within the secondary structure within this region and therefore could impact on interactions with ligand, as well as receptor activation. Despite the effects of P360A on hCT and pCT affinity, remarkably, mutation of this residue has no effect on sCT, which is consistent with single mutations throughout this study and others (Dal Maso *et al.*, 2018b, Dal Maso *et al.*, 2019) having little effect on the overall affinity of this ligand.

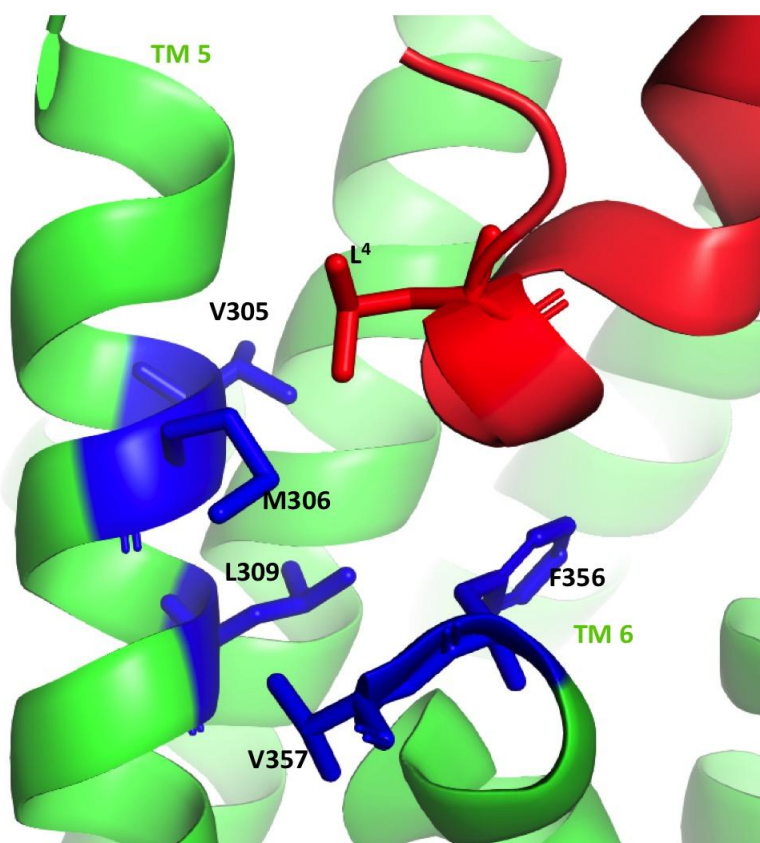


Figure 4.36. 3D model showing hydrophobic residues in proximity of M306. Ribbon representation of the TM bundle of the sCT-CTR complex based on the active Cryo-EM structure of CTR in complex with sCT (Dal Maso et. al., 2019). Receptor is shown in green and ligand is shown in red with M306 and hydrophobic residues in its proximity are shown as sticks.

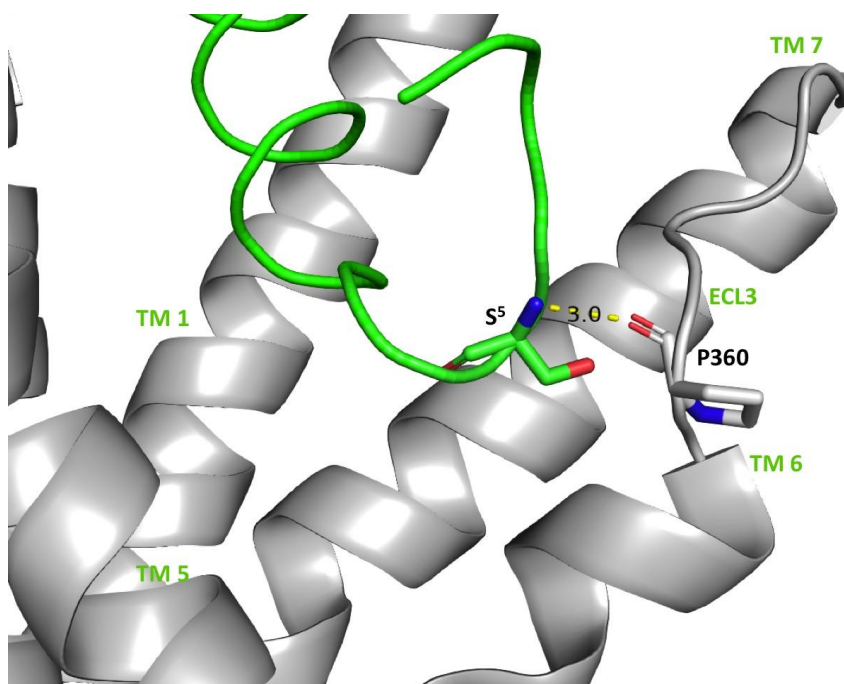


Figure 4.37. 3D model showing proximity between P360 of the CTR and S⁵ of the peptide. Ribbon representation of the TM bundle of the sCT-CTR complex based on the active Cryo-EM structure of CTR in complex with sCT (Dal Maso et. al., 2019). Receptor is shown in gray and ligand is shown in green ribbon. The distance measured between the atoms is shown by the yellow dash and equals 3.0 Å.

D373A (D^{7.39}A) showed decreased global affinity for hCT and pCT, but not for sCT, which is partially consistent with previous data where D373A (D^{7.39}A) decreased affinity across all the three calcitonin agonists (Figures 4.12 – 4.14) (Dal Maso *et al.*, 2018b). Removal of the negative charge from the aspartic acid due to the mutation appears to disrupt specific ligand interactions. One potential interaction is a salt bridge between D373 (D^{7.39}) and the K¹¹ of sCT, which are about 5 Å apart, as captured in the CTR cryo-EM structure (Figure 4.38). It should also be noted that receptors are dynamic rather than static structures and it is possible that K¹¹ and D373 (D^{7.39}) can move closer together to form a stronger salt bridge interaction depending on receptor's conformational state. A salt bridge was proposed between the same residue D366 (D^{7.39}) of CGRP (CLR/RAMP1) and D³ of α CGRP based on the cryo-EM map. Interestingly, hydrogen bond formation was also predicted between R¹¹ of α CGRP and D366 (D^{7.39}) of the receptor, but, similarly to the CTR, this interaction is not seen in the cryo-EM map (Liang *et al.*, 2018a). hCT and pCT have T¹¹ and A¹¹ residues at position 11 of the peptide, indicating that other interactions might be in place for D373 (D^{7.39}), which we, however, could not identify based on the available structural data.

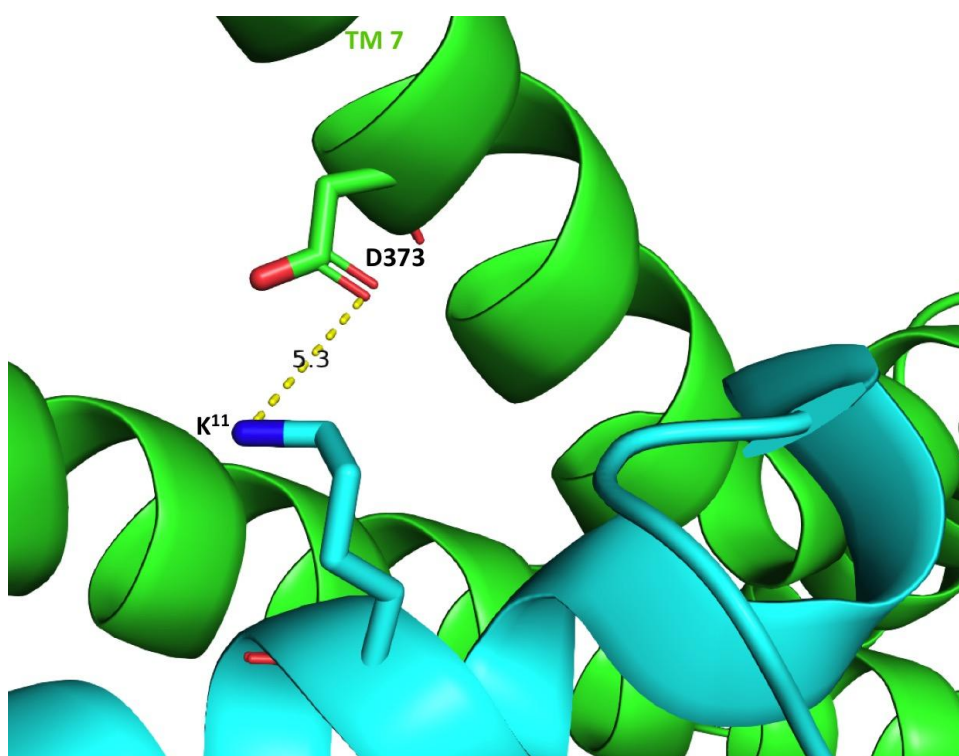


Figure 4.38. 3D model showing proximity between D373 of the CTR and K¹¹ of the peptide. Ribbon representation of the TM bundle of the sCT-CTR complex based on the active Cryo-EM structure of CTR in complex with sCT (Dal Maso *et. al.*, 2019). Receptor is shown in green and ligand is shown in cyan. The distance measured between the atoms is shown by the yellow dash and equals 5.3 Å.

I380A (I^{7.46}A) trended towards increased affinity for hCT and pCT, however, it only reached statistical significance for pCT pK_i (Figures 4.13 – 4.14). Exchange of I for a shorter amino acid A possibly removes steric constraints, thus improving affinity.

Our results show that, apart from the K220A (K^{3.30}A) mutation which had global effect on CTR functional affinity across all three calcitonin peptides, the majority of the analysed residues within the TMs 2, 3, 5, 6 and 7 had ligand-specific effects on CTR binding and functional affinity, with mutation of the residues mentioned above having effects on the CTR lower affinity peptides, such as hCT and pCT, but limited disruption to binding of the higher affinity agonist, sCT. These results imply that CTR engages differentially with its individual agonists, for example, by utilizing distinct amino acid residues networks or that the stable interaction made by sCT with the receptor is less susceptible to disruption by single amino acid substitutions.

Comparison of the static cryo-EM structures of sCT-CTR and hCT-CTR complexes shows little difference in CTR-ligand interactions overall, however there are indications of differential contribution of residues within CTs N-terminal ring to their affinity. For example, consecutive truncation of the residues from N-terminus of sCT results in transition from full agonist to partial agonist while truncation of 7 to 8 amino acids results in competitive antagonists (Feyen *et al.*, 1992). Presence of the N-terminal helical structure has been shown to be important for hCT potency in cAMP signalling, but not for sCT (Orlowski *et al.*, 1987). This is consistent with our results demonstrating that sCT is less sensitive to the individual Ala mutations introduced within the CTR TM region, compared to hCT and pCT, which were both more generally more sensitive to the individual Ala substitutions. sCT is characterised by a slower binding dissociation rate, and in some reports approaches pseudo-irreversible binding, compared to hCT ($T_{1/2}$ = 4.4 minutes for hCT versus and $T_{1/2}$ =41 minutes for sCT (reported by Furness *et al.*, 2016). MD simulations performed on the CTR-sCT and CTR-hCT showed distinct dynamics of the CTR-sCT and CTR-hCT complexes (Dal Maso *et al.*, 2018b). In these simulations sCT trended to form relatively stable and persistent interactions with the receptor, whereas hCT interacted with similar residues but was more conformationally dynamic, forming less persistent interactions with the receptor side chains. These differences extend to the receptor itself, such that in complex with sCT the top of the receptor TM bundle is less mobile compared with the situation when hCT is bound. It seems likely that the formation of more stable interactions with the binding pocket can make the sCT-CTR complex more tolerant to single mutations, as seen in the mutagenesis data, and that perhaps multiple interactions need to be disrupted before any effects in the mutagenesis are observed.

Another distinct feature of CT agonists is the ability of sCT mid-region to form an alpha helix that is also supported by the current CTR model. This secondary structure of the sCT seems to add additional constraints on how sCT is positioned within the CTR binding pocket and thus might affect sCT affinity (Hilton *et al.*, 2000, Meadows *et al.*, 1991). On the other hand, this ability of sCT from form secondary structure translates into its distinct binding kinetics (Sexton *et al.*, 1999, Furness *et al.*, 2016).

Hence, our data supports distinct interaction modes between the CTR and its individual agonists. This can a result from either distinct conformations that the CTR adopts when interacting with each agonists and/or from distinct residency times of each agonist that causes different strength of interactions between the receptor and the ligand.

4.3.3 EFFECTS OF THE CTR TM MUTATIONS ON CTs pERK1/2 FUNCTIONAL AFFINITY

CTR pERK1/2 response represents a convergent response from multiple signalling pathways, including PKC, PI3K and PLC (Morfis *et al.*, 2008), where multiple G proteins can be involved. Effects of the mutations on pERK1/2 pK_A were dissimilar to the cAMP pK_A changes, with the majority of mutants displaying either slightly enhanced or slightly reduced functional affinity for pERK1/2 response (depending on the operational fit for the pERK1/2 data) (Figures 4.12 – 4.14, 4.26 – 4.28, 4.15, 4.31, Supplementary figure 4, Appendix 1). Thus, comparing pK_A effects between the two different signalling pathways, cAMP and pERK1/2, demonstrates that same mutations can have differential effects on functional affinity for coupling to distinct signalling pathways. Mapping the CTR mutational effects for the CTR ECD (ECLs 1, 2 and 3 and the top of TM1) also revealed differences in patterns of pK_A effects (as well as the direction of effects for select ECD regions) between pERK1/2 and cAMP pathways. This implies that distinct amino acid networks are engaged for coupling to different downstream signalling effectors.

While applying the operational model has allowed us to derive the functional affinity (pK_A) for each individual mutant for pERK1/2 pathway, there is a significant kinetic difference in the way the data was acquired for measurements of pERK1/2 compared with those used for radioligand binding and cAMP assays. With K_{off} of 4.4 minutes and 41 minutes for hCT and sCT (when assessed at room temperature), respectively, under our experimental conditions, all agonists are expected to be at, or close to equilibrium for occupancy at the WT receptor in the radioligand binding (incubation for 16 hours at 4°C) and the cAMP assay (incubation for 30 minutes at 37°C) (Furness *et al.*, 2016). Activation of pERK1/2 is a transient response, peaking at a ~5 minutes and at this time, sCT will not be close to occupancy equilibrium, while hCT and pCT will be closer to occupancy equilibrium at the WT receptor. Therefore, if any of the CTR

mutants resulted in substantial changes in binding kinetics, and in particular, K_{off} , this could lead to disproportionate changes in pERK1/2 pK_A (especially for sCT), i.e. these mutants will be closer to the occupancy equilibrium than the WT receptor at the time of the assay readout. To test whether this might be the case, measuring ligand binding kinetics for each mutant would be required.

The majority of CTR mutants had good agreement between the pK_i and cAMP pK_A , indicating that these assays, performed at conditions either at or close to equilibrium, provide a good estimate for CTR affinity. For the CTR pERK1/2 pK_A , further experiments are required in order to assess the contribution of kinetic differences observed with non-equilibrium measurements and their contribution to the mutation-dependent observed changes in pK_A for pERK1/2. These differences between pK_i and pERK1/2 pK_A values could also indicate that the affinity of CT agonists is not affected by the effectors (pathways) leading to pERK1/2 phosphorylation, but that pK_i is largely influenced by receptor coupling to G_s -mediated pathways.

Although our pERK1/2 operational analysis resulted in ΔpK_A patterns with pERK1/2 functional affinity being increased relative to the WT for the majority of mutants for CT agonists, these results need to be interpreted with caution due to certain limitations in our analysis. And, therefore, as discussed in the results section, we performed a comparison of different fits for the operational model to see which is a better representation for our data. Because of the heterogeneity of pERK1/2 concentration responses (both biphasic and monophasic concentration responses) an operational fit with a common mechanism (common transducer slope) resulted in fits with varying degrees of goodness. Either sharing or constraining the transducer slope results in operational fits better representing some data sets, while poorly representing others (i.e. the goodness of fit). While under such circumstances there is no ideal way to fit these data onto the operational model, we considered a number of options for the analysis, each having its strengths and limitations. Operational analysis that is described in the main Chapters 4 and 5 was chosen based on a shared transducer slope globally fitted to all data sets from the WT and each mutant. However, this analysis does appear to underestimate pK_A for the WT, resulting in ΔpK_A profiles where mutant receptors had slightly increased pK_A relative to the WT (although, the majority of these effects did not reach significance). Another approach was to constrain the transducer slope n to 1 as we did for the 2 other agonists – α CGRP and rAMY (the data for α CGRP and rAMY was better fitted using monophasic concentration response curves). This approach resulted in a poor fit for WT with the fit not passing through most of the data points (Supplementary figure 6, Appendix 1), therefore we dismissed this option. The third approach was constraining the transducer slope n to 0.4 and increasing E_{max} to

200 (as described in the results section), which resulted in a reasonably good fits for CTs at WT (although the fit did miss some data points for pCT) (Supplementary figures 1–3, Appendix 1) with apparent higher pK_A and a slightly changed pattern of ΔpK_A effects (Supplementary figure 4, Appendix 1).

We therefore, compared the ΔpK_A profiles obtained for the two different fits to see how these influenced our data interpretation. When comparing the results of ΔpK_A effects across the two fits (globally fitted transducer slope versus one constrained to 0.4 (see above) and comparing figures 4.26 – 4.28 with Supplementary figure 4, Appendix 1), it could be seen that the patterns of the mutational effects trended in opposite directions, however, the overall magnitude of effects was very modest, with only few effects reaching significance for the fit with shared transducer slope and none with the alternative fit. In spite of this general trend for apparent reversal of pK_A depending on the model fitted, mutants K220A ($K^{3.30}A$), I301A ($I^{5.39}A$) and H302A ($H^{5.40}A$) all showed an apparent increase in sCT dependent pK_A regardless of model. This supports that the interactions of sCT for pERK1/2 coupling are somewhat different to the other CT ligands and that overall (for all ligands) the resulting pattern of effects of TM mutations on pERK1/2 pK_A are still different from that of pK_i and cAMP pK_A effects. This supports our previous conclusions regarding distinct amino acid networks being important for coupling to different downstream signalling effectors (cAMP versus pERK1/2) for the CTR.

4.3.4 EFFECTS OF CTR TM MUTATIONS ON THE CTR CAMP AND pERK1/2 FUNCTIONAL AFFINITY IN RESPONSE TO α CGRP AND rAMY

Overall, the pattern of cAMP pK_A values for α CGRP and rAMY resembled that of the low affinity CT agonists, hCT and pCT, with the magnitude of effects being most similar to hCT. We observed both common and ligand-specific effects of the selected mutations on CTR affinity when comparing this data against the affinity data from other CT ligands (as described above) (Figures 4.12 – 4.14, 4.18 – 4.19). Among residues with common effects on the CTR affinity was K220A ($K^{3.30}A$), which reduced cAMP functional affinity for all 5 studied CTR agonists, including sCT. K220 ($K^{3.30}A$) is located at the top of TM3 where it can potentially form interactions with residues of the ECL2, and through this, affect CTR binding affinity. This theory is supported by studies assessing ECL2 that identified it as a critical domain for CT peptide binding affinity (Dal Maso *et al.*, 2018b, Dal Maso *et al.*, 2019). ECL2 has also been identified as a crucial domain across all class B GPCRs (and many class A GPCRs) where it has been studied to date, highlighting a common role of ECL2 in class B GPCR function. In the current literature, mutation of the same, $K^{3.30}A$ in CGRP receptor (CLR/RAMP1) showed no significant effects on potency of the cAMP response to α CGRP (Barwell *et al.*, 2011). The

recently published CGRP receptor structure (Liang *et al.*, 2018a) revealed that the RAMP1 protein plays a role in ECL2 stability and therefore may account for a more limited role of the K220 side chain in stability of this loop that is required for function. In contrast, this residue stabilises ECL2 in both the CTR and GLP-1R structures that do not contain and RAMP, and mutation to alanine alters function of all agonists assessed to date (Wootten *et al.*, 2016b, Siu *et al.*, 2013), including in this study.

Similar to the lower affinity CT agonists (hCT and pCT), central polar network residues N194A (N^{2.60}A), N233A (N^{3.43}A), Q355A (Q^{6.52}A) (only α CGRP) as well as F356A (F^{6.53}A) (a non-polar side chain residue in proximity of the central polar network) were important for α CGRP and rAMY pK_A (Figures 4.12 – 4.14, 4.18 – 4.19). As discussed above, hCT data suggests that N233A (N^{3.43}A), Q355A (Q^{6.52}A) and F356A (F^{6.53}A) are specifically involved in G_s coupling affinity. Q^{6.52}A and F^{6.53}A decreased potency of AM cAMP response for AM1 (CLR/RAMP2) and AM2 (CLR/RAMP3) receptors; Q^{6.52}A also decreased potency of α CGRP response to CGRP receptor (CLR/RAMP1); while N^{3.43}A caused small increase in potency of AM response for all three CLR receptors (CLR/RAMP1; CLR/RAMP2 and CLR/RAMP3) (Woolley *et al.*, 2017b). Interestingly, as assessed by radioligand binding assay, these mutations didn't affect the binding affinity for AM at AM1 receptor (Woolley *et al.*, 2017b). This indicates, that for CLR these mutations can affect either affinity of G_s coupling affinity or cAMP efficacy, suggesting that the these polar network residues are involved in allosteric networks that control G_s coupling affinity for both CTR and CLR.

Mutagenesis studies were performed on CLR in complex with RAMP1 to assess effects on CGRP receptor ECL1, ECL2 and ECL3 and adjacent parts of TMs to determine effects on receptor expression, internalisation and on cAMP response (Barwell *et al.*, 2011b, Woolley *et al.*, 2013). For the same residues that overlap with the current study (K^{3.30}, Q^{3.33}, H^{3.36}, L^{3.37}, I^{5.39}, I^{6.56}, P^{6.57}, M^{7.42} and H^{7.43}) there were limited common effects seen across the CLR and CTR studies. Thus, there was a 126-fold decrease in radioligand binding affinity (pIC₅₀) for H^{3.36}A mutant in the CLR which correlates poorly with a 10-fold decrease in pK_i seen for hCT (not statistically significant), and a 3-fold decrease in pK_i seen for pCT (statistically significant); although no pK_A effects for this mutation were seen for either α CGRP, or rAMY, for this mutant in CTR in the absence of RAMPs. L^{3.37}A in CGRP receptor also decreased radioligand binding affinity (pIC₅₀) for 1.1-fold. In the CTR this correlated with a 4-fold decrease in pCT binding affinity (although, this result didn't reach statistical significance). The CLR study was conducted in presence of RAMP1 (which is known to allosterically modulate CLR and therefore alter the shape of the binding pocket). In both CGRP receptor and CTR structures, the residues discussed above are positioned in a similar way. The CTR when coupled with RAMPs (either RAMP1, 2

or 3) forms a higher affinity AMY receptor, with lower affinity for hCT. CTR/RAMP1 also has higher affinity for CGRP than the CTR alone. For a more direct comparison of the role of these residues between CLR/RAMP complexes, it would be interesting to compare effects of the same mutations on CTR affinity when it is co-expressed with RAMP1, 2 or 3. Whereas CLR does not form functional receptor in the absence of RAMPs, experiments assessing effects of same mutations when CTR is co-expressed with RAMPs would be required to test if the observed differences between the CTR and CLR effects are caused by allosteric effects of RAMP co-expression, or whether it is the result receptor-specific differences in the binding pocket conformation. Previous work examining ECLs 2 and 3 of the CTR revealed distinct patterns in terms of direction and magnitudes of effects on cAMP pK_A for CTR alone and when it is allosterically modulated by RAMP3 (Dal Maso, *et al.*, 2018b, Pham *et al.*, 2019).

Due to weak coupling and low affinity of α CGRP and rAMY, pK_A effects for pERK1/2 pathway could be calculated only for a limited number of mutants (Figures 4.29 – 4.30). The direction of mutational effects on pERK1/2 pK_A for α CGRP and rAMY differed from the pERK1/2 pK_A pattern for CTs (which displayed increased pK_A), with all pK_A effects trending towards decreased pK_A , (Figures 4.26 – 4.30, 4.31 – 4.32). For rAMY, pERK1/2 pK_A pattern was somewhat similar to cAMP pK_A pattern for this agonist (although, pERK1/2 pK_A couldn't be calculated for about half of the mutants). This data suggests that there might be differences in the residue networks involved in pERK1/2 coupling affinity for CT agonists versus α CGRP and rAMY. On the other hand it is to be verified whether there is any kinetic aspect of α CGRP and rAMY residency time that contributed to this obvious difference to CT agonists. Noticeably, α CGRP and rAMY had higher pERK1/2-derived pK_A than CT agonists. α CGRP and rAMY are weak CTR agonists with equilibrium affinity lower than that of CT agonists. This difference could arise from either kinetic shortcoming of measuring pERK1/2 response at non-equilibrium state, or from the limitations associated with fitting these data onto the operational model (as ΔpK_A profiles obtained for the CTs when using an alternative operational fit (with $n=0.4$) correlated better with these for α CGRP and rAMY (Figures 4.29 – 4.30, Supplementary figure 4, Appendix 1)).

We are not able to directly compare α CGRP and rAMY functional affinity effects to the effects of these ligands on equilibrium affinity, as pK_i for α CGRP and rAMY couldn't be determined at the concentrations tested. However, since N194A ($N^{2.60}A$) cAMP pK_A change was of same direction and similar magnitude as pK_A change for pERK1/2 pathway (Figures 4.18 – 4.19 and 4.29 – 4.30) and since N194A ($N^{2.60}A$) showed detrimental effects on pK_i for sCT(8-32), hCT and pCT (as was previously discussed), it could be speculated the affinity effects seen for both cAMP and ERK1/2 pK_A for rAMY reflect N194A ($N^{2.60}A$) effects on equilibrium

binding affinity. Therefore, N194A (N^{2.60}A) is involved in important contacts that maintain receptor optimal conformation for binding of sCT(8-32), hCT, pCT as well as rAMY.

Thus, for weak CTR agonists, α CGRP and rAMY we observed both ligand- and pathway specific effects of the CTR TM mutants on the receptor affinity. Our data suggests that the overall conformation of the CTR binding pocket is largely shared between its agonists, including hCT, pCT, α CGRP and rAMY, that is supported by close profiles of cAMP pK_A effects for these 4 agonists, (with sCT being the least sensitive to the individual Ala substitutions). On the other had, pERK1/2 pK_A profiles were of opposite direction for α CGRP, rAMY when compared to CT agonists. Whether this is due to ligand-specific downstream coupling activation, or it is associated with pERK1/2 assay kinetics, will require further investigation. Limitations in the operational fitting of the data for CT agonists could also impact on the comparison across different CTR agonists.

4.4 SUMMARY

1. CTR agonists displayed both global and ligand-specific effects on the CTR binding and functional affinity.
2. The interactions between the deep TM receptor binding pocket residues and the peptide N-terminus are important for binding, at least for the lower affinity CTR agonists, hCT and pCT as well as for α CGRP and rAMY. For these agonists interactions with CTR TM region had greater effects on affinity, both pK_i and cAMP pK_A, than for sCT which was more tolerant to individual mutations of the CTR TM binding site.
3. Central polar network residues were important for affinity (pK_i and cAMP pK_A) of hCT and pCT and for weak CTR agonists, α CGRP and rAMY.
4. Comparing cAMP pK_A effects against pK_i allowed us to separate global affinity effects and effects on the G_s coupling affinity for a number of mutants identifying residues that are potentially linked to the allosteric networks that propagate the activation of signal from the ligand orthosteric binding pocket site to the G_s protein binding site.
5. Distinct structures of the CTR ligands (higher alpha-helicity of sCT mid-region) may translate in differential orientation and interactions of the peptide N-terminal ring with the surrounding receptor environment. On the other hand, differential kinetics of interactions with the receptor for different ligands may also translate into distinct modes of ligand-receptor interactions or distinct requirements of individual amino acids.
6. CTR agonists displayed pathway-specific effects on pK_A for cAMP and pERK1/2, indicating that receptor is utilizing distinct amino acid networks to activate different signalling effectors. pERK1/2 response was measured at non-equilibrium conditions and

kinetic effects on pK_A values should be considered; effects of CTR mutants on individual ligands residency times require additional interrogation.

CHAPTER 5

Effects of alanine mutations of residues within calcitonin receptor (hCTR) binding pocket on intracellular signalling to cAMP and ERK pathways

5.1 INTRODUCTION

Previous studies of the analogous TM binding pocket residues in various class B receptors provide strong evidence of the important role these residues play in binding and signalling. Of particular interest are conserved polar residue networks that play important roles in transmission of conformational changes associated with receptor transition between inactive and active states. These residues have been extensively studied for a number of class B GPCRs and shown to alter receptor function when mutated to Ala. GLP-1R studies using receptor agonists with different sequence and structure revealed that the central polar network residues and their interactions are important for modulating effector coupling specificity and biased signalling (Wootten *et al.*, 2016b, Furness *et al.*, 2018).

Previous studies revealed that a naturally occurring CTR polymorphism (in the ICL1) as well as introduced Ala mutations in the CTR extracellular loops (ECL2 and ECL3) can alter CTR signalling in ligand- and pathway-specific manners (Dal Maso *et al.*, 2018b, Dal Maso *et al.*, 2018a). In this study, we extend the work reported in Chapter 4 to assess the role of receptor mutants in transmission of signalling.

Upon CTR activation, both TM6 and TM7 are known to undergo the major conformational reorganisation that includes a large outward movement of the intracellular part of the TM6 that is necessary to enable G protein engagement. Toward the extracellular end of TM6, there is an outward movement as well as disordering and unwinding of this helix correlated with $\sim 60^\circ$ kink at the centre of TM6 formed around Pro^{6.47}-X-X-Gly^{6.50}. There are also significant outward movements in both extracellular and intracellular regions of the TM7. The tops of TMs 6 and 7, along with ECL3, play important roles in CTR activation and signalling, and this was previously confirmed for the CTR and other class B receptors. There is also an inward movement at the top of TM1 and a small outward movement at the top of TM5.

In order to assess the effects of mutations within the TM peptide binding pocket (TM 3, 5, 6 and 7) and central polar network of CTR on initiation and propagation of intracellular signalling, two pathways were evaluated – cAMP and ERK1/2 phosphorylation. Concentration response data were generated for each pathway (Figures 5.1 – 5.3, 5.5 – 5.6 and 5.8 – 5.10, 5.15 – 5.16) as per the previous chapter and these data were analysed using the Black and Leff operational model of agonism to derive affinity-independent measures of intrinsic efficacy (τ) for each mutant and for each peptide agonist for each signalling pathway. Corrected for the cell surface expression, τ_c values can then be used to directly evaluate changes in the efficiency with which each mutant receptor can transduce a signal (that comes from receptor activation by a specific agonist) relative to the WT receptor.

This study aimed to provide a more detailed mechanistic understanding on how signalling is propagated within the CTR and how this relates to the existing knowledge on other class B receptors. Identifying residues with either ligand- or pathway-specific effects provides a framework with which to understand the networks of residues engaged by particular agonists in order to couple to downstream effectors and may also be useful for the future design of biased agonists with desired pharmacological properties.

Chapter 5 utilized analysis of the original cAMP and pERK1/2 concentration-response data, alongside with efficacy (τ) analysis to identify CTR TM residues responsible for signaling. As previously mentioned in the introduction to Chapter 4, there is some redundancy between the two chapters in terms of analyzing the same data sets, however Chapter 5 focusses on characterizing signal transduction, rather than binding *per se*.

5.2 RESULTS

5.2.1 EFFECTS OF THE CTR TM MUTATIONS ON CTR CAMP SIGNALLING

5.2.1.1 CAMP SIGNALLING IN RESPONSE TO CALCITONINS

cAMP response for each mutant and the WT receptor was measured and data was fitted to three-parameter logistic curves that were normalized to WT maximal response (Figures 5.1 – 5.3), this is a re-analysis of data from chapter 4. Values for pEC_{50} and E_{max} were derived from the curves and are reported in Table 5.1. Efficacy values were derived using Black and Leff operational model with transducer slope $n=1$ (as the operational fit was used with $n=1$, the curves looked identical to the three-parameter fit (Figures 5.1 – 5.3). Since many of the introduced TM mutations had detrimental effects on cell surface expression, correction for the cell surface expression was subsequently applied to $\log\tau$ values to obtain corrected values $\log\tau_c$ and errors were propagated accordingly (Table 5.2). $\Delta\log\tau_c$ value for each mutant was obtained by subtracting WT $\log\tau$ from each mutant's $\log\tau_c$ value (Figure 5.4).

There were many mutations that had statistically significant effects on the potency or maximal response induced by calcitonin peptides relative to the WT receptor (Table 5.1). However, application of the operational model allowed us to separate effects that were due to altered functional affinities (described in the previous chapter) and effects that were due to efficacy. Consistent with decreased expression of the TM mutants, many of the observed E_{max} effects were a result of decreased expression (reported in the previous chapter) rather than reduced efficacy. Application of cell surface correction allowed us to identify mutants that had genuine changes in efficacy (Table 5.2).

Interestingly, residues important for cAMP efficacy seemed to be largely conserved across calcitonin peptide agonists. The mutation of K220A (K^{3.30}A) resulted in a statistically significant increase in efficacy for all CT agonists (Table 5.2 and Figure 5.4). A number of other residues also increased cAMP efficacy across all three CT agonists (sCT, hCT and pCT): N194A (N^{2.60}A), I301A (I^{5.39}A), V305A (V^{5.43}A), F356A (F^{6.56}A), P363A (P^{6.60}A), D373A (D^{7.39}A), I380A (I^{7.46}A) and Q383A (Q^{7.49}A), although none of these reached significance (Table 5.2 and Figure 5.4). While F359A (F^{6.56}A), P360A (P^{6.57}A) and W361A (W^{6.58}A) decreased cAMP efficacy for all three agonists. For other residues the pattern of cAMP efficacy effects was similar for all CTs (Figure 5.4).

K220A (K^{3.30}A) was only residue that had significant effect on the cAMP efficacy was mapped onto a hCTR model (pdb 6NIY) (dal Maso *et al.*, 2019) in order to better visualise where this residue is positioned within the structure (Figure 5.5).

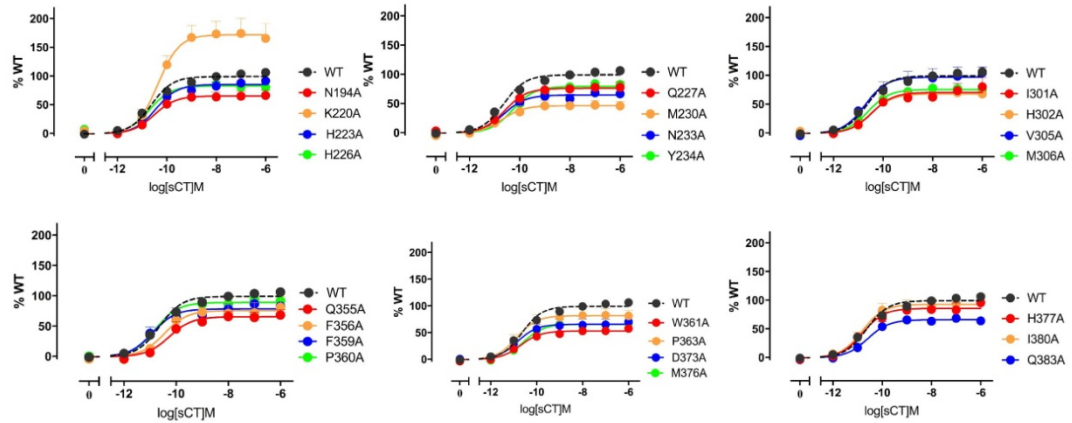


Figure 5.1. *cAMP accumulation profiles in response to sCT in CV-1-FlpIn cells stably expressing hCTRαLeu single alanine mutations in the receptor TM region.* *cAMP formation in the presence of sCT was fit using three parameter logistic equation and normalized to WT receptor response. The Black and Leff operational model, with a hill slope of 1, was applied to separate efficacy (τ) and functional affinity (pK_A). All values are mean+S.E.M. of 3 to 5 independent experiments conducted in duplicate; for some data points error bars are not shown as they are smaller than the height of the symbol.*

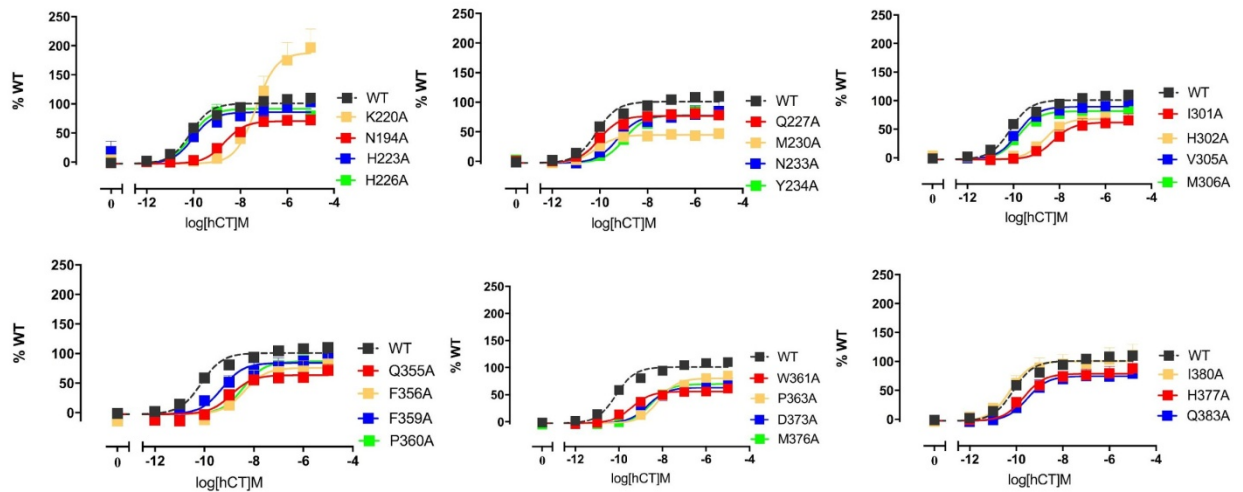


Figure 5.2. *cAMP accumulation profiles in response to hCT in CV-1-FlpIn cells stably expressing hCTRαLeu single alanine mutations in the receptor TM region.* *cAMP formation in the presence of hCT was fit using three parameter logistic equation and normalized to WT receptor response. The Black and Leff operational model, with a hill slope of 1, was applied to separate efficacy (τ) and functional affinity (pK_A). All values are mean+S.E.M. of 3 to 5 independent experiments conducted in duplicate; for some data points error bars are not shown as they are smaller than the height of the symbol.*

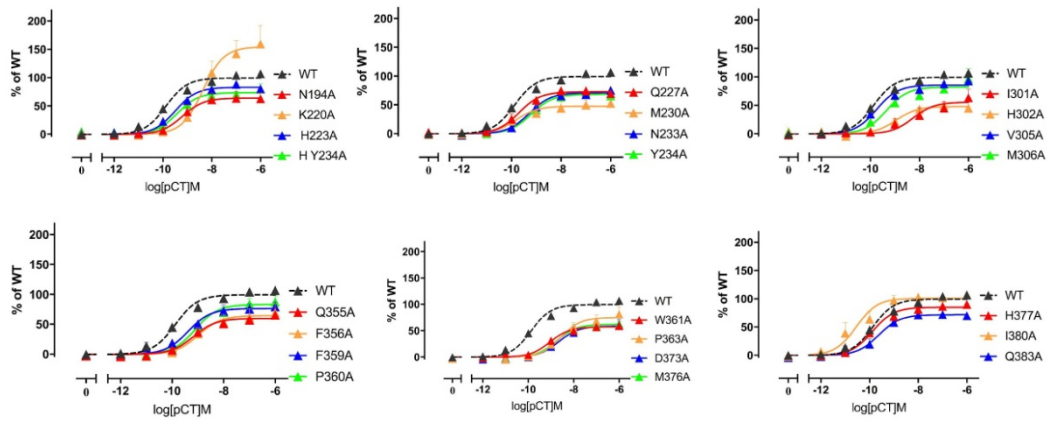


Figure 5.3. *cAMP accumulation profiles in response to pCT in CV-1-FlpIn cells stably expressing hCTRαLeu single alanine mutations in the receptor TM region. cAMP formation in the presence of pCT was fit using three parameter logistic equation and normalized to WT receptor response. The Black and Leff operational model, with a hill slope of 1, was applied to separate efficacy (τ) and functional affinity (pK_A). All values are mean+S.E.M. of 3 to 5 independent experiments conducted in duplicate; for some data points error bars are not shown as they are smaller than the height of the symbol.*

Table 5.1. Effect of single alanine CTR TM region mutation on cAMP potency (EC_{50}) and maximal response to CT agonists (sCT, hCT and pCT) in CV-1-FlpIn cells stably expressing hCTR α Leu.

	sCT			hCT			pCT		
	pEC ₅₀		E _{max}	pEC ₅₀		E _{max}	pEC ₅₀		E _{max}
WT	10.61	± 0.04	99 ± 1	10.08	± 0.05	101 ± 1	9.84	± 0.05	100 ± 2
N194A(N ^{2.60} A)	10.55	± 0.18	65* ± 3	8.60*	± 0.18	71* ± 4	9.22*	± 0.22	64* ± 5
K220A(K ^{3.30} A)	10.35	± 0.20	172* ± 9	7.29*	± 0.17	189* ± 13	8.36*	± 0.20	155* ± 11
H223A(H ^{3.33} A)	10.41	± 0.14	85 ± 3	9.70	± 0.24	87 ± 5	9.44	± 0.10	83 ± 2
H226A(H ^{3.36} A)	10.63	± 0.15	83 ± 3	10.02	± 0.20	92 ± 5	9.35	± 0.26	74* ± 6
Q227A(Q ^{3.37} A)	10.53	± 0.13	76* ± 2	9.96	± 0.16	77* ± 3	9.66	± 0.10	73* ± 2
M230A(M ^{3.40} A)	10.79	± 0.27	46* ± 3	10.13	± 0.23	45* ± 3	9.84	± 0.31	48* ± 5
N233A (N ^{3.43} A)	10.72	± 0.17	64* ± 3	9.31*	± 0.24	77* ± 5	9.32*	± 0.14	71* ± 3
Y234A (Y ^{3.44} A)	10.18	± 0.12	80* ± 2	8.88*	± 0.14	79* ± 4	9.17	± 0.07	69* ± 2
I301A (I ^{5.39} A)	10.52	± 0.26	70 ± 5	8.29*	± 0.22	62* ± 5	8.19*	± 0.30	56* ± 6
H302A (H ^{5.40} A)	10.46	± 0.16	68* ± 3	8.53*	± 0.17	69* ± 4	8.94*	± 0.18	48* ± 3
V305A (V ^{5.43} A)	10.78	± 0.19	96 ± 5	9.89	± 0.15	89 ± 4	9.81	± 0.18	85 ± 5
M306A(M ^{5.44} A)	10.61	± 0.15	75* ± 3	9.70	± 0.17	82 ± 3	9.26	± 0.25	83 ± 6
Q355A (Q ^{6.52} A)	10.36	± 0.20	65* ± 4	9.12*	± 0.16	63* ± 4	9.23*	± 0.16	59* ± 3
F356A (F ^{6.53} A)	10.54	± 0.30	75* ± 6	8.58*	± 0.26	75* ± 7	9.04*	± 0.23	64* ± 5
F359A (F ^{6.56} A)	10.95	± 0.18	78* ± 4	9.29*	± 0.20	84* ± 5	9.35*	± 0.16	76* ± 4
P360A (P ^{6.57} A)	10.81	± 0.15	89 ± 3	8.51*	± 0.17	86 ± 5	9.12*	± 0.14	83* ± 4
W361A(W ^{6.58} A)	10.77	± 0.13	53* ± 2	9.44*	± 0.12	56* ± 2	9.07*	± 0.17	57* ± 3
P363A (P ^{6.60} A)	10.93	± 0.19	81* ± 4	8.34*	± 0.16	79* ± 4	8.64*	± 0.17	74* ± 5
D373A (D ^{7.39} A)	10.84	± 0.22	66* ± 4	8.86*	± 0.17	62* ± 4	8.74*	± 0.21	58* ± 4
M376A(M ^{7.42} A)	10.64	± 0.12	65* ± 2	8.53*	± 0.09	70* ± 2	8.81*	± 0.14	62* ± 3
H377A (H ^{7.43} A)	10.84	± 0.20	86 ± 4	9.76	± 0.20	79* ± 4	9.89	± 0.17	85* ± 4
I380A (I ^{7.46} A)	10.82	± 0.18	93 ± 4	10.22	± 0.24	101 ± 6	10.45	± 0.19	102 ± 5
Q383A (Q ^{7.49} A)	10.66	± 0.13	66* ± 2	9.56	± 0.19	74* ± 4	9.65	± 0.13	72* ± 3

cAMP formation in the presence of CT agonists was fit using 3-parameter logistic curves and normalized to WT receptor response. All values are mean±S.E.M. of 3 to 5

*independent experiments conducted in duplicate. Significance of changes in pEC_{50} and E_{max} values were calculated via comparison of mutant pEC_{50} and E_{max} values to the WT pEC_{50} and E_{max} respective values in a one-way Anova analysis of variance with Dunnett's post-hoc test with significant changes $P<0.05$ denoted by *.*

Table 5.2. Effect of single alanine mutation in the CTR TM region on cAMP efficacy ($\log\tau_c$) of CT agonists.

	sCT	hCT	pCT
WT	-0.08 \pm 0.02	-0.06 \pm 0.02	-0.08 \pm 0.02
N194A(N ^{2.60} A)	0.13 \pm 0.10	0.20 \pm 0.10	0.13 \pm 0.11
K220A(K ^{3.30} A)	0.88* \pm 0.13	1.10* \pm 0.16	0.70* \pm 0.13
H223A(H ^{3.33} A)	-0.17 \pm 0.07	-0.16 \pm 0.08	-0.19 \pm 0.08
H226A(H ^{3.36} A)	-0.16 \pm 0.04	-0.08 \pm 0.04	-0.24 \pm 0.05
Q227A(Q ^{3.37} A)	-0.04 \pm 0.13	-0.02 \pm 0.13	-0.07 \pm 0.13
M230A(M ^{3.40} A)	-0.19 \pm 0.15	-0.19 \pm 0.15	-0.17 \pm 0.15
N233A(N ^{3.43} A)	-0.08 \pm 0.06	0.05 \pm 0.05	-0.02 \pm 0.06
Y234A(Y ^{3.44} A)	-0.14 \pm 0.10	-0.14 \pm 0.11	-0.24 \pm 0.10
I301A(I ^{5.39} A)	0.41 \pm 0.31	0.24 \pm 0.31	0.18 \pm 0.31
H302A(H ^{5.40} A)	0.50 \pm 0.72	0.52 \pm 0.72	0.30 \pm 0.72
V305A(V ^{5.43} A)	0.19 \pm 0.10	0.14 \pm 0.10	0.09 \pm 0.11
M306A(M ^{5.44} A)	-0.03 \pm 0.11	0.03 \pm 0.11	0.03 \pm 0.11
Q355A(Q ^{6.52} A)	N.D.	N.D.	N.D.
F356A(F ^{6.53} A)	0.37 \pm 0.37	0.38 \pm 0.37	0.27 \pm 0.37
F359A(F ^{6.56} A)	-0.34 \pm 0.05	-0.28 \pm 0.06	-0.36 \pm 0.06
P360A(P ^{6.57} A)	-0.21 \pm 0.04	-0.21 \pm 0.05	-0.26 \pm 0.05
W361A(W ^{6.58} A)	-0.52 \pm 0.07	-0.48 \pm 0.07	-0.48 \pm 0.07
P363A(P ^{6.60} A)	0.13 \pm 0.10	0.13 \pm 0.10	0.07 \pm 0.10
D373A(D ^{7.39} A)	0.17 \pm 0.17	0.16 \pm 0.17	0.10 \pm 0.18
M376A(M ^{7.42} A)	0.07 \pm 0.18	0.12 \pm 0.18	0.04 \pm 0.18
H377A(H ^{7.43} A)	-0.12 \pm 0.06	-0.17 \pm 0.06	-0.13 \pm 0.06
I380A(I ^{7.46} A)	0.15 \pm 0.07	0.21 \pm 0.07	0.21 \pm 0.07
Q383A(Q ^{7.49} A)	0.35 \pm 0.11	0.44 \pm 0.11	0.40 \pm 0.11

cAMP formation in the presence of CT agonists was fit using three-parameter logistic equation and normalized to WT receptor response. The Black and Leff operational model, with a hill slope of 1, was applied to separate efficacy (τ) and functional affinity (pK_A). All log values were corrected for the cell surface expression to result $\log\tau_c$ and errors were propagated. Significance of changes in $\log\tau_c$ values were calculated via comparison of mutant $\log\tau_c$ values to the WT $\log\tau_c$ in a one-way Anova analysis of variance with Dunett's post-hoc test with significant changes $P < 0.05$ denoted by *. All values are mean \pm S.E.M. of 3 to 5 independent experiments conducted in duplicate. We were unable to obtain $\log\tau_c$ value for the Q355A as it had undetectable cell surface expression.

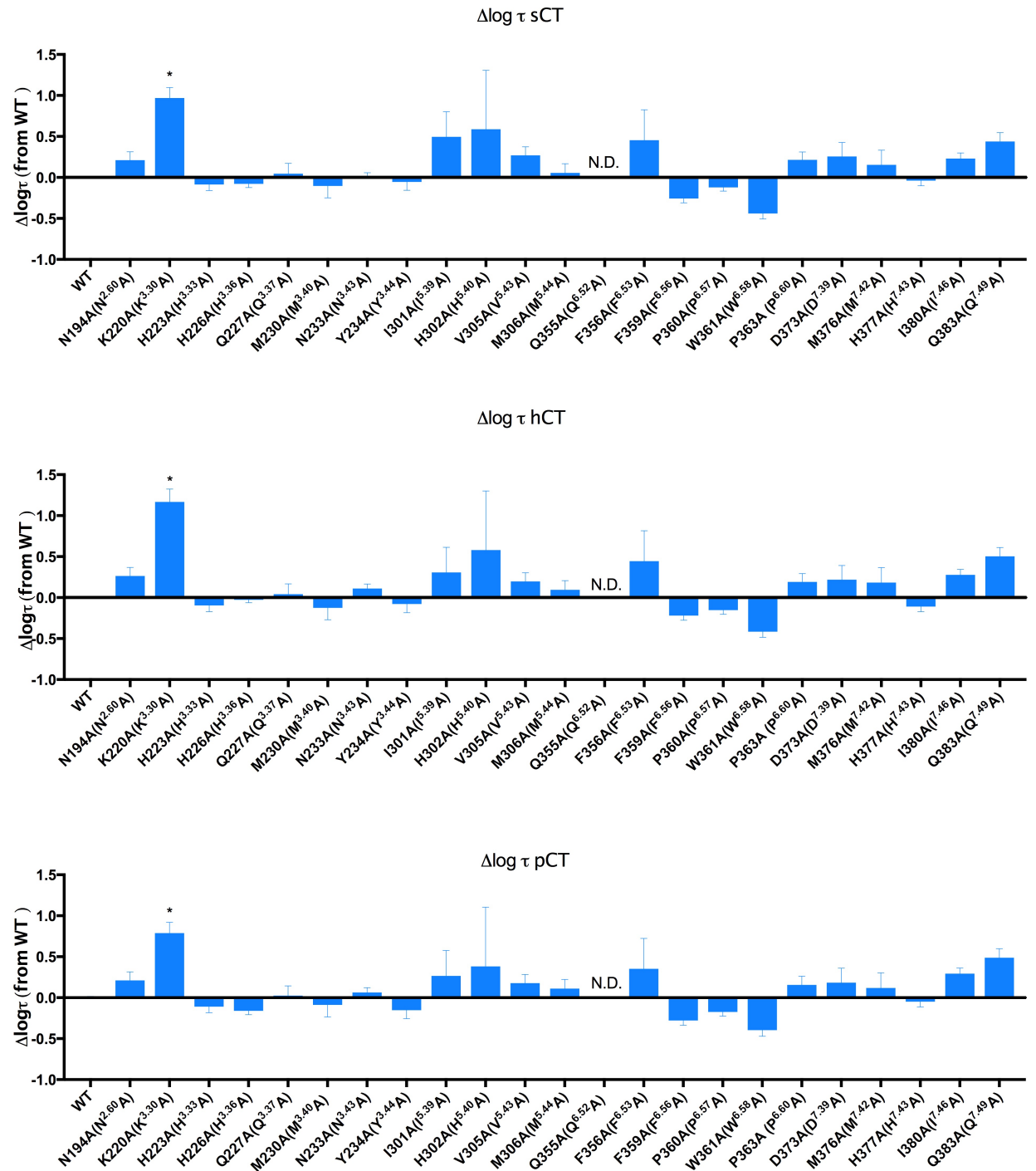
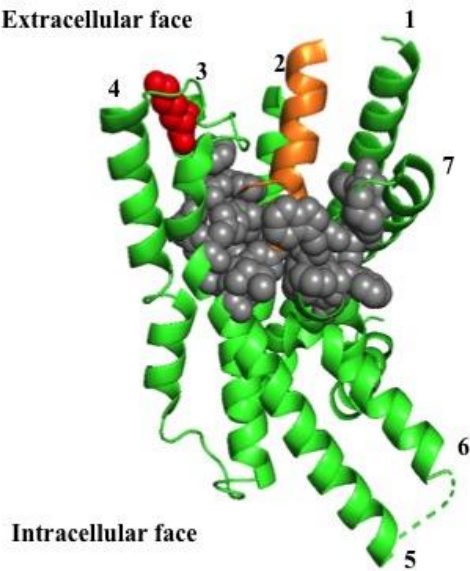


Figure 5.4. $\Delta\log\tau$ CT agonists (sCT, hCT and pCT) for cAMP. $\Delta\log\tau_c$ value for each mutant was obtained by subtracting WT $\log\tau$ from each mutant's $\log\tau_c$ value. All values are mean+S.E.M. of 3 to 5 independent experiments conducted in duplicate. Significance of changes were calculated via comparison of mutant's $\log\tau$ values to the WT receptor $\log\tau$ values in a one-way Anova analysis of variance with Dunnett's post-hoc test with significant changes ($P<0.05$ denoted by *). We were unable to obtain $\log\tau_c$ value for the Q355A as it had undetectable cell surface expression.

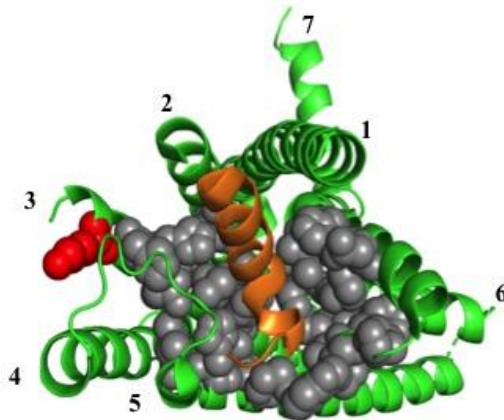
sCT, hCT, pCT

Extracellular face

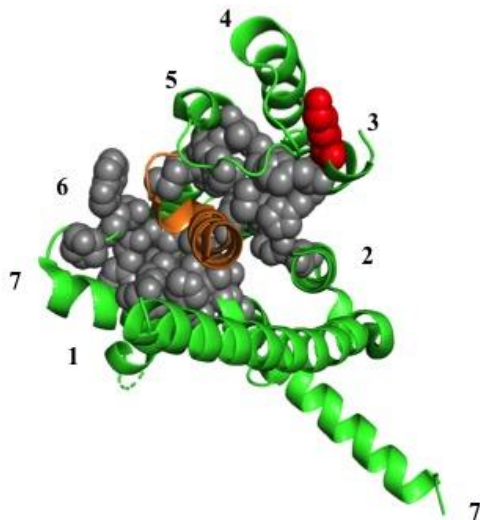


Orientation 1
(side view)

Intracellular face



Orientation 2
(oblique view)
looking down on
the CTR TM
bundle from the
extracellular side



Orientation 3
(top view)
looking down on
the CTR TM
bundle from the
extracellular side

Figure 5.5. Effect of the CTR TM mutations on cAMP efficacy for CT peptides. Residues are mapped onto the active Cryo-EM structure of CTR in complex with sCT and G_s protein (G_s protein and CTR N-terminal domain are not shown) (Dal Maso et. al., 2019). The receptor is shown in green and sCT ligand is shown in orange. K220A that significantly increased efficacy for all 3 CTs (sCT, hCT and pCT) is coloured in either red. Residues that produced no significant change in efficacy were coloured in gray.

5.2.1.2 cAMP SIGNALLING IN RESPONSE TO α CGRP AND rAMY

cAMP response for each mutant and the WT receptor to α CGRP and rAMY was measured and data were fitted to three-parameter logistic curves that were normalized to WT maximal response (Figures 5.6 and 5.7), this is a re-analysis of data from chapter 4. Values for the EC_{50} and E_{max} were derived from the curves and are reported in Table 5.3. Efficacy values were derived using the Black and Leff operational model with transducer slope $n=1$ (as the operational fit was used with $n=1$, the curves looked identical to the three-parameter fit (Figures 5.6 and 5.7)). Correction for the cell surface expression was subsequently applied to $\log\tau$ values to obtain corrected values $\log\tau_c$ (Table 5.4). $\Delta\log\tau_c$ value for each mutant was obtained by subtracting WT $\log\tau$ from each mutant's $\log\tau_c$ value (Figure 5.8). Similarly to CT agonists, many mutants exhibited impaired concentration response data, either reducing potency, E_{max} or both, however following application of the operational model to derive efficacy parameters and correcting these for changes in cell surface expression revealed that many of the observed E_{max} effects were the result of reduced cell surface expression.

For rAMY, statistically significant changes in efficacy were seen for the mutants: K220A ($K^{3.30}A$), F356A ($F^{6.53}A$), M376A ($M^{7.42}A$) and Q383A ($Q^{7.49}A$), all increasing cAMP efficacy (these residues were mapped onto a hCTR model (pdb 6NIY) (dal Maso *et al.*, 2019) (Figure 5.9). None of cAMP efficacy effects reached statistical significance for α CGRP, however the magnitude and direction of change was similar to that seen with rAMY (Figure 5.8, Table 5.4).

Concentration response and operational fitting was not carried out where there was inadequate data to support that the curve fit had passed the inflection point such that there was limited confidence in the curve-fit estimate for the E_{max} . These included datasets: P363A ($P^{6.60}A$) and D373A ($D^{7.39}A$) (α CGRP); H302A ($H^{5.40}A$), P363A ($P^{6.60}A$), D373A ($D^{7.39}A$) (rAMY). Additionally, we were unable to obtain cell surface corrected $\log\tau_c$ value for the Q355A ($Q^{6.52}A$) as it had undetectable cell surface expression.

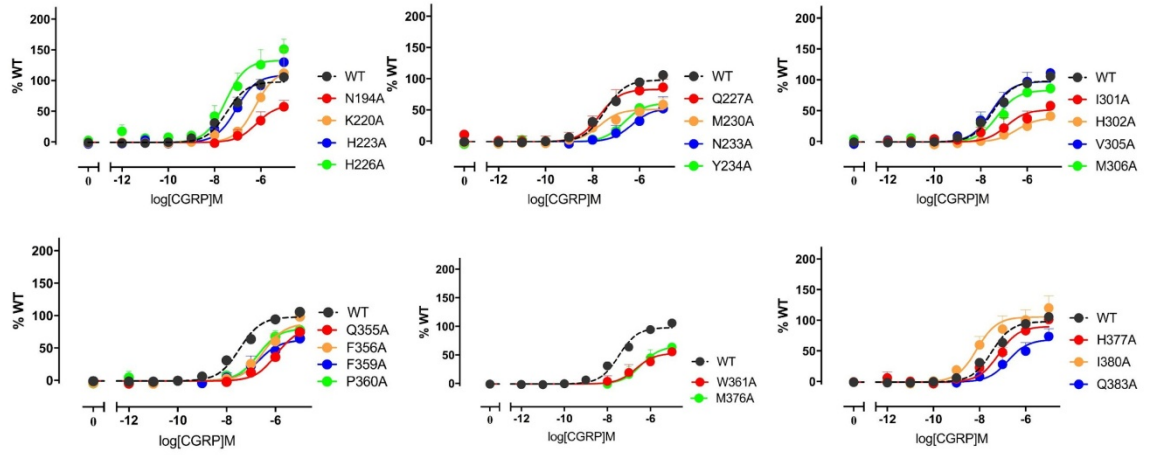


Figure 5.6. *cAMP accumulation profiles in response to α CGRP in CV-1-FlpIn cells stably expressing hCTR α Leu single alanine mutations in the receptor TM region. cAMP formation in the presence of α CGRP was fit using three-parameter logistic equation and normalized to WT receptor response. The Black and Leff operational model, with a hill slope of 1, was applied to separate efficacy (τ) and functional affinity (pK_A). All values are mean+S.E.M. of 3 to 5 independent experiments conducted in duplicate; for some data points error bars are not shown as they are smaller than the height of the symbol.*

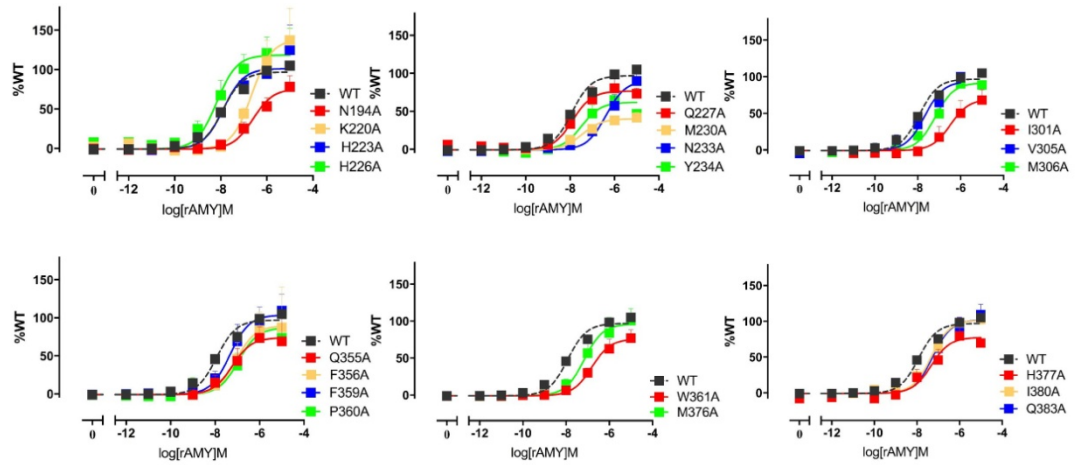


Figure 5.7. *cAMP accumulation profiles in response to rAMY in CV-1-FlpIn cells stably expressing hCTR α Leu single alanine mutations in the receptor TM region. cAMP formation in the presence of rAMY was fit using three-parameter logistic equation and normalized to WT receptor response. The Black and Leff operational model, with a hill slope of 1, was applied to separate efficacy (τ) and functional affinity (pK_A). All values are mean+S.E.M. of 3 to 5 independent experiments conducted in duplicate; for some data points error bars are not shown as they are smaller than the height of the symbol.*

Table 5.3. Effect of single alanine CTR TM region mutation on cAMP potency (EC_{50}) and maximal response to α CGRP and rAMY.

	α CGRP		rAMY	
	pEC ₅₀	E _{max}	pEC ₅₀	E _{max}
WT	7.42 \pm 0.06	99 \pm 2	7.88 \pm 0.06	97 \pm 2
N194A(N ^{2.60} A)	6.30* \pm 0.26	59* \pm 8	6.55* \pm 0.21	76* \pm 7
K220A(K ^{3.30} A)	6.21* \pm 0.19	118 \pm 14	6.64* \pm 0.20	139* \pm 14
H223A(H ^{3.33} A)	7.02 \pm 0.16	110 \pm 9	7.85 \pm 0.16	102 \pm 6
H226A(H ^{3.36} A)	7.35 \pm 0.22	137 \pm 12	8.05 \pm 0.21	120 \pm 9
Q227A(Q ^{3.37} A)	7.62 \pm 0.26	84 \pm 7	7.81 \pm 0.24	77 \pm 6
M230A(M ^{3.40} A)	7.77 \pm 0.25	50* \pm 5	7.74 \pm 0.17	39* \pm 3
N233A (N ^{3.43} A)	6.51* \pm 0.37	51* \pm 9	6.32* \pm 0.21	92 \pm 9
Y234A (Y ^{3.44} A)	6.67* \pm 0.13	61* \pm 4	7.55 \pm 0.18	62* \pm 5
I301A (I ^{5.39} A)	6.64* \pm 0.32	54* \pm 7	6.59 \pm 0.28	68* \pm 9
H302A (H ^{5.40} A)	6.75* \pm 0.28	35* \pm 6	N.D.	N.D.
V305A (V ^{5.43} A)	7.47 \pm 0.21	98 \pm 8	7.67 \pm 0.15	94 \pm 6
M306A(M ^{5.44} A)	7.06 \pm 0.23	86 \pm 7	7.18* \pm 0.13	92 \pm 5
Q355A (Q ^{6.52} A)	6.07* \pm 0.11	77* \pm 8	7.39 \pm 0.26	72* \pm 9
F356A (F ^{6.53} A)	6.59* \pm 0.15	85 \pm 8	7.14* \pm 0.29	89 \pm 13
F359A (F ^{6.56} A)	6.82 \pm 0.25	61* \pm 7	7.30* \pm 0.24	104 \pm 9
P360A (P ^{6.57} A)	6.72* \pm 0.17	80 \pm 8	6.93* \pm 0.21	87 \pm 10
W361A(W ^{6.58} A)	6.87* \pm 0.24	51* \pm 6	6.80 \pm 0.17	76* \pm 6
P363A (P ^{6.60} A)	N.D.	N.D.	N.D.	N.D.
D373A (D ^{7.39} A)	N.D.	N.D.	N.D.	N.D.
M376A(M ^{7.42} A)	6.64 \pm 0.22	62* \pm 7	7.16* \pm 0.21	96 \pm 8
H377A (H ^{7.43} A)	7.08 \pm 0.16	92 \pm 7	7.51 \pm 0.28	75* \pm 9
I380A (I ^{7.46} A)	8.13 \pm 0.21	106 \pm 8	7.31 \pm 0.11	102 \pm 4
Q383A (Q ^{7.49} A)	6.85 \pm 0.25	68* \pm 8	7.22 \pm 0.18	103 \pm 7

cAMP formation in the presence of CT agonists was fit using 3-parameter logistic curves and normalized to WT receptor response. All values are mean \pm S.E.M. of 3 to 5 independent experiments conducted in duplicate. Significance of changes in pEC₅₀ and E_{max} values were calculated via comparison of mutant pEC₅₀ and E_{max} values to the WT pEC₅₀ and E_{max} respective values in a one-way Anova analysis of variance with Dunett's post-hoc test with significant changes $P < 0.05$ denoted by *.

Table 5.4. Effect of single alanine mutation in the CTR TM region on cAMP efficacy ($\log\tau_c$) of α CGRP and rAMY.

	\langle CGRP	rAMY
WT	-0.21 \pm 0.02	-0.18 \pm 0.02
N194A(N ^{2.60} A)	0.00 \pm 0.14	0.17 \pm 0.12
K220A(K ^{3.30} A)	0.25 \pm 0.16	0.45* \pm 0.14
H223A(H ^{3.33} A)	-0.11 \pm 0.10	-0.13 \pm 0.08
H226A(H ^{3.36} A)	0.08 \pm 0.06	0.03 \pm 0.05
Q227A(Q ^{3.37} A)	-0.09 \pm 0.13	-0.10 \pm 0.13
M230A(M ^{3.40} A)	-0.22 \pm 0.15	-0.32 \pm 0.18
N233A (N ^{3.43} A)	-0.29 \pm 0.11	0.07 \pm 0.10
Y234A (Y ^{3.44} A)	-0.40 \pm 0.16	-0.36 \pm 0.14
I301A (I ^{5.39} A)	0.04 \pm 0.31	0.24 \pm 0.32
H302A (H ^{5.40} A)	0.10 \pm 0.74	N.D.
V305A (V ^{5.43} A)	0.07 \pm 0.12	0.08 \pm 0.13
M306A(M ^{5.44} A)	-0.07 \pm 0.12	0.03 \pm 0.12
Q355A (Q ^{6.52} A)	N.D.	N.D.
F356A (F ^{6.53} A)	0.37 \pm 0.39	0.41* \pm 0.38
F359A (F ^{6.56} A)	-0.58 \pm 0.09	-0.22 \pm 0.06
P360A (P ^{6.57} A)	-0.39 \pm 0.10	-0.30 \pm 0.10
W361A(W ^{6.58} A)	-0.61 \pm 0.11	-0.37 \pm 0.08
P363A (P ^{6.60} A)	N.D.	N.D.
D373A (D ^{7.39} A)	N.D.	N.D.
M376A(M ^{7.42} A)	-0.03 \pm 0.20	0.25* \pm 0.18
H377A (H ^{7.43} A)	-0.20 \pm 0.09	-0.26 \pm 0.11
I380A (I ^{7.46} A)	0.12 \pm 0.07	0.13 \pm 0.09
Q383A (Q ^{7.49} A)	0.28 \pm 0.13	0.58* \pm 0.11

cAMP formation in the presence of α CGRP and rAMY agonists was fit using three-parameter logistic equation and normalized to WT receptor response. The Black and Leff operational model, with a hill slope of 1, was applied to separate efficacy (τ) and functional affinity (pK_A). All values are mean \pm S.E.M. of 3 to 5 independent experiments conducted in duplicate. All $\log\tau$ were corrected for the cell surface expression to result $\log\tau_c$ values and errors were propagated. Significance of changes in $\log\tau_c$ values were calculated via comparison of mutant $\log\tau_c$ values to the WT $\log\tau_c$ in a one-way Anova analysis of variance with Dunett's post-hoc test with significant changes $P<0.05$ denoted by *.

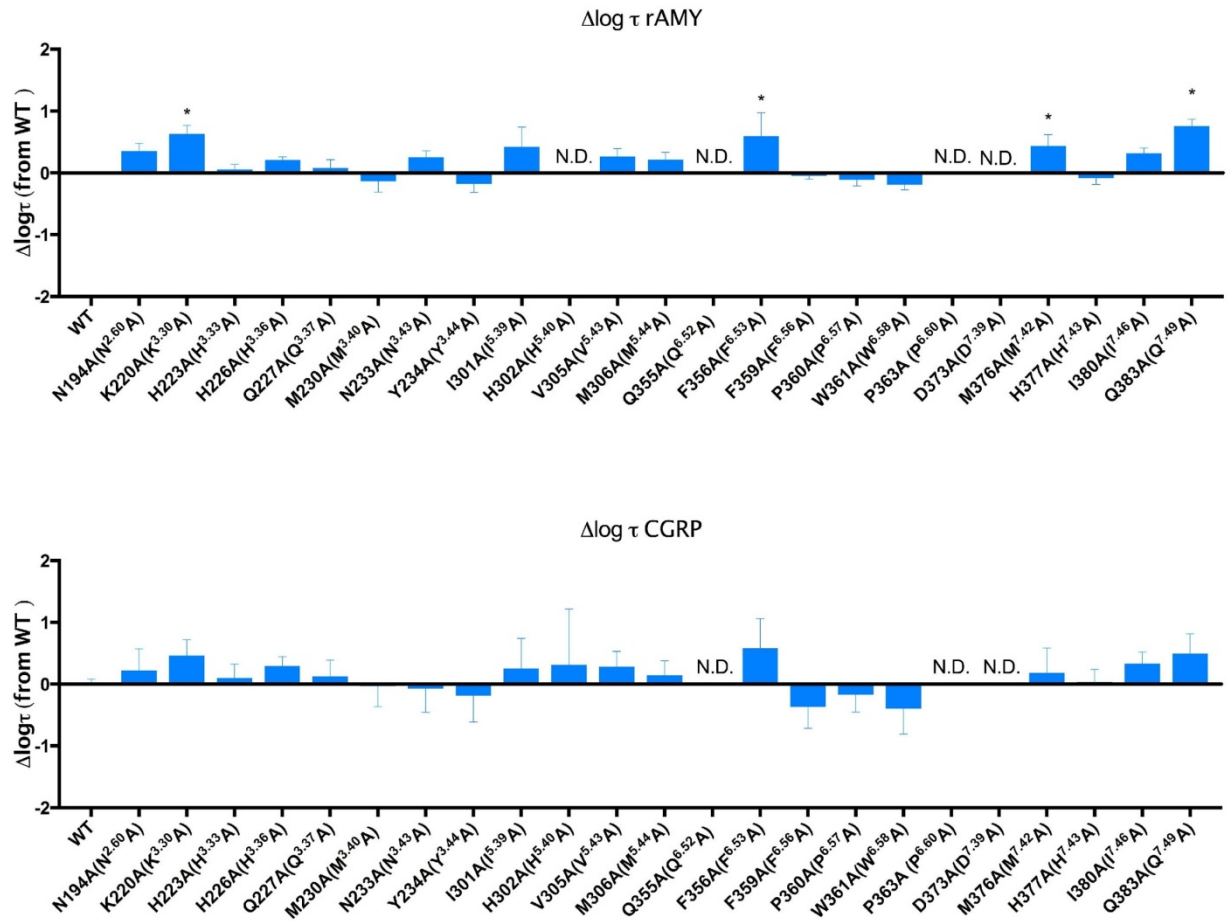


Figure 5.8. $\Delta\log\tau$ for α CGRP and rAMY for cAMP. $\Delta\log\tau_c$ value for each mutant was obtained by subtracting WT $\log\tau$ from each mutant's $\log\tau_c$ value. All values are mean+S.E.M. of 3 to 5 independent experiments conducted in duplicate. Significance of changes were calculated via comparison of mutant's $\log\tau$ values to the WT receptor $\log\tau$ values in a one-way Anova analysis of variance with Dunett's post-hoc test with significant changes $P<0.05$ denoted by *.

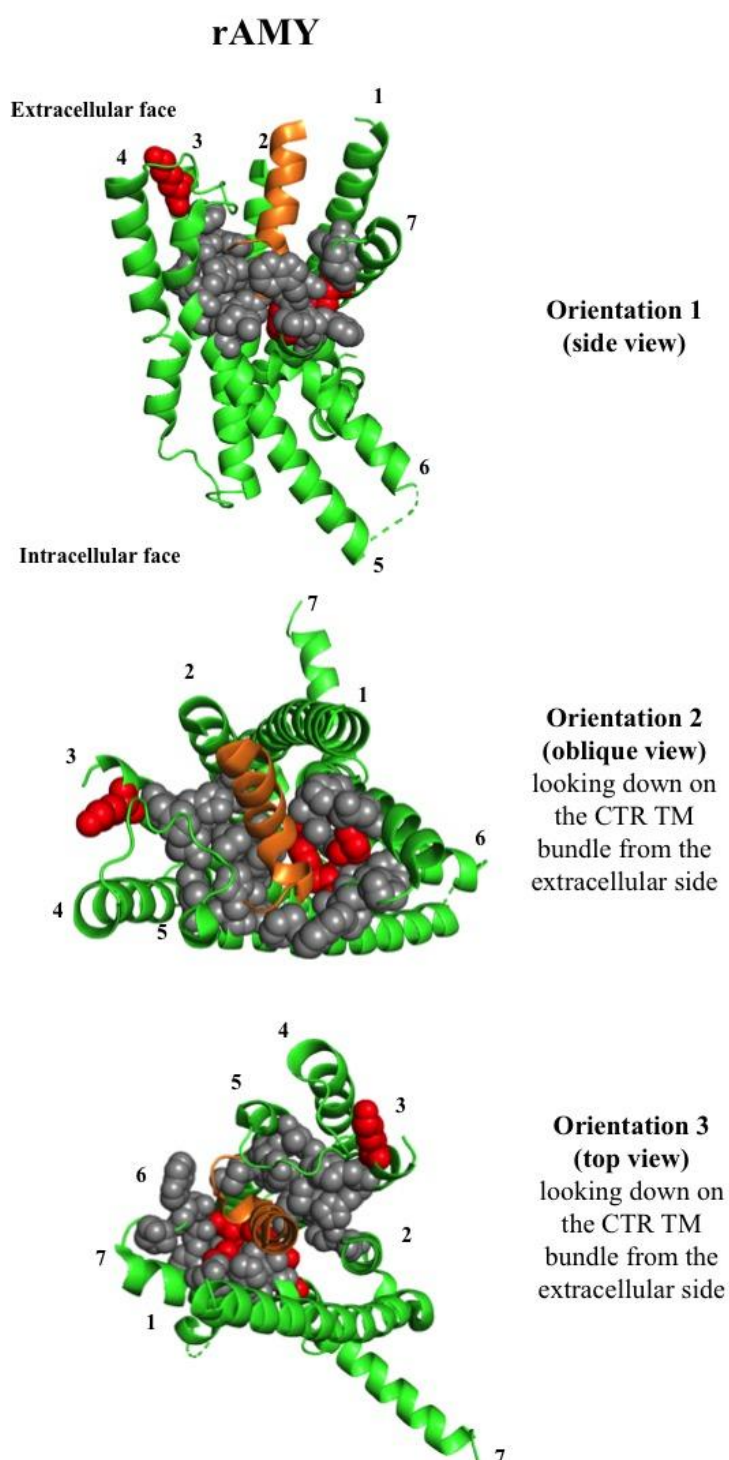


Figure 5.9. Effect of the CTR TM mutations on cAMP efficacy for rAMY. Residues are mapped onto a CTR model based on the active Cryo-EM structure of CTR in complex with sCT and G_s protein (G_s protein and CTR N-terminal domain are not shown) (Dal Maso et. al., 2019). The receptor is shown in green and sCT ligand is shown in orange. Residues that produced significant changes in efficacy were coloured in red (<10 times increase in efficacy) and are shown as space-fill side chains. Residues that produced no significant change in efficacy were coloured in gray.

5.2.2 EFFECTS OF THE CTR TM MUTATIONS ON CTR PERK1/2 SIGNALLING

5.2.2.1 ASSESSMENT OF PERK1/2 IN RESPONSE TO CALCITONINS

A pERK1/2 time-course was performed for each mutant and for the WT receptor in presence of 100 nM sCT, 1 μ M hCT, 1 μ M pCT in order to determine the peak response time and to assess if the time to peak was altered by any of the introduced mutations. The time course experiment revealed that, for all CTR agonists, pERK1/2 peak response time for all mutants as well as the WT receptor was between 5-6 minutes (Figures 5.10 – 5.12). Therefore, all subsequent concentration response experiments were performed at a 5 minute time point.

Interestingly, pERK1/2 response to CT agonists for the WT receptor and for some of the mutants was better fit with a biphasic concentration response curve. Therefore, for all CT agonists pERK1/2 response was fit to either three-parameter logistic equation or a two-site (biphasic) fit based on F-test with a P-value cutoff for the preferred model of < 0.05 (Figures 5.13 – 5.15) this is a re-analysis of data from chapter 4. It should be noted that the concentration response curves were composed of only 6 ligand concentrations and distinct phases of the biphasic response, especially the higher concentration responses, often only entailed one or two points. Hence, to truly sample the significance of the biphasic effects a larger number of concentrations would need to be tested in the concentration response curves.

Values for EC_{50} and E_{max} were derived from the curves and are reported in Table 5.5. In pERK1/2 assay we measured a transient response under non-equilibrium conditions. Presence of biphasic pERK1/2 concentration curves indicates that there are two receptor pools that are essentially non-interchangeable over the timescale of this experiment. It is also possible that each phase of pERK1/2 response corresponds to a distinct upstream signalling pathway.

Efficacy values were derived for the pERK1/2 data using the Black and Leff operational model of agonism. This model assumes that the mechanism is shared for all receptor mutants and thus the transducer slope must be the same. In addition, it is not possible to fit biphasic concentration-response curves using this model. Thus, to allow comparison across mutants, the data was fit with a shared variable transducer slope (Figures 5.16 – 5.18), however this necessitated excluding data for which a second inflection point was not evident when a shared (low transducer slope) was fitted. Correction for cell surface expression was applied for all log τ values to give log τ_c values (Table 5.6). Δ log τ_c value for each mutant was obtained by subtracting WT log τ from each mutant's log τ_c value (Figure 5.19). Significant effects of the Ala TM mutations on the CTR pERK1/2 pathway for CT agonists were mapped onto a hCTR model (pdb 6NIY) (Dal Maso *et al.*, 2019) (Figure 5.20).

Overall, mutations of the CTR TM residues have more profound effects on the CTR efficacy for the pERK1/2 pathway compared to the cAMP pathway. Thus, statistically significant reductions in sCT dependent pERK1/2 efficacy were seen for the following residues: N194A (N^{2.60}A), K220A (K^{3.30}A), H226A (H^{3.36}A), Q227A (Q^{3.37}A), M230A (M^{3.40}A), N233A (N^{3.43}A), I301A (I^{5.39}A), H302A (H^{5.40}A), V305A (V^{5.43}A), M306A (M^{5.44}A), F356A (F^{6.53}A), D373A (D^{7.39}A) and Q383A (Q^{7.49}A) (Figure 5.19, Table 5.6). hCT and pCT had similar patterns to sCT (Figure 5.19, Table 5.6). Operational fitting was not carried out where there was inadequate data to confidently estimate the E_{\max} . These included datasets: Q355A (Q^{6.52}A), F359A (F^{6.56}A) and M376A (M^{7.42}A) (for sCT); Y234A (Y^{3.44}A), P360A (P^{6.57}A), W361A (W^{6.58}A) and D373A (D^{7.39}A) (for hCT); H223A (H^{3.33}A), H226A (H^{3.36}A), N233A (N^{3.43}A), Q355A (Q^{6.52}A), F359A (F^{6.56}A), M376A (M^{7.42}A) and Q383A (Q^{7.49}A) (for pCT). Additionally, we were unable to obtain cell surface corrected $\log\tau_c$ value for the Q355A as it had undetectable cell surface expression.

Although, we were not able to quantify $\log\tau_c$ for W361A (W^{6.58}A) and D373A (D^{7.39}A) for hCT, the changes that these mutants have on the concentration response curves (decreased potency and severely reduced maximal response (expression was only about 30% of the WT), (Figures 5.13 – 5.15), suggest that these mutations affect hCT pERK1/2 efficacy in the same way they did for sCT and pCT (Figure 5.19).

Because of detrimental effects on pERK1/2 signalling, the data for the mutants H223A (H^{3.33}A), H226A (H^{3.36}A) and N233A (N^{3.43}A) for pCT could not be fitted to the operational model. According to the concentration response curves for these three residues, all three of them severely decreased pERK1/2 potency while H223A (H^{3.33}A) and N233A (N^{3.43}A) also decreased E_{\max} (Figure 5.15). H223A (H^{3.33}A) and H226A (H^{3.36}A) displayed cell surface expression not significantly different from the WT CTR, whereas N233A (N^{3.43}A) showed 50% of the WT decreased expression (Figure 5.15). Therefore, these 3 residues are likely to be important for pERK1/2 efficacy. Because H223A (H^{3.33}A) decreased E_{\max} while its expression was not significantly different from the WT, this residue is also important for pCT efficacy, albeit we were unable to quantify this effect.

As we considered an alternative operational fitting for pERK1/2 data (constraining the transducer slope (n) to 0.4 and increasing E_{\max} to 200, as previously discussed in Chapter 4), we calculated $\Delta\log\tau_c$ for this alternative fit (Supplementary figure 5, Appendix 1). $\Delta\log\tau_c$ values obtained for the alternative fit were largely consistent with the results obtained from the original fit (shared transducer slope globally fitted to all data sets from the WT and each mutant): the pattern and the direction of effects was the same between the two fits, although the magnitude of

the effects was smaller for the alternative fit. Since the overall pattern of the effects was similar between the two fits, it did not affect our data interpretation.

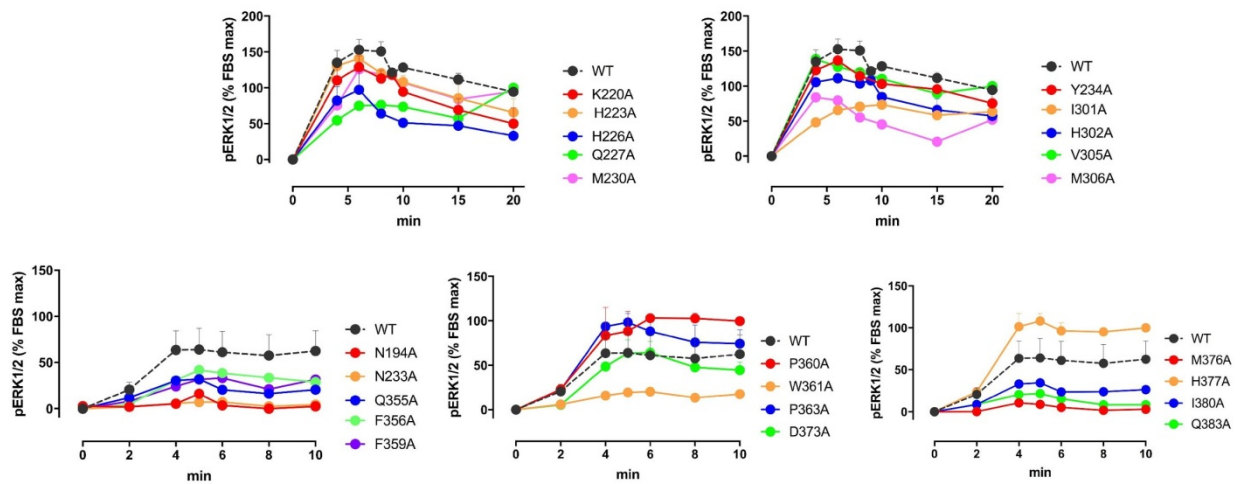


Figure 5.10. *pERK1/2* time course response profiles to 100 nM sCT in CV-1-FlpIn cells stably expressing hCTRαLeu mutations in the receptor TM region. *pERK1/2* response in the presence of 100 nM sCT was measured as indicated and normalized at 8 min FBS and vehicle responses. All values are mean of either 1 or 2 (mean +SD) independent experiments conducted in duplicate (for the experiments that are an N of 1, only the mean of the replicates with no error is shown).

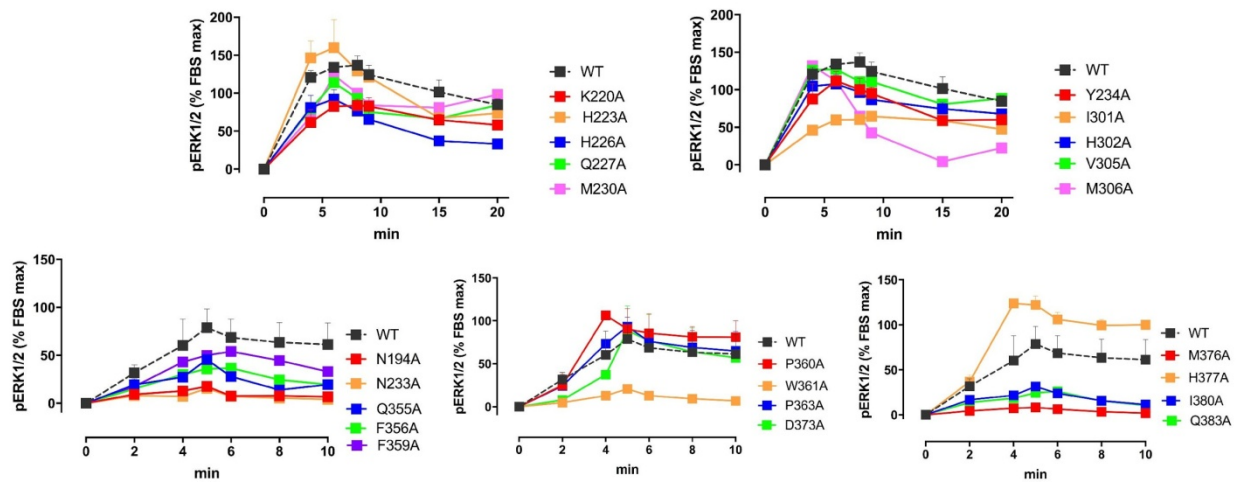


Figure 5.11. *pERK1/2* time course response profiles to 1 μM hCT in CV-1-FlpIn cells stably expressing hCTRαLeu mutations in the receptor TM region. *pERK1/2* response in the presence of 1 μM hCT was measured as indicated and normalized at 8 min FBS and vehicle responses. All values are mean of either 1 or 2 (mean+SD) independent experiments conducted in duplicate (for the experiments that are an N of 1, only the mean of the replicates with no error is shown).

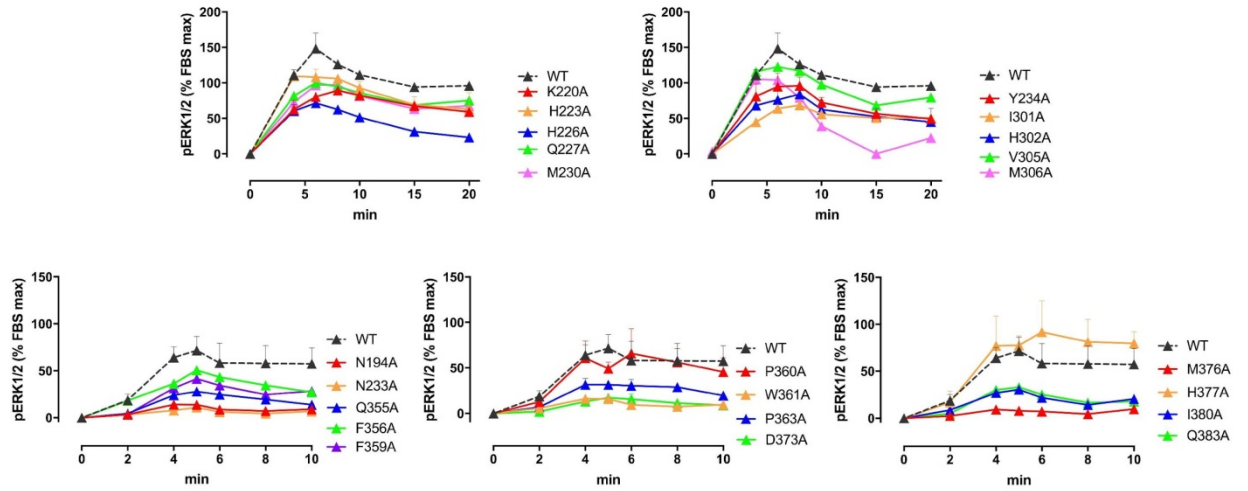


Figure 5.12. *pERK1/2 time course response profiles to 1 μ M pCT in CV-1-FlpIn cells stably expressing hCTRaLeu mutations in the receptor TM region.* *pERK1/2 response in the presence of 1 μ M pCT was measured as indicated and normalized at 8 min FBS and vehicle responses. All values are mean of either 1 or 2 (mean +SD) independent experiments conducted in duplicate (for the experiments that are an N of 1, only the mean of the replicates with no error is shown).*

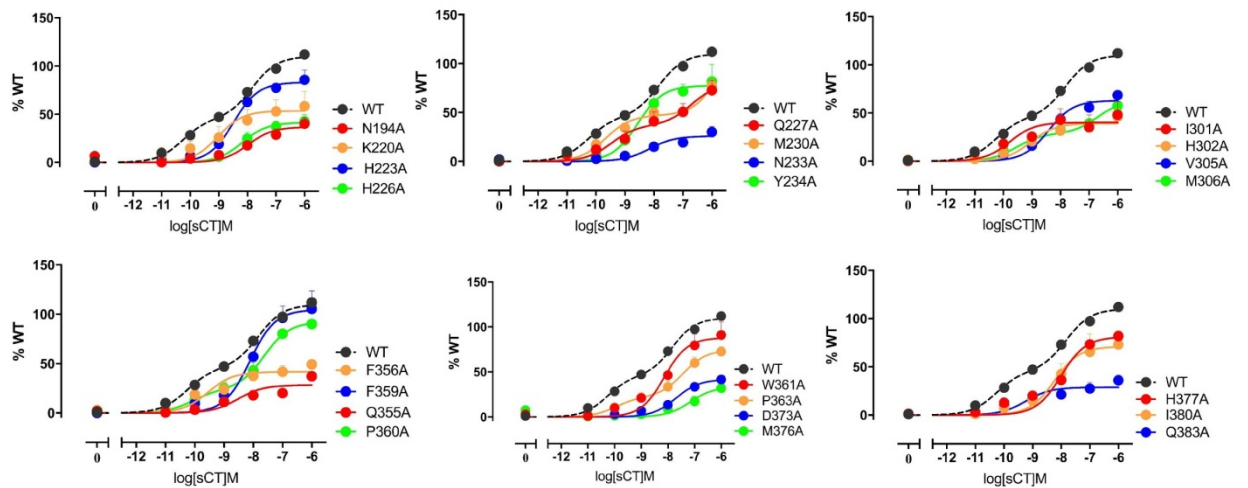


Figure 5.13. *pERK1/2 concentration response to sCT in CV-1-FlpIn cells stably expressing hCTRaLeu mutations in the receptor TM region.* *pERK1/2 response in presence of sCT was fit to either three-parameter logistic equation or a two-site (biphasic) fit and normalized to WT receptor response. The choice of data fit was determined using an F-test with a P-value cutoff for the preferred model of < 0.05. All values are mean+S.E.M. of 3 to 5 independent experiments conducted in duplicate; for some data points error bars are not shown as they are smaller than the height of the symbol.*

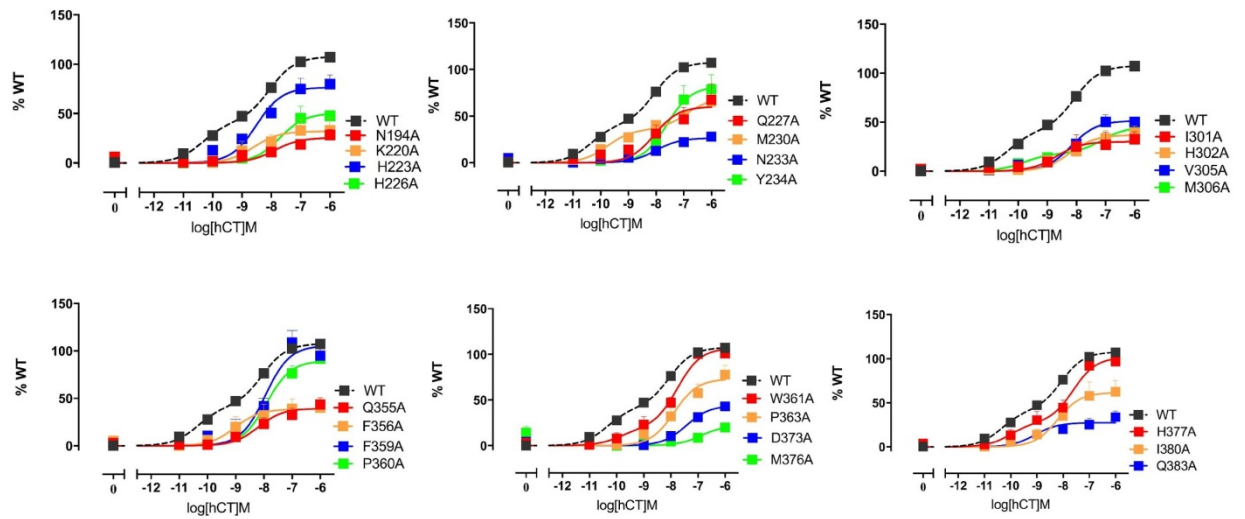


Figure 5.14. *pERK1/2* concentration response to hCT in CV-1-FlpIn cells stably expressing hCTR α Leu mutations in the receptor TM region. *pERK1/2* response in presence of hCT was fit to either three-parameter logistic equation or a two-site (biphasic) fit and normalized to WT receptor response. The choice of data fit was determined using an F-test with a P-value cutoff for the preferred model of < 0.05. All values are mean+S.E.M. of 3 to 5 independent experiments conducted in duplicate; for some data points error bars are not shown as they are smaller than the height of the symbol.

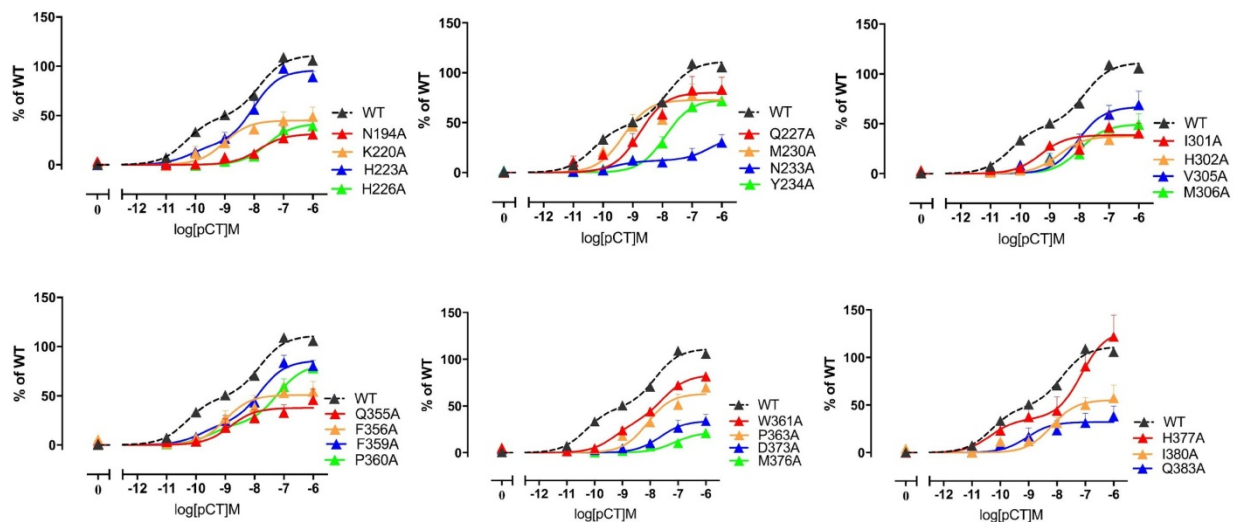


Figure 5.15. *pERK1/2* concentration response to pCT in CV-1-FlpIn cells stably expressing hCTR α Leu mutations in the receptor TM region. *pERK1/2* response in presence of pCT was fit to either three-parameter logistic equation or a two-site (biphasic) fit and normalized to WT receptor response. The choice of data fit was determined using an F-test with a P-value cutoff for the preferred model of < 0.05. All values are mean+S.E.M. of 3 to 5 independent experiments conducted in duplicate; for some data points error bars are not shown as they are smaller than the height of the symbol.

Table 5.5. Effect of single alanine CTR TM region mutation on pERK1/2 potency (EC_{50}) and maximal response to calcitonin agonists (sCT, hCT and pCT)

	sCT				hCT				pCT			
	pEC50 ₁	pEC50 ₂	fraction	E _{max}	pEC50 ₁	pEC50 ₂	fraction	E _{max}	pEC50 ₁	pEC50 ₂	fraction	E _{max}
WT	10.23±0.17	7.84±0.15	0.44±0.05	109±3	10.38±0.19	8.08±0.13	0.38±0.05	108±3	10.32±0.18	7.83±0.15	0.57±0.05	111 ±3
N2.60 (194)A	7.98±0.21	_____	_____	37*±3	7.89±0.27	_____	_____	26*±2	7.84±0.29	_____	_____	31±4
K3.30 (220)A	5.56±0.29	_____	_____	54*±5	8.75±0.3	_____	_____	33*±4	9.02±0.24	_____	_____	45*±4
H3.33 (223)A	8.77±0.15	_____	_____	81±4	10.54±0.73	8.17±0.25	0.24±0.11	80±4	10.2±0.72	8.02±0.21	0.21±0.11	96±5
H3.36 (226)A	8.18±0.19	_____	_____	41*±3	7.72±0.19	_____	_____	51*±5	7.55±0.19	_____	_____	42*±4
Q3.37 (227)A	9.69±0.36	6.91±0.29	0.49±0.1	76*±9	8.22±0.25	_____	_____	59*±6	8.76±0.22	_____	_____	80±6
M3.40 (230)A	9.67±0.19	5.68±2.24	0.66±0.74	61*±4	9.76±0.18	6.92±0.26	0.51±0.05	69*±5	9.32±0.23	_____	_____	73*±9
N3.43 (233)A	8.15±0.22	_____	_____	26*±2	8±0.21	_____	_____	27**±3	9.7±0.78	6.37±1.01	0.31±0.14	38*±19
Y3.44 (234)A	8.76±0.19	_____	_____	75*±5	7.65±0.16	_____	_____	77*±6	7.88±0.17	_____	_____	73*±6
I5.39 (301)A	9.78±0.37	_____	_____	40*±5	8.69±0.43	_____	_____	30*±5	9.3±0.36	_____	_____	39*±5
H5.40 (302)A	9.42±0.26	_____	_____	42*±3	8.59±0.25	_____	_____	41*±4	8.7±0.19	_____	_____	38*±3
V5.43 (305)A	8.43±0.12	_____	_____	63*±3	8.17±0.14	_____	_____	52*±3	8.04±0.19	_____	_____	67*±6
M5.44 (306)A	9.56±0.41	6.7±0.54	0.45±0.1	63*±10	9.81±0.36	7.12±0.32	0.4±0.08	45*±4	7.97±0.24	_____	_____	50*±5
Q6.52(355)A	8.53±0.25	_____	_____	28*±3	8.2±0.23	_____	_____	39*±4	8.83±0.32	_____	_____	38*±4
F6.53 (356)A	8.03±0.41	10.53±0.54	0.59±0.13	49*±4	8.9±0.28	_____	_____	40*±4	9±0.25	_____	_____	51*±5
F6.56 (359)A	8.12±0.14	_____	_____	105±6	7.88±0.17	_____	_____	73±6	9.85±0.63	7.82±0.25	0.25±0.12	86±5
P6.57 (360)A	10.1±0.45	-7.63±0.2	0.25±0.07	92±5	7.91±0.12	_____	_____	90±5	9.5±0.67	7.21±0.29	0.26±0.11	82±7
W6.58 (361)A	8.14±0.16	_____	_____	88±6	9.89±0.72	7.76±0.19	0.17±0.09	107±5	9.28±0.36	7.54±0.3	0.4±0.13	83±4
P6.60 (363)A	9.95±0.48	7.43±0.29	0.3±0.09	74*±5	7.88±0.17	_____	_____	73*±6	8.11±0.25	_____	_____	63*±7
D7.39 (373)A	7.7±0.13	_____	_____	42*±3	7.43±0.1	_____	_____	44*±2	7.64±0.29	_____	_____	34*±5
M7.42 (376)A	7.16±0.27	_____	_____	33*±5	6.87±0.49	_____	_____	22*±7	7.13±0.28	_____	_____	22*±4
H7.43 (377)A	10.39±0.43	7.63±0.14	0.21±0.05	84±3	10.01±0.55	7.61±0.27	0.27±0.1	102±7	10.35±0.73	7.15±0.36	0.27±0.09	128±16
I7.46 (380)A	8.24±0.24	_____	_____	71*±7	8.21±0.25	_____	_____	62*±6	8.2±0.23	_____	_____	55*±5
Q7.49 (383)A	10.09±0.42	6.98±0.57	0.51±0.11	38*±6	9.07±0.31	_____	_____	27*±3	9.05±0.38	_____	_____	32*±4

pERK1/2 response in presence of CT agonists was fit to either three-parameter logistic equation or a two-site (biphasic) fit and normalized to WT receptor response. The choice of data fit was determined using an F-test with a P-value cutoff for the preferred model of < 0.05. For biphasic response curves pEC₅₀ for high (pEC50₁) and low (pEC50₂) sites and the fraction of maximal response due to the more potent phase (fraction) are shown. All values are mean±S.E.M. of 3 to 5 independent experiments conducted in duplicate. Significance of changes in E_{max} values were calculated via comparison of mutant E_{max} values to the WT E_{max} respective values in a one-way Anova analysis of variance with Dunett's post-hoc test with significant changes P<0.05 denoted by *.

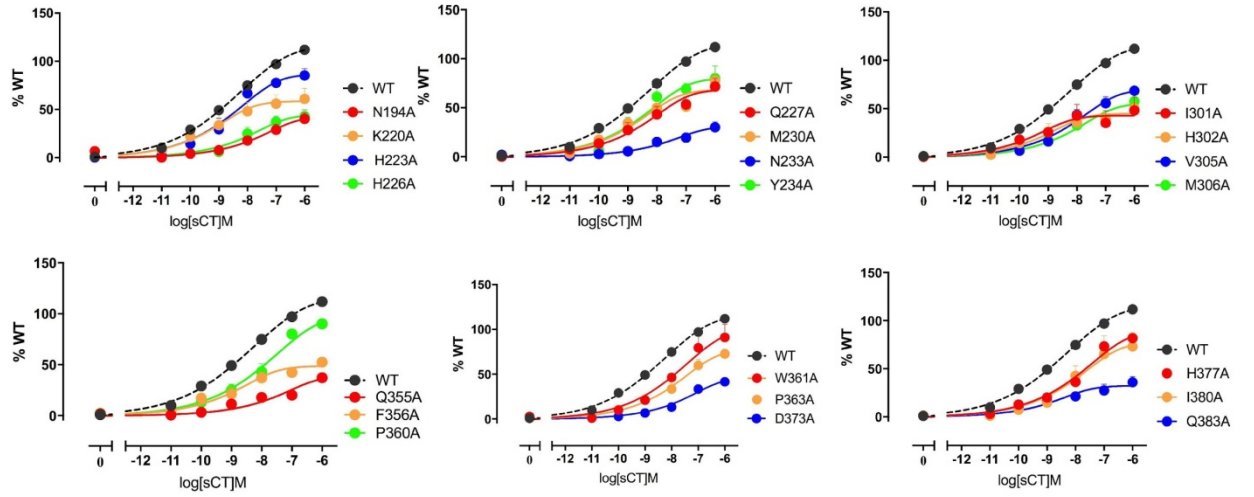


Figure 5.16. *pERK1/2* concentration response to *sCT* in *CV-1-FlpIn* cells stably expressing *hCTRαLeu* mutations in the receptor TM region. *pERK1/2* response in the presence of *sCT* was fit using Black and Leff operational model with a variable transducer slope and normalized to WT receptor response. All values are mean+S.E.M. of 3 to 5 independent experiments conducted in duplicate; for some data points error bars are not shown as they are smaller than the height of the symbol.

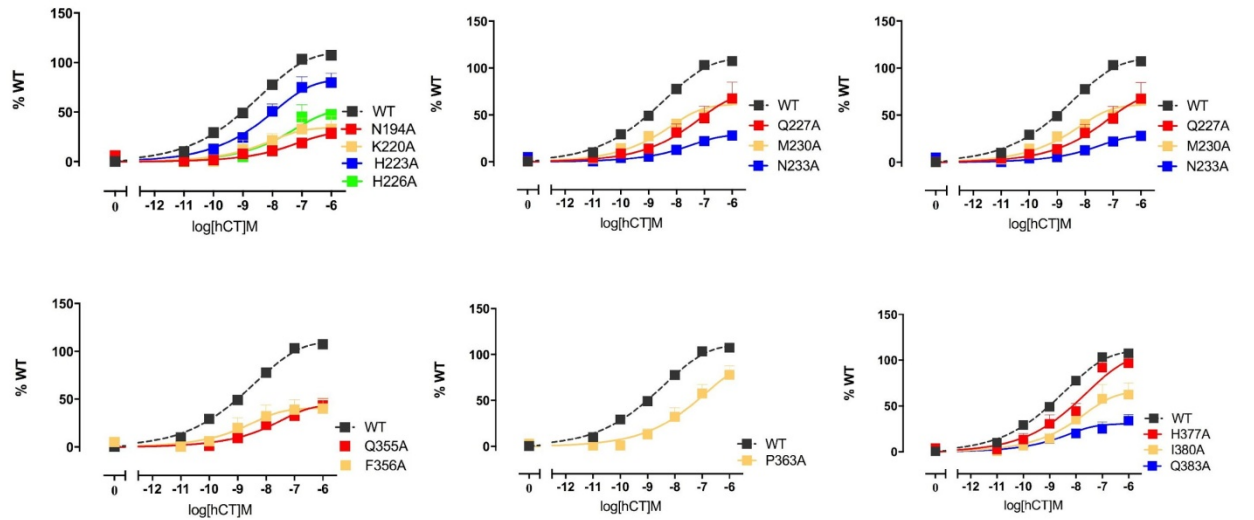


Figure 5.17. *pERK1/2* concentration response to *hCT* in *CV-1-FlpIn* cells stably expressing *hCTRαLeu* mutations in the receptor TM region. *pERK1/2* response in the presence of *sCT* was fit using Black and Leff operational model with a variable transducer slope and normalized to WT receptor response. All values are mean+S.E.M. of 3 to 5 independent experiments conducted in duplicate; for some data points error bars are not shown as they are smaller than the height of the symbol.

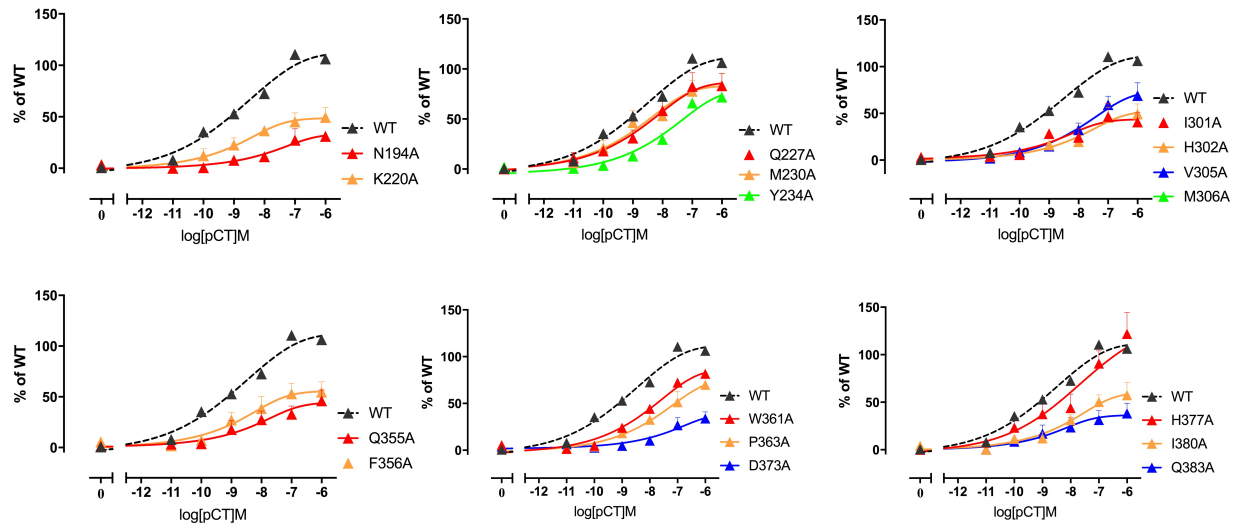


Figure 5.18. *pERK1/2 concentration response to pCT in CV-1-FlpIn cells stably expressing hCTRαLeu mutations in the receptor TM region. pERK1/2 response in the presence of pCT was fit using Black and Leff operational model with a variable transducer slope and normalized to WT receptor response. All values are mean±S.E.M. of 3 to 5 independent experiments conducted in duplicate; for some data points error bars are not shown as they are smaller than the height of the symbol.*

Table 5.6. Effect of single alanine mutation in the CTR TM region on pERK1/2 efficacy ($\log\tau_c$) of CT agonists.

	sCT	hCT	pCT
WT	1.96 \pm 0.29	1.66 \pm 0.21	1.98 \pm 0.36
N194A(N ^{2.60} A)	-0.53* \pm 0.45	-1.09* \pm 0.55	-1.06* \pm 0.65
K220A(K ^{3.30} A)	-0.09* \pm 0.20	-1.06* \pm 0.33	-0.51* \pm 0.30
H223A(H ^{3.33} A)	0.65 \pm 0.25	0.50 \pm 0.26	N.D.
H226A(H ^{3.36} A)	-0.91* \pm 0.29	-0.55* \pm 0.40	N.D.
Q227A(Q ^{3.37} A)	0.19* \pm 0.22	0.34* \pm 0.36	0.95 \pm 0.31
M230A(M ^{3.40} A)	0.33* \pm 0.23	0.08* \pm 0.24	0.96 \pm 0.33
N233A (N ^{3.43} A)	-1.30* \pm 0.51	-1.35* \pm 0.46	N.D.
Y234A (Y ^{3.44} A)	0.49 \pm 0.24	N.D.	0.57 \pm 0.68
I301A (I ^{5.39} A)	-0.41* \pm 0.35	-0.90* \pm 0.40	-0.45* \pm 0.42
H302A (H ^{5.40} A)	-0.10* \pm 0.74	-0.27* \pm 0.79	0.17 \pm 0.83
V305A (V ^{5.43} A)	0.29* \pm 0.31	-0.29* \pm 0.30	0.50 \pm 0.59
M306A(M ^{5.44} A)	-0.27* \pm 0.28	-0.76* \pm 0.29	-0.43* \pm 0.42
Q355A (Q ^{6.52} A)	N.D.	N.D.	N.D.
F356A (F ^{6.53} A)	-0.15* \pm 0.42	-0.46* \pm 0.44	0.10 \pm 0.49
F359A (F ^{6.56} A)	N.D.	N.D.	N.D.
P360A (P ^{6.57} A)	1.05 \pm 0.49	N.D.	N.D.
W361A(W ^{6.58} A)	1.15 \pm 0.66	N.D.	0.29 \pm 0.64
P363A (P ^{6.60} A)	0.62 \pm 0.34	1.14 \pm 0.81	0.24 \pm 0.69
D373A (D ^{7.39} A)	-0.37* \pm 0.45	N.D.	-1.25* \pm 0.68
M376A(M ^{7.42} A)	N.D.	N.D.	N.D.
H377A (H ^{7.43} A)	0.79 \pm 0.41	1.47 \pm 0.56	-0.62 \pm 0.60
I380A (I ^{7.46} A)	0.56 \pm 0.34	0.14 \pm 0.29	-0.52* \pm 0.44
Q383A (Q ^{7.49} A)	-0.81* \pm 0.30	-0.86* \pm 0.31	-1.15* \pm 0.39

*pERK1/2 response in the presence of CT agonists was fit using Black and Leff operational model to derive $\log\tau$ values. All values are mean \pm S.E.M. of 3 to 5 independent experiments conducted in duplicate. All $\log\tau$ were corrected for the cell surface expression to result $\log\tau_c$ values and errors were propagated. Significance of changes in $\log\tau_c$ values were calculated via comparison of mutant $\log\tau_c$ values to the WT $\log\tau_c$ in a one-way Anova analysis of variance with Dunnett's post-hoc test with significant changes $P<0.05$ denoted by *.*

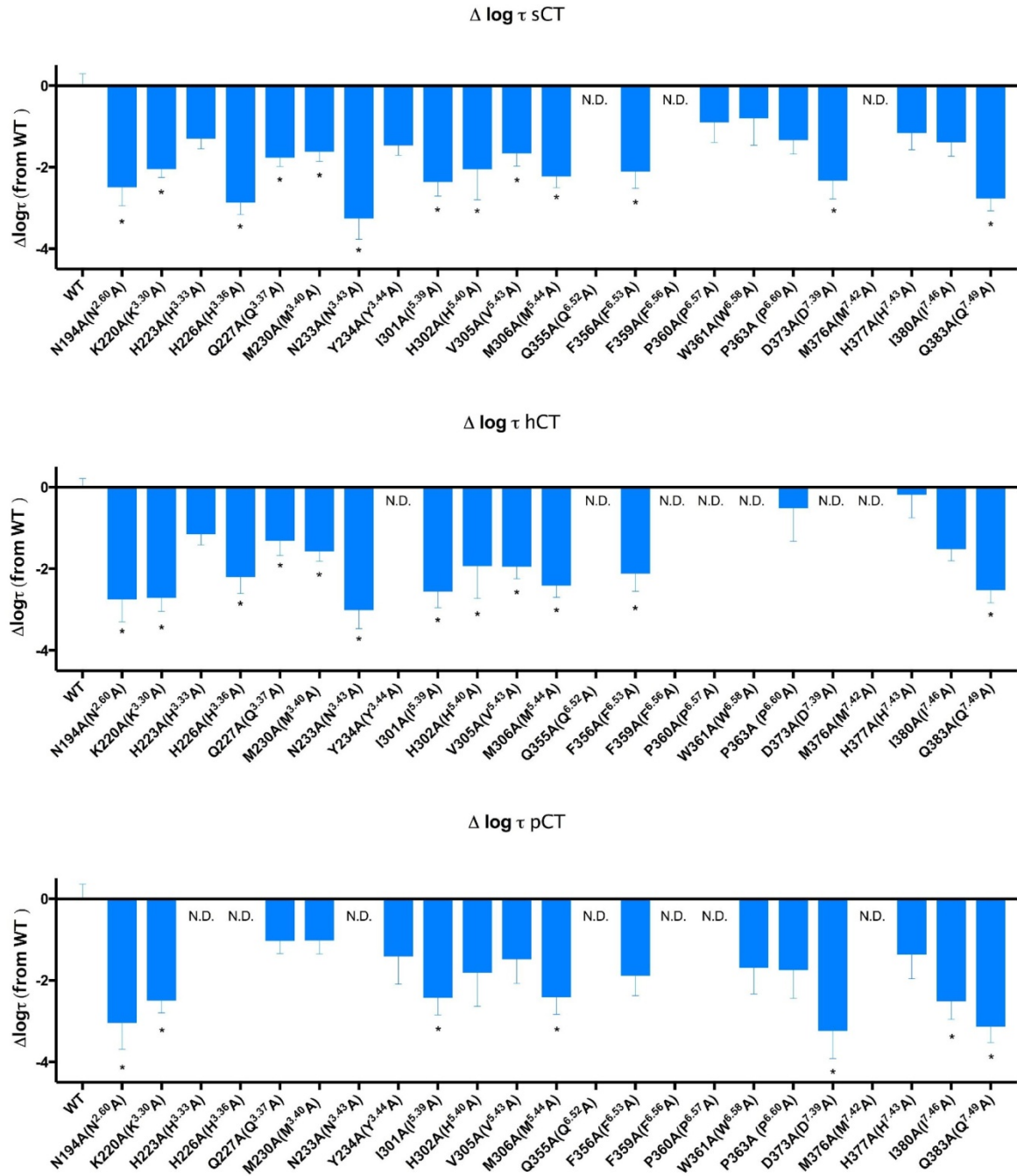


Figure 5.19. Δlogτ CT agonists (sCT, hCT and pCT) values for pERK1/2 pathway. . Δlogτ_c value for each mutant was obtained by subtracting WT logτ from each mutant's logτ_c value. All values are mean+S.E.M. of 3 to 5 independent experiments conducted in duplicate. Significance of changes were calculated via comparison of mutant's logτ values to the WT receptor logτ values in a one-way Anova analysis of variance with Dunett's post-hoc test with significant changes $P < 0.05$ denoted by *.

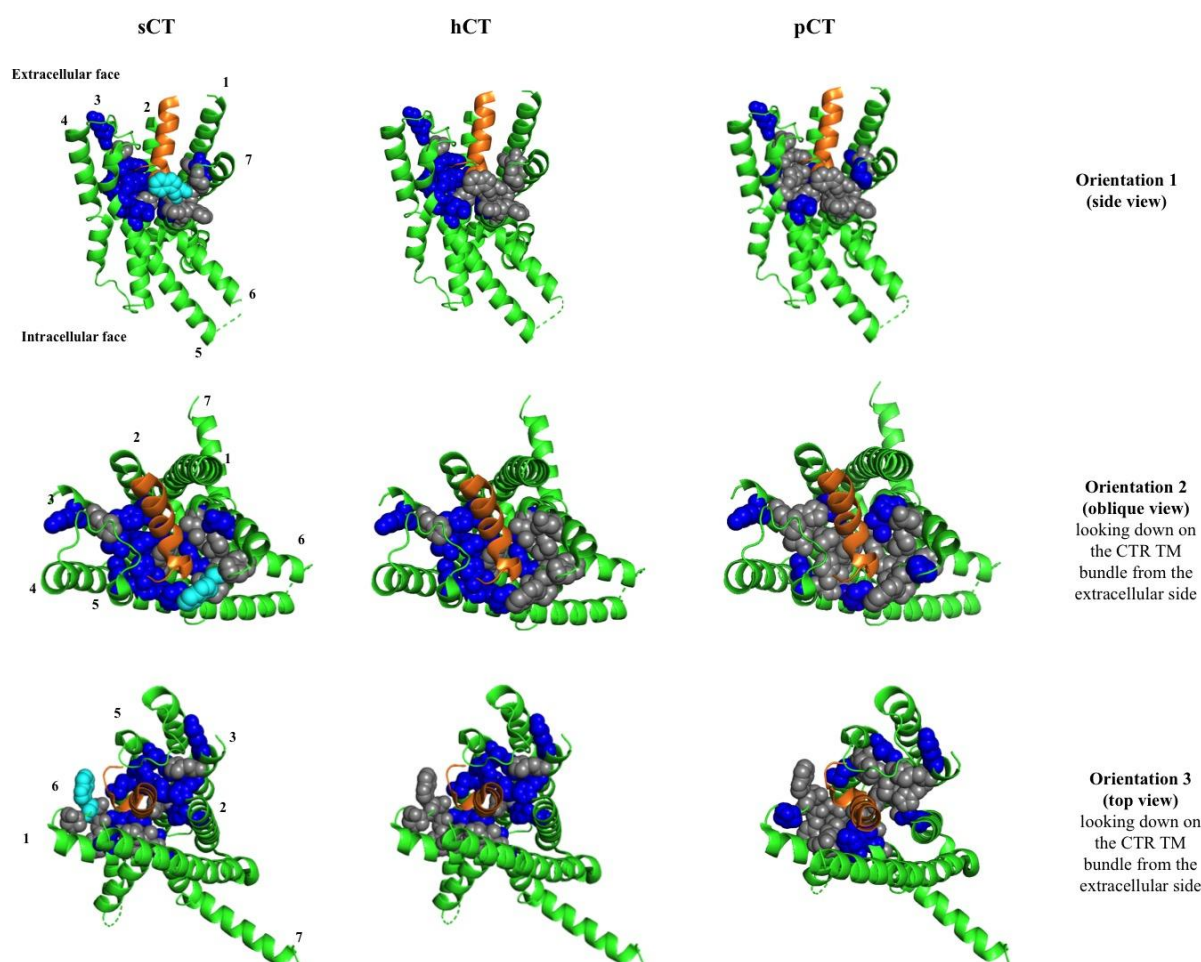


Figure 5.20. Effect of the CTR TM mutations on pERK1/2 efficacy for CT peptides. Residues for sCT and pCT are mapped onto a Cryo-EM structure of CTR in complex with sCT and G_s protein (G_s protein and CTR N-terminal domain are not shown) (Dal Maso et. al., 2019) and for hCT onto a provisional Cryo-EM structure of CTR in complex with hCT and G_s protein (G_s protein and CTR N-terminal domain are not shown) (not published). The receptor is shown in green and sCT ligand is shown in orange. Residues that produced significant changes in efficacy were coloured in either blue (<10 times decrease in efficacy); or cyan (<10 times decrease in efficacy) and are shown as space-fill side chains. Residues that produced no significant change in efficacy were coloured in gray.

5.2.2.2 ASSESSMENT OF pERK1/2 IN RESPONSE TO α CGRP AND rAMY

pERK1/2 time course was performed for each mutant/WT receptor in presence 1 μ M α CGRP and 1 μ M rAMY. Similarly to CT agonists pERK1/2 maximum response was observed around 5-6 minutes (Figures 5.21 – 5.22). Therefore, all subsequent concentration course experiments were all performed at 5 minutes time point.

pERK1/2 concentration response data for α CGRP and rAMY was fit using a three-parameter curve (Figures 5.23 – 5.24). Values for EC_{50} and E_{max} were derived from the curves and are reported in Table 5.7. Since only monophasic curves were evident α CGRP and rAMY at the concentrations tested, efficacy values were derived using Black and Leff operational model with the transducer slope $n=1$ (with the operational curves looked identical to the three-parameter fit (Figures 5.23 – 5.24)). Obtained $\log\tau$ values were corrected for the cell surface expression to obtain $\log\tau_c$ values for each mutant (Table 5.8). $\Delta\log\tau_c$ value for each mutant was obtained by subtracting WT $\log\tau$ from each mutant's $\log\tau_c$ value (Figure 5.25).

pERK1/2 is a less strongly coupled pathway than cAMP for the CTR, and α CGRP and rAMY are weak CTR agonists. Therefore, it was problematic to achieve robust operational fits for a subset of low expressing mutants or for some of those mutants that had highly detrimental effects on pERK1/2 response. Although, our statistical analysis revealed no significant effects on pERK1/2 efficacy, there were some residues that decreased pERK1/2 efficacy ≥ 5 -fold. These included H226A ($H^{3.36}A$), Y234A ($Y^{3.44}A$) and F359A ($F^{6.56}A$) for α CGRP and F359A ($F^{6.56}A$) for rAMY (Figure 5.25, Table 5.8). Concentration response and operational fitting was not carried out where there was inadequate data to support that the curve fit had passed the second inflection point such that there was limited confidence in the curve-fit estimate for the E_{max} . These included datasets: N194A ($N^{2.60}A$), K220A ($K^{3.30}A$), N233A ($N^{3.43}A$), I301A ($I^{5.39}A$), Q355A ($Q^{6.52}A$), D373A ($D^{7.39}A$) and M376A ($M^{7.42}A$) for α CGRP; H226A ($H^{3.36}A$), N233A ($N^{3.43}A$), H302A ($H^{5.40}A$), V305A ($V^{5.43}A$), Q355A ($Q^{6.52}A$), P360A ($P^{6.57}A$), W361A ($W^{6.58}A$), P363A ($D^{7.39}A$), D373A ($D^{7.39}A$), M376A ($M^{7.42}A$) and Q383A ($Q^{7.49}A$) for rAMY.

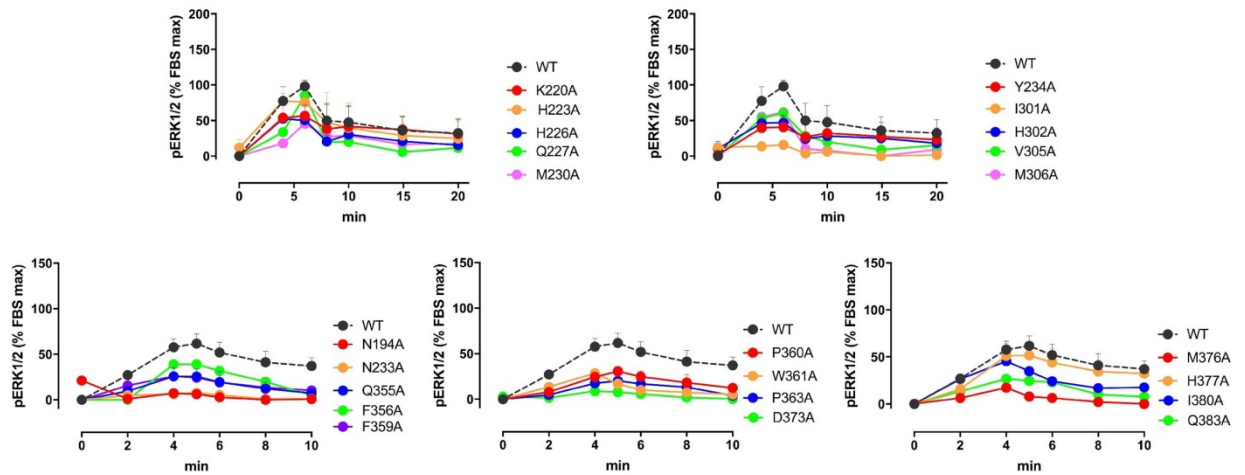


Figure 5.21. *pERK1/2 time course response profiles to 1 μ M α CGRP in CV-1-FlpIn cells stably expressing hCTR α Leu mutations in the receptor TM region. pERK1/2 response in the presence of 1 μ M α CGRP was measured as indicated and normalized at 8 min FBS and vehicle responses. All values are mean of either 1 or 2 (mean +SD) independent experiments conducted in duplicate (for the experiments that are an N of 1, only the mean of the replicates with no error is shown).*

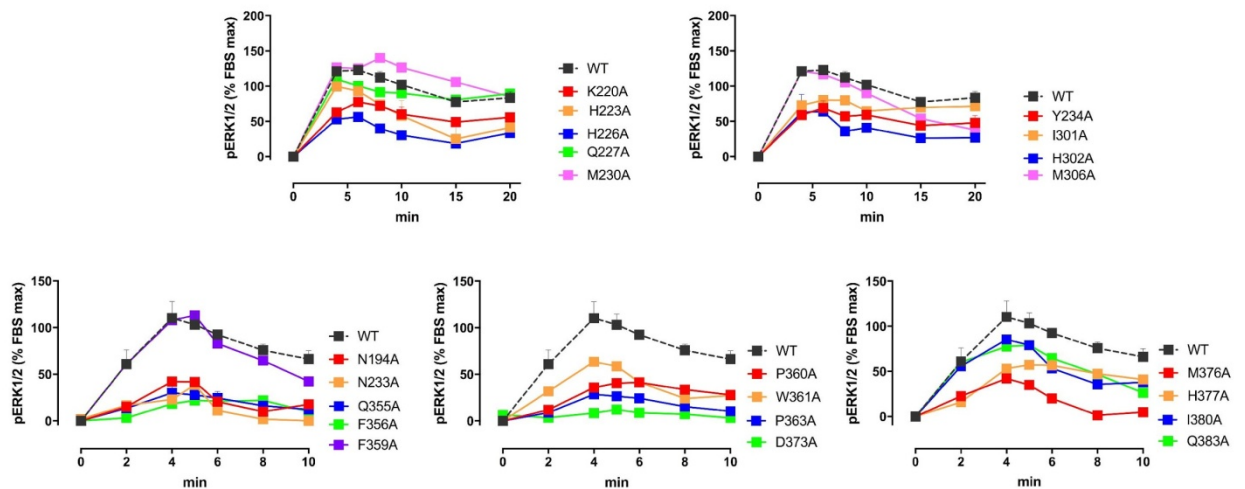


Figure 5.22. *pERK1/2 time course response profiles to 1 μ M rAMY in CV-1-FlpIn cells stably expressing hCTR α Leu mutations in the receptor TM region. pERK1/2 response in the presence of 1 μ M rAMY was measured as indicated and normalized at 8 min FBS and vehicle responses. All values are mean of either 1 or 2 (mean +SD) independent experiments conducted in duplicate (for the experiments that are an N of 1, only the mean of the replicates with no error is shown).*

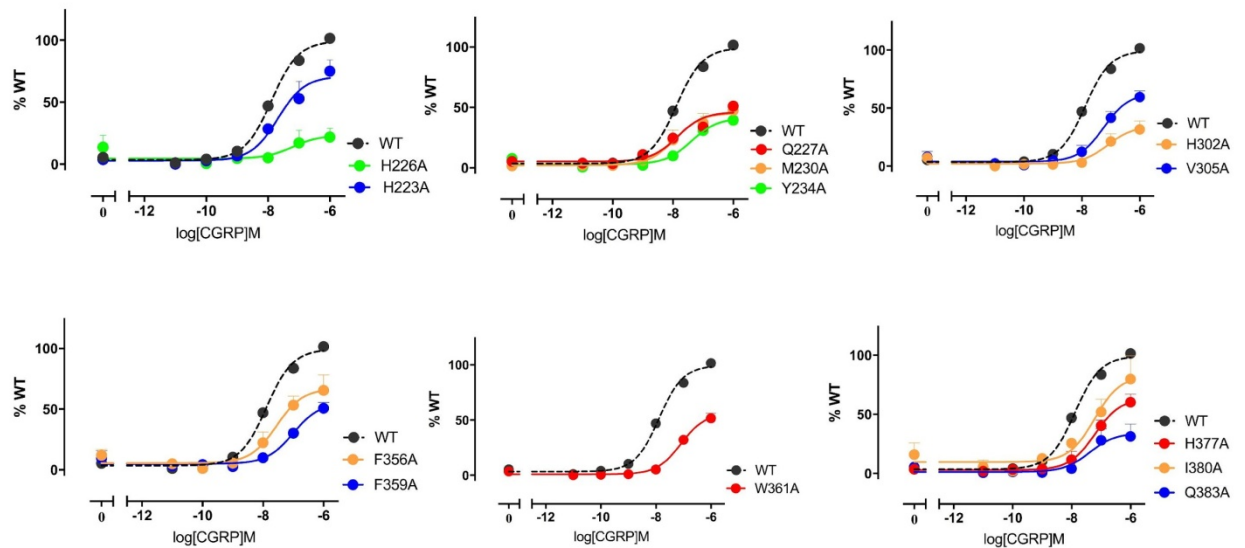


Figure 5.23. *pERK1/2 concentration response to α CGRP in CV-1-FlpIn cells stably expressing hCTR α Leu single alanine mutations in the receptor TM region.* *pERK1/2 response in the presence of α CGRP was fit using three-parameter logistic equation and normalized to WT receptor response. The Black and Leff operational model, with a hill slope of 1, was applied to separate efficacy (τ) and functional affinity (pK_A). All values are mean+S.E.M. of 3 to 5 independent experiments conducted in duplicate; for some data points error bars are not shown as they are smaller than the height of the symbol.*

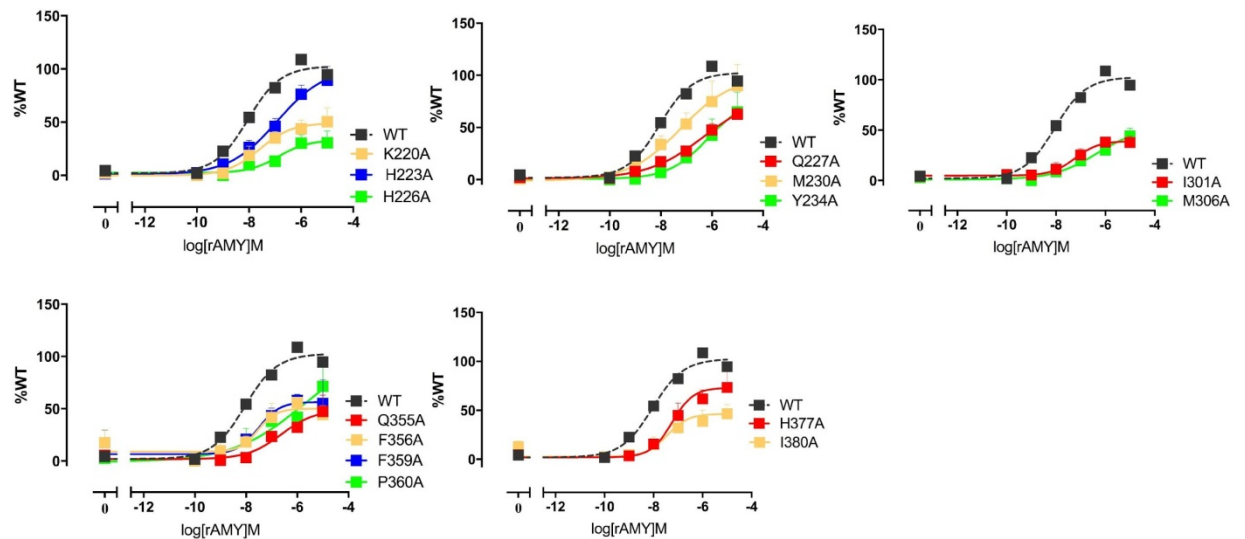


Figure 5.24. *pERK1/2 concentration response to rAMY in CV-1-FlpIn cells stably expressing hCTR α Leu single alanine mutations in the receptor TM region.* *cAMP formation in the presence of rAMY was fit using three-parameter logistic equation and normalized to WT receptor response. The Black and Leff operational model, with a hill slope of 1, was applied to separate efficacy (τ) and functional affinity (pK_A). All values are mean+S.E.M. of 3 to 5 independent experiments conducted in duplicate; for some data points error bars are not shown as they are smaller than the height of the symbol.*

Table 5.7. Effect of single alanine CTR TM region mutation on pERK1/2 potency (EC_{50}) and maximal response to α CGRP and rAMY.

	α CGRP		rAMY	
	pEC ₅₀	E _{max}	pEC ₅₀	E _{max}
WT	7.95 \pm 0.06	99 \pm 2	8.15 \pm 0.07	98 \pm 2
N194A(N ^{2.60} A)	N.D.	N.D.	7.0* \pm 0.54	28* \pm 7
K220A(K ^{3.30} A)	7.87 \pm 0.23	58* \pm 6	7.74 \pm 0.26	46* \pm 4
H223A(H ^{3.33} A)	7.77 \pm 0.17	75* \pm 6	7.27* \pm 0.16	83 \pm 6
H226A(H ^{3.36} A)	7.53 \pm 0.60	22* \pm 6	7.01* \pm 0.36	32* \pm 5
Q227A(Q ^{3.37} A)	8.12 \pm 0.19	45* \pm 4	7.04* \pm 0.15	58* \pm 4
M230A(M ^{3.40} A)	8.01 \pm 0.18	45* \pm 4	7.73 \pm 0.27	79* \pm 8
N233A (N ^{3.43} A)	N.D.	N.D.	6.17* \pm 0.64	26* \pm 9
Y234A (Y ^{3.44} A)	7.51 \pm 0.24	41* \pm 5	6.56* \pm 0.31	63* \pm 9
I301A (I ^{5.39} A)	N.D.	N.D.	7.50 \pm 0.26	38* \pm 4
H302A (H ^{5.40} A)	7.87 \pm 0.33	32* \pm 5	6.37* \pm 0.30	32* \pm 5
V305A (V ^{5.43} A)	7.36 \pm 0.15	62* \pm 5	7.75 \pm 0.25	33* \pm 3
M306A(M ^{5.44} A)	7.40 \pm 0.38	21* \pm 4	6.97* \pm 0.17	40* \pm 3
Q355A (Q ^{6.52} A)	6.72* \pm 0.28	31* \pm 6	7.03* \pm 0.22	42* \pm 4
F356A (F ^{6.53} A)	7.61 \pm 0.23	60* \pm 7	7.80 \pm 0.32	50* \pm 6
F359A (F ^{6.56} A)	7.17 \pm 0.16	53* \pm 5	7.70 \pm 0.33	56* \pm 7
P360A (P ^{6.57} A)	6.82* \pm 0.25	54* \pm 9	7.52 \pm 0.34	55* \pm 7
W361A(W ^{6.58})	7.12 \pm 0.08	56* \pm 3	7.53 \pm 0.16	41* \pm 2
P363A (P ^{6.60} A)	7.04* \pm 0.29	26* \pm 4	6.77* \pm 0.25	41* \pm 5
D373A (D ^{7.39} A)	N.D.	N.D.	6.00* \pm 0.29	20* \pm 4
M376A(M ^{7.42} A)	N.D.	N.D.	6.73* \pm 0.44	23* \pm 5
H377A (H ^{7.43} A)	7.29 \pm 7.34	63* \pm 5	7.34 \pm 0.21	68* \pm 6
I380A (I ^{7.46} A)	7.58 \pm 7.68	76* \pm 10	7.68 \pm 0.33	42* \pm 5
Q383A (Q ^{7.49} A)	7.43 \pm 7.92	34* \pm 6	7.92 \pm 0.28	30* \pm 3

pERK1/2 response in the presence of α CGRP and rAMY was fit using three-parameter logistic equation and normalized to WT receptor response. The Black and Leff operational model, with a transducer slope of 1, was applied to separate efficacy (τ) and functional affinity (pK_A). All values are mean \pm S.E.M. of 3 to 5 independent experiments conducted in duplicate. Significance of changes in pEC₅₀ and E_{max} values were calculated via comparison of mutant pEC₅₀ and E_{max} values to the WT pEC₅₀ and E_{max} respective values in a one-way Anova analysis of variance with Dunett's post-hoc test with significant changes $P < 0.05$ denoted by *.

Table 5.8. Effect of single alanine mutation in the CTR TM region on pERK1/2 efficacy ($\log\tau_c$) of α CGRP and rAMY.

	α CGRP	rAMY
WT	-0.22 ± 0.04	0.02 ± 0.03
N194A (N ^{2.60} A)	N.D.	-0.30 ± 0.35
K220A (K ^{3.30} A)	N.D.	-0.22 ± 0.16
H223A (H ^{3.33} A)	-0.58 ± 0.16	-0.09 ± 0.10
H226A (H ^{3.36} A)	-0.73 ± 0.21	N.D.
Q227A (Q ^{3.37} A)	-0.48 ± 0.18	-0.15 ± 0.15
M230A (M ^{3.40} A)	-0.36 ± 0.21	0.24 ± 0.16
N233A (N ^{3.43} A)	N. D.	N.D.
Y234A (Y ^{3.44} A)	-0.70 ± 0.28	-0.20 ± 0.17
I301A (I ^{5.39} A)	N.D.	-0.06 ± 0.33
H302A (H ^{5.40} A)	-0.01 ± 0.77	N.D.
V305A (V ^{5.43} A)	-0.25 ± 0.20	N.D.
M306A (M ^{5.44} A)	N.D.	-0.35 ± 0.21
Q355A (Q ^{6.52} A)	N.D.	N.D.
F356A (F ^{6.53} A)	0.08 ± 0.40	0.14 ± 0.39
F359A (F ^{6.56} A)	-0.71 ± 0.24	-0.52 ± 0.11
P360A (P ^{6.57} A)	N.D.	N.D.
W361A (W ^{6.58} A)	-0.63 ± 0.24	N.D.
P363A (P ^{6.60} A)	N.D.	N.D.
D373A (D ^{7.39} A)	N.D.	N.D.
M376A (M ^{7.42} A)	N.D.	N.D.
H377A (H ^{7.43} A)	-0.46 ± 0.17	-0.21 ± 0.11
I380A (I ^{7.46} A)	-0.09 ± 0.15	-0.33 ± 0.15
Q383A (Q ^{7.49} A)	-0.22 ± 0.35	N.D.

*cAMP formation in the presence of α CGRP or rAMY was fit using Black and Leff operational model to derive $\log\tau$ values. All values are mean+S.E.M. of 3 to 5 independent experiments conducted in duplicate. All $\log\tau$ values were corrected for the cell surface expression to result $\log\tau_c$ values and errors were propagated. Significance of changes in $\log\tau_c$ values were calculated via comparison of mutant $\log\tau_c$ values to the WT $\log\tau_c$ in a one-way Anova analysis of variance with Dunnett's post-hoc test with significant changes $P<0.05$ denoted by *.*

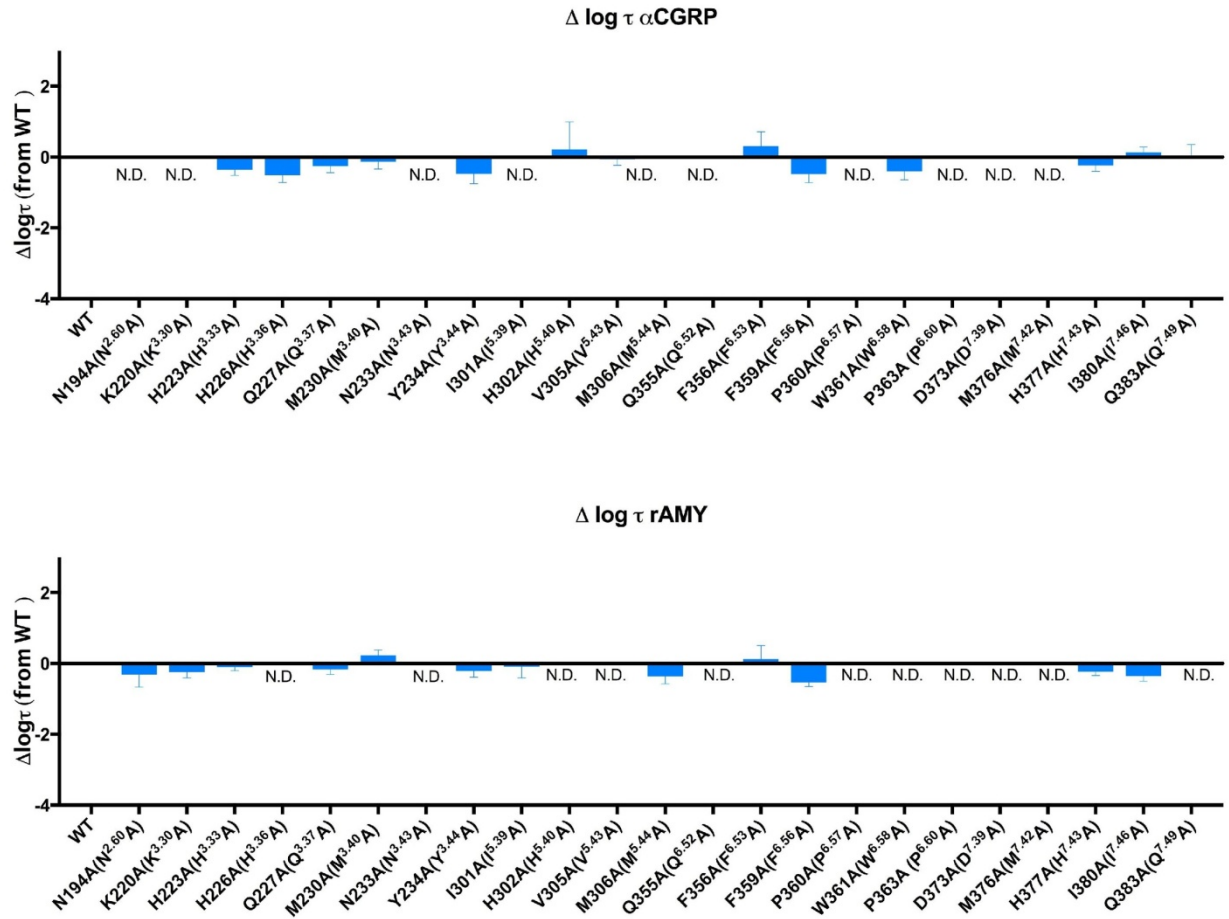


Figure 5.25. $\Delta \log \tau$ for α CGRP and rAMY for pERK1/2 pathway. $\Delta \log \tau_c$ value for each mutant was obtained by subtracting WT $\log \tau$ from each mutant's $\log \tau_c$ value. All values are mean+S.E.M. of 3 to 5 independent experiments conducted in duplicate. Significance of changes were calculated via comparison of mutants $\log \tau$ values to the WT receptor $\log \tau$ values in a one-way Anova analysis of variance with Dunett's post-hoc test with significant changes $P < 0.05$ denoted by *.

5.3 DISCUSSION

EFFECTS OF THE CTR TM MUTATIONS ON CTR cAMP AND pERK1/2 EFFICACY

For the majority of the tested CTR TM mutants changes in cAMP efficacy do not reach significance. One of the potential reasons for this is that efficacy is a composite measurement, and therefore is prone to false negative results, especially in those instances when the magnitude of effects is small.

Out of the 23 selected residues that were included in this study within the CTR TMs 2, 3, 5, 6 and 7 it was interesting to find that, for different CTR agonists including rAMY and α CGRP (although the latter had high error associated with its values), individual amino acid mutations resulted in largely similar patterns of efficacy effects across cAMP pathway with N194A (N^{2.60}A), K220A (K^{3.30}A), H301A (I^{5.39}A), H302A (H^{5.40}A) (ND for rAMY), F356A (F^{6.53}A), I380A (I^{7.46}A) and Q383A (Q^{7.49}A) increasing and F359A (F^{6.56}A) and W361A (W^{6.58}A) decreasing cAMP efficacy (Figures 5.4, 5.8). Additionally, M376A (M^{7.42}A) significantly increased rAMY efficacy for cAMP (4.4-fold), whereas for other agonists the magnitude of efficacy increase was less than 2-fold (Figure 5.8). Mutations of residues in the top of TM1 also resulted in similar cAMP efficacy profiles for CT agonists and rAMY, with only α CGRP showing distinct pattern (Dal Maso *et al.*, 2019). This data suggests common conformational change in the TM region of the CTR (and hence the conservation of amino acid networks) important for cAMP signal transmission for different CTR ligands.

The conservation of networks of residues important for cAMP efficacy in both hCT and sCT correlates with the structural data that showed low divergence in the TM region structures of the CTR in complex with G_s and either sCT (Liang *et al.*, 2017) or hCT (preliminary data from our laboratory). Our cAMP efficacy data suggests that the hotspots for cAMP efficacy (in the TM region) are largely located in the TMs 6 and 7 as well as one residue in the top of TM3, K220 (K^{3.30}A). The importance of TM6 and TM7 regions in cAMP efficacy is consistent with both extracellular and intracellular regions of TM6 and TM7 undergoing major structural reorganization upon CTR activation (Liang *et al.*, 2017).

Whereas CTR cAMP response is downstream of G_s protein activation, CTR pERK1/2 signalling results from convergent activation of multiple upstream pathways. In our systems we are not able to detect coupling of CTR to β -arrestin signalling (Dal Maso *et al.*, 2018a), and CTR pERK1/2 response is predicted to result from the activation of several G proteins, with at least some contribution from G_q signalling (Morfis *et al.*, 2008, Dal Maso *et al.*, 2018b).

I analysed the data using an operational fit and global mapping of pERK1/2 efficacy effects resulted in similar patterns for pERK1/2 efficacy across CT agonists, with the same

direction and similar magnitudes of mutations effects (Figures 5.19, 5.20). Similarly if, instead of considering operational fitting, the switch from biphasic to monophasic response is considered, again mutants that switched the response to a monophasic one did so for all calcitonin peptides (Figures 5.13 – 5.15).

As noted above, the fact that the wild-type receptor exhibits a biphasic response to the CT peptides for pERK1/2 indicates that there are 2 receptor populations that do not appreciably interchange at the timescale of this assay. A number of receptor mutants appeared to alter the response from biphasic to monophasic (Figures 5.13 – 5.15), which could be consistent with either an increase in exchange rates between the receptor populations or a loss of one of the response phases (although these may not be mutually exclusive). In the former case this would suggest that the normal role of the residue in question is to constrain the exchange of the receptor between different states. In the latter case, this would suggest loss of coupling of the receptor to one of the upstream pathways that converges on pERK1/2 (e.g. specific loss of G_q coupling whilst sparing G_s coupling). Either mechanism suggests additional texture in the way this receptor can respond to its ligand(s) but would require extensive biophysical and reductionist signalling experiments to understand properly.

In contrast to the cAMP pathway that revealed only limited effects on efficacy of small magnitude, all tested, operationally-fitted mutations reduced pERK1/2 efficacy to some degree, with many effects reaching statistical significance (Figures 5.4, 5.19). In addition, there were many mutants that switched the pharmacology from a biphasic to a monophasic curve (Figures 5.13 – 5.15). Perhaps because the pERK1/2 signal is a composite of several convergent pathways, more residues seemed to play role in efficacy for this pathway, compared to the cAMP pathway. This data implies CTR TM region plays role in the regulation of lower efficacy non- G_s signalling pathways.

Only switches from biphasic to monophasic responses for certain mutants relative to the WT receptor (WT showed biphasic pERK1/2 response to all 3 CTs: sCT, hCT and pCT) were observed for pERK1/2. There was no direct correlation between the switch from biphasic to monophasic response and decreased efficacy (for, example, K220A displayed monophasic response while it showed increased efficacy for all 3 CTs). It's worth noting that comparing concentration response curves versus analyzing the data with the Operational Model represent the 2 different ways to analyse the same data.

Whereas there was an overlap in residues involved in efficacy across both signalling pathways, the direction of effects for cAMP and pERK1/2 was generally opposed. For example, K220A ($K^{3.30}A$), I380 ($I^{7.46}A$) and Q383A ($Q^{7.49}A$) increased efficacy for cAMP while these mutants decreased efficacy at pERK1/2 (Figures 5.4, 5.19). This supports a model in which

different conformations of the receptor are sampled to allow coupling to pERK1/2 and cAMP pathways resulting in differential involvement of the CTR TM residues in each signalling pathway. Particular mutations can shift the conformational selection towards one that is better coupled to cAMP signalling output (higher efficiency of the interaction with G_{as} (via either improved G_{as} affinity or higher GTP turnover), while decreasing pERK1/2 signalling output. As pERK1/2 response arises from multiple pathways, the assumption would be that the efficiency of CTR interactions with some of its signalling transducers is decreased (for example, decreased efficiency of the interaction with G_q) to give a total decreased pERK1/2 efficacy. This data is consistent with the previous mutagenesis data for the CTR extracellular region, including the top of TM1, that showed the conformations linked to the different CTR signalling pathways are frequently mutually exclusive (Dal Maso *et al.*, 2018b, Dal Maso *et al.*, 2019). Differential engagement of segments of receptor extracellular regions for different pathways has also been previously shown for GLP-1R, (Wootten *et al.*, 2016). In order to gain more mechanistical understanding it would be useful to employ methods that enable direct measurement of the recruitment of various G proteins (i.e. G protein BRET or FRET sensors) as well as those that measure the rate of nucleotide exchange at a G protein.

Although the magnitude of effect was small for both pathways for α CGRP and rAMY, similarly to CT agonists, the overall pattern and direction of efficacy changes was the same as that seen for the clacitonins and was frequently in the opposite direction for cAMP compared with pERK1/2. This further implies a conserved mechanism of signalling activation for the TM region of the CTR for different ligands for multiple transducers that converge to activate the pERK1/2 pathway. In additional, this data supports CTR coupling to distinct pathways via adopting differential conformations.

Collectively, our data supports that particular residues can participate in signal transduction across two different signalling pathways (cAMP and pERK1/2) in a pathway-dependent manner.

We could identify only limited direct interactions for the studied TM residues based on our CTR cryo-EM structures complexed with either sCT, or hCT and some of these have been already discussed in Chapter 4 (including K220A ($K^{3.30}A$), M306A ($M^{5.44}A$) and D373A ($D^{7.39}A$)). Below we speculate about potential interactions that some of the CTR TM residues (not listed in Chapter 4) might be involved in based on our static cryo-EM structures.

W361 ($W^{6.58}$), a hydrophobic residue in the ECL3 region (proximal to the top of TM6), oriented towards the peptide in both CTR-sCT and CTR-hCT structures, where it could potentially interact with L^4 of the peptide (Figure 5.26). Consistent with being involved in direct interaction with the peptide, W361A ($W^{6.58}A$) decreased affinity for a number of CTR agonists

and also decreased efficacy for both cAMP and pERK1/2 pathways (although, not all of these effects reached statistical significance).

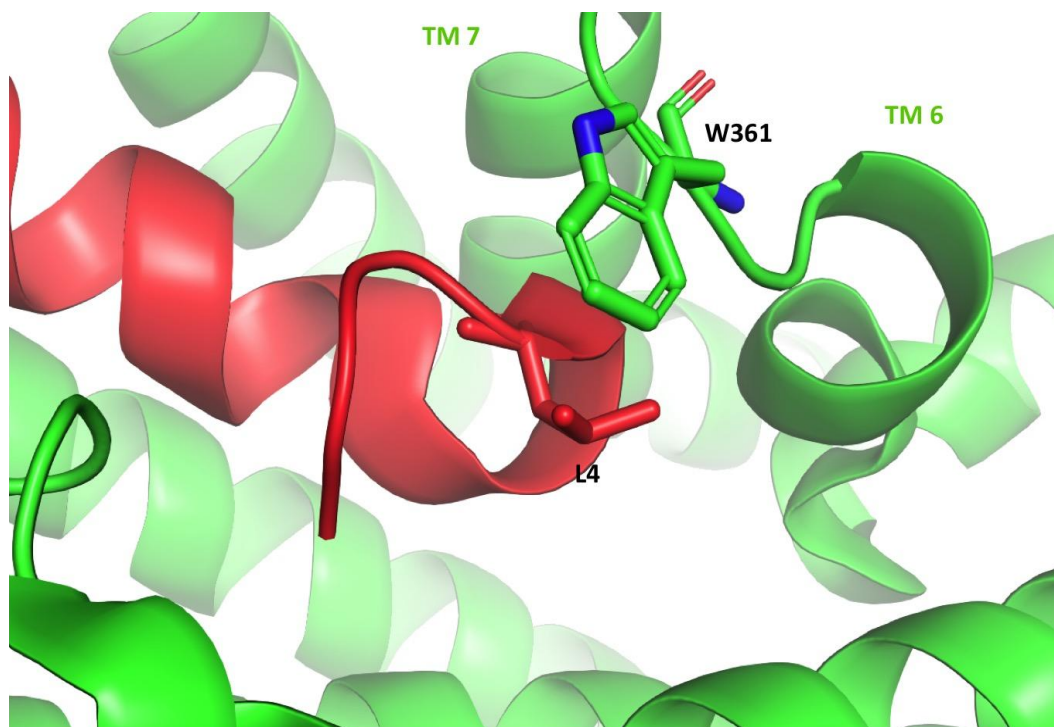


Figure 5.26. 3D model showing proximity between W361 and L⁴ of sCT. Ribbon representation of the TM bundle of the sCT-CTR complex based on the active Cryo-EM structure of CTR in complex with sCT (Dal Maso *et al.*, 2019). Receptor is shown in green and sCT is shown in red.

K220 (K^{3.30}A) is a residue that is a conserved positive side chain in all class B GPCRs (either lysine or arginine). In the CTR we predicted that K220 (K^{3.30}) may stabilize ECL2 via contact with D287^{ECL2} (Figure 4.35, Chapter 4). K220A (K^{3.30}A) was the only residue in this study that had global effects on both pathways (efficacy and functional affinity) across all agonists, including α CGRP and rAMY. While the direction of effect was the same across ligands for each pathway, the effect direction was opposed when comparing one signalling pathway to another and when comparing functional affinity versus efficacy for each pathway. While decreasing cAMP and improving pERK1/2 functional affinity (pK_A) K220A (K^{3.30}A) improved cAMP and decreased pERK1/2 efficacy. Residue D287^{ECL2}, proposed to interact with K220 (K^{3.30}), was previously assessed using mutational analysis of the ECL2 (Dal Maso *et al.*, 2018). There is a very strong correlation not only between the direction but also the magnitude of effect caused by mutation of either K220A (K^{3.30}A) or D287A on cAMP functional affinity and efficacy for each ligand. This is consistent with the proposed interaction between the two residues and the effect on cAMP coupling and signalling when this interaction between K220A (K^{3.30}A) and D287^{ECL2} is disrupted. For the pERK1/2 pathway the correlation between the

mutational effects for the two residues was not as clear (pERK1/2 pK_A for D287A was decreased and there were no significant effects on pERK1/2 efficacy for D287A, although pERK1/2 efficacy was decreased for K220A (K^{3.30}A). Perhaps, these results indicate that while the K220-D287 interaction is important for the cAMP pathway; there might be other factors and/or interactions that differentially contribute to pERK1/2 signalling for each of these residues. To further confirm the model in which K220 (K^{3.30}A) interaction with D287^{ECL2} is important for cAMP signalling, recovery of wild type signalling profile with a charge swap experiment (i.e. double mutant of K220D plus D287K) would be very informative and, if our model is correct, would be predicted to rescue the effect of each individual mutant. In GLP-1R K^{3.30}A decreased cAMP efficacy for GLP-1(1-36)NH₂ and GLP-1(1-37) but produced no effect on pERK1/2 efficacy for either ligand (Furness *et al.*, 2018). Collectively, these data indicate that K220 (K^{3.30}) can be differentially engaged in signal transmission in a receptor-, ligand- and pathway-specific manner.

There are a number of histidines surrounding the binding pocket of CTR for which we examined possible interactions based on our cryo-EM structures.

H302 (H^{5.40}) is predicted to form direct contact with T⁶ of the peptide. Very low expression of this mutant resulted in high error for the efficacy values (after error propagation was applied to correct for cell surface expression). For the three-parameter curve fit, H302A (H^{5.40}A) strongly reduced both cAMP and pERK1/2 potency for CTs and α CGRP (effects on sCT cAMP potency were smaller compared to other ligands and we were not able to fit the response for rAMY), consistent with this mutant decreasing affinity. Although cAMP efficacy for this mutant trended towards an increase, the magnitude of error was as big as the efficacy change. Reduction in pERK1/2 efficacy was more obvious for all three CTs, with sCT and hCT pERK1/2 effects reaching statistical significance. In the GLP-1R, R^{5.40} is predicted to directly interact with peptides N-terminus: (E¹ in exendin P⁵ (Liang *et al.*, 2018b) and H⁷ of GLP-1 (Dods *et al.*, 2016). For the GLP-1R this residue was important for the cAMP pathway for endogenous and biased agonists and it also showed differential effects in cAMP efficacy for extended GLP-1 peptides, while decreasing pERK1/2 efficacy for all peptides (Furness *et al.*, 2018). The mutation of the corresponding residue (H^{5.40}A) also decreased pEC₅₀ and E_{max} of cAMP response to α CGRP and AM in the CGRP receptor (CLR/RAMP1), as well as pEC₅₀ of cAMP response to AM in AM2 receptor (CLR/RAMP3) and E_{max} of cAMP response to AM in AM1 receptor (CLR/RAMP2) (Woolley *et al.*, 2017b). Hence, our data supports that H302 (H^{5.40}A) has conserved role in ligand binding (Chapter 4) and signal transmission in the class B receptors.

Mutation of histidines H223A (H^{3.33}A) and H226A (H^{3.36}A) had no effect on either affinity or cAMP efficacy for the peptides tested at the CTR but decreased pERK1/2 efficacy in a ligand-dependent manner. Histidines H223 (H^{3.33}), H226 (H^{3.36}) sit one helical turn apart from each other. H223 (H^{3.33}) is about one helical turn below K220 (K^{3.30}) and is in proximity of ECL2. We predict H223 (H^{3.33}) to form direct hydrogen bond with the backbone of W290^{ECL2}, this potential interaction is observed in both sCT and hCT structures (Figure 5.27). ECL2 is essential for propagation of pERK1/2 signalling in the CTR, but not cAMP (Dal Maso *et al.*, 2018b) and therefore we speculate that these histidines are important for modulating pERK1/2 signalling through their interactions with ECL2.

A number of hydrophobic residues line the CTR binding pocket. These include I301 (I^{5.39}), V305 (V^{5.43}), M306 (M^{5.44}) and M230 (M^{3.40}). Except for I301A (I^{5.39}A), whose mutation decreased affinity, mutation of the remaining residues did not alter equilibrium affinity but rather pERK1/2 efficacy.

Ala mutants I301A (I^{5.39}A), V305A (V^{5.43}A) and M306A (M^{5.44}A) and M230A (M^{3.40}A) had detrimental effects on pERK1/2 efficacy. These data suggest that the resulting active state conformation for these mutants was less productive in activating pERK1/2 response (compared to the WT receptor). M230A (M^{3.40}A) and I301A (I^{5.39}A) are hydrophobic TM3 and TM5 residues that are located towards the bottom of the binding pocket. Whereas V305A (V^{5.43}A) in TM5, is located below the binding pocket in proximity to other hydrophobic residues, such as I301 (I^{5.39}), M230 (M^{3.40}) and A231 (A^{3.41}) (Figure 5.28). M306 (M^{5.44}) is also located towards the bottom of the binding pocket where it can interact with hydrophobic residues V305 (V^{5.43}), L309 (L^{5.47}), F356 (F^{6.53}) and V357 (V^{6.53}), and the L⁴ of the peptide (Figure 4.36, Chapter 4). Hydrophobic residues are located at these positions in other class B GPCRs and undergo a reorganisation when comparing the available inactive state X-ray structures of TM bundles to cryo-EM structures of activated class B TM bundles (Hollenstein *et al.*, 2013, Siu *et al.*, 2013, Liang *et al.*, 2017, Liang *et al.*, 2018b, Liang *et al.*, 2018a, Zhang *et al.*, 2017b) and are likely to play important roles in stabilisation of both inactive and active state conformations. The data obtained here implies that at least for the pERK1/2 pathway, removal of the side chain of these residues disrupts the active state receptor conformation (by removing interactions stabilising the active conformation) and therefore reduce the overall efficacy of the receptor.

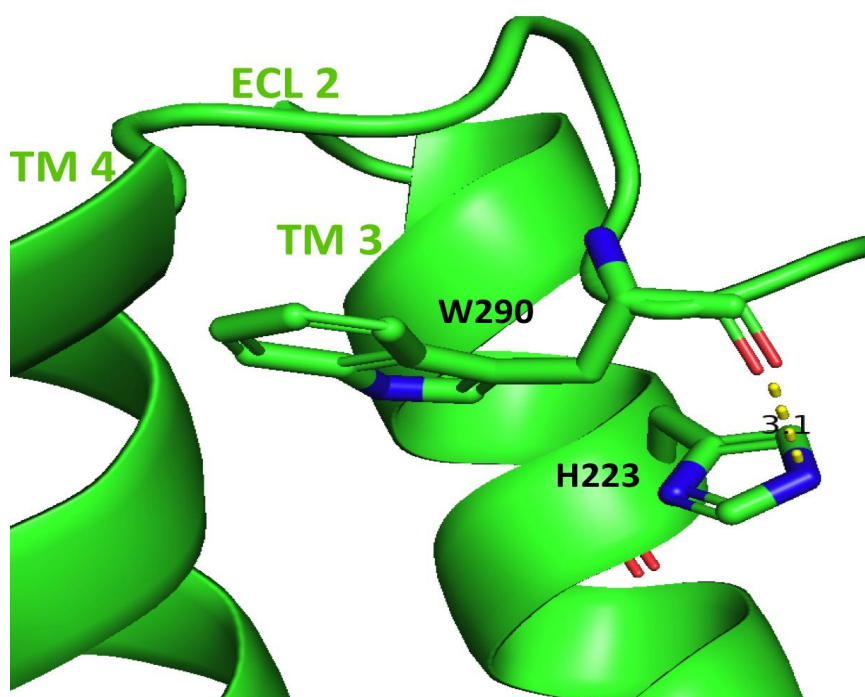


Figure 5.27. 3D model showing proximity between H223 and W290. Ribbon representation of the TM bundle of the sCT-CTR complex based on the active Cryo-EM structure of CTR in complex with sCT (Dal Maso et al., 2019). Receptor is shown in green and sCT is shown in red. The distance measured between the atoms is shown by the yellow dash and equals 3.1 Å.

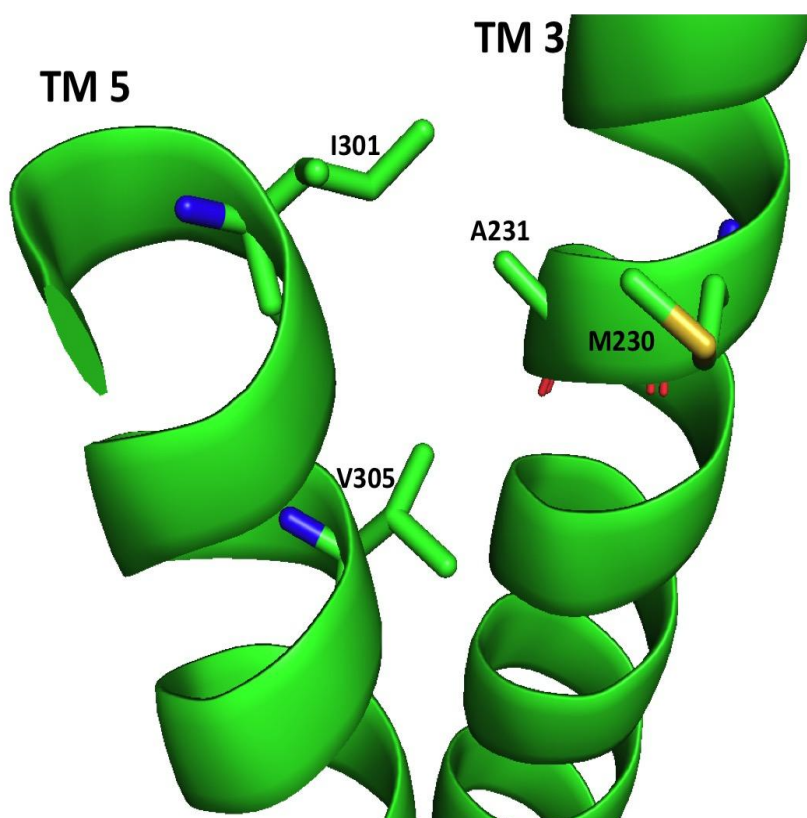


Figure 5.28. 3D model showing hydrophobic residues in proximity of I301. Ribbon representation of the TM bundle of the sCT-CTR complex based on the active Cryo-EM structure of CTR in complex with (Dal Maso et al., 2019). Receptor is shown in green and ligand is shown in red with I301 and hydrophobic residues in its proximity are shown as sticks.

Another cluster of residues with hydrophobic side chains that are predicted to pack together are F356 (F^{6.53}) and F359 (F^{6.56}) and M376 (M^{7.42}). While decreasing functional affinity for hCT and pCT, F359A (F^{6.56}A) is and F356A (F^{6.53}A) improved cAMP efficacy. Apart from the hydrophobic interactions, these residues are positioned in TMs 6 and 7, the region that undergoes major conformational reorganisation upon receptor activation (as we know from the active CTR structure complexed with G_s protein). Hence, our data suggests that mutation of these residues affected the interactions in this region in a manner that improved G_s coupling. Improved G_s coupling might happen as a result of the conformational selection that leads to either improved affinity of the receptor to the transducer (G_{as}) or via acceleration of the rate of nucleotide exchange at G_{as} (Furness *et al.*, 2016).

Polar network residues (K/R/N^{2.60}; N^{3.43}; Y/F^{3.44}; H/T/Q/E^{6.52}; and Q/H^{7.49}) are conserved in all class B receptors. Comparison of active cryo-EM structures of CTR and GLP-1R against inactive class B structures (GCGR and CRF-1R) (Zhang *et al.*, 2017b, Liang *et al.*, 2017, Liang *et al.*, 2018b, Siu *et al.*, 2013, Dore *et al.*, 2017) concluded that agonist binding results in large movements within the extracellular ends of TM6, TM7 and TM1 that induces an unwinding of the top of TM6. Upon these movements, the central polar network undergoes a rearrangement. This new packing arrangement within the polar network stabilizes the active state structure. It is interesting, that while we observed N194A (N^{2.60}A), N233A (N^{3.43}A) and Q355A (Q^{6.52}A) involvement in either equilibrium pK_i or functional cAMP affinity (pK_A), these residues had no measurable effect on cAMP efficacy, suggesting that while mutations of these residues result in a receptor with lower agonist affinity the ability of these mutated receptors to propagate ligand binding to transducer coupling was unaffected. It is quite surprising that disruption of these polar network residues did not directly affect CTR cAMP efficacy, as the mutation of analogous residues did so in other class B GPCRs (as reviewed by (de Graaf *et al.*, 2017)). Q383 (Q^{7.49}) was not important for functional affinity for the cAMP pathway, but was the only residue out of the polar residue network, whose mutation increased efficacy for cAMP pathway. Interestingly, for pERK1/2 efficacy, N194A (N^{2.60}A), N233A (N^{3.43}A), Y234A (Y^{3.44}A) and Q383A (Q^{7.49}A) all had detrimental effects (where efficacy could be determined). These data show that particular central polar network residues are differentially involved in the CTR binding and signal transmission across distinct signalling pathways. It also confirms differential mechanisms for signal transmission for the cAMP pathway compared to that for pERK1/2 activation.

For comparison, in GLP-1R, an alanine substitution at R^{2.60} differentially affected cAMP efficacy (decreased GLP-1(7-36)NH₂ and exendin, but increased oxyntomodulin); and increased pERK1/2 efficacy for oxyntomodulin. Mutation of N^{3.43} to Ala decreased cAMP efficacy for GLP-1(7-36)NH₂ and pERK1/2 efficacy for exendin-4; and Q^{7.49}A decreased cAMP efficacy for

GLP-1(7-36)NH₂ and oxyntomodulin and decreased pERK1/2 efficacy for GLP-1(7-36)NH₂. For Q355 (Q^{6.52}) in the CTR, functional affinity effects for either signalling pathway could not be determined as CTR with this mutation had undetectable cell surface expression and thus even where this mutant resulted in decreased E_{max} for the concentration-response curves, we can not rule out that these effects were due to the reduced expression. In GLP-1R, H^{6.52}A decreased cAMP efficacy for 3 GLP-1 agonists (GLP-1(7-36)NH₂, exendin-4 and oxyntomodulin) and decreased pERK1/2 efficacy for GLP-1(7-36)NH₂ and exendin-4. Y234 (Y^{3.44}) is also considered to be involved in the central polar network in the CTR. Hence, while being important for ligand binding and signalling activation in class B receptors, central polar network controls ligand binding and signalling transmission in both ligand- and pathway-dependent manners, and the exact role of this network differs for each receptor. These differences perhaps reflect the distinct features of the binding pocket organization for different class B receptors (for example, in GLP-1R the central polar network is close enough for direct interactions with the peptide, whereas in the CTR this network sits about one helical turn below precluding direct interactions with the peptide) as well as the distinct structure of the various class B ligands (such as for example, N-terminal cysteine ring for CTR agonists). In addition, while the network is conserved as polar, the exact nature of the individual residues at each location differs between receptors (for sequence alignment see Supplementary Figure 7, Appendix1). Thus, this could play a role in the differences observed in signal propagation upon mutation of individual positions, between different receptors.

While low potency and poor expression limited our analysis, the impact of the tested CTR TM mutants on α CGRP and rAMY signalling was broadly consistent with the results for CT agonists. RAMP3 has been shown to alter how ECL2 and ECL3 contribute to the signalling propagation through the CTR (Pham *et al.*, 2019). Further investigation of RAMP effects on the CTR TM mutants signalling, would provide us with new insights on how the presence of RAMPs allosterically modulate the CTR binding pocket.

5.4 SUMMARY

1. Mutations in the deep binding pocket and in the central polar network of CTR are important for cAMP functional affinity, but had only a limited effect on cAMP efficacy.
2. Mutations of the CTR TM residues resulted in largely similar patterns of cAMP efficacy effects for all CTR agonists, highlighting the potentially universal role of these residues for signal transduction.
3. The proportion of residues that, when mutated, altered CTR signalling efficacy at the pERK1/2 pathway was much greater than the proportion that altered cAMP signalling. It is possible that

this reflects the complex convergent nature of the pERK1/2 response being the result of activation of multiple signalling pathways. Many mutants that changed efficacy at both cAMP and ERK1/2 pathways did so in opposite directions. This suggests that the transducers that are involved in pERK1/2 signalling have a different mode of engagement with the receptor compared with those involved in the cAMP pathway.

4. A switch from biphasic to monophasic curves for pERK1/2 experiments for CTs may suggest that the mutations helped to promote the exchange of the receptor between different states (that was otherwise constrained by the TM residues). It could also indicate that the mutations resulted in CTR decoupling from one of the upstream pathways that converges on pERK1/2 signalling.
5. Comparison of efficacy effects of the analogous mutations between CTR and other class B receptors revealed only limited conservation of the exact role of individual residues involved in signalling propagation; implying that different class B receptors regulate its ligand binding and signalling in a ligand-, pathway- and receptor-specific manner.

CHAPTER 6

General discussion and future directions

6.1 RESEARCH FOCUS

The CTR is a class B (secretin-like) GPCR and is involved in calcium and bone homeostasis by regulating osteoclast activity and renal calcium excretion. The CTR is also expressed in haematopoietic precursors, the central nervous system, and is implicated in regulating the progression of several cancers (Fujikawa *et al.*, 1996, Nakamura *et al.*, 2007, Shah *et al.*, 2008, Wookey *et al.*, 2012, Tolcos *et al.*, 2003, Wookey *et al.*, 2009). In the first project of my thesis, I assessed CTR's role in the deadly brain tumour, glioblastoma multiforme. By measuring CTR signalling in GBM cells I aimed to understand how CTR regulates secondary messenger systems in GBM cancer cells to explore whether CTR could be a useful target for GBM treatment.

CTR signalling has been shown to be both receptor subtype (distinct CTR isoforms and splice variants), ligand- and cellular background dependent (Dal Maso *et al.*, 2018a). Additionally, CTR can form heteromeric complexes with single pass transmembrane receptor activity modifying proteins (RAMPs) that result in AMY receptors with distinct pharmacological profiles (Christopoulos *et al.*, 1999, Morfis *et al.*, 2008). CTR is pleiotropically coupled to multiple signalling pathways, including cAMP (mediated by G_{as}), intracellular Ca^{2+} mobilisation (mediated by G_{aq}) and pERK1/2. In the last decade, much work has been done to understand GPCR structure and the relationship between structure and receptor's downstream signalling. Large-scale mutagenesis of receptor signalling domains helps to identify the networks of amino acids that initiate and propagate signalling and to separate out these networks into individual pathways. In order to better understand how calcitonin peptides interact with the receptor to initiate different effector coupling/signalling at molecular level I undertook structure-function studies using large-scale mutagenesis of the CTR transmembrane binding domain (project II). This knowledge is important for designing better therapeutics using structure-based drug design approach.

6.2 CTR ROLE IN GBM SIGNALLING AND PROLIFERATION: MAIN FINDINGS AND DISCUSSION

Glioblastoma multiforme is the most common and aggressive type of primary brain cancer. GBM arises from transformed precursors of astrocytes and is characterized by high proliferation, vascularization and resistance to apoptosis (Louis *et al.*, 2007, Kleihues *et al.*, 1999, Sanai *et al.*, 2005). With median survival of less than 15 months, identification and validation of new GBM therapeutic targets is of critical importance (Louis *et al.*, 2007). Studies involving breast cancer, prostate cancer and glioma cell lines show that tumor invasiveness, metastatic potential and angiogenesis can be modulated by stimulation of CTR/CLR with their

agonists/ antagonists (Venkatanarayan *et al.*, 2015, Nakamura *et al.*, 2007, Hay *et al.*, 2011). Adrenomedullin and CGRP are thought to be involved in cancer progression both directly (stimulating cancer cell proliferation) and indirectly (promoting tumor angiogenesis); with these effects mediated by their respective receptors (Hay *et al.*, 2011). CTR expression by immunohistochemistry was reported in the majority of glioblastoma tumor biopsies (12 out of 14, $P < 0.05$) with low or undetectable CTR expression in adjacent non-tumor tissue (Wookey *et al.*, 2012), other public databases report the presence of CTR mRNA in either 28% (IVY-GAP) or 76% (TCGA) of tissue samples. Of note GBM is primarily a tumour of the cerebral cortex (Davis, 2016, Larjavaara *et al.*, 2007) whereas CTR is normally only expressed in a subset of regions within the brain-stem (Hilton *et al.*, 1995, Sexton *et al.*, 1991, Sexton *et al.*, 1993). A single report showed that second messenger systems could be activated by calcitonin in the GBM-derived A172 cell line (Wookey *et al.*, 2012). Prior to the work presented here this was the extent of knowledge regarding CTR in glioblastoma.

As we showed, not all high-grade glioma cell lines in this study appeared to express functional CTR (as assessed by second messenger coupling). Only one of the four studied high-grade glioma cell lines expressed functional CTR (as supported by its ability to activate cAMP response upon stimulation with CT agonists (sCT and hCT). sCT and hCT in the Sb2B cell line showed distinct profiles with hCT having lower potency of response compared to sCT which is in agreement with anticipated low receptor expression levels in these GBM cell lines and the known affinities for these two ligands. CTR present in SB2b cell line showed no detectable signalling across other known, CTR- coupled pathways, such as Ca^{2+} , pERK1/2, p38 kinase. Our inability to measure response to less strongly CTR coupled pathways could easily be the result of low receptor expression levels.

Our exome sequencing data failed to account for the discrepancy between functional data and expression on the cell lines that do not respond to calcitonin(s) with no deleterious non-synonymous polymorphisms detected, suggesting that other factors may be at play, such as alternative splicing or rapid constitutive receptor internalization. While we tried 3 different approaches to measure cell proliferation, no effects on cell proliferation mediated pharmacologically through the CTR in SB2b cell line were detected.

No correlation between GBM subtype and the expression profile has been observed between our samples. Additionally, our analysis of published CTR expression from IVY-GAP or TCGA databases does not support a correlation between CTR expression and patient outcome.

We would therefore argue that CTR expression, while common in primary GBM tumors, is unlikely to be tractable to pharmacological intervention but may be suitable as a target for delivering cytotoxic agents. This study shows that GPCR signaling can display significant

variation depending on cellular system used, and effects seen in model recombinant cell lines or tumor cell lines are not always reproduced in a more physiologically relevant system and vice versa.

There are a number of additional experiments that might be performed to clarify discrepancy between the data, though these are beyond the scope of this thesis. Performing FACS or immunohistochemistry using anti-CTR antibodies targeted against the extracellular domain may help to understand what proportion of the receptor is reaching the surface, given we are able to detect the receptor in immunoblots from cell membrane fractions. Ligand binding experiments, although technically very challenging with low endogenous expression would be very useful to try and characterize both cell surface receptor pools and apparent receptor affinity. RT-PCR or RNase protection could be used as methods to assess which CTR splice variant(s) are expressed in these model cell lines. These approaches may resolve the observed lack of signaling in the three cell lines (PB1, JK2 and WK1) where inability to measure functional cAMP response to CTs was a result of lack of receptor trafficking to the cell surface, severely reduced coupling due to expression of the insert positive splice variant or where CTR in those cell lines has impaired binding properties. Impaired binding in conjunction with preserved cell surface expression would be difficult to reconcile with our exome sequencing data but may be the result of defects in receptor glycosylation, as glycosylation, at least at asparagine 130 (N130), is required for full receptor affinity for sCT (Ho *et al.*, 1999, Lee *et al.*, 2017). Abundant CGRP (CLR/RAMP) receptor expression in the GBM cell lines makes it tempting to think that this might be a suitable alternative target for pharmacological intervention in glioblastoma but the widespread expression throughout the brain and central involvement in pain transmission pathways means that this is unlikely to be a pharmacologically tractable target.

6.3 MUTAGENESIS OF CTR BINDING POCKET: MAIN FINDINGS AND DISCUSSION

It is now well established in the field that CTR, as well as other class B GPCRs interact with their peptide agonists via a 2 domain mechanism in which the NTD of the receptor provides a high affinity interaction site for the C-terminal end of an agonist and the N-terminal end of the peptide interacts with the receptor transmembrane binding pocket (Culhane *et al.*, 2015, Pal *et al.*, 2012). This is supported by the cryo-EM structures for CTR, GLP-1R and CGRP receptors (Liang *et al.*, 2018a, Liang *et al.*, 2018b, Liang *et al.*, 2017, Zhang *et al.*, 2017b). According to our cryo-EM structural models of CTR, sCT and hCT are predicted to form interactions with tops of all CTR TMs, except for TM4. TM6 and TM7 are especially important as the whole region, including TM6-ECL3-TM7, is thought to undergo a major conformational rearrangement (Liang *et al.*, 2017). At the base of the binding pocket there is a central network of polar residues

conserved in class B GPCRs (Liang *et al.*, 2017, Wootten *et al.*, 2013, Wootten *et al.*, 2016a). These residues have previously been demonstrated to play both global and ligand-specific roles in ligand binding and propagation of signaling in other class B GPCRs (Wootten *et al.*, 2013, Wootten *et al.*, 2016a, Wootten *et al.*, 2017). To further explore, at a molecular level, how different ligands initiate and propagate signalling, residues located in the CTR TM binding pocket were evaluated to determine their contribution to binding and signalling using alanine scanning mutagenesis.

According to the earlier model of CTR interaction with its agonists, the mid-region and C-terminus of CT agonists are predominantly important for affinity, while peptide N-terminus is responsible for receptor activation (Hilton *et al.*, 2000, Furness *et al.*, 2016). Collectively, our recent data shows that the interactions between the deep TM receptor binding pocket residues and the peptide N-terminus are also important for binding, at least for the lower affinity CTR agonists, hCT and pCT.

Effects of mutation of individual TM residues on ligand affinity at different class B receptors were previously studied elsewhere. There are some overlaps between the affinity effects of TM mutations observed for CTR and other class B receptors. For example, N194A (N^{2.60}A) had detrimental effects on the CTR binding affinity at 4 out of 5 tested CTR agonists (hCT, pCT, CGRP and rAMY). The equivalent residue-mutation was previously reported to reduce affinity for GLP-1R (Yang *et al.*, 2016, Coopman *et al.*, 2011, Wootten *et al.*, 2013), GCGR (Siu *et al.*, 2013), VPAC1-R (Solano *et al.*, 2001), secretin (Di Paolo *et al.*, 1998) and GIPR (Yaqub *et al.*, 2010) (for secretin and GIPR detrimental effects on cAMP potency (decreased EC₅₀) were reported). Interestingly, this appears to be the only polar network residue that consistently reduced affinity across different class B GPCRs, including CTR. While N240A (N^{3.43}A) differentially decreased affinity between the different GLP-1R agonists (Wootten *et al.*, 2013) (as well as potency of GIPR cAMP response to GIP) (Yaqub *et al.*, 2010)), and H363A (H^{6.52}A) was globally important in pK_i of GLP-1R agonists (Wootten *et al.*, 2013, Coopman *et al.*, 2011) and GCGR pK_i (less than 4-fold change of potency) (Siu *et al.*, 2013), our radioligand competition binding data did not support the role of these two central polar network residues in CTR binding affinity, although N233 (N^{3.43}) and Q355 (Q^{6.52}) were both important for hCT, CGRP and rAMY functional affinity for cAMP pathway. According to our data, mutation of Q383A (Q^{7.49}A) had no effect on binding of CTR ligands. Consistent with this, the corresponding Q^{7.39}A mutation did not alter ligand affinity at the GLP-1R (Wootten *et al.*, 2013). Y234A (Y^{3.44}A) is considered to be a part of the central polar network. I found that Y234A (Y^{3.44}A) was important for both hCT and pCT CTR affinity, and the equivalent mutation had moderate effects on affinity in GLP-1R and GCGR (Siu *et al.*, 2013, Yang *et al.*, 2016).

Other TM residues whose mutation was commonly important for ligand affinity at both CTR and other class B receptors affinity were H^{3.36}, Y^{3.44}, H^{5.40}, F^{6.56} and D^{3.39}. The mutation H226A (H^{3.36}A) in CTR only reduced pK_i for pCT yet the corresponding mutation decreased ligand affinity for GCGR (Yang *et al.*, 2016, Siu *et al.*, 2013), GLP-1R (Yang *et al.*, 2016) and GIPR (decreased EC₅₀) (Yaqub *et al.*, 2010). H302A (H^{5.40}A) mutation decreased CTR affinity for hCT and the corresponding residue was also important for ligand affinity at both GLP-1R, CGRP (Wootten *et al.*, 2013, Coopman *et al.*, 2011, Dods *et al.*, 2016, Siu *et al.*, 2013) and GIPR (decreased EC₅₀) (Yaqub *et al.*, 2010). Another residue that was important for hCT CTR affinity, F359 (F^{6.56}), was also involved in GCGR (Siu *et al.*, 2013), GLP-1R (Yang *et al.*, 2016), GIPR (EC₅₀) (Yaqub *et al.*, 2010) and secretin (Cordomí *et al.*, 2015) pK_i (EC₅₀ for GIPR). D373A (D^{7.39}) was detrimental for both hCT, pCT affinity at the CTR, and it also had effects on GCGR (Siu *et al.*, 2013) and GLP-1R (Yang *et al.*, 2016) affinities. Interestingly, I380A, that increased pCT affinity for the CTR, also increased affinity of GIPR receptor (Cordomí *et al.*, 2015), but had a small decrease of GCGR (Siu *et al.*, 2013); and GLP-1 (Coopman *et al.*, 2011) affinities. Overall the changes in affinity seen at these CTR mutants were broadly similar to those seen for other class B receptors if the affinity for sCT was not considered. This suggests that the nature of the affinity determining interactions for sCT are substantially different than those for other CTR, and indeed other class B receptor, ligands, and perhaps that these are responsible for its unusual off-rate kinetics. Alternatively, as MD simulations indicate (Dal Maso *et al.*, 2018), sCT forms a substantially more stable interaction with CTR when compared with hCT and thus its binding may be much less susceptible to the effects of single mutations.

R227A (K^{3.30}) was globally important for ligand affinity at the GLP-1R (Wootten *et al.*, 2013, Furness *et al.*, 2018) and the mutation of the corresponding residue also decreased GCGR affinity (Siu *et al.*, 2013). In this study mutation of K220A (K^{3.30}A) resulted in global effects on functional cAMP affinity (across all agonists), while pK_i couldn't be robustly determined. F356 (F^{6.53}) was also important for CTR functional cAMP affinity for hCT, CGRP and rAMY, but showed no effects on pK_i. Whereas the corresponding residue, when mutated, decreased affinity for GCGR (Siu *et al.*, 2013), GLP-1R and GIPR (decreased EC₅₀) (Cordomí *et al.*, 2015, Coopman *et al.*, 2011, Yang *et al.*, 2016, Yaqub *et al.*, 2010).

An interesting and important observation was the overall higher sensitivity of lower affinity CT agonists (hCT and pCT) to individual Ala mutations compared to sCT. The fact that there are only subtle differences between the CTR-sCT and CTR-hCT cryo-EM structures indicates that there might be differences in the kinetics of interactions between CTR and different calcitonin ligands. MD simulations provide some evidence for this. The MD simulations performed on sCT-CTR and hCT-CTR models (Dal Maso *et al.*, 2018b) support

more transient nature of hCT-CTR interactions. Taken together with the fact that total equilibrium affinity for this agonist is lower compared to sCT, the transient nature of interactions can make the interaction with hCT less stable, and thus more sensitive to single mutations. Because of making more stable contacts with the receptor, sCT appears to be less sensitive to removal of a single interaction and might require substitution of several residues in order to see the effects on affinity.

The differences observed for different CTR ligands require further investigation. Only a limited number of direct interactions with receptor and ligands are supported by our sCT-CTR and hCT-CTR cryo-EM data. As all GPCRs are dynamic rather than static structures and detergents used to obtain receptor structures represent an artificial system, it is important to understand that, while providing us with valuable information, X-ray and cryo-EM structures do not provide us with information about all possible receptor conformations. Therefore, other aspects of the receptor-ligand interactions might come in play, such as the kinetics of interaction (as discussed above). Protein dynamics methods are an emerging new paradigm that helps to provide additional structural insights about GPCR activation and signalling as well energy state transitions associated with this (Deupi *et al.*, 2010). These include NMR spectroscopy (can be used to address specific questions about receptor conformational dynamics, particularly the exchange rate between different conformational states and may allow subtle conformational changes within a protein to be measured); site-directed spin labelling (SDSL) with double electron-electron resonance (DEER) spectroscopy (can be used to map distances between two different probes); fluorescence spectroscopy, including methods based on fluorescence resonance energy transfer and fluorescence quenching (to test protein-protein interactions and structural reorganisations within protein domains); hydrogen-deuterium exchange (HDX) spectroscopy (allows to define the conformational flexibility in receptors at a global level, and through the use of selective labels in proteins) (as reviewed by (Stevens *et al.*, 2013, Wishart, 2011, Jeschke, 2012, Lohse *et al.*, 2008, Lohse *et al.*, 2012). Thus, using methods of protein dynamics to compare CTR interactions with its various ligands could provide additional insights into the process of activation and visualisation of the energy landscapes that CTR undergoes during the activation process. MD simulations complement these studies providing a full atomic-level picture of the structure as it changes over time.

Differences seen in pCT affinity profile (compared to sCT and hCT) in our study are in agreement with the distinct binding profile for pCT previously observed in the ECL2/3 study (Dal Maso *et al.*, 2018b). The mechanism explaining these differences for pCT requires further investigation. One approach is running MD simulations for pCT. This would provide additional information about CTR-pCT interactions and how this is different from sCT and hCT.

Chicken calcitonin (cCT), which was not included into this study, has a sequence and properties (higher potency compared to hCT and pCT) similar to sCT. Performing a comparable analysis as I have done here with cCT at the various CTR TM mutants could be another possibility to better understand how differences in CTR agonist structure influence its interactions with the receptor. Another approach is to use peptides chimeras in pair with mutant receptors (sCT-hCT chimeric receptors were described by (Hilton *et al.*, 2000, Furness *et al.*, 2016)).

Fluorescence polarisation technique could be used to test whether introducing single Ala substitutions in the CTR TM region changes the kinetics of the CTR-ligand interactions. For example, we know that sCT has an unusually long residency time at the CTR (over 30 mins). Therefore, we could measure K_{on} and K_{off} for K220A ($K^{3.30}A$) mutant versus for the WT receptor to look for any changes in K_{on} and K_{off} resulting from K220 ($K^{3.30}A$) Ala substitution. We have a fluorescently labeled sCT(8-32) and an optimized protocol for measuring CTR interaction kinetics (residency time) with its ligands (Furness *et al.*, 2016) allowing real-time binding kinetics and full determination of unlabeled ligand K_{on} and K_{off} using the Matoulsky-Mahan kinetic competition method (Matoulsky and Mahan, 1984). Radioligand binding kinetics experiments as well as nanoBRET may also employed to answer the same question. The main disadvantage of the radioligand binding method is that it is difficult to obtain reproducible fast kinetic data. For NanoBRET development of protocol and optimization are needed along with acquisition of nLuc tagged receptor construct.

There was a good correlation between cAMP functional affinity data (pK_A) values for individual mutants and the pK_i values. However, for pERK1/2 pathway the correlation between the pK_i and pK_A was low. On one hand, these differences between pK_i and pERK1/2 pK_A may be a reflection of the differences in our assay systems (both pK_i and cAMP pK_A were measured under either equilibrium or close to equilibrium conditions for receptor occupancy while pERK1/2 assay was performed under non-equilibrium conditions). On the other hand, these results might also indicate that the affinity of CT agonists is primarily driven by G_s coupling and not by the effectors (pathways) leading to pERK1/2 phosphorylation.

Mutational effects on the CTR efficacy were clearly pathway-dependant, indicating that distinct signalling transducers are involved in cAMP and pERK1/2 pathways. There were very few effects on CTR cAMP efficacy, indicating that the functional effects on CTR cAMP signalling primarily result from functional affinity changes (as discussed above). For the majority of mutants for pERK1/2 pathway efficacy was profoundly decreased across all ligands. Collectively our pERK1/2 data suggests that while Ala substitutions enabled better CTR

coupling to the pERK1/2 pathway (and thus increased pK_A values), pERK1/2 signalling output for the mutant receptors was, in fact, decreased compared to the WT receptor.

Comparison of efficacy effects between the CTR and other B GPCRs was limited, as the majority of previous studies did not separate efficacy effects from affinity, with functional effects being commonly reported as EC_{50} changes for cAMP pathway. Data on residue mutations of GLP-1R, where the Operational Model had been applied to separate efficacy effects, were used for the comparison of efficacy effects.

Efficacy data for corresponding residues between this study (CTR) and previous studies (GLP-1R) were available for K^{3.30}, H^{5.40}, N^{2.60}, N^{3.43}, H^{6.52} and Q^{7.49}. Mutations at these residues supported a model in which there is somewhat limited similarity between the networks of the TM residues that these two receptors use for their signaling pathway activation (Wootten *et al.*, 2013, Wootten *et al.*, 2016b, Furness *et al.*, 2018). As reported previously, in a comparison between signalling at CTR and GLP-1R mutants in ECL2 and 3 (Dal Maso *et al.*, 2018b), this study also shows only limited conservation of the effect of deep-binding pocket mutations on CTR versus GLP-1R activation and signaling; implying that different class B receptors regulate its ligand binding and signaling in a ligand-specific pathway- and receptor-specific manner.

Allosteric influence of RAMPs on the CTR signalling is of interest as presence of RAMPs induces new CTR phenotypes. It was recently shown that ECL2/3 mutations in the AMY3 (CTR/RAMP3) receptor result in highly ligand-specific effects on CTR agonists efficacy to both cAMP and pERK1/2 pathways and that for analogous ECL2/3 mutants, signal propagation is fundamentally altered compared to the CTR receptor alone (Pham *et al.*, 2019, Dal Maso *et al.*, 2018b). Investigating effects of the analogous TM mutations in the context of RAMPs will allow us to reveal the changes in CTR binding and signalling induced by CTR-RAMP association. As it was previously demonstrated, including the work on CTR in GBM, CTR co-expression with RAMPs is physiologically relevant and commonly occurs in nature, so understanding CTR signalling in the context of co-expression with RAMPs is important.

6.4 CONCLUDING REMARKS

In the first project of my thesis, I have investigated CTR expression in high grade glioma cell lines and showed that CTR is unlikely to be a tractable pharmacological target in GBM, although it may still be targeted by cytotoxic agents. While awareness and appreciation of CT and CTR being much more than just regulators of bone and calcium homeostasis is constantly growing, we are still in the very early phase of understanding of all physiological and pathophysiological repertoire for this hormone-receptor pair. Investigation of mechanisms of how CTR is involved in the cell growth and development, wound healing and immune system,

the CNS, regulation of cell cycle and cancer are required and may lead to interesting and important findings. Our results also emphasize the importance of using physiologically relevant systems versus recombinant cell lines in addressing questions on GPCR (patho)physiology.

Solving of the CTR ternary cryo-EM structure provided a big advance not only in the CTR field, but for all GPCR biology. Mutagenesis studies were undertaken in order to better understand how CTR extracellular domain contribute to the receptor activation and signaling for distinct CTR ligands (these interactions represent the first step of the class B two-domain activation mechanism) (Dal Maso *et al.*, 2018b, Dal Maso *et al.*, 2019). Analysis of analogous ECL2 and 3 mutants was conducted in the presence and absence of RAMPs demonstrating that RAMP3 fundamentally altered propagation of signaling for the CTR (Pham *et al.*, 2019). To further investigate the second stage of the two-domain activation mechanism for the CTR, I undertook a mutational analysis of the selected residues located in TMs 2,3,5,6 and 7 of the CTR, and this represents the second project of my PhD thesis. My data showed that the CTR TM region is not only important for efficacy, but it is important for the affinity of ligand binding (at least for lower affinity CTR ligands, hCT and pCT) as well as for functional coupling affinity. This is an important outcome that correlates with data on other class B GPCRs and further supports the two-domain model of the class B activation, highlighting the conservation of certain TM residues (and particularly those that are a part of the central polar network) within class B GPCRs. I have observed both ligand- and pathway-specific effects on affinity for the CTR indicating distinct modes of interactions with the receptor for individual CTR ligands. Efficacy effects of the CTR TM mutations were similar across CT ligands but strikingly pathway-specific, indicating differential transducers involved in the CTR signaling to distinct signaling pathways. When interacting with the CTR, rAMY and CGRP utilized amino acid networks that only partially overlap with that of the CT agonists which is consistent with low sequence homology between rAMY, CGRP and CT agonists. With future studies, this data will help to reveal the role of RAMPs as modulators of the CTR signaling.

Advances in structural biology provided us with long-awaited data on the structure of class B GPCRs, and CTR in particular. CTR activation and signaling to multiple pathways can now be characterized using various molecular pharmacology tools. We are just starting to dissect the mechanisms of CTR activation and signaling, yet the current picture that we have is far from being complete. We are yet to understand what structure characteristics of the CTR ligands are responsible for stabilizing specific receptor conformations and what is the contribution of differential ligand-receptor kinetics in this process. On the other hand, understanding of how molecular signaling effects observed at the CTR in recombinant cellular systems contribute to whole animal physiology and what are the roles of CT and CTR expression at various sites of the

body unrelated to bone physiology, including CTR expression at certain (patho)physiological conditions (such as morphogenesis, sepsis, cancer, etc.) is of paramount importance. Recent development of viable CALCA- and CTR- knock-out mouse models, can be a very useful tool to help address these questions in future studies.

REFERENCES

- ADELHORST, K., HEDEGAARD, B. B., KNUDSEN, L. B. & KIRK, O. 1994. Structure-activity studies of glucagon-like peptide-1. *J Biol Chem*, 269, 6275-8.
- ALBRANDT, K., BRADY, E. M., MOORE, C. X., MULL, E., SIERZEGA, M. E. & BEAUMONT, K. 1995. Molecular cloning and functional expression of a third isoform of the human calcitonin receptor and partial characterization of the calcitonin receptor gene. *Endocrinology*, 136, 5377-84.
- ALJAMEELI, A., THAKKAR, A. & SHAH, G. 2017. Calcitonin receptor increases invasion of prostate cancer cells by recruiting zonula occludens-1 and promoting PKA-mediated TJ disassembly. *Cell Signal*, 36, 1-13.
- ALJAMEELI, A., THAKKAR, A., THOMAS, S., LAKSHMIKANTHAN, V., ICZKOWSKI, K. A. & SHAH, G. V. 2016. Calcitonin Receptor-Zonula Occludens-1 Interaction Is Critical for Calcitonin-Stimulated Prostate Cancer Metastasis. *PLOS ONE*, 11, e0150090.
- AMARA, S. G., JONAS, V., ROSENFELD, M. G., ONG, E. S. & EVANS, R. M. 1982. Alternative RNA processing in calcitonin gene expression generates mRNAs encoding different polypeptide products. *Nature*, 298, 240.
- ANDREASSEN, K. V., HJULER, S. T., FURNESS, S. G., SEXTON, P. M., CHRISTOPOULOS, A., NOSJEAN, O., KARSDAL, M. A. & HENRIKSEN, K. 2014. Prolonged calcitonin receptor signaling by salmon, but not human calcitonin, reveals ligand bias. *PLoS One*, 9, e92042.
- ANGERS, S., SALAHPOUR, A. & BOUVIER, M. 2002. Dimerization: an emerging concept for G protein-coupled receptor ontogeny and function. *Annu Rev Pharmacol Toxicol*, 42, 409-35.
- ARDAILLOU, R. 1975. Kidney and calcitonin. *Nephron*, 15, 250-60.
- ARDAILLOU, R., VUAGNAT, P., MILHAUD, G. & RICHET, G. 1967. [Effects of thyrocalcitonin on the renal excretion of phosphates, calcium and hydrogen ions in man]. *Nephron*, 4, 298-314.
- ASSIL-KISHAWI, I., SAMRA, T. A., MIERKE, D. F. & ABOU-SAMRA, A. B. 2008. Residue 17 of sauvagine cross-links to the first transmembrane domain of corticotropin-releasing factor receptor 1 (CRFR1). *The Journal of biological chemistry*, 283, 35644-35651.
- ASSICOT, M., GENDREL, D., CARSIN, H., RAYMOND, J., GUILBAUD, J. & BOHUON, C. 1993. High serum procalcitonin concentrations in patients with sepsis and infection. *Lancet*, 341, 515-8.
- AXELROD, J., BURCH, R. M. & JELSEMA, C. L. 1988. Receptor-mediated activation of phospholipase A2 via GTP-binding proteins: arachidonic acid and its metabolites as second messengers. *Trends Neurosci*, 11, 117-23.
- AYERS, K. L. & THEROND, P. P. 2010. Evaluating Smoothed as a G-protein-coupled receptor for Hedgehog signalling. *Trends Cell Biol*, 20, 287-98.
- BALLESTEROS, J. A., JENSEN, A. D., LIAPAKIS, G., RASMUSSEN, S. G., SHI, L., GETHER, U. & JAVITCH, J. A. 2001. Activation of the beta 2-adrenergic receptor involves disruption of an ionic lock between the cytoplasmic ends of transmembrane segments 3 and 6. *J Biol Chem*, 276, 29171-7.
- BALLESTEROS, J. A. & WEINSTEIN, H. 1995. [19] Integrated methods for the construction of three-dimensional models and computational probing of structure-function relations in G protein-coupled receptors. In: SEALFON, S. C. (ed.) *Methods in Neurosciences*. Academic Press.
- BARWELL, J., CONNER, A. & POYNER, D. R. 2011. Extracellular loops 1 and 3 and their associated transmembrane regions of the calcitonin receptor-like receptor are needed for CGRP receptor function. *Biochimica et biophysica acta*, 1813, 1906-1916.
- BAVEC, A., HALLBRINK, M., LANGE, U. & ZORKO, M. 2003. Different role of intracellular loops of glucagon-like peptide-1 receptor in G-protein coupling. *Regul Pept*, 111, 137-44.

- BEAUDREUIL, J., BALASUBRAMANIAN, S., CHENAIS, J., TABOULET, J., FRENKIAN, M., ORCEL, P., JULLIENNE, A., HORNE, W. C., DE VERNEJOUL, M. C. & CRESSANT, M. 2004. Molecular characterization of two novel isoforms of the human calcitonin receptor. *Gene*, 343, 143-51.
- BECKER, K. L., NYLÉN, E. S., WHITE, J. C., MÜLLER, B. & SNIDER, J. R. H. 2004. Procalcitonin and the Calcitonin Gene Family of Peptides in Inflammation, Infection, and Sepsis: A Journey from Calcitonin Back to Its Precursors. *The Journal of Clinical Endocrinology & Metabolism*, 89, 1512-1525.
- BECKER, K. L., SNIDER, R. & NYLEN, E. S. 2010. Procalcitonin in sepsis and systemic inflammation: a harmful biomarker and a therapeutic target. *Br J Pharmacol*, 159, 253-64.
- BELL, D. & MCDERMOTT, B. J. 1996. Calcitonin gene-related peptide in the cardiovascular system: characterization of receptor populations and their (patho)physiological significance. *Pharmacol Rev*, 48, 253-88.
- BENOVIC, J. L., PIKE, L. J., CERIONE, R. A., STANISZEWSKI, C., YOSHIMASA, T., CODINA, J., CARON, M. G. & LEFKOWITZ, R. J. 1985. Phosphorylation of the mammalian beta-adrenergic receptor by cyclic AMP-dependent protein kinase. Regulation of the rate of receptor phosphorylation and dephosphorylation by agonist occupancy and effects on coupling of the receptor to the stimulatory guanine nucleotide regulatory protein. *J Biol Chem*, 260, 7094-101.
- BERGWITZ, C., GARDELLA, T. J., FLANNERY, M. R., POTTS, J. T., JR., KRONENBERG, H. M., GOLDRING, S. R. & JUPPNER, H. 1996. Full activation of chimeric receptors by hybrids between parathyroid hormone and calcitonin. Evidence for a common pattern of ligand-receptor interaction. *J Biol Chem*, 271, 26469-72.
- BLACK, J. W. & LEFF, P. 1983. Operational models of pharmacological agonism. *Proc R Soc Lond B Biol Sci*, 220, 141-62.
- BODY, J. J., GLIBERT, F., NEJAI, S., FERNANDEZ, G., VAN LANGENDONCK, A. & BORKOWSKI, A. 1990. Calcitonin receptors on circulating normal human lymphocytes. *J Clin Endocrinol Metab*, 71, 675-81.
- BOOE, J. M., WALKER, C. S., BARWELL, J., KUTEYI, G., SIMMS, J., JAMALUDDIN, M. A., WARNER, M. L., BILL, R. M., HARRIS, P. W., BRIMBLE, M. A., POYNER, D. R., HAY, D. L. & PIOSZAK, A. A. 2015. Structural Basis for Receptor Activity-Modifying Protein-Dependent Selective Peptide Recognition by a G Protein-Coupled Receptor. *Mol Cell*, 58, 1040-52.
- BOOE, J. M., WARNER, M. L., ROEHRKASSE, A. M., HAY, D. L. & PIOSZAK, A. A. 2018. Probing the Mechanism of Receptor Activity-Modifying Protein Modulation of GPCR Ligand Selectivity through Rational Design of Potent Adrenomedullin and Calcitonin Gene-Related Peptide Antagonists. *Molecular Pharmacology*, 93, 355.
- BORTOLATO, A., DORÉ, A. S., HOLLENSTEIN, K., TEHAN, B. G., MASON, J. S. & MARSHALL, F. H. 2014. Structure of Class B GPCRs: new horizons for drug discovery. *Br J Pharmacol*, 171, 3132-45.
- BOUVIER, M., HAUSDORFF, W. P., DE BLASI, A., O'DOWD, B. F., KOBILKA, B. K., CARON, M. G. & LEFKOWITZ, R. J. 1988. Removal of phosphorylation sites from the beta 2-adrenergic receptor delays onset of agonist-promoted desensitization. *Nature*, 333, 370-3.
- BROULIK, P. 2010. [Calcitonin and his role in regulation of calcium-phosphate metabolism]. *Cas Lek Cesk*, 149, 285-7.
- BUNEMANN, M., GERHARDSTEIN, B. L., GAO, T. & HOSEY, M. M. 1999. Functional regulation of L-type calcium channels via protein kinase A-mediated phosphorylation of the beta(2) subunit. *J Biol Chem*, 274, 33851-4.
- BURGEN, A. S. 1981. Conformational changes and drug action. *Fed Proc*, 40, 2723-8.

- BURKHOLDER, A. C. & HARTWELL, L. H. 1985. The yeast alpha-factor receptor: structural properties deduced from the sequence of the STE2 gene. *Nucleic Acids Res*, 13, 8463-75.
- CABRERA-VERA, T. M., VANHAUWE, J., THOMAS, T. O., MEDKOVA, M., PREININGER, A., MAZZONI, M. R. & HAMM, H. E. 2003. Insights into G protein structure, function, and regulation. *Endocr Rev*, 24, 765-81.
- CADIGAN, K. M. & NUSSE, R. 1997. Wnt signaling: a common theme in animal development. *Genes Dev*, 11, 3286-305.
- CAFFORIO, P., DE MATTEO, M., BRUNETTI, A. E., DAMMACCO, F. & SILVESTRIS, F. 2009. Functional expression of the calcitonin receptor by human T and B cells. *Hum Immunol*, 70, 678-85.
- CALEBIRO, D., NIKOLAEV, V. O., PERSANI, L. & LOHSE, M. J. 2010. Signaling by internalized G-protein-coupled receptors. *Trends Pharmacol Sci*, 31, 221-8.
- CHABARDES, D., IMBERT-TEBOUL, M., MONTEGUT, M., CLIQUE, A. & MOREL, F. 1976. Distribution of calcitonin-sensitive adenylate cyclase activity along the rabbit kidney tubule. *Proc Natl Acad Sci U S A*, 73, 3608-12.
- CHABRE, O., CONKLIN, B. R., LIN, H. Y., LODISH, H. F., WILSON, E., IVES, H. E., CATANZARITI, L., HEMMINGS, B. A. & BOURNE, H. R. 1992. A recombinant calcitonin receptor independently stimulates 3',5'-cyclic adenosine monophosphate and Ca²⁺/inositol phosphate signaling pathways. *Molecular Endocrinology*, 6, 551-556.
- CHAFTARI, A. M., HACHEM, R., REITZEL, R., JORDAN, M., JIANG, Y., YOUSIF, A., GAROGE, K., DESHMUKH, P., AL HAMAL, Z., JABBOUR, J., HANANIA, A., RAAD, S., JAMAL, M. & RAAD, I. 2015. Role of Procalcitonin and Interleukin-6 in Predicting Cancer, and Its Progression Independent of Infection. *PLoS One*, 10, e0130999.
- CHAMBERS, T. J., MCSHEEHY, P. M., THOMSON, B. M. & FULLER, K. 1985. The effect of calcium-regulating hormones and prostaglandins on bone resorption by osteoclasts disaggregated from neonatal rabbit bones. *Endocrinology*, 116, 234-9.
- CHEN, Y., SHYU, J. F., SANTHANAGOPAL, A., INOUE, D., DAVID, J. P., DIXON, S. J., HORNE, W. C. & BARON, R. 1998. The calcitonin receptor stimulates Shc tyrosine phosphorylation and Erk1/2 activation. Involvement of Gi, protein kinase C, and calcium. *J Biol Chem*, 273, 19809-16.
- CHENG, L., HUANG, Z., ZHOU, W., WU, Q., DONNOLA, S., LIU, J. K., FANG, X., SLOAN, A. E., MAO, Y., LATHIA, J. D., MIN, W., MCLENDON, R. E., RICH, J. N. & BAO, S. 2013. Glioblastoma stem cells generate vascular pericytes to support vessel function and tumor growth. *Cell*, 153, 139-52.
- CHENG, X., JI, Z., TSALKOVA, T. & MEI, F. 2008. Epac and PKA: a tale of two intracellular cAMP receptors. *Acta Biochim Biophys Sin (Shanghai)*, 40, 651-62.
- CHIEN, J., REN, Y., QING WANG, Y., BORDELON, W., THOMPSON, E., DAVIS, R., RAYFORD, W. & SHAH, G. 2001. Calcitonin is a prostate epithelium-derived growth stimulatory peptide. *Mol Cell Endocrinol*, 181, 69-79.
- CHO, E. Y., CHO, D. I., PARK, J. H., KUROSE, H., CARON, M. G. & KIM, K. M. 2007. Roles of protein kinase C and actin-binding protein 280 in the regulation of intracellular trafficking of dopamine D3 receptor. *Mol Endocrinol*, 21, 2242-54.
- CHRISTOPOULOS, G., PERRY, K. J., MORFIS, M., TILAKARATNE, N., GAO, Y., FRASER, N. J., MAIN, M. J., FOORD, S. M. & SEXTON, P. M. 1999. Multiple amylin receptors arise from receptor activity-modifying protein interaction with the calcitonin receptor gene product. *Mol Pharmacol*, 56, 235-42.
- CHUNG, C. Y., POTIKYAN, G. & FIRTEL, R. A. 2001. Control of Cell Polarity and Chemotaxis by Akt/PKB and PI3 Kinase through the Regulation of PAKa. *Molecular Cell*, 7, 937-947.

- CLAPHAM, D. E. & NEER, E. J. 1997. G protein beta gamma subunits. *Annu Rev Pharmacol Toxicol*, 37, 167-203.
- COCHRAN, M., PEACOCK, M., SACHS, G. & NORDIN, B. E. 1970. Renal effects of calcitonin. *Br Med J*, 1, 135-7.
- CONLON, J. M., GRIMELIUS, L. & THIM, L. 1988. Structural characterization of a high-molecular-mass form of calcitonin [procalcitonin-(60-116)-peptide] and its corresponding N-terminal flanking peptide [procalcitonin-(1-57)-peptide] in a human medullary thyroid carcinoma. *Biochem J*, 256, 245-50.
- CONNER, A. C., SIMMS, J., CONNER, M. T., WOOTTEN, D. L., WHEATLEY, M. & POYNER, D. R. 2006. Diverse functional motifs within the three intracellular loops of the CGRP1 receptor. *Biochemistry*, 45, 12976-85.
- CONNER, M., HICKS, M. R., DAFFORN, T., KNOWLES, T. J., LUDWIG, C., STADDON, S., OVERDUIN, M., GUNTHER, U. L., THOME, J., WHEATLEY, M., POYNER, D. R. & CONNER, A. C. 2008. Functional and biophysical analysis of the C-terminus of the CGRP-receptor; a family B GPCR. *Biochemistry*, 47, 8434-44.
- COPP, D. H., CAMERON, E. C., CHENEY, B. A., DAVIDSON, A. G. & HENZE, K. G. 1962. Evidence for calcitonin--a new hormone from the parathyroid that lowers blood calcium. *Endocrinology*, 70, 638-49.
- COOPMAN, K., WILLARS, G. B., TIMMS, D., WILKINSON, G. F., WALLIS, R., BROWN, A. J. H. & ROBB, G. 2011. Residues within the Transmembrane Domain of the Glucagon-Like Peptide-1 Receptor Involved in Ligand Binding and Receptor Activation: Modelling the Ligand-Bound Receptor. *Molecular Endocrinology*, 25, 1804-1818.
- CORDOMÍ, A., ISMAIL, S., MATSOUKAS, M.-T., ESCRIEUT, C., GHERARDI, M.-J., PARDO, L. & FOURMY, D. 2015. Functional elements of the gastric inhibitory polypeptide receptor: Comparison between secretin- and rhodopsin-like G protein-coupled receptors. *Biochemical Pharmacology*, 96, 237-246.
- CUBILLOS, S., NORGAUER, J. & LEHMANN, K. 2010. Toxins-useful biochemical tools for leukocyte research. *Toxins (Basel)*, 2, 428-52.
- CULHANE, K. J., LIU, Y., CAI, Y. & YAN, E. C. 2015. Transmembrane signal transduction by peptide hormones via family B G protein-coupled receptors. *Front Pharmacol*, 6, 264.
- CYPESS, A. M., UNSON, C. G., WU, C. R. & SAKMAR, T. P. 1999. Two cytoplasmic loops of the glucagon receptor are required to elevate cAMP or intracellular calcium. *J Biol Chem*, 274, 19455-64.
- DACQUIN, R., DAVEY, R. A., LAPLACE, C., LEVASSEUR, R., MORRIS, H. A., GOLDRING, S. R., GEBRE-MEDHIN, S., GALSON, D. L., ZAJAC, J. D. & KARSENTY, G. 2004. Amylin inhibits bone resorption while the calcitonin receptor controls bone formation in vivo. *J Cell Biol*, 164, 509-14.
- DAL MASO, E., GLUKHOVA, A., ZHU, Y., GARCIA-NAFRIA, J., TATE, C., ATANASIO, S., ARTHUR REYNOLDS, C., RAMÍREZ-APORTELA, E., CARAZO, J.-M., A. HICK, C., FURNESS, S., L. HAY, D., LIANG, Y.-L., J. MILLER, L., CHRISTOPOULOS, A., WANG, M.-W., WOOTTEN, D. & M. SEXTON, P. 2019. *The molecular control of calcitonin receptor (CTR) signaling*.
- DAL MASO, E., JUST, R., HICK, C., CHRISTOPOULOS, A., SEXTON, P. M., WOOTTEN, D. & FURNESS, S. G. B. 2018a. Characterization of signalling and regulation of common calcitonin receptor splice variants and polymorphisms. *Biochem Pharmacol*, 148, 111-129.
- DAL MASO, E., ZHU, Y., PHAM, V., REYNOLDS, C. A., DEGANUTTI, G., HICK, C. A., YANG, D., CHRISTOPOULOS, A., HAY, D. L., WANG, M. W., SEXTON, P. M., FURNESS, S. G. B. & WOOTTEN, D. 2018b. Extracellular loops 2 and 3 of the calcitonin receptor selectively modify agonist binding and efficacy. *Biochem Pharmacol*, 150, 214-244.

- DAS, S. & MARSDEN, P. A. 2013. Angiogenesis in Glioblastoma. *N Engl J Med*, 369, 1561-3.
- DAVENPORT, A. P., ALEXANDER, S. P., SHARMAN, J. L., PAWSON, A. J., BENSON, H. E., MONAGHAN, A. E., LIEW, W. C., MPAMHANGA, C. P., BONNER, T. I., NEUBIG, R. R., PIN, J. P., SPEDDING, M. & HARMAR, A. J. 2013. International Union of Basic and Clinical Pharmacology. LXXXVIII. G protein-coupled receptor list: recommendations for new pairings with cognate ligands. *Pharmacol Rev*, 65, 967-86.
- DAVEY, R. A., TURNER, A. G., MCMANUS, J. F., CHIU, W. S., TJAHYONO, F., MOORE, A. J., ATKINS, G. J., ANDERSON, P. H., MA, C., GLATT, V., MACLEAN, H. E., VINCENT, C., BOUXSEIN, M., MORRIS, H. A., FINDLAY, D. M. & ZAJAC, J. D. 2008. Calcitonin receptor plays a physiological role to protect against hypercalcemia in mice. *J Bone Miner Res*, 23, 1182-93.
- DAVIS, M. E. 2016. Glioblastoma: Overview of Disease and Treatment. *Clinical journal of oncology nursing*, 20, S2-S8.
- DAVIS, N. S., DISANT'AGNESE, P. A., EWING, J. F. & MOONEY, R. A. 1989. The neuroendocrine prostate: characterization and quantitation of calcitonin in the human gland. *J Urol*, 142, 884-8.
- DAY, B. W., STRINGER, B. W., WILSON, J., JEFFREE, R. L., JAMIESON, P. R., ENSBEY, K. S., BRUCE, Z. C., INGLIS, P., ALLAN, S., WINTER, C., TOLLESSON, G., CAMPBELL, S., LUCAS, P., FINDLAY, W., KADRIAN, D., JOHNSON, D., ROBERTSON, T., JOHNS, T. G., BARTLETT, P. F., OSBORNE, G. W. & BOYD, A. W. 2013. Glioma surgical aspirate: a viable source of tumor tissue for experimental research. *Cancers (Basel)*, 5, 357-71.
- DE GRAAF, C., SONG, G., CAO, C., ZHAO, Q., WANG, M. W., WU, B. & STEVENS, R. C. 2017. Extending the Structural View of Class B GPCRs. *Trends Biochem Sci*, 42, 946-960.
- DE LEAN, A., STADEL, J. M. & LEFKOWITZ, R. J. 1980. A ternary complex model explains the agonist-specific binding properties of the adenylate cyclase-coupled beta-adrenergic receptor. *J Biol Chem*, 255, 7108-17.
- DEFEA, K. A., ZALEVSKY, J., THOMA, M. S., DERY, O., MULLINS, R. D. & BUNNETT, N. W. 2000. beta-arrestin-dependent endocytosis of proteinase-activated receptor 2 is required for intracellular targeting of activated ERK1/2. *J Cell Biol*, 148, 1267-81.
- DELGHANDI, M. P., JOHANNESSEN, M. & MOENS, U. 2005. The cAMP signalling pathway activates CREB through PKA, p38 and MSK1 in NIH 3T3 cells. *Cell Signal*, 17, 1343-51.
- DEUPI, X. & KOBILKA, B. K. 2010. Energy landscapes as a tool to integrate GPCR structure, dynamics, and function. *Physiology (Bethesda)*, 25, 293-303.
- DHANASEKARAN, N. & DERMOTT, J. M. 1996. Signaling by the G12 class of G proteins. *Cell Signal*, 8, 235-45.
- DI PAOLO, E., DE NEEF, P., MOGUILEVSKY, N., PETRY, H., BOLLEN, A., WAELBROECK, M. & ROBBERECHT, P. 1998. Contribution of the second transmembrane helix of the secretin receptor to the positioning of secretin. *FEBS Lett*, 424, 207-10.
- DI PAOLO, E., PETRY, H., MOGUILEVSKY, N., BOLLEN, A., DE NEEF, P., WAELBROECK, M. & ROBBERECHT, P. 1999. Mutations of aromatic residues in the first transmembrane helix impair signalling by the secretin receptor. *Receptors Channels*, 6, 309-15.
- DODS, R. L. & DONNELLY, D. 2016. The peptide agonist-binding site of the glucagon-like peptide-1 (GLP-1) receptor based on site-directed mutagenesis and knowledge-based modelling. *Biosci Rep*, 36, e00285.
- DONG, M., XU, X., BALL, A. M., MAKHOUL, J. A., LAM, P. C. H., PINON, D. I., ORRY, A., SEXTON, P. M., ABAGYAN, R. & MILLER, L. J. 2012. Mapping spatial approximations between the amino terminus of secretin and each of the extracellular loops of its receptor using cysteine trapping. *The FASEB Journal*, 26, 5092-5105.
- DONG, C., FILIPEANU, C. M., DUVERNAY, M. T. & WU, G. 2007. Regulation of G protein-coupled receptor export trafficking. *Biochimica et biophysica acta*, 1768, 853-870.

- DONG, M., KOOLE, C., WOOTTEN, D., SEXTON, P. M. & MILLER, L. J. 2014. Structural and functional insights into the juxtamembranous amino-terminal tail and extracellular loop regions of class B GPCRs. *Br J Pharmacol*, 171, 1085-101.
- DONG, M., LAM, P. C., ORRY, A., SEXTON, P. M., CHRISTOPOULOS, A., ABAGYAN, R. & MILLER, L. J. 2016. Use of Cysteine Trapping to Map Spatial Approximations between Residues Contributing to the Helix N-capping Motif of Secretin and Distinct Residues within Each of the Extracellular Loops of Its Receptor. *J Biol Chem*, 291, 5172-84.
- DONG, M., LAM, P. C., PINON, D. I., HOSOHATA, K., ORRY, A., SEXTON, P. M., ABAGYAN, R. & MILLER, L. J. 2011. Molecular basis of secretin docking to its intact receptor using multiple photolabile probes distributed throughout the pharmacophore. *J Biol Chem*, 286, 23888-99.
- DORE, A. S., BORTOLATO, A., HOLLENSTEIN, K., CHENG, R. K. Y., READ, R. J. & MARSHALL, F. H. 2017. Decoding Corticotropin-Releasing Factor Receptor Type 1 Crystal Structures. *Curr Mol Pharmacol*, 10, 334-344.
- DOWNES, G. B. & GAUTAM, N. 1999. The G protein subunit gene families. *Genomics*, 62, 544-52.
- DROR, R. O., ARLOW, D. H., MARAGAKIS, P., MILDORF, T. J., PAN, A. C., XU, H., BORHANI, D. W. & SHAW, D. E. 2011. Activation mechanism of the β 2-adrenergic receptor. *Proc Natl Acad Sci U S A*, 108, 18684-9.
- DURHAM, P. L. 2006. Calcitonin gene-related peptide (CGRP) and migraine. *Headache*, 46 Suppl 1, S3-8.
- EHRENMANN, J., SCHÖPPE, J., KLENK, C., RAPPAS, M., KUMMER, L., DORÉ, A. S. & PLÜCKTHUN, A. 2018. High-resolution crystal structure of parathyroid hormone 1 receptor in complex with a peptide agonist. *Nature Structural & Molecular Biology*, 25, 1086-1092.
- EICHEL, K. & VON ZASTROW, M. 2018. Subcellular Organization of GPCR Signaling. *Trends Pharmacol Sci*, 39, 200-208.
- EMESON, R. B., HEDJIRAN, F., YEAKLEY, J. M., GUISE, J. W. & ROSENFELD, M. G. 1989. Alternative production of calcitonin and CGRP mRNA is regulated at the calcitonin-specific splice acceptor. *Nature*, 341, 76-80.
- ESSEN, L.-O., PERISIC, O., KATAN, M., WU, Y., ROBERTS, M. F. & WILLIAMS, R. L. 1997. Structural Mapping of the Catalytic Mechanism for a Mammalian Phosphoinositide-Specific Phospholipase C. *Biochemistry*, 36, 1704-1718.
- FEINSTEIN, T. N., YUI, N., WEBBER, M. J., WEHBI, V. L., STEVENSON, H. P., KING, J. D., JR., HALLOWS, K. R., BROWN, D., BOULEY, R. & VILARDAGA, J. P. 2013. Noncanonical control of vasopressin receptor type 2 signaling by retromer and arrestin. *J Biol Chem*, 288, 27849-60.
- FERRANDON, S., FEINSTEIN, T. N., CASTRO, M., WANG, B., BOULEY, R., POTTS, J. T., GARDELLA, T. J. & VILARDAGA, J. P. 2009. Sustained cyclic AMP production by parathyroid hormone receptor endocytosis. *Nat Chem Biol*, 5, 734-42.
- FERGUSON, S. S., DOWNEY, W. E., 3RD, COLAPIETRO, A. M., BARAK, L. S., MENARD, L. & CARON, M. G. 1996. Role of beta-arrestin in mediating agonist-promoted G protein-coupled receptor internalization. *Science*, 271, 363-6.
- FERGUSON, S. S., ZHANG, J., BARAK, L. S. & CARON, M. G. 1998. Molecular mechanisms of G protein-coupled receptor desensitization and resensitization. *Life Sci*, 62, 1561-5.
- FEYEN, J. H., CARDINAUX, F., GAMSE, R., BRUNS, C., AZRIA, M. & TRECHSEL, U. 1992. N-terminal truncation of salmon calcitonin leads to calcitonin antagonists. Structure activity relationship of N-terminally truncated salmon calcitonin fragments in vitro and in vivo. *Biochem Biophys Res Commun*, 187, 8-13.

- FEVE, M., SALIOU, J. M., ZENIOU, M., LENNON, S., CARAPITO, C., DONG, J., VAN DORSSELAER, A., JUNIER, M. P., CHNEIWEISS, H., CIANFERANI, S., HAIECH, J. & KILHOFFER, M. C. 2014. Comparative expression study of the endo-G protein coupled receptor (GPCR) repertoire in human glioblastoma cancer stem-like cells, U87-MG cells and non malignant cells of neural origin unveils new potential therapeutic targets. *PLoS One*, 9, e91519.
- FINDLAY, D. M., HOUSSAMI, S., CHRISTOPOULOS, G. & SEXTON, P. M. 1996. Homologous regulation of the rat C1a calcitonin receptor (CTR) in nonosteoclastic cells is independent of CTR messenger ribonucleic acid changes and cyclic adenosine 3',5'-monophosphate-dependent protein kinase activation. *Endocrinology*, 137, 4576-85.
- FINDLAY, D. M. & MARTIN, T. J. 1984. Relationship between internalization and calcitonin-induced receptor loss in T 47D cells. *Endocrinology*, 115, 78-83.
- FINDLAY, D. M., MICHELANGELI, V. P., MOSELEY, J. M. & MARTIN, T. J. 1981. Calcitonin binding and degradation by two cultured human breast cancer cell lines (MCF 7 and T 47D). *Biochem J*, 196, 513-20.
- FINDLAY, D. M., NG, K. W., NIALI, M. & MARTIN, T. J. 1982. Processing of calcitonin and epidermal growth factor after binding to receptors in human breast cancer cells (T 47D). *Biochem J*, 206, 343-50.
- FORCE, T., BONVENTRE, J. V., FLANNERY, M. R., GORN, A. H., YAMIN, M. & GOLDRING, S. R. 1992. A cloned porcine renal calcitonin receptor couples to adenylyl cyclase and phospholipase C. *Am J Physiol*, 262, F1110-5.
- FRANK, G. A., SHUKLA, S., RAO, P., BORGNIA, M. J., BARTESAGHI, A., MERK, A., MOBIN, A., ESSER, L., EARL, L. A., GOTTESMAN, M. M., XIA, D., AMBUDKAR, S. V. & SUBRAMANIAM, S. 2016. Cryo-EM Analysis of the Conformational Landscape of Human P-glycoprotein (ABCB1) During its Catalytic Cycle. *Mol Pharmacol*, 90, 35-41.
- FREDRIKSSON, R., LAGERSTROM, M. C., LUNDIN, L. G. & SCHIOTH, H. B. 2003. The G-protein-coupled receptors in the human genome form five main families. Phylogenetic analysis, paralogon groups, and fingerprints. *Mol Pharmacol*, 63, 1256-72.
- FRIEDMAN, J. & RAISZ, L. G. 1965. Thyrocalcitonin: inhibitor of bone resorption in tissue culture. *Science*, 150, 1465-7.
- FRIMURER, T. M. & BYWATER, R. P. 1999. Structure of the integral membrane domain of the GLP1 receptor. *Proteins*, 35, 375-86.
- FRITZE, O., FILIPEK, S., KUKSA, V., PALCZEWSKI, K., HOFMANN, K. P. & ERNST, O. P. 2003. Role of the conserved NPxxY(x)5,6F motif in the rhodopsin ground state and during activation. *Proc Natl Acad Sci U S A*, 100, 2290-5.
- FROMM, C., COSO, O. A., MONTANER, S., XU, N. & GUTKIND, J. S. 1997. The small GTP-binding protein Rho links G protein-coupled receptors and Galpha12 to the serum response element and to cellular transformation. *Proc Natl Acad Sci U S A*, 94, 10098-103.
- FUJIKAWA, Y., QUINN, J. M., SABOKBAR, A., MCGEE, J. O. & ATHANASOU, N. A. 1996a. The human osteoclast precursor circulates in the monocyte fraction. *Endocrinology*, 137, 4058-60.
- FUJIKAWA, Y., SABOKBAR, A., NEALE, S. & ATHANASOU, N. A. 1996. Human osteoclast formation and bone resorption by monocytes and synovial macrophages in rheumatoid arthritis. *Ann Rheum Dis*, 55, 816-22.
- FUJIOKA, S., SASAKAWA, O., KISHIMOTO, H., TSUMURA, K. & MORII, H. 1991. The antihypertensive effect of calcitonin gene-related peptide in rats with norepinephrine- and angiotensin II-induced hypertension. *J Hypertens*, 9, 175-9.
- FUKUHARA, S., CHIKUMI, H. & GUTKIND, J. S. 2001. RGS-containing RhoGEFs: the missing link between transforming G proteins and Rho? *Oncogene*, 20, 1661-8.

- FUNADA, M., SUZUKI, T., NARITA, M., MISAWA, M. & NAGASE, H. 1993. Modification of morphine-induced locomotor activity by pertussis toxin: Biochemical and behavioral studies in mice. *Brain Research*, 619, 163-172.
- FURNESS, S. G. B., CHRISTOPOULOS, A., SEXTON, P. M. & WOOTTEN, D. 2018. Differential engagement of polar networks in the glucagon-like peptide 1 receptor by endogenous variants of the glucagon-like peptide 1. *Biochemical Pharmacology*, 156, 223-240.
- FURNESS, S. G. B., LIANG, Y. L., NOWELL, C. J., HALLS, M. L., WOOKEY, P. J., DAL MASO, E., INOUE, A., CHRISTOPOULOS, A., WOOTTEN, D. & SEXTON, P. M. 2016. Ligand-Dependent Modulation of G Protein Conformation Alters Drug Efficacy. *Cell*, 167, 739-749.e11.
- GALANTE, L., HORTON, R., JOPLIN, G. F., WOODHOUSE, N. J. & MACINTYRE, I. 1971. Comparison of human, porcine and salmon synthetic calcitonins in man and in the rat. *Clin Sci*, 40, 9p-10p.
- GAO, H., SUN, Y., WU, Y., LUAN, B., WANG, Y., QU, B. & PEI, G. 2004. Identification of beta-arrestin2 as a G protein-coupled receptor-stimulated regulator of NF-kappaB pathways. *Mol Cell*, 14, 303-17.
- GAUTAM, N., DOWNES, G. B., YAN, K. & KISSELEV, O. 1998. The G-protein betagamma complex. *Cell Signal*, 10, 447-55.
- GELLING, R. W., WHEELER, M. B., XUE, J., GYOMOREY, S., NIAN, C., PEDERSON, R. A. & MCINTOSH, C. H. 1997. Localization of the domains involved in ligand binding and activation of the glucose-dependent insulinotropic polypeptide receptor. *Endocrinology*, 138, 2640-3.
- GENG, Y., BUSH, M., MOSYAK, L., WANG, F. & FAN, Q. R. 2013. Structural mechanism of ligand activation in human GABA(B) receptor. *Nature*, 504, 254-9.
- GENG, Y., MOSYAK, L., KURINOV, I., ZUO, H., STURCHLER, E., CHENG, T. C., SUBRAMANYAM, P., BROWN, A. P., BRENNAN, S. C., MUN, H. C., BUSH, M., CHEN, Y., NGUYEN, T. X., CAO, B., CHANG, D. D., QUICK, M., CONIGRAVE, A. D., COLECRAFT, H. M., MCDONALD, P. & FAN, Q. R. 2016. Structural mechanism of ligand activation in human calcium-sensing receptor. *Elife*, 5.
- GEORGE, S. R., O'DOWD, B. F. & LEE, S. P. 2002. G-protein-coupled receptor oligomerization and its potential for drug discovery. *Nat Rev Drug Discov*, 1, 808-20.
- GESTY-PALMER, D., FLANNERY, P., YUAN, L., CORSINO, L., SPURNEY, R., LEFKOWITZ, R. J. & LUTTRELL, L. M. 2009. A beta-arrestin-biased agonist of the parathyroid hormone receptor (PTH1R) promotes bone formation independent of G protein activation. *Sci Transl Med*, 1, 1ra1.
- GILABERT-ORIOL, R., FURNESS, S. G. B., STRINGER, B. W., WENG, A., FUCHS, H., DAY, B. W., KOURAKIS, A., BOYD, A. W., HARE, D. L., THAKUR, M., JOHNS, T. G. & WOOKEY, P. J. 2017. Dianthin-30 or gelonin versus monomethyl auristatin E, each configured with an anti-calcitonin receptor antibody, are differentially potent in vitro in high-grade glioma cell lines derived from glioblastoma. *Cancer Immunol Immunother*, 66, 1217-1228.
- GKOUNTELIS, K., TSELIOS, T., VENIHAKI, M., DERAOS, G., LAZARIDIS, I., RASSOULI, O., GRAVANIS, A. & LIAPAKIS, G. 2009. Alanine scanning mutagenesis of the second extracellular loop of type 1 corticotropin-releasing factor receptor revealed residues critical for peptide binding. *Mol Pharmacol*, 75, 793-800.
- GOEL, R., PHILLIPS-MASON, P. J., GARDNER, A., RABEN, D. M. & BALDASSARE, J. J. 2004. Alpha-thrombin-mediated phosphatidylinositol 3-kinase activation through release of Gbetagamma dimers from Galphaq and Galphai2. *J Biol Chem*, 279, 6701-10.

- GOLDRING, S. R., DAYER, J.-M., AUSIELLO, D. A. & KRANE, S. M. 1978. A cell strain cultured from porcine kidney increases cyclic AMP content upon exposure to calcitonin or vasopressin. *Biochemical and Biophysical Research Communications*, 83, 434-440.
- GOLDSMITH, Z. G. & DHANASEKARAN, D. N. 2007. G protein regulation of MAPK networks. *Oncogene*, 26, 3122-42.
- GOODMAN, O. B., JR., KRUPNICK, J. G., SANTINI, F., GUREVICH, V. V., PENN, R. B., GAGNON, A. W., KEEN, J. H. & BENOVIĆ, J. L. 1996. Beta-arrestin acts as a clathrin adaptor in endocytosis of the beta2-adrenergic receptor. *Nature*, 383, 447-50.
- GORN, A. H., LIN, H. Y., YAMIN, M., AURON, P. E., FLANNERY, M. R., TAPP, D. R., MANNING, C. A., LODISH, H. F., KRANE, S. M. & GOLDRING, S. R. 1992. Cloning, characterization, and expression of a human calcitonin receptor from an ovarian carcinoma cell line. *J Clin Invest*, 90, 1726-35.
- GOSNEY, J. R., SISSONS, M. C. & O'MALLEY, J. A. 1985. Quantitative study of endocrine cells immunoreactive for calcitonin in the normal adult human lung. *Thorax*, 40, 866-9.
- GUIDOBONO, F., BETTICA, P., VILLA, I., PAGANI, F., NETTI, C., SIBILIA, V. & PECILE, A. 1991a. Treatment with pertussis toxin does not prevent central effects of eel calcitonin. *Peptides*, 12, 549-53.
- GUIDOBONO, F., NETTI, C., VILLANI, P., BETTICA, P. & PECILE, A. 1991b. Antinociceptive activity of eel calcitonin, injected into the inflamed paw in rats. *Neuropharmacology*, 30, 1275-8.
- HAAS, H. G., DAMBACHER, M. A., GUNCAGA, J. & LAUFFENBRUGER, T. 1971. Renal effects of calcitonin and parathyroid extract in man. Studies in hypoparathyroidism. *J Clin Invest*, 50, 2689-702.
- HALLBRINK, M., HOLMQVIST, T., OLSSON, M., OSTENSON, C. G., EFENDIC, S. & LANGEL, U. 2001. Different domains in the third intracellular loop of the GLP-1 receptor are responsible for Galpha(s) and Galpha(i)/Galpha(o) activation. *Biochim Biophys Acta*, 1546, 79-86.
- HAMANN, J., AUST, G., ARAÇ, D., ENGEL, F. B., FORMSTONE, C., FREDRIKSSON, R., HALL, R. A., HARTY, B. L., KIRCHHOFF, C., KNAPP, B., KRISHNAN, A., LIEBSCHER, I., LIN, H. H., MARTINELLI, D. C., MONK, K. R., PEETERS, M. C., PIAO, X., PRÖMEL, S., SCHÖNEBERG, T., SCHWARTZ, T. W., SINGER, K., STACEY, M., USHKARYOV, Y. A., VALLON, M., WOLFRUM, U., WRIGHT, M. W., XU, L., LANGENHAN, T. & SCHIÖTH, H. B. 2015. International Union of Basic and Clinical Pharmacology. XCIV. Adhesion G protein-coupled receptors. *Pharmacol Rev*, 67, 338-67.
- HAMM, H. E. 2001. How activated receptors couple to G proteins. *Proc Natl Acad Sci U S A*, 98, 4819-21.
- HARDY, A. R., CONLEY, P. B., LUO, J., BENOVIĆ, J. L., POOLE, A. W. & MUNDELL, S. J. 2005. P2Y1 and P2Y12 receptors for ADP desensitize by distinct kinase-dependent mechanisms. *Blood*, 105, 3552-60.
- HART, M. J., JIANG, X., KOZASA, T., ROSCOE, W., SINGER, W. D., GILMAN, A. G., STERNWEIS, P. C. & BOLLAG, G. 1998. Direct Stimulation of the Guanine Nucleotide Exchange Activity of p115 RhoGEF by Gα₁₃. *Science*, 280, 2112.
- HAUSDORFF, W. P., CAMPBELL, P. T., OSTROWSKI, J., YU, S. S., CARON, M. G. & LEFKOWITZ, R. J. 1991. A small region of the beta-adrenergic receptor is selectively involved in its rapid regulation. *Proc Natl Acad Sci U S A*, 88, 2979-83.
- HAUSDORFF, W. P., CARON, M. G. & LEFKOWITZ, R. J. 1990. Turning off the signal: desensitization of beta-adrenergic receptor function. *The FASEB Journal*, 4, 2881-2889.
- HAY, D. L., GARELJA, M. L., POYNER, D. R. & WALKER, C. S. 2018. Update on the pharmacology of calcitonin/CGRP family of peptides: IUPHAR Review 25. *Br J Pharmacol*, 175, 3-17.

- HAY, D. L. & WALKER, C. S. 2017. CGRP and its receptors. *Headache*, 57, 625-636.
- HAY, D., WALKER, C., J GINGELL, J., LADDS, G., REYNOLDS, C. & POYNER, D. 2016. *Receptor activity-modifying proteins: Multifunctional G protein-coupled receptor accessory proteins*.
- HAY, D. L., WALKER, C. S. & POYNER, D. R. 2011. Adrenomedullin and calcitonin gene-related peptide receptors in endocrine-related cancers: opportunities and challenges. *Endocr Relat Cancer*, 18, C1-14.
- HE, R., BROWNING, D. D. & YE, R. D. 2001. Differential Roles of the NPXXY Motif in Formyl Peptide Receptor Signaling. *The Journal of Immunology*, 166, 4099.
- HENKE, H., TOBLER, P. H. & FISCHER, J. A. 1983. Localization of salmon calcitonin binding sites in rat brain by autoradiography. *Brain Res*, 272, 373-7.
- HILTON, J. M., DOWTON, M., HOUSSAMI, S. & SEXTON, P. M. 2000. Identification of key components in the irreversibility of salmon calcitonin binding to calcitonin receptors. *J Endocrinol*, 166, 213-26.
- HILTON, J. M., CHAI, S. Y. & SEXTON, P. M. 1995. In vitro autoradiographic localization of the calcitonin receptor isoforms, C1a and C1b, in rat brain. *Neuroscience*, 69, 1223-37.
- HINSON, J. P., KAPAS, S. & SMITH, D. M. 2000. Adrenomedullin, a multifunctional regulatory peptide. *Endocr Rev*, 21, 138-67.
- HIRSCH, P. F. & MUNSON, P. L. 1969. Thyrocalcitonin. *Physiol Rev*, 49, 548-622.
- HO, H. H., GILBERT, M. T., NUSSENZVEIG, D. R. & GERSHENGORN, M. C. 1999. Glycosylation is important for binding to human calcitonin receptors. *Biochemistry*, 38, 1866-72.
- HOFF, A. O., CATALA-LEHNEN, P., THOMAS, P. M., PRIEMEL, M., RUEGER, J. M., NASONKIN, I., BRADLEY, A., HUGHES, M. R., ORDONEZ, N., COTE, G. J., AMLING, M. & GAGEL, R. F. 2002. Increased bone mass is an unexpected phenotype associated with deletion of the calcitonin gene. *J Clin Invest*, 110, 1849-57.
- HOLLENSTEIN, K., DE GRAAF, C., BORTOLATO, A., WANG, M. W., MARSHALL, F. H. & STEVENS, R. C. 2014. Insights into the structure of class B GPCRs. *Trends Pharmacol Sci*, 35, 12-22.
- HOLLENSTEIN, K., KEAN, J., BORTOLATO, A., CHENG, R. K., DORE, A. S., JAZAYERI, A., COOKE, R. M., WEIR, M. & MARSHALL, F. H. 2013. Structure of class B GPCR corticotropin-releasing factor receptor 1. *Nature*, 499, 438-43.
- HOLTMANN, M. H., HADAC, E. M. & MILLER, L. J. 1995. Critical contributions of amino-terminal extracellular domains in agonist binding and activation of secretin and vasoactive intestinal polypeptide receptors. Studies of chimeric receptors. *J Biol Chem*, 270, 14394-8.
- HOLZMANN, B. 2013. Antiinflammatory activities of CGRP modulating innate immune responses in health and disease. *Curr Protein Pept Sci*, 14, 268-74.
- HOUSSAMI, S., FINDLAY, D. M., BRADY, C. L., MYERS, D. E., MARTIN, T. J. & SEXTON, P. M. 1994. Isoforms of the rat calcitonin receptor: consequences for ligand binding and signal transduction. *Endocrinology*, 135, 183-90.
- HSIEH, J. C., RATTNER, A., SMALLWOOD, P. M. & NATHANS, J. 1999. Biochemical characterization of Wnt-frizzled interactions using a soluble, biologically active vertebrate Wnt protein. *Proc Natl Acad Sci U S A*, 96, 3546-51.
- HUANG, P., ZHENG, S., WIERBOWSKI, B. M., KIM, Y., NEDELCO, D., ARAVENA, L., LIU, J., KRUSE, A. C. & SALIC, A. 2018. Structural Basis of Smoothed Activation in Hedgehog Signaling. *Cell*, 175, 295-297.
- HUYNH, J., THOMAS, W. G., AGUILAR, M.-I. & PATTENDEN, L. K. 2009. Role of helix 8 in G protein-coupled receptors based on structure-function studies on the type 1 angiotensin receptor. *Molecular and Cellular Endocrinology*, 302, 118-127.

- IKEGAME, M., EJIRI, S. & OZAWA, H. 1994. Histochemical and autoradiographic studies on calcitonin internalization and intracellular movement in osteoclasts. *J Bone Miner Res*, 9, 25-37.
- ISHIKAWA, T., OKAMURA, N., SAITO, A., MASAKI, T. & GOTO, K. 1988. Positive inotropic effect of calcitonin gene-related peptide mediated by cyclic AMP in guinea pig heart. *Circ Res*, 63, 726-34.
- ITOH, N., OBATA, K., YANAIHARA, N. & OKAMOTO, H. 1983. Human preprovasoactive intestinal polypeptide contains a novel PHI-27-like peptide, PHM-27. *Nature*, 304, 547-9.
- IWASAKI, Y., IWASAKI, J. & FREAKER, H. C. 1983. Growth inhibition of human breast cancer cells induced by calcitonin. *Biochemical and Biophysical Research Communications*, 110, 235-242.
- GINGELL, J., SIMMS, J., BARWELL, J., POYNER, D. R., WATKINS, H. A., PIOSZAK, A. A., SEXTON, P. M. & HAY, D. L. 2016. An allosteric role for receptor activity-modifying proteins in defining GPCR pharmacology. *Cell Discovery*, 2, 16012.
- JAEGGER, P., JONES, W., CLEMENS, T. L. & HAYSLETT, J. P. 1986. Evidence that calcitonin stimulates 1,25-dihydroxyvitamin D production and intestinal absorption of calcium in vivo. *J Clin Invest*, 78, 456-61.
- JENSEN, D. D., LIEU, T., HALLS, M. L., VELDHUIS, N. A., IMLACH, W. L., MAI, Q. N., POOLE, D. P., QUACH, T., AURELIO, L., CONNER, J., HERENBRINK, C. K., BARLOW, N., SIMPSON, J. S., SCANLON, M. J., GRAHAM, B., MCCLUSKEY, A., ROBINSON, P. J., ESCRIOU, V., NASSINI, R., MATERAZZI, S., GEPPETTI, P., HICKS, G. A., CHRISTIE, M. J., PORTER, C. J. H., CANALS, M. & BUNNETT, N. W. 2017. Neurokinin 1 receptor signaling in endosomes mediates sustained nociception and is a viable therapeutic target for prolonged pain relief. *Sci Transl Med*, 9.
- JESCHKE, G. 2012. DEER distance measurements on proteins. *Annu Rev Phys Chem*, 63, 419-46.
- JIMENO, A., GARCIA-VELASCO, A., DEL VAL, O., GONZALEZ-BILLALABEITIA, E., HERNANDO, S., HERNANDEZ, R., SANCHEZ-MUNOZ, A., LOPEZ-MARTIN, A., DURAN, I., ROBLES, L., CORTES-FUNES, H. & PAZ-ARES, L. 2004. Assessment of procalcitonin as a diagnostic and prognostic marker in patients with solid tumors and febrile neutropenia. *Cancer*, 100, 2462-9.
- JOHANSSON, E., HANSEN, J. L., HANSEN, A. M., SHAW, A. C., BECKER, P., SCHÄFFER, L. & REEDTZ-RUNGE, S. Type II Turn of Receptor-bound Salmon Calcitonin Revealed by X-ray Crystallography.
- JOHANSSON, E., HANSEN, J. L., HANSEN, A. M. K., SHAW, A. C., BECKER, P., SCHÄFFER, L. & REEDTZ-RUNGE, S. 2016. Type II Turn of Receptor-bound Salmon Calcitonin Revealed by X-ray Crystallography. *The Journal of biological chemistry*, 291, 13689-13698.
- JONG, Y. I., HARMON, S. K. & O'MALLEY, K. L. 2018. GPCR signalling from within the cell. *Br J Pharmacol*, 175, 4026-4035.
- JOHNSON, R. L., SAXE, C. L., 3RD, GOLLOP, R., KIMMEL, A. R. & DEVREOTES, P. N. 1993. Identification and targeted gene disruption of cAR3, a cAMP receptor subtype expressed during multicellular stages of Dictyostelium development. *Genes Dev*, 7, 273-82.
- JOYCE, C. D., FISCUS, R. R., WANG, X., DRIES, D. J., MORRIS, R. C. & PRINZ, R. A. 1990. Calcitonin gene-related peptide levels are elevated in patients with sepsis. *Surgery*, 108, 1097-101.
- KANG, J., SHI, Y., XIANG, B., QU, B., SU, W., ZHU, M., ZHANG, M., BAO, G., WANG, F., ZHANG, X., YANG, R., FAN, F., CHEN, X., PEI, G. & MA, L. 2005. A nuclear function of beta-

- arrestin1 in GPCR signaling: regulation of histone acetylation and gene transcription. *Cell*, 123, 833-47.
- KANIS, J. A. & MCCLOSKEY, E. V. 1999. Effect of calcitonin on vertebral and other fractures. *QJM: An International Journal of Medicine*, 92, 143-150.
- KATAFUCHI, T., YASUE, H., OSAKI, T. & MINAMINO, N. 2009. Calcitonin receptor-stimulating peptide: Its evolutionary and functional relationship with calcitonin/calcitonin gene-related peptide based on gene structure. *Peptides*, 30, 1753-62.
- KATRITCH, V., CHEREZOV, V. & STEVENS, R. C. 2013. Structure-function of the G protein-coupled receptor superfamily. *Annu Rev Pharmacol Toxicol*, 53, 531-56.
- KAWASAKI, H., SAITO, A. & TAKASAKI, K. 1990. Age-related decrease of calcitonin gene-related peptide-containing vasodilator innervation in the mesenteric resistance vessel of the spontaneously hypertensive rat. *Circ Res*, 67, 733-43.
- KELLER, J., CATALA-LEHNEN, P., HUEBNER, A. K., JESCHKE, A., HECKT, T., LUETH, A., KRAUSE, M., KOEHNE, T., ALBERS, J., SCHULZE, J., SCHILLING, S., HABERLAND, M., DENNINGER, H., NEVEN, M., HERMANS-BORGMAYER, I., STREICHERT, T., BREER, S., BARVENCIK, F., LEVKAU, B., RATHKOLB, B., WOLF, E., CALZADA-WACK, J., NEFF, F., GAILUS-DURNER, V., FUCHS, H., DE ANGELIS, M. H., KLUTMANN, S., TSOURDI, E., HOFBAUER, L. C., KLEUSER, B., CHUN, J., SCHINKE, T. & AMLING, M. 2014. Calcitonin controls bone formation by inhibiting the release of sphingosine 1-phosphate from osteoclasts. *Nat Commun*, 5, 5215.
- KELLEY, G. G., REKS, S. E. & SMRCKA, A. V. 2004. Hormonal regulation of phospholipase Cepsilon through distinct and overlapping pathways involving G12 and Ras family G-proteins. *Biochem J*, 378, 129-39.
- KELLY, E., BAILEY, C. P. & HENDERSON, G. 2008. Agonist-selective mechanisms of GPCR desensitization. *Br J Pharmacol*, 153 Suppl 1, S379-88.
- KENAKIN, T. 2002. Efficacy at G-protein-coupled receptors. *Nat Rev Drug Discov*, 1, 103-10.
- KENAKIN, T. 2011. Functional selectivity and biased receptor signaling. *J Pharmacol Exp Ther*, 336, 296-302.
- KENAKIN, T. & CHRISTOPOULOS, A. 2013. Signalling bias in new drug discovery: detection, quantification and therapeutic impact. *Nat Rev Drug Discov*, 12, 205-16.
- KENAKIN, T. & MILLER, L. J. 2010. Seven transmembrane receptors as shapeshifting proteins: the impact of allosteric modulation and functional selectivity on new drug discovery. *Pharmacol Rev*, 62, 265-304.
- KENAKIN, T., WATSON, C., MUNIZ-MEDINA, V., CHRISTOPOULOS, A. & NOVICK, S. 2012. A simple method for quantifying functional selectivity and agonist bias. *ACS Chem Neurosci*, 3, 193-203.
- KEUTMANN, H. T., PARSONS, J. A., POTTS, J. T., JR. & SCHLUETER, R. J. 1970. Isolation and chemical properties of two calcitonins from salmon ultimobranchial glands. *J Biol Chem*, 245, 1491-6.
- KITAMURA, K., KANGAWA, K. & ETO, T. 2002. Adrenomedullin and PAMP: discovery, structures, and cardiovascular functions. *Microsc Res Tech*, 57, 3-13.
- KITAMURA, K., KANGAWA, K., KAWAMOTO, M., ICHIKI, Y., NAKAMURA, S., MATSUO, H. & ETO, T. 1993. Adrenomedullin: a novel hypotensive peptide isolated from human pheochromocytoma. *Biochem Biophys Res Commun*, 192, 553-60.
- KLEIHUES, P. & OHGAKI, H. 1999. Primary and secondary glioblastomas: from concept to clinical diagnosis. *Neuro Oncol*, 1, 44-51.
- KLEIN, P. S., SUN, T. J., SAXE, C. L., 3RD, KIMMEL, A. R., JOHNSON, R. L. & DEVREOTES, P. N. 1988. A chemoattractant receptor controls development in Dictyostelium discoideum. *Science*, 241, 1467-72.

- KLEPPINGER, E. L. & VIVIAN, E. M. 2003. Pramlintide for the treatment of diabetes mellitus. *Ann Pharmacother*, 37, 1082-9.
- KNIAZEFF, J., PREZEAU, L., RONDARD, P., PIN, J. P. & GOUDET, C. 2011. Dimers and beyond: The functional puzzles of class C GPCRs. *Pharmacol Ther*, 130, 9-25.
- KOOLE, C., WOOTTEN, D., SIMMS, J., MILLER, L. J., CHRISTOPOULOS, A. & SEXTON, P. M. 2012a. Second extracellular loop of human glucagon-like peptide-1 receptor (GLP-1R) has a critical role in GLP-1 peptide binding and receptor activation. *J Biol Chem*, 287, 3642-58.
- KOOLE, C., WOOTTEN, D., SIMMS, J., SAVAGE, E. E., MILLER, L. J., CHRISTOPOULOS, A. & SEXTON, P. M. 2012b. Second extracellular loop of human glucagon-like peptide-1 receptor (GLP-1R) differentially regulates orthosteric but not allosteric agonist binding and function. *J Biol Chem*, 287, 3659-73.
- KOZASA, T., JIANG, X., HART, M. J., STERNWEIS, P. M., SINGER, W. D., GILMAN, A. G., BOLLAG, G. & STERNWEIS, P. C. 1998. p115 RhoGEF, a GTPase activating protein for G α 12 and G α 13. *Science*, 280, 2109-11.
- KRUGER, D. F. & GLOSTER, M. A. 2004. Pramlintide for the treatment of insulin-requiring diabetes mellitus: rationale and review of clinical data. *Drugs*, 64, 1419-32.
- KUESTNER, R. E., ELROD, R. D., GRANT, F. J., HAGEN, F. S., KUIJPER, J. L., MATTHEWES, S. L., O'HARA, P. J., SHEPPARD, P. O., STROOP, S. D., THOMPSON, D. L. & ET AL. 1994. Cloning and characterization of an abundant subtype of the human calcitonin receptor. *Mol Pharmacol*, 46, 246-55.
- LACROIX, M., SIWEK, B. & BODY, J. J. 1998. Breast cancer cell response to calcitonin: modulation by growth-regulating agents. *Eur J Pharmacol*, 344, 279-86.
- LAGERSTROM, M. C. & SCHIOTH, H. B. 2008. Structural diversity of G protein-coupled receptors and significance for drug discovery. *Nat Rev Drug Discov*, 7, 339-57.
- LAPORTE, S. A., OAKLEY, R. H., ZHANG, J., HOLT, J. A., FERGUSON, S. S., CARON, M. G. & BARAK, L. S. 1999. The beta2-adrenergic receptor/betaarrestin complex recruits the clathrin adaptor AP-2 during endocytosis. *Proc Natl Acad Sci U S A*, 96, 3712-7.
- LARJAVAARA, S., MANTYLA, R., SALMINEN, T., HAAPASALO, H., RAITANEN, J., JAASKELAINEN, J. & AUVINEN, A. 2007. Incidence of gliomas by anatomic location. *Neuro Oncol*, 9, 319-25.
- LEE, S.-M., BOOE, J. M., GINGELL, J. J., SJOELUND, V., HAY, D. L. & PIOSZAK, A. A. 2017. N-Glycosylation of Asparagine 130 in the Extracellular Domain of the Human Calcitonin Receptor Significantly Increases Peptide Hormone Affinity. *Biochemistry*, 56, 3380-3393.
- LEENDERS, A. G. & SHENG, Z. H. 2005. Modulation of neurotransmitter release by the second messenger-activated protein kinases: implications for presynaptic plasticity. *Pharmacol Ther*, 105, 69-84.
- LEFKOWITZ, R. J. 1993. G protein-coupled receptor kinases. *Cell*, 74, 409-12.
- LEFKOWITZ, R. J. 1998. G protein-coupled receptors. III. New roles for receptor kinases and beta-arrestins in receptor signaling and desensitization. *J Biol Chem*, 273, 18677-80.
- LEI, S., CLYDESDALE, L., DAI, A., CAI, X., FENG, Y., YANG, D., LIANG, Y. L., KOOLE, C., ZHAO, P., COUDRAT, T., CHRISTOPOULOS, A., WANG, M. W., WOOTTEN, D. & SEXTON, P. M. 2018. Two distinct domains of the glucagon-like peptide-1 receptor control peptide-mediated biased agonism. *J Biol Chem*, 293, 9370-9387.
- LERNER, U. H. 2006. Deletions of genes encoding calcitonin/alpha-CGRP, amylin and calcitonin receptor have given new and unexpected insights into the function of calcitonin receptors and calcitonin receptor-like receptors in bone. *J Musculoskelet Neuronal Interact*, 6, 87-95.
- LEUTHAUSER, K., GUJER, R., ALDECOA, A., MCKINNEY, R. A., MUFF, R., FISCHER, J. A. & BORN, W. 2000. Receptor-activity-modifying protein 1 forms heterodimers with

- two G-protein-coupled receptors to define ligand recognition. *Biochem J*, 351 Pt 2, 347-51.
- LIANG, Y.-L., KHOSHOU EI, M., RADJAINIA, M., ZHANG, Y., GLUKHOVA, A., TARRASCH, J., THAL, D. M., FURNESS, S. G. B., CHRISTOPOULOS, G., COUDRAT, T., DANEV, R., BAUMEISTER, W., MILLER, L. J., CHRISTOPOULOS, A., KOBILKA, B. K., WOOTTEN, D., SKINIOTIS, G. & SEXTON, P. M. 2017. Phase-plate cryo-EM structure of a class B GPCR-G-protein complex. *Nature*, 546, 118-123.
- LIANG, Y. L., KHOSHOU EI, M., DEGANUTTI, G., GLUKHOVA, A., KOOLE, C., PEAT, T. S., RADJAINIA, M., PLITZKO, J. M., BAUMEISTER, W., MILLER, L. J., HAY, D. L., CHRISTOPOULOS, A., REYNOLDS, C. A., WOOTTEN, D. & SEXTON, P. M. 2018a. Cryo-EM structure of the active, Gs-protein complexed, human CGRP receptor. *Nature*, 561, 492-497.
- LIANG, Y. L., KHOSHOU EI, M., GLUKHOVA, A., FURNESS, S. G. B., ZHAO, P., CLYDESDALE, L., KOOLE, C., TRUONG, T. T., THAL, D. M., LEI, S., RADJAINIA, M., DANEV, R., BAUMEISTER, W., WANG, M. W., MILLER, L. J., CHRISTOPOULOS, A., SEXTON, P. M. & WOOTTEN, D. 2018b. Phase-plate cryo-EM structure of a biased agonist-bound human GLP-1 receptor-Gs complex. *Nature*, 555, 121-125.
- LOPEZ, J. & MARTINEZ, A. 2002. Cell and molecular biology of the multifunctional peptide, adrenomedullin. *Int Rev Cytol*, 221, 1-92.
- LOHSE, M. J., HEIN, P., HOFFMANN, C., NIKOLAEV, V. O., VILARDAGA, J. P. & BUNEMANN, M. 2008. Kinetics of G-protein-coupled receptor signals in intact cells. *Br J Pharmacol*, 153 Suppl 1, S125-32.
- LOHSE, M. J., NUBER, S. & HOFFMANN, C. 2012. Fluorescence/bioluminescence resonance energy transfer techniques to study G-protein-coupled receptor activation and signaling. *Pharmacol Rev*, 64, 299-336.
- LOUIS, D. N., OHGAKI, H., WIESTLER, O. D., CAVENEE, W. K., BURGER, P. C., JOUVET, A., SCHEITHAUER, B. W. & KLEIHUES, P. 2007. The 2007 WHO classification of tumours of the central nervous system. *Acta Neuropathol*, 114, 97-109.
- LU, Y., WU, J., DONG, Y., CHEN, S., SUN, S., MA, Y. B., OUYANG, Q., FINLEY, D., KIRSCHNER, M. W. & MAO, Y. 2017. Conformational Landscape of the p28-Bound Human Proteasome Regulatory Particle. *Mol Cell*, 67, 322-333.e6.
- LUAN, B., ZHANG, Z., WU, Y., KANG, J. & PEI, G. 2005. Beta-arrestin2 functions as a phosphorylation-regulated suppressor of UV-induced NF-kappaB activation. *Embo j*, 24, 4237-46.
- LUCHETTI, G., SIRCAR, R., KONG, J. H., NACHTERGAELE, S., SAGNER, A., BYRNE, E. F., COVEY, D. F., SIEBOLD, C. & ROHATGI, R. 2016. Cholesterol activates the G-protein coupled receptor Smoothed to promote Hedgehog signaling. *Elife*, 5.
- LUPULESCU, A. & HABOWSKY, J. 1978. Effects of calcitonin on wound healing: a morphological study in rabbits. *J Surg Res*, 25, 260-8.
- LUTTRELL, L. M., DAAKA, Y., DELLA ROCCA, G. J. & LEFKOWITZ, R. J. 1997. G protein-coupled receptors mediate two functionally distinct pathways of tyrosine phosphorylation in rat 1a fibroblasts. Shc phosphorylation and receptor endocytosis correlate with activation of Erk kinases. *J Biol Chem*, 272, 31648-56.
- LUTTRELL, L. M. & LEFKOWITZ, R. J. 2002. The role of beta-arrestins in the termination and transduction of G-protein-coupled receptor signals. *J Cell Sci*, 115, 455-65.
- LUTTRELL, L. M., ROUDABUSH, F. L., CHOY, E. W., MILLER, W. E., FIELD, M. E., PIERCE, K. L. & LEFKOWITZ, R. J. 2001. Activation and targeting of extracellular signal-regulated kinases by beta-arrestin scaffolds. *Proc Natl Acad Sci U S A*, 98, 2449-54.
- MA, J. N., CURRIER, E. A., ESSEX, A., FEDDOCK, M., SPALDING, T. A., NASH, N. R., BRANN, M. R. & BURSTEIN, E. S. 2004. Discovery of novel peptide/receptor interactions:

- identification of PHM-27 as a potent agonist of the human calcitonin receptor. *Biochem Pharmacol*, 67, 1279-84.
- MAGALHAES, A. C., DUNN, H. & FERGUSON, S. S. 2012. Regulation of GPCR activity, trafficking and localization by GPCR-interacting proteins. *Br J Pharmacol*, 165, 1717-1736.
- MANGLIK, A., KIM, T. H., MASUREEL, M., ALTENBACH, C., YANG, Z., HILGER, D., LERCH, M. T., KOBILKA, T. S., THIAN, F. S., HUBBELL, W. L., PROSSER, R. S. & KOBILKA, B. K. 2015. Structural Insights into the Dynamic Process of β 2-Adrenergic Receptor Signaling. *Cell*, 161, 1101-1111.
- MARINISSEN, M. J. & GUTKIND, J. S. 2001. G-protein-coupled receptors and signaling networks: emerging paradigms. *Trends Pharmacol Sci*, 22, 368-76.
- MARSH, L. & HERSKOWITZ, I. 1988. STE2 protein of *Saccharomyces kluyveri* is a member of the rhodopsin/beta-adrenergic receptor family and is responsible for recognition of the peptide ligand alpha factor. *Proc Natl Acad Sci U S A*, 85, 3855-9.
- MARTIN, T. J., FINDLAY, D. M., MACINTYRE, I., EISMAN, J. A., MICHELANGELI, V. P., MOSELEY, J. M. & PARTRIDGE, N. C. 1980. Calcitonin receptors in a cloned human breast cancer cell line (MCF 7). *Biochemical and Biophysical Research Communications*, 96, 150-156.
- MARY, S., DAMIAN, M., LOUET, M., FLOQUET, N., FEHRENTZ, J. A., MARIE, J., MARTINEZ, J. & BANÈRES, J. L. 2012. Ligands and signaling proteins govern the conformational landscape explored by a G protein-coupled receptor. *Proc Natl Acad Sci U S A*, 109, 8304-9.
- MARY, S., FEHRENTZ, J. A., DAMIAN, M., VERDIE, P., MARTINEZ, J., MARIE, J. & BANERES, J. L. 2013. How ligands and signalling proteins affect G-protein-coupled receptors' conformational landscape. *Biochem Soc Trans*, 41, 144-7.
- MASI, L., BECHERINI, L., GENNARI, L., COLLI, E., MANSANI, R., FALCHETTI, A., CEPOLLARO, C., GONNELLI, S., TANINI, A. & BRANDI, M. L. 1998. Allelic Variants of Human Calcitonin Receptor: Distribution and Association with Bone Mass in Postmenopausal Italian Women. *Biochemical and Biophysical Research Communications*, 245, 622-626.
- MAYO, K. E., MILLER, L. J., BATAILLE, D., DALLE, S., GÖKE, B., THORENS, B. & DRUCKER, D. J. 2003. International Union of Pharmacology. XXXV. The Glucagon Receptor Family. *Pharmacological Reviews*, 55, 167.
- MCLATCHIE, L. M., FRASER, N. J., MAIN, M. J., WISE, A., BROWN, J., THOMPSON, N., SOLARI, R., LEE, M. G. & FOORD, S. M. 1998. RAMPs regulate the transport and ligand specificity of the calcitonin-receptor-like receptor. *Nature*, 393, 333-9.
- MEADOWS, R. P., NIKONOWICZ, E. P., JONES, C. R., BASTIAN, J. W. & GORENSTEIN, D. G. 1991. Two-dimensional NMR and structure determination of salmon calcitonin in methanol. *Biochemistry*, 30, 1247-54.
- METELLUS, P., VOUTSINOS-PORCHE, B., NANNI-METELLUS, I., COLIN, C., FINA, F., BERENGUER, C., DUSSAULT, N., BOUDOURESQUE, F., LOUNDOU, A., INTAGLIATA, D., CHINOT, O., MARTIN, P. M., FIGARELLA-BRANGER, D. & OUAFIK, L. 2011. Adrenomedullin expression and regulation in human glioblastoma, cultured human glioblastoma cell lines and pilocytic astrocytoma. *Eur J Cancer*, 47, 1727-35.
- MIAO, Y., NICHOLS, S. E., GASPER, P. M., METZGER, V. T. & MCCAMMON, J. A. 2013. Activation and dynamic network of the M2 muscarinic receptor. *Proc Natl Acad Sci U S A*, 110, 10982-7.
- MICHELANGELI, V. P., FINDLAY, D. M., MOSELEY, J. M. & MARTIN, T. J. 1983. Mechanisms of calcitonin induction of prolonged activation of adenylate cyclase in human cancer cells. *J Cyclic Nucleotide Protein Phosphor Res*, 9, 129-41.

- MILLER, J.L., CHEN, Q., C-H LAM, P., I PINON, D., SEXTON, P., ABAGYAN, R. & DONG, M. 2011. *Refinement of Glucagon-like Peptide 1 Docking to Its Intact Receptor Using Mid-region Photolabile Probes and Molecular Modeling.*
- MILLIGAN, G. & KOSTENIS, E. 2006. Heterotrimeric G-proteins: a short history. *Br J Pharmacol*, 147 Suppl 1, S46-55.
- MOLLER, T. C., MORENO-DELGADO, D., PIN, J. P. & KNIAZEFF, J. 2017. Class C G protein-coupled receptors: reviving old couples with new partners. *Biophys Rep*, 3, 57-63.
- MONTANELLI, L., J J VAN DURME, J., SMITS, G., BONOMI, M., RODIEN, P., DEVOR, E., MOFFAT-WILSON, K., PARDO, L., VASSART, G. & COSTAGLIOLA, S. 2004. *Modulation of Ligand Selectivity Associated with Activation of the Transmembrane Region of the Human Follitropin Receptor.*
- MOON, M. J., LEE, Y. N., PARK, S., REYES-ALCARAZ, A., HWANG, J. I., MILLAR, R. P., CHOE, H. & SEONG, J. Y. 2015. Ligand binding pocket formed by evolutionarily conserved residues in the glucagon-like peptide-1 (GLP-1) receptor core domain. *J Biol Chem*, 290, 5696-706.
- MOORE, E. E., KUESTNER, R. E., STROOP, S. D., GRANT, F. J., MATTHEWES, S. L., BRADY, C. L., SEXTON, P. M. & FINDLAY, D. M. 1995. Functionally different isoforms of the human calcitonin receptor result from alternative splicing of the gene transcript. *Mol Endocrinol*, 9, 959-68.
- MORAN, J., HUNZIKER, W. & A FISCHER, J. 1978. *Calcitonin and calcium ionophores: Cyclic AMP responses in cells of a human lymphoid line.*
- MORFIS, M., TILAKARATNE, N., FURNESS, S. G., CHRISTOPOULOS, G., WERRY, T. D., CHRISTOPOULOS, A. & SEXTON, P. M. 2008. Receptor activity-modifying proteins differentially modulate the G protein-coupling efficiency of amylin receptors. *Endocrinology*, 149, 5423-31.
- MORLEY, J. & F. FLOOD, J. 1991. *Amylin decreases food intake in mice.*
- MORLEY, J. E., LEVINE, A. S. & SILVIS, S. E. 1981. Intraventricular calcitonin inhibits gastric acid secretion. *Science*, 214, 671.
- MOSCAT, J., DIAZ-MECO, M. T. & RENNERT, P. 2003. NF-kappaB activation by protein kinase C isoforms and B-cell function. *EMBO Rep*, 4, 31-6.
- MUFF, R., BORN, W. & FISCHER, J. A. 1995. Calcitonin, calcitonin gene-related peptide, adrenomedullin and amylin: homologous peptides, separate receptors and overlapping biological actions. *Eur J Endocrinol*, 133, 17-20.
- MULDERRY, P. K., GHATEI, M. A., SPOKES, R. A., JONES, P. M., PIERSON, A. M., HAMID, Q. A., KANSE, S., AMARA, S. G., BURRIN, J. M., LEGON, S. & ET AL. 1988. Differential expression of alpha-CGRP and beta-CGRP by primary sensory neurons and enteric autonomic neurons of the rat. *Neuroscience*, 25, 195-205.
- MULLER, B., BECKER, K. L., SCHACHINGER, H., RICKENBACHER, P. R., HUBER, P. R., ZIMMERLI, W. & RITZ, R. 2000. Calcitonin precursors are reliable markers of sepsis in a medical intensive care unit. *Crit Care Med*, 28, 977-83.
- MURPHY, E., CHAMBERLIN, M. E. & MANDEL, L. J. 1986. Effects of calcitonin on cytosolic Ca in a suspension of rabbit medullary thick ascending limb tubules. *Am J Physiol*, 251, C491-5.
- NAKAMURA, M., HAN, B., NISHISHITA, T., BAI, Y. & KAKUDO, K. 2007. Calcitonin targets extracellular signal-regulated kinase signaling pathway in human cancers. *J Mol Endocrinol*, 39, 375-84.
- NAKAMURA, M., HASHIMOTO, T., NAKAJIMA, T., ICHII, S., FURUYAMA, J., ISHIHARA, Y. & KAKUDO, K. 1995. A new type of human calcitonin receptor isoform generated by alternative splicing. *Biochem Biophys Res Commun*, 209, 744-51.

- NAKAMURA, M., MORIMOTO, S., ZHANG, Z., UTSUNOMIYA, H., INAGAMI, T., OGIHARA, T. & KAKUDO, K. 2001. Calcitonin receptor gene polymorphism in Japanese women: correlation with body mass and bone mineral density. *Calcif Tissue Int*, 68, 211-5.
- NAKAMURA, M., ZHANG, Z. Q., SHAN, L., HISA, T., SASAKI, M., TSUKINO, R., YOKOI, T., KANAME, A. & KAKUDO, K. 1997. Allelic variants of human calcitonin receptor in the Japanese population. *Hum Genet*, 99, 38-41.
- NAKAMURA, T. & GOLD, G. H. 1987. A cyclic nucleotide-gated conductance in olfactory receptor cilia. *Nature*, 325, 442-4.
- NAKAYAMA, N., MIYAJIMA, A. & ARAI, K. 1985. Nucleotide sequences of STE2 and STE3, cell type-specific sterile genes from *Saccharomyces cerevisiae*. *The EMBO journal*, 4, 2643-2648.
- NARO, F., PEREZ, M., MIGLIACCIO, S., GALSON, D. L., ORCEL, P., TETI, A. & GOLDRING, S. R. 1998. Phospholipase D- and protein kinase C isoenzyme-dependent signal transduction pathways activated by the calcitonin receptor. *Endocrinology*, 139, 3241-8.
- NEUBIG, R. R., SPEDDING, M., KENAKIN, T. & CHRISTOPOULOS, A. 2003. International Union of Pharmacology Committee on Receptor Nomenclature and Drug Classification. XXXVIII. Update on terms and symbols in quantitative pharmacology. *Pharmacol Rev*, 55, 597-606.
- NEUMANN, J. M., COUVINEAU, A., MURAIL, S., LACAPERE, J. J., JAMIN, N. & LABURTHE, M. 2008. Class-B GPCR activation: is ligand helix-capping the key? *Trends Biochem Sci*, 33, 314-9.
- NICHOLS, A. S., FLOYD, D. H., BRUINSMA, S. P., NARZINSKI, K. & BARANSKI, T. J. 2013. Frizzled receptors signal through G proteins. *Cell Signal*, 25, 1468-75.
- NICOLE, P., LINS, L., ROUYER-FESSARD, C., DROUOT, C., FULCRAND, P., THOMAS, A., COUVINEAU, A., MARTINEZ, J., BRASSEUR, R. & LABURTHE, M. 2000. Identification of key residues for interaction of vasoactive intestinal peptide with human VPAC1 and VPAC2 receptors and development of a highly selective VPAC1 receptor agonist. Alanine scanning and molecular modeling of the peptide. *J Biol Chem*, 275, 24003-12.
- NICOSIA, S., GUIDOBONO, F., MUSANTI, M. & PECILE, A. 1986. Inhibitory effects of calcitonin on adenylate cyclase activity in different rat brain areas. *Life Sci*, 39, 2253-62.
- NORDSTRÖM, K. J. V., LAGERSTRÖM, M. C., WALLÉR, L. M. J., FREDRIKSSON, R. & SCHIÖTH, H. B. 2009. The Secretin GPCRs Descended from the Family of Adhesion GPCRs. *Molecular Biology and Evolution*, 26, 71-84.
- NUSSE, R. & VARMUS, H. E. 1992. Wnt genes. *Cell*, 69, 1073-87.
- NUSSLEIN-VOLHARD, C. & WIESCHAUS, E. 1980. Mutations affecting segment number and polarity in *Drosophila*. *Nature*, 287, 795-801.
- NYLEN, E. S., WHANG, K. T., SNIDER, R. H., JR., STEINWALD, P. M., WHITE, J. C. & BECKER, K. L. 1998. Mortality is increased by procalcitonin and decreased by an antiserum reactive to procalcitonin in experimental sepsis. *Crit Care Med*, 26, 1001-6.
- OAKLEY, R. H., LAPORTE, S. A., HOLT, J. A., BARAK, L. S. & CARON, M. G. 1999. Association of beta-arrestin with G protein-coupled receptors during clathrin-mediated endocytosis dictates the profile of receptor resensitization. *J Biol Chem*, 274, 32248-57.
- OAKLEY, R. H., LAPORTE, S. A., HOLT, J. A., CARON, M. G. & BARAK, L. S. 2000. Differential affinities of visual arrestin, beta arrestin1, and beta arrestin2 for G protein-coupled receptors delineate two major classes of receptors. *J Biol Chem*, 275, 17201-10.
- O'DOR, R. K., PARKES, C. O. & COPP, D. H. 1969. Amino acid composition of salmon calcitonin. *Can J Biochem*, 47, 823-5.

- OFFERMANN, S. 2003. G-proteins as transducers in transmembrane signalling. *Prog Biophys Mol Biol*, 83, 101-30.
- OGOSHI, M. 2016. Subchapter 27C - Calcitonin Receptor-Stimulating Peptide. In: TAKEI, Y., ANDO, H. & TSUTSUI, K. (eds.) *Handbook of Hormones*. San Diego: Academic Press.
- OLDHAM, W. M. & HAMM, H. E. 2008. Heterotrimeric G protein activation by G-protein-coupled receptors. *Nature Reviews Molecular Cell Biology*, 9, 60.
- ORLOWSKI, R. C., EPAND, R. M. & STAFFORD, A. R. 1987. Biologically potent analogues of salmon calcitonin which do not contain an N-terminal disulfide-bridged ring structure. *Eur J Biochem*, 162, 399-402.
- OSTROVSKAYA, A., FINDLAY, D. M., SEXTON, P. M. & FURNESS, S. G. B. 2017. Calcitonin. *Reference Module in Neuroscience and Biobehavioral Psychology*. Elsevier.
- OTJACQUES, E., BINSFELD, M., NOEL, A., BEGUIN, Y., CATALDO, D. & CAERS, J. 2011. Biological aspects of angiogenesis in multiple myeloma. *Int J Hematol*, 94, 505-18.
- OUAFIK, L., SAUZE, S., BOUDOURESQUE, F., CHINOT, O., DELFINO, C., FINA, F., VUAROQUEAUX, V., DUSSERT, C., PALMARI, J., DUFOUR, H., GRISOLI, F., CASELLAS, P., BRUNNER, N. & MARTIN, P. M. 2002. Neutralization of adrenomedullin inhibits the growth of human glioblastoma cell lines in vitro and suppresses tumor xenograft growth in vivo. *Am J Pathol*, 160, 1279-92.
- OVERGAARD, K. 1994. Effect of intranasal salmon calcitonin therapy on bone mass and bone turnover in early postmenopausal women: a dose-response study. *Calcif Tissue Int*, 55, 82-6.
- PACE, N. C. & MARTIN SCHOLTZ, J. 1998. A Helix Propensity Scale Based on Experimental Studies of Peptides and Proteins. *Biophysical Journal*, 75, 422-427.
- PAL, K., MATHUR, M., KUMAR, P. & DEFEA, K. 2013. Divergent beta-arrestin-dependent signaling events are dependent upon sequences within G-protein-coupled receptor C termini. *J Biol Chem*, 288, 3265-74.
- PAL, K., MELCHER, K. & XU, H. E. 2012. Structure and mechanism for recognition of peptide hormones by Class B G-protein-coupled receptors. *Acta Pharmacol Sin*, 33, 300-11.
- PALCZEWSKI, K., KUMASAKA, T., HORI, T., BEHNKE, C. A., MOTOSHIMA, H., FOX, B. A., LE TRONG, I., TELLER, D. C., OKADA, T., STENKAMP, R. E., YAMAMOTO, M. & MIYANO, M. 2000. Crystal structure of rhodopsin: A G protein-coupled receptor. *Science*, 289, 739-45.
- PARTHIER, C., REEDTZ-RUNGE, S., RUDOLPH, R. & STUBBS, M. T. 2009. Passing the baton in class B GPCRs: peptide hormone activation via helix induction? *Trends Biochem Sci*, 34, 303-10.
- PATOUT, M., SALAUN, M., BRUNEL, V., BOTA, S., CAULIEZ, B. & THIBERVILLE, L. 2014. Diagnostic and prognostic value of serum procalcitonin concentrations in primary lung cancers. *Clin Biochem*, 47, 263-7.
- PERRET, J., VAN CRAENENBROECK, M., LANGER, I., VERTONGEN, P., GREGOIRE, F., ROBBERECHT, P. & WAELEBROECK, M. 2002. Mutational analysis of the glucagon receptor: similarities with the vasoactive intestinal peptide (VIP)/pituitary adenylate cyclase-activating peptide (PACAP)/secretin receptors for recognition of the ligand's third residue. *Biochem J*, 362, 389-94.
- PHILIPP, M. & CARON, M. G. 2009. Hedgehog signaling: is Smo a G protein-coupled receptor? *Curr Biol*, 19, R125-7.
- PILKIS, S. J., CLAUS, T. H. & EL-MAGHRABI, M. R. 1988. The role of cyclic AMP in rapid and long-term regulation of gluconeogenesis and glycolysis. *Adv Second Messenger Phosphoprotein Res*, 22, 175-91.
- PIU, F., GAUTHIER, N. K. & WANG, F. 2006. Beta-arrestin 2 modulates the activity of nuclear receptor RAR beta2 through activation of ERK2 kinase. *Oncogene*, 25, 218-29.

- POVSIC, T. J., KOHOUT, T. A. & LEFKOWITZ, R. J. 2003. Beta-arrestin1 mediates insulin-like growth factor 1 (IGF-1) activation of phosphatidylinositol 3-kinase (PI3K) and anti-apoptosis. *J Biol Chem*, 278, 51334-9.
- POYNER, D. R., SEXTON, P. M., MARSHALL, I., SMITH, D. M., QUIRION, R., BORN, W., MUFF, R., FISCHER, J. A. & FOORD, S. M. 2002. International Union of Pharmacology. XXXII. The mammalian calcitonin gene-related peptides, adrenomedullin, amylin, and calcitonin receptors. *Pharmacol Rev*, 54, 233-46.
- POZVEK, G., HILTON, J. M., QUIZA, M., HOUSSAMI, S. & SEXTON, P. M. 1997. Structure/function relationships of calcitonin analogues as agonists, antagonists, or inverse agonists in a constitutively activated receptor cell system. *Mol Pharmacol*, 51, 658-65.
- PHAM, V., ZHU, Y., DAL MASO, E., REYNOLDS, C. A., DEGANUTTI, G., ATANASIO, S., HICK, C. A., YANG, D., CHRISTOPOULOS, A., HAY, D. L., FURNESS, S. G. B., WANG, M.-W., WOOTTEN, D. & SEXTON, P. M. 2019. Deconvoluting the Molecular Control of Binding and Signaling at the Amylin 3 Receptor: RAMP3 Alters Signal Propagation through Extracellular Loops of the Calcitonin Receptor. *ACS Pharmacology & Translational Science*.
- QING, H., ARDESHIRPOUR, L., PAJEVIC, P. D., DUSEVICH, V., JÄHN, K., KATO, S., WYSOLMERSKI, J. & BONEWALD, L. F. 2012. Demonstration of osteocytic perilacunar/canalicular remodeling in mice during lactation. *J Bone Miner Res*, 27, 1018-29.
- RAGGATT, L. J., EVDOKIOU, A. & FINDLAY, D. M. 2000. Sustained activation of Erk1/2 MAPK and cell growth suppression by the insert-negative, but not the insert-positive isoform of the human calcitonin receptor. *J Endocrinol*, 167, 93-105.
- RAISZ, L. G. & NIEMANN, I. 1969. Effect of phosphate, calcium and magnesium on bone resorption and hormonal responses in tissue culture. *Endocrinology*, 85, 446-52.
- RAMOS-ÁLVAREZ, I., MANTEY, S. A., NAKAMURA, T., NUCHE-BERENGUER, B., MORENO, P., MOODY, T. W., MADERDRUT, J. L., COY, D. H. & JENSEN, R. T. 2015. A structure-function study of PACAP using conformationally restricted analogs: Identification of PAC1 receptor-selective PACAP agonists. *Peptides*, 66, 26-42.
- RASMUSSEN, S. G., CHOI, H. J., FUNG, J. J., PARDON, E., CASAROSA, P., CHAE, P. S., DEVREE, B. T., ROSENBAUM, D. M., THIAN, F. S., KOBILKA, T. S., SCHNAPP, A., KONETZKI, I., SUNAHARA, R. K., GELLMAN, S. H., PAUTSCH, A., STEYAERT, J., WEIS, W. I. & KOBILKA, B. K. 2011a. Structure of a nanobody-stabilized active state of the beta(2) adrenoceptor. *Nature*, 469, 175-80.
- RASMUSSEN, S. G., DEVREE, B. T., ZOU, Y., KRUSE, A. C., CHUNG, K. Y., KOBILKA, T. S., THIAN, F. S., CHAE, P. S., PARDON, E., CALINSKI, D., MATHIESEN, J. M., SHAH, S. T., LYONS, J. A., CAFFREY, M., GELLMAN, S. H., STEYAERT, J., SKINIOTIS, G., WEIS, W. I., SUNAHARA, R. K. & KOBILKA, B. K. 2011b. Crystal structure of the beta2 adrenergic receptor-Gs protein complex. *Nature*, 477, 549-55.
- RASK-ANDERSEN, M., MASURAM, S. & SCHIOTH, H. B. 2014. The druggable genome: Evaluation of drug targets in clinical trials suggests major shifts in molecular class and indication. *Annu Rev Pharmacol Toxicol*, 54, 9-26.
- REDA, T. K., GELIEBTER, A. & PI-SUNYER, F. X. 2002. Amylin, food intake, and obesity. *Obes Res*, 10, 1087-91.
- REN, Y., CHIEN, J., SUN, Y. P. & SHAH, G. V. 2001. Calcitonin is expressed in gonadotropes of the anterior pituitary gland: its possible role in paracrine regulation of lactotrope function. *J Endocrinol*, 171, 217-28.
- RHEE, S. G. & CHOI, K. D. 1992. Regulation of inositol phospholipid-specific phospholipase C isozymes. *J Biol Chem*, 267, 12393-6.

- RICCI-VITIANI, L., PALLINI, R., BIFFONI, M., TODARO, M., INVERNICI, G., CENCI, T., MAIRA, G., PARATI, E. A., STASSI, G., LAROCCA, L. M. & DE MARIA, R. 2010. Tumour vascularization via endothelial differentiation of glioblastoma stem-like cells. *Nature*, 468, 824-8.
- RICHARDSON, J. S. 1981. The Anatomy and Taxonomy of Protein Structure. In: ANFINSEN, C. B., EDSALL, J. T. & RICHARDS, F. M. (eds.) *Advances in Protein Chemistry*. Academic Press.
- RIZZO, A. J. & GOLTZMAN, D. 1981. Calcitonin receptors in the central nervous system of the rat. *Endocrinology*, 108, 1672-7.
- ROBERTS, A. N., LEIGHTON, B., TODD, J. A., COCKBURN, D., SCHOFIELD, P. N., SUTTON, R., HOLT, S., BOYD, Y., DAY, A. J. & FOOT, E. A. 1989. Molecular and functional characterization of amylin, a peptide associated with type 2 diabetes mellitus. *Proc Natl Acad Sci U S A*, 86, 9662-6.
- ROBINSON, M. J. & COBB, M. H. 1997. Mitogen-activated protein kinase pathways. *Curr Opin Cell Biol*, 9, 180-6.
- ROED, S. N., ORGAARD, A., JORGENSEN, R. & DE MEYTS, P. 2012. Receptor oligomerization in family B1 of G-protein-coupled receptors: focus on BRET investigations and the link between GPCR oligomerization and binding cooperativity. *Front Endocrinol (Lausanne)*, 3, 62.
- ROH, J., CHANG, C. L., BHALLA, A., KLEIN, C. & HSU, S. Y. 2004. Intermedin is a calcitonin/calcitonin gene-related peptide family peptide acting through the calcitonin receptor-like receptor/receptor activity-modifying protein receptor complexes. *J Biol Chem*, 279, 7264-74.
- ROVATI, G. E., CAPRA, V. & NEUBIG, R. R. 2007. The highly conserved DRY motif of class A G protein-coupled receptors: beyond the ground state. *Mol Pharmacol*, 71, 959-64.
- RUNGE, S., GRAM, C., BRAUNER-OSBORNE, H., MADSEN, K., KNUDSEN, L. B. & WULFF, B. S. 2003. Three distinct epitopes on the extracellular face of the glucagon receptor determine specificity for the glucagon amino terminus. *J Biol Chem*, 278, 28005-10.
- RYAN, G., BRISCOE, T. A. & JOBE, L. 2008. Review of pramlintide as adjunctive therapy in treatment of type 1 and type 2 diabetes. *Drug Des Devel Ther*, 2, 203-14.
- SABBISSETTI, V. S., CHIRUGUPATI, S., THOMAS, S., VAIDYA, K. S., REARDON, D., CHIRIVAI-INTERNATI, M., ICZKOWSKI, K. A. & SHAH, G. V. 2005. Calcitonin increases invasiveness of prostate cancer cells: role for cyclic AMP-dependent protein kinase A in calcitonin action. *Int J Cancer*, 117, 551-60.
- SAMURA, A., WADA, S., SUDA, S., IITAKA, M. & KATAYAMA, S. 2000. Calcitonin Receptor Regulation and Responsiveness to Calcitonin in Human Osteoclast-Like Cells Prepared in Vitro using Receptor Activator of Nuclear Factor- κ B Ligand and Macrophage Colony-Stimulating Factor. *Endocrinology*, 141, 3774-3782.
- SANAI, N., ALVAREZ-BUYLLA, A. & BERGER, M. S. 2005. Neural stem cells and the origin of gliomas. *N Engl J Med*, 353, 811-22.
- SATO, M. 2013. Roles of accessory proteins for heterotrimeric G-protein in the development of cardiovascular diseases. *Circ J*, 77, 2455-61.
- SATOH, M., OKU, R., MAEDA, A., FUJII, N., OTAKA, A., FUNAKOSHI, S., YAJIMA, H. & TAKAGI, H. 1986. Possible mechanisms of positive inotropic action of synthetic human calcitonin gene-related peptide in isolated rat atrium. *Peptides*, 7, 631-635.
- SAULIERE, A., BELLOT, M., PARIS, H., DENIS, C., FINANA, F., HANSEN, J. T., ALTIE, M. F., SEGUELAS, M. H., PATHAK, A., HANSEN, J. L., SENARD, J. M. & GALES, C. 2012. Deciphering biased-agonism complexity reveals a new active AT1 receptor entity. *Nat Chem Biol*, 8, 622-30.

- SAXE, C. L., 3RD, GINSBURG, G. T., LOUIS, J. M., JOHNSON, R., DEVREOTES, P. N. & KIMMEL, A. R. 1993. CAR2, a prestalk cAMP receptor required for normal tip formation and late development of Dictyostelium discoideum. *Genes Dev*, 7, 262-72.
- SCHINKE, T., LIESE, S., PRIEMEL, M., HABERLAND, M., SCHILLING, A. F., CATALA-LEHNEN, P., BLICHARSKI, D., RUEGER, J. M., GAGEL, R. F., EMESON, R. B. & AMLING, M. 2004. Decreased bone formation and osteopenia in mice lacking alpha-calcitonin gene-related peptide. *J Bone Miner Res*, 19, 2049-56.
- SCHIPANI, E., JENSEN, G. S., PINCUS, J., NISSENSON, R. A., GARDELLA, T. J. & JUPPNER, H. 1997. Constitutive activation of the cyclic adenosine 3',5'-monophosphate signaling pathway by parathyroid hormone (PTH)/PTH-related peptide receptors mutated at the two loci for Jansen's metaphyseal chondrodysplasia. *Mol Endocrinol*, 11, 851-8.
- SCHWARTZ, K. E., ORLOWSKI, R. C. & MARCUS, R. 1981. des-Ser2 salmon calcitonin: a biologically potent synthetic analog. *Endocrinology*, 108, 831-5.
- SCHWINDINGER, W. F. & ROBISHAW, J. D. 2001. Heterotrimeric G-protein betagamma-dimers in growth and differentiation. *Oncogene*, 20, 1653-60.
- SECK, T., BARON, R. & HORNE, W. C. 2003. Binding of filamin to the C-terminal tail of the calcitonin receptor controls recycling. *J Biol Chem*, 278, 10408-16.
- SECK, T., PELLEGRINI, M., FLOREA, A. M., GRIGNOUX, V., BARON, R., MIERKE, D. F. & HORNE, W. C. 2005. The delta e13 isoform of the calcitonin receptor forms a six-transmembrane domain receptor with dominant-negative effects on receptor surface expression and signaling. *Mol Endocrinol*, 19, 2132-44.
- SEGAWA, N., NAKAMURA, M., NAKAMURA, Y., MORI, I., KATSUOKA, Y. & KAKUDO, K. 2001. Phosphorylation of mitogen-activated protein kinase is inhibited by calcitonin in DU145 prostate cancer cells. *Cancer Res*, 61, 6060-3.
- SEIDEL, L., ZARZYCKA, B., ZAIDI, S. A., KATRITCH, V. & COIN, I. 2017. Structural insight into the activation of a class B G-protein-coupled receptor by peptide hormones in live human cells. *Elife*, 6.
- SEINO, S., TAKAHASHI, H., FUJIMOTO, W. & SHIBASAKI, T. 2009. Roles of cAMP signalling in insulin granule exocytosis. *Diabetes Obes Metab*, 11 Suppl 4, 180-8.
- SEN, R. & BALTIMORE, D. 1986. Inducibility of kappa immunoglobulin enhancer-binding protein NF-kappa B by a posttranslational mechanism. *Cell*, 47, 921-8.
- SEXTON, P. M., FINDLAY, D. M. & MARTIN, T. J. 1999. Calcitonin. *Curr Med Chem*, 6, 1067-93.
- SEXTON, P. M., HOUSAMI, S., HILTON, J. M., O'KEEFFE, L. M., CENTER, R. J., GILLESPIE, M. T., DARCY, P. & FINDLAY, D. M. 1993. Identification of brain isoforms of the rat calcitonin receptor. *Mol Endocrinol*, 7, 815-21.
- SEXTON, P. M., SCHNEIDER, H. G., D'SANTOS, C. S., MENDELSON, F. A., KEMP, B. E., MOSELEY, J. M., MARTIN, T. J. & FINDLAY, D. M. 1991. Reversible calcitonin binding to solubilized sheep brain binding sites. *Biochem J*, 273(Pt 1), 179-84.
- SHAH, G. V., THOMAS, S., MURALIDHARAN, A., LIU, Y., HERMONAT, P. L., WILLIAMS, J. & CHAUDHARY, J. 2008. Calcitonin promotes in vivo metastasis of prostate cancer cells by altering cell signaling, adhesion, and inflammatory pathways. *Endocr Relat Cancer*, 15, 953-64.
- SHEN, H., ZHENG, S., CHEN, R., JIN, X., XU, X., JING, C., LIN, J., ZHANG, J., ZHANG, M., ZHANG, L., XIE, X., GUO, K., REN, Z., LIN, S. & ZHANG, B. 2017. Prognostic significance of serum procalcitonin in patients with unresectable hepatocellular carcinoma treated with transcatheter arterial chemoembolization: A retrospective analysis of 509 cases. *Medicine (Baltimore)*, 96, e7438.
- SHI, L., LIAPAKIS, G., XU, R., GUARNIERI, F., BALLESTEROS, J. A. & JAVITCH, J. A. 2002. Beta2 adrenergic receptor activation. Modulation of the proline kink in transmembrane 6 by a rotamer toggle switch. *J Biol Chem*, 277, 40989-96.

- SHYU, F. J., INOUE, D., BARON, R. & C HORNE, W. 1997. *The Deletion of 14 Amino Acids in the Seventh Transmembrane Domain of a Naturally Occurring Calcitonin Receptor Isoform Alters Ligand Binding and Selectively Abolishes Coupling to Phospholipase C.*
- SILVESTRONI, L., MENDITTO, A., FRAJESE, G. & GNESSI, L. 1987. Identification of calcitonin receptors in human spermatozoa. *J Clin Endocrinol Metab*, 65, 742-6.
- SIMON, M. I., STRATHMANN, M. P. & GAUTAM, N. 1991. Diversity of G proteins in signal transduction. *Science*, 252, 802-8.
- SIU, F. Y., HE, M., DE GRAAF, C., HAN, G. W., YANG, D., ZHANG, Z., ZHOU, C., XU, Q., WACKER, D., JOSEPH, J. S., LIU, W., LAU, J., CHEREZOV, V., KATRITCH, V., WANG, M.-W. & STEVENS, R. C. 2013. Structure of the human glucagon class B G-protein-coupled receptor. *Nature*, 499, 444.
- SKINNER, J. P., ZAJAC, J. D., CLARKE, M. V., RUSSELL, P. K., SASTRA, S., DAVEY, R. A., FINDLAY, D. M., ATKINS, G. J. & ANDERSON, P. H. 2015. A Role for the Calcitonin Receptor to Limit Bone Loss During Lactation in Female Mice by Inhibiting Osteocytic Osteolysis. *Endocrinology*, 156, 3203-3214.
- SMITH, J. S. & RAJAGOPAL, S. 2016. The beta-Arrestins: Multifunctional Regulators of G Protein-coupled Receptors. *J Biol Chem*, 291, 8969-77.
- SODA, Y., MARUMOTO, T., FRIEDMANN-MORVINSKI, D., SODA, M., LIU, F., MICHIE, H., PASTORINO, S., YANG, M., HOFFMAN, R. M., KESARI, S. & VERMA, I. M. 2011. Transdifferentiation of glioblastoma cells into vascular endothelial cells. *Proceedings of the National Academy of Sciences*, 108, 4274-4280.
- SOLANO, R. M., LANGER, I., PERRET, J., VERTONGEN, P., JUARRANZ, M. G., ROBBERECHT, P. & WAELBROECK, M. 2001. Two basic residues of the h-VPAC1 receptor second transmembrane helix are essential for ligand binding and signal transduction. *J Biol Chem*, 276, 1084-8.
- SONG, G., YANG, D., WANG, Y., DE GRAAF, C., ZHOU, Q., JIANG, S., LIU, K., CAI, X., DAI, A., LIN, G., LIU, D., WU, F., WU, Y., ZHAO, S., YE, L., HAN, G. W., LAU, J., WU, B., HANSON, M. A., LIU, Z. J., WANG, M. W. & STEVENS, R. C. 2017. Human GLP-1 receptor transmembrane domain structure in complex with allosteric modulators. *Nature*, 546, 312-315.
- SPYRIDAKI, K., MATSOUKAS, M. T., CORDOMI, A., GKOUNTELIS, K., PAPADOKOSTAKI, M., MAVROMOUSTAKOS, T., LOGOTHETIS, D. E., MARGIORIS, A. N., PARDO, L. & LIAPAKIS, G. 2014. Structural-functional analysis of the third transmembrane domain of the corticotropin-releasing factor type 1 receptor: role in activation and allosteric antagonism. *J Biol Chem*, 289, 18966-77.
- STERNINI, C. & ANDERSON, K. 1992. Calcitonin gene-related peptide-containing neurons supplying the rat digestive system: differential distribution and expression pattern. *Somatosens Mot Res*, 9, 45-59.
- STEVENS, R. C., CHEREZOV, V., KATRITCH, V., ABAGYAN, R., KUHN, P., ROSEN, H. & WÜTHRICH, K. 2013. The GPCR Network: a large-scale collaboration to determine human GPCR structure and function. *Nat Rev Drug Discov*, 12, 25-34.
- STRITTMATTER, S. M., FISHMAN, M. C. & ZHU, X. P. 1994. Activated mutants of the alpha subunit of G(o) promote an increased number of neurites per cell. *J Neurosci*, 14, 2327-38.
- STRITTMATTER, S. M., VALENZUELA, D., KENNEDY, T. E., NEER, E. J. & FISHMAN, M. C. 1990. G0 is a major growth cone protein subject to regulation by GAP-43. *Nature*, 344, 836.
- STROOP, S. D., KUESTNER, R. E., SERWOLD, T. F., CHEN, L. & MOORE, E. E. 1995. Chimeric human calcitonin and glucagon receptors reveal two dissociable calcitonin interaction sites. *Biochemistry*, 34, 1050-7.

- SUN, L. & YE, R. D. 2012. Role of G protein-coupled receptors in inflammation. *Acta Pharmacol Sin*, 33, 342-50.
- SUZUKI, M., KAWAGUCHI, Y., KURIHARA, S. & MIYAHARA, T. 1989. *Heterogeneous response of cytoplasmic free Ca²⁺ in proximal convoluted and straight tubule cells in primary culture.*
- SUZUKI, Y., OGASAWARA, T., TANAKA, Y., TAKEDA, H., SAWASAKI, T., MOGI, M., LIU, S. & MAEYAMA, K. 2018. Functional G-Protein-Coupled Receptor (GPCR) Synthesis: The Pharmacological Analysis of Human Histamine H1 Receptor (HRH1) Synthesized by a Wheat Germ Cell-Free Protein Synthesis System Combined with Asolectin Glycosomes. *Frontiers in pharmacology*, 9, 38-38.
- TABOULET, J., FRENKIAN, M., FRENDON, J. L., FEINGOLD, N., JULLIENNE, A. & DE VERNEJOL, M. C. 1998. Calcitonin receptor polymorphism is associated with a decreased fracture risk in post-menopausal women. *Hum Mol Genet*, 7, 2129-33.
- TAKAHASHI, S., GOLDRING, S., KATZ, M., HILSENBECK, S., WILLIAMS, R. & ROODMAN, G. D. 1995. Downregulation of calcitonin receptor mRNA expression by calcitonin during human osteoclast-like cell differentiation. *J Clin Invest*, 95, 167-71.
- TAUSSIG, R., INIGUEZ-LLUHI, J. A. & GILMAN, A. G. 1993. Inhibition of adenylyl cyclase by Gi alpha. *Science*, 261, 218-21.
- TAYLOR, M. M., BAGLEY, S. L. & SAMSON, W. K. 2005a. Intermedin/adrenomedullin-2 acts within central nervous system to elevate blood pressure and inhibit food and water intake. *Am J Physiol Regul Integr Comp Physiol*, 288, R919-27.
- TAYLOR, M. M. & SAMSON, W. K. 2005b. Stress hormone secretion is altered by central administration of intermedin/adrenomedullin-2. *Brain Res*, 1045, 199-205.
- TERRILLON, S. & BOUVIER, M. 2004. Roles of G-protein-coupled receptor dimerization. *EMBO Rep*, 5, 30-4.
- THAKKAR, A., ALJAMEELI, A., THOMAS, S. & SHAH, G. V. 2016. A-kinase anchoring protein 2 is required for calcitonin-mediated invasion of cancer cells. *Endocr Relat Cancer*, 23, 1-14.
- THOMAS, S., ANBALAGAN, M. & SHAH, G. 2008. *Knock-down of calcitonin receptor expression induces apoptosis and growth arrest of prostate cancer cells.*
- THOMAS, S., CHIGURUPATI, S., ANBALAGAN, M. & SHAH, G. 2006. Calcitonin increases tumorigenicity of prostate cancer cells: evidence for the role of protein kinase A and urokinase-type plasminogen receptor. *Mol Endocrinol*, 20, 1894-911.
- THOMAS, S. & SHAH, G. 2005. Calcitonin induces apoptosis resistance in prostate cancer cell lines against cytotoxic drugs via the Akt/survivin pathway. *Cancer Biol Ther*, 4, 1226-33.
- TILAKARATNE, N., CHRISTOPOULOS, G., ZUMPE, E. T., FOORD, S. M. & SEXTON, P. M. 2000. Amylin receptor phenotypes derived from human calcitonin receptor/RAMP coexpression exhibit pharmacological differences dependent on receptor isoform and host cell environment. *J Pharmacol Exp Ther*, 294, 61-72.
- TOLCOS, M., TIKELLIS, C., REES, S., COOPER, M. & WOOKEY, P. 2003. Ontogeny of calcitonin receptor mRNA and protein in the developing central nervous system of the rat. *J Comp Neurol*, 456, 29-38.
- TSAI, F. J., CHEN, W. C., CHEN, H. Y. & TSAI, C. H. 2003. The ALUI calcitonin receptor gene polymorphism (TT) is associated with low bone mineral density and susceptibility to osteoporosis in postmenopausal women. *Gynecol Obstet Invest*, 55, 82-7.
- TSENG, C. C. & LIN, L. 1997. A point mutation in the glucose-dependent insulinotropic peptide receptor confers constitutive activity. *Biochem Biophys Res Commun*, 232, 96-100.
- TUTEJA, N. 2009. Signaling through G protein coupled receptors. *Plant Signal Behav*, 4, 942-7.

- TWERY, M. J., SEITZ, P. K., ALLEN NICKOLS, G., COOPER, C. W., GALLAGHER, J. P. & ORLOWSKI, R. C. 1988. Analogue separates biological effects of salmon calcitonin on brain and renal cortical membranes. *European Journal of Pharmacology*, 155, 285-292.
- UEDA, Y., HIRAI, S., OSADA, S., SUZUKI, A., MIZUNO, K. & OHNO, S. 1996. Protein kinase C activates the MEK-ERK pathway in a manner independent of Ras and dependent on Raf. *J Biol Chem*, 271, 23512-9.
- UNSON, C. G., WU, C. R., JIANG, Y., YOO, B., CHEUNG, C., SAKMAR, T. P. & MERRIFIELD, R. B. 2002. Roles of specific extracellular domains of the glucagon receptor in ligand binding and signaling. *Biochemistry*, 41, 11795-803.
- VALENTINE, K. G., LIU, S. F., MARASSI, F. M., VEGLIA, G., OPELLA, S. J., DING, F. X., WANG, S. H., ARSHAVA, B., BECKER, J. M. & NAIDER, F. 2001. Structure and topology of a peptide segment of the 6th transmembrane domain of the *Saccharomyces cerevisiae* alpha-factor receptor in phospholipid bilayers. *Biopolymers*, 59, 243-256.
- VENKATANARAYAN, A., RAULJI, P., NORTON, W., CHAKRAVARTI, D., COARFA, C., SU, X., SANDUR, S. K., RAMIREZ, M. S., LEE, J., KINGSLEY, C. V., SANANIKONE, E. F., RAJAPAKSHE, K., NAFF, K., PARKER-THORNBURG, J., BANKSON, J. A., TSAI, K. Y., GUNARATNE, P. H. & FLORES, E. R. 2015. IAPP-driven metabolic reprogramming induces regression of p53-deficient tumours in vivo. *Nature*, 517, 626-30.
- VENKATANARAYAN, A., RAULJI, P., NORTON, W. & FLORES, E. R. 2016. Novel therapeutic interventions for p53-altered tumors through manipulation of its family members, p63 and p73. *Cell Cycle*, 15, 164-71.
- VERHAAK, R. G. W., HOADLEY, K. A., PURDOM, E., WANG, V., QI, Y., WILKERSON, M. D., MILLER, C. R., DING, L., GOLUB, T., MESIROV, J. P., ALEXE, G., LAWRENCE, M., O'KELLY, M., TAMAYO, P., WEIR, B. A., GABRIE, S., WINCKLER, W., GUPTA, S., JAKKULA, L., FEILER, H. S., HODGSON, J. G., JAMES, C. D., SARKARIA, J. N., BRENNAN, C., KAHN, A., SPELLMAN, P. T., WILSON, R. K., SPEED, T. P., GRAY, J. W., MEYERSON, M., GETZ, G., PEROU, C. M. & HAYES, D. N. 2010. An integrated genomic analysis identifies clinically relevant subtypes of glioblastoma characterized by abnormalities in PDGFRA, IDH1, EGFR and NF1. *Cancer Cell*, 17, 98.
- VILARDAGA, J. P., ROMERO, G., FRIEDMAN, P. A. & GARDELLA, T. J. 2011. Molecular basis of parathyroid hormone receptor signaling and trafficking: a family B GPCR paradigm. *Cell Mol Life Sci*, 68, 1-13.
- VIOLIN, J. D., CROMBIE, A. L., SOERGEL, D. G. & LARK, M. W. 2014. Biased ligands at G-protein-coupled receptors: promise and progress. *Trends in Pharmacological Sciences*, 35, 308-316.
- VOHRA, S., TADDESE, B., CONNER, A. C., POYNER, D. R., HAY, D. L., BARWELL, J., REEVES, P. J., UPTON, G. J. & REYNOLDS, C. A. 2013a. Similarity between class A and class B G-protein-coupled receptors exemplified through calcitonin gene-related peptide receptor modelling and mutagenesis studies. *J R Soc Interface*, 10, 20120846.
- WADA, S., MARTIN, T. J. & FINDLAY, D. M. 1995. Homologous regulation of the calcitonin receptor in mouse osteoclast-like cells and human breast cancer T47D cells. *Endocrinology*, 136, 2611-21.
- WADA, S., UDAGAWA, N., NAGATA, N., MARTIN, T. J. & FINDLAY, D. M. 1996. Physiological levels of calcitonin regulate the mouse osteoclast calcitonin receptor by a protein kinase Alpha-mediated mechanism. *Endocrinology*, 137, 312-20.
- WADA, S., YASUDA, S., NAGAI, T., MAEDA, T., KITAHAMA, S., SUDA, S., FINDLAY, D. M., IITAKA, M. & KATAYAMA, S. 2001. Regulation of Calcitonin Receptor by Glucocorticoid in Human Osteoclast-Like Cells Prepared in Vitro Using Receptor Activator of Nuclear Factor- κ B Ligand and Macrophage Colony-Stimulating Factor*. *Endocrinology*, 142, 1471-1478.

- WALKER, C. S., EFTEKHARI, S., BOWER, R. L., WILDERMAN, A., INSEL, P. A., EDVINSSON, L., WALDVOGEL, H. J., JAMALUDDIN, M. A., RUSSO, A. F. & HAY, D. L. 2015. A second trigeminal CGRP receptor: function and expression of the AMY1 receptor. *Ann Clin Transl Neurol*, 2, 595-608.
- WALKER, C. S., RADDANT, A. C., WOOLLEY, M. J., RUSSO, A. F. & HAY, D. L. 2018. CGRP receptor antagonist activity of olcegepant depends on the signalling pathway measured. *Cephalalgia*, 38, 437-451.
- WALKER, C. S., SUNDRUM, T. & HAY, D. L. 2014. PACAP receptor pharmacology and agonist bias: analysis in primary neurons and glia from the trigeminal ganglia and transfected cells. *Br J Pharmacol*, 171, 1521-33.
- WALTEREIT, R. & WELLER, M. 2003. Signaling from cAMP/PKA to MAPK and synaptic plasticity. *Molecular Neurobiology*, 27, 99-106.
- WANG, Q., MULLAH, B. K. & ROBISHAW, J. D. 1999. Ribozyme approach identifies a functional association between the G protein beta1gamma7 subunits in the beta-adrenergic receptor signaling pathway. *J Biol Chem*, 274, 17365-71.
- WANG, R., CHADALAVADA, K., WILSHIRE, J., KOWALIK, U., HOVINGA, K. E., GEBER, A., FLIGELMAN, B., LEVERSHA, M., BRENNAN, C. & TABAR, V. 2010. Glioblastoma stem-like cells give rise to tumour endothelium. *Nature*, 468, 829-33.
- WANG, X., NAKAMURA, M., MORI, I., TAKEDA, K., NAKAMURA, Y., UTSUNOMIYA, H., YOSHIMURA, G., SAKURAI, T. & KAKUDO, K. 2004. Calcitonin receptor gene and breast cancer: quantitative analysis with laser capture microdissection. *Breast Cancer Res Treat*, 83, 109-17.
- WANG, Y., MACKE, J. P., ABELLA, B. S., ANDREASSON, K., WORLEY, P., GILBERT, D. J., COPELAND, N. G., JENKINS, N. A. & NATHANS, J. 1996. A large family of putative transmembrane receptors homologous to the product of the *Drosophila* tissue polarity gene *frizzled*. *J Biol Chem*, 271, 4468-76.
- WESTERMARK, P., WERNSTEDT, C., WILANDER, E. & SLETTEN, K. 1986. A novel peptide in the calcitonin gene related peptide family as an amyloid fibril protein in the endocrine pancreas. *Biochem Biophys Res Commun*, 140, 827-31.
- WHANG, K. T., STEINWALD, P. M., WHITE, J. C., NYLEN, E. S., SNIDER, R. H., SIMON, G. L., GOLDBERG, R. L. & BECKER, K. L. 1998. Serum calcitonin precursors in sepsis and systemic inflammation. *J Clin Endocrinol Metab*, 83, 3296-301.
- WILKINSON, R. 1984. Treatment of hypercalcaemia associated with malignancy. *Br Med J (Clin Res Ed)*, 288, 812-3.
- WILLIAMS, C. P., MEACHIM, G. & TAYLOR, W. H. 1978. Effect of calcitonin treatment on osteoclast counts in Paget's disease of bone. *J Clin Pathol*, 31, 1212-7.
- WISHART, D. S. 2011. Interpreting protein chemical shift data. *Prog Nucl Magn Reson Spectrosc*, 58, 62-87.
- WOLF, S. & GRUNEWALD, S. 2015. Sequence, structure and ligand binding evolution of rhodopsin-like G protein-coupled receptors: a crystal structure-based phylogenetic analysis. *PLoS One*, 10, e0123533.
- WOLFE, L. A., 3RD, FLING, M. E., XUE, Z., ARMOUR, S., KERNER, S. A., WAY, J., RIMELE, T. & COX, R. F. 2003. In vitro characterization of a human calcitonin receptor gene polymorphism. *Mutat Res*, 522, 93-105.
- WONGSURAWAT, N. & ARMBRECHT, H. J. 1991. Calcitonin stimulates 1,25-dihydroxyvitamin D production in diabetic rat kidney. *Metabolism*, 40, 22-5.
- WOOKEY, P. J., MCLEAN, C. A., HWANG, P., FURNESS, S. G., NGUYEN, S., KOURAKIS, A., HARE, D. L. & ROSENFELD, J. V. 2012. The expression of calcitonin receptor detected in malignant cells of the brain tumour glioblastoma multiforme and functional properties in the cell line A172. *Histopathology*, 60, 895-910.

- WOOKEY, P. J., ZULLI, A., BUXTON, B. F. & HARE, D. L. 2008. Calcitonin receptor immunoreactivity associated with specific cell types in diseased radial and internal mammary arteries. *Histopathology*, 52, 605-12.
- WOOKEY, P., ZULLI, A., LO, C., HARE, D., P. SCHWARER, A., DARBY, I. & LEUNG, A. 2009. Calcitonin Receptor Expression in Embryonic, Foetal and Adult Tissues: Developmental and Pathophysiological Implications.
- WOOLLEY, M. J. & CONNER, A. C. 2017a. Understanding the common themes and diverse roles of the second extracellular loop (ECL2) of the GPCR super-family. *Mol Cell Endocrinol*, 449, 3-11.
- WOOLLEY, M. J., REYNOLDS, C. A., SIMMS, J., WALKER, C. S., MOBAREC, J. C., GARELJA, M. L., CONNER, A. C., POYNER, D. R. & HAY, D. L. 2017b. Receptor activity-modifying protein dependent and independent activation mechanisms in the coupling of calcitonin gene-related peptide and adrenomedullin receptors to Gs. *Biochem Pharmacol*, 142, 96-110.
- WOOLLEY, M. J., WATKINS, H. A., TADDESE, B., KARAKULLUKCU, Z. G., BARWELL, J., SMITH, K. J., HAY, D. L., POYNER, D. R., REYNOLDS, C. A. & CONNER, A. C. 2013. The role of ECL2 in CGRP receptor activation: a combined modelling and experimental approach. *J R Soc Interface*, 10, 20130589.
- WOOTEN, D., CHRISTOPOULOS, A., MARTI-SOLANO, M., BABU, M. M. & SEXTON, P. M. 2018. Mechanisms of signalling and biased agonism in G protein-coupled receptors. *Nat Rev Mol Cell Biol*, 19, 638-653.
- WOOTEN, D., MILLER, L. J., KOOLE, C., CHRISTOPOULOS, A. & SEXTON, P. M. 2017. Allostery and Biased Agonism at Class B G Protein-Coupled Receptors. *Chem Rev*, 117, 111-138.
- WOOTEN, D., REYNOLDS, C. A., KOOLE, C., SMITH, K. J., MOBAREC, J. C., SIMMS, J., QUON, T., COUDRAT, T., FURNESS, S. G., MILLER, L. J., CHRISTOPOULOS, A. & SEXTON, P. M. 2016a. A Hydrogen-Bonded Polar Network in the Core of the Glucagon-Like Peptide-1 Receptor Is a Fulcrum for Biased Agonism: Lessons from Class B Crystal Structures. *Mol Pharmacol*, 89, 335-47.
- WOOTEN, D., REYNOLDS, C. A., SMITH, K. J., MOBAREC, J. C., FURNESS, S. G., MILLER, L. J., CHRISTOPOULOS, A. & SEXTON, P. M. 2016b. Key interactions by conserved polar amino acids located at the transmembrane helical boundaries in Class B GPCRs modulate activation, effector specificity and biased signalling in the glucagon-like peptide-1 receptor. *Biochem Pharmacol*, 118, 68-87.
- WOOTEN, D., REYNOLDS, C. A., SMITH, K. J., MOBAREC, J. C., KOOLE, C., SAVAGE, E. E., PABREJA, K., SIMMS, J., SRIDHAR, R., FURNESS, S. G. B., LIU, M., THOMPSON, P. E., MILLER, L. J., CHRISTOPOULOS, A. & SEXTON, P. M. 2016c. The Extracellular Surface of the GLP-1 Receptor Is a Molecular Trigger for Biased Agonism. *Cell*, 165, 1632-1643.
- WOOTEN, D., SIMMS, J., MILLER, L. J., CHRISTOPOULOS, A. & SEXTON, P. M. 2013. Polar transmembrane interactions drive formation of ligand-specific and signal pathway-biased family B G protein-coupled receptor conformations. *Proc Natl Acad Sci U S A*, 110, 5211-6.
- WU, G., BURZON, D. T., DI SANT'AGNESE, P. A., SCHOEN, S., DEFTOS, L. J., GERSHAGEN, S. & COCKETT, A. T. 1996. Calcitonin receptor mRNA expression in the human prostate. *Urology*, 47, 376-81.
- XU, J., WANG, F., VAN KEYMEULEN, A., HERZMARK, P., STRAIGHT, A., KELLY, K., TAKUWA, Y., SUGIMOTO, N., MITCHISON, T. & BOURNE, H. R. 2003. Divergent Signals and Cytoskeletal Assemblies Regulate Self-Organizing Polarity in Neutrophils. *Cell*, 114, 201-214.

- YAMAGUCHI, M. 1989. Effect of calcitonin on exchangeable calcium transport in isolated rat hepatocytes. *Mol Cell Endocrinol*, 62, 313-8.
- YAMAGUCHI, M. 1991. Stimulatory effect of calcitonin on Ca^{2+} inflow in isolated rat hepatocytes. *Mol Cell Endocrinol*, 75, 65-70.
- YAMAGUCHI, M., WATANABE, Y., OHTANI, T., UEZUMI, A., MIKAMI, N., NAKAMURA, M., SATO, T., IKAWA, M., HOSHINO, M., TSUCHIDA, K., MIYAGOE-SUZUKI, Y., TSUJIKAWA, K., TAKEDA, S., YAMAMOTO, H. & FUKADA, S. 2015. Calcitonin Receptor Signaling Inhibits Muscle Stem Cells from Escaping the Quiescent State and the Niche. *Cell Rep*, 13, 302-14.
- YAN, K., KALYANARAMAN, V. & GAUTAM, N. 1996. Differential ability to form the G protein beta gamma complex among members of the beta and gamma subunit families.
- YANG, D., DE GRAAF, C., YANG, L., SONG, G., DAI, A., CAI, X., FENG, Y., REEDTZ-RUNGE, S., HANSON, M. A., YANG, H., JIANG, H., STEVENS, R. C. & WANG, M. W. 2016. Structural Determinants of Binding the Seven-transmembrane Domain of the Glucagon-like Peptide-1 Receptor (GLP-1R). *J Biol Chem*, 291, 12991-3004.
- YANG-SNYDER, J., MILLER, J. R., BROWN, J. D., LAI, C. J. & MOON, R. T. 1996. A frizzled homolog functions in a vertebrate Wnt signaling pathway. *Curr Biol*, 6, 1302-6.
- YAQUB, T., TIKHONOVA, I. G., LÄTTIG, J., MAGNAN, R., LAVAL, M., ESCRIEUT, C., BOULÈGUE, C., HEWAGE, C. & FOURMY, D. 2010. Identification of Determinants of Glucose-Dependent Insulinotropic Polypeptide Receptor That Interact with N-Terminal Biologically Active Region of the Natural Ligand. *Molecular Pharmacology*, 77, 547.
- ZAIDI, M., MOONGA, B. S. & ABE, E. 2002. Calcitonin and bone formation: a knockout full of surprises. *J Clin Invest*, 110, 1769-71.
- ZHANG, H., QIAO, A., YANG, D., YANG, L., DAI, A., DE GRAAF, C., REEDTZ-RUNGE, S., DHARMARAJAN, V., ZHANG, H., HAN, G. W., GRANT, T. D., SIERRA, R. G., WEIERSTALL, U., NELSON, G., LIU, W., WU, Y., MA, L., CAI, X., LIN, G., WU, X., GENG, Z., DONG, Y., SONG, G., GRIFFIN, P. R., LAU, J., CHEREZOV, V., YANG, H., HANSON, M. A., STEVENS, R. C., ZHAO, Q., JIANG, H., WANG, M.-W. & WU, B. 2017a. Structure of the full-length glucagon class B G-protein-coupled receptor. *Nature*, 546, 259-264.
- ZHANG, H., QIAO, A., YANG, L., VAN EPS, N., FREDERIKSEN, K. S., YANG, D., DAI, A., CAI, X., ZHANG, H., YI, C., CAO, C., HE, L., YANG, H., LAU, J., ERNST, O. P., HANSON, M. A., STEVENS, R. C., WANG, M.-W., REEDTZ-RUNGE, S., JIANG, H., ZHAO, Q. & WU, B. 2018. Structure of the glucagon receptor in complex with a glucagon analogue. *Nature*, 553, 106.
- ZHANG, Y., SUN, B., FENG, D., HU, H., CHU, M., QU, Q., TARRASCH, J. T., LI, S., SUN KOBILKA, T., KOBILKA, B. K. & SKINIOTIS, G. 2017b. Cryo-EM structure of the activated GLP-1 receptor in complex with a G protein. *Nature*, 546, 248-253.
- ZHANG, Z., HERNANDEZ-LAGUNAS, L., HORNE, W. C. & BARON, R. 1999. Cytoskeleton-dependent tyrosine phosphorylation of the p130(Cas) family member HEF1 downstream of the G protein-coupled calcitonin receptor. Calcitonin induces the association of HEF1, paxillin, and focal adhesion kinase. *J Biol Chem*, 274, 25093-8.
- ZOLNIEROWICZ, S., CRON, P., SOLINAS-TOLDO, S., FRIES, R., LIN, H. Y. & HEMMINGS, B. A. 1994. Isolation, characterization, and chromosomal localization of the porcine calcitonin receptor gene. Identification of two variants of the receptor generated by alternative splicing. *J Biol Chem*, 269, 19530-8.

APPENDIX 1

Supplementary Table 1. DNA sequence hCTRaLeu variant. Highlighted in magenta is the cMyc tag.

1	ATG	AGG	TTC	ACA	TTT	ACA	AGC	CGG	TGC	TTG	GCA	CTG	TTT	CTT	CTT	CTA
17	AAT	CAC	CCA	ACC	CCA	ATT	CTG	CCT	GAG	CAG	AAG	CTT	ATC	AGC	GAG	GAG
33	GAC	CTG	GCC	TTT	TCA	AAT	CAA	ACC	TAT	CCA	ACA	ATA	GAG	CCC	AAG	CCA
49	TTT	CTT	TAC	GTC	GTA	GGA	CGA	AAG	AAG	ATG	ATG	GAT	GCA	CAG	TAC	AAA
65	TGC	TAT	GAC	CGA	ATG	CAG	CAG	TTA	CCC	GCA	TAC	CAA	GGA	GAA	GGT	CCA
81	TAT	TGC	AAT	CGC	ACC	TGG	GAT	GGA	TGG	CTG	TGC	TGG	GAT	GAC	ACA	CCG
97	GCT	GGA	GTA	TTG	TCC	TAT	CAG	TTC	TGC	CCA	GAT	TAT	TTT	CCG	GAT	TTT
113	GAT	CCA	TCA	GAA	AAG	GTT	ACA	AAA	TAC	TGT	GAT	GAA	AAA	GGT	GTT	TGG
129	TTT	AAA	CAT	CCT	GAA	AAC	AAT	CGA	ACC	TGG	TCC	AAC	TAT	ACT	ATG	TGC
145	AAT	GCT	TTC	ACT	CCT	GAG	AAA	CTG	AAG	AAT	GCA	TAT	GTT	CTG	TAC	TAT
161	TTG	GCT	ATT	GTG	GGT	CAT	TCT	TTG	TCA	ATT	TTC	ACC	CTA	GTG	ATT	TCC
177	CTG	GGG	ATT	TTC	GTG	TTT	TTC	AGG	AGC	CTT	GGC	TGC	CAA	AGG	GTA	ACC
193	CTG	CAC	AAG	AAC	ATG	TTT	CTT	ACT	TAC	ATT	CTG	AAT	TCT	ATG	ATT	ATC
209	ATC	ATC	CAC	CTG	GTT	GAA	GTA	GTA	CCC	AAT	GGA	GAG	CTC	GTG	CGA	AGG
225	GAC	CCG	GTG	AGC	TGC	AAG	ATT	TTG	CAT	TTT	TTC	CAC	CAG	TAC	ATG	ATG
241	GCC	TGC	AAC	TAT	TTC	TGG	ATG	CTC	TGT	GAA	GGG	ATC	TAT	CTT	CAT	ACA
257	CTC	ATT	GTC	GTG	GCT	GTG	TTT	ACT	GAG	AAG	CAA	CGC	TTG	CGG	TGG	TAT
273	TAT	CTC	TTG	GGC	TGG	GGG	TTC	CCG	CTG	GTG	CCA	ACC	ACT	ATC	CAT	GCT
289	ATT	ACC	AGG	GCC	GTG	TAC	TTC	AAT	GAC	AAC	TGC	TGG	CTG	AGT	GTG	GAA
305	ACC	CAT	TTG	CTT	TAC	ATA	ATC	CAT	GGA	CCT	GTC	ATG	GCG	GCA	CTT	GTG
321	GTC	AAT	TTC	TTC	TTT	TTG	CTC	AAC	ATT	GTC	CGG	GTG	CTT	GTG	ACC	AAA

337 ATG AGG GAA ACC CAT GAG GCG GAA TCC CAC ATG TAC CTG AAG GCT
 GTG
 353 AAG GCC ACC ATG ATC CTT GTG CCC CTG CTG GGA ATC CAG TTT GTC
 GTC
 369 TTT CCC TGG AGA CCT TCC AAC AAG ATG CTT GGG AAG ATA TAT GAT
 TAC
 385 GTG ATG CAC TCT CTG ATT CAT TTC CAG GGC TTC TTT GTT GCG ACC
 ATC
 401 TAC TGC TTC TGC AAC AAT GAG GTC CAA ACC ACC GTG AAG CGC CAA
 TGG
 417 GCC CAA TTC AAA ATT CAG TGG AAC CAG CGT TGG GGG AGG CGC CCC
 TCC
 433 AAC CGC TCT GCT CGC GCT GCA GCC GCT GCT GCG GAG GCT GGC GAC
 ATC
 449 CCA ATT TAC ATC TGC CAT CAG GAG CTG AGG AAT GAA CCA GCC AAC
 AAC
 465 CAA GGC GAG GAG AGT GCT GAG ATC ATC CCT TTG AAT ATC ATA GAG
 CAA
 481 GAG TCA TCT GCT TGA

Supplementary Table 2. Amino acid sequence of the hCTRaLeu variant. Highlighted in magenta is the cMyc tag.

```

1  M R F T F T S R C L A L F L L L N H P T P I L P E Q K L I S E
E
33 D L A F S N Q T Y P T I E P K P F L Y V V G R K K M M D A Q Y
K
65 C Y D R M Q Q L P A Y Q G E G P Y C N R T W D G W L C W D D T
P
97 A G V L S Y Q F C P D Y F P D F D P S E K V T K Y C D E K G V
W
129 F K H P E N N R T W S N Y T M C N A F T P E K L K N A Y V L Y
Y
161 L A I V G H S L S I F T L V I S L G I F V F F R S L G C Q R V
T
193 L H K N M F L T Y I L N S M I I I I H L V E V V P N G E L V R
R
225 D P V S C K I L H F F H Q Y M M A C N Y F W M L C E G I Y L H
T
257 L I V V A V F T E K Q R L R W Y Y L L G W G F P L V P T T I H
A
289 I T R A V Y F N D N C W L S V E T H L L Y I I H G P V M A A L
V
321 V N F F F L L N I V R V L V T K M R E T H E A E S H M Y L K A
V
353 K A T M I L V P L L G I Q F V V F P W R P S N K M L G K I Y D
Y
385 V M H S L I H F Q G F F V A T I Y C F C N N E V Q T T V K R Q
W
417 A Q F K I Q W N Q R W G R R P S N R S A R A A A A A A E A G D
I
449 P I Y I C H Q E L R N E P A N N Q G E E S A E I I P L N I I E
Q
481 E S S A

```

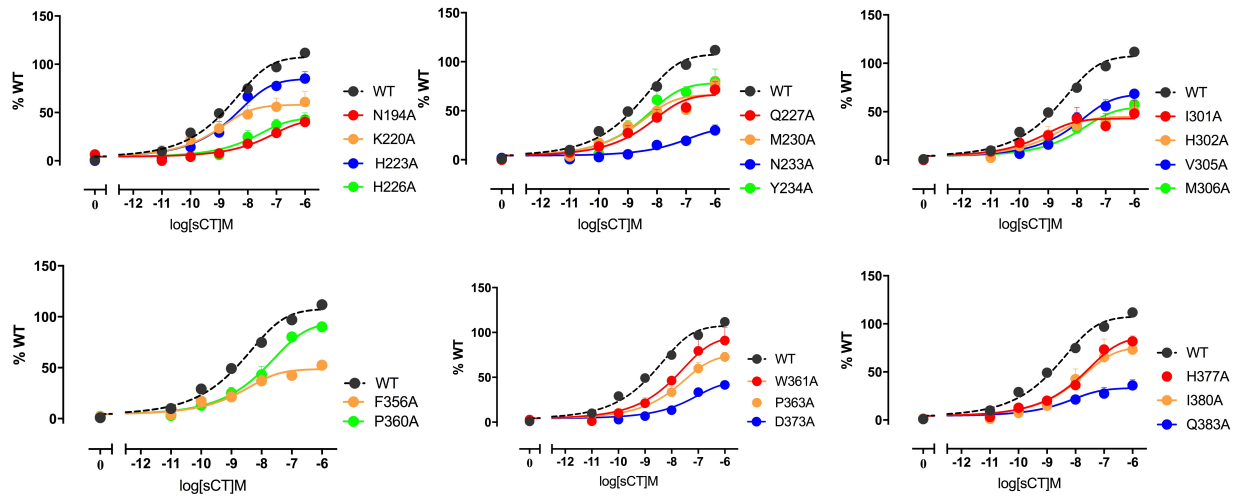
Supplementary Table 3. Nucleotide sequence of the primers used to confirm single point mutations introduced into CALCR gene.

Sequencing primer:	Nucleotide sequence:
pENTR11 forward	AGGCTTCGAAGGAGATAGAACC
pENTR11 reverse	GTGCAATGTAACATCAGAGATTTTGAG
BGH	CAACTAGAAGGCACAGTCGAGGCTGAT
T7	TAATACGACTCACTATAGGG

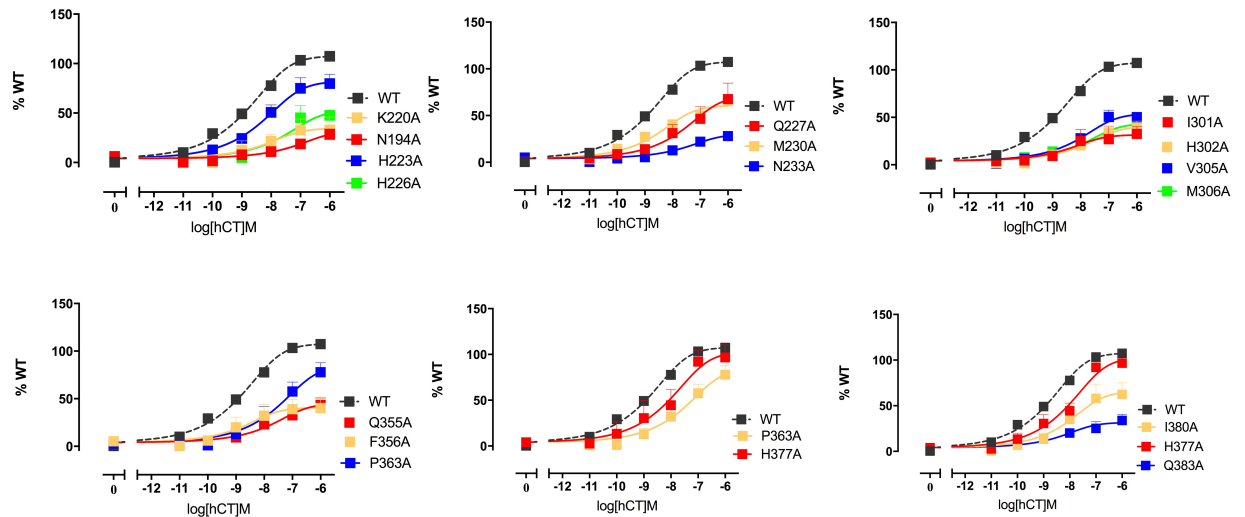
Supplementary Table 4. Nucleotide sequence of the primers used to introduce single point mutations into CALCR gene.

Residue location:	Residue:	Primer Nucleotide sequence:
TM1	T138A (T ^{2.29} A)	Forward: CTATGTGCAATGCTTTCGCTCCTGAGAACTGAAG Reverse: CTTCAAGTTTCTCAGGAGCGAAAGCATTGCACATAG
	K141A (K ^{1.32} A)	Forward: CAATGCTTTCCTCCTGAGGCACTGAAGAATGCATATGTTT Reverse: GAACATATGCATTCTTCAGTGCCTCAGGAGTGAAAGCATTG
	A145L (A ^{1.36} L)	Forward: CCTGAGAACTGAAGAATCTATATGTTCTGTAC Reverse: GTACAGAACATATAGAATCTTCAGTTTCTCAGG
	A145S (A ^{1.36} S)	Forward: CCTGAGAACTGAAGAATTCATATGTTCTGTAC Reverse: GTACAGAACATATGAAATCTTCAGTTTCTCAGG
	Y149A (Y ^{1.40} A)	Forward: GAAGAATGCATATGTTCTGGCCTATTTGGCTATTGTGGG Reverse: CCCACAATAGCCAAATAGGCCAGAACATATGCATTCTTC
	A152L (A ^{1.43} L)	Forward: CTGTACTATTTGCTTATTGTGGGTCATTC Reverse: GAATGACCCACAATAAGCAAATAGTACAG
	A152S (A ^{1.43} S)	Forward: CTGTACTATTTGTCTATTGTGGGTC Reverse: GACCCACAATAGACAAATAGTACAG
	H156A (H ^{1.47} A)	Forward: CTATTGTGGGTGCTTCTTTGTCAATTTTC Reverse: GAAAATTGACAAAGAAGCACCCACAATAG
TM2	Y191A (Y ^{2.57} A)	Forward: CATGTTTCTTACTGCCATTCTGAATTCTATG Reverse: CATAGAATTCAGAATGGCAGTAAGAAACATG
	N194A (N ^{2.60A})	Forward : CTTACATTCTGGCTTCTATGATTATCATC Reverse: GATGATAATCATAGAAGCCAGAATGTAAG
	I198A (I ^{2.64} A)	Forward: GAATTCTATGATTGCCATCATCCACCTGG Reverse: CCAGGTGGATGATGGCAATCATAGAATTC
	H201A (H ^{2.67} A)	Forward: GATTATCATCATCGCCCTGGTTGAAGTAG Reverse: CTAATTCAACCAGGGCGATGATGATAATC
	L202A (L ^{2.68} A)	Forward: CTATGATTATCATCATCCACGCGTTGAAGTAGTACCCAATG Reverse: CATTGGGTACTACTTCAACCGCGTGGATGATGATAATCATAG
	V205A (V ^{2.71} A)	Forward: CACCTGGTTGAAGCAGTACCCAATGGAG Reverse: CTCCATTGGGTACTGCTTCAACCAGGTG
TM3	K220A (K ^{3.30} A)	Forward: CGGTGAGCTGCGCCATTTTGCATTTTTC Reverse: GAAAAAATGCAAAATGGCGCAGCTCACCG
	H223A (H ^{3.33} A)	Forward: GCAAGATTTTGGCTTTTTTCCACCAGTAC Reverse: GTACTGGTGGAAGGAAAGCCAAAATCTTGC

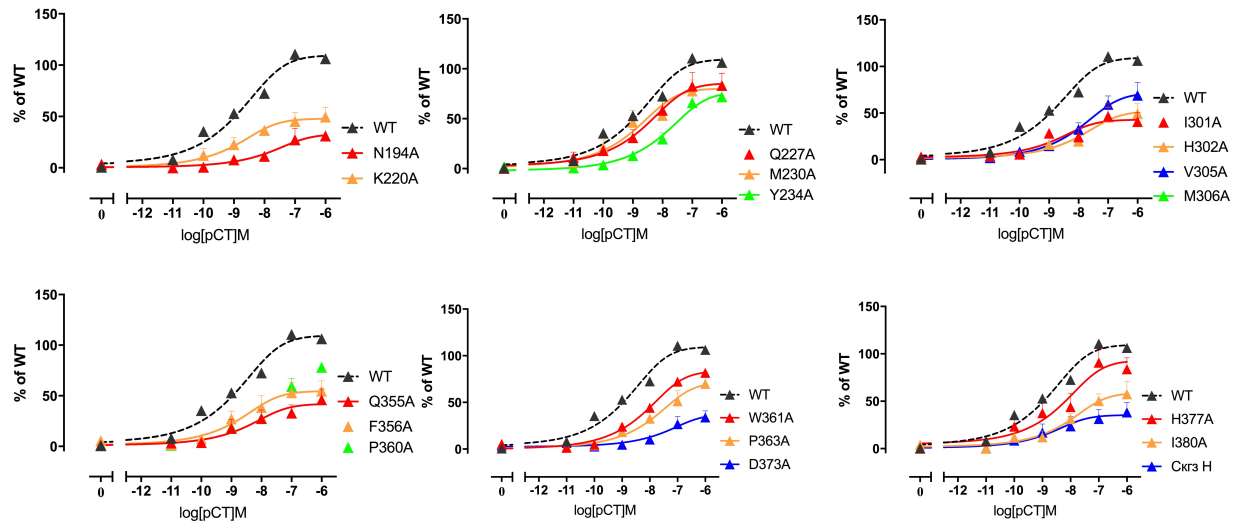
	H226A (H ^{3.36} A)	Forward: GATTTTGCATTTTTTCGCCAGTACATGATG Reverse: CATCATGTACTGGGCGAAAAAATGCAAAATC
	Q227A (Q ^{3.37} A)	Forward: GATTTTGCATTTTTTCCACGCTTACATGATGGCC Reverse: GCCATCATGTAAAGCGTGAAAAAATGCAAAATC
	M230A (M ^{3.40} A)	Forward: CACCAGTACATGGCCGCTGCAACTATTTC Reverse: GAAATAGTTGCAGGCGGCCATGTACTGGTG
	N233A (N ^{3.43} A)	Forward: CATGATGGCCTGCGCCTATTTCTGGATG Reverse: CATCCAGAAATAGGCGCAGGCCATCATG
	Y234A (Y ^{3.44} A)	Forward: GATGGCCTGCAACGCTTTCTGGATGCTC Reverse: CATCCAGAAATAGGCGCAGGCCATCATG
TM5	I301A (I ^{5.39} A)	Forward: CATTTGCTTTACATAGCCCATGGACCTGTC Reverse: GACAGGTCCATGGGCTATGTAAAGCAAATG
	H302A (H ^{5.40} A)	Forward: GCTTTACATAATCGCTGGACCTGTCATGG Reverse: CCATGACAGGTCCAGCGATTATGTAAAGC
	V305A (V ^{5.43} A)	Forward: CCATGGACCTGCTATGGCGGCACTTG Reverse: CAAGTGCCGCCATAGCAGGTCCATGG
	M306A (M ^{5.44} A)	Forward: CCATGGACCTGTCGCTGCGGCACTTGTGGTC Reverse: GACCACAAGTGCCGCAGCGACAGGTCCATGG
TM6	Q355A (Q ^{6.52} A)	Forward: CTGCTGGGAATCGCCTTTGTCGTCTTTC Reverse: GAAAGACGACAAAGGCGATTCCCAGCAG
	F356A (F ^{6.53} A)	Forward: CTGCTGGGAATCCAGGCTGTCGTCTTTCCTG Reverse: CAGGGAAAGACGACAGCCTGGATTCCCAGCAG
	F359A (F ^{6.56} A)	Forward: GAATCCAGTTTGTCTGCTCCCTGGAGACCTTCC Reverse: GGAAGGTCTCCAGGGAGCGACGACAACTGGATTCC
	P360A (P ^{6.57} A)	Forward: GTTTGTCTGCTTTTGCCTGGAGACCTTCC Reverse: GGAAGGTCTCCAGGCAAAGACGACAAAC
	W361A (W ^{6.58} A)	Forward: GTTTGTCTGCTTTTCCCGCGAGACCTTCCAACAAG Reverse: CTTGTTGGAAGGTCTCGCGGAAAGACGACAAAC
	P363A (P ^{6.60} A)	Forward: GTCTTTCCCTGGAGAGCTTCCAACAAGATG Reverse: CATCTTGTTGGAAGCTCTCCAGGGAAAGAC
TM7	D373A (D ^{7.39} A)	Forward: CTTGGGAAGATATATGCTTACGTGATGCACTC Reverse: GAGTGCATCACGTAAGCATATATCTTCCCAAG
	M376A (M ^{7.42} A)	Forward: GAAGATATATGATTACGTGGCGCACTCTCTGATTCAATTC Reverse: GAAATGAATCAGAGAGTGCGCCACGTAATCATATATCTTC
	H377A (H ^{7.43} A)	Forward: TTACGTGATGgccTCTCTGATTCAATTC Reverse: GAAATGAATCAGAGAggcCATCACGTAA
	I380A (I ^{7.46} A)	Forward: GATGCACTCTCTGGCTCATTTCCAGGG Reverse: CCCTGGAAATGAGCCAGAGAGTGCATC
	Q383A (Q ^{7.49} A)	Forward: CTCTGATTCAATTCGCCGGCTTCTTTGTTGC Reverse: GCAACAAAGAAGCCGGCGAAATGAATCAGAG



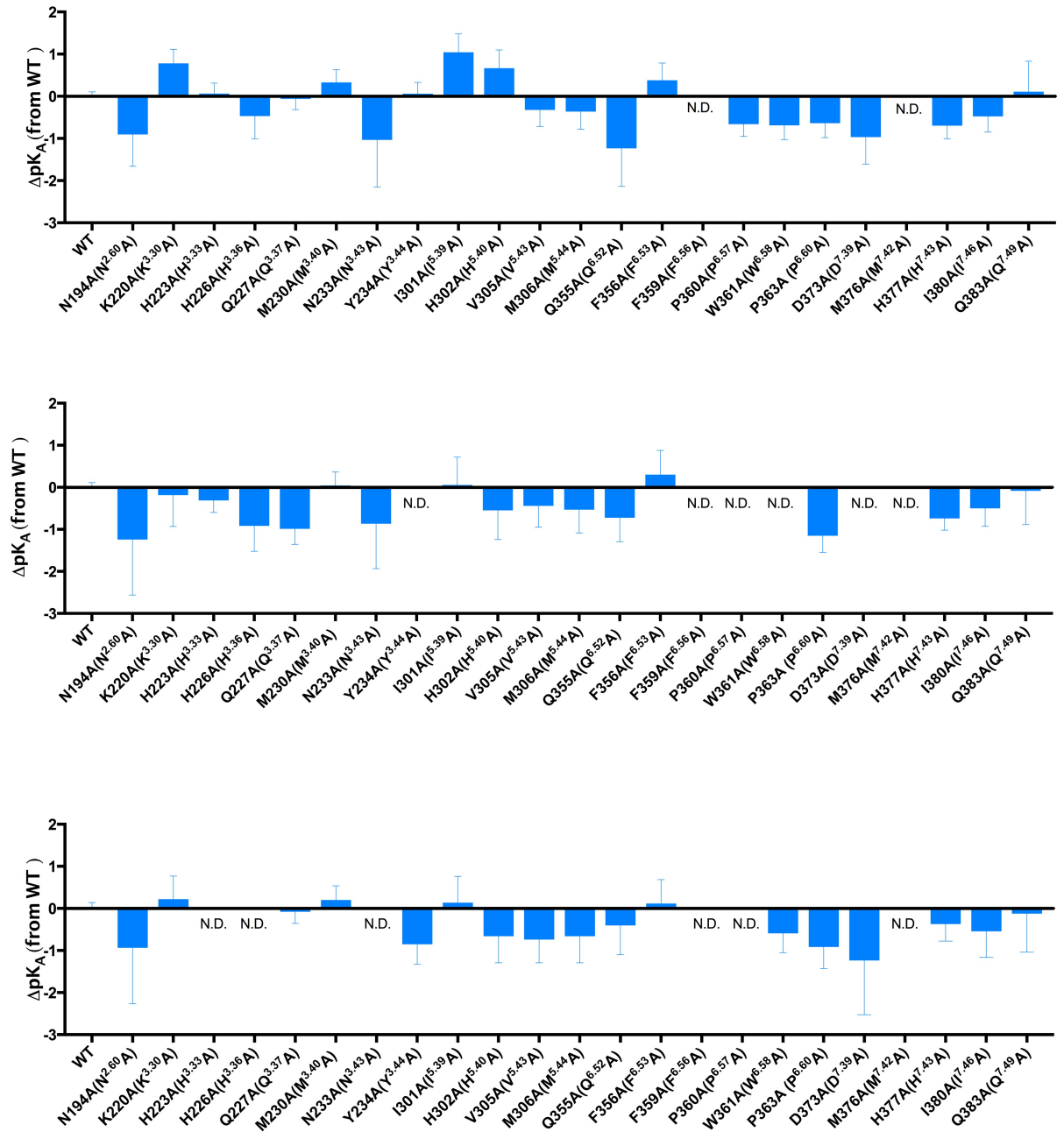
Supplementary figure 1. Alternative fit of Black and Leff operational model for pERK1/2 concentration response to sCT in CV-1-FlpIn cells stably expressing hCTRaLeu mutations in the receptor TM region. pERK1/2 response in the presence of sCT was fit using Black and Leff operational model with hill slope $n=0.4$ and normalized to WT receptor response. All values are mean \pm S.E.M. of 3 to 5 independent experiments conducted in duplicate; for some data points error bars are not shown as they are smaller than the height of the symbol.



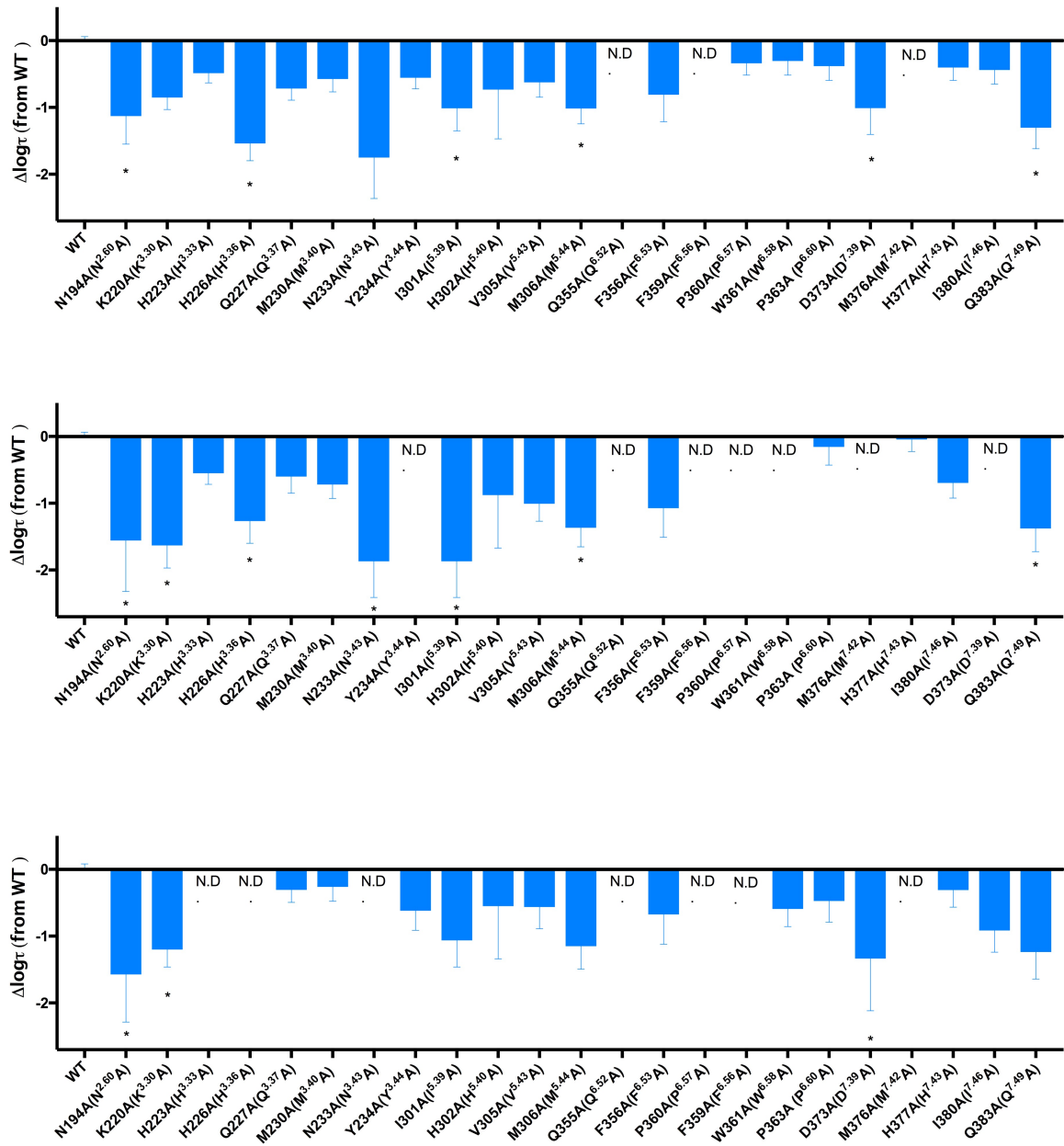
Supplementary figure 2. Alternative fit of Black and Leff operational model for pERK1/2 concentration response to hCT in CV-1-FlpIn cells stably expressing hCTRaLeu mutations in the receptor TM region. pERK1/2 response in the presence of hCT was fit using Black and Leff operational model with hill slope $n=0.4$ and normalized to WT receptor response. All values are mean \pm S.E.M. of 3 to 5 independent experiments conducted in duplicate; for some data points error bars are not shown as they are smaller than the height of the symbol.



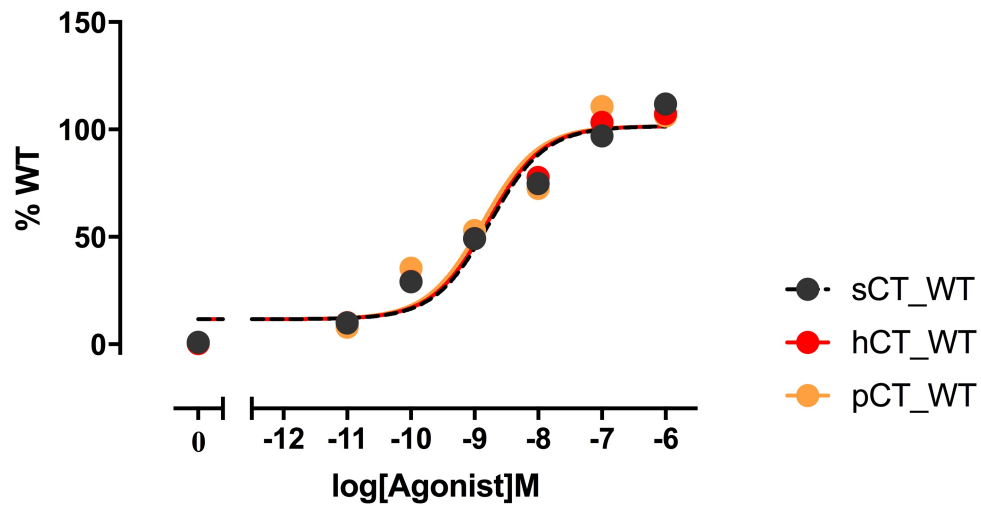
Supplementary figure 3. Alternative fit of Black and Leff operational model for pERK1/2 concentration response to pCT in CV-1-FlpIn cells stably expressing hCTRaLeu mutations in the receptor TM region. pERK1/2 response in the presence of sCT was fit using Black and Leff operational model with hill slope $n=0.4$ and normalized to WT receptor response. All values are mean \pm S.E.M. of 3 to 5 independent experiments conducted in duplicate; for some data points error bars are not shown as they are smaller than the height of the symbol.



Supplementary figure 4. pERK1/2 ΔpK_A values for CT agonists (sCT, hCT and pCT) calculated based on the alternative fit for the Black and Leff operational model with $n=0.4$ (as per supplementary figures 1-3). ΔpK_A value for each mutant was obtained by subtracting WT pK_A from each mutant's pK_A value. All values are mean \pm S.E.M. of 3 to 5 independent experiments conducted in duplicate. Significance of changes were calculated via comparison of mutants pK_A to the WT receptor pK_A values in a one-way analysis of variance (ANOVA) with Dunett's post-hoc test with significant changes ($P < 0.05$ denoted by *).



Supplementary figure 5. pERK1/2 $\Delta\log\tau$ CT agonists (sCT, hCT and pCT) calculated based on the alternative fit for the operational model with $n=0.4$ (as per supplementary figures 1-3) . $\Delta\log\tau_c$ value for each mutant was obtained by subtracting WT $\log\tau$ from each mutant's $\log\tau_c$ value. All values are mean \pm S.E.M. of 3 to 5 independent experiments conducted in duplicate. Significance of changes were calculated via comparison of mutants $\log\tau$ to the WT receptor $\log\tau$ values in a one-way analysis of variance (ANOVA) with Dunnett's post-hoc test with significant changes ($P < 0.05$ denoted by *).



Supplementary figure 6. Fitting of Black and Leff operational model with $n=1$ for pERK1/2 concentration response to WT sCT, hCT and pCT in CV-1-FlpIn cells stably expressing hCTRaLeu mutations in the receptor TM region. pERK1/2 response for WT CTR in the presence of either sCT, hCT or pCT was fit using Black and Leff operational model with a hill slope $n=1$. All values are mean \pm S.E.M. of 3 to 5 independent experiments conducted in duplicate; for some data points error bars are not shown as they are smaller than the height of the symbol.

Class B (Wootten) residue numbering	2.60	3.43	5.40	6.52	7.52
CT receptor	N	N	H	Q	Q
Calcitonin receptor-like receptor	N	N	H	E	Q
CRF1 receptor	R	N	Q	T	Q
CRF2 receptor	R	N	Q	T	Q
GHRH receptor	R	N	K	H	Q
GIP receptor	R	N	R	H	Q
GLP-1 receptor	R	N	R	H	Q
GLP-2 receptor	R	N	R	H	H
Glucagon receptor	R	N	R	H	Q
Secretin receptor	R	N	R	H	Q
PTH1 receptor	R	N	Q	H	Q
PTH2 receptor	R	N	Q	H	Q
PAC1 receptor	R	N	K	H	Q
VPAC1 receptor	R	N	K	H	Q
VPAC2 receptor	R	N	R	H	Q
Consensus	R	N	R	H	Q

Supplementary figure 7. Class B GPCRs select TM residues sequence alignment showing the nature of amino acid properties. The alignment is based on Class B GPCRs TM and H8 sequence alignment (adopted from (Liang et al., 2018)). Chemically similar amino acids are of the same colour. The colour scheme is according to default settings in GPCRdb (<http://gpcrdb.org/>): polar positively charged amino acids are coloured in blue and light-blue, polar negatively charged amino acids are coloured in red; polar neutral amino acids are coloured in purple. The consensus sequence is displayed at the bottom of the alignment.

APPENDIX 2

Expression and activity of the calcitonin receptor family in a sample of primary human high-grade gliomas

(Additional Files)

Supplementary Figure 1

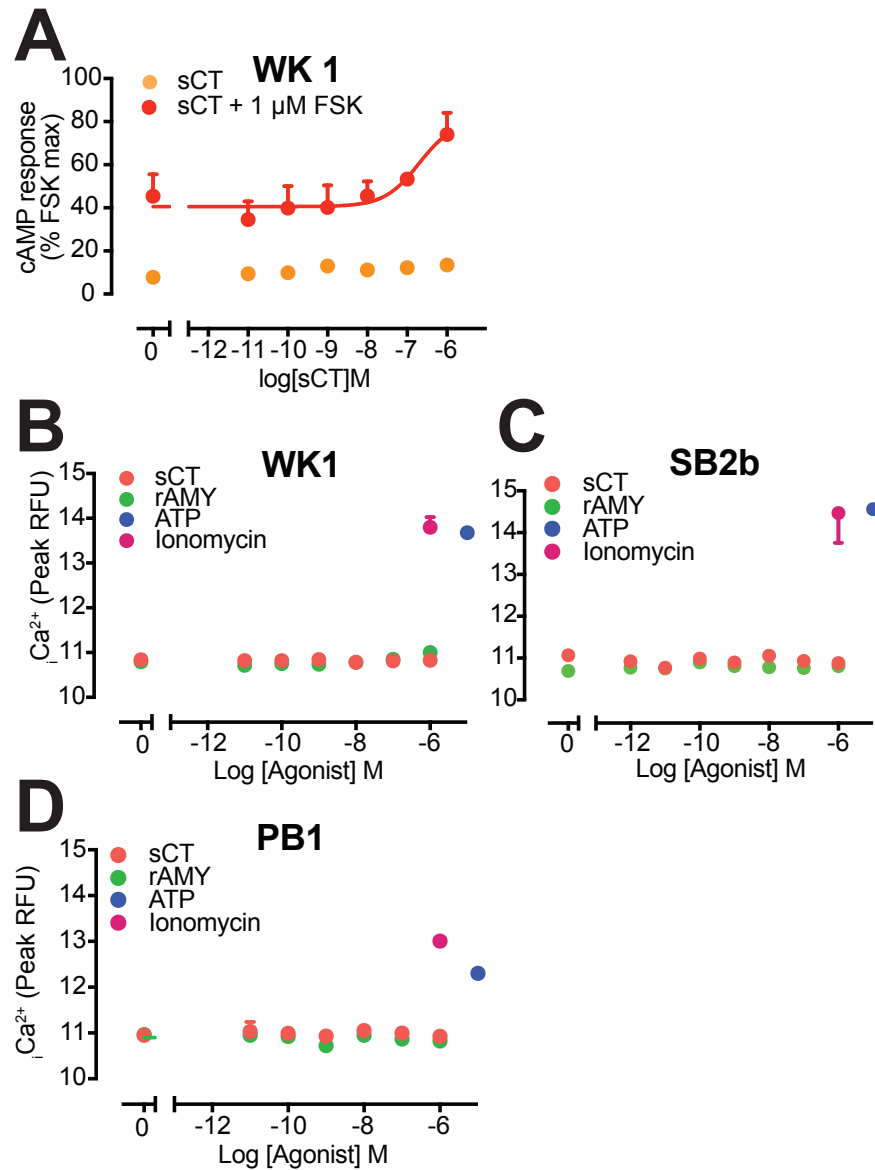


Figure S1. cAMP and iCa^{2+} mobilization in response to CTR agonists. A, Characterization of cAMP accumulation (30 min) in WK1 cells in response to stimulation by sCT alone or in presence of 1 μ M forskolin. Data are presented as mean \pm S.E.M. of 3 replicates of a representative experiment. Absence of intracellular calcium mobilization response to sCT and rAMY in WK1 (B), SB2b (C) and PB1(D) cell lines while maintaining robust response to 10 μ M ATP and 1 μ M ionomycin. Data are presented as peak values of response measured in relative fluorescence units. Data are presented as mean \pm or - S.E.M. of 3 replicates of a representative experiment.

Supplementary Figure 2

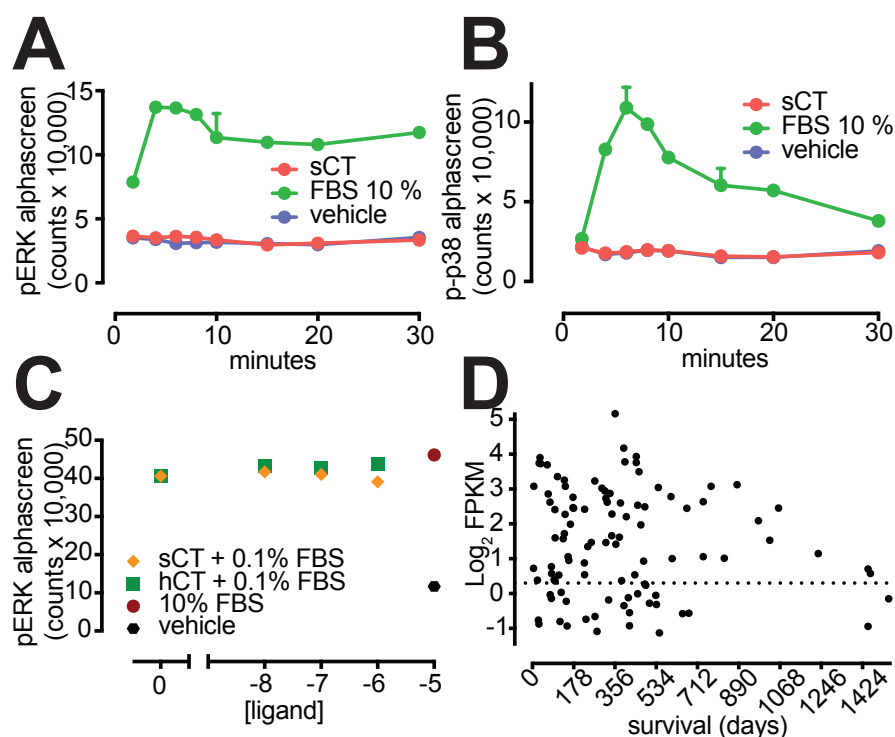


Figure S2. MAP kinase response to sCT in SB2b cells and TCGA survival data. No detectable ERK1/2 phosphorylation (A) or p38 (B) in response to stimulation with 1 μ M sCT in SB2b cell line while a robust response to 10% FBS is seen; Data are presented as mean + S.E.M. of 3 replicates of a representative experiment. (C) ERK1/2 Phosphorylation response in SB2b cell line was induced by 0.1% FBS. No suppression of the induced response after stimulation sCT or hCT was seen at the concentrations tested (C). Data are presented as mean + S.E.M. of 3 replicates of a representative experiment. (D) Log₂ expression (FPKM) of CALCR transcript in patients with survival data from the TCGA database plotted as a scatter plot against survival.

Supplementary Figure 3

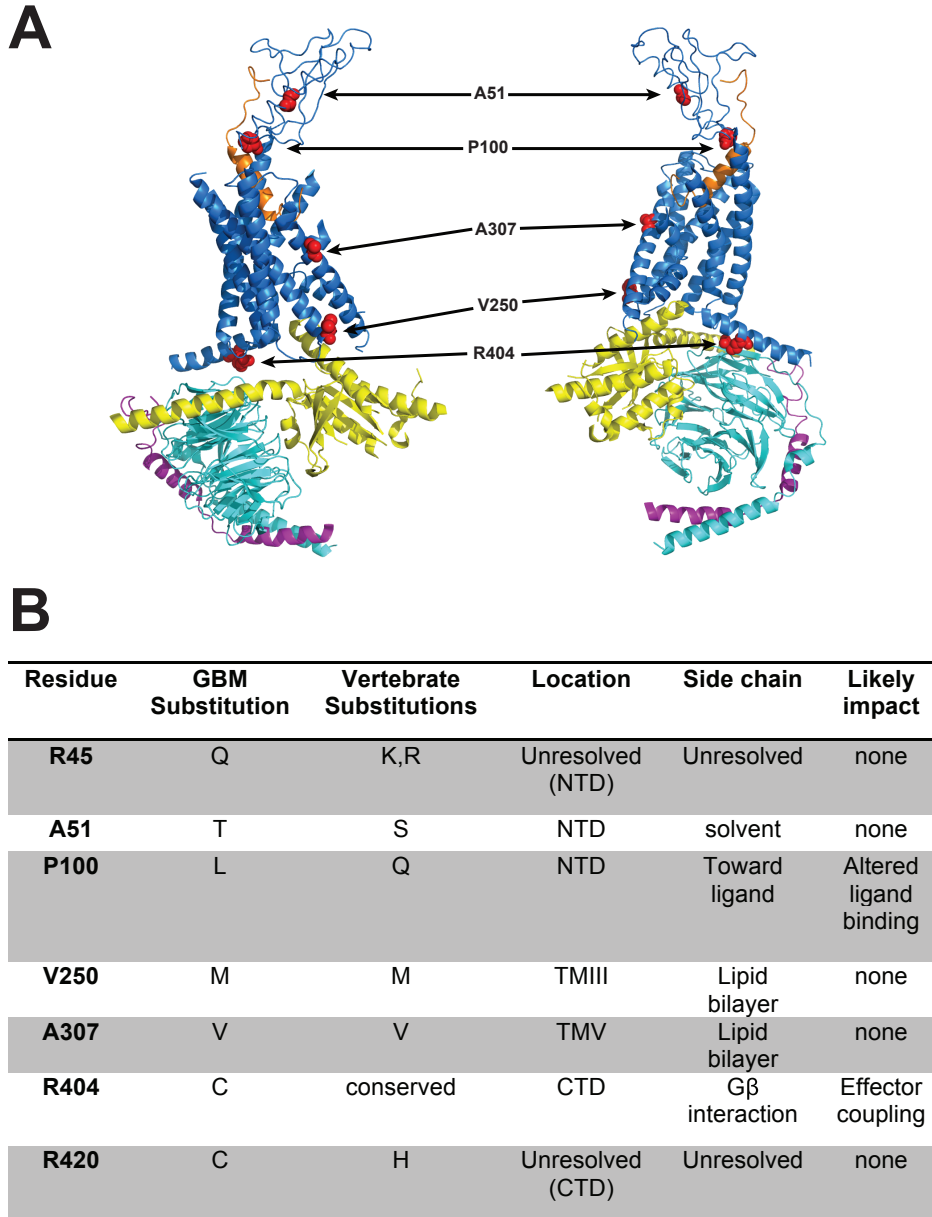


Figure S3. Mapping reported CTR mutations to our a molecular model of the CTR [48]. A, mutations reported to be associated with LOF at the CTR are shown in space fill red, mapped onto our active, G protein bound, model derived from Cryo-EM data,; the peptide (sCT) is shown in orange, receptor in blue, G α subunit in yellow, G β in teal and G γ in purple. B, the reported LOF residues, their substitution, mammalian conservation structural location, potential side-chain interaction and likely effect on receptor function are shown as a table.

Xenopus tropicalis	-----MKMVSSDVRDKTVRKHVEHCFL-VIVVIRMVPGFAST---VDP-TLMPIVNEEY	50	amphibian
Thamnophis sirtalis	-----MNKKSSG-YFLLIILLIRMAPSFPTTVSYVDP-TLESMT--EYS	39	
Anolis carolinensis	-----MDKKNNGCCLL-MILLIRMAPTSSSTVSYTDP-TLAPVATEHS	41	reptiles
Serinus canaria	-----MKKTQSCFLLI-ILLTRIVPSLSAVNYTDP-TLEPVVTENS	41	
Corvus brachyrhynchos	-----MKKTQSCFLLI-ILLTRIVPSLSSTVNYTDP-TLEPVVTENS	41	
Ficedula albicollis	-----MKKTQTCFLLI-ILLTRIVPSLSSTVNYTDP-TLEPVVTENS	41	
Anser cygnoides domesticus	-----MKKTTHSCFLLI-ILLIRMVPSLTATVNYTDP-TLEPVVTENS	41	
Anas platyrhynchos	-----MKKTTHGCFLLI-ILLIRMVPSLTATVNYTDP-TLEPVVTENS	41	
Apteryx australis mantelli	-----MKKTTHSCFLLI-ILLIRMVPSLTSTVNYTDP-TLEPVVTENS	41	
Gallus gallus	-----MKKTTHSCFLLI-ILLIRMVPSLTATVNYTDP-TLEPVVTENS	41	
Picoides pubescens	-----MKKTTHGCFLLV-ILLIRMVPSLSSTVNYTDP-TLEPLVTENS	41	
Chaetura pelagica	-----MKKTQSCILLI-ILLIRMVPSLSSTVNYTDP-TLEPVVTENS	41	
Apaloderma vittatum	-----MKKRTTHSCFLLI-ILLTRMVPSLSSTVNYTDP-TLEPVVTENS	41	
Balearica regulorum gibbericeps	-----MKKTTHSCFLLI-ILLIRMVPSLSSTVNYTDP-TLEPVVTENS	41	aves
Cuculus canorus	-----MKKTTHSCFLLV-ILLIKMVPTLSSTVNYTDP-TLEPVVTENS	41	
Caprimulgus carolinensis	-----MKKTTHSCFLI-IILLMRMVPSLSSTVNYTDP-TLEPVVTENS	41	
Calypte anna	-----MKKTAHSCILL-IILLIRMAPSLSTVNYTDP-TLEPVVTENS	41	
Pygoscelis adeliae	-----MKKTTHSCFLV-IILLIRMVSPSSTVNYTDP-TLEPVVTENS	41	
Egretta garzetta	-----MKKTTHICFLL-VILLIRMVPSLSSTVNYTDP-TLEPVVNENS	41	
Nipponia nippon	-----MKKVTHS-FLLIILLIRMVPSLSSTVNYTDP-TLEPVVTENS	41	
Charadrius vociferus	-----MVPSLSSTVNYTDP-TLEPVVTENS	24	
Aquila chrysaetos canadensis	-----MKKTTHSCFLLIIFLTRMVPSLSSTVNYTDP-TLEPVVTENS	42	
Phalacrocorax carbo	-----MVPSLSSTVNYTDP-TLEPVATENS	24	
Sus scrofa	-----MRFTLTRWCLTLFIFLNRPLPVLPSADGAHTPTLEPEFFLYI	43	
Mus musculus	-----MRFLLVNRFTLLLLLVSPPTVLPVQAPTNLTDG-GLDQEPFLYL	42	
Rattus norvegicus	MTPRSRMKRRNLKPKMRFLLLNRFTLLLLLVSPPTVLPVQAPTNLTDG-GLDQEPFLYL	59	
Jaculus jaculus	-----MKLSLTLRVAGLFILLNQPSALPYFSNFTLPTNEPEFFLYT	43	
Pteropus vampyrus	-----MKFTLTRWCFVLFIFLNHPTPVLPTSSNNTYSPALESPEFFLYV	43	
Cavia porcellus	-----MRFTFTTRQFLAFFILISNPASILPRSENLTFFP-TFEPEPYLYS	42	
Galeopterus variegatus	-----MRLRVTCRLALFVLLNHPTPILPAFSNQTFP-TLDSEPEFFLYI	42	mammals
Oryctolagus cuniculus	MAHLPPSRMKRDLQPKMKFTLTWRCFALFLLHQPTPVNPASSNDTHP-TVEPEFFLYV	59	
Colobus angolensis palliatus	-----MKFTFTRCFALFLLLNHPILPAFSNQTFP-TIEPEFFLYV	42	
Homo sapiens	-----MRFTFTRCFALFLLLNHPILPAFSNQTFP-TIEPKPFLLYV	42	
Pan troglodytes	-----MRFTFTRCFALFLLLNHPILPAFSNQTFP-TIEPEFFLYV	42	
Canis lupus familiaris	-----MKFTLTRRCLVLFIFLNHPTPVLPAFSNDTYPPNMESEFFLYV	43	
Equus caballus	-----MKFSLTRRCLVLFIFLNHPTPILPASSNDTYPPNMESEFFLYV	43	
Ceratotherium simum simum	-----MKFSLTRRCLVLFIFLNHPTPILPAFSNDTYPPNMESEFFLYV	43	

Species	Sequence	Position	Class
Xenopus_tropicalis	DPTERASKYCDENGWNFQHPESNRTWSNYTLCNSPTSEKLKMAIILYYMAIVGHALSIVS	170	amphibian
Thamnophis_sirtalis	DPTEIATKYCDKTGTWFRHPENRTWSNYKRCNSPTNEKKRMIFIVYMTIAGHVLMSVS	159	
Anolis_carolinensis	DPETATKYCDKTGTWFRHPESNRTWSNYTRCNSPTNEKKRMVFILYYMTIVGHALSITS	161	reptiles
Serinus_canaria	DPTERASKYCDGTGNWFRHPESNRTWSNYTLCNSPTSEKLKMAFILYYMAIVGHALSITS	161	
Corvus_brachyrhynchus	DPTERASKYCDGTGNWFRHPESNRTWSNYTLCNSPTSEKLKMAFILYYMAIVGHALSITS	161	
Ficedula_albicollis	DPTERASKYCDGTGNWFRHPESNRTWSNYTLCNSPTSEKLKMAFILYYMAIVGHALSITS	161	
Anser_cygnoides_domesticus	DPTERASKYCDGTGNWFRHPESNRTWSNYTLCNSPTSEKLKMAFILYYMAIVGHALSITS	161	
Anas_platyrhynchus	DPTERASKYCDGTGNWFRHPESNRTWSNYTLCNSPTSEKLKMAFILYYMAIVGHALSITS	161	
Apteryx_australis_mantelli	DPTERASKYCDGTGNWFRHPESNRTWSNYTLCNSPTSEKLKMAFILYYMAIVGHALSITS	161	
Gallus_gallus	DPTERASKYCDGTGNWFRHPESNRTWSNYTLCNSPTSEKLKMAFILYYMAIVGHALSITS	161	
Picoides_pubescens	DPTERASKYCDGTGNWFRHPESNRTWSNYTLCNSPTSEKLKMAFILYYMAIVGHALSITS	161	
Chaetura_pelagica	DPTERASKYCDENGWNFQHPESNRTWSNYTLCNSPTSEKLKMAFILYYMAIVGHALSITS	161	
Apaloderma_vittatum	DPTERASKYCDGTGNWFRHPESNRTWSNYTLCNSPTSEKLKMAFILYYMAIVGHALSITS	161	aves
Balearica_regulorum_gibbericeps	DPTERASKYCDGTGNWFRHPESNRTWSNYTLCNSPTSEKLKMAFILYYMAIVGHALSTAS	161	
Cuculus_canorus	DPTERASKYCDGTGNWFRHPESNRTWSNYTLCNSPTSEKLKMAFILYYMAIVGHALSTAS	161	
Caprimulgus_carolinensis	DPTERASKYCDGTGNWFRHPESNRTWSNYTLCNSPTSEKLKMAFILYYMAIVGHALSITS	161	
Calypte_anna	DPTERASKYCDGTGNWFRHPESNRTWSNYTLCNSPTSEKLKMAFILYYMAIVGHALSITS	161	
Pygoccelis_adeliae	DPTERASKYCDGTGNWFRHPESNRTWSNYTLCNSPTSEKLKMAFILYYMAIVGHALSITS	161	
Egretta_garzetta	DPTERASKYCDGTGNWFRHPESNRTWSNYTLCNSPTSEKLKMAFILYYMAIVGHALSITS	161	
Nipponia_nippon	DPTERASKYCDGTGNWFRHPESNRTWSNYTLCNSPTSEKLKMAFILYYMAIVGHALSITS	161	
Charadrius_vociferus	DPTERASKYCDGTGNWFRHPESNRTWSNYTLCNSPTSEKLKMAFILYYMAIVGHALSITS	144	
Aquila_chrysaetos_canadensis	DPTERASKYCDGTGNWFRHPESNRTWSNYTLCNSPTSEKLKMAFILYYMAIVGHALSITS	162	
Phalacrocorax_carbo	DPTEARSKYCDGTGNWFRHPESNRTWSNYTLCNSPTSEKLKMAFILYYMAIVGHALSITS	144	
Sus_scrofa	DAAEKVTKYCGEDGDWYFRHPESNISWSNYTMCNAFTPDQKLNAYILYLYLAIVGHSLSILT	163	
Mus_musculus	DAEKVSKYCDENGGEWFRHPDSNRTWSNYTLCNAFTSEKLQNAVYVLYYLAIVGHSLSIAA	162	
Rattus_norvegicus	DPTEKVSKYCDENGGEWFRHPDSNRTWSNYTLCNAFTPDQKLNAYVLYYLAIVGHSMSIAA	179	
Jaculus_jaculus	DPAESVTKYCDENGWDWFRHPDSNRTWSNYTMCNAFTPDQKLNAYVLYYLAIVGHSLSIFT	163	
Pteropus_vampyrus	DPTEKATRYCDENGWDYKHPEYNRTWSNYSMCNAFTPEKLNAYVLYYLAIVGHSVSIAI	163	
Cavia_porcellus	DPTEKVTKYCDSEGVWFKHPENNRTWSNYTLCNAFTPEKLNAYVLYYLAIVGHSMSIIT	162	
Galeopterus_variegatus	DPTEKVTKYCDSEGVWFKHPENNRTWSNYTMCNAFTPEKLNAYVLYYLAIVGHSLSIFT	163	
Oryctolagus_cuniculus	DPTEKVTKYCDSEGVWFKHPGNNRTWSNYTMCNAFTPEKLNAYVLYYLAIVGHSLSIFT	179	mammals
Colobus_angolensis_palliatius	DPSEKVTKYCDENGWVFKHPENNRTWSNYTMCNAFTPEKLNAYVLYYLAIVGHSLSIFT	162	
Homo_sapiens	DPSEKVTKYCDSEGVWFKHPENNRTWSNYTMCNAFTPEKLNAYVLYYLAIVGHSLSIFT	162	
Pan_troglodytes	DPSEKVTKYCDSEGVWFKHPENNRTWSNYTMCNAFTPEKLNAYVLYYLAIVGHSLSIFT	162	
Canis_lupus_familiaris	DPSEKVTKYCDSEGVWFKHPENNRTWSNYTMCNAFTPEKLNAYVLYYLAIVGHSLSIFT	163	
Equus_caballus	DPAEKVTKYCDSEGVWFKHPENNRTWSNYTMCNAFTPEKLNAYVLYYLAIVGHSLSIFT	163	
Ceratotherium_simum_simum	DPAEKVTKYCDSEGVWFKHPENNRTWSNYTMCNAFTPEKLNAYVLYYLAIVGHSLSIFT	163	

Xenopus_tropicalis	LMISLGIFFFYFKSLSCQRITLHKNLF	TSYVLNSVFTIVHLTAVVPD	TDLVRSDPVSCVKL	230	amphibian
Thamnophis_sirtalis	LLISLGIFFFYFKSLSCQRITLHKNLF	CSYVLNSVFTLAHLIAVVPD	QELVKKDPISCKVL	219	reptiles
Anolis_carolinensis	LLISLGIFFFYFKSLSCQRITLHKNLF	FSYVLNSVFTLAHLIAVVS	DRDLVKNDPVSCVKL	221	
Serinus_canaria	LLISLAIFFFYFKSLSCQRITLHKNLF	FSYVLNSMFTIAHLIAVVPN	PGLVKRDPVSCVKL	221	
Corvus_brachyrhynchos	LLISLAIFFFYFKSLSCQRITLHKNLF	FSYVLNSMFTIAHLIAVVPN	PGLVKRDPVSCVKL	221	
Ficedula_albicollis	LLISLAIFFFYFKSLSCQRITLHKNLF	FSYVLNSMFTIAHLIVVVPN	PGLVKRDPVSCVKL	221	aves
Anser_cygnoides_domesticus	LLISLAIFFFYFKSLSCQRITLHKNLF	FSYVLNSVFTIAHLIAVVPN	PGLVKRDPVSCVKL	221	
Anas_platyrhynchos	LLISLAIFFFYFKSLSCQRITLHKNLF	FSYVLNSVFTIAHLIAVVPN	PGLVKRDPVSCVKL	221	
Apteryx_australis_mantelli	LLISLAIFFFYFKSLSCQRITLHKNLF	FSYVLNSVFTIAHLIAVVPN	PGLVKRDPVSCVKL	221	
Gallus_gallus	LLISLAIFFFYFKSLSCQRITLHKNLF	FSYVLNSMFTIAHLIVVVPN	PGLVKRDPVSCVKL	221	
Picoides_pubescens	LLISLAIFFFYFKSLSCQRITLHKNLF	FSYVLNSVFTIAHLIAVVPN	PGLVKRDPVSCVKL	221	
Chaetura_pelagica	LLISLAIFFFYFKSLSCQRITLHKNLF	FSYVLNSVFTIAHLIAVVPN	PGLVKRDPVSCVKL	221	
Apaloderma_vittatum	LLISLAIFFFYFKSLSCQRITLHKNLF	CSYVLNSVFTIAHLIAVVPN	PGLVKRDPVSCVKL	221	
Balearica_regulorum_gibbericeps	LLISLAIFFFYFKSLSCQRITLHKNLF	FSYVLNSMFTIAHLIAVVPN	PGLVKRDPVSCVKL	221	
Cuculus_canorus	LLISLAIFFFYFKSLSCQRITLHKNLF	FSYVLNSMFTIAHLIAVVPN	PGLVKRDPVSCVKL	221	
Caprimulgus_carolinensis	LLISLAIFFFYFKSLSCQRITLHKNLF	FSYVLNSMFTIAHLIAVVPN	PGLVKRDPVSCVKL	221	
Calypte_anna	LLISLAIFFFYFKSLSCQRITLHKNLF	FSYVLNSMFTIAHLIAVVPN	PGLVKRDPVSCVKL	221	
Pygoscelis_adeliae	LLISLAIFFFYFKSLSCQRITLHKNLF	FSYVLNSVFTIAHLIAVVPN	PGLVKRDPVSCVKL	221	
Egretta_garzetta	LLISLAIFFFYFKSLSCQRITLHKNLF	FSYVLNSVFTIAHLIAVVPN	PGLVKRDPVSCVKL	221	
Nipponia_nippon	LLISLAIFFFYFKSLSCQRITLHKNLF	FSYVLNSVFTIAHLIAVVPN	PGLVKRDPVSCVKL	221	
Charadrius_vociferus	LLISLAIFFFYFKSLSCQRITLHKNLF	FSYVLNSVFTIAHLIAVVPN	PGLVKRDPVSCVKL	204	
Aquila_chrysaetos_canadensis	LLISLAIFFFYFKSLSCQRITLHKNLF	FSYVLNSMFTIAHLIAVVPN	PGLVKRDPVSCVKL	222	
Phalacrocorax_carbo	LLISLAIFFFYFKSLSCQRITLHKNLF	FSYVLNSMFTIAHLIAVVPN	PDVKRDPVSCVKL	204	mammals
Sus_scrofa	LLISLGIFMFLRSIS	QQRVTLHKNMFLTYVLNSIII	IVHLVVI	223	
Mus_musculus	LVASMLIFWIFKNL	SCQRVTLHKNMFLTYILNSIII	IHLVEVVPNGDLVRRDPISCKVL	222	
Rattus_norvegicus	LIASMGIFLFFKNL	SCQRVTLHKNMFLTYILNSIII	IHLVEVVPNGDLVRRDPISCKIL	239	
Jaculus_jaculus	LVISLGIFVCFRSL	SCQRVTLHKNMFLTYILNSMII	IHLVEVVPNGDLVRRDPVSCKIL	223	
Pteropus_vampyrus	LVISLGIFMYFKSL	GCQRVTLHKNMFLTYILNSMII	IHLVEVVPNGELVRQDPVSCKIL	223	
Cavia_porcellus	LVVSLGIFVYFRSL	GCQRVTLHKNMFLTYILNSMII	IHLVEVVPNGELVRKDPVSCKIL	222	
Galeopterus_variegatus	LVISLGIFMFYRNL	SCQRVTLHKNMFLTYILNSMII	IHLVEVVPNGDLVRRDPVSCKIL	222	
Oryctolagus_cuniculus	LVISLGIFMCFRSL	GCQRVTLHKNMFLTYILNSMII	IHLVEVVPNGELVRRDPVSCVKL	239	
Colobus_angolensis_palliatu	LVISLGIFVFFKSL	GCQRVTLHKNMFLTYILNSMII	IHLVEVVPNGELVRRDPVSCKIL	222	
Homo_sapiens	LVISLGIFVFFRSL	GCQRVTLHKNMFLTYILNSMII	IHLVEVVPNGELVRRDPVSCKIL	222	
Pan_troglodytes	LVISLGIFVFFRSL	GCQRVTLHKNMFLTYILNSMII	IHLVEVVPNGELVRRDPVSCKIL	222	
Canis_lupus_familiaris	LVISLGIFVFFKSL	GCQRVTLHKNMFLTYILNSMII	IHLVEVVPNGELVRRDPLSCKIL	223	
Equus_caballus	LVISLGIFMFFKSL	GCQRVTLHKNMFLTYILNSMII	IHLVEVVPNGELVRRDPVSCKIL	223	
Ceratotherium_simum_simum	LVISLGIFVFFKSL	GCQRVTLHKNMFLTYILNSMII	IHLVEVVPNGELVRRDPVSCKIL	223	

TMI

TMII

Xenopus_tropicalis	QFFSQYMLGCNYFWMLCEGIYLHTLIVVAVFAEEQRLHWYLLGWGFPLVPASIHAFART	290	amphibian
Thamnophis_sirtalis	QFFHQYTMGCNYFWMLCEGIYLHTLIVVAVFAEEQRLHWYLLGWGFPLVPASIHAVARA	279	reptiles
Anolis_carolinensis	QFFHQYMMGCNYFWMLCEGIYLHTLIVVAVFAEEQRLHWYLLGWGFPLVPASIHAVART	281	
Serinus_canaria	QFFHQYMLGCNYFWMLCEGIYLHTLIVVAVFAEEQRLHWYLLGWGFPLVPASIHAVARA	281	
Corvus_brachyrhynchos	QFFHQYMLGCNYFWMLCEGIYLHTLIVVAVFAEEQRLHWYLLGWGFPLVPASIHAVARA	281	
Ficedula_albicollis	QFFHQYMLGCNYFWMLCEGIYLHTLIVVAVFAEEQRLHWYLLGWGFPLVPASIHAVARA	281	aves
Anser_cygnoides_domesticus	QFFHQYMLGCNYFWMLCEGIYLHTLIVVAVFAEEQRLHWYLLGWGFPLVPASIHAVARA	281	
Anas_platyrhynchos	QFFHQYMLGCNYFWMLCEGIYLHTLIVVAVFAEEQRLHWYLLGWGFPLVPASIHAVARA	281	
Apteryx_australis_mantelli	QFFHQYMLGCNYFWMLCEGIYLHTLIVVAVFAEEQRLHWYLLGWGFPLVPASIHAIARA	281	
Gallus_gallus	QFFHQYMLGCNYFWMLCEGIYLHTLIVVAVFAEEQRLHWYLLGWGFPLVPASIHAVARA	281	
Picoides_pubescens	QFFHQYMLGCNYFWMLCEGIYLHTLIVVAVFAEEQRLHWYLLGWGFPLVPASIHAVARA	281	
Chaetura_pelagica	QFFHQYMLGCNYFWMLCEGIYLHTLIVVAVFAEEQRLHWYLLGWGFPLVPASIHAIARA	281	
Apaloderma_vittatum	QFFHQYMLGCNYFWMLCEGIYLHTLIVVAVFAEEQRLHWYLLGWGFPLVPASIHAVARA	281	
Balearica_regulorum_gibbericeps	QFFHQYMLGCNYFWMLCEGIYLHTLIVVAVFAEEQRLHWYLLGWGFPLVPASIHAVARA	281	
Cuculus_canorus	QFFHQYMLGCNYFWMLCEGIYLHTLIVVAVFAEEQRLHWYLLGWGFPLVPASIHAVARA	281	
Caprimulgus_carolinensis	QFFHQYMLGCNYFWMLCEGIYLHTLIVVAVFAEEQRLHWYLLGWGFPLVPASIHAVARA	281	
Calypte_anna	QFFHQYMLGCNYFWMLCEGIYLHTLIVVAVFAEEQRLHWYLLGWGFPLVPASIHAVARA	281	
Pygoscelis_adeliae	QFFHQYMLGCNYFWMLCEGIYLHTLIVVAVFAEEQRLHWYLLGWGFPLVPASIHAVARA	281	
Egretta_garzetta	QFFHQYMLGCNYFWMLCEGIYLHTLIVVAVFAEEQRLHWYLLGWGFPLVPASIHAVARA	281	
Nipponia_nippon	QFFHQYMLGCNYFWMLCEGIYLHTLIVVAVFAEEQRLHWYLLGWGFPLVPASIHAVARA	281	
Charadrius_vociferus	QFFHQYMLGCNYFWMLCEGIYLHTLIVVAVFAEEQRLHWYLLGWGFPLVPASIHAVARA	264	
Aquila_chrysaetos_canadensis	QFFHQYMLGCNYFWMLCEGIYLHTLIVVAVFAEEQRLHWYLLGWGFPLVPASIHAVARA	282	mammals
Phalacrocorax_carbo	QFFHQYMLGCNYFWMLCEGIYLHTLIVVAVFAEEQRLHWYLLGWGFPLVPASIHAVARA	264	
Sus_scrofa	HFFHQYMMSCNYFWMLCEGVYLTLLIVSVFAEGQRLWYHVLGWGFPLIPTTAHAITRA	283	
Mus_musculus	HFLHQYMMSCNYFWMLCEGIYLHTLIVMAVFTDEQRLRWYLLGWGFPLVPTTIHAITRA	282	
Rattus_norvegicus	HFFHQYMMACNYFWMLCEGIYLHTLIVMAVFTEDQRLRWYLLGWGFPLVPTTIHAITRA	299	
Jaculus_jaculus	HFFHQYMMACNYFWMLCEGIYLHTLIVSVFTTEEQLRYYFLGWGFPLVPTVIHAITRA	283	
Pteropus_vampyrus	HFFHQYMMACNYFWMLCEGIYLHTLIVVAVFAEKQHRWYLLGWGFPLVPTTIHAITRA	283	
Cavia_porcellus	HFFHQYMMACNYFWMLCEGIYLHTLIVSVFNEAKHLRWYLLGWGFPLVPTTIHAITRA	282	
Galeopterus_variegatus	HFFHQYMMACNYFWMLCEGIYLHTLIVVAVFSGEQHLRWYLLGWGFPLVPTTIHAITRA	282	
Oryctolagus_cuniculus	HFFHQYMMSCNYFWMLCEGIYLHTLIVVAVFAKQHLRWYLLGWGFPLVPTTIHAITRA	299	
Colobus_angolensis_palliatu	HFFHQYMMACNYFWMLCEGIYLHTLIVMAVFTTEKQRLRWYLLGWGFPLVPTTIHAITRA	282	
Homo_sapiens	HFFHQYMMACNYFWMLCEGIYLHTLIVVAVFTEKQRLRWYLLGWGFPLVPTTIHAITRA	282	
Pan_troglodytes	HFFHQYMMACNYFWMLCEGIYLHTLIVVAVFTEKQRLRWYLLGWGFPLVPTTIHAITRA	282	
Canis_lupus_familiaris	HFFHQYMMACNYFWMLCEGIYLHTLIVVAVFTEEHLRWYLLGWGFPLVPTTIHAITRA	283	
Equus_caballus	HFFHQYMMACNYFWMLCEGIYLHTLIVVAVFTEEQLRWYLLGWGFPLVPTTIHAITRA	283	
Ceratotherium_simum_simum	HFFHQYMMACNYFWMLCEGIYLHTLIVVAVFTEEQLRWYLLGWGFPLVPTTIHAITRA	283	

: ** :.***:*****:*** :: **:*****:*** **:***:

TMIII

TMIV

Xenopus_tropicalis	KYFNDNCWMSVETHLLYIVHGPVMAALLVNFLLNIIVRLVTKLRDTHRAESNMYMKAV	350	amphibians
Thamnophis_sirtalis	RYFNDNCWISVDTHLLYIVHGPVMAALLVNFLLNIIVRLVTKLRDTHRAESNMYMKAV	339	
Anolis_carolinensis	KYFNDNCWISVDTHLLYIVHGPVMAALLVNFLLNIIVRLVTKLRDTHRAESNMYMKAV	341	reptiles
Serinus_canaria	RYFNDNCWMSVDTHLLYIVHGPVMAALLVNFLLNIIVRLVTKLRDTHRAESNMYMKAV	341	
Corvus_brachyrhynchos	RYFNDNCWMSVDTHLLYIVHGPVMAALLVNFLLNIIVRLVTKLRDTHRAESNMYMKAV	341	aves
Ficedula_albicollis	RYFNDNCWMSVDTHLLYIVHGPVMAALLVNFLLNIIVRLVTKLRDTHRAESNMYMKAV	341	
Anser_cygnoides_domesticus	KYFNDNCWMSVDTHLLYIVHGPVMAALLVNFLLNIIVRLVTKLRDTHRAESNMYMKAV	341	
Anas_platyrhynchos	KYFNDNCWMSVDTHLLYIVHGPVMAALLVNFLLNIIVRLVTKLRDTHRAESNMYMKAV	341	
Apteryx_australis_mantelli	KYFNDNCWMSVDTHLLYIVHGPVMAALLVNFLLNIIVRLVTKLRDTHRAESNMYMKAV	341	
Gallus_gallus	KYFNDNCWMSVDTHLLYIVHGPVMAALLVNFLLNIIVRLVTKLRDTHRAESNMYMKAV	341	
Picoides_pubescens	KYFNDNCWMSVDTHLLYIVHGPVMAALLVNFLLNIIVRLVTKLRDTHRAESNMYMKAV	341	
Chaetura_pelagica	KYFNDNCWMSVDTHLLYIVHGPVMAALLVNFLLNIIVRLVTKLRDTHRAESNMYMKAV	341	
Apaloderma_vittatum	RYFNDNCWMSVDTHLLYIVHGPVMAALLVNFLLNIIVRLVTKLRDTHRAESNMYMKAV	341	
Balearica_regulorum_gibbericeps	KYFNDNCWMSVDTHLLYIVHGPVMAALLVNFLLNIIVRLVTKLRDTHRAESNMYMKAV	341	
Cuculus_canorus	KYFNDNCWMSVDTHLLYIVHGPVMAALLVNFLLNIIVRLVTKLRDTHRAESNMYMKAV	341	mammals
Caprimulgus_carolinensis	KYFNDNCWMSVDTHLLYIVHGPVMAALLVNFLLNIIVRLVTKLRDTHRAESNMYMKAV	341	
Calypte_anna	KYFNDNCWMSVDTHLLYIVHGPVMAALLVNFLLNIIVRLVTKLRDTHRAESNMYMKAV	341	
Pygoscelis_adeliae	RYFNDNCWMSVDTHLLYIVHGPVMAALLVNFLLNIIVRLVTKLRDTHRAESNMYMKAV	341	
Egretta_garzetta	RYFNDNCWMSVDTHLLYIVHGPVMAALLVNFLLNIIVRLVTKLRDTHRAESNMYMKAV	341	
Nipponia_nippon	RYFNDNCWMSVDTHLLYIVHGPVMAALLVNFLLNIIVRLVTKLRDTHRAESNMYMKAV	341	
Charadrius_vociferus	KYFNDNCWMSVDTHLLYIVHGPVMAALLVNFLLNIIVRLVTKLRDTHRAESNMYMKAV	324	
Aquila_chrysaetos_canadensis	RYFNDNCWMSVDTHLLYIVHGPVMAALLVNFLLNIIVRLVTKLRDTHRAESNMYMKAV	342	
Phalacrocorax_carbo	RYFNDNCWMSVDTHLLYIVHGPVMAALLVNFLLNIIVRLVTKLRDTHRAESNMYMKAV	324	
Sus_scrofa	VLFNDNCWLSVDTHLLYIIHGPVMAALVNFLLNIIVRLVTKLRDTHRAESNMYMKAV	343	
Mus_musculus	LYFNDNCWLSAETHLLYIIHGPVMAALVNFLLNIIVRLVTKMRQTHEAESYMYLKAV	342	
Rattus_norvegicus	VYFNDNCWLSSTETHLLYIIHGPVMAALVNFLLNIIVRLVTKMRQTHEAEAYMYLKAV	359	
Jaculus_jaculus	LYYDNCWLSVETHLLYIIHGPVMAALVNFLLNIIVRLVTKMRQTHEAESHYMYLKAV	343	
Pteropus_vampyrus	LYFNDNCWLSVETHLLYIIHGPVMAALVNFLLNIIVRLVTKMRQTHEAESHYMYLKAV	343	
Cavia_porcellus	LYFNDNCWISVDTHLLYIIHGPVMAALVNFLLNIIVRLVTKMRQTHEAESYMYLKAV	342	
Galeopterus_variegatus	LYFNDNCWLSVETHLLYIIHGPVMAALVNFLLNIIVRLVTKMRQTHEAESQMYLKAV	342	
Oryctolagus_cuniculus	IYFNDNCWMSVETHLLYIIHGPVMAALVNFLLNIIVRLVTKMRQTHEAESHYMYLKAV	359	
Colobus_angolensis_palliatu	VYFNDNCWLSVETHLLYIIHGPVMAALVNFLLNIIVRLVTKMRQTHEAESHYMYLKAV	342	
Homo_sapiens	VYFNDNCWLSVETHLLYIIHGPVMAALVNFLLNIIVRLVTKMRQTHEAESHYMYLKAV	342	
Pan_troglodytes	VYFNDNCWLSVETHLLYIIHGPVMAALVNFLLNIIVRLVTKMRQTHEAESHYMYLKAV	342	
Canis_lupus_familiaris	LYFNDNCWLSVETHLLYIIHGPVMAALVNFLLNIIVRLVSKMRQTHEAESHYMYLKAV	343	
Equus_caballus	LYFNDNCWLSVETHLLYIIHGPVMAALVNFLLNIIVRLVSKMRQTHEAESHYMYLKAV	343	
Ceratotherium_simum_simum	LYFNDNCWLSVETHLLYIIHGPVMAALVNFLLNIIVRLVSKMRQTHEAESHYMYLKAV	343	

*****.* ***:***:***:***:*****:***.*:*****:***:***

TMV

TMVI

<i>Xenopus_tropicalis</i>	RATLILVPLLGIQFVIFPWRPDRTRLAGEIYDYIMHILMHYQGLLVATIFCFNFGEVQGA	410	amphibians
<i>Thamnophis_sirtalis</i>	RATLILVPLLGIQFVIFPWRPENRLAGEIYDYIMHILMHYQGLLVATIFCFNFGEVQGT	399	
<i>Anolis_carolinensis</i>	RATLILVPLLGIQFVIFPWRPENRLAGEIYDYIMHILMHYQGLLVATIFCFNFGEVQGA	401	reptiles
<i>Serinus_canaria</i>	RATLILVPLLGIQFVIFPWRPENRLAGEIYDYIMHILMHYQGLLVATIFCFNFGEVQGA	401	
<i>Corvus_brachyrhynchus</i>	RATLILVPLLGIQFVIFPWRPENRLAGEIYDYIMHILMHYQGLLVATIFCFNFGEVQGA	401	aves
<i>Ficedula_albicollis</i>	RATLILVPLLGIQFVIFPWRPENRLAGEIYDYIMHILMHYQGLLVATIFCFNFGEVQGA	401	
<i>Anser_cygnoides_domesticus</i>	RATLILVPLLGIQFVIFPWRPENRLAGEIYDYIMHILMHYQGLLVATIFCFNFGEVQGA	401	
<i>Anas_platyrhynchus</i>	RATLILVPLLGIQFVIFPWRPENRLAGEIYDYIMHILMHYQGLLVATIFCFNFGEVQGA	401	
<i>Apteryx_australis_mantelli</i>	RATLILVPLLGIQFVIFPWRPENRLAGEIYDYIMHILMHYQGLLVATIFCFNFGEVQGA	401	
<i>Gallus_gallus</i>	RATLILVPLLGIQFVIFPWRPENRLAGEIYDYIMHILMHYQGLLVATIFCFNFGEVQGA	401	
<i>Picoides_pubescens</i>	RATLILVPLLGIQFVIFPWRPENRLAGEIYDYIMHILMHYQGLLVATIFCFNFGEVQGA	401	
<i>Chaetura_pelagica</i>	RATLILVPLLGIQFVIFPWRPENRLAGEIYDYIMHILMHYQGLLVATIFCFNFGEVQGA	401	
<i>Apaloderma_vittatum</i>	RATLILVPLLGIQFVIFPWRPENRLAGEIYDYIMHILMHYQGLLVATIFCFNFGEVQGT	401	
<i>Balearica_regularum_gibbericeps</i>	RATLILVPLLGIQFVIFPWRPENRLAGEIYDYIMHILMHYQGLLVATIFCFNFGEVQGA	401	
<i>Cuculus_canorus</i>	RATLILVPLLGIQFVIFPWRPENRLAGEIYDYIMHILMHYQGLLVATIFCFNFGEVQGA	401	
<i>Caprimulgus_carolinensis</i>	RATLILVPLLGIQFVIFPWRPENRLAGEIYDYIMHILMHYQGLLVATIFCFNFGEVQGA	401	
<i>Calypte_anna</i>	RATLILVPLLGIQFVIFPWRPENRLAGEIYDYIMHILMHYQGLLVATIFCFNFGEVQGA	401	
<i>Pygoscelis_adeliae</i>	RATLILVPLLGIQFVIFPWRPENRLAGEIYDYIMHILMHYQGLLVATIFCFNFGEVQGA	401	
<i>Egretta_garzetta</i>	RATLILVPLLGIQFVIFPWRPENRLAGEIYDYIMHILMHYQGLLVATIFCFNFGEVQGA	401	
<i>Nipponia_nippon</i>	RATLILVPLLGIQFVIFPWRPENRLAGEIYDYIMHILMHYQGLLVATIFCFNFGEVQGA	401	
<i>Charadrius_vociferus</i>	RATLILVPLLGIQFVIFPWRPENRLAGEIYDYIMHILMHYQGLLVATIFCFNFGEVQGA	384	
<i>Aquila_chrysaetos_canadensis</i>	RATLILVPLLGIQFVIFPWRPENRLAGEIYDYIMHILMHYQGLLVATIFCFNFGEVQGA	402	
<i>Phalacrocorax_carbo</i>	RATLILVPLLGIQFVIFPWRPENRLAGEIYDYIMHILMHYQGLLVATIFCFNFGEVQGA	384	
<i>Sus_scrofa</i>	RATLILVPLLGQFVVFVLPWRPSTPLLGKIYDYVMHSLIHFQGGFFVAVIYCFNCNHEVQGA	403	mammals
<i>Mus_musculus</i>	KATMVLVPLLGQFVVFVLPWRPSNKVLGKIYDYVMHSLIHFQGGFFVATIYCFNCNHEVQTT	402	
<i>Rattus_norvegicus</i>	KATMVLVPLLGQFVVFVLPWRPSNKVLGKIYDYVMHSLIHFQGGFFVATIYCFNCNHEVQTT	419	
<i>Jaculus_jaculus</i>	KATMVLVPLLGQFVVFVLPWRPSNKILGKIYDYVMHSLIHFQGGFFVATIYCFNCNHEVQTT	403	
<i>Pteropus_vampyrus</i>	RATLILVPLLGQFVVFVLPWRPSNKVLGKIYDYVMHSLIHFQGGFFVAVIYCFYNSEVQTAV	403	
<i>Cavia_porcellus</i>	KATMILVPLLGQFVVFVLPWRPSNKVLGKIYDYVMHSLIHFQGGFFVATIYCFNCNHEVQTT	402	
<i>Galeopterus_variegatus</i>	KATMILVPLLGQFVVFVLPWRPSNKILGKIYDYVMHSLIHFQGGFFVATIYCFNCNHEVQTT	402	
<i>Oryctolagus_cuniculus</i>	KATMILVPLLGQFVVFVLPWRPSNKILGKIYDYVMHSLIHFQGGFFVATIYCFNCNHEVQTT	419	
<i>Colobus_angolensis_palliatu</i>	KATMILVPLLGQFVVFVLPWRPSNKMLGKIYDYVMHSLIHFQGGFFVATIYCFNCNHEVQTT	402	
<i>Homo_sapiens</i>	KATMILVPLLGQFVVFVLPWRPSNKMLGKIYDYVMHSLIHFQGGFFVATIYCFNCNHEVQTT	402	
<i>Pan_troglodytes</i>	KATMILVPLLGQFVVFVLPWRPSNKMLGKIYDYVMHSLIHFQGGFFVATIYCFNCNHEVQTT	402	mammals
<i>Canis_lupus_familiaris</i>	RATLILVPLLGQFVVFVLPWRPSNKMLGKIYDYVMHSLIHFQGGFFVAVIYCFNCNHEVQTT	403	
<i>Equus_caballus</i>	RATLILVPLLGQFVVFVLPWRPSNKMLGKIYDYVMHSLIHFQGGFFVAVIYCFNCNHEVQTT	403	
<i>Ceratotherium_simum_simum</i>	RATLILVPLLGQFVVFVLPWRPSNKMLGKIYDYVMHSLIHFQGGFFVAVIYCFNCNHEVQTT	403	

Xenopus_tropicalis	KRQWMQYKTQWGQRRREHCSTRSTSCT-----ATSITEVPIYLYHHDSSNEQ--LN	459	amphibian
Thamnophis_sirtalis	KRQWMQYKTQWGQRRREHCSTRSTSCT-----ATSITEVPIYLYHHDSSNEH--LN	448	reptiles
Anolis_carolinensis	KRQWMQYKTQWGQRRREHCSTRSTSCT-----ATSITEVPIYLYHHDSSSEQ--FN	450	
Serinus_canaria	KRQWAQYKTQWGQRRREHCSTRSTSCT-----ATSITEVPIYLYHHDSSNEH--LN	450	aves
Corvus_brachyrhynchos	KRQWAQYKTQWGQRRREHCSTRSTSCT-----ATSITEVPIYLYHHDSSNEQ--LN	450	
Ficedula_albicollis	KRQWTQYKTQWGQRRREHCSTRSTSCT-----ATSITEVPIYLYHHDSSNEQ--LN	450	
Anser_cygnoides_domesticus	KRQWTQYKTQWGQRRREHCSTRSTSCT-----ATSITEVPIYLYHHDSSNEQ--LN	450	
Anas_platyrhynchos	KRQWTQYKTQWGQRRREHCSTRSTSCT-----ATSITEVPIYLYHHDSSNEQ--LN	450	
Apteryx_australis_mantelli	KRQWTQYKTQWGQRRREHCSTRSTSCT-----ATSITEVPIYLYHHDSSNEQ--LN	450	
Gallus_gallus	KRQWTQYKTQWGQRRREHCSTRSTSCT-----ATSITEVPIYLYHHDSSNEQ--LN	450	
Picoides_pubescens	KRQWTQYKTQWGQRRREHCSTRSTSCT-----ATSITEVPIYLYHHDSSNEQ--FN	450	
Chaetura_pelagica	KRQWTQYKTQWGQRRREHCSTRSTSCT-----ATSITEVPIYLYHHDSSNEQ--IN	450	
Apaloderma_vittatum	KRQWTQYKTQWGQRRREHCSTRSTSCT-----ATSITEVPIYLYHHDSSNEQ--LN	450	
Balearica_regulorum_gibbericeps	KRQWTQYKTQWGQRRREHCSTRSTSCT-----ATSITEVPIYLYHHDSSNEQ--LN	450	mammals
Cuculus_canorus	KRQWTQYKTQWGQRRREHCSTRSTSCT-----ATSITEVPIYLYHHDSSNEQ--LN	450	
Caprimulgus_carolinensis	KRQWTQYKTQWGQRRREHCSTRSTSCT-----ATSITEVPIYLYHHDSSNEQ--LN	450	
Calypte_anna	KRQWTQYKTQWGQRRREHCSTRSTSCT-----ATSITEVPIYLYHHDSSNEQ--LN	450	
Pygoscelis_adeliae	KRQWAQYKTQWGQRRREHCSTRSTSCT-----ATSITEVPIYLYHHDSSNEQ--LN	450	
Egretta_garzetta	KRQWTQYKTQWGQRRREHCSTRSTSCT-----ATSITEVPIYLYHHDSSNEQ--LN	450	
Nipponia_nippon	KRQWTQYKTQWGQRRREHCSTRSTSCT-----ATSITEVPIYLYHHDSSNEQ--LN	450	
Charadrius_vociferus	KRQWTQYKTQWGQRRREHCSTRSTSCT-----ATSITEVPIYLYHHDSSNEQ--LN	433	
Aquila_chrysaetos_canadensis	KRQWTQYKTQWGQRRREHCSTRSTSCT-----ATSITEVPIYLYHHDSSNEQ--LN	451	
Phalacrocorax_carbo	KRQWTQYKTQWGQRRREHCSTRSTSCT-----ATSITEVPIYLYHHDSSNEQ--LN	433	
Sus_scrofa	KRQWNQYQAQ---RWAGRRSTRAANAAAAAATAAAAAAETVEIPVYICHQEPREEPAGEE	460	
Mus_musculus	KRQWTQFKIQWQQRGR---RPTN---RVVSAPRAVAFEPDGLPIYICHQEPN-NPPISN	457	
Rattus_norvegicus	KRQWAQFKIQWQSHRWGRRRRPTN---RVVSAPRAVAFEPDGLPIYICHQEPN-NPPVSN	475	
Jaculus_jaculus	KRQWTQFKLQ---HWGTAALNRTAP-QASPAATASAEAGDIDLPIYICHREPPRA----N	455	
Pteropus_vampyrus	KRQWIQFKIQWQQRGRNRRPHF-HAAAAAAAEAEAGDIPVYICHQEPN-NNEPAI	461	
Cavia_porcellus	KRQWAQFKIQWQQRGRNRRPHF-HAAAAAAAEAEAGDIPVYICHQEPN-NNEPPN	457	
Galeopterus_variegatus	KRHWAQLRIQWQQRGRNRRPHF-HAAAAAAAEAEAGDIPVYICHPEPEPRNEPAG	455	
Oryctolagus_cuniculus	KRQWVQFKIQWQQRGRNRRPHF-HAAAAAAAEAEAGDIPVYICHQEPN-NNEPAI	470	
Colobus_angolensis_palliatu	KRQWVQFKIQWQQRGRNRRPHF-HAAAAAAAEAEAGDIPVYICHQEPN-NNEPAI	452	
Homo_sapiens	KRQWAQFKIQWQQRGRNRRPHF-HAAAAAAAEAEAGDIPVYICHQEPN-NNEPAI	453	
Pan_troglodytes	KRQWAQFKIQWQQRGRNRRPHF-HAAAAAAAEAEAGDIPVYICHQEPN-NNEPAI	453	
Canis_lupus_familiaris	KRQWAQFKIQWQQRGRNRRPHF-HAAAAAAAEAEAGDIPVYICHQEPN-NNEPAI	455	
Equus_caballus	KRHWAQFKIQWQQRGRNRRPHF-HAAAAAAAEAEAGDIPVYICHQEPN-NNEPAI	454	
Ceratotherium_simum_simum	KRHWAQFKIQWQQRGRNRRPHF-HAAAAAAAEAEAGDIPVYICHQEPN-NNEPAI	454	
**:* * : * :			

Xenopus_tropicalis	-GKYGDESEITALNSG--DTYA	478	amphibian
Thamnophis_sirtalis	-GKYIHDSELVALKSG--ETSA	467	reptiles
Anolis_carolinensis	-GKYIDDSELVALKSG--ETSA	469	
Serinus_canaria	-GRYVEDSELVALKSG--DTSA	469	
Corvus_brachyrhynchos	-GRYVEDSELVALKSG--ETSA	469	
Ficedula_albicollis	-GRYLEDSSELVALKSG--ETSA	469	aves
Anser_cygnoides_domesticus	-GRYIDDSELVALKSG--ETSA	469	
Anas_platyrhynchos	-GRYIDDSELVALKSG--ETSA	469	
Apteryx_australis_mantelli	-GRYIDDSELVALKSG--ETSA	469	
Gallus_gallus	-GRYVDDSELVALKSG--ETSA	469	
Picoides_pubescens	-GRYTEDSELVALKSG--ETSA	469	
Chaetura_pelagica	-GRYTEDSELVALKSG--ETSA	469	
Apaloderma_vittatum	-GRYVEDSELVALKSG--ETSA	469	
Balearica_regulorum_gibbericeps	-GRYIEDSELVALKSG--ETSA	469	
Cuculus_canorus	-GRYVEDSELVALKSG--ETSA	469	
Caprimulgus_carolinensis	-GRYVEDSELVALKPG--ETSA	469	
Calypte_anna	-GRYTEDSELVALKSG--ETSA	469	
Pygoscelis_adeliae	-GRYIEDSELVALKSG--ETSA	469	
Egretta_garzetta	-GRYTEDSELVALKSG--ETSA	469	
Nipponia_nippon	-GRYAEDSELVALKSG--ETSA	469	
Charadrius_vociferus	-GRYVEDSELVALKSG--ETSA	452	
Aquila_chrysaetos_canadensis	-GRYVEDSELVALKSG--ETSA	470	
Phalacrocorax_carbo	-GRYVEDSELVALKSG--ETSA	452	
Sus_scrofa	PVVEVEGVEVIAMEVLEQETSA	482	mammals
Mus_musculus	-NEGEESTEMIPMNVIQQDASA	478	
Rattus_norvegicus	-NEGEEGTEMIPMNVIQQDSSA	496	
Jaculus_jaculus	-NQVLEGAEIIPLNTVEQESSA	476	
Pteropus_vampyrus	-NLGEEGAEDIPMEIEQESCA	482	
Cavia_porcellus	-NQGEEGAEMIVLNIEKESSA	478	
Galeopterus_variegatus	-NEGERGAELIPLNIEHESSA	476	
Oryctolagus_cuniculus	-SLGEEGAELIPLNIEQESSA	491	
Colobus_angolensis_palliatu	-NQGEESAEIIPLNIEQETSA	473	
Homo_sapiens	-NQGEESAEIIPLNIEQESSA	474	
Pan_troglodytes	-NQGEESAEIIPLNIEQESSA	474	
Canis_lupus_familiaris	-NLGEEGAEVIALEIEQESSA	476	
Equus_caballus	-NLGGEGAEVIALEIEQESSA	475	
Ceratotherium_simum_simum	-NLGGEGAEVIALEIEQESSA	475	

* :: :: *

Figure S4. Alignment of vertebrate CTR sequences. Alignment of a subset of validated and predicted CTR sequences from mammals and aves with reptile and amphibian sequences used as outgroups. Sequences were obtained from NCBI homologue filtering for reference sequences only. These were then manually curated and an alignment was performed using Clustalw Omega. Conserved asparagine (yellow) and cysteine (purple) residues in the N-terminus have been manually annotated and TMMHM used to predict TM helices which were manually curated and are indicated in blue. Putative LOF mutations are highlighted in red.

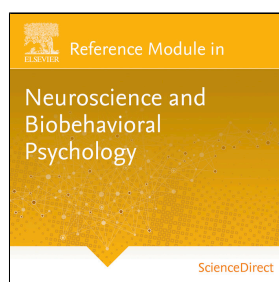
APPENDIX 3

Calcitonin

A Ostrovskaya, DM Findlay, PM Sexton and SGB. Furness

**Provided for non-commercial research and educational use.
Not for reproduction, distribution or commercial use.**

This article was originally published in the online Reference Module in Neuroscience and Biobehavioral Psychology, published by Elsevier, and the attached copy is provided by Elsevier for the author's benefit and for the benefit of the author's institution, for non-commercial research and educational use including without limitation use in instruction at your institution, sending it to specific colleagues who you know, and providing a copy to your institution's administrator.



All other uses, reproduction and distribution, including without limitation commercial reprints, selling or licensing copies or access, or posting on open internet sites, your personal or institution's website or repository, are prohibited. For exceptions, permission may be sought for such use through Elsevier's permissions site at:

<http://www.elsevier.com/locate/permissionusematerial>

From Ostrovskaya, A., Findlay, D.M., Sexton, P.M., Furness, S.G.B. Calcitonin. In Reference Module in Neuroscience and Biobehavioral Psychology, Elsevier, 2017. ISBN 9780128093245

ISBN: 9780128093245

© 2017 Elsevier Inc. All rights reserved.
Elsevier

Calcitonin[☆]

A Ostrovskaya, Monash University, Parkville, VIC, Australia
DM Findlay, University of Adelaide, Adelaide, SA, Australia
PM Sexton and SGB Furness, Monash University, Parkville, VIC, Australia

© 2017 Elsevier Inc. All rights reserved.

Calcitonin Family of Peptides	1
Chemistry	3
Biosynthesis	4
Sites of Production	4
Metabolism	4
Biological Actions	5
Bone Actions of Calcitonin	5
Renal Actions of Calcitonin	6
Central Actions of Calcitonin	6
Calcitonin Role in Cancer	6
Other Actions of Calcitonin	7
Mechanisms of Action	7
Receptors	7
Receptor Isoforms	8
Calcitonin Receptor Signaling	9
Receptor Regulation	10
Summary	11
Further Reading	11

Glossary

Calcitonin A 32-amino acid peptide hormone produced by the C cells of the thyroid. Immunologically similar molecules have also been identified in other tissues, suggesting additional local autocrine or paracrine actions of calcitonin.

G proteins Family of intracellular proteins that act as linking molecules or adapters to link receptors to effector molecules. G proteins are heterotrimers of $\alpha\beta\gamma$ subunits and are activated by receptor binding, which enables them to bind GTP and to dissociate into α and $\beta\gamma$ subunits, which in turn activate molecules such as adenylate cyclase and phospholipase C. Activation is terminated by hydrolysis of GTP to GDP.

Isoforms Different but related forms of protein molecules. Different isoforms of the calcitonin receptor arise by

differential splicing of the primary mRNA transcript and through interaction with RAMPs.

Osteoclasts Large, multinucleated cells that are responsible for the resorption of bone in the cycle of bone turnover that comprises bone removal and bone formation. Osteoclasts are sensitive to CT, which rapidly and potently inhibits their bone-resorbing activity.

Receptor A protein molecule that recognizes and binds its cognate ligand with high affinity and specificity. The calcitonin receptor is a cell surface receptor with extracellular domains that interact with the calcitonin molecule (ligand). The intracellular domains interact with intracellular signal transduction molecules to translate ligand binding into cellular actions.

Calcitonin Family of Peptides

Calcitonin (CT) belongs to a family of molecules that are structurally related but biologically diverse, comprising CT, calcitonin gene-related peptides (CGRPs), amylin, and adrenomedullin (see footnotes for further reading). The CT family of peptides shares a common disulfide bridge and C-terminal amidation, which is required for activity (Fig. 1); beyond this the sequence homology is low.

[☆]Change History: May 2016. Anna Ostrovskaya, David M. Findlay, Patrick M. Sexton and Sebastian G.B. Furness made some changes to the text and updated all the figures.

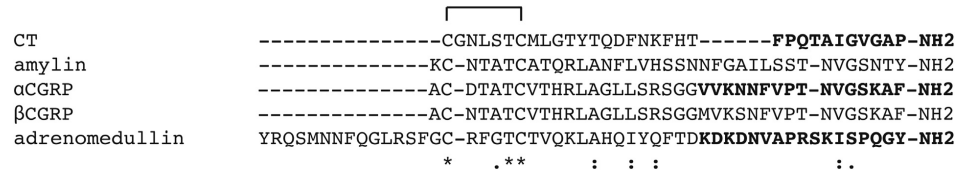


Figure 1 Primary amino acid sequence alignment for the mature human calcitonin, amylin, calcitonin gene-related peptides, and adrenomedullin peptides, which form the calcitonin family. Note the low sequence conservation but the absolute conservation of the cysteine disulfide toward the N-terminal and C-terminal amidation. The sequences highlighted in bold are those that have been shown by crystallography to make contacts with the receptor N-terminal domain. For all peptides, truncation after the second cysteine generates an antagonist, highlighting the importance of the peptide N-terminus in activating the receptor.

CT is a 32-amino acid peptide best known for its synthesis in mammals by the C cells of the thyroid gland. CT lowers blood Ca^{2+} levels by direct inhibition of osteoclast-mediated bone resorption and by enhancing calcium excretion by the kidney. It has been used clinically in the treatment of bone disorders, including Paget's disease, osteoporosis, and hypercalcemia due to malignancy. The receptor for CT [calcitonin receptor (CTR)] is a G protein-coupled receptor (GPCR) belonging to the secretin-like family, which is also known as class B. For many years, the research on CTR and CT was largely focused on their function in calcium homeostasis. Since the initial discovery of CT, expression of CT and its receptors has been demonstrated in many cell types and tissues other than bone. This suggests additional, biologically diverse roles for CT, including functions in brain, kidney, and cell differentiation and tissue morphogenesis.

CT is processed from a 141 amino acid pre-pro-peptide encoded by the CALCA gene; several other processed peptides have also been identified in human plasma. Procalcitonin (pro-CT; Fig. 2) is a 116-amino acid peptide that is found in plasma of healthy individuals at about 10% of the level of mature CT. During sepsis, pro-CT becomes expressed and secreted throughout the body, with levels rising to several hundred to thousand fold that of healthy individuals. Septic levels of pro-CT show a strong

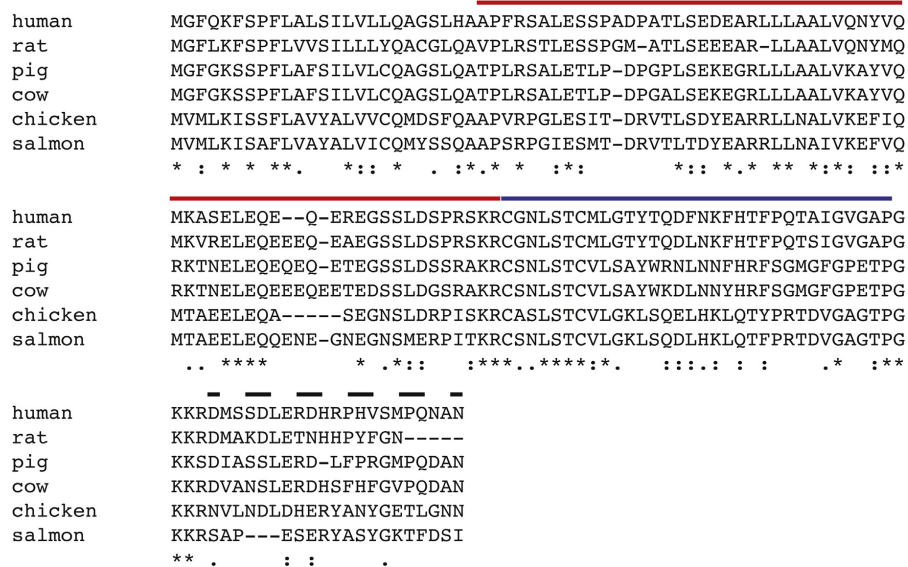


Figure 2 Primary amino acid sequence alignment of the sequences for the predicted pre-pro-calcitonin (CT) peptide from various species. The first 25 amino acids comprise a signal peptide. Highlighted in red is the sequence for the N-terminus of pro-CT (which continues to the very C-terminus), blue is fully processed CT while in black dashes is katacalcin.

positive correlation with mortality, and in a variety of animal models, administration of pro-CT increases septic mortality while immunoneutralization reduces mortality. Indeed, serum pro-CT levels are a significantly better diagnostic indicator of sepsis than plasma C-reactive protein, interleukin-6, or lactate levels, and its level is now used clinically to diagnose bacterial sepsis and for differential diagnosis of bacterial versus viral meningitis and pneumonia. The receptor for pro-CT is not well characterized, but pro-CT is a potent partial agonist for the CGRP₁ receptor (see below) and a weak partial agonist for the AMY₁ receptor (below). Secretion of pro-CT by a variety of neuroendocrine tumors and breast cancers has also been reported, with serum levels correlating positively with disease progression/remission. Katalcacin [also known as CCP-1 (calcitonin carboxypeptide-1)] comprises the last 21 amino acids of pro-CT (Fig. 2). Katalcacin is present in plasma at roughly equimolar concentrations to CT and is cosecreted from the thyroid. It has no sequence homology to the other mature CT family peptides, shows poor sequence conservation across species (Fig. 2), and its receptor is unknown. An early report that katalcacin mimics CT's hypocalcemic activity was subsequently repudiated, and the only reported activity at physiologically relevant concentrations is as a macrophage chemoattractant.

α -Calcitonin gene-related peptide (α CGRP) is also encoded by the same gene as CT and arises through tissue-specific alternative splicing of the primary mRNA transcript. The CT/ α CGRP gene was one of the first recognized examples of a cellular gene exhibiting alternative, tissue-specific processing and has served as an important paradigm to study the molecular mechanisms of RNA splicing. Processing of the premessenger RNA to the CT mRNA transcript involves usage of exon 4 as a 3' terminal exon, with concomitant polyadenylation at the end of exon 4. Processing to produce the α CGRP mRNA involves the exclusion of exon 4 and direct ligation of exon 3 to exon 5, with polyadenylation at the end of exon 6. The resulting α CGRP transcript encodes a 128 amino acid pre-pro-peptide sharing the same signal peptide and most of the same N-terminal pro-peptide as CT, before diverging in sequence. Mature α CGRP is a 37-amino acid peptide with low sequence homology to CT but sharing cysteine cyclization at the amino end and amidated C-terminus (Fig. 1). α CGRP is predominantly produced in the nervous system. It is a potent vasodilator and is strongly implicated in the pathophysiology of migraine. α CGRP's inotropic actions on the heart are mediated through activation of the sympathetic nervous system. Of note, α CGRP expression and secretion is upregulated in a wide range of tissues during sepsis and, in animal models, has a protective effect against septic mortality. This is supportive of an interaction between α CGRP and pro-CT at the same receptor. β CGRP is encoded by a different, but closely related gene with the mature peptide identical at 34 of 37 residues (Fig. 1). β CGRP is expressed in the gastrointestinal tract and has a role in modulating gastric motility and gastric acid secretion. Historically the primary receptor for the CGRPs was considered to be the CGRP₁ receptor. This is a heteromeric receptor composed of the calcitonin-like receptor (CLR) of the secretin-like family of GPCRs and a single transmembrane spanning protein called RAMP1 (receptor activity modifying protein 1). It is now accepted in the GPCR field that the AMY₁ (amylin 1) receptor, comprising CTR and RAMP1, is also a receptor for the CGRPs.

Adrenomedullin (AM), initially identified from the adrenal medulla of a patient with pheochromocytoma, is widely distributed and produced predominantly in vascular smooth muscle and endothelial cells. Mature AM is a 52-amino acid peptide that is amidated at the C-terminus with a single disulfide bond between residues 16 and 21. It is produced from a 185-amino acid pre-pro-peptide. Much like α CGRP, AM is a potent vasodilator. Other important actions include bronchodilation, natriuresis as well as regulation of cell growth, differentiation, and apoptosis. Like the receptors for the CGRPs, there are two accepted receptors for AM both comprising heteromers. In this case the AM₁ receptor comprises CLR and RAMP2, with CLR/RAMP3 forming the AM₂ receptor.

Amylin (AMY) is cosecreted with insulin from pancreatic β -cells and acts to inhibit gastric emptying and signal satiety, thus reducing postprandial glucose excursion. In common with the other CT family members, the mature 37-amino acid amylin hormone is C-terminally amidated and has an internal disulfide bond between residues 2 and 6, and is produced from a pre-pro-peptide of 89 amino acids. Its stable analogue, pramlintide, is used in combination therapy with insulin for treatment of types 1 and 2 diabetes. There are three recognized receptors for amylin, AMY₁ (CTR/RAMP1), AMY₂ comprising CTR/RAMP2, and AMY₃ comprising CTR/RAMP3, although AMY₂ is rather poorly characterized and may not be a physiologically relevant receptor for AMY.

Several novel peptides with the ability to stimulate CTR have been reported. One of them is PHM-27 that is synthesized from the precursor protein pre-pro-VIP and was found in human neuroblastoma and neuroendocrine tumors. PHM-27 and hCT share limited sequence homology. PHM-27 has been published to be full agonist of hCTR with potency and efficacy similar to hCT, although in our hands this peptide acts as a weak partial agonist in all pathways tested.

A family of peptides that are most closely related to the CT/ α CGRP primary transcript, known as CTR-stimulating peptides (CRSPs), CRSP-1, CRSP-2, and CRSP-3, have been identified in the brain and the thyroid gland of the pig, dog, and cow, but not in man and mouse. CRSP-1 has been shown to transiently decrease plasma calcium concentration when administered into rats. CRSP peptides bind effectively to CTR and stimulate cAMP (cyclic adenosine monophosphate) production in COS-7 cells expressing recombinant CTR.

Chemistry

The CT sequence has been determined for many species and shows considerable divergence, with the common features being that all sequences contain 32 amino acids, a carboxy-terminal proline amide, and a disulfide bridge between cysteine residues at positions 1 and 7 (Figs. 1 and 2). Based on their amino acid sequence homologies, CTs from different species are classified into three groups. The first is the artiodactyl group, which includes porcine, bovine, and ovine CT; within this group each CT differs by four amino acids. The second group is the primate/rodent group, which includes human and rat CT, and these differ within the group by two amino acids. The third group is the teleost/avian group, which includes salmon, eel, goldfish, and chicken CT, each differing

within the group by four amino acids. The order of biological potency of the CTs, with respect to a hypocalcemic response, is teleost \geq artiodactyl \geq human, although absolute biological activities vary considerably among different animal species.

Studies of substituted, deleted, and otherwise modified CTs have provided considerable information regarding structure–activity relationships of the CT peptide. For example, stabilization of the N-terminal ring structure, by substitution of the disulfide bridge with an ethylene linkage or an acetylenic bridge, leads to greatly improved stability of the salmon calcitonin (sCT) molecule and retention of biological potency. Despite this, analogues of sCT that lack the ring structure can retain full potency, in terms of hypocalcemic activity. However, the N-terminal amino acids are critical for the agonist activity of CT. Progressive truncation of this region of sCT leads to generation of, first, weak or partial agonists and then, with deletion of six or seven amino acids, to peptides with antagonist activity. Deamidation of the amino terminus can increase the potency of CT peptides *in vivo*, perhaps by increasing their resistance to degrading endopeptidases. Modifications of CT peptide length from the C-terminal end, either by deletion or elongation, are poorly tolerated. Additionally, the C-terminal amide is required, with the COOH form having markedly reduced activity (see below). The lower *in vivo* potency of human CT (hCT), compared with teleost CTs, is due partly to its increased rate of metabolic degradation and clearance, contributed to by the methionine in position 8, which is susceptible to oxidation.

Circular dichroism studies indicate that sCT exhibits considerable secondary structure in the presence of lipid and predicts the generation of an amphipathic α -helix between residues 8 and 22, in proximity to the cell membrane. The less potent hCT has reduced propensity to form this secondary structure. In addition, amino acid substitutions that enhance the formation of an α -helix between residues 8 and 16 also increase the hypocalcemic potency of the peptide. However, modifications of residues in the 8–22 sequence that alter the ability of sCT or hCT to form a helical secondary structure have yielded conflicting results in terms of the biological significance of this structure, which may be explicable on the basis of differences between CTR subtypes in the model animal studied. In rat tissues, two CTR subtypes have been described: the first, designated CT-H [for helical (subsequently C1a)], displays high-affinity interaction only for peptides with a strong potential to form helical secondary structure; the other, designated CT-L [for linear (subsequently C1b)], is capable of high-affinity interaction with both helical and nonhelical peptides. These differ by alternative splicing, which leads to insertion of an additional 37 amino acids in the second extracellular domain of the C1b receptor. This isoform has not been identified in humans.

Biosynthesis

Sites of Production

Elevation of circulating calcium concentrations stimulates sCT release from the C cells of the thyroid, and low serum calcium levels inhibit release. Sensitivity by thyroïdal C cells to circulating calcium levels appears to be mediated by the same extracellular calcium-sensing receptor that is found in parathyroid cells, another GPCR known as the calcium-sensing receptor. The basal concentration of hCT in human blood in normal individuals is very low (<10 pg/mL or 3pM). Size fractionation analysis of CT extracted from plasma and tissues demonstrates the presence of multiple immunoreactive forms of CT. In addition to the CT monomer (~3500 Da), a number of high-molecular-weight forms exist in certain situations. These forms probably correspond to pro-CT and dimers and other aggregates of the CT molecule and have poorly defined biological activity. In several pathological states, such as CT-secreting medullary thyroid carcinomas (MTCs), circulating levels of CT are increased. Conditions of stress, such as some chronic lung problems, burns, acute pancreatitis, and certain infections/inflammatory conditions, are characterized by high circulating levels of pro-CT.

CT synthesis also occurs in extrathyroidal sites. For example, assays using specific anti-hCT serum have detected hCT-like immunoreactivity (hCT-i) in the blood and urine of patients after total thyroidectomy, which may constitute CT or pro-CT. In fact, significant amounts of (pro)-CT have been found in many human tissues. Thyroid and prostate gland contain the highest levels of hCT-i, and significant amounts are also extractable from the gastrointestinal tract, thymus, bladder, lung, and central nervous system (CNS). Little is known of the physiological role of CT in these extrathyroidal tissues. However, CT-producing cells in extrathyroidal sites do not appear to respond to elevation in serum calcium, suggesting that CT produced in these sites is not involved in calcium homeostasis.

Both hCT-i and salmon CT-i (sCT-i) have been found in the CNS of vertebrate and invertebrate species, the latter again consistent with roles for CT unrelated to osteoclast inhibition. hCT-i is detectable in human cerebrospinal fluid and in extracts of postmortem human brain. In addition, a low level of peptide, immunologically similar to sCT-i, is found in the hypothalamus, which also contains high densities of CTRs. Release of as CT-like peptide from cultured rat anterior pituitary cells has been described, and a cell line derived from a mouse pituitary carcinoma produces abundant CT-i activity. CTRs are present in the intermediate pituitary, thus CT-like material present at this site may act as a paracrine regulator in this tissue. In accord with this, both anti-sCT and anti-hCT antisera were shown to significantly increase the release of prolactin from cultured anterior pituitary cells, presumably by neutralizing the effects of endogenously produced CT.

Metabolism

CT is rapidly cleared from the circulation at a rate that depends on the species of CT, the route of administration, and the preparation of administered peptide. This clearance has implications for the use of CT clinically, and CT is usually injected

intramuscularly in vehicles that maintain useful serum levels for 4–8 h after injection. Degradation of the CT molecule into inactive fragments occurs in various organs, with the kinetics and sites of inactivation being different for different species of CT. The hypocalcemic activity of CT is reduced by incubation, *in vitro*, in serum at 37°C, with relative rates of loss in the following order: porcine CT > hCT = rat CT > sCT >> chicken CT. For sCT, the half-life of elimination from plasma *in vivo* is about 90 min and the metabolic clearance rate is around 200 mL/min. Incubation of CT with extracts of liver, kidney, or spleen showed that hypocalcemic activity was lost most rapidly in liver and kidney extracts due to a thermolabile degrading factor, with different rates of degradation for different CTs. The primary sites of CT degradation are extravascular, mainly in the liver for porcine CT and mainly in the kidney for hCT and sCT. Impaired renal function results in delayed elimination of human and sCT.

Biological Actions

Bone Actions of Calcitonin

The first discovered physiological role of CT is its ability to acutely inhibit bone resorption under conditions of elevated plasma calcium. This effect has been widely observed in model animals and decreases significantly with age. This role is likely to be relevant at times of stress on skeletal calcium conservation, such as pregnancy, lactation, and growth, when bone remodeling by osteoclasts and consequent release of calcium stores in bone needs to be tightly regulated to prevent unnecessary bone loss.

In adult humans, serum calcium levels are maintained in a narrow concentration “window” and gross pathological changes such as thyroidectomy or MTC that cause large decreases, or increases in circulating CT do not cause overt changes in serum calcium levels or bone pathologies. In thyroidectomized patients the decrease in serum calcium levels in response to short-term intravenous calcium infusion is delayed compared with patients with an intact thyroid, showing the role of CT in the acute control of bone resorption. The human CTR is polymorphic in the C-terminal tail, with strong racial association between the two variants. A number of studies have attempted to link this polymorphism with osteoporotic risk, but the association remains weak. Isolated human osteoclasts are very sensitive to inhibition by CT but in adults the rate of bone turnover is relatively slow, so it may be unsurprising that large changes in serum CT have little effect on serum calcium levels. In spite of this, and because of the known action to inhibit osteoclast-mediated bone resorption, CT has been used clinically for treatment of osteoporosis, Paget’s disease, prevention of bone loss due to sudden immobilization, and hypercalcemia of malignancy. Recently the European Medicines Agency undertook a large metaanalysis of data relating to the clinical use of CTs. The report concluded that there was limited evidence demonstrating improvements in osteoporosis, Paget’s disease, and bone loss due to sudden immobilization but did conclude that there is evidence for benefit in treating hypercalcemia of malignancy. It did note that there is evidence that pharmacological use of CT is associated with increased risk of several cancers (see below). In the United States, CT is no longer used for treatment of osteoporosis or Paget’s disease. It seems likely that the physiological activity of CT in humans with respect to bone is limited to development and protection from bone loss during lactation and that CT should be regarded as a regulator of the rate of bone remodeling (see below).

The genetic disruption of CT and its receptor in mice would seem to provide the most direct means for analysis of the physiological actions of CT (at least in a model organism). Disruption of *CALCA* leads to loss of both CT and α CGRP, and these mice display increased bone density and increased bone turnover with age suggesting that the action of CT is to regulate the rate of bone turnover. The authors of these papers also developed mice, in which a translational termination codon was introduced into exon 5, effectively producing a functional deletion of α CGRP without affecting CT. These mice displayed a mild loss of bone density at all ages (osteopenia) due to decreased bone formation, arguing for a role of α CGRP in antagonizing CT action on osteoclasts. At 3 months of age these mice displayed increased bone density and there were no changes in osteoclast number, bone resorption, or serum calcium levels; however, at 12 months there were increased osteoclast numbers and increased bone resorption, even though there was still increased bone density. This suggests that the physiological role of CT is to decrease the overall rate of bone turnover. Since α CGRP-deleted mice display decreased bone formation and there are no CTRs on osteoblasts, CT must exert an indirect anabolic effect on bone. Two groups have developed CTR knockout mice. The first group reported that global knockout resulted in embryonic lethality; however, haploinsufficient mice showed normal serum calcium levels but developed high bone density due to increased bone formation. Through the use of conditional knockout techniques, this group was able to generate animals that had >94 and <100% functional deletion of CTR. Consistent with their haploinsufficient animals disruption, these animals displayed normal serum calcium and increased bone density due to increased bone formation. A second group generated CTR knockouts by using a conditional knockout strategy to remove the same exons; in contrast to the first group, global functional deletion was not embryonic lethal. These mice displayed normal plasma calcium and increased bone formation leading to increased bone density from 3 to 18 months. This group then generated mice with osteoclast-specific disruption of CTR and was able to show that CT, acting through CTR on osteoclasts, inhibited sphingosine 1-phosphate release, which acts on osteoblasts to increase their activity. These data therefore support the role of CT, acting through the CTR as a modulator of bone remodeling rather than a regulator of plasma calcium levels and is consistent with observations in humans (above).

The preceding discussion relates largely to CT bone physiology in nonstress situations. In mice bearing the *CALCA* disruption, challenge with parathyroid hormone (PTH) or 1,25-dihydroxyvitamin D₃ resulted in short-term elevation of serum calcium caused by excess bone resorption and this could be corrected by pharmacological dosing of CT. Similarly, mouse models in which CTR was disrupted in osteoclasts there was impaired acute regulation of serum calcium levels in response to 1,25-dihydroxyvitamin D₃. This supports the idea that CT provides acute regulation of serum calcium via its actions at the CTR to inhibit osteoclast-mediated bone resorption. During lactation there are large demands for calcium, which are largely met by mobilization of calcium stores. Qing et al.

showed that osteocytes also play an important role during lactation by a PTH-mediated mobilization of calcium from their surrounding bone matrix, through a process termed osteocytic osteolysis. Subsequently evidence from global CTR knockout mice implicated a role for CT in protecting the maternal skeleton during lactation by modulating this process, consistent with the reported expression of the CTR on osteocytes, was obtained.

Renal Actions of Calcitonin

CT has been reported to have several effects in the kidney. These include an increase in the urinary excretion rate of sodium, potassium, phosphorus, chloride, and magnesium. sCT was much more potent than porcine CT or hCT when administered subcutaneously into rats. A transient increase in calcium excretion, due probably to inhibition of renal tubular calcium reabsorption, has not usually been regarded as an important effect of CT, although recent observations link it to the calcium-lowering effect of CT in hypercalcemic patients with metastatic bone disease, in addition to inhibition of osteolysis by CT. CTRs have been demonstrated in the kidney, and a further action on the kidney is to enhance 1-hydroxylation of 25-hydroxyvitamin D in the proximal straight tubule of the kidney by stimulating the expression of 25-hydroxyvitamin D1 α -hydroxylase (CYP27B1). These results suggest that CT is involved in the regulation of vitamin D production.

Central Actions of Calcitonin

In addition to their presence in kidney and bone, CTRs are also abundant in the CNS. Central administration of CT and pro-CT in rats generates potent effects that include analgesia and inhibition of appetite and gastric acid secretion. The centrally mediated actions of CT correlate well with the location of CT-binding sites. The periaqueductal gray is important in central regulation of pain, and CT binding within this region is likely to be involved in CT-induced analgesia, although other brain regions have also been implicated. The recent identification of mouse CTR mRNA in serotonergic neurons, which are known to project into the spinal cord, forming a descending inhibitory system against pain transmission, also strongly supports a central analgesic role for CT. Administration of CT in clinical situations of bone pain can be very effective in ameliorating the pain symptoms. The hypothalamic binding parallels the multiple hypothalamic actions of CT, which include modulation of hormone release, decreased appetite, gastric acid secretion, and intestinal motility. There are also high densities of receptors in the subfornical organ (SFO), the vascular organ of the lamina terminalis (VOLT), and the area postrema, which, as circumventricular organs, are directly accessible to thyroïdally derived, bloodborne CT. The area postrema may contribute similarly to the anorexia of peripherally administered CT, although it has recently been demonstrated that CTR is expressed in enteric neurons of the mouse, which, coupled with gastrointestinal CT expression, may suggest involvement of CT in the brain–gut axis. The SFO and VOLT are involved in fluid and electrolyte homeostasis and thus are potential targets for CT-induced alteration in drinking behavior in animal models. sCT, when injected into the lateral part of the paraventricular nucleus of the hypothalamus in rats, reduced sleep duration and profoundly affected sleep cycles, producing prolonged insomnia, a major reduction of slow-wave sleep, and a long period of alternation of rapid eye movement (REM) sleep and awakening. The recent development of CALCA-disrupted and CTR-disrupted mice provides an excellent opportunity to further understand the physiology of CT in the CNS.

Calcitonin Role in Cancer

Neuroendocrine tumors including pheochromocytoma, small cell lung cancer, pancreatic islet, gastrointestinal and lung carcinoid as well as both neuroendocrine and nonneuroendocrine breast tumors have been reported as secreting high levels of pro-CT. Levels of pro-CT present in plasma from cancer patients are elevated compared with healthy individuals, and the levels are positively correlated with disease stage. The role of pro-CT in this broad range of cancers is unknown, but a number of both prospective and retrospective studies have shown positive correlation with disease progression and morbidity. This has led a number of clinical researchers to propose the use of pro-CT as a prognostic indicator. As mentioned above, serum pro-CT levels are also massively increased by sepsis, and studies of cancer patients demonstrate that even with elevated baseline pro-CT, elevated pro-CT is still prognostic for septic infection.

MTCs secrete high levels of CT. It is widely assumed that this is simply a consequence of the tumor origin and there is currently no evidence that CT secretion is consequential to the disease pathology. On the other hand, CT is a useful biomarker for confirming complete surgical resection.

The expression of CTR has been demonstrated in a number of cancer cell lines and primary cancers including breast, prostate, thymic lymphoma, and glioblastoma. Research on the role of CTR expression in cancer has been fragmentary, and any role for CTR in cancer pathology seems to be entirely dependent on the cancer type.

CTR mRNA is expressed in normal ductal cells but not elsewhere in the breast. CT has been found to be a potent inhibitor of the growth and invasion of a model human breast cancer cell line (MB-MDA-231) in vitro. This is due to the ability of CT to suppress high basal MAPK (mitogen-activated protein kinase) activity as well as reducing expression of urokinase plasminogen activator (uPA), a protease at the top of the extracellular matrix degradation pathway. Further, CT inhibits growth of tumors of MB-MDA-231 in a mouse xenograft model. In less invasive human breast cancer model cell lines, such as T47D and MCF-7, binding and activity data support the presence of CTR as AMY receptors. The level of CTR in these cells is suppressed by estradiol, and CT is not reported to affect growth of these cells. A study of CTR in surgically obtained human breast cancers identified receptor mRNA

production in all cases examined, regardless of breast cancer subtype. CTR expression by nonductal tumors possibly represents a recapitulation of fetal expression, and it was recently reported that the CTR is expressed in several fetal tissues in the mouse, including the developing mammary gland, although it is absent in the same tissues postnatally. There are no data on the developmental expression of the CTR in humans, but it is reasonable to speculate that CTR expression in certain tumors represents a reappearance of fetal expression. Of note, pro-CT is present at elevated levels in the serum of patients suffering from breast cancer.

Basal epithelial cells of the prostate express mRNA for both CT and CTR, and primary prostate cells in culture secrete CT. There is no evidence for expression of either CT or CTR elsewhere in normal prostate tissue. In prostate tumor biopsies there is a strong positive correlation between histological scoring of disease progression and coexpression of both CT and CTR mRNA. The LNCaP model human prostate cell line expresses CTR but not CT and responds to CT with increased growth. The PC-3 model cell line secretes CT but does not express CTR, on the other hand a highly metastatic clone PC-3M and the highly metastatic line DU-145 express both CT and CTR. In support of paracrine/autocrine signaling of CT/CTR, in vitro proliferation and invasiveness of LNCaP cells is increased by enforced expression of CT. Similarly, the proliferation and invasiveness of the PC-3 cell line could be increased by enforced CTR expression and that of the PC-3M line decreased by downregulation of either CT or CTR. In these cell lines, autocrine CT/CTR signaling via PKA stimulates expression of uPA to promote correlates of invasiveness. In addition, CT activated CTR, via its C-terminal PDZ (PSD95, Dsg1, zo-1) docking site, destabilizes tight junctions, which would also contribute to invasiveness. These data are consistent with the European Medicines Agency report, recommending close monitoring of prostate cancer during the clinical use of CT.

CTR is functionally expressed on normal B and T lymphocytes from healthy individuals as well as on B and T cells from leukemic patients and transformed lymphoid cell lines. In a genetically modified mouse model of thymic lymphoma, it has been shown that the p53 family of tumor suppressors are upstream of amylin expression. CTR is expressed on malignant cells with RAMP3 as the AMY₃ receptor. Stimulation of these lymphomas with pramlintide (a synthetic amylin analogue) causes CTR-dependent tumor regression via changes to cellular metabolism. This work was extended to show that a range of model human cancers also undergo a switch from glycolysis to mitochondrial respiration in response to amylin signaling via CTR/AMY₃ and that this leads to increased oxidative stress and apoptosis. There are currently no data that address how signaling from CTR/AMY₃ couples to changes in cellular metabolism and whether CT would also produce these effects.

In primary glioblastoma tumor biopsies, high CTR expression is reported in the majority of samples from patients, with low or undetectable expression in adjacent nontumour tissue. There are currently no data that address a potential role for CT/CTR in the progression of glioblastoma.

Given the wide expression of pro-CT/CT/CTR in a variety of cancers and the differing effects observed, significantly more work needs to be done. Clearly, there needs to be better assessment of the potential receptor(s) for pro-CT and a better understanding of its possible metabolism to products with different activity. In addition, significantly more work is required to understand the coupling of CTR and AMY receptors in different cell backgrounds if expression of pro-CT, CT, or CTR is to be leveraged in cancer treatment.

Other Actions of Calcitonin

As discussed above and using various experimental approaches, CT and its receptors have been identified in a large number of cell types and tissue sites, suggesting multiple roles for the CT/CTR. CT-binding sites include kidney, brain, pituitary, testis, prostate, spermatozoa, lung, and lymphocytes. In spite of this, and as discussed above, mice bearing a functional deletion of CT have no overt phenotype outside bone. The most thorough published data on mice carrying functional deletion of CTR in mice also show no overt phenotype in any of the above tissues. Thus, physiological roles for CT/CTR outside bone homeostasis are likely to be to do with environmental adaptation. That there is a massive upregulation of pro-CT expression during sepsis and that neutralization of serum pro-CT improves outcome speaks to some involvement of (pro)-CT in immune modulation. Indeed, expression of CTR is a characteristic of most hematopoietic lineages and this expression occurs in two phases, one in very early precursors and another implicated in recruitment of mature cells to target tissues. Similarly, there have been a number of reports that CTR is upregulated during wound healing and CT signaling may be involved in this process. Lastly CTR is expressed on muscle satellite cells, and CT signaling appears to play a role in maintaining their quiescence.

Mechanisms of Action

Receptors

CT is known to act by binding to receptors on the plasma membrane of responsive cells. Our knowledge of the molecular basis of CT action, both in terms of ligand-binding and postbinding events, has been greatly assisted by the cloning of the CTR gene from several species. The first receptor cloned, in 1991, was the porcine CTR, which was isolated by expression cloning from a cDNA library derived from a renal epithelial cell line. Subsequently, human, rat, mouse, rabbit, and guinea pig CTR cDNAs were isolated. Analysis of the proteins translated from the CTR cDNA sequences revealed that these receptors comprise approximately 500 amino acids and belong to the class B subclass of GPCRs, which also includes the receptors for other peptide hormones such as secretin, PTH, glucagon, glucagon-like peptide-1, vasoactive intestinal polypeptide, pituitary adenylate cyclase-activating peptide, and gastric inhibitory peptide. The human CTR gene is located on chromosome 7 at 7q21.3. In the mouse it is in the proximal

region of chromosome 6, and in chromosomal band 9q11–q12 in the pig, which are homologous to the 7q location in humans. The CTR gene, like the genes for other class B GPCRs, is complex, comprising at least 14 exons with introns ranging in size from 78 nucleotides to >20,000 nucleotides. The total receptor gene is estimated to exceed 70 kb in length. There is no indication that there is any other high-affinity receptor for CT.

The CTR has an N-terminal signal peptide, followed by an approximately 120-amino acid extracellular N-terminal domain (NTD), a seven transmembrane bundle and a relatively long C-terminal tail of approximately 90 amino acids. There are four N-linked glycosylation sites in the NTD, and mutagenesis studies show that three of these are dispensable for high-affinity ligand binding but that all assist with expression and folding. Common with all class B GPCRs, CTR has three conserved disulfide bonds that stabilize the NTD and a further extracellular disulfide between extracellular loop 1 and 2. A wide range of mutagenic, chimeric, and photo-crosslinking data indicate that CT interacts with CTR via a two-domain mechanism in which the NTD provides a high-affinity interaction site for the C-terminal end of CT and the N-terminal end of CT interacts with the transmembrane bundle. This mechanism is common to all family B GPCRs. There is no published structure of full-length CTR, although there is a structure of the isolated NTD in complex with truncated sCT. There are also structures for the NTD of CLR:RAMP1 (CGRP₁) and CLR:RAMP2 (AMY₁) bound to truncated CGRP and AM. Together these provide useful information on differences between binding of CT family peptides to their receptors compared with other family B GPCRs. These structures reveal that CT family peptides occupy a similar cleft in the NTD of the receptor but unlike other class B peptides they do not adopt an extended alpha helix. These peptides do not adopt any strong secondary structure when bound, with the exception of a β -turn at their extreme C-terminus. This β -turn allows the C-terminal amide in all three structures to bury into a pocket that allows hydrogen bonding with the receptor backbone carbonyl group and complementary hydrogen bonding between the receptor backbone amide and the ligand C-terminal carbonyl. This appears to explain the observed requirement for C-terminal amidation among all CT family peptides.

Clearly the agonist–receptor relationships within this family are complex due to the ability of CTR and CLR to form heterodimers with the RAMPs, and alternative splicing of CALCA. While RAMPs engender significant pharmacology switches to these receptors, all current evidence points to this occurring via allosteric modulation of the receptor ligand-binding site. In the published CLR–RAMP–ligand complexes, interactions between the ligand and RAMPs contribute <10% to the buried surface. In spite of this, the structural data point to the requirement for C-terminal amidation for high-affinity ligand interaction. This leaves the physiological relevance of the observed high plasma concentrations of pro-CT completely unresolved.

Receptor Isoforms

There are reports of the existence of at least five isoforms of the human receptor that arise from alternative splicing of the CTR gene. The supporting data for most of these variants are poor and they are likely to represent aberrant mRNA from transformed cell lines. The only human splice variant, for which there is convincing evidence, is one in which an additional 48 nucleotide exon is added between exons 7 and 8 of the more predominant form. This leads to an additional 16 amino acids in intracellular loop 1 of the receptor (CTR_{i1+}, Fig. 3). Alternate splicing to yield a 16-amino acid insert form also occurs in the pig CTR. However, splicing

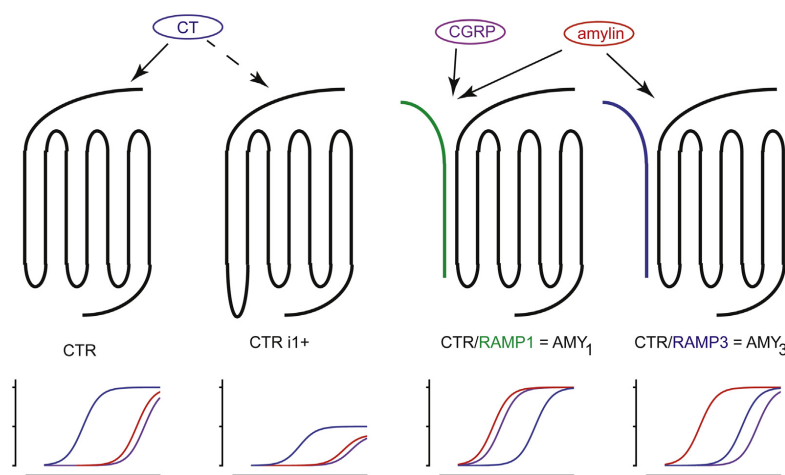


Figure 3 Schematic showing the different calcitonin receptor (CTR) variants and their pharmacology. Far left is the predominant form of CTR, which responds primarily to calcitonin (CT) (blue) and weakly to calcitonin gene-related peptide (CGRP) (purple) and amylin (red). The CTR_{i1+} variant shows profound reduction in cellular response, in contrast AMY₁ and AMY₃ receptors that arise as a consequence of heterodimerization with RAMP1 (green) and RAMP3 (blue) show reduced response to (human) CT but increased response to amylin and CGRP (AMY₁ only).

of the pig CTR primary transcript differs slightly from that in the human transcript, in that the insert arises from alternate splicing within exon 8 of the pig gene, whereas the insert is encoded by a separate exon in the human. Presence of the 16-amino acid insert leads to complete loss of CT-induced intracellular calcium mobilization and profoundly reduced stimulation of cAMP production in response to CT. The physiological significance of the two CTR isoforms remains to be established. However, receptor isoforms are differentially expressed in different cell types, suggesting that alternative splicing is highly regulated and that receptor variants do have physiological roles.

As mentioned earlier, the CTR contains a common single nucleotide polymorphism in the coding sequence that results in either a leucine (T) or a proline (C) at amino acid 447 (463 for IL1 insert positive) in the C-terminal tail. This polymorphism is more commonly leucine in Caucasian populations and much more commonly proline in Asian populations. In other mammals this residue is proline. In Asian populations there are reports of association with predisposition to osteoporosis in postmenopausal women. Some studies have shown that, in those (Asian) populations, women with leucine homozygote (TT) displayed lower spine bone density compared to either proline (CC) homozygotes or heterozygotes. In vitro studies have not confirmed any statistically significant difference between the polymorphs with respect to their binding characteristics or their ability to signal when stimulated with CT. Variants were examined individually, as well as in combination at ratios of 1:1, 3:1, and 1:3, in an effort to mimic heterozygous states. No binding or functional differences were found between any of the combinations tested, when compared to each of the homozygous variants alone. No statistically significant difference in the constitutive receptor activity to stimulate production of basal levels of cAMP in the absence of agonist stimulation was observed between the proline and leucine forms.

The function of CTR can also be influenced by the coexpression of RAMPs. RAMPs are single-pass transmembrane proteins with ~100-amino acid extracellular N-terminal domains and very short C-terminal cytoplasmic domains. In recombinant cell lines, heterodimerization of CTR with RAMPs causes very large shifts in receptor pharmacology. AMY₁ (CTR/RAMP1) and AMY₃ (CTR/RAMP3) receptors no longer show high-affinity binding, nor high-efficacy signaling from hCT but instead become high-affinity and high-efficacy receptors for amylin/CGRP and amylin, respectively (Fig. 3). This modulation of activity and binding appears to occur via an allosteric change to the CTR ligand-binding domain that is induced by the RAMP partner protein. Physiologically, amylin acts as a glucoregulatory hormone to slow gastric emptying, increase satiety, and inhibit glucagon secretion. It is assumed but not shown that this is via central actions of the hormone on CTR containing amylin receptors in privileged areas of the brain. It has also recently been shown that amylin/AMY₃ act as a tumor suppressor pair through metabolic reprogramming of tumor cells. Given the glucoregulatory role of amylin and its clinical use in treatment of insulin-dependent diabetics, there is an urgent need to understand how this hormone operates to modulate cellular activity. The recent development of viable CTR knockout mice would allow this to be tested and would help greatly in trying to dissect the underlying signaling and physiology of the CT/CTR/amylin system.

Calcitonin Receptor Signaling

The molecular mechanisms underlying CTR-mediated signaling inside cells to produce cellular effects are still being elucidated. However, the signaling pathways appear to depend on the cell type as well as on the animal species. As with most other GPCRs, the CTR can couple to multiple members of the heterotrimeric guanosine triphosphate (GTP)-regulated G protein family. In many cell types, activation of the CTR results in its ability to interact with G_{2s}, which leads, in turn, to activation of adenylate cyclase and elevated intracellular levels of cAMP (Fig. 4). The action of CT in osteoclasts to inhibit bone resorption is accompanied by increased cAMP levels. In addition, both forskolin, which directly activates adenylate cyclase, and dibutyryl cAMP, which elevates intracellular cAMP independent of adenylate cyclase action, inhibit bone resorption. CT also stimulates adenylate cyclase activity in the kidney, with the pattern of CT responsiveness paralleling the distribution of CTRs in this tissue. CT induction of cAMP has now been documented in a large number of cultured CTR-bearing cells, including LLC-PK1 pig kidney cells, and in cancers of lung, breast, brain, and bone. Receptor cloning and expression studies have confirmed that cAMP production is an important component of CTR-mediated signaling in many cell types.

Activation of the insert-negative isoform of the CTR can also induce mobilization of intracellular calcium. In osteoclasts, there is evidence that signaling through both cAMP and intracellular calcium is important in CT action. Inhibition of osteoclast-mediated bone resorption by CT can be mimicked by dibutyryl cAMP and phorbol esters, or blocked by protein kinase inhibitors. Thus, coupling of the CTR to different G proteins can activate adenylate cyclase as well as phospholipase C. In the latter case, coupling of the CTR to G_{2q} can lead to increased intracellular inositol-triphosphate levels and thence to increased cytosolic calcium, which, together with liberated diacylglycerol, activates protein kinase C (PKC) (Fig. 4). In brain tissue, CT apparently couples primarily to G proteins other than G_{2s}, based on the limited evidence of activation of adenylate cyclase in neural tissue. In hepatocytes, CT-induced activation of adenylate cyclase has not been shown, but CT, even at very low concentrations, is capable of increasing cytosolic calcium, and CT-induced differentiation of early rat embryos is dependent on intracellular calcium mobilization. In LLC-PK1, pig kidney cells, CT can induce changes mediated by either cAMP or intracellular calcium, in a cell cycle-dependent manner. Expression of cloned receptors in a wide variety of cell types has conclusively shown that CTR is capable of signaling through both cAMP- and calcium-activated second messenger systems.

An interesting "calcium-sensing" function of the CTR has been reported, whereby CTR-bearing cells are rendered sensitive to extracellular calcium in terms of increased cytosolic calcium. Thus, CT treatment of CTR-bearing cells, in the presence of extracellular calcium, initiates a sustained rise in intracellular calcium level, the extent of which is dependent on the concentration of the extracellular calcium. Because osteoclasts, which express high levels of CTR, are reportedly exposed to calcium concentrations as high as

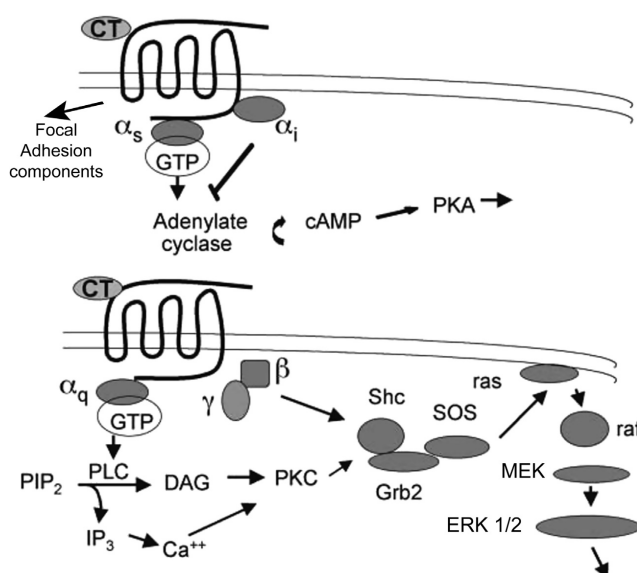


Figure 4 Signaling capability of the calcitonin receptor (CTR), showing some of the major intracellular signaling pathways that are activated on binding of calcitonin (CT) to the CTR. Ligand binding causes a conformational change in the receptor that enables it to bind to [and to activate, by allowing the binding of guanosine triphosphate (GTP)] a number of heterotrimeric G proteins. These G proteins then dissociate into α and $\beta\gamma$ subunits, which act as adapter molecules that in turn bind and activate effector molecules, such as phospholipase C (PLC) and adenylyl cyclase. Downstream pathways activated include those involving protein kinase C (PKC), protein kinase A (PKA), mitogen-activated protein kinase (extracellular signal-related kinase, ERK), and components of the focal adhesions.

26 mM during bone resorption, this phenomenon may have particular relevance for this cell type. In fact, CT and extracellular calcium can both cause intracellular calcium transients in isolated osteoclasts and, interestingly, CT and extracellular calcium greatly augment the signal produced by either agent alone. In addition to cAMP- and Ca²⁺-mediated signaling, CTR-mediated activation of the MAPK pathway has also been described. Rapid or sustained activation of MAPK has been observed under different circumstances, the former apparently involving both G_{xi} and G_{12/13} mechanisms. A sustained activation of the Erk1/2 MAPK pathway and cell growth suppression by CT was also associated with growth inhibition and accumulation of cells in G2 phase.

Evidence for coupling of CTR to G_{xi} was seen in cells overexpressing the insert-negative CTR isoform, in which pertussis toxin enhanced the cAMP response to CT. The means by which CTR activation leads to MAPK activation requires further examination, and, in particular, consideration of a possible role for $\beta\gamma$ G protein subunits, as is commonly the case for other GPCRs. There is also evidence that CT, acting via CTR, can influence cell-cell and cell-extracellular matrix interactions. This can occur by modulating components of focal adhesions and the cytoskeleton as well as tight junction components. CT can induce phosphorylation of the focal adhesion-associated protein, human enhancer of filamentum 1 (HEF1), paxillin, and focal adhesion kinase (FAK), and the association of these latter two proteins with HEF1. This effect of CT requires cell attachment and the integrity of the cytoskeleton and involves c-Src. CT-activated CTR can also destabilize tight junctions and this requires its C-terminal PDZ docking site. CT treatment of cells can thus result in changes in cell adhesion and although it is not yet clear how these *in vitro* results relate to the actions of CT; *in vivo* this effect may have relevance to cancer.

Overall there is a lack of clear understanding of how molecular signaling events at the various isoforms of the CTR contribute to whole animal physiology.

Receptor Regulation

The cell surface expression of receptors is, in general, tightly regulated and as can be seen from the ability of RAMP proteins to influence CTR pharmacology so can receptor affinity. The CTR is subject to regulation both by CT (homologous regulation) and by other agents (heterologous regulation). CT-induced CTR downregulation has been demonstrated in various transformed CTR-expressing cell lines, primary kidney cell cultures and osteoclasts. The CT-induced loss of CTRs in osteoclasts has been proposed as a mechanism to account for the well-known loss of responsiveness to CT by patients on repeated administration clinically. Downregulation

of the CTR is mediated by specific loss of cell surface receptors, which occurs by an energy-dependent internalization of the ligand–receptor complex. Prevention of lysosomal degradation also prevents loss of cell surface receptors, indicating that the principal internalization pathway involves processing of the receptor–ligand complex into lysosomes and subsequent degradation of the receptor. Prevention of lysosomal recycling does not influence receptor levels, suggesting that the CTRs are unlikely to be recycled. Downregulation of CTRs *in vivo* has been observed in the kidney, in animals chronically administered CT and in animals with CT-secreting tumors. Downregulation of CTRs is accompanied by desensitization of responses to CT, in particular activation of adenylyl cyclase. This presumably occurs via uncoupling of the CTR from G proteins.

Acutely, downregulation of receptors is not mimicked by activators of either protein kinase A (PKA) or PKC, and may be dependent on G protein receptor kinases. The intracellular C-terminal tail of the CTR is subject to phosphorylation by second messenger-dependent and second messenger-independent kinases following agonist activation of the receptor, and it has been shown that integrity of the C-terminal tail is important for cellular internalization of the CTR. However, the mechanisms of regulation of CTR expression by homologous downregulation appear to be cell type dependent. For example, in mouse or rat osteoclasts, a potent downregulation of CTR mRNA appears to be mediated by a cAMP-dependent mechanism, in addition to downregulation of the receptor by internalization. The mechanism of CT-induced receptor mRNA loss in osteoclasts is due principally to destabilization of receptor mRNA. The 3′-untranslated regions of mouse and rat CTR mRNAs contain four AUUUA motifs, as well as other A/U-rich domains and a large number of poly (U) regions. Such motifs, commonly found in cytokines and oncogenes, function as signals for rapid mRNA inactivation. Interestingly, CTR regulation in human osteoclasts differs from that in mice, in that receptor downregulation and CT-induced receptor mRNA loss appear to be due to PKC-mediated events, rather than involving cAMP. In nonosteoclastic cells, regulation of the CTR was found to be mechanistically distinct from that in osteoclasts. In a number of cell types, CTR downregulation was cAMP independent and did not involve reduced CTR mRNA levels. It has now been found that the CTR gene in the mouse has at least three promoters and that one of these, P3, appears specific for osteoclasts. Different promoter usage may provide a mechanism for the tissue-specific regulation of the CTR.

An additional interesting aspect of CT-induced CTR regulation in osteoclasts is that glucocorticoid treatment can substantially prevent the loss of CTRs. In the mouse, glucocorticoid treatment was shown by nuclear run-on analysis to increase transcription of the CTR gene. It is worth noting that clinical evidence suggests that glucocorticoids, when administered with CT, might prevent, to some extent, the CT-induced resistance to its own action. It is also worth noting that the degree of internalization of human CTRs appears to be isoform specific, with the insert positive variant being resistant to internalization. Thus, the regulation of receptors, and consequently peptide responses, may also vary according to the level of specific receptor isoforms present in each tissue.

Heterologous regulation of the CTR by other agents has also been found. As previously indicated, in mouse and human osteoclast cultures, glucocorticoids increase the level of cell surface CTR expression following upregulation of receptor mRNA levels; this is an effect mediated at the level of transcription. Similarly, the CT-mediated decrease in cell surface receptors and mRNAs is attenuated by dexamethasone. Increased production of CTRs in response to glucocorticoid stimulation also occurs in the human T47D breast cancer cell line, which requires cortisol for expression of CTRs, suggesting that this may be a common regulatory mechanism for induction of CTR expression, while estradiol suppresses CTR expression in both T47D and MCF-7 cells. Transforming growth factor- β (TGF- β) also increases CTR levels in human blood monocyte cultures; this is perhaps related to induction of cellular differentiation toward the osteoclast lineage. As with homologous CTR regulation, responses to heterologous agents are cell type specific. Thus, in UMR 106-06 cells, TGF- β reduces the cell surface CTR levels. CTR expression is a nearly marker for differentiation of cells toward osteoclasts and indeed is considered the most reliable marker for monitoring osteoclast differentiation. Thus, factors that promote osteoclast differentiation induce CTRs as part of this process. A recent example of this is the combination of macrophage colony-stimulating factor (M-CSF) and the soluble osteoclast differentiation factor, RANK ligand, which can induce CTR expression in human or mouse monocytes or mouse spleen cells, secondary to promotion of osteoclast differentiation.

Summary

There is much yet to learn about the actions and role of CT. It will be important to better understand the physiochemistry of CT–CTR interactions, and the complex interactions between CT, CGRP, and amylin at the CTR, AMY₁ and AMY₃ receptors. An understanding of the actions of CT in inflammation and stress, in the CNS, in cancer, and in cell growth and morphogenesis could well have interesting and unexpected consequences. The study of CT in, and well beyond, its role as a calcium-regulating and bone-sparing hormone will continue to provide insights of biological interest and of importance in our understanding of health and disease.

Further Reading

- Becker, K.L., Snider, R., Nylén, E.S., January 1, 2010. Procalcitonin in sepsis and systemic inflammation: a harmful biomarker and a therapeutic target. *Br. J. Pharmacol.* 159 (2), 253–264. <http://dx.doi.org/10.1111/j.1476-5381.2009.00433.x>. Epub 2009 Nov 27. Review. PubMed PMID: 20002097; PubMed Central PMCID: PMC2825349.
- Booe, J.M., Walker, C.S., Barwell, J., Kuteyi, G., Simms, J., Jamaluddin, M.A., Warner, M.L., Bill, R.M., Harris, P.W., Brimble, M.A., Poyner, D.R., Hay, D.L., Pioszak, A.A., June 18, 2015. Structural basis for receptor activity-modifying protein-dependent selective peptide recognition by a G protein-coupled receptor. *Mol. Cell.* 58 (6), 1040–1052. <http://dx.doi.org/10.1016/j.molcel.2015.04.018>. Epub 2015 May 14. PubMed PMID: 25982113; PubMed Central PMCID: PMC4504005.

- Chaftari, A.M., Hachem, R., Reitzel, R., Jordan, M., Jiang, Y., Yousif, A., Garoge, K., Deshmukh, P., Al Hamal, Z., Jabbour, J., Hanania, A., Raad, S., Jamal, M., Raad, I., July 6, 2015. Role of procalcitonin and Interleukin-6 in predicting cancer, and its progression independent of infection. *PLoS One* 10 (7), e0130999. <http://dx.doi.org/10.1371/journal.pone.0130999> eCollection 2015. PubMed PMID: 26148092; PubMed Central PMCID: PMC4492776.
- Chambers, T.J., Magnus, C.J., January 1982. Calcitonin alters behaviour of isolated osteoclasts. *J. Pathol.* 136 (1), 27–39. PubMed PMID: 7057295.
- Clarke, M.V., Russell, P.K., Findlay, D.M., Sastra, S., Anderson, P.H., Skinner, J.P., Atkins, G.J., Zajac, J.D., Davey, R.A., September 2015. A role for the calcitonin receptor to limit bone loss during lactation in female mice by inhibiting osteocytic osteolysis. *Endocrinology* 156 (9), 3203–3214. <http://dx.doi.org/10.1210/en.2015-1345>. Epub 2015 Jul 2. PubMed PMID: 26135836.
- Davey, R.A., Findlay, D.M., May 2013. Calcitonin: physiology or fantasy? *J. Bone Min. Res.* 28 (5), 973–979. <http://dx.doi.org/10.1002/jbmr.1869>. PubMed PMID: 23519892.
- Davey, R.A., Turner, A.G., McManus, J.F., Chiu, W.S., Tjahjono, F., Moore, A.J., Atkins, G.J., Anderson, P.H., Ma, C., Glatt, V., MacLean, H.E., Vincent, C., Bouxsein, M., Morris, H.A., Findlay, D.M., Zajac, J.D., August 2008. Calcitonin receptor plays a physiological role to protect against hypercalcemia in mice. *J. Bone Min. Res.* 23 (8), 1182–1193. <http://dx.doi.org/10.1359/jbmr.080310>. PubMed PMID: 18627265; PubMed Central PMCID: PMC2680171.
- Gooi, J.H., Pompolo, S., Karsdal, M.A., Kulkarni, N.H., Kalajic, I., McAhren, S.H., Han, B., Onyia, J.E., Ho, P.W., Gillespie, M.T., Walsh, N.C., Chia, L.Y., Quinn, J.M., Martin, T.J., Sims, N.A., June 2010. Calcitonin impairs the anabolic effect of PTH in young rats and stimulates expression of sclerostin by osteocytes. *Bone* 46 (6), 1486–1497. <http://dx.doi.org/10.1016/j.bone.2010.02.018>. Epub 2010 Feb 24. PubMed PMID: 20188226.
- Hay, D.L., Walker, C.S., Gingell, J.J., Ladds, G., Reynolds, C.A., Poyner, D.R., April 15, 2016. Receptor activity-modifying proteins; multifunctional G protein-coupled receptor accessory proteins. *Biochem. Trans.* 44 (2), 568–573. <http://dx.doi.org/10.1042/BST20150237>. Review. PubMed PMID: 27068971.
- Johansson, E., Hansen, J.L., Hansen, A.M., Shaw, A.C., Becker, P., Schäffer, L., Reedt-Runge, S., May 4, 2016. Type II turn of receptor-bound salmon calcitonin revealed by X-ray crystallography. *J. Biol. Chem.* pii: jbc.M116.726034. [Epub ahead of print] PubMed PMID: 27189946.
- Keller, J., Catala-Lehnen, P., Huebner, A.K., Jeschke, A., Heckt, T., Lueth, A., Krause, M., Koehne, T., Albers, J., Schulze, J., Schilling, S., Haberland, M., Denninger, H., Neven, M., Hermans-Borgmeyer, I., Streichert, T., Breer, S., Barvencik, F., Levkau, B., Rathkolb, B., Wolf, E., Calzada-Wack, J., Neff, F., Gailus-Durner, V., Fuchs, H., de Angelis, M.H., Klutmann, S., Tsoudi, E., Hofbauer, L.C., Kleuser, B., Chun, J., Schinke, T., Amling, M., October 21, 2014. Calcitonin controls bone formation by inhibiting the release of sphingosine 1-phosphate from osteoclasts. *Nat. Commun.* 5, 5215. <http://dx.doi.org/10.1038/ncomms6215>. PubMed PMID: 25333900; PubMed Central PMCID: PMC4205484.
- Lin, H.Y., Harris, T.L., Flannery, M.S., Aruffo, A., Kaji, E.H., Gorn, A., Kolakowski Jr., L.F., Lodish, H.F., Goldring, S.R., November 15, 1991. Expression cloning of an adenylate cyclase-coupled calcitonin receptor. *Science* 254 (5034), 1022–1024. PubMed PMID: 1658940.
- Pal, K., Melcher, K., Xu, H.E., March 2012. Structure and mechanism for recognition of peptide hormones by class B G-protein-coupled receptors. *Acta Pharmacol. Sin.* 33 (3), 300–311. <http://dx.doi.org/10.1038/aps.2011.170>. Epub 2012 Jan 23. Review. PubMed PMID: 22266723; PubMed Central PMCID: PMC3690506.
- Sexton, P.M., Moris, M., Tilakaratne, N., Hay, D.L., Udawela, M., Christopoulos, G., Christopoulos, A., July 2006. Complexing receptor pharmacology: modulation of family B G protein-coupled receptor function by RAMPs. *Ann. N.Y. Acad. Sci.* 1070, 90–104. Review. PubMed PMID: 16888151.
- Walker, C.S., Eftekhari, S., Bower, R.L., Wilderman, A., Insel, P.A., Edvinsson, L., Waldvogel, H.J., Jamaluddin, M.A., Russo, A.F., Hay, D.L., June 2015. A second trigeminal CGRP receptor: function and expression of the AMY1 receptor. *Ann. Clin. Transl. Neurol.* 2 (6), 595–608. <http://dx.doi.org/10.1002/acn3.197>. Epub 2015 Apr 1. PubMed PMID: 26125036; PubMed Central PMCID: PMC4479521.
- Zaidi, M., Moonga, B.S., Abe, E., December 2002. Calcitonin and bone formation: a knockout full of surprises. *J. Clin. Invest.* 110 (12), 1769–1771. PubMed PMID: 12488426; PubMed Central PMCID: PMC151662.